# HYGROTHERMAL PERFORMANCE OF HEMP BASED THERMAL INSULATION MATERIALS IN THE UK


**ESHRAR LATIF**

MSc Planning Practice and Research
MSc Architecture: Advanced Environmental and Energy Studies
Bachelor of Architecture

**A thesis submitted in partial fulfilment of the requirements of the School of Architecture, Computing and Engineering, University of East London for the degree of Doctor of Philosophy**

**February 2013**

## Abstract

This thesis explores the hygrothermal performance of hemp insulation in the context of the United Kingdom. The key objectives of this investigation were to assess the heat and moisture management capacities of hemp insulations in two constructions typical to the UK, of timber frame and solid brick walls and to put the findings of the assessment into the greater context of conventional insulation materials by comparing hemp insulation's performance with that of stone wool. The assessments were performed by means of laboratory-based experiments, in situ experimental monitoring and computer based numerical hygrothermal simulations. The most important finding during the laboratory-based experiment is that, in high relative humidity, the likelihood and frequency of interstitial condensation is higher in stone wool insulation than in hemp insulation. In terms of the material properties, one of the key findings during the laboratory-based experiment is the high level of moisture buffering capacities of hemp insulations, and therefore their potential in managing moisture in buildings. The in situ assessment of hygrothermal properties of hemp and stone wool insulations confirms the findings of the laboratory based experiments of the corresponding moisture management capacities of these two insulation materials. Parametric analysis of the in situ data shows that mould spore germination is possible in the insulations in vapour open walls although the visual observation has not confirmed the outcome of this analysis. In terms of thermal conductivity, the important finding is that the equivalent thermal conductivity of hemp and stone wool insulations are always equal or below the manufacturers' declared thermal conductivity values. Long-term hygrothermal performances of hemp and stone wool insulation in timber frame and solid brick walls have been also assessed using a numerical hygrothermal simulation tool (WUFI). As far as the WUFI predictions are concerned, the application of the hemp or stone wool insulation on solid brick wall does not seem to be feasible with reference to condensation and mould growth in the insulations.



**Keywords:** Sustainability, thermal insulation, bio-based insulation, hemp, stone wool, thermal conductivity, condensation, moisture buffering, moisture adsorption, heat flux.

# Table of contents


Abstract ii
Table of contents iii
List of Figures xv
List of Tables xxxiii
List of abbreviations and acronyms xxxvi
Acknowledgment xxxix

**1 Introduction 1**

**1.1 Background 1**

**1.2 Research Hypothesis 7**

**1.3 Aim and objectives of the research 7**

**1.4 Outline of the materials and research methods 8**

1.4.1 Materials 8
1.4.2 Outline of the research methods 10

**1.5 Boundaries of research 10**

1.5.1 Boundary of research activities 10
1.5.2 Boundary of location 11

**1.6 Contribution to knowledge 11**

1.6.1 Experimental setup and equipment 11
1.6.2 Experimental method for laboratory and in situ tests 11
1.6.3 Research Outcome 11

**1.7 Structure of the thesis 12**

**2 Literature review of hygrothermal properties of fibrous insulations with particular focus on hemp 15**

**2.1 Heat and thermal mass 15**

2.1.1 Material level 15
2.1.2 Assembly or system level 18
2.1.3 Variable heat capacity 19
2.1.4 Heat of Wetting 20

**2.2 Moisture flux and moisture mass in buildings 21**

2.2.1 Hygrothermal performance of typical UK houses 22
2.2.2 Moisture in loft space, roof and implications 23
2.2.3 Structural moisture and implications 23
2.2.4 Indoor moisture and implications 26

**2.3 Moisture adsorption and Buffering 28**
2.3.1 Moisture adsorption 28
2.3.2 Moisture buffering 30

**2.4 Mould Growth 32**

**2.5 Summary of the literature review 35**
2.5.1 Heat 35
2.5.2 Moisture 35
2.5.3 Mould 36

**2.6 Summary of the key knowledge gaps 37**

**3 Definitions and theories related to heat, air and mass transfer and mould growth 38**

**3.1 Heat, air and moisture transfer 38**

3.1.1 Moisture transfer 38
3.1.2 Heat transfer 39
3.1.3 Heat and Moisture Balance Equation 39
3.1.4 Air balance equation 40

**3.2 Thermal conductivity 40**

3.2.1 Definition of thermal conductivity 40
3.2.2 Governing thermal equations 41

3.2.3 Thermal conductivity of moist materials 42
3.2.4 Equivalent thermal conductivity 43

**3.3 Adsorption isotherm of fibrous insulation materials 44**

3.3.1 Adsorption and adsorption isotherm 44
3.3.2 Morphology of bio-based fibres and adsorption 46
3.3.3 Adsorption mechanism 48
3.3.4 Hygroscopic region 49
3.3.5 Types of adsorption isotherms 51
3.3.6 Hysteresis 52
3.3.6.1 The incomplete wetting theory 53
3.3.6.2 The bottle neck theory 54
3.3.6.3 The open pore theory 54
3.3.6.4 The sorption site availability theory 55
3.3.7 Heat of wetting or heat of sorption 55
3.3.8 Variations in adsorption isotherms 56
3.3.9 Theories of adsorption 57
3.3.9.1 The Langmuir Isotherm 57
3.3.9.2 The Brunauer, Emmett and Teller isotherm 58
3.3.9.3 The Guggenheim/ Andersen/ de Boer isotherm 59
3.3.9.4 Hailwood and Horrobin model 59

**3.4 Moisture buffering 60**

3.4.1 Introduction 60
3.4.2 Application of moisture buffering capacity of materials 60
3.4.3 Levels of moisture buffering 61
3.4.4 Moisture penetration depth 62
3.4.5 The methods and units of moisture buffering capacity 63
3.4.5.1 Nordtest units 63
3.4.5.2 'Buf' Value 65
3.4.6 The Japanese Standard and the Nordtest method 67

**3.5 Water absorption coefficient 68**

**3.6 Vapour permeability and vapour diffusion resistance factor 68**
**3.7 Prediction of mould growth 70**
**3.8 Chapter summary 72**

**4 Research Methodology: materials, equipment, test methods and numerical simulation software 74**

**4.1 Introduction 74**

**4.2 The methodological philosophy 74**

**4.3 Outline of research methods 77**

4.3.1 The material level and research methods 77

4.3.2 The system level and research methods 78

**4.4 Material selection 80**

4.4.1 Hemp Insulation 93
4.4.2 Stone Wool Insulation 94
4.4.3 Sheep Wool Insulation 94
4.4.4 Wood fibre Insulation 95

**4.5 Use of equipment 95**

4.5.1 Standard equipment 95
4.5.1.1 The TAS climate chamber 95
4.5.1.2 The Feutron climate chamber 96
4.5.1.3 Measurement and control module 97
4.5.1.4 Temperature probes 98
4.5.1.5 Temperature and relative humidity sensors 99
4.5.1.6 Heat flux sensors 100
4.5.1.7 Water content reflectometer 100
4.5.1.8 Isomet heat transfer analyser 101
4.5.1.9 Precision weighing scales 102
4.5.1.10 Flir i7 thermal imaging camera 103
4.5.1.11 Digital microscope 104
4.5.1.12 Cirrus 40 fan heater 104

4.5.1.13 Fox 600 guarded hot plate 105
4.5.1.14 Century 4 industrial humidifier 105
4.5.1.15 TH-810H plug-in humidistat 106

4.5.2 Specialist equipment 106
4.5.2.1 Data acquisition and temperature control unit 106
4.5.2.2 Data acquisition unit 107
4.5.2.3 The dynamic hygrothermal hotbox 107

**4.6 Chapter Summary 108**

**5 Standard steady state tests 110**

**5.1 Introduction 110**

**5.2 Determination of adsorption-desorption Isotherm 110**

5.2.1 Method of determination 110
5.2.2 Method of analysis of the adsorption-desorption data 111
5.2.3 Results and discussion 112
5.2.4 Adsorption isotherms in terms of weight and volume 119
5.2.5 Hysteresis 121
5.2.6 Summary of adsorption-desorption isotherm 121

**5.3 Determination of moisture buffering capacity 122**

**5.4 Determination of vapour diffusion resistance factor 126**

**5.5 Determination of water absorption coefficient 130**

**5.6 Chapter summary 136**

**6 Dynamic and quasi steady state experiments 139**

**6.1 Introduction to the dynamic and quasi steady state experiments. 139**

**6.2 Dynamic hygrothermal performance of hemp-2 and stone wool insulation materials. 142**

6.2.1 Introduction 142
6.2.2 The sample insulation materials 142
6.2.3 The experimental setup 142
6.2.3.1 The dynamic hygrothermal hot box 143
6.2.3.2 The air conditioner 143
6.2.3.3 Temperature and relative humidity sensors 143
6.2.3.4 Heat flux sensors 144
6.2.3.5 Isomet needle probe 144
6.2.3.6 CR1000 data logger 144
6.2.4 Material preparation and instrumentation 144
6.2.5 Insulation installation 147
6.2.6 Experimental method 148
6.2.7 Results and discussion 152
6.2.7.1 Relative humidity and interstitial condensation 152
6.2.7.2 Heat Flux and thermal conductivity 161
6.2.8 Summary of the dynamic experiment 172

**6.3 Hygrothermal performance of hemp-2 and stone wool insulation materials in quasi steady state hygrothermal conditions 173**

6.3.1 The insulation samples 174
6.3.2 Instrumentation and experimental setup 174
6.3.2.1 Feutron dual climate chamber 174
6.3.2.2 Temperature and relative humidity sensors 174
6.3.2.3 Heat flux sensors 174
6.3.2.4 CR1000 data logger 175
6.3.2.5 Sample Installation 175

6.3.3 Experimental method 179
6.3.4 Results and discussion 180
6.3.4.1 Relative humidity and interstitial condensation 180
6.3.4.2 Heat flux and equivalent thermal conductivity 188
6.3.5 Summary of the quasi steady state tests 198

**6.4 An experimental assessment of the conventional method of measuring thermal conductivity of moistened insulations 200**

6.4.1 Introduction 200
6.4.2 Method 199
6.4.3 Conditioning and preparation of the insulations 201
6.4.4 Setup and instrumentation 201
6.4.5 Measurement of thermal Conductivity 203
6.4.6 Results and discussion 205
6.4.7 Summary of the assessment 209

**6.5 Insulation in lofts: experimental simulation of moisture management and thermal conductivity 209**

6.5.1 Introduction 209
6.5.2 Material selection 210
6.5.3 Experimental method 210
6.5.4 The Experimental Protocol 218
6.5.5 Results and discussion 218
6.5.5.1 Likelihood of condensation 218
6.5.5.2 Equivalent thermal conductivity 223
6.5.6 Summary of the loft experiment 225

**6.6 Chapter summary 226**

**7 In situ tests to determine hygrothermal properties of insulation materials in service conditions 228**

**7.1 Introduction 228**

**7.2 Outline of the in situ tests 229**

7.2.1 Test-1 229
7.2.2 Test-2 229
7.2.3 Test-3 229

**7.3 The test building and the test panels 230**

7.3.1 The test building 230
7.3.2 The test panels 234

**7.4 Theory** **237**

7.4.1 Theory on thermal conductivity and mould spore germination 237

7.4.2 Mould spore germination: hygrothermal conditions 238

**7.5 Operational errors in heat flux measurement** **239**

7.5.1 Operational errors in heat flux measurement in assembly-1 239

7.5.2 Operational errors in heat flux measurement in assembly-2 240

**7.6 In situ test-1: Hygrothermal performance of hemp insulation in timber frame structures with and without vapour barrier** **240**

7.6.1 Introduction 240

7.6.2 Test Materials and test panels 241

7.6.2.1 The test materials 241

7.6.2.2 The test panels 241

7.6.3 Research Method 241

7.6.3.1 Experimental protocol 241

7.6.3.2 Assessment of thermal performance and mould growth conditions 244

7.6.4 Results test-1.1 and test-1.2 245

7.6.4.1 Temperature and relative humidity 245

7.6.4.2 Heat flux, U-value and thermal conductivity 246

7.6.4.3 Hygric conditions 248

7.6.5 Discussion 249

7.6.5.1 Thermal properties 249

7.6.5.2 Relative humidity and prediction of mould growth 251

**7.7 In situ test-2: Hygrothermal performances of two hemp insulations in a vapour open timber frame structure** **255**

7.7.1 Introduction 255

7.7.2 Test materials and experimental setup 256

7.7.2.1 Test materials 256
7.7.2.2 The test panels 257

7.7.3 Research Method 257
7.7.3.1 Experimental protocol 257
7.7.3.2 Assessment of thermal performance and mould growth conditions 258

7.7.4 Results of the in situ experiment 258
7.7.4.1 Temperature and relative humidity 258
7.7.4.2 Heat flux, U-value and thermal conductivity 258
7.7.4.3 Hygric conditions 260

7.7.5 Discussion 261
7.7.5.1 Thermal properties 261
7.7.5.2 Relative humidity and prediction of mould growth 262

**7.8 In situ Test-3: Hygrothermal performance of hemp-2 and stone wool insulation materials 264**

7.8.1 Introduction 264
7.8.2 Test materials and experimental setup 265
7.8.2.1 Test materials 265
7.8.2.2 The test panels, instrumentation 265
7.8.3 Research Method 266
7.8.3.1 Experimental protocol 266
7.8.3.2 Assessment of thermal performance and mould growth conditions 266
7.8.4 Results 267
7.8.4.1 Temperature and relative humidity 267
7.8.4.2 Heat flux, U-value and thermal conductivity 267

7.8.5 Discussion 269
7.8.5.1 Thermal properties 269

7.8.5.2 Relative humidity and prediction of mould spore germination 270

**7.9 Chapter summary 275**

**8 Hygrothermal simulations using test reference year data from two UK sites 277**

**8.1 Introduction 277**

**8.2 Validation of WUFI software and parameter sensitivity analysis 278**

8.2.1 Validation of the WUFI software 278

8.2.2 Parameter sensitivity analysis 279

**8.3 Material selection and wall types 284**

8.3.1 Materials 284

8.3.2 Wall types 284

**8.4 Boundary conditions 290**

8.4.1 Interior temperature and relative humidity 290

8.4.2 Weather Data 290

**8.5 Method of hygrothermal simulation 291**

8.5.1 Material data 291

8.5.2 Simulation period 291

8.5.3 Data analysis and comparison 292

**8.6 Results and discussion 293**

8.6.1 Timber Frame Wall in Edinburgh **293**

8.6.1.1 Relative humidity conditions 294

8.6.1.2 Water content 296

8.6.1.3 Mould spore germination and mould growth 299

8.6.1.4 Mould index and mould growth 306

8.6.1.5 Thermal conductivity of the insulations 307

8.6.2 Timber frame walls in Birmingham 308

8.6.2.1 Relative humidity 308

8.6.2.2 Water content 313

8.6.2.3 Mould spore germination and mould growth 316

8.6.2.4 Mould index and mould growth 322

8.6.2.5 Thermal conductivity of the insulations 324

8.6.3 Solid Brick Wall in Edinburgh 325
8.6.3.1 Relative humidity 325
8.6.3.2 Mould spore germination and mould growth 329
8.6.3.3 Equivalent U-value of the walls 331

8.6.4 Solid Brick Wall in Birmingham 333
8.6.4.1 Relative humidity 333
8.6.4.2 Mould spore germination and mould growth 335
8.6.4.3 Equivalent U-value of the walls 337

**8.7 Summary of the numerical simulations using the WUFI software 339**

8.7.1 Condensation, mould spore germination and growth 339
8.7.2 Equivalent thermal conductivity and U-value 340

**9 Conclusions and recommendations 342**

**9.1 Overall conclusions 342**
9.1.1 Hygric material properties of hemp insulations 343
9.1.2 Moisture management of hemp insulations 344
9.1.3 Mould spore germination and mould growth 345
9.1.4 Thermal conductivity and U-value 346

**9.2 Contribution to knowledge 349**

9.2.1 Moisture management of hemp insulation 349
9.2.2 Experimental setup for visual inspection of condensation 349
9.2.3 Experimental determination of the equivalent thermal conductivity of hemp insulations in the laboratory 350
9.2.4 In situ measurement of equivalent thermal conductivity of hemp insulations 350

**9.3 Industrial benefit from the research 351**

**9.4 Recommendations for further work 351**
9.4.1 Improvement of the dual insulation set up 351
9.4.2 Long-term monitoring of hygrothermal performance 351

9.4.3 Hygrothermal simulation in a heat, air and mass (HAM) transfer software 352

**References** **353**

**Appendix A** Hot wire method for measuring thermal conductivity **366**

**Appendix B** Thermal conductivity of insulation materials: comparison of the results obtained by using an Isomet 2104 heat transfer analyser with the results obtained from Fox 600 hot plate **369**

**Appendix C** Some proposed 'rule of thumb' methods of measuring moisture dependent thermal conductivity of hemp **372**

**Appendix D** Thermal and daylight images of the test building **376**

**Appendix E** Whole building energy use **377**

**Appendix F** Sensitivity analysis data **384**

**Appendix G** Conference presentation and publication **386**

**Appendix H** Reference of current research **388**

**Appendix I** Published work **389**

# List of Figures


Figure 1.1: Built environment and CO2 emission (IGT, 2010) 03

Figure 1.2: Heat loss through the envelope of an uninsulated home (after McMullan, 2007) 04

Figure 1.3: Insulation measures (Utley and Shorrock, 2012) 05

Figure 1.4: Outline of the structure of the thesis 14

Figure 2.1: Thermal conductivity of hemp samples (Korjenic *et al*., 2011) 16

Figure 2.2: Heat of wetting of flax fibre (Hill, Norton and Newman, 2009) 21

Figure 2.3: Relative humidity in a residential space adjacent to the bathroom (Hill, Norton and Newman, 2009) 23

Figure 2.4: Health and emission risk related to different humidity regimes (Modified from Arundel *et al.*, 1986) 27

Figure 2.5: Adsorption isotherm of some natural fibres (Hill, Norton and Newman, 2009) 29

Figure 2.6: Sorption kinetics of hemp fibres (Xie *et al.*, 2011) 30

Figure 3.1: Scanning electron microscopy (SEM) images of hemp bast fibres, Scale bar: 10μm (Garcia-Jaldon, Dupeyre and Vignon, 1998) 46

Figure 3.2: Structure of hemp fibres (Norton, 2008) 47

Figure 3.3: A schematic diagram of direct and indirect moisture sorption onto (1) external surface, (2) amorphous regions, (3) inner surface of voids and (4) crystallites (Okubayashia,Griesserb and Bechtolda, 2004) 48

Figure 3.4: Adsorption regions (Kunzel, 1995) 50

Figure 3.5: Monolayer and multilayer adsorption (after Osborne, 2004) 51

Figure 3.6: Physisorption (after Condon, 2006) 52

Figure 3.7: Types of hysterisis loops (Donohue, 2012) 53

Figure 3.8: Relative energy (enthalpy) levels of vapour, liquid water, frozen and bound water as a function of moisture content (Skaar, 1998 in Time, 1998) 56

Figure 3.9: Three levels of moisture buffering (Nordtest, 2005) 61

Figure 3.10: Moisture penetration depth (Time, 1998) 62

Figure 3.11: Moisture buffering Equivalent volume (Padfield and Jensen, 2009) 66
Figure 3.12: Tortuosity (Hens, 2007) 70
Figure 3.13: Sedlbauer's isopleth system for substrate class I (Vereecken, 2012) 71
Figure 4.1: The research methods and their relationship 76
Figure 4.2: Schematic diagram of the research method 79
Figure 4.3: The material assessment pyramid 80
Figure 4.4: Illustration of hemp samples; (a) hemp-1, (b) hemp-2, (c) hemp-3, (d) hemp-4, (e) hemp-5, (f) perspective image of hemp-2. Scale bar: 1 cm 83
Figure 4.5: Illustration of wood fibre insulation sample. Scale bar: 1 cm 84
Figure 4.6: Illustration of sheep wool insulation sample. Scale bar: 1 cm 84
Figure 4.7: Illustration of stone wool insulation sample. Scale bar: 1 cm 84
Figure 4.8: Microscopic image of the sample of the hemp-1 insulation. Scale bar: 100 μm 85
Figure 4.9: Microscopic image of the sample of the hemp-1 insulation. Scale bar: 100 μm 85
Figure 4.10: Microscopic image of the sample of the hemp-2 insulation. Scale bar: 100 μm 86
Figure 4.11: Microscopic image of the sample of the hemp-2 insulation. Scale bar: 100 μm 86
Figure 4.12: Microscopic image of the sample of the hemp-3 insulation. Scale bar: 100 μm 87
Figure 4.13: Microscopic image of the sample of the hemp-3 insulation. Scale bar: 100 μm 87
Figure 4.14: Microscopic image of the sample of the hemp-4 insulation. Scale bar: 100 μm 88
Figure 4.15: Microscopic image of the sample of the hemp-4 insulation. Scale bar: 100 μm 88
Figure 4.16: Microscopic image of the sample of the hemp-5 insulation. Scale bar: 100 μm 89
Figure 4.17: Microscopic image of the sample of the hemp-5 insulation. Scale bar: 100 μm 89

Figure 4.18: Microscopic image of the sample of the stone wool insulation. Scale bar: 100 μm 90
Figure 4.19: Microscopic image of the sample of the stone wool insulation. Scale bar: 100 μm 90
Figure 4.20: Microscopic image of the sample of the wood fibre insulation. Scale bar: 100 μm 91
Figure 4.21: Microscopic image of the sample of the wood fibre insulation. Scale bar: 100 μm 91
Figure 4.22: Microscopic image of the sample of the sheep wool insulation. Scale bar: 100 μm 92
Figure 4.23: Microscopic image of the sample of the sheep wool insulation. Scale bar: 100 μm 92
Figure 4.24: TheTAS climate chamber 96
Figure 4.25: The Feutron dual climate chamber 97
Figure 4.26: The CR100 measurement and control module (CR1000: Specifications and Technical Data, 2013) 98
Figure 4.27: The 107 thermistor probes 99
Figure 4.28: The CS215 Temperature & Relative Humidity Sensors 100
Figure 4.29: The HFP01 heat flux sensor 100
Figure 4.30: The CS616 water content reflectometer 101
Figure 4.31: The Isomet heat transfer analyser 102
Figure 4.32: The surface and needle probes of the Isomet heat transfer analyser 102
Figure 4.33: The PGW 4502e precision balance 103
Figure 4.34: The Flir i7 thermal imaging camera 103
Figure 4.35: The digital microscope 104
Figure 4.36: The Cirrus 40 fan heater 104
Figure 4.37: The Fox 600 hot plate 138
Figure 4.38: The Century 4 industrial humidifier 106
Figure 4.39: The TH-810H plug-in humidistat 106
Figure 4.40: Thee dynamic hygrothermal hot box 108
Figure 5.1: The test equipment for determination of adsorption-desorption isotherm 111

Figure 5.2: Adsorption of Moisture in the insulation materials in terms of average moisture content by weight (AMCw) of each of the insulation types with 1 standard deviation 113
Figure 5.3: Adsorption of Moisture in the insulation materials in terms of average moisture content by volume (AMCv) of each of the insulation types with 1 standard deviation 114
Figure 5.4: Adsorption Isotherms of insulation materials by average moisture content by weight (AMCw) 115
Figure 5.5: Adsorption Isotherms of insulation materials by average moisture content by volume (AMCv) 115
Figure 5.6: Adsorption-desorption isotherm of hemp-1 with GAB fit in relation to average moisture content by weight (AMCw) 116
Figure 5.7: Adsorption-desorption isotherm of hemp-2 with GAB fit in relation to average moisture content by weight (AMCw) 116
Figure 5.8: Adsorption-desorption isotherm of hemp-3 with GAB fit in relation to average moisture content by weight (AMCw) 117
Figure 5.9: Adsorption-desorption isotherm of hemp-4 with GAB fit in relation to average moisture content by weight (AMCw) 117
Figure 5.10: Adsorption-desorption isotherm of hemp-5 with GAB fit in relation to average moisture content by weight (AMCw) 118
Figure 5.11: Adsorption-desorption isotherm of wood fibre with GAB fit in relation to average moisture content by weight (AMCw) 118
Figure 5.12: Adsorption-desorption isotherm of sheep wool with GAB fit in relation to average moisture content by weight (AMCw) 119
Figure 5.13: Modified classification of type 2 isotherms (Blahovic and Yanniotis, 2008) 120
Figure 5.14: Moisture buffering test setup showing hemp, sheep wool and wood fibre samples 123
Figure 5.15: Moisture buffering values with one standard deviation 124
Figure 5.16: Wood fibre insulation with three layers and hemp-2 insulation 126
Figure 5.17: Test setup for assessing vapour diffusion resistance factor 127
Figure 5.18: Mean μ value with one standard deviation determined by wet cup tests 129
Figure 5.19: Mean μ value of the insulations determined by dry cup test 130

Figure 5.20: Setup for assessing water absorption coefficient or A-value 131
Figure 5.21: Δmt versus √s plot for hemp-1 insulation, average of 3 samples 133
Figure 5.22: Δmt versus √s plot for hemp-2 insulation, average of 3 samples 165
Figure 5.23: Δmt versus √s plot for hemp-3 insulation, average of 3 samples 134
Figure 5.24: Δmt versus √s plot for hemp-4 insulation, average of 3 samples 134
Figure 5.25: Δmt versus √s plot for hemp-5 insulation, average of 3 samples 135
Figure 5.26: A value of Hemp insulations with 1 standard deviation 135
Figure 6.1: The cross section of the setup showing the dynamic hygrothermal hot box and the air-conditioner 143
Figure 6.2: Installation of sensors inside the insulation 145
Figure 6.3: The cross section of the insulation sample showing the position of the sensor and probes 145
Figure 6.4: The front elevation of the dual-insulation setup 146
Figure 6.5: The installed samples 146
Figure 6.6: The experimental setup 148
Figure 6.7: Relative humidity and vapour pressure inside the dynamic hot box and in the insulation external surfaces during test-1 153
Figure 6.8: Relative humidity and vapour pressure inside the dynamic hot box and in the insulation external surfaces during the test-2 153
Figure 6.9: Condensation is observed in (stone wool)–acrylic interface (a) while hemp-acrylic interface (b) remains dry 154
Figure 6.10: Dew point temperatures of hemp-2 and stone wool and the acrylic surface temperature during condensation (test-1) 156
Figure 6.11: Dew point temperatures of hemp-2 and stone wool and the acrylic surface temperature during condensation (test-2) 156
Figure 6.12: Calculated dew point temperature along the depth of the hemp-2 and stone wool insulations and the surface temperatures at those points 157
Figure 6.13: Relative humidity distribution in the insulation materials during test-2 158

Figure 6.14: Adsorption isotherms of hemp-2 and stone wool insulation in terms of average moisture content by volume (AMCv) 159
Figure 6.15: Water absorption of hemp in relation to √s 159
Figure 6.16: Comparison of WUFI numerical simulations and experimental results during test-2 in terms of relative humidity and water content in the insulation-acrylic interface 160
Figure 6.17: Effective equivalent thermal conductivity of hemp-2 and stone wool insulations during test-1 162
Figure 6.18: Effective equivalent thermal conductivity of hemp-2 and stone wool insulations during test-2 162
Figure 6.19: Equivalent thermal conductivity values of hemp-2 and stone wool Insulations 163
Figure 6.20: Correlation between ambient temperature difference and heat flux in hemp-2 and stone wool during test-1 166
Figure 6.21: Correlation between the ambient temperature difference and heat flux in hemp-2 and Stone wool during test-2 167
Figure 6.22: Relative humidity in the hot box and heat flux in hemp-2 and stone wool insulation during test-1 167
Figure 6.23: Relative humidity in the hot box and heat flux in hemp-2 and stone wool insulation during test-2 168
Figure 6.24: Vapour pressure difference and heat flux in hemp-2 and Stone wool insulation during test-1 168
Figure 6.25: Vapour pressure difference and heat flux in hemp-2 and stone wool insulation during test-2 169
Figure 6.26: Experimental data and numerical predictions (WUFI) of heat flux during test-2 170
Figure 6.27: Correlation between ranges of average relative humidity and equivalent thermal conductivity of hemp-2 171
Figure 6.28: Ranges of average relative humidity and corresponding equivalent thermal conductivity of stone wool 172
Figure 6.29: Correlation between ranges of adsorbed moisture content and equivalent thermal conductivity of hemp-2 172
Figure 6.30: Front elevation and cross section of the insulation setup 175
Figure 6.31: Cross section of the dual climate chamber 176

Figure 6.32: Insulation materials to be placed on the EPS frameworks 177
Figure 6.33: The XPS framework and the partition frame 177
Figure 6.34: The insulation materials placed between the hot and cold chamber 178
Figure 6.35: The insulation materials between the hot and cold chamber with all the sensors installed 178
Figure 6.36: The temperature and humidity profile of the climate chamber 180
Figure 6.37: Relative humidity in the middle and in the surface of hemp insulation 181
Figure 6.38: Relative humidity in the middle and in the surface of stone wool insulation 182
Figure 6.39: Relative humidity in the insulation-acrylic interface and in the hot chamber 182
Figure 6.40: Dew formed in acrylic inner surface of stone wool insulation and foggy patches in acrylic inner surface of hemp-2 insulation 183
Figure 6.41: Relative humidity in the insulation-acrylic interface and in the warm chamber during the laboratory experiment and simulation in the WUFI software 184
Figure 6.42: Internal surface temperatures of the acrylic and the insulation-acrylic dew point temperatures 185
Figure 6.43: Insulation-acrylic interface air temperature and dew point temperature 187
Figure 6.44: WUFI simulation data of water content in insulation external surfaces and insulation-acrylic interfaces 188
Figure 6.45: Equivalent thermal conductivity values of hemp-2 and stone wool insulation along with the values of interior and insulation-acrylic interface relative humidity 190
Figure 6.46: Equivalent thermal conductivity values of hemp-2 and stone wool Insulations 191
Figure 6.47: Equivalent thermal conductivity of hemp-2 plotted against relative humidity 192
Figure 6.48: Equivalent thermal conductivity of stone wool plotted against relative humidity 192

Figure 6.49 Equivalent thermal conductivity plotted against adsorbed water 193
Figure 6.50: Interior relative humidity and heat flux in hemp-2 and stone wool insulation 194
Figure 6.51: Vapour pressure difference and heat flux in hemp-2 and stone wool insulation 194
Figure 6.52: Experimental and WUFI simulation of heat flux in the cold side of hemp insulation (external surface of the acrylic) 195
Figure 6.53: Experimental and WUFI simulation of heat flux in the cold side of stone wool insulation (external surface of the acrylic) 196
Figure 6.54: Experimental and WUFI simulation of heat flux in the warm side surface of hemp insulation 197
Figure 6.55: Experimental and WUFI simulation of heat flux in the warm side surface of stone wool insulation 197
Figure 6.56: The front elevation of the dual-insulation setup 202
Figure 6.57: The cross section of the dual-insulation setup 203
Figure 6.58: Thermal conductivity measurement of hemp-2 at 80 EMC with EPS insulation as a control (40 hours) 205
Figure 6.59: Thermal conductivity measurement of hemp-2 at 95 EMC with EPS insulation as a control (24 hours measurement) 206
Figure 6.60: Thermal conductivity measurement of hemp-2 at 95 EMC with EPS insulation as a control (40 hours measurement) 206
Figure 6.61: The typical hygrothermal condition in the ‘problem loft’ 211
Figure 6.62: The conceptual diagram of the lab-based experiment 213
Figure 6.63: The cross section of the experimental set up 214
Figure 6.64: Completed installation of the experimental setup 215
Figure 6.65: The plan view of the setup 215
Figure 6.66: Installation process of the sensors 216
Figure 6.67: Installation of insulation and temperature and relative humidity sensors 216
Figure 6.68: Installation of the breather membrane box 217
Figure 6.69: Condensed moisture on the acrylic inner surface after the experiment with stone wool 219
Figure 6.70: Close-up image of condensed moisture on the acrylic inner surface after the experiment with stone wool 219

Figure 6.71: Mass change in the experimental setups for the insulation materials 221
Figure 6.72: Relative humidity distribution during the stone wool test 221
Figure 6.73: Relative humidity distribution during the sheep wool test 222
Figure 6.74: Relative humidity distribution during the hemp-1 test 222
Figure 6.75: Relative humidity distribution during the Hemp-4 test 223
Figure 6.76: Equivalent thermal conductivity of the insulations with error bar 224
Figure 6.77: Heat flux and temperature difference in stone wool and hemp-4 225
Figure 7.1: The test building showing the test wall 230
Figure 7.2: The plan of the test building 231
Figure 7.3: Three dimensional computer image of the test building with the roof removed 231
Figure 7.4: Construction of the outer layer of the test building 232
Figure 7.5: Installation of the EPS insulation and breather membrane 232
Figure 7.6: Installation of the OSB boards and timber frames for wall panels 233
Figure 7.7: Installation of the EPS insulation in the eastern wall 233
Figure 7.8: Horizontal cross section showing panel A and pane B and sensor locations in assembly-1 235
Figure 7.9: Horizontal cross section showing panel A and panel B and sensor locations in assembly-2 236
Figure 7.10: Sedlbauer's isopleth system for substrate class I 238
Figure 7.11: The setup process showing the inner OSB linings and the temperature and relative humidity sensors 243
Figure 7.12: The installation of the inner layer of the insulation with the sensors 243
Figure 7.13: The installation of the outer layer of the insulation 244
Figure 7.14: The installation of the surface lining and the sensors 244
Figure 7.15: Surface temperatures in OSB inner lining, (a) panel A and (b) panel B 245
Figure 7.16: Temperature and relative humidity during the test-1.1 246
Figure 7.17: Temperature and relative humidity during the test-1.2 246
Figure 7.18: Heat flux in panels with plasterboard lining during test-1.1 247

Figure 7.19: Heat flux in panels with plasterboard lining during test-1.2 247
Figure 7.20: Relative humidity and soil moisture content equivalent in hemp-PB interfaces and interior relative humidity during test-1.1 248
Figure 7.21: Relative humidity and soil moisture content equivalent in hemp-PB interfaces and interior relative humidity during test-1.2 249
Figure 7.22: Equivalent thermal conductivity values (λequi) with error bar during test-1.1 250
Figure 7.23: Equivalent thermal conductivity values (λequi) with error bar during test-1.2 250
Figure 7.24: Average equivalent thermal conductivity values (λequi) with error bar during test-1.1 and test-1.2. 251
Figure 7.25: (Hemp-1)-OSB interface conditions against Sedlbauer's isopleth during the test-1.1 252
Figure 7.26: 11 days' conditions of (hemp-1)-OSB interface condition against Sedlbauer's 8 day isopleth line during test-1.1 253
Figure 7.27: (Hemp-1)-OSB interface condition against Sedlbauer's isopleth during test-1.2 254
Figure 7.28: The vertical cross section of the wall panel 256
Figure 7.29: Hem-1 and hemp-2 insulation materials respectively 257
Figure 7.30: The temperature and relative humidity boundary conditions during the experiment 258
Figure 7.31: Heat Flux data gathered from the surface of the plasterboards during test-2 259
Figure 7.32: Heat flux data gathered from insulation-OSB interfaces during test-2 259
Figure 7.33: Relative humidity and moisture content in the insulation-OSB interface during test-2 260
Figure 7.34: Equivalent thermal conductivity values with error bar 262
Figure 7.35: Adsorption isotherms of hemp-1 and hemp-2 263
Figure 7.36: Hygrothermal conditions in the insulation-OSB interface in conjunction with spore germination isopleths 264
Figure 7.37: The hygrothermal boundary conditions 267

Figure 7.38: Heat Flux in panel A (hemp-2) and panel B (stone wool) based on the heat flux sensors located on the inner plaster board surfaces 268
Figure 7.39: Heat Flux in panel A (hemp-2) and panel B (stone wool) based on the heat flux sensors located in the insulation-OSB interfaces 268
Figure 7.40: The equivalent thermal conductivity values of the Insulations 270
Figure 7.41: The relative humidity conditions at insulation-OSB interfaces 270
Figure 7.42: The insulation-OSB interface hygric conditions 271
Figure 7.43: The insulation-OSB interface hygric conditions 272
Figure 7.44: 39 Days' Hygrothermal Condition in (stone wool)-OSB Interface 273
Figure 7.45: Continuous 11 days hygrothermal condition in (stone wool)-OSB interface 273
Figure 7.46: 40 Days' Hygrothermal Condition in (hemp-2)-OSB Interface 274
Figure 7.47: Continuous 11 days hygrothermal condition in (hemp-2)-OSB interface 274
Figure 8.1: Moisture distribution in the slab in 7 days, 30 days and 365 days (Benchmark Test of EN 15026, 2012) 278
Figure 8.2: Temperature distribution in the slab in 7 days, 30 days and 365 days (Benchmark Test of EN 15026, 2012) 279
Figure 8.3: Effect of (%) change of parameters on (%) change of water content in Hemp-2 from base case 281
Figure 8.4: Effect of (%) change of parameters on (%) change of water content in (hemp-2)-OSB interface from base case 282
Figure 8.5: Effect of (%) changes of parameters on (%) changes of relative humidity in (hemp-2)-OSB interface from base case 282
Figure 8.6: Effect of (%) changes of parameters on (%) changes of relative humidity in (Hemp-2)-OSB interface from base case (ranges of y axis narrowed down to ±1%) 283

Figure 8.7: Effect of (%) changes of parameters on (%) changes of temperature in hemp-2 from base case 283
Figure 8.8: Effect of (%) changes of parameters on (%) changes of temperature in hemp-2 from base case(ranges of y axis narrowed down to ±1%) 284
Figure 8.9: The vertical cross section of the timber frame wall assembly without vapour barrier (wall-1) 285
Figure 8.10: The vertical cross section of the timber frame wall assembly with vapour barrier (wall-2) 286
Figure 8.11: The vertical cross section of the solid brick wall assembly without vapour barrier (wall-3) 287
Figure 8.12: The vertical cross section of the solid brick wall assembly with vapour barrier (wall-4) 288
Figure 8.13: The vertical cross section of the solid brick wall assembly (with air gap) without vapour barrier (wall-5) 288
Figure 8.14: The vertical cross section of the solid brick wall assembly (with air gap) assembly with vapour barrier (wall-6) 289
Figure 8.15: The vertical cross section of the solid brick wall assembly (with lime plaster) without vapour barrier (wall-7) 289
Figure 8.16: The vertical cross section of the solid brick wall assembly (with lime plaster) with vapour barrier (wall-8) 290
Figure 8.17: The study of an insulated solid brick wall to explore the time required to reach hygrotheral equilibrium 292
Figure 8.18: Relative humidity conditions in (hemp-1)-OSB interfaces in wall-1 and wall-2 in Edinburgh 293
Figure 8.19: Relative humidity conditions in the (hemp-2)-OSB interfaces in wall-1 and wall-2 in Edinburgh 294
Figure 8.20: Relative humidity conditions in the (stone wool)-OSB interfaces in wall-1 and wall-2 in Edinburgh 294
Figure 8.21: Relative humidity conditions in the Insulation OSB interfaces in wall-1 and Wall-2 in Edinburgh 295
Figure 8.22: Relative humidity conditions in the inner surfaces of the hemp-1 insulations in wall-1 and wall-2 in Edinburgh 295

Figure 8.23: Relative humidity conditions in the inner surfaces of the hemp-2 insulations in wall-1 and wall-2 in Edinburgh 296
Figure 8.24: Relative humidity conditions in the inner surfaces of the stone wool insulations in wall-1 and wall-2 in Edinburgh 296
Figure 8.25: Water content in the (hemp-1)-OSB interfaces of wall-1 and wall-2 in Edinburgh 297
Figure 8.26: Water content in the (hemp-2)-OSB interfaces of wall-1 and wall-2 in Edinburgh 297
Figure 8.27: Water content in the stone wool-OSB interfaces of wall-1 and wall-2 in Edinburgh 298
Figure 8.28: Water content in the insulation-OSB interfaces of wall-1 and wall-2 in Edinburgh 298
Figure 8.29: Estimated and critical water content in the mould spore in The (hemp-1)-OSB interface of the timber frame walls without vapour barrier (wall-1) in Edinburgh 300
Figure 8.30: Estimated and critical water content in the mould spore in the (hemp-1)-OSB interface of the timber frame walls with vapour barrier(wall-2) in Edinburgh 300
Figure 8.31: Estimated and critical water content in the mould spore in the (hemp-2)-OSB interface of the timber frame walls without vapour barrier (wall-1) in Edinburgh 301
Figure 8.32: Estimated and critical water content in the mould spore in the (hemp-2)-OSB interface of the timber frame walls with vapour barrier (wall-2) in Edinburgh 301
Figure 8.33: Estimated and critical water content in the mould spore in the (stone wool)-OSB interface of the timber frame walls without vapour barrier (wall-1) in Edinburgh 302
Figure 8.34: Estimated and critical water content in the mould spore in the (stone wool)-OSB interface of the timber frame walls with vapour (wall-2) barrier in Edinburgh 302
Figure 8.35: Hygrothermal condition in the (hemp-1)-OSB interface of timber frame walls without vapour barrier (wall-1) In Edinburgh 303

Figure 8.36: Hygrothermal condition in the (hemp-1)-OSB interface of timber frame walls with vapour barrier (wall-2) in Edinburgh 303
Figure 8.37: Hygrothermal condition in the (hemp-2)-OSB interface of frame timber walls without vapour (wall-1) barrier in Edinburgh 304
Figure 8.38: Hygrothermal condition in the (hemp-2)-OSB interface of timber frame walls with vapour barrier (wall-2) in Edinburgh 304
Figure 8.39: Hygrothermal condition in the (stone wool)-OSB interface of timber frame walls without vapour barrier (wall-1) in Edinburgh 305
Figure 8.40: Hygrothermal condition in the (stone wool)-OSB interface of timber frame walls with vapour barrier (wall-2) in Edinburgh 305
Figure 8.41: Mould index in insulation-OSB interfaces for different insulations in Edinburgh 306
Figure 8.42: Mould growth in insulation-OSB interfaces for different insulations in Edinburgh 307
Figure 8.43: Equivalent thermal conductivity values of the insulations in Edinburgh 308
Figure 8.44: Relative humidity conditions in the (hemp-1)-OSB interfaces for timber frame walls with and without vapour barrier in Birmingham 309
Figure 8.45: Relative humidity conditions in the (hemp-2)-OSB interfaces in wall-1 and wall-2 in Birmingham 310
Figure 8.46: Relative humidity conditions in the (stone wool)-OSB interfaces in wall-1 and wall-2 in Birmingham 310
Figure 8.47: Relative Humidity conditions in the inner surfaces of the hemp-1 insulations in wall-1 and wall-2 in Birmingham 311
Figure 8.48: Relative Humidity conditions in the inner surfaces of the hemp-2 insulations in wall-1 and wall-2 in Birmingham 311
Figure 8.49: The relative humidity conditions in the inner surfaces of the stone wool insulations in wall-1 and wall-2 in Birmingham 312
Figure 8.50: Relative humidity conditions in the inner surfaces of the insulations in wall-1 and wall-2 in Birmingham 312
Figure 8.51: Water content in the (hemp-1)-OSB interfaces in wall-1 and wall-2 in Birmingham 313

Figure 8.52: Water content in the (hemp-2)-OSB interfaces in wall-1 and wall-2 in Birmingham 314
Figure 8.53: Water content in the (stone wool)-OSB interfaces in wall-1 and wall-2 in Birmingham 314
Figure 8.54: Water content in the insulation-OSB interfaces in wall-1 in Birmingham 315
Figure 8.55: Water content in the insulation-OSB interfaces in wall-2 in Birmingham 315
Figure 8.56: Estimated and critical water content in the mould spore in the (hemp-1)-OSB interfaces in wall-1 in Birmingham 316
Figure 8.57: Estimated and critical water content in the mould spore in the (hemp-1)-OSB interface in wall-2 in Birmingham 317
Figure 8.58: Estimated and critical water content in the mould spore in the (hemp-2)-OSB interface in wall-1 in Birmingham 317
Figure 8.59: Estimated and critical water content in the mould spore in the (hemp-2-OSB) interface in wall-2 in Birmingham 318
Figure 8.60: Estimated and critical water content in the mould spore in the (stone wool)-OSB interface in wall-1 in Birmingham 318
Figure 8.61: Estimated and critical water content in the mould spore in the (stone wool)-OSB interface in wall-2 in Birmingham 319
Figure 8.62: Hygrothermal condition in the (hemp-1)-OSB in wall-1 in Birmingham 319
Figure 8.63: Hygrothermal condition in the (hemp-1)-OSB interface in wall-2 in Birmingham 319
Figure 8.64: Hygrothermal condition in the (hemp-2)-OSB interface in wall-1 in Birmingham 320
Figure 8.65: Hygrothermal condition in the (hemp-2)-OSB interface in wall-2 in Birmingham 321
Figure 8.66: Hygrothermal condition in the (stone wool)-OSB in wall-1 in Birmingham 321
Figure 8.67: Hygrothermal condition in the (stone wool)-OSB interface in wall-1 in Birmingham 322
Figure 8.68: Predicted mould index in the insulation-OSB interfaces of wall-1 and wall-2 in Birmingham 323

Figure 8.69: Predicted mould growth in the insulation-OSB interfaces of timber frame walls (Birmingham) 323
Figure 8.70: Equivalent thermal conductivity values of the insulations in wall-1 and wall-2 in Birmingham 324
Figure 8.71: Relative humidity in (hemp-1)-Brick, (hemp-1)-air and (hemp-1)-lime interfaces in walls with and without vapour barrier in Edinburgh 326
Figure 8.72: Relative humidity in (hemp-2)-Brick, (hemp-2)-air and (hemp-2)-lime interfaces in walls with and without vapour barrier in Edinburgh 326
Figure 8.73: Relative humidity in(stone wool)-Brick, (stone wool)-air and (stone wool)-lime interfaces in walls with and without vapour barrier in Edinburgh 327
Figure 8.74: Relative humidity in the hemp-2 inner surface of the wall-7 and wall-8 in Edinburgh during October 1991 to November 1995 328
Figure 8.75: Relative humidity in the hemp-2 inner surface of the wall-7 and wall-8 in Edinburgh during 1994 328
Figure 8.76: Hygrothermal condition in the (hemp-2)-air interface of wall-5 in Edinburgh 329
Figure 8.77: Estimated and critical water content in the mould spore in the (hemp-2)-air interface of wall-5 in Edinburgh 330
Figure 8.78: Predicted mould index in the (hemp-2)-air interface of wall-5 in Edinburgh 330
Figure 8.79: Predicted mould growth in the (hemp-2)-air interface of wall-5 in Edinburgh 331
Figure 8.80: Equivalent U-values of walls incorporating hemp-1 insulations in Edinburgh 331
Figure 8.81: Equivalent U-values of walls incorporating hemp-2 insulations in Edinburgh 332
Figure 8.82: Equivalent U-values of walls incorporating stone wool insulations in Edinburgh 332
Figure 8.83: Relative humidity in the (hemp-1)-brick, (hemp-1)-air and (hemp-1)-lime interfaces of solid brick walls in Birmingham 333

Figure 8.84: Relative humidity in the (hemp-2)-brick, (hemp-2)-air and (hemp-2)-lime interfaces of solid brick walls in Birmingham 334
Figure 8.85: Relative humidity in the (stone wool)-brick, (stone wool)-air and (stone wool)-lime interfaces of solid brick walls in Birmingham 334
Figure 8.86: Hygrothermal condition in the (hemp-2)-air interface of the wall-5 in Birmingham 335
Figure 8.87: Estimated and critical water content in the mould spore in the (hemp-2)-air interface of wall-5 in Birmingham 336
Figure 8.88: Predicted mould index in the (hemp-2)-air interface of wall-5 in Birmingham 336
Figure 8.89: Predicted mould growth in the (hemp-2)-air interface of wall-5 in Birmingham 337
Figure 8.90: Equivalent U-values of walls incorporating hemp-1 insulations in Birmingham 337
Figure 8.91: Equivalent U-values of walls incorporating hemp-2 insulations in Birmingham 338
Figure 8.92: Equivalent U-values of walls incorporating stone wool insulations in Birmingham 338
Figure 8.93: The relative humidity the insulation-air interfaces of wall-5 in Edinburgh and Birmingham 340
Figure A.1: Transient hot wire apparatus 367
Figure A.2: Isomet heat analyser at CAT 368
Figure B.1: Conductivity readings at 23 °C temperature and 50% relative humidity 370
Figure B.2: Conductivity readings at 90 °C temperature and 10% relative humidity 370
Figure B.3: Conductivity readings at 10 °C temperature and 80% relative humidity 371
Figure C.1: Thermal conductivity of hemp insulation determined by using supplement 375
Figure D.1: Thermal images showing (a) wall panel location (b) eastern wall, without insulations 376
Figure D.2: Thermal images showing (a) wall panel location (b) eastern wall, with insulations 376

Figure D.3: Illustration showing the test and the residential building 376
Figure E.1: The wall section 378
Figure E.2: Moisture content in hemp-2 insulation 379
Figure E.3: The plan of the notional building for the IES software 380
Figure E.4: The IES software image of the simulated buildings 380
Figure E.5: The monthly space conditioning sensible loads of the selected buildings in Edinburgh 381
Figure E.6: The monthly space conditioning sensible loads of the selected buildings in Birmingham 382
Figure E.7: The yearly space conditioning sensible loads of the selected buildings in Edinburgh and Birmingham, respectively 382

# List of Tables


| | | |
|---|---|---|
| Table 2.1: | Thermal conductivity values of the insulations (adapted from Ye *et al*., 2005) | 17 |
| Table 2.2: | Thermal properties of some building materials | 19 |
| Table 3.1: | Mould spore germination conditions in IEA-Annex 14 | 71 |
| Table 4.1: | Summary of the properties of the hemp insulations | 93 |
| Table 4.2: | Summary of the properties of stone wool insulation | 94 |
| Table 4.3: | Summary of the properties of the sheep wool insulation | 94 |
| Table 4.4: | Summary of the properties of the wood fibre insulation | 95 |
| Table 4.5: | Dimensions of the TAS climate chamber | 95 |
| Table 4.6: | Range and accuracy of conditioning of the TAS climate chamber | 96 |
| Table 4.7: | Dimensions of the Feutron dual climate chamber | 96 |
| Table 4.8: | Range and accuracy of conditioning of the chambers | 97 |
| Table 4.9: | Technical details of the CR100 measurement and control module | 98 |
| Table 4.10: | Technical details of CS616 water content reflectometer | 101 |
| Table 4.11: | Range and accuracy of conditioning of the chambers | 101 |
| Table 4.12: | Capacity and accuracy of the precision weighing scale | 102 |
| Table 4.13: | Technical details of the Flir i7 thermal imaging camera | 103 |
| Table 4.14: | Technical details of the HooToo digital microscope. | 104 |
| Table 4.15: | Technical details of the Fox 600 hot plate | 105 |
| Table 5.1: | The test conditions for all insulation samples | 122 |
| Table 5.2: | Mean practical moisture buffer value of the Hemp insulations | 124 |
| Table 5.3: | Ranges for practical Moisture Buffer Value classes (Rode, 2005) | 125 |
| Table 5.4: | μ values and Sd values of the insulations | 129 |
| Table 5.5: | Mean Aw,24 value of the Hemp insulations | 136 |
| Table 6.1: | Overview of the experimental tests | 140 |
| Table 6.2: | Equivalent and design values of thermal conductivity of hemp-2 and stone wool insulation materials | 165 |

| | | |
|---|---|---|
| Table 6.3: | The average heat flux values of hemp-2 and stone wool insulation materials | 169 |
| Table 6.4: | The average interior relative humidity and the corresponding equivalent thermal conductivity values of hemp-2 insulation along with adsorption water content | 171 |
| Table 6.5: | The temperature and relative humidity profile of the climate chamber | 179 |
| Table 6.6: | Experimental and design value of thermal conductivity with standard deviations | 191 |
| Table 6.7: | Moisture migration during conductivity measurements of hemp-2 at 85 EMC during test-1 | 207 |
| Table 6.8: | Moisture migration during conductivity measurements of hemp-2 at 95 EMC during test-2 | 208 |
| Table 6.9: | Different values of thermal conductivity | 209 |
| Table 6.10: | Representative data for experimental simulation of the loft hygrothermal conditions | 212 |
| Table 6.11: | The experimental protocol | 218 |
| Table 6.12: | Moisture accumulation in the acrylic, the breather membrane box and in the insulation materials | 220 |
| Table 6.13: | Equivalent thermal conductivity of the insulations | 224 |
| Table 7.1: | Average external temperatures (temp) in the UK and Wales during January, February, July and August | 234 |
| Table 7.2: | The test setup and duration | 241 |
| Table 7.3: | U-value of the wall panel A and panel B and equivalent thermal conductivity of the hemp insulation measured according to the ISO 9869 | 248 |
| Table 7.4: | The setup and duration of test-2 | 255 |
| Table 7.5: | U-value of the wall panel A and panel B and equivalent thermal conductivity of the hemp insulation measured according to the ISO 9869 | 260 |
| Table 7.6: | The test setup and duration | 265 |
| Table 7.7: | The relative humidity protocol | 266 |

Table 7.8: U-values of the wall panel A (hemp-1) and panel B (stone wool) and λequi values of hemp-2 and stone wool insulation materials 269
Table B.1: Material properties of the insulations 369
Table C.1: Thermal conductivity of hemp insulation determined by using thermal conductivity supplement 372
Table C.2: Thermal conductivity of hemp insulation determined by using effective thermal conductivity value 373
Table C.3: Design values of thermal conductivity of hemp insulation 374
Table F.1: Effect of change of parameter values (%) on change of water content (%) in hemp-2 from the base case 384
Table F.2: Effect of change of parameter values (%) on change of relative humidity (%) in (hemp-2)-OSB interface from the base case 384
Table F.3: Effect of change of parameter values (%) on change of water content (%) in (hemp-2)-OSB interface from the base case 385
Table F.4: Effect of change of parameter values (%) on change of temperature (%) in hemp-2 from the base case 385

# List of Abbreviations and Acronyms

| | |
|---|---|
| ACC | Aerated cellular concrete |
| ACE | Association for the Conservation of Energy |
| ASTM | American Society of Testing and Materials |
| BET | Brunauer, Emmett and Teller |
| BMP | Bitmap image file |
| BRE | Building Research Establishment |
| BREAM | Building Research Establishment Environmental Assessment Method |
| BS | British Standards |
| DCLG | Department for Communities and Local Government |
| DECC | Department of Energy and Climate Change |
| DETR | Department of the Environment, Transport and the Regions |
| EEP | Extruded polystyrene |
| EMC | Equilibrium moisture content |
| EN | European Standards |
| EPS | Expanded polystyrene |
| FSP | Fibre saturation point |
| GAB | Guggenheim/ Andersen/ de Boer |
| GP | Gypsum plaster |
| IEA | International Energy Agency |
| IES | Integrated Environmental Solutions |
| IGT | Innovation and Growth Team |

| | |
|---|---|
| IPCC | Intergovernmental Panel on Climate Change |
| ISO | International Organization for Standardization |
| IUPAC | International Union of Pure and Applied Chemistry |
| JPEG | Joint Photographic Experts Group |
| LIM | Lowest isopleth for mould |
| MBV | Moisture buffer value |
| MFA | Microfibril angle |
| MMC | Modern method of construction |
| MMF | Man-made fibre |
| N-DEEM | Non-Domestic building Energy and Emissions Model |
| NIST | National Institute of Standards and Technology |
| Nordtest | Nordic organisation for cooperation within the area of testing |
| NPL | National Physical Laboratory |
| NTP | National Toxicology Program |
| OH | Hydroxyl |
| OSB | Oriented strand board |
| PE | Polyethylene |
| PF | Polyurethane foam |
| ppm | Parts per million |
| PW | Plywood |
| RH | Relative humidity |
| SPSS | Statistical Package for the Social Sciences |
| TAS | Temperature Applied Sciences Limited |

| | |
|---|---|
| TSB | Technology Strategy Board |
| UNEP | United Nations Environment Programme |
| VB | Vapour barrier |
| VO | Vapour open |
| VWC | Volumetric water content |
| WFB | Wood fibreboard |
| WHO | World Health Organization |
| WUFI | Wärme und Feuchte instationär |
| XPS | Extruded polystyrene |

# Acknowledgements

I am greatly indebted to Dr Mihaela Anca Ciupala, Dr Simon Tucker, Mr Darryl Newport and Professor D C Wijeyesekera for their meticulous supervision and continued encouragement.

I would like to thank the Technology Strategy Board, the University of East London and the other partners of the 'Energy Efficient Bio-based Natural Fibre Insulation' project for the PhD studentship and continued support without which this work would not have been possible. Grateful thanks are extended to the Centre for Alternative Technology (CAT) where I was on secondment during the whole period of my doctoral studies.

I am grateful to the Faculty of Civil Engineering and Building Services of 'Gheorghe Asachi' Technical University of Iași, Romania, for allowing me to use their climate chamber. I would like to thank Dr Mihaela Anca Ciupala again for being instrumental in arranging this travel and introducing me to the 'Going Global' travel grant.

Particular thanks must go to Professor Tom Woolley, Dr Robert Elias, Dr Andrew Hewitt, Dr Marian Pruteanu, Dr Arthur Butler, Mr Giles Ranyl Rhydwen, Mr Gary Newman, Ms Ceri Loxton, Mr Christof Fehr, Ms Blanche Cameron, Ms Paula Amani, Ms Linda Day and Mr Will Bryson for their kind support at various stages of the research. I would also like to convey my gratitude to Mr Neil May for sharing his wealth of knowledge on natural building materials and for providing the wood fibre samples.

The thesis would not have been possible without the constant support and encouragement from my wife Deepa, family and friends.

To

My parents, wife and children

# Chapter 1

# Introduction

## 1.1 Background

This thesis explores the hygrothermal performance of bio-based fibrous thermal insulations with particular reference to the use of hemp in the UK. The rationale for the research is rooted in the global context of concerted efforts to mitigate the adverse effects of climate change and resource depletion.

Among the bio-based thermal insulation materials, the hemp insulation is of particular importance in the UK. Hemp is a high yield and low input crop with the additional advantages of being a break crop in cereal rotations. Other benefits include excellent weed control and less field operation (Hemp Technology, 2012a). The largest hemp fibre processing plant in the world with the highest production capacity is located in the UK from where much of the locally grown hemp fibres are processed and supplied to the domestic and international market. Hemp fibre is a renewable, sustainable and carbon negative material (Hemp Technology, 2012b). The aforementioned agricultural, processing and environmental benefits of hemp make hemp insulation potentially relevant to the UK construction sector.

The 'Earth System' is facing unprecedented threats from human interference. Anthropogenic activities, with 90% probability (IPCC, 2007), are changing the dynamics of atmospheric, geological, hydrological, biological and other Earth System processes (UNEP, 2012). Most evident of the changes are the rise in global average air and sea level temperature and ocean acidification, both triggered by increasing greenhouse gas emission, especially carbon and methane (UNEP, 2012). Sea level is rising at the average rate of 3.1 mm per year with thermal expansion contributing about 57%, melting of glacier and ice caps about 28% and decrease of polar ice sheet contributing the remainder to the total rise (IPCC, 2007).

From a pre-industrial value of about 280 ppm (parts per million), the global atmospheric concentration of carbon has increased to about 379 ppm in 2005

resulting in about 20% increase in radiative forcing (IPCC, 2007). The best estimate predicts that 450 ppm of $CO_2$ equivalent radiative forcing will increase the global mean equilibrium surface temperature by 2.1 °C over the pre-industrial level (IPCC, 2007). More than 2°C rise in global temperature is described as the 'dangerous anthropogenic interference with the climate system' (UNEP, 2010) beyond which the risk of severe damage to ecosystem and of nonlinear responses are expected rapidly (IPCC, 2007). The business as usual scenario is a 6 °C rise in temperature by the end of the century (IEA, 2008).

Two-thirds of the anthropogenic contributor to $CO_2$ emission is fossil fuel, of which about 37% of the emission is from oil, 43% from coal/peat and 14% from natural gas (IEA, 2011). To avert the global temperature rise to a dangerous level, a paradigm shift from human civilization's dependence on hydrocarbon based energy to clean energy is apparently inevitable.

Yet climate change is not the only risk necessitating immediate mitigating action. Human consumptions are not in harmony with the earth's natural support system. Twenty per cent of the world's seven billion population are consuming seventy seven per cent of the earth's resources at a pace and intensity that outdo the earth's capacity to neutralize the adverse effects (Kummel, 2011). Resource depletion and degradation at a planetary scale are gradually pushing the human civilization to the edge of catastrophe. Production of oil and 'non-renewable water' (Palaniappan and Gleick, 2009) are predicted to reach their peak nearly at the same time (Brown, 2011) irrespective of one being stock-limited and the other being flow-limited.

Against this overwhelmingly challenging backdrop, the United Kingdom has made the legally binding commitment to reduce greenhouse gas emissions by 80% compared to the 1990 baseline by the year 2050 (Great Britain. *Climate Change Act 2008)*. Any deep cut in $CO_2$ emission in the UK requires involving the construction sector, since about 55% of the total $CO_2$ emission from the UK is directly related to the emission from domestic and non-domestic buildings and construction process (IGT, 2010). The domestic buildings are liable for 27%, non-domestic buildings for 18% and construction process for 10% of the total emission in terms of operational energy use (Figure 1.1).

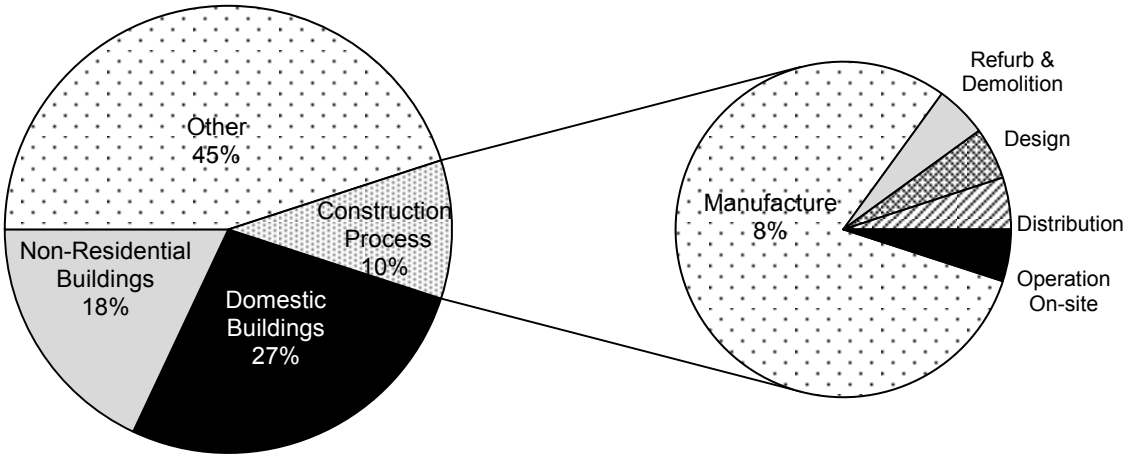


**Figure 1.1: Built environment and $CO_2$ emission (IGT, 2010).**

Within the domestic sector in the UK, the highest amount of energy is being used for space heating (IGT, 2010) which can be explained by the fact that 75% of the existing domestic buildings were built before energy efficiency was taken into consideration in the building regulations in 1975 (Utley and Shorrock, 2012, Mackenzie *et al.*, 2010). It has been estimated that there is a technical potential of 40% reduction of $CO_2$ emission of these houses of which 20% is achievable by adopting cost effective measures such as using energy efficient boilers and appliances and improving insulation standards (Mackenzie *et al.*, 2010). Among the cost effective measures, improving insulation standards can contribute to about 65% of total carbon reduction (Halliday, 2008). Studies suggests that most of the 7.7 million houses with solid brick walls and about 7.6 million of the 19 million houses with cavity walls are uninsulated (DECC, 2012) while about 9 million lofts are inadequately insulated. About 25 million out of existing 26.7 million houses will still be present in 2050 (Boardman, 2007; DECC, 2012; ACE, 2012). Subsequently, these housing stocks need to be thermally upgraded to become energy efficient in line with the carbon reduction target set by the UK government. One-quarter of the 2050 housing stock, consisting of post-2010 houses, will be gradually built with an annual construction rate of 240,000 houses to meet the demand of about 31.8 million houses by 2050. These houses will be built by the standards set in the Code for Sustainable Homes

(DCLG, 2006), particularly by the Code Level 6 from 2016 onward. At any rate, the building fabrics of these housing stocks have to be well insulated. Apart from this, increasing interest in Passivhaus design standards (Passivhaus, 2012) will mean that many of the fabrics of the houses will potentially be built with very high amount of thermal insulations. For the insulation market, it implies that there will be a steady demand for thermal insulations for next 40 years.

The importance of thermal insulation particularly in the lofts and walls can be understood from Figure 1.2 (after McMullan, 2007).

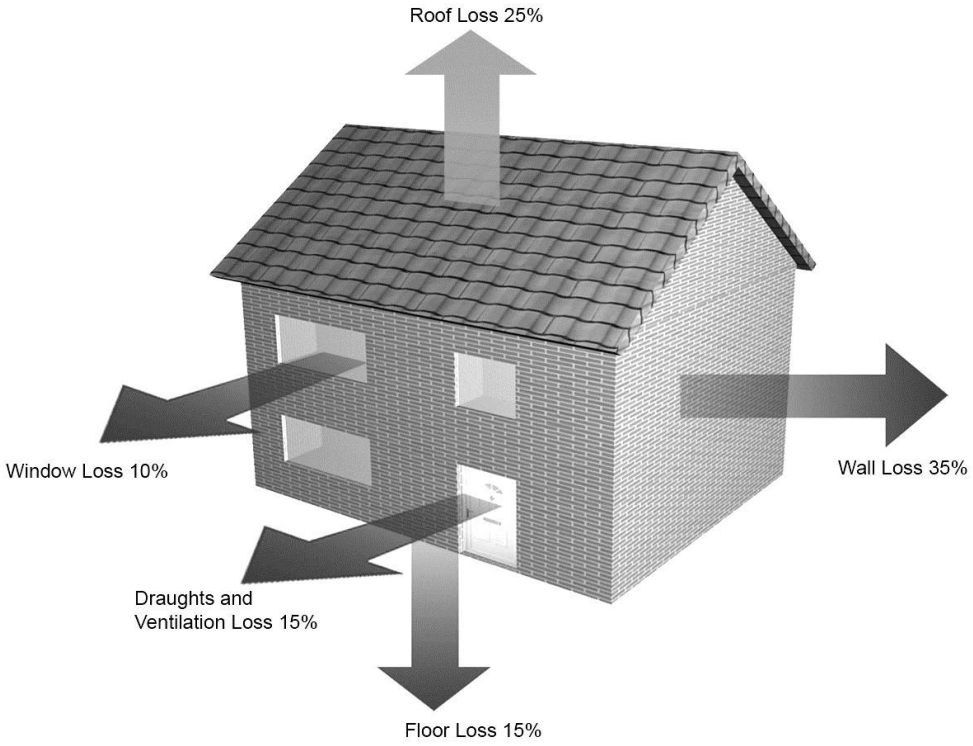


**Figure 1.2: Heat loss through the envelope of an uninsulated home (after McMullan, 2007).**

This figure shows that, in an uninsulated home, heat loss through the roof is 25%, through the walls is 35%, through the windows is 10%, through the floor is 15% and due to draught and ventilation is 15%. However, Figure 1.3 shows that there is a particular lag in the rate of uptake of wall insulation (Utley and Shorrock, 2012). In terms of loft insulation, only 62% of the houses are installed with adequate thickness of insulation (DECC, 2012). The adoption of tougher building regulations will mean that either the thickness or the performance of the insulations have to be increased to reduce heat loss through the building envelope.

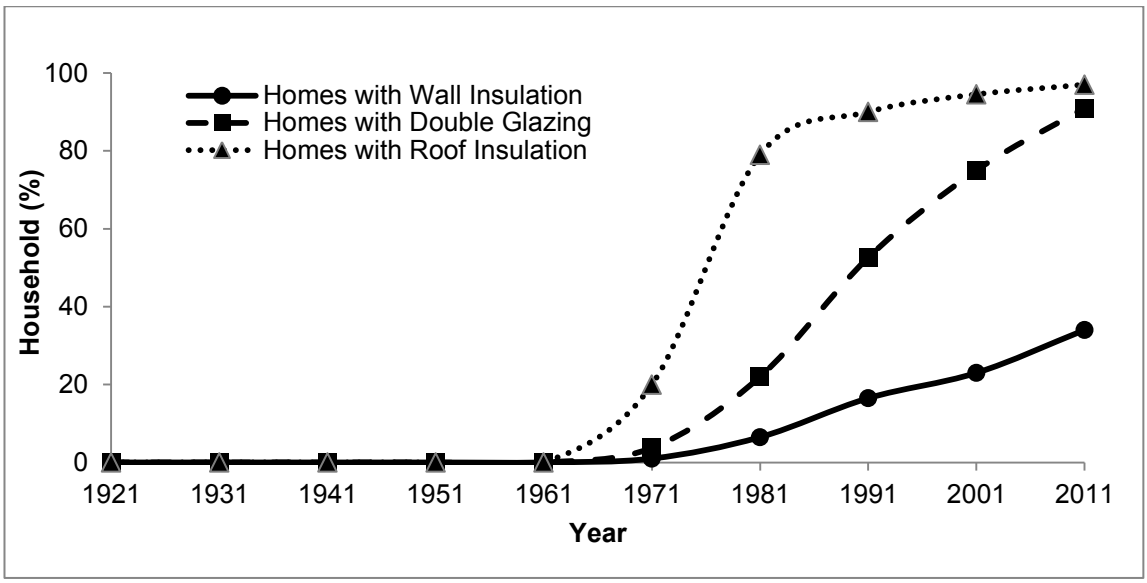


**Figure 1.3: Insulation measures (Utley and Shorrock, 2012).**

Among the non-domestic buildings, about 60% of the existing stock will remain in 2050 and many will require upgrade in terms of energy use (Mackenzie *et al.*, 2010). Fabric insulation in the existing non-domestic buildings can save around 4.7 Mt (million tons) $CO_2$/year (Caleb, 2012). The new non-domestic buildings, on the other hand, will be built according to the energy efficiency measures set in the building regulations.

The Use of higher amount of insulation materials can potentially increase the embodied carbon of the building. It has been suggested that between 2%- 36% of the lifetime energy demand of a conventional house is attributable to the embodied energy of the building materials and this can increase to 9%-46% for a low energy building (Monahan and Powell, 2011). However, the amount of embodied carbon can be kept low by using low energy and renewable materials. The Centre for the Built Environment of the University of East Anglia (2013) observed that an average low energy house built with conventional building materials, to attain the Code Level 6, can contain about 50 tonne (t) $CO_2$ as embodied carbon compared to the 18 tonne $CO_2$ in a low energy house built with renewable materials designed according to the Code Level 4.

To reduce the embodied and operational energy of the buildings, thermal insulations need to be produced from low-energy and renewable materials and should meet the key operational performance criteria. The key performance criteria of thermal insulation materials are to control heat flow through the building envelope and to manage moisture. Additionally, thermal insulation

materials have to meet some secondary performance criteria based on how the products sustain and fail in terms of their physical structure, as described in the British Standard (BS ISO 2219, 2010). For an eco-friendly insulation material, some further performance criteria can be developed based on the life cycle assessment method, as developed by the International Organization for Standardization (ISO 14040, 2006).

Bio-based thermal insulation materials, as opposed to synthetic and mineral thermal insulations, are produced from renewable materials and carry lower embodied energy. The principal bio-based thermal insulations that are available in the UK market are cellulose, hemp, flax, wood fibre and sheep wool insulations. Among these thermal insulations, hemp insulation has high production potential in the UK. According to a 2008 estimate, only 0.064% of all UK agricultural land is required to produce enough hemp insulation to meet the yearly demand for loft insulation (Murphy and Norton, 2008). Hemp comes from renewable sources and is biodegradable. Hemp plants are high-yield and require very little amount of fertiliser (Roulac and Hemptech, 1997). In addition, hemp fibre is one of the strongest natural fibres in the world (Bourie, 2003). All these attributes make hemp insulation a likely candidate for being identified as a 'green' insulation material that can contribute to sustainable construction process.

In terms of key functional performance, in the literature there are limited data available about the embodied energy and life cycle analysis of hemp insulation of particular make (Norton, 2008) and adsorption isotherm and vapour diffusion resistance factor of some hemp insulations (Collet *et al.*, 2011).

However, there is lack of data on the heat and moisture management capacity of hemp insulations. To the present author's knowledge, there is no data available about the dynamic hygrothermal performance of hemp insulations in laboratory conditions, in situ conditions and in terms of data gathered from numerical hygrothermal simulations. There is also a lack of data on the steady state hygric properties of hemp insulation such as moisture buffering value and water absorption coefficient.

Insufficient research, therefore lack of data and evidence in terms of the hygrothermal performance of hemp insulations, is regarded among the key

market barriers for the use of sustainable materials (Glass, Dainty and Gibb, 2008). In addition to this barrier, natural insulations also face barriers in relation to the assessment method applied in ranking them amongst the green building materials. Many natural insulation materials are not included in the Green Guide due to lack of robust data on their functional performance. This creates in turn a serious market barrier for these products despite the presence of apparently wider market for them (May and Newman, 2008).

Consequently, this thesis attempts to fill the gap of knowledge about the hygrothermal performance of hemp insulations in building envelopes through a number of laboratory-based and in situ experiments and through numerical hygrothermal simulations. Analyses of the data gathered from these experiments and numerical simulations can create new knowledge about the hygrothermal performance potential of hemp insulations in the UK.

### 1.2. Research hypothesis

Based on the key performance criteria, which are to manage heat and moisture transfer through the building envelope, the following hypothesis has been formulated and tested:

*Hemp insulation has a hygrothermal performance potential that is equal to or better than that of conventional fibrous thermal insulation materials in building envelope applications.*

### 1.3 Aim and objectives of the research

The overarching aim of the research is to investigate the hygrothermal performance of fibrous hemp insulations in the context of the UK and compare this performance with that of other conventional insulation materials.

In line with the aforementioned aim of the research, following objectives of the present study were identified:

*1.3.1 To determine the thermal conductivity values and heat flux management capacity of hemp insulation for a range of hygrothermal boundary conditions relevant to the UK climatic conditions. This is achieved through a*

*variety of laboratory-based experiments, computer based numerical simulations and full scale in situ studies.*

*1.3.2 To determine the moisture management capacity of hemp insulation in a range of hygrothermal boundary conditions relevant to the UK climatic conditions. This is achieved through a variety of laboratory-based experiments, computer based numerical simulations and full scale in situ studies.*

*1.3.3 To acquire relevant data of the hygrothermal performance of some other conventional insulation materials. This is achieved through a variety of laboratory-based experiments, computer based numerical simulations and full scale in situ studies.*

## 1.4 Outline of the materials and research methods

The aim of this research is to evaluate the hygrothermal performance of hemp insulations. However, some other insulation materials have also been tested at various stages of the research to compare the hygrothermal performance of hemp insulations with that of the other insulation materials. These insulations are sheep wool, wood fibre and stone wool. The brief outline of the materials and method has been presented here. Detailed descriptions of the materials and methods are provided in chapter five.

### *1.4.1 Materials*

A brief description of the insulation materials that have been used during the course of the research are provided below:

- *Hemp insulation*

Hemp insulations produced by five different manufacturers have been tested in the different stages of the research. The apparent density of the insulations varies between 45 kg/m$^3$ and 57 kg/m$^3$ and manufacturers' declared thermal conductivity varies between 0.038 W/mK and 0.043 W/mK.

- *Sheep wool insulation*

The Sheep wool insulation used in this research is produced from 95% natural fibre and 5 % adhesive. The apparent density of the insulation is 19 kg/m$^3$ and the manufacturer's declared thermal conductivity is 0.039 W/mK. Sheep wool is

an animal derived bio-insulation and the structure of the fibre is different from plant-derived bio-insulations such as hemp. Sheep wool has been selected to find out how the hygrothermal properties of plant-derived bio-insulation like hemp compares with those of animal-derived insulations.

- *Wood fibre insulation*

The raw materials for wood fibre boards consist of splinters and wood chips of softwoods which are the by-products in sawmills. The apparent density of the insulation is 170 kg/m$^3$ and the manufacturer's declared thermal conductivity is 0.042 W/mK. Wood fibre has been selected to determine how the hygrothermal properties of a medium density plant-derived bio-insulation like hemp compares with those of a high density plant-derived insulation like wood fibre.

- *Stone wool insulation*

Stone wool accounts for 35% of the European thermal insulation market (Karamanos, Hadiarakou and Papadopoulos, 2008). In the UK, stone wool and glass wool together represent 40% of the thermal insulation market (Great Britain. Office of Fair Trading, 2012). The apparent density of stone wool insulation is 23 kg/m$^3$ and the manufacturer's declared thermal conductivity is 0.038 W/mK. Since stone wool is one of the major mainstream fibrous insulation materials in the UK, the comparison of the hygrothermal properties of stone wool and hemp will potentially highlight the strength and weaknesses of hemp insulations.

The study involved the **laboratory testing** of the following thermal insulation materials:

- Hemp
- Stone wool
- Sheep wool
- Wood fibre

In addition to laboratory testing, the study involved numerical **computer simulations** using the 'Wärme und Feuchte instationär - Transient Heat and Moisture' (WUFI) software for assessing the hygrothermal behaviour of the following thermal insulation materials:

- Hemp

- Stone wool

In addition to the laboratory testing and computer based numerical simulations, the study also involved the **in situ testing** of the following materials:

- Hemp
- Stone wool

### *1.4.2 Outline of the research methods*

Thermal properties of the insulation materials have been studied through literature review, experimental works, computer simulations and in situ testing of a full scale test building. Moisture related properties of the insulation materials have been studied through literature review, experimental works, computer simulations and in situ testing of a full scale building. The long-term hygrothermal performance of the building envelope have been studied through computer based numerical hygrothermal simulations for walls including various types of insulation materials

## 1.5 Boundaries of research

The research hypothesis has been tested within the constraints of the following boundaries of research:

### *1.5.1 Boundary of research activities*

The following properties of the insulations have been assessed through laboratory-based experiments: adsorption-desorption isotherm, vapour diffusion resistance factor, water absorption coefficient, moisture buffering value, equivalent thermal conductivity at a range of relative humidity, likelihood of condensation and mould spore germination in the insulation interface.

During the in situ tests in timber frame wall panels, the equivalent thermal conductivity, likelihood of condensation and mould spore germination in hemp and stone wool insulation were assessed. The computer based numerical hygrothermal simulations have been carried out to study the following long-term hygrothermal performance of hemp and stone wool insulations in timber frame and solid brick walls: equivalent thermal conductivity, likelihood of interstitial condensation, likelihood of mould spore germination and mould growth.

Due to the constraint of time, instruments and opportunities, the following issues and applications could not be addressed in this research:

- Durability of hemp insulation
- External application of hemp insulation
- Non-fibrous bio-insulations

### *1.5.2 Boundary of location*

The research study was based on the climatic conditions of the UK and thereby may not be relevant to other climatic contexts. The numerical simulations were based on the external climatic conditions of Edinburgh and Birmingham.

## 1.6 Contribution to knowledge

As a result of this research, the following key contributions are made to the existing knowledge:

### *1.6.1 Experimental setup and equipment*

- Development of an innovative hygrothermal hotbox to study the heat and moisture management capacity of the insulations materials in dynamic hygrothermal conditions.
- Development of an acrylic-faced dual insulation holder as a part of the dynamic hygrothermal hot box for visual identification of condensation in the insulation materials.

### *1.6.2 Experimental method for laboratory and in situ tests*

- Development of a new experimental method of determining equivalent thermal conductivity and moisture management capacity of hemp insulations in vapour open conditions and in a range of relative humidity conditions.

### *1.6.3 Research outcomes*

- Hemp insulation, compared to stone wool insulation, reduces the frequency and magnitude of interstitial condensation in the building envelope.

- The average equivalent thermal conductivity values of hemp insulations do not exceed the manufacturers' declared thermal conductivity values.
- The average equivalent thermal conductivity values of hemp insulations are similar for timber frame constructions, both with and without a vapour barrier.
- In situ thermal conductivity values of any hemp insulation can depend on the placement of the heat flux meter, either on the inner surface or on the junction between the exterior surface of the insulation and the oriented strand board (OSB).
- Analysis of hygrothermal data of the in situ experiments and hygrothermal simulations show that there is a likelihood of interstitial mould growth in the interfaces between the exterior surface of the insulation and the oriented strand board (OSB) regardless of whether the walls have or not a vapour barrier. This finding applies to both hemp and stone wool insulations. However, visual observations during the in situ experiments do not support the aforementioned finding.

### 1.7 Structure of the thesis

The thesis contains 9 chapters. Its schematic structure is shown in Figure 1.4.

**Chapter One** includes the introduction, background, aim and objectives, hypothesis, the boundaries of the research and the brief description of the contribution to knowledge as a result of this research.

**Chapter Two** critically reviews the work done by other researchers on hygrothermal properties and mould growth potentials of hemp insulation. Where data is not available on hemp insulation, research works on other cellulose based fibrous insulations are critically reviewed. The gaps in the present knowledge related to the hygrothermal potential of hemp insulation are then identified.

**Chapter Three** presents the science of heat and moisture flow through fibrous thermal insulation materials.

**Chapter four** provides the overview of materials, equipment and research methodologies used in this study.

**Chapter five** describes the experimental programme, testing techniques, apparatus and materials used to investigate the adsorption-desorption isotherm, moisture buffering capacity, vapour diffusion resistance factor and water absorption coefficient of the selected insulation materials.

**Chapter six** describes the experimental programme, testing techniques, apparatus and materials used to investigate the dynamic and quasi steady state hygrothermal performance of hemp and stone wool insulations in the laboratory.

**Chapter seven** describes the protocol, testing technique and materials used for the in situ tests of timber frame wall panels incorporating hemp and stone wool insulations.

**Chapter eight** describes the material, research method and the results of numerical hygrothermal simulations of timber frame and solid brick walls incorporating hemp and stone wool insulations.

**Chapter nine** presents the overall conclusions of the study, the contribution to knowledge and the suggestions for future research.

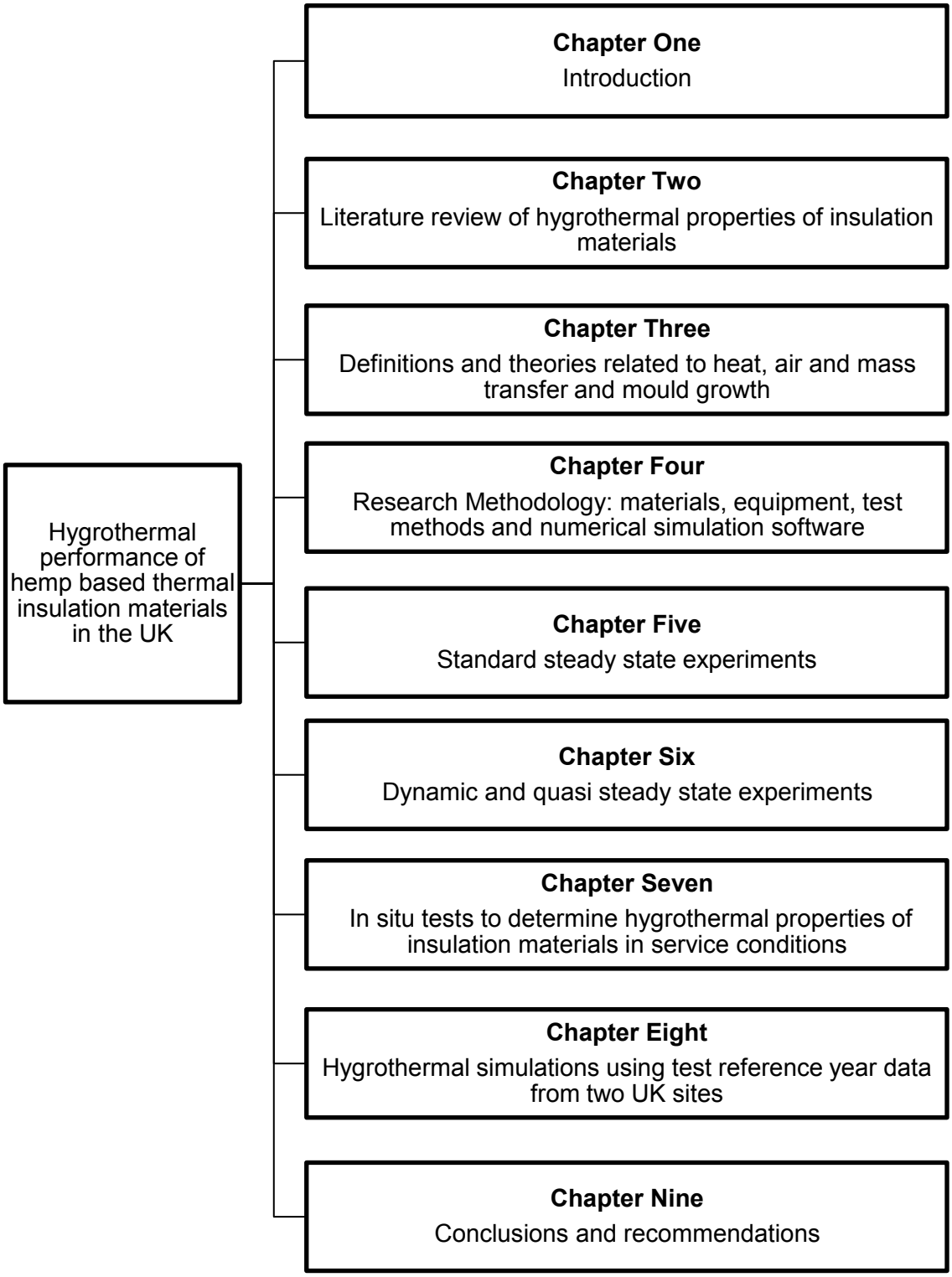


**Figure 1.4: Outline of the structure of the thesis.**

# Chapter 2

# Literature Review of Hygrothermal Properties of Fibrous Insulations with Particular Focus on Hemp

In this chapter, thermal insulations have been critically assessed in terms of their hygrothermal properties. Particular emphasis has been given to fibrous hemp insulations. Since research works on fibrous hemp insulations are scarce, examples are also drawn from research works on other bio-insulations due to their closeness to hemp in physical structure. Literature reviews of experimental and in situ monitoring methods are more overarching since some research methodologies can be reasonably generic in their applications. The following hygrothermal aspects in relation to thermal insulations are discussed: heat transfer and thermal mass, moisture transfer and moisture mass, mould growth. Where information is available, each topic has been discussed both at material and at assembly or system level. The theoretical and numeric aspects of heat, air and mass transfer and mould growth are discussed in chapter three.

## 2.1 Heat and thermal mass

### *2.1.1 Material level*

At material level, a number of researchers have carried out the determination of heat transfer properties of hemp and other bio insulations. Among them, Korjenic *et al.* (2011) measured moisture dependent thermal conductivity of two types of hemp insulations in a heat flow meter as shown in Figure 2.1. Type 1 (Hemp 1A and 1B) contained 48% natural fibre, 20% binder and 32% shives while type 2 (hemp 2A and 2B) contained 64% hemp, 20% binder and 16% shives. Insulations were moistened to several moisture levels between 0% and 14%. The moisture level was based on the ratio of the weight of the moisture content and the dry weight of the insulations. The samples were enclosed in foils and thermal conductivity was measured according to ISO 8301 (1991). Substantial variations were observed between the thermal conductivity of the

hemp samples, even between the two samples of similar type of hemp insulations, as shown in Figure 2.1. However, no explanation was offered by the authors' about the reasons for the variations. The material data provided by the authors' shows that the adsorption isotherms of the insulations are nearly similar. However, there are considerable variations in the corresponding vapour diffusion resistance factors. The vapour diffusion resistance factor of hemp 2B is twice the value of that of hemp 2A and 70% higher than that of hemp 1A. Thermal conductivity of hemp 2B is about 5-7% higher than that of hemp 1B while the vapour diffusion resistance factor of hemp 2B is also only 5% higher than that of hemp 1B.

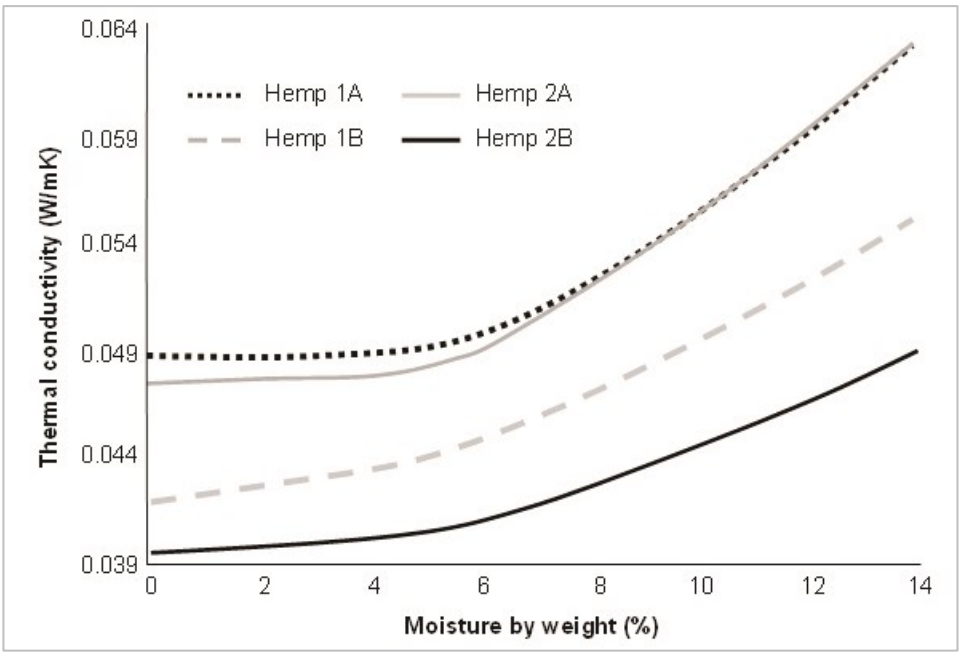


**Figure 2.1: Thermal conductivity of hemp samples (after Korjenic *et al.*, 2011)**

Moisture can evaporate from the warm side of the heat flow meter and condense at the cold side during the standard tests and thus vapour diffusion is highly likely. When moisture adsorption capacities are similar, the rate of vapour diffusion depends on the vapour diffusion resistance factors of the insulations and the temperature gradient along the insulation thickness. This can partly explain why heat flux is higher in the insulations with lower vapour diffusion resistance factor and lower in the insulations with higher vapour diffusion resistance factor, resulting in different thermal conductivity values. However, if this assumption is correct then the thermal conductivity values determined are not moisture dependent thermal conductivity, they should be treated rather as

equivalent thermal conductivity values. Theoretical aspects of equivalent thermal conductivity are discussed in section 3.2 of chapter three.

The comprehensive description of the measurement of thermal conductivity of moistened sheep wool insulations by Ye *et al*. (2005) provides additional perspective about the implications of the aforementioned standard measurement method of determining heat transfer properties. Ye *et al.* moistened the insulation by 10% to 30% moisture content by weight. Insulations were wetted by spraying water on the insulation surface facing the warm side of the guarded hot box. Insulations were sealed with plastic film and conductivity was measured both for vertical (as inside a wall) and horizontal (as in a loft space) placement of the insulations. In case of the horizontal placement of insulation, according to the authors, the condensed water came back to the warm side to be evaporated again and thus evaporation-condensation cycle emerged. During the tests on the vertical orientation of the insulations, moisture started diffusing from warm side to the cold side and a certain amount of water was condensed on the plastic film in the cold side. The amount of the condensed water was deducted from the original amount of sprayed water to determine the final quantity of moisture for which the conductivity was measured. For example, when sprayed moisture content in the insulation was 30% and deposited moisture content in the plastic film was 10%, the net moisture content in the insulation was assumed as 20%. Thus the thermal conductivity value was determined for the insulation with 20% moisture content. Table 2.1 shows some results of the test.

**Table 2.1: Thermal conductivity values of the insulations (adapted from Ye *et al.*, 2005).**

| Moisture content by Weight (%) | λ at Horizontal Placement (W/mK) | λ at Vertical Placement (W/mK) |
|---|---|---|
| 0 | 0.047 | 0.047 |
| 20 | 0.05 | 0.049 |

This method can provide uncertain results as the moisture gradient and moisture phase in the insulation are unknown and it is likely that most of the moisture is moved to the cold side of the insulation by the time steady state is

reached, this means that the insulation is measured in almost a dry state for conductivity with some wetness near the cold surface. Additionally, in case of the assumptions of condensation-evaporation cycle during the horizontal test, due to constant movement of vapour, it is difficult to know what is being measured, whether it is insulation with vapour or with liquid water, or whether the insulation contains a certain ratio of vapour and water. The thermal conductivity of vapour is about 0.028 W/mK whereas the thermal conductivity of water is about 0.065 W/mK and therefore the phase of moisture is an important factor in measuring thermal conductivity.

In chapter six, these aspects of moisture migration are experimentally tested with hemp insulations and it is also shown that moisture migration is less severe in vapour open hemp insulation than in stone wool insulation.

### *2.1.2 Assembly or system level*

No published work has been found in terms of assessing the thermal conductivity of hemp insulations at assembly level, either in laboratory experiments or in service conditions. This is pertinent for both wall panels, with and without vapour barriers. However, it is possible to gain some methodological insight into the in situ determination of thermal transmittance from the work of Nicolajsen (2005) on cellulose and stone wool insulations. Nicolajsen compared thermal transmittance of cellulose loose-fill insulation and stone wool insulation installed in a north facing timber frame wall in Denmark. Interior temperature and relative humidity were maintained at around 20 °C and 60%, respectively. Stone wool insulation was tested in wall panels with vapour retarder and cellulose insulation was tested in wall panels with and without vapour retarder. The average thermal transmittance of the panels with 285 mm cellulose insulation for both panels was 0.14 W/m$^2$K (which equates to an equivalent insulation thermal conductivity of about 0.04 W/m-K). The thermal transmittance value for stone wool was 0.12 W/m$^2$K (which equates to an equivalent insulation thermal conductivity of about 0.04 W/m-K). For both applications of cellulose insulations, it was noted that the maximum moisture contents were similar and within the safe range (18% moisture content by volume). However, while the moisture content was presented by Nicolajsen as the moisture content of the total insulation, judging by the placement of the moisture dowels, it can be said that the moisture content should represent only

the state at the insulation-oriented strand board (OSB) interface. While Nicolajsen's study focused only on 60% interior relative humidity, it is more useful to include the effect of changes in internal relative humidity to understand its effect on heat flux and interstitial relative humidity of wall panels in full scale and experimental tests. Some interior spaces are subject to sudden fluctuation of relative humidity. For example, adjacent areas of kitchen and bathroom can become very humid while in operation. It is worthwhile therefore to assess the effect of the dynamic or quasi steady state relative humidity on average heat flux through the thermal envelope and on the likelihood of increased moisture content and mould growth.

### *2.1.3 Variable heat capacity*

The contribution of thermal mass in moderating fluctuating temperature is undisputed and is the crux of the debate between the efficiency of the lightweight and heavy weight constructions. Two determining characteristics of thermal mass are specific heat capacity and density. Table 2.2 shows the specific heat capacity, density and diffusivity of some building materials. Most of the data are taken from the database of the 'Wärme und Feuchte instationär' (WUFI) software and the hemp data are taken from the manufacturer's literature. The diffusivity data are calculated from volume heat capacity and thermal conductivity. It is interesting to note that hemp and wood fibre have the lowest diffusivity value in dry condition despite concrete being the densest among the selected materials.

**Table 2.2: Thermal properties of some building materials.**

| | Density ($Kg/m^3$) | Thermal conductivity (W/mK) | Heat capacity (J/kgK) | Diffusivity ($m^2/s$) |
|---|---|---|---|---|
| Concrete | 2200 | 1.6 | 850 | 8.5561E-07 |
| Stone wool | 60 | 0.04 | 850 | 7.8431E-07 |
| Hemp | 45 | 0.039 | 2200 | 3.9394E-07 |
| Wood fibre board | 168 | 0.044 | 2100 | 1.2472E-07 |

In moist conditions, the heat capacity is likely to increase and the diffusivity is likely to decrease further in accordance with the materials' corresponding

moisture adsorption capacities. In high relative humidity, hemp insulations adsorb moisture of about 30% -55% of its dry weight. The specific heat capacity of water is about 4200 J/KgK. Obviously at high relative humidity, the specific heat capacity of hemp-moisture matrix will increase in relation to the amount of water that is condensed during adsorption.

Krus and Sedlbauer (2012) argue that the results of the laboratory measurements in relation to the increase of thermal conductivity of moistened bio-insulations should be carefully assessed for two reasons. Firstly, the increased reading is due to the moisture migration caused by the measurement method and secondly, this increased thermal conductivity does not represent the thermal activity during dynamic boundary conditions where heat capacity plays an equally dominant role. It implies that in real life the net heat loss/gain may not be represented by the moisture dependent thermal conductivity values determined in the laboratory. However, the effect of dynamic specific heat capacity of moistened insulation can be assessed through dynamic energy simulations.

### *2.1.4 Heat of wetting*

Heat of wetting resulting from moisture adsorption by natural insulations may have considerable contribution to heat flux. Theoretical aspects of the heat of wetting are further discussed in chapter three.

Figure 2.2 shows the heat of wetting of flax fibre determined by Hill, Norton and Newman (2009) using the Calsius-Clapeyron equation. Norton (2008) states that heat of wetting can make significant difference in the internal temperature of a building when large quantities of natural fibres are used. Norton carried out an approximate calculation to determine the impact of adsorption in a 40 $m^2$ loft space insulated with 320 kg of hemp insulation using the heat of wetting data of flax fibre as surrogate. For a relative humidity change from 30% to 60% between day and night, it was found that 156,600 Jules of energy would be released equating to about 4% of the total daily energy use of an energy efficient home, assuming an energy use of 1000 watt hour per day.

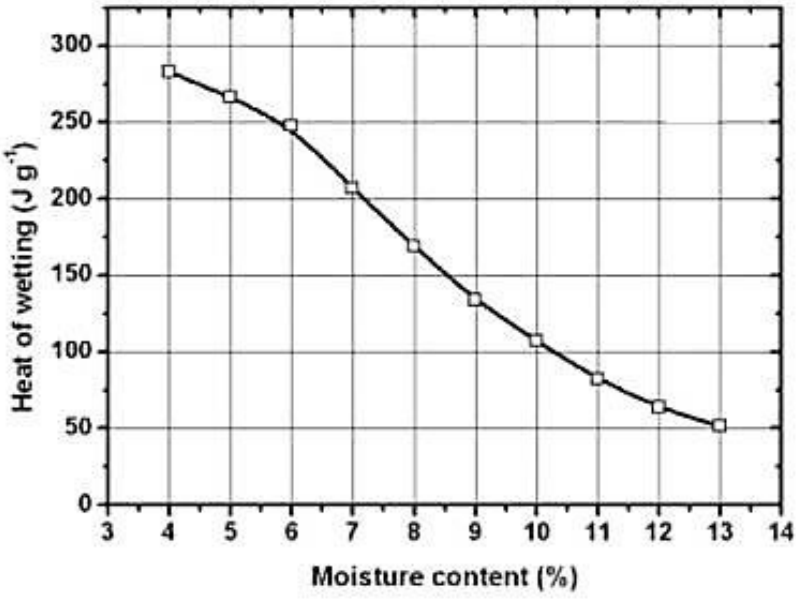


**Figure 2.2: Heat of wetting of flax fibre (Hill, Norton and Newman, 2009).**

However, heat of wetting is not much focused in heat, air and moisture calculations. While explaining the heat flux in moist insulations materials, heat of wetting is not much discussed because it is perceived as a process not as much linked to mineral materials as it is to the bio-based materials. Kunzel (1995), while deriving heat transfer equation of building components, disregarded heat of sorption on the basis that it was negligible compared to enthalpy of condensation/evaporation (based on works with mineral materials). However, contrary to Kunzel's assumptions, condensation/ evaporation may be secondary to adsorption in highly hygroscopic insulations where heat of wetting can play an important role. This is particularly important in loft spaces where the upper surfaces of the insulations are exposed and full advantages of their buffering capacities can be exploited.

## 2.2 Moisture flux and moisture mass in buildings

Moisture problems have two dimensions: indoor moisture problem and structural moisture problem. Indoor moisture problem is more severe than structural moisture problem (Tsongas, 2009) if human health and comfort are given the priority in the scheme of the concerns. On the other hand, condensation inside the building envelope can deteriorate the performance of the building structure and the building elements. The literature review will

concentrate on the causes and implications of moisture in the loft space, indoor moisture problem and structural moisture problem.

### *2.2.1 Hygrothermal performance of typical UK houses*

The problem of high relative humidity and mould growth is most prevalent in low income households in the UK Therefore, as far as addressing the problems of high relative humidity and mould growth are concerned, low income households are most representative of the UK houses and require further attention (Oreszczyn *et al.*, 2006).

A comprehensive analysis of the hygrothermal conditions of the low income households of the UK was conducted by Oreszczyn *et al.* (2006). The study involved 1604 dwellings and the study was conducted during the winters of 2001-02 and 2002-03 in the following five urban areas: Birmingham, Liverpool, Manchester, Newcastle and Southampton. The data were standardised for the external temperature of 5°C and external relative humidity of 80%. The median standardized living room relative humidity was 42.8% (5th centile 32.3%, 95th centile 59.8%) and the median standardised bedroom relative humidity was 49.2% (5th centile 34.8%, 95th centile 66.3%). The median standardised living room temperature was 19.1°C (5th to 95th centile range: 13.5 to 23.0°C) and the median standardized bedroom temperature was 17.1°C (5th to 95th centile range: 12.1 to 21.8°C).

In this study it can be observed that the relative humidity conditions in the bedrooms can be as high as 66.3% in the low income houses. Since the relative humidity value was standardised, the actual relative humidity could have been higher when the external vapour pressure was higher.

The aforementioned study did not take into account the relative humidity conditioned in the bathrooms and kitchens where relative humidity could be potentially higher due to intermittent production of steam during water related activities such as having a hot shower and boiling a kettle, respectively. During those periods, relative humidity can be as high as 100% (Padfield, 1998), resulting in potential interstitial and surface condensations in the building envelope. An in situ monitoring of the relative hygrothermal conditions of a residence in LLanberis was conducted by Ceri and Newman (2011). The result shows that the relative humidity in the lobby near the bathroom can remain

between 80%-95% during the whole period of the monitoring as shown in Figure 2.3. Therefore, 80%-95% relative humidity conditions can be considered as high relative humidity conditions for hygrothermal studies.

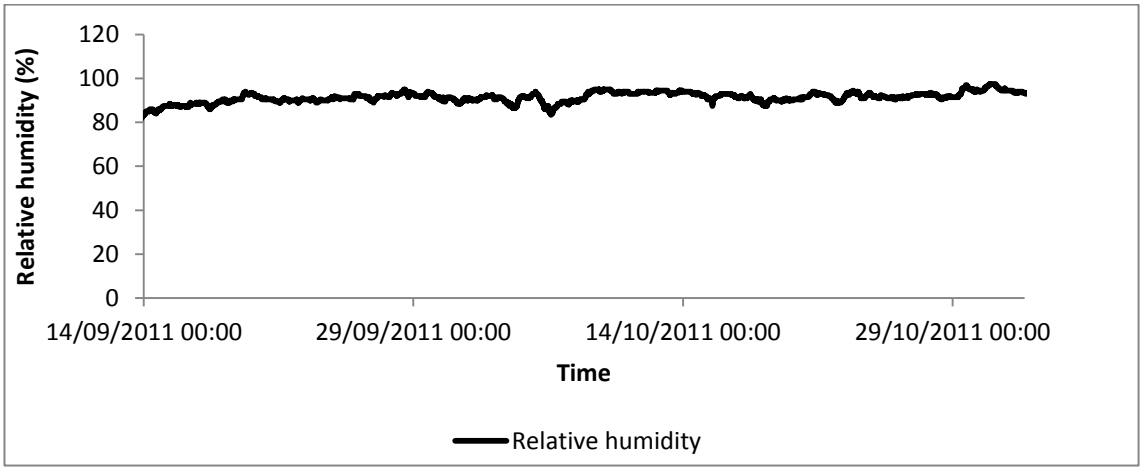


**Figure 2.3: Relative humidity in a residential space adjacent to the bathroom (Hill, Norton and Newman, 2009).**

### *2.2.2 Moisture in loft space, roof and implications*

Moisture problems in ventilated and non-ventilated loft space are due to exfiltration of moist air through ceiling bypasses and vapour penetrations. In certain cases, cold roof sheathings can act as condensing surface. Air leakage is thought to be the governing mechanism of moisture flow (Tobiasson, 2009) rather than vapour diffusion while both mechanisms are active at the same time.

A case of severe moisture in the roof was that of Smithsonian Institute in Washington (Padfield, 1998) where there were occurrences of internal raining from the roof only during bright and sunny weather. The ceiling was built of the following materials from inside to outside: plywood, vapour barrier, glass fibre insulation, plywood, tarred paper and lead coated copper. During the winter, moisture came from the interior through the accidental and other gaps by upward air flow and was adsorbed inside the upper ply board. During the summer, the moisture diffused and condensed in the inner vapour barrier and, subsequently, dripping of this condensed water through the downstream breaks caused raining.

### *2.2.3 Structural moisture and implications*

Occurrence of liquid water in building envelopes can generally be attributed to rainwater penetration, capillary suction, and condensation by advection

(combined vapour diffusion and convection). The individual contribution of these factors varies for different weather conditions, construction details and construction faults. In the United States, air leakage into building envelopes is found to be a more powerful mechanism of vapour transport than vapour diffusion (Bomberg, Trechsel and Achenbach, 2009). It is estimated that 75-80% envelope failures are caused by excessive moisture (Bomberg and Brown 1993, cited in Heseltine and Rosen, 2009), although the number of the structural failure is very low compared to the numbers of structures that operate properly. Dampness can also pose risk to structural integrity by inducing rot in wood, corrosion in metal, and by freeze-thaw cycles in masonry (Trechsel and Vigener, 2009). However, there is no evidence of significantly elevated mould concentration in indoors due to interstitial mould growth in building envelope (Tsongas, 2009).

Moisture activity in vapour open walls is an area of particular interest to researchers and building professionals. This issue may attract further attention in the future with the risk of reverse condensation in walls with vapour barrier as a result of increasing cooling degree days. Tsongas, Odell and Thompson (2009) carried out an extensive field survey on 96 houses with vapour open walls in 1979 in the United States. The timber frame walls of these houses were retrofitted, at least three years prior to the survey, with different insulations (stone wool, cellulose and urea-formaldehyde foam) without any vapour barrier. The most vulnerable parts of the walls in terms of moisture damage were identified, opened up and individual elements (timber stud and insulation) were tested visually and more thoroughly in the laboratory for excessive moisture content and decay fungi. However, negligible number of cases of high moisture content, moisture damage or decay fungi was detected. Langlais and kiersfield (1984) conducted experimental and natural climatic tests in France to assess the hygric performance of glass fibre insulation internally retrofitted on hollow and solid concrete block walls. No condensation was observed in the insulation, but nearly saturation humidity condition was observed on the internal surface of the masonry walls in spring during the natural climatic test (in steady temperature of 20 °C and relative humidity of 60%). However, because of day-night and seasonal cycles, and the lower quantity of the moisture accumulation, the condensate was easily absorbed by the masonry during the

day-night cycle and was fully evaporated out in the summer. The aforementioned studies clearly indicate the potential of effective use of vapour open construction.

Pavlik and Cerny's (2009) work explains the process and results of testing an innovative vapour-open wall system that incorporates specially developed hygrophilic stone wool insulation with vapour diffusion resistance factor of 7.1 and cement-glue based vapour retarder. A computer simulation tool was used to study the hygrothermal behaviour of the initial wall system and to improve the system through optimization. The parameters developed from the simulation were used to manufacture the hygrophilic stone wool insulation and the vapour retarder. Thermal conductivity, vapour permeability and other related data were obtained by testing the real materials and the data were fed into the computer simulation tool to determine the hygrothermal performance of the system in winter climate in Prague. Experimental work was then carried out in a climate chamber where the climate inside the chamber simulated the external winter climate of Prague. The climate inside the laboratory (which is usually 23°C temperature and 50-60% relative humidity) represented the interior condition. In both computer simulation and laboratory experiments, it was found that the new system was capable of absorbing and releasing moisture without creating any interstitial condensation in the wall system. This study concentrated on stone wool insulation which had negligible moisture adsorption capacity and was modified to have about seven times higher vapour diffusion resistance factor compared to conventional stone wool insulations. The finding of this experiment may not be applicable to hemp insulations because of hemp's higher moisture adsorption capacity and lower vapour diffusion resistance factor (usually between 1 and 2). It can be assumed that hemp will adsorb moisture from the cement-glue based vapour retarder which was not the case for stone wool insulation.

Nicolajsen's (2005) study has been discussed in section 2.1.2. Both Nicolajsen (2005), Langlais and kiersfield (1984) and Pavlik and Cerny's (2009) study focused only on 60% interior relative humidity boundary condition and the insulations used in the studies did not include hemp. It is important to include the effect of change in internal relative humidity on heat flux and interstitial relative humidity of wall panels in full scale tests. There are spaces in the

residential buildings that are subject to sudden fluctuation of relative humidity, which is needed to be incorporated in the tests.

Unlike typical direction of vapour flux and resulting interstitial condensation, 'summer condensation' or 'reverse condensation' is less emphasized. Nevertheless, summer condensation may become more prevalent with increasing cooling degree days as a direct result of global warming. While typical condensation occurs when the interior temperature is warmer than the exterior temperature, summer condensation happens when water evaporates from warmer exterior wall or wind barrier, diffuses through the insulation layer and condenses on the cooler and impermeable surface of vapour barrier near the inner lining. Due to very high diffusion resistance factor of the vapour barrier, the condensate can run downward and can be deposited on structural elements and can cause damages similar to those discussed earlier in this section. Southern's (1986) experimental study on summer condensation in solid concrete block wall retrofitted with glass wool, expanded polystyrene (EPS), extruded polystyrene (EEP) and polyurethane foam (PF) insulations unfolds the gravity of the problem. Southern installed insulation on the internal surface of solid concrete block wall panels and applied vapour barrier on insulation leaving an air gap of 25 mm between the insulation and the vapour barrier. The experiment was conducted between May and June. Condensation was observed on the vapour barrier of the panels with glass wool, EEP, PF insulations within 3 hours of the start of the experiment. When the air gap between the PF insulation and the vapour barrier was ventilated outside, the frequency of the occurrence of condensation was reduced and rate of drying up was increased. The findings in this example are similar to those in the example of the roof that rained (although the earlier example resembled light weight construction), as discussed in section 2.2.1, and highlights the challenges that occur when highly vapour permeable and highly vapour impermeable materials are combined in an envelope system.

### *2.2.4 Indoor moisture and implications*

Indoor moisture problem is caused by excessive relative humidity largely generated from the following sources (Christian, 2009):

- Built-in moisture of construction materials

- Moisture from interior activities (cooking and gas combustion in kitchen, baths and showers in the bathroom, water emission from plants, evaporation from wet surfaces and respiration and perspiration of human beings)
- Immediate surrounding exterior (rain, snow, dew, fog, flood, capillary, humid air)
- Adjacent soil (migration of moisture from surrounding soil to the foundation and conditioned spaces)

Moisture, mould and other forms of microbial contamination are regarded as the most severe indoor air quality issues (Flanagan and Jewell, 2003). Figure 2.4 (after Arundel *et al.*, 1986) shows some health and emission risks related to different humidity regimes.

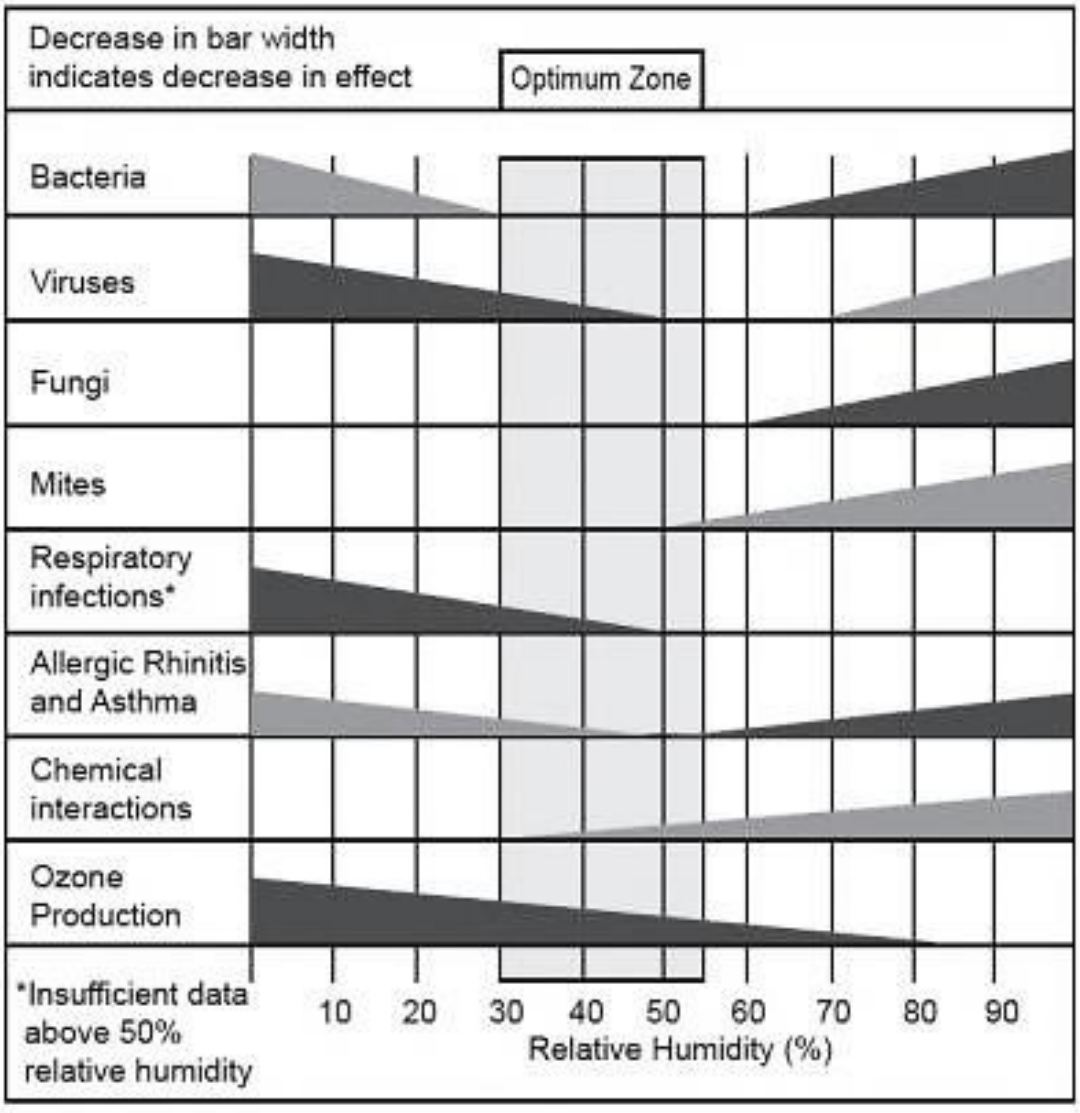


**Figure 2.4: Health and emission risk related to different humidity regimes (after Arundel *et al.*, 1986).**

A detailed and comprehensive discussion on indoor air quality can be found in the World Health Organization (WHO) guidelines for indoor air quality (Heseltine and Rosen, 2009). WHO guideline shows that 20% houses in several European countries, Canada and the United States has one or more sign of indoor dampness. Dampness is defined by qualitative indicators such as water leakage or damage, visible mould growth in indoor walls, floors or ceilings, bubbles or discolouration of floor coverings, condensation in windowpane and walls. Dampness and excess moisture are suspected to increase the concentration of dust mites and fungi. Dust mites and fungi produce allergens and many fungi also produce toxins and irritants, all of which affect respiratory health. Excess moisture also results in emission of potentially harmful volatile organic compounds like formaldehyde from the building materials.

## 2.3 Moisture adsorption and buffering

### *2.3.1 Moisture adsorption*

Research on moisture management of insulation materials are mostly focused on moisture buffering and moisture adsorption capacity. The materials with better adsorption and buffering capacity also delay interstitial condensation more effectively than the materials with poor adsorption and buffering capacity provided that the respective materials do not have disproportionately differing vapour diffusion resistance factors and densities. This assumption is tested and explained for hemp and stone wool insulations in sections 6.1 and 6.2 of chapter six.

Norton and Newman (2009) studied the moisture adsorption-desorption behaviour of natural fibres such as jute, coir flax, Sitka spruce, in a dynamic vapour sorption apparatus (Figure 2.5).

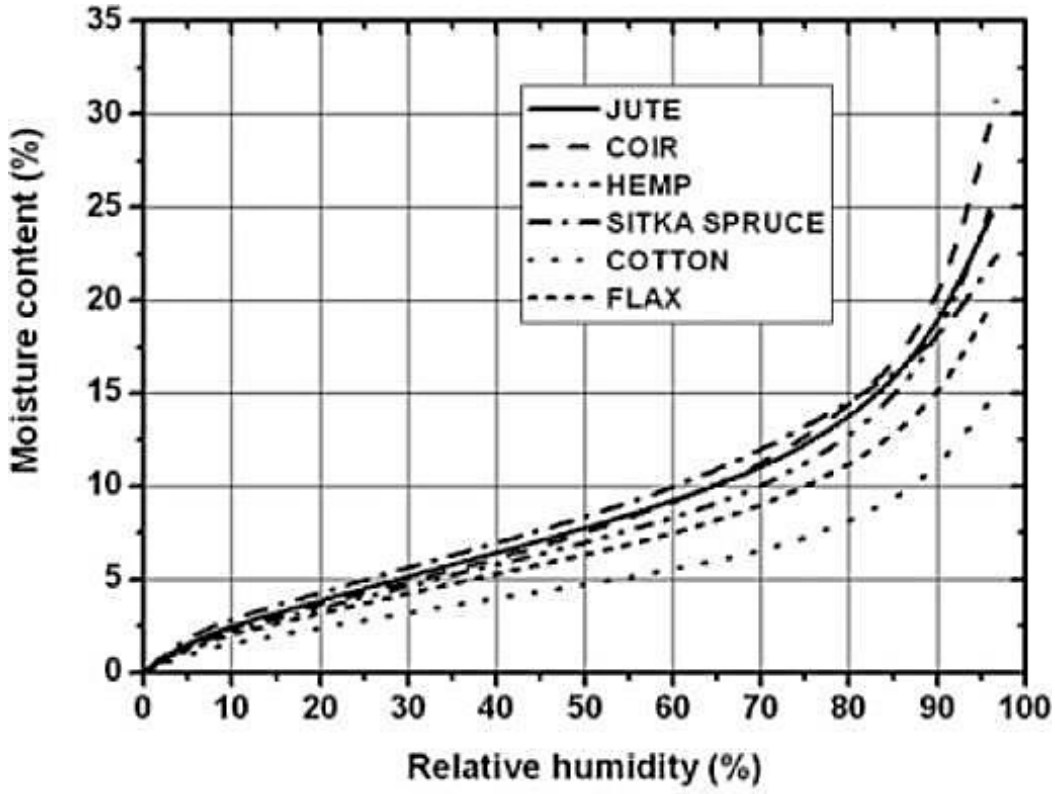


**Figure 2.5: Adsorption isotherms of some natural fibres (Hill, Norton and Newman, 2009).**

Considerable differences in adsorption and hysteresis were found among the fibres, with fibres containing high lignin level (jute, coir and Sitka spruce) showing higher moisture adsorption-desorption capacity during the process.

The contribution of lignin to moisture adsorption was also studied by Kostic *et al.* (2010). They found that the removal of lignin decreased and removal of hemicellulose increased the moisture and iodine adsorption of hemp fibres. Hill Norton and Newman (2009) found that hemp had higher moisture content in the capillary condensation region. This is important in terms of managing interstitial condensation, as hemp fibres will adsorb more moisture within its pore system under critical relative humidity conditions. Equilibrium moisture content (EMC) in hemp fibre during adsorption can significantly vary depending on the time of harvesting the crop and the process of fibre separation. Unretted fibres show higher EMC and quicker mould growth at high EMC (Kymalainen *et al*., 2001). Xie *et al.*(2011) studied the rate of sorption of hemp fibre. Their study, as shown in Figure 2.6, reveals that, from the onset of 70% relative humidity exposure, the rate of sorption starts to increase.

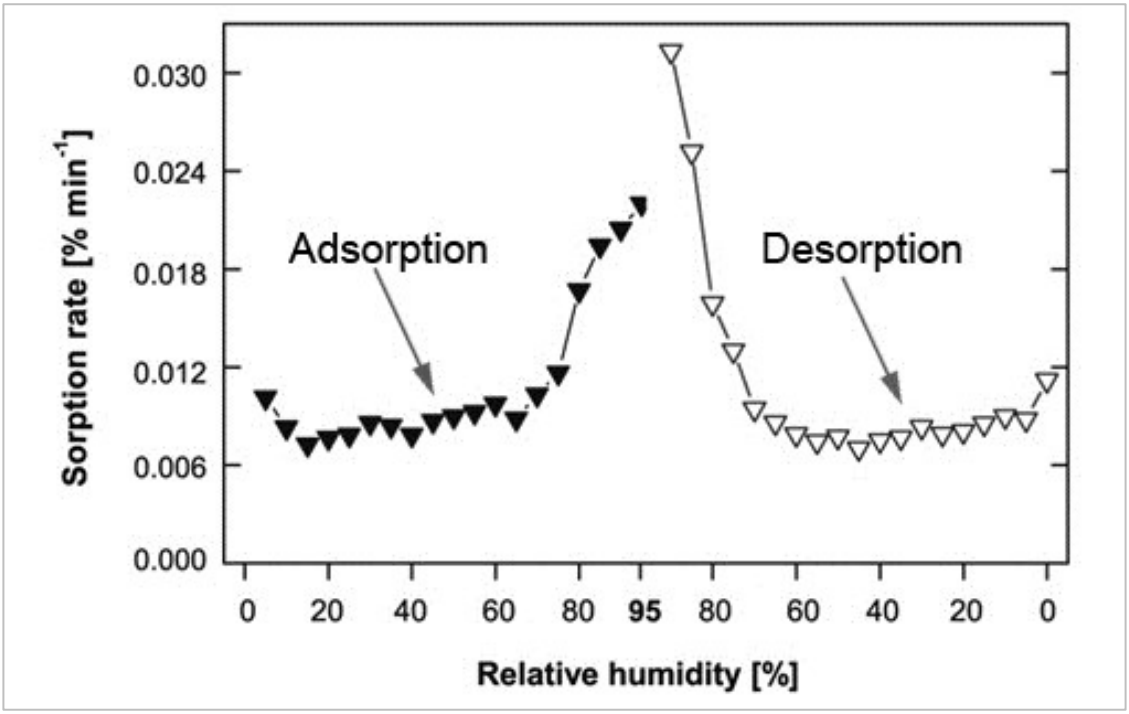


**Figure 2.6: Sorption kinetics of hemp fibre (Xie *et al.* 2011).**

At material level, Collet *et al.* (2011) determined the adsorption isotherms of two hemp insulations, HW1 and HW2, containing organic and polyester binders. HW1 and HW2 had corresponding densities of 40 and 45 Kg/m$^3$. At 95% relative humidity, HW1 adsorbed about twice the amount of moisture (about 26% weight gains by volume) that HW2 adsorbed (about 14% weight gain by volume). The authors assumed correlation between type of binder and adsorption. However, there can be many other causes for difference in the amount of adsorption, like processing method of the fibre, amount of lignin and hemicellulose in the fibre, available surface area for adsorption, type of fire retardant used in the fibre, variations in swelling of the fibres during capillary condensation.

### *2.3.2 Moisture buffering*

While the ability of thermal mass to moderate undesired temperature change is a widely discussed and established fact, the ability of hygric mass to moderate undesired humidity changes through moisture buffering is yet to be fully explored. Hygric inertia prevents surface and interstitial condensation (Hens, 2007). With increasing air tightness and draft proofing of interior spaces, interior relative humidity has also increased. Increased relative humidity can cause surface condensation, interstitial condensation and health risks. However, the risk of surface condensation and surface mould growth can be mitigated by

maintaining steady relative humidity near the interior surfaces by utilising the moisture buffering capacities of building envelopes. In terms of roof and attic applications, there are many incidences where ventilated loft spaces still require dehumidification due to excessive internal relative humidity. In such cases moisture buffering capacity of thermal insulations can potentially lessen the risk and rate of condensation provided that the insulation surfaces are exposed to the internal boundary conditions of the attic. Moisture buffering of these interior spaces can be performed by soft furnishes and wall materials. However, exploiting the potential of hygroscopic insulations is problematic in the interior spaces as insulations will be covered by dry lining and the moisture penetration depth of the dry lining will be a determining factor unless perforated inner lining is used. Two of the key areas for applying the potential of moisture buffering are museums and achieves where certain humidity conditions are needed to be maintained to preserve the integrity of the archival items (Padfield, 1998).

Unlike adsorption isotherm, no work on moisture buffering of hemp insulations has been found in published literature, which clearly indicates a gap of knowledge in this particular area. Nevertheless, a discussion of the moisture buffering values of some other bio based and mineral materials, determined by a number of researchers, is useful in terms of getting a broad-brush perspective on the methods and the performances of the materials.

When Padfield (1998) determined the moisture buffering values of brick, cellular concrete, wood, earth, lime mortar, gypsum plaster and wool insulation, a novel climate chamber was used where excessive vapour beyond the level of saturation vapour pressure could be pumped into the chamber. This technical ability to control moisture flux helped to simulate a state where there was a sudden flux of huge amount of moisture in the air as it happened during boiling a kettle or taking a hot shower. The most common buffering test incorporated a 24-hour cycle and relative humidity values varied approximately in the following pattern 60%-90% for 6 hours, 90%-60% for 6 hours, 60%-20% for 6 hours, 20%-60% for 6 hours. Wood provided the best buffer value when its longitudinal direction was perpendicular to the exposed surface. Clay mixed with organic materials and clay mixed with inorganic materials also showed good buffering performance. However, no buffering test was performed on hemp insulations.

Cereloni *et al.* (2008) used the method developed by the Nordic organisation for cooperation within the area of testing (Rode, 2005) to determine the buffering capacity of the following materials: sodium polyacrylate, cellulose-based material, perlite and gypsum. Cellulose-based material (cellulose and super adsorbent polymers) showed best buffer performances. Sodium polyacrylate, although a good adsorbent, showed considerable amount of hysteresis, which, according to the authors, might cause decreasing buffering performance. The moisture buffering performance of cellulose-based materials indicates that hemp, as cellulose based fibrous insulation, may have significant moisture buffering capacity.

Yoshino, Mitamura and Hasegawa (2009) explored the relationship between moisture buffering, ventilation rate and volume rate (ratio of hygrothermal area to room volume).Three ventilation regimes ware chosen: no ventilation, 1 air change per hour and 5 air change per hour. They found that moisture buffering had an inverse relationship with ventilation rate and a positive correlation with volume rate.

Since there is a lack of knowledge on the moisture buffering performance of hemp insulations with moisture buffering capability being one of the key characteristics of hygroscopic materials, this knowledge gap needs to be addressed.

### *2.4 Mould growth*

Mould growth can damage building materials and mould spores can be a health hazard. There are various reasons for mould growth in building materials, which are mostly related to humidity, dampness and supply of nutrients. Some of the research works on mould growth on building materials are discussed in this subsection.

Nykter (2006) focused on the microbial quality and microbial risks in the primary production chain of hemp and flax fibres and fibrous insulation products. Nykter's key findings can be summed up as follows:

- Humidity and wetness encourage the formation of spores in the fibres.
- Limit value for equilibrium relative humidity for fungal growth in building material is 70% -90%, depending on materials and fungal species.

- Dry weather encourages distribution of spores in air, not humid weather.
- Mould needs little amount of nutrient to colonise and multiply.
- Flax and hemp bio insulations already contain microbes through processing chain.
- Humidity level and required exposure time for mould growth is higher for mineral insulation than bio-based insulations.
- Water damaged and aged organic materials containing cellulose are most susceptible to mould growth.
- Not only spores but also fungal fragments are released into air from contaminated insulation materials.
- Hemp fibres contain cellulose, hemicelluloses and lignin. Due to containing nutrient in the matrix, it is difficult to remove microbes completely from these insulations even by using anti- fungal agents. However, fungal growth can be regulated.
- If amount of nutrient are minimized during retting of crop, the processed fibre becomes better fungal resistant.

At material level, Klamer *et al.* (2004) tested commercially available paper, flax, rock wool and glass wool insulations to assess their sensitivity to moisture and the ability of fungi to grow on them under different moisture regimes. The materials were wetted with a mixture of fungi and incubated at 26 °C in boxes with high moisture levels for 4 weeks. The highest amount of fungal growth was found on paper and flax insulation materials, which were initially conditioned to ambient moisture levels. Glass and rock wools showed good moisture resistance and minimal fugal growth and loss of dry mass.

Hoang *et al.* (2010) tested building materials for natural and artificial inoculations. The so called ‘green materials’ that were tested for mould growth were sunflower board (G-Sunflower), bamboo flooring (G-Bamboo), inorganic ceiling tile (G-Ceiling), and paperless drywall (G-Drywall). The non-green materials (as denoted by Hoang *et al.*) were particle board (C-Particle), hardwood flooring (C-Hardwood), ceiling tile (C-Ceiling), and gypsum board (C-Gypsum). The key finding was that there is no higher likelihood of mould growth in green building materials than in non-green materials. However, cellulose based materials (both green and non-green) are more prone to fungal growth.

All the materials required at least 20 days exposure to 85%-95% relative humidity for fungal growth. The amount of time could be shortened by half if the materials were directly exposed to liquid water at the beginning. They also found that the presence of external nutrient could promote the growth of fungi.

At assembly level, Rao *et al.* (2009) experimentally evaluated the potential transport of mould spores from mouldy studs to the interior environment. They used a full size wall assembly for the experiment. Different wall assemblies were used with or without vapour barrier, glass wool insulation, and clear studs or visibly mouldy studs. The rate of air leakage was controlled through pressurization system. Some tests were carried out in dry wall assembly and some tests were carried out after having the wall system moistened with 90% relative humidity for 6 weeks. The research did not find any statistically significant spore movement to the interior environment due to using mouldy studs. However, if the walls without vapour barriers are taken separately, higher level of spore concentration was observed inside and outside the building envelope. This implies that, although there is no statistically significant change in spore concentration in indoor as a whole, envelopes without vapour barrier should still be examined cautiously for its role in possible increase of microbial emission.

At assembly level, Rasmussen and Nicolajsen (2005) tested the performance of organic and mineral-based insulation products in exterior walls and attics in a traditional Danish housing estate. They focused on the performance of the materials once installed and exposed to the normal use of the dwellings in Danish weather conditions over a 2-year period. Evaluations were based on on-site observations, thermographic observations and measurements of temperature and moisture conditions in the building and inside the envelope. They used six organic and two mineral fibre materials in the form of loose-fills and rigid shapes. The eight different products were installed in 16 dwellings by having two neighbouring dwellings insulated with each product. Exterior walls were constructed without Polyethylene (PE) vapour barriers while ceilings were constructed with PE. The resulting moisture conditions in either exterior walls or attics did not show any mould growth in the thermal insulation material.

## 2.5 Summary of the literature review

Thermal insulations can be related to energy use, buildings' structural integrity and human health, through the following hygrothermal interactions:

### *2.5.1 Heat*

Laboratory tests, as discussed in this literature review, show a correlation between the increases in heat flux with the increase in the moisture content in insulations. However, during in situ tests, no increase in thermal conductivity was noticed in various insulations during prolonged exposure of the assembly to 60% relative humidity. There is a clear gap in knowledge in terms of in situ experiments in high relative humidity exposures though. Experimental works on the effects of vapour diffusion seems incomplete without considering 80%-95% relative humidity exposures as subsection 2.3.2 shows that the presence of this range of relative humidity is plausible in residential interiors. As far as fibrous hemp insulations are concerned, no published work has been found on in situ determination of thermal transmittance and conductivity of insulation at 80%-95% internal relative humidity exposures.

The ability of bio-insulations like hemp to increase the heat capacity of the matrix by adsorbing moisture and its effect on dynamic heat transfer cannot be appreciated from the conventionally determined moisture dependent thermal conductivity values. The method of determining moisture dependent thermal conductivity itself is not highly reliable due to the thermal gradient induced moisture transfer. Dynamic energy simulations can be useful to understand the effect of variable heat capacity of hygroscopic insulation materials on heat transfer through the building envelope.

### *2.5.2 Moisture*

Hemp is a highly adsorptive insulation material and the amount of adsorption may vary depending on the fibre extraction and the insulation manufacturing process. Variations between the adsorption isotherms of some hemp insulations are shown in section 5.2 of chapter five. These variations, more pronounced when different fibres are mixed together at different ratios with different amount of fire retardants and binders, imply that for similar relative humidity exposure, different hemp insulations may adsorb varying amount of moisture content. For this reason, in a vapour open construction, humidity dependent conductivity will

be a more important factor in terms of comparing the performances of adsorptive insulations. However, it is always possible to relate relative humidity to moisture content and vice versa if the adsorption isotherm is known and the insulation is exposed to the specific relative humidity for adequate amount of time to reach equilibrium moisture content (EMC).

High relative humidity in the insulation seems to be more of a concern than condensation if human health is given the highest priority. Moisture buffering can moderate internal relative humidity. Between vapour diffusion and air leakage, the latter is assumed to be the dominant factor for excessive moisture concentration and interstitial condensation. In a comprehensive survey (Oreszczyn *et al.*, 2006), no evidence of interstitial condensation was found either in lightweight or in masonry walls which may be due to the drying out of condensed water by absorption by the wind barrier or the masonry and then external evaporation by diurnal and seasonal cycles.

In contrast, reverse condensation is a more plausible phenomenon in constructions with vapour barrier when increasingly warming future climate is considered. Water damage can happen not only by vapour diffusion but also by accidental rainwater penetration. In addition to the thermal expansion and contraction of the building materials and the resulting cracks, one can always expect that workmanship could be inadequate. The ‘defensive’ role of building envelope materials is needed to be assessed. As far as fibrous hemp insulation is concerned, there is no published work available in this area.

In terms of internal relative humidity, moisture buffering capacities of hygrothermal insulations can be explored both in room interiors and in loft spaces. Moisture buffering values of hemp insulations need to be determined as no published data are available.

### *2.5.3 Mould*

Mould and microbial emission can be damaging to both human health and building structure. The relative humidity linked to the onset of mould spore germination and mould growth can vary with mould species. As far as hemp insulations are concerned, studies have found that it is difficult to decontaminate hemp fibres from microbes completely. However, further studies are needed to explore the mould growth potentials in hemp insulation in building assemblies.

This can be done in terms of in situ investigation, parametric analysis and bio-hygrothermal simulations.

### 2.6 Summary of the key knowledge gaps

As a result of the literature review of the hygrothermal properties of hemp and related bio-insulations, the following key gaps in knowledge are identified:

- There is a lack of data on the following hygric properties of hemp insulations that can be determined by standard steady state tests: moisture buffer value, water absorption coefficient. The data of vapour diffusion resistance factor and adsorption-desorption isotherm are available on limited types of hemp insulations which may not be available in the UK.
- No laboratory based experiment has been carried out to determine the equivalent thermal conductivity of hemp insulation in vapour open condition for dynamic and quasi steady state hygrothermal boundary conditions.
- No laboratory based experiment has been carried out to determine the likelihood of interstitial condensation in hemp insulation in vapour open condition for dynamic and quasi steady state hygrothermal boundary conditions.
- There is no data available about the in situ equivalent thermal conductivity of hemp insulations.
- There is no data available about the likelihood of interstitial condensation in hemp insulations with respect to in situ conditions.
- Limited information is available about mould growth in hemp fibre. No information is available about mould growth in hemp insulation during service conditions.
- No numerical simulations have been conducted to investigate the long term hygrothermal performance of hemp insulation.

All of the aforementioned limitations are addressed in this study using laboratory based experiments, in situ experiments and numerical hygrothermal simulations.

# Chapter 3

# Definitions and Theories Related to Heat, Air and Mass Transfer and Mould Growth

This chapter discusses the key theoretical and numerical aspects of heat, air and mass transfer, which will be relevant during the analysis and discussion of the experimental and numerical results. Adsorption isotherm is given particular emphasis in the discussion in this chapter as it is a defining hygric property of fibrous bio-based insulations and it can potentially play a key role in moderating moisture fluctuation and lessening the frequency of condensation. Adsorption also influences heat flux by the process of heat of wetting and moisture induced change in thermal conductivity and diffusivity.

## 3.1 Heat, air and moisture transfer

### *3.1.1 Moisture transfer*

Moisture flow (g) through a building envelope can be divided into vapour and liquid flow and can be expressed as follows:

$$g = g_V + g_l \quad [3.1]$$

Where,

$g_v$ is vapour flow (Kg/m$^2$S) and $g_l$ (Kg/m$^2$S) is liquid flow.

Vapour flow $g_v$ can be expressed as follows:

$$g_v = (-\delta_P)\nabla p + r_a v_a \quad [3.2]$$

where,

$\delta_P$ = Water vapour permeability of building material (Kg/msPa), $v_a$ is the humidity by volume of air (Kg/m$^3$) and $r_a$ is the density of air flow rate (m$^3$/m$^2$s), and $r_a$ is further described by the following equation:

$$r_a = -K_a\nabla(P_a - \rho_a g z U_z) \quad [3.3]$$

Where $K_a$ is air permeance (s), $P_a$ is the overall air pressure (Pa), $\rho_a$ is the density of air (kg/m$^3$), g is acceleration due to gravity (m/s$^2$), z is height above a Datum level (m) and Uz is the unit vector in the vertical direction.

Liquid flow $g_l$ can be expressed as:

$$g_l = K.\nabla P_{SUC} \quad [3.4]$$

Where K is the coefficient of liquid permeability (Kg/msPa), $P_{SUC}$ is capillary suction stress (Pa).

### *3.1.2 Heat transfer*

Heat flow consists of conductive, convective and diffusive part

$$q = q_{cond} + q_{conv} + q_{diff} \quad [3.5]$$

Where $q_{cond}$ is heat flux due to conduction (W/m$^2$), $q_{conv}$ is heat flux due to convection (W/m$^2$), and $q_{diff}$ is heat flux due to diffusion (W/m$^2$).

$$q_{cond} = -\lambda\nabla T \quad [3.6]$$

Where λ is the thermal conductivity (W/mK) of the material, T is the temperature (°C).

The convective and diffusive parts of the heat flow can be combined as:

$$q_{(conv+diff)} = g_v L = \left((-\delta_P)\nabla p + r_a v_a\right) \quad [3.7]$$

It follows from the sum of equations [3.6] and [3.7]:

$$q = -\lambda\nabla T + g_v L \quad [3.8]$$

Where L is the evaporation enthalpy of water (J/kg).

### *3.1.3 Heat and moisture balance equation*

Heat and moisture balance equation have been expressed in terms of various state variables. Classical models take into account temperature and moisture gradient. WUFI, the transient heat and moisture transfer simulation software (Kunzel, 1995) which is being used in this thesis takes temperature and relative humidity gradient as the state variables. The following coupled heat and moisture balance equations are used and the solutions are obtained by finite volume method:

$$\frac{dH}{dT}\frac{\partial T}{\partial t} = \nabla.(\lambda^{*}\nabla T) + L_{lv}\,\nabla.\left(\delta p \nabla(\varphi \rho_{sat})\right) \quad [3.9]$$

$$\frac{dw}{d\varphi}\frac{\partial \varphi}{\partial t} = \nabla.\left(D\varphi \nabla\varphi + \delta p \nabla(\varphi \rho_{sat})\right) \quad [3.10]$$

Where

$\frac{dH}{dT}$ = heat storage capacity of moist building material (J/m$^3$K)

$\frac{dw}{d\varphi}$ = moisture storage capacity of building material (Kg/m$^3$)

λ*= thermal conductivity of moist material (W/mK)

$D\varphi$ = liquid conduction coefficient of building material (kg/ms)

$\delta p$ = Water vapour permeability of building material (Kg/msPa)

$L_{lv}$ = evaporation enthalpy of water (J/kg)

$\rho_{sat}$ = saturation vapour pressure (Pa)

T = temperature (°C)

φ = relative humidity (-)

### *3.1.4 Air balance equation*

Air balance equation is important in many cases where there is air flow through the cracks and holes in the building envelopes. Air flow may also contribute to heat and moisture flows through the building envelopes without vapour barriers.

Under small pressure difference air compression and storage is negligible, therefore the air balance equation can be written as:

$$\nabla\left(K_a \nabla(P_a - \rho_a g z U_z)\right) = 0 \quad [3.11]$$

## 3.2 Thermal conductivity

### *3.2.1 Definition of thermal conductivity*

Thermal conductivity is defined as the rate of heat transfer through the unit thickness of a material per unit area per unit temperature difference. The unit of thermal conductivity is W/mK. Thermal conductivity is lowest in gas phase of a

material and highest in solid phase. Heat conduction in a solid phase occurs through the energy transport by free flow of electrons and through the vibration of the lattice-like structure of the molecules. In steady state condition, thermal conductivity is a good indicator of the heat conduction through a material, but in transient condition where temperature difference varies in time, diffusivity (α in $m^2/s$) of a material gives a better indication of how quickly heat propagates through a material. In transient condition thermal conductivity data of a material is still needed since diffusivity is a function of conductivity and volume heat capacity. Thermal conductivity also depends on ambient temperature, density, and moisture content of a material.

Thermal conductivity is usually measured in a steady state condition. However, the process is time consuming and complex, especially in case of materials with higher heat capacity. Conventional steady state instruments are not very suitable for routine measurements of conductivity in a research and development environment, since a lot of samples are needed to be tested in a short period of time. A quicker method requires the measurement of heat transfer in transient condition since steady state cannot be reached in a short period of time. The transient method of measuring thermal conductivity is described in appendix A.

### *3.2.2 Governing thermal equations*

The primary equations of one dimensional thermal conductivity at macroscopic level and based on Fourier's law are:

$$\mathrm{Q}_x = -\lambda_X A \frac{\partial \mathrm{T}}{\partial \mathrm{X}} = -\lambda_X \mathrm{A} \nabla \mathrm{T} \qquad [3.12]$$

$$\mathrm{q}_x = -\lambda_X \frac{\partial \mathrm{T}}{\partial \mathrm{X}} = -\lambda_X \nabla \mathrm{T} \qquad [3.13]$$

Where $\mathrm{Q}_x$ is heat transfer (W) rate in x direction and $\mathrm{q}_x$ is heat transfer rate ($W/m^2$) in x direction per unit area (normal to the direction of heat flow); the coefficient $\lambda_X$ is thermal conductivity (W/m.K) towards the x direction and $\partial T/\partial x$ is the temperature gradient in the same direction.

The internal thermal conductivity derived from the equations 3.12 or 3.13 is for steady state heat flow and temperature variations. Based on the Fourier's' law

and the first law of thermodynamics, the following partial differential heat equation is developed for one dimensional transient heat flow, where heat capacity of the conductive material is taken into account:

$$\frac{\partial^2 T}{\partial X^2} + \frac{g}{K} = \frac{1}{\alpha} \frac{\partial T}{\partial t} \quad [3.14]$$

Where α is the diffusivity of the conductive material, ∂T is differential temperature, ∂X is the differential thickness of the material, ∂t is the differential time, K is thermal conductivity and g is internal heat generation.

For three dimensional Cartesian co-ordinate system, the heat balance equation is as follows:

$$\frac{\partial^2 T}{\partial X^2} + \frac{\partial^2 T}{\partial Y^2} + \frac{\partial^2 T}{\partial Z^2} + \frac{g}{K} = \frac{1}{\alpha} \frac{\partial T}{\partial t} \quad [3.15]$$

In steady state condition, temperature difference is not changing in time (∂T/∂t), and if there is no internal heat generation, equations 3.14 and 3.15 can be written respectively as:

$$\frac{\partial^2 T}{\partial X^2} = 0 \quad [3.16]$$

$$\frac{\partial^2 T}{\partial X^2} + \frac{\partial^2 T}{\partial Y^2} + \frac{\partial^2 T}{\partial Z^2} = 0 \quad [3.17]$$

### *3.2.3 Thermal conductivity of moist materials*

Thermal conductivity of moist material can be expressed through the following equation:

$$q_{cond} = -\lambda^* \nabla T \quad [3.18]$$

Where,

λ* = thermal conductivity of moist material (W/mK)

ISO 10051 (1996) is the approved test method for determining the thermal conductivity of moist materials in steady state condition in a guarded hot plate or a heat flow meter. Test materials can be conditioned to the expected moisture content by adsorption in humid air, water immersion, spraying of

water, exposing the specimen to a temperature gradient or by the combination of the methods. Materials are enclosed in vapour tight envelopes and are tested in steady state condition.

### *3.2.4 Equivalent thermal conductivity*

Heat flux in a thermal envelope occurs due to conduction, convection, vapour diffusion and radiation. The conventional method of measuring dry thermal conductivity treats conductive, convective and radiative heat flux between the pore walls as thermal conduction at macro scale. Radiation only becomes a dominant driver at macro level at very high temperature during industrial usage, as shown by Karamanos, Papadopoulos and Anastasellos (2012). Vapour diffusion can play an active role in heat transfer in a vapour open wall and air flow can become important when there is significant level of air infiltration.

If two similar types of wall panels, insulated with different insulation materials, are exposed to similar kind of heat, air and moisture boundary conditions, their thermal performance can be compared in terms of their respective heat flux values. If these values are multiplied by similar temperature difference and divided by similar thickness, yet the values will be comparable according to the similar measure. The new value can be defined as 'equivalent thermal conductivity' meaning that this would have been the actual thermal conductivity if there were equivalent heat flux due to thermal conduction. The term 'equivalent thermal conductivity' is taken from Sandberg (2009). Sandberg included heat flux due to moisture dependent conduction and vapour diffusion in equivalent thermal conductivity. Convection was ignored due to its minimal influence in a reasonably air tight wall. Hence equivalent thermal conductivity does not represent the physical phenomenon of 'thermal conduction', it is a combination of heat flux due to dry and moisture dependent conduction and heat flux due to other processes namely vapour diffusion and convection.

According to Sandberg (2009), one obtains:

$$g_v \approx -\rho_l D_{TV} \nabla T \qquad [3.19]$$

Where,

$\rho_l$= density of liquid (kg/m$^3$)

$D_{TV}$ = thermal moisture diffusivity ($m^2/sK$)

From equation 3.19 one obtains:

$$\lambda_{equi} = -\lambda^* + \rho_l L \nabla T \qquad [3.20]$$

Where,

$\lambda$equi is the equivalent thermal conductivity (W/mK),

L is the evaporation enthalpy of water (J/kg).

## 3.3 Adsorption isotherm of fibrous insulation materials

### *3.3.1 Adsorption and adsorption isotherm*

Adsorption is defined as an increase in the concentration of dissolved substance at the interface of a condensed (stationary phase) and a liquid or a gaseous phase (mobile phase) due to the operation of surface forces (IUPAC, 2012).

As far as insulation materials are concerned, adsorption describes the addition of water vapour to the solid surfaces of the insulation matrix. The partial pressure of vapour in the matrix determines the quantity of water molecules that will adsorb to the solid surfaces. At constant temperature, partial pressure will be a function of relative humidity.

In fibrous bio-insulation, water can be present in three forms. These are: free water, water vapour and hygroscopic (bound) water. Water vapour, as a gaseous phase, contains the highest amount of potential energy, free water contains lower potential energy and bound water contains the lowest potential energy (Norton, 2008). Adsorption involves accumulation of bound water and, in higher vapour pressure, increase of free water.

Adsorption has many important and broader industrial applications. These include safe and efficient storage and transport of gasses (Donohue, 2012) and removal of organic molecules and matters causing odour and toxicity from water (Snoeyink and Summers 1999) and other substances. Knowledge of adsorption isotherm is an important part of storage and shelf life of food stuffs.

For insulation materials, the importance of moisture adsorption capacity lies in its potential of regulating the fluctuation of relative humidity of the surrounding environment and of minimising the risk of interstitial condensation in the thermal envelopes of buildings. Thus, adsorption/desorption isotherms can provide an initial idea of the insulation materials' moisture management capacity.

An adsorption isotherm can be defined as the constant temperature relationship between the amount of adsorbate accumulated by the unit quantity of adsorbent and the unit quantity of adsorbent in equilibrium condition in a range of partial pressure (Snoeyink and Summers 1999). To experimentally determine the adsorption isotherm, the relationship between the relative humidity and the adsorbed water content of a material is determined at a constant temperature.

For hygroscopic building materials, the adsorbed water content is measured in terms of Equilibrium Moisture Content (EMC). A material can be described as in EMC when the moisture content being accumulated in a constant temperature and vapour pressure does not vary in time (Kumaran *et al*., 2006). During the state of EMC, vapour pressure within the material is equal to the vapour pressure of the surrounding air. Brooker *et al.* (1992, cited in Nilsson, Svennerstedt and Wretfors, 2005) defined EMC of biological material as the accumulated moisture content of the material after it has been exposed to a certain temperature and humidity for infinity.

Moisture content in building materials, according to Kumaran (2006), can be defined in the following three ways:

- Mass of moisture in unit volume of dry material
- Mass of moisture in unit mass of dry material
- Volume of condensed moisture in unit volume of dry material

In terms of determining adsorption/desorption isotherms of insulation materials, first two definitions of moisture content have been used in this thesis. The first definition helps explore the effect of variable density on adsorption capacity and the second definition can be used to compare the adsorption performance of the existing insulation of particular densities.

### *3.3.2 Morphology of bio-based fibres and adsorption*

Before discussing any further details of adsorption isotherm in general, it is worth knowing the mechanism of adsorption in hemp fibre. The moisture adsorption process in hemp fibres is related to the morphological structure of hemp fibre through physical and chemical interactions.

The structure of hemp stem is consisted of the bark and the core. The bark contains the bast fibres and the core contains the wood cells. Bast fibres contain the outer primary and the inner secondary fibres. Primary bast fibres are 5 mm- 40 mm long and secondary bast fibres are 4 mm long. The elementary fibres of hemp (fibre cell) are bonded together with pectin and lignin to form technical fibre. As shown in Figures 3.1 and 3.2, each fibre cell consists of the primary layer, the secondary layer and the lumen.

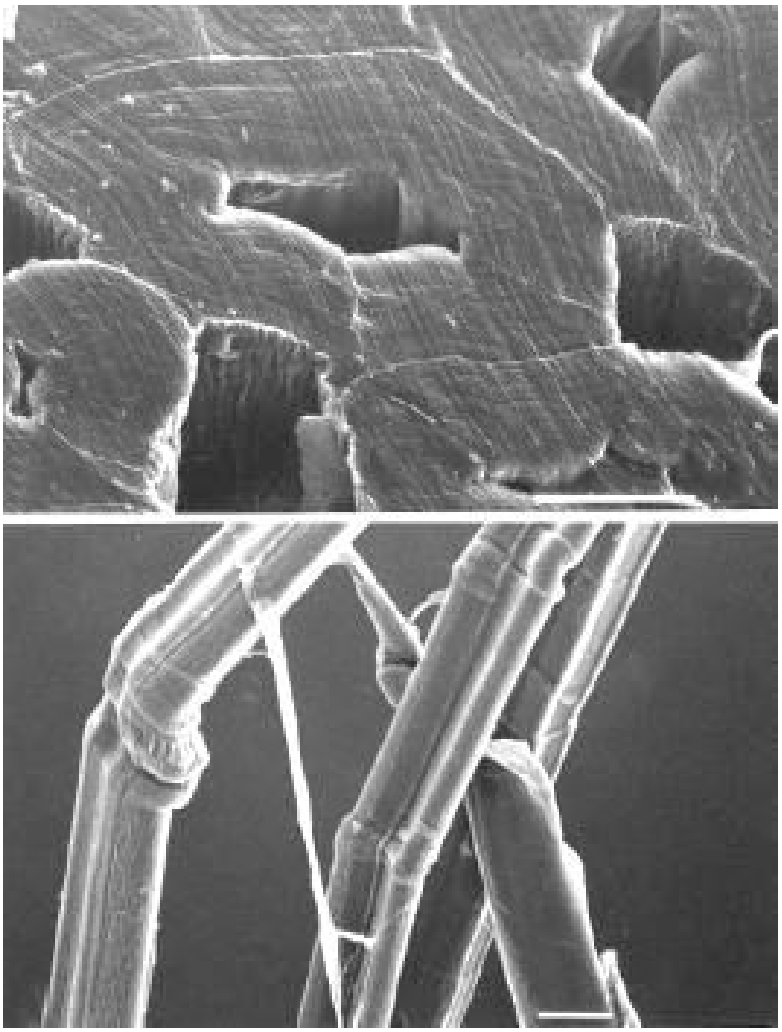

**Figure 3.1: Scanning electron microscopy (SEM) images of hemp bas fibres, Scale bar: 10 µm (Garcia-Jaldon, Dupeyre and Vignon, 1998).**

The secondary wall is divided into further 3 layers, S1, S2 and S3, S2 being the thickest of the layers. The secondary layer consists of fibrils and fibrils accommodate mostly crystalline cellulose microfibrils. The microfibril angle (MFA) is also shown in Figure 3.2.

These crystalline cellulose microfibrils are surrounded by matrix of amorphous lignin, hemicellulose, and pectic components in the fibrils. The difference between crystalline and amorphous polymers is in the arrangement of molecules. In crystalline polymer the long strands of molecules are ordered evenly whereas in amorphous polymers the stands of molecules are ordered unevenly.

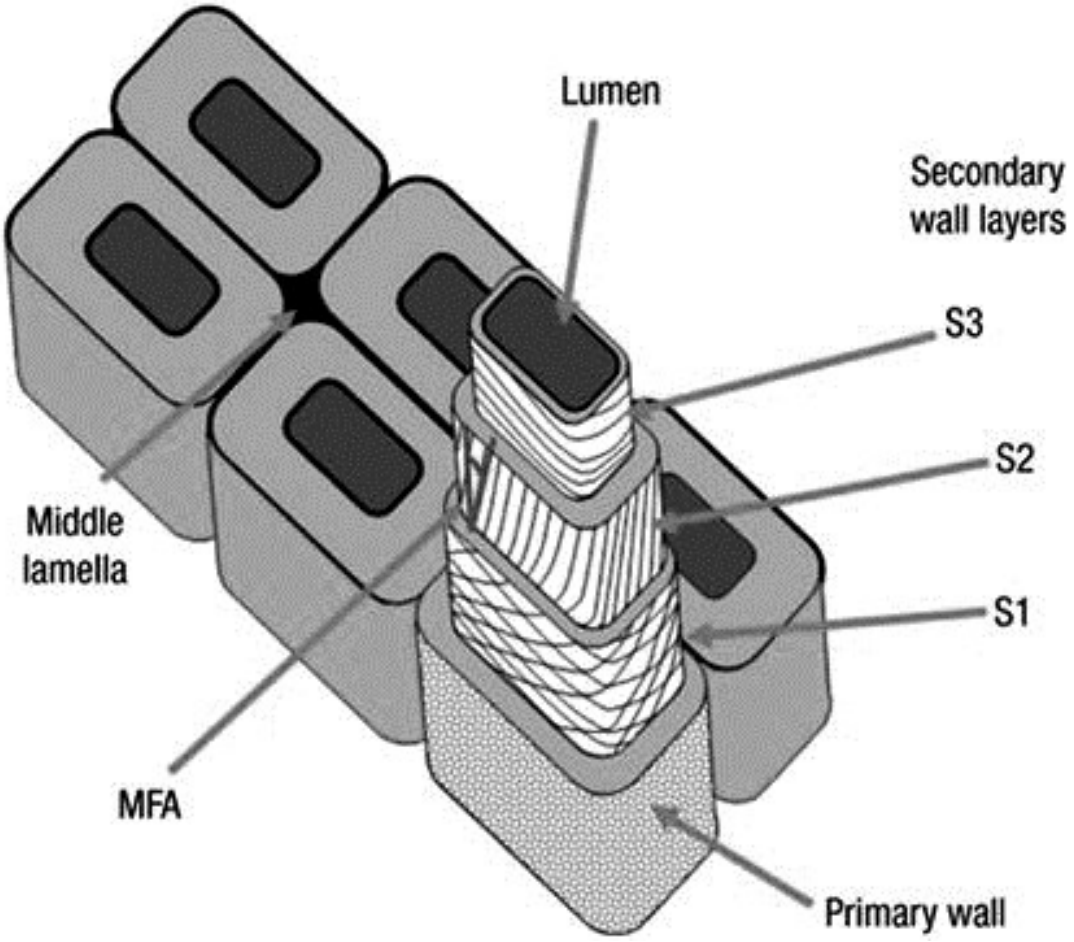


**Figure 3.2: Structure of hemp fibres (Norton, 2008).**

Cellulose, hemicellulose and lignin molecules contain hydroxyl (OH) groups in their structures. These hydroxyl groups, along with carboxyl and sulfonic acid groups, cause affinity to hydroxyl containing materials like water. For example, cellulose can adsorb between one molecular layer and several molecular layers

of water in normal ambient environment (Skaar, 1992 cited in Gardner *et al.*, 2008). However, in cellulose, not all hydroxyl are available to water molecules. In general, hydroxyl groups in amorphous areas have free sorption sites available in contrast with crystalline areas (Time, 1998). Thus, high crystalline part of cellulose is inaccessible to water molecules whereas paracrystalline and amorphous part can be accessible to water molecules. Figure 3.3 shows the sorption sites in internal and external surfaces of a natural fibre available for hydroxyl bonding.

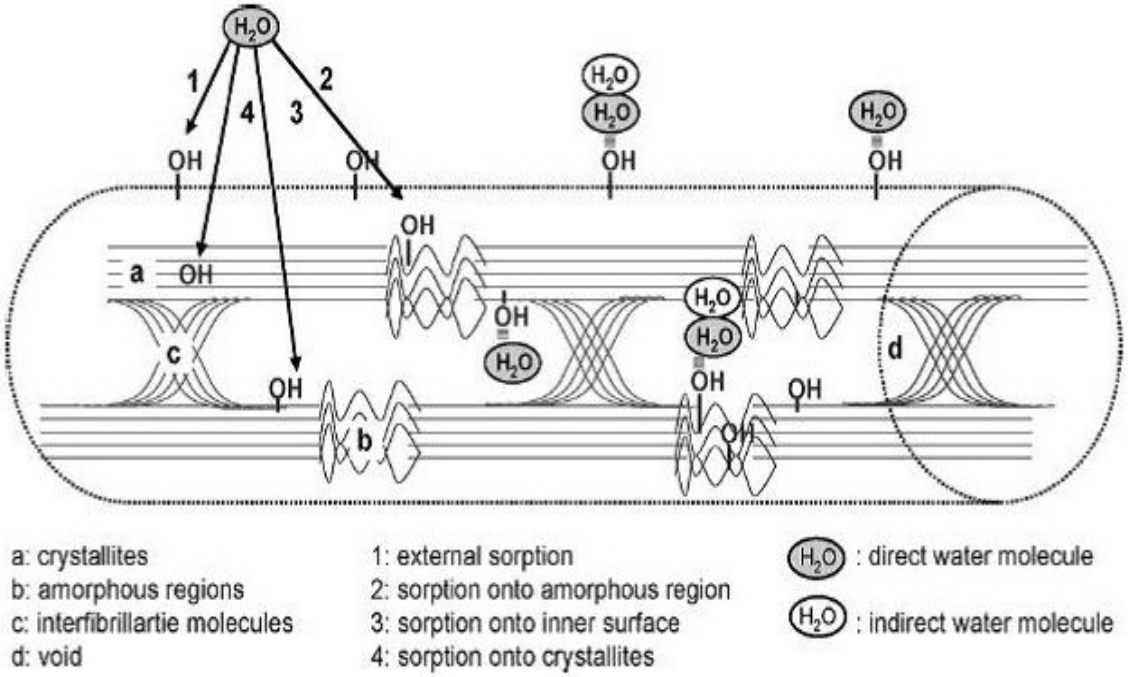


**Figure 3.3: A schematic diagram of direct and indirect moisture sorption onto (1) external surface, (2) amorphous regions, (3) inner surface of voids and (4) crystallites (Okubayashia, Griesserb and Bechtolda, 2004).**

The hemicellulose and pectic component has high OH to C ratio and is highly accessible to water molecules (Hill, Norton and Newman, 2009). As far as insulation materials are concerned, the improvement of overall sorption performance will require knowledge of the effect of these bio-components on the sorption performance of individual fibres.

### *3.3.3 Adsorption mechanism*

In a multilayer sorption, the primary molecules are strongly bonded to the dry surface while the secondary molecules show weak bonding to the wet surface. It is assumed that during sorption/ desorption, energy required for

attachment/ removal of secondary molecules is similar to that of condensation/ evaporation. However, energy required for the removal of primary water molecules is far higher than that needed for the removal of secondary molecules. Primary molecules can be bonded to the surface either by chemisorption or by physisorption or by a combination of both mechanisms. Chemisorption bonding is more energy intensive than physisorption bonding, therefore requires further energy interaction during sorption and desorption. These issues are more highlighted in the discussion of hysteresis and different models of sorption in subsections 3.3.6 and 3.3.7, respectively.

The space taken by adsorbed water molecules in the cell walls of plant-derived materials create transient microcapillary network, which as a result expands the cells' volume. In terms of building insulation materials, the swelling may result into the lessening of porosity, since the voids between the individual fibres are inevitably reduced.

In general, the adsorption/ desorption isotherms are measured up to 95% (98% according to Time, 1998) relative humidity. This is because it is difficult to measure sorption isotherm accurately above this value without using pressure plate, tension plate or pressure membrane measurement methods (Hill, Norton and Newman, 2009). Adsorption value in cellulosic and lingo-cellulosic fibres extrapolated for 100% relative humidity is defined as fibre saturation point or FSP (Hill, Norton and Newman, 2009). This is a term originated in wood science but is also applicable to other plant-derived fibres. At FSP, the cell walls are saturated with water (bound water) but there is no free water in cell cavities and macro voids (Smith, 2012). Beyond FSP, 'free water' or 'absorbed water' accumulates in cell lumens (Forest Product Laboratory, 1944).

### *3.3.4 Hygroscopic region*

A sorption isotherm can be divided into three distinct regions in relation to water storage function as shown in Figure 3.4.

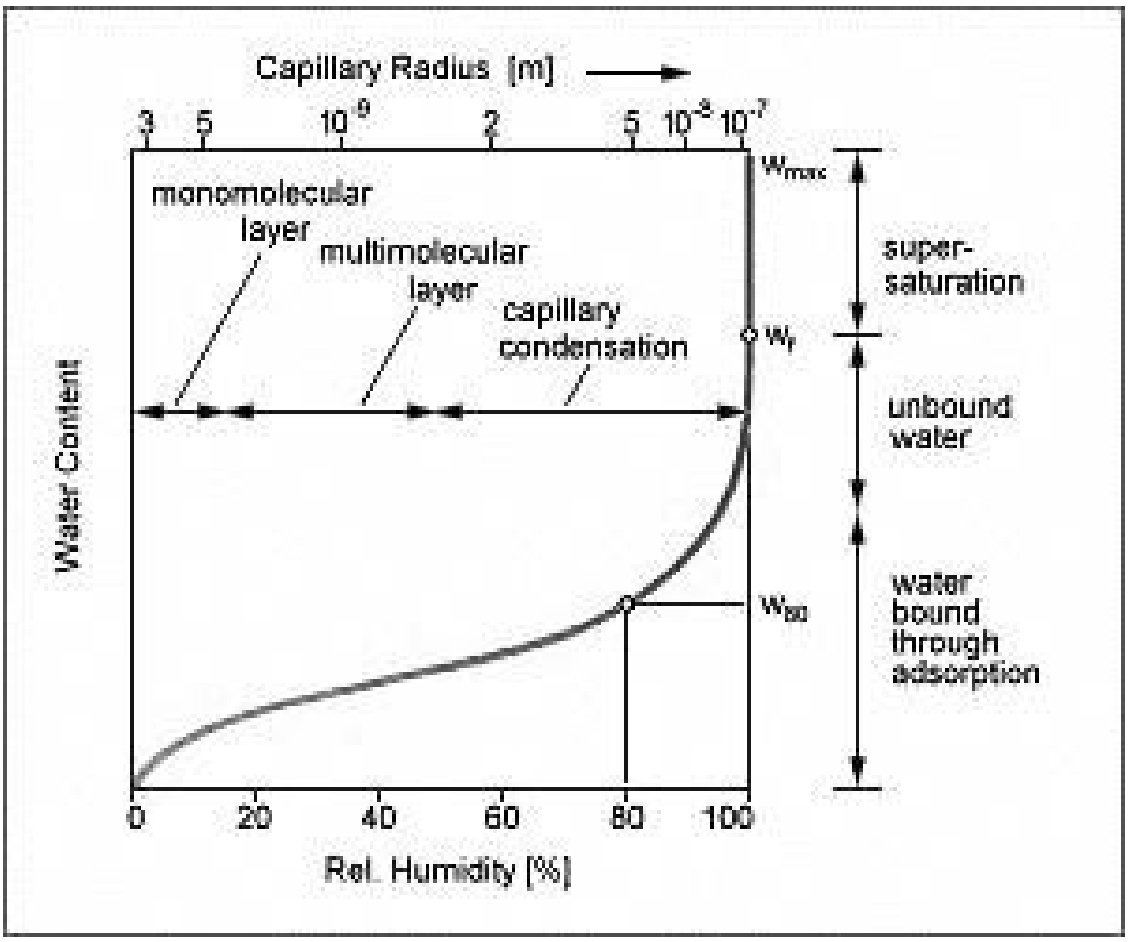


**Figure 3.4: Adsorption regions (Kunzel, 1995).**

At lower relative humidity, water molecules are adsorbed in a monolayer (solid solution) on to the internal surfaces of the cell wall. The relative humidity range is 0%-15% according to Hill, Norton and Newman (2009) and 5%-35% according to Collet *et al.* (2011). The variations in the relative vapour pressure range for monolayer sorption is due to the overlap between the boundaries of relative pressure ranges of monolayer and multilayer sorption. Between 15% and 70% relative humidity, the multi-molecular layer of water is formed on the cell wall micro-capillaries, while capillary condensation occurs at further higher relative humidity ranges. The area covered by 0% to 95-98% relative humidity is defined as hygroscopic region. The adsorption mechanism is graphically represented in Figure 3.5.

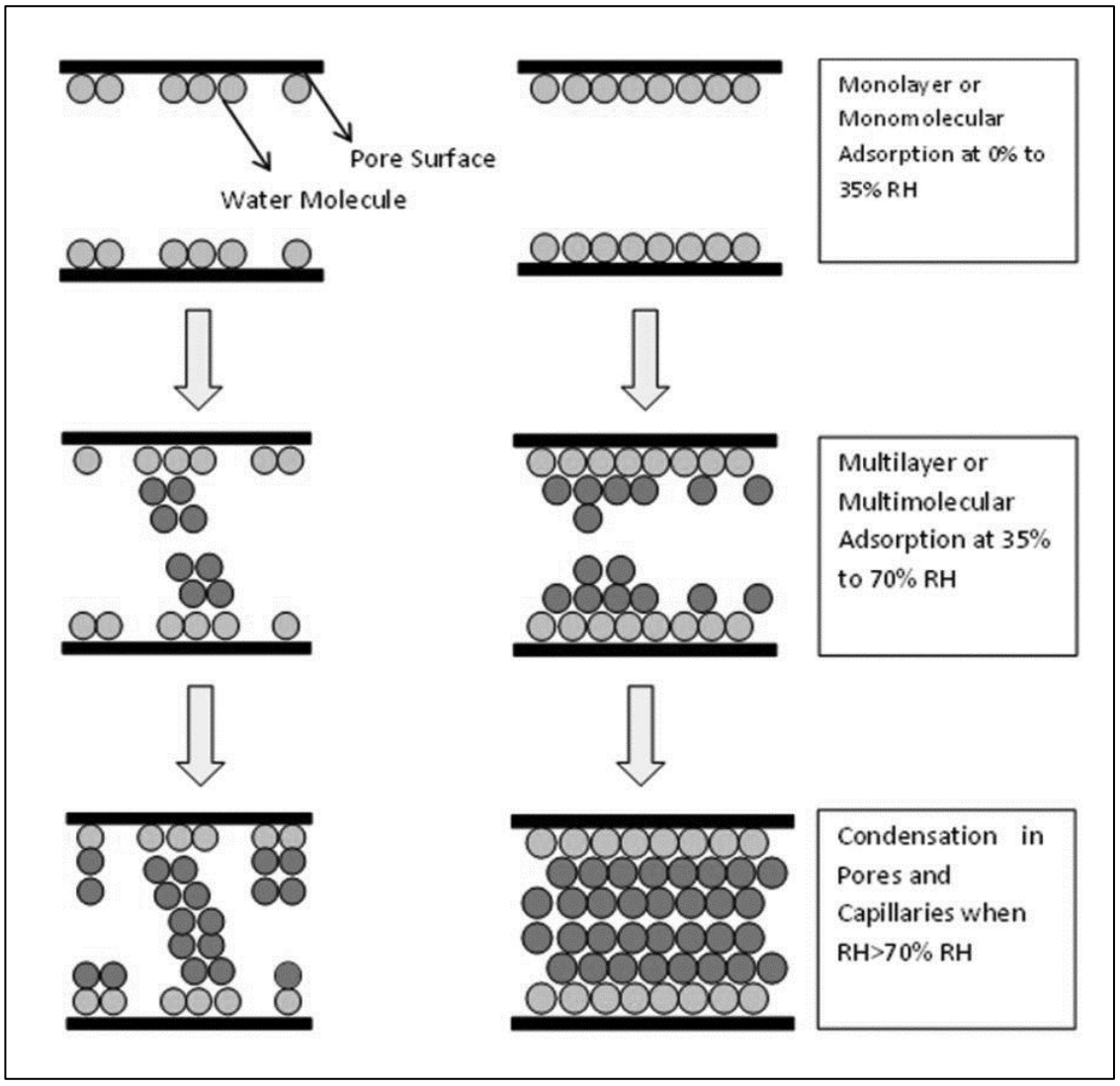


**Figure 3.5: Monolayer and multilayer adsorption (after Osborne, 2004).**

### *3.3.5 Types of adsorption isotherms*

Adsorption isotherms in subcritical temperature are classified by International Union of Pure and Applied Chemistry ( IUPAC) into six distinct types as shown in Figure 3.6. The characteristics of each of these types, after Condon (2006) are described as follows:

- **Type 1** corresponds to Langmuir isotherm, describing monolayer adsorption on microporous (pore widths below 2 nm) adsorbent.
- **Type 2** describes adsorption on macroporous adsorbent with adsorbent-adsorbate interaction. There is initial formation of monolayer and subsequent formation of multilayer.
- **Type 3** describes multilayer isotherm on macroporous absorbent with week adsorbent-adsorbate interaction.

- **Type 4 and 5** represents adsorption isotherm with hysteresis. Capillary condensation occurs in mesopores (pore widths from 2 nm to 50 nm) in these two types.
- **Type 6** includes steps that occur due to phase transition of adsorbed molecular layer or due to adsorption on different faces of crystalline solids.

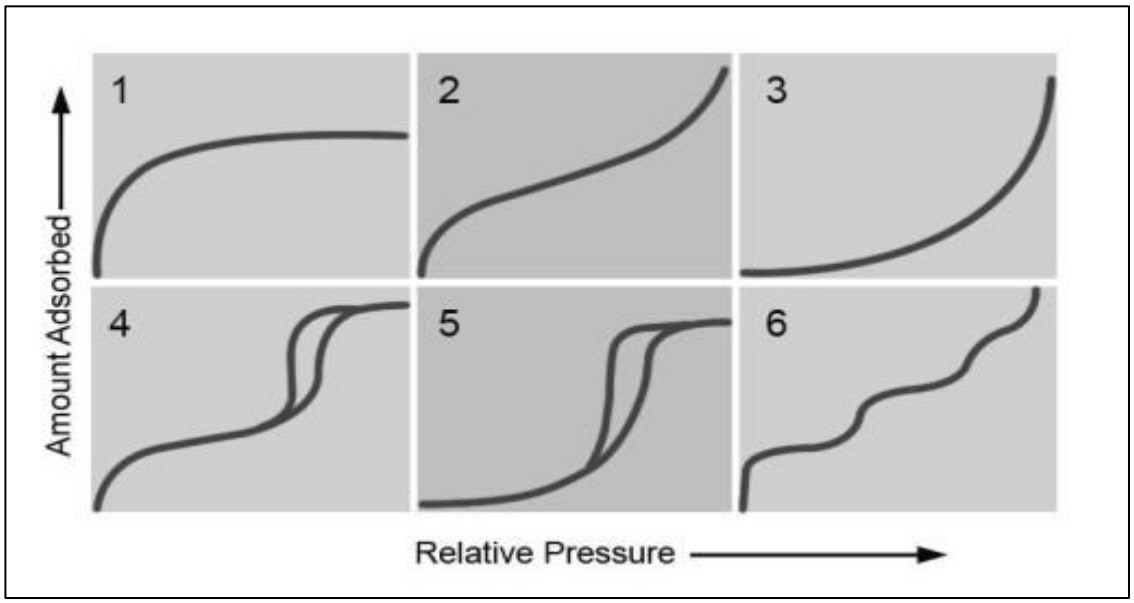


**Figure 3.6: Physisorption (after Condon, 2006).**

### *3.3.6 Hysteresis*

Hysteresis denotes the dependence of a value of a material quantity on the direction of change from a previous value, therefore adsorption hysteresis occurs when there is difference between adsorption and desorption values (IUPAC, 2012). The various types of hysteresis loops are shown in Figure 3.7. Knowledge of hysteresis in an insulation material is helpful as the occurrence of hysteresis also implies that capillary condensation has happened in the micro-voids of fibres during adsorption (Snoeyink, 2012), although these hypothesis is not adequate as will be explained later. As a result of this perceived relation to condensation, hysteresis may have implications on thermal conductivity and moisture buffering capacity of a material assuming that condensed water will increase the thermal conductivity and will also be unavailable for moisture release during desorption in normal ambient temperature. For bio-based fibrous insulations, if the difference between sorption and desorption is too prominent then the data for only adsorption will not be adequate as input parameter for

hygrothermal simulation of building envelopes as Fick's equation will not be valid anymore (Salin, 2010).

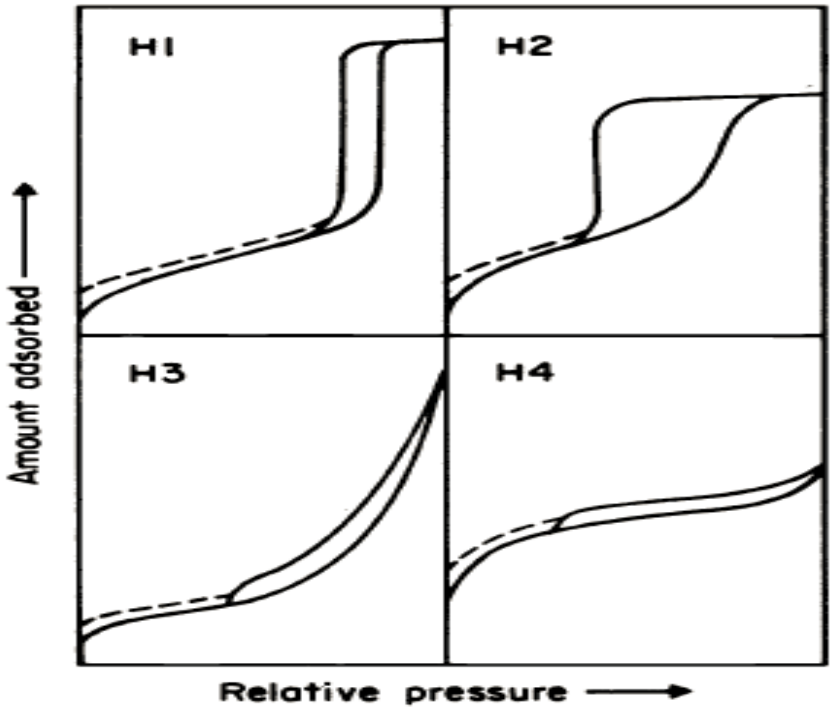


**Figure 3.7: Types of hysterisis loops (Donohue, 2012).**

Some of the longstanding theories that explain the cause of hysteresis are detailed in the following subsections.

#### *3.3.6.1 The incomplete wetting theory*

This theory, by Zigmondy (Cohan, 1938), is based on the assumption that hysteresis is caused by the different value of θ, angle of contact between the surface of the liquid and the walls of the capillary, of the following Kelvin's equation:

$$P = p_s exp\left(\frac{-2\sigma V cos\theta}{r_c RT}\right) \quad [3.21]$$

Where,

σ= surface tension, V= volume of the liquid, $r_c$= radius of the capillary, θ= angle of contact between the surface of the liquid and the walls of the capillary.

According to this theory, hysteresis occurs when the value of θ is higher during adsorption than during desorption. The physical implication of this difference is explained in terms of the presence of impurities (e.g. air) in the surface. During

adsorption process, wetting of the wall is incomplete due to already adsorbed impurities in some sorption sites. However, when vapour pressure is lowered during desorption, the impurities are removed and full wetting of liquid takes place. Hence less moisture is released during desorption. Thus, according to this theory, desorption curve is the true representation of adsorption curve, which is however only valid when hysteresis is irreversible.

#### *3.3.6.2 The bottle neck theory*

According to Kraemer and McBain (Cohan, 1938), reversible hysteresis occurs due to the bottle neck shape of the pores. If the radius of the body of the pore is $r_b$ and the radius of the neck of the pore is $r_n$, condensation occurs inside the body of the pore at pressure p, which can be expressed as follows:

$$P = p_s exp\left(\frac{-2\sigma V cos\theta}{r_b RT}\right) \quad [3.22]$$

After the pore is filled, desorption cannot occur until the pressure $P$ goes down to the level where the value of $r_b$ in equation 3.22 is replaced by the value of $r_n$.

Thus, according to this theory, pore geometry with small opening and large body will result in hysteresis loops during adsorption-desorption cycles, and pore geometry with large opening and small body will not have any hysteresis.

#### *3.3.6.3 The open pore theory*

According to open pore theory by Fosters (Cohan, 1938), hysteresis in open pores occurs as the formation of meniscus is delayed during adsorption process. The pore surface is initially covered with adsorbed film of water molecules. When the meniscus is created, condensation takes place. The pressure at which the annular ring of adsorbed water is formed can be expressed through the following equation:

$$P_a = p_s exp\left(\frac{-2\sigma V cos\theta}{rRT}\right) \quad [3.23]$$

Where, r is the inner radius of the annular ring (the sorbed film).

The pressure during desorption when meniscus is formed can be expressed as follows:

$$P_d = p_s exp\left(\frac{-\sigma V}{r_m RT}\right) \quad [3.24]$$

Eventually, all pores are covered with water at saturation vapour pressure. Therefore, during adsorption both adsorption and capillary condensation is represented in the curve, but during desorption only capillary condensation is represented.

#### *3.3.6.4 The sorption site availability theory*

This theory, developed by Urquhart and Williams (Time, 1998), is particularly relevant to wood science. According to this theory, during the drying up of water saturated wood, as a result of shrinkage, some hydroxyl groups come closer to each other and create bonds between them. As a result these hydroxyl groups or sorption sites are not fully available for moisture adsorption and thus hysteresis loop is created. However, some of the bonds break due to swelling pressure during adsorption and becomes available again.

This theory is different from other theories in terms of relating hysteresis to sorption site availability instead of condensation. Since in some cases, hysteresis, also takes place in low relative humidity ranges, it is difficult to explain the phenomenon completely in terms of condensation-based theories.

### *3.3.7 Heat of wetting or heat of sorption*

As mentioned in subsection 3.3.1, adsorbed water in bio-based insulation materials can be present as bound water and as liquid water. Water can also present in vapour form in the open spaces. The energy state of bound water is comparable to that of frozen water. The heat of wetting is defined as the difference of energy between the following two transformations: transforming bound water into vapour and transforming liquid water into vapour. Thus, it is the energy required to transform the energy state of bound water into the energy state of liquid, which explains why it is called ‘heat of wetting’.

Figure 3.8 shows the analogy between relative energy levels of water vapour, liquid water and frozen water and their equivalent in plant fibre. $Q_0$ is the relative energy level of vapourisation of liquid water, $Q_f$ is the relative energy level of frozen water, $Q_u$ is the relative energy level of vaporization of frozen water. Following the similar phases changes of water in the fibre, $Q_s$ is the relative energy level of sorption of liquid water by the fibre or the wetting of bound

water, it is also called the differential heat of wetting. $Q_v$ is the relative energy level of vapourisation of bound water.

It can be noted that heat of wetting is a significant phenomenon during sorption and desorption of wood based fibrous materials. Therefore, the heat of wetting may be needed to be taken into account when considerable amount of hygroscopic thermal insulation materials are used in the building fabric and in the loft.

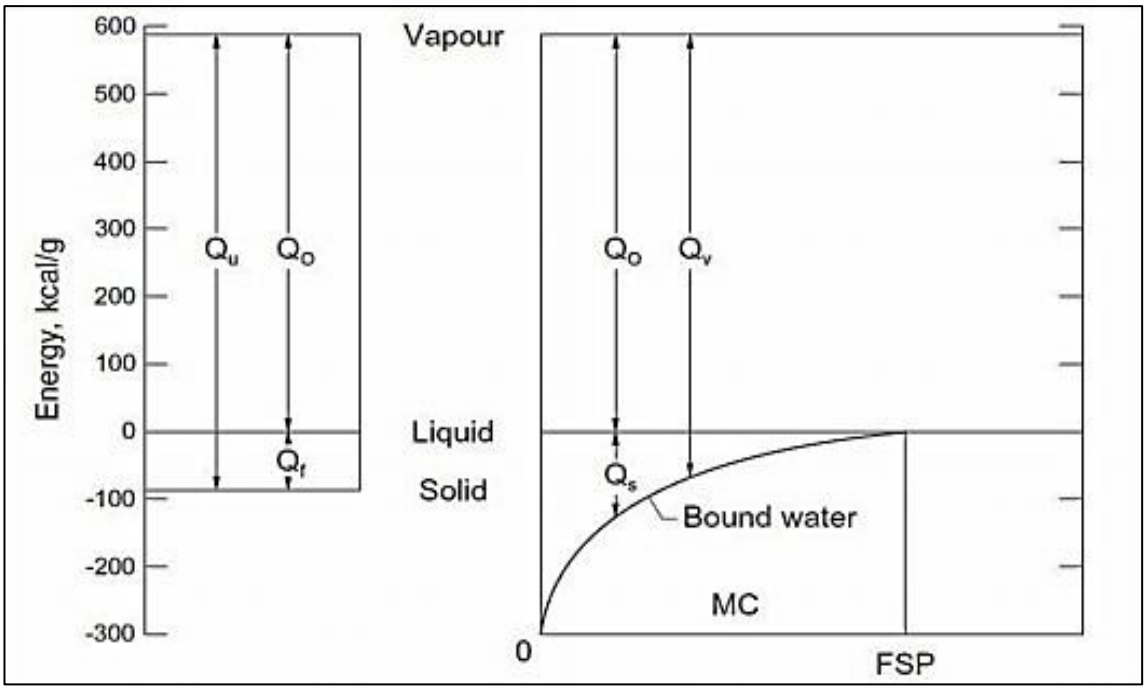


**Figure 3.8: Relative energy (enthalpy) levels of vapour, liquid water, frozen and bound water as a function of moisture content (Skaar, 1998 in Time, 1998).**

### *3.3.8 Variations in adsorption isotherms*

Determining adsorption isotherms of a hygroscopic material can yield differing results. For a particular sample, it can happen due to the difference between fast sorption and slow sorption methods (Xie et al, 2010). For plant derived fibres, variations in adsorption isotherms can be observed as a result of the difference in fibre extraction and processing (Nilsson, Svennerstedt and Wretfors, 2005). Adsorption isotherm can also vary due to the heterogeneity of the adsorbing material resulting in varying pore sizes, pore distribution, active adsorption sites, and presence of blocked or interconnected pores (Balbuena and Gubbins, 1993). Therefore, it is always possible that the adsorption properties of insulations made from same fibres but obtained from different

sources will vary as they may have different initial processing history and different amount of constituent in the final products.

### *3.3.9 Theories of adsorption*

Various numerical models have been developed to describe moisture adsorption by biological materials. Time (1998) has divided the models into following four categories:

- Monolayer adsorption models
- Multilayer adsorption models
- Sorption models in polymer science
- Empirical models

The most representative models are briefly described in the following subsections.

#### *3.3.9.1 The Langmuir isotherm*

The Langmuir isotherm is the first model of adsorption isotherm describing a monolayer or monomolecular adsorption. The Langmuir isotherm is based on the hypothesis of dynamic equilibrium between the adsorbed phase and the gaseous phase meaning that the rate of evaporation from adsorbed molecules is equal to the rate of condensation from the gaseous molecules. The following assumptions are made:

- There is no lateral interaction between adsorbed molecules.
- The heat of adsorption is constant and independent of coverage.
- Each adsorbate molecule occupies only one site.
- The adsorbed molecule remains at the site of adsorption until it is desorbed.

The type 1 shown in Figure 3.6 represents a typical example of the Langmuir isotherm. The governing equation for Langmuir Isotherm is:

$$\theta = \frac{K_a \varphi}{(K_d + K_a \varphi)} \qquad [3.25]$$

Where θ = fraction of the surface covered by adsorbate, $\varphi$ = relative pressure of relative humidity, $K_d$, Ka = proportionality constants.

Equation 3.25 is applicable to monolayer adsorption, which occurs, as already mentioned, at the lower range of relative humidity.

### *3.3.9.2 The Brunauer, Emmett and Teller isotherm*

The Brunauer, Emmett and Teller (BET) isotherm is an extension of the Langmuir isotherm. This represents multilayer sorption of gas on a surface. The following assumptions are made:

- The surface is homogeneous.
- There is no lateral interaction between adsorbed molecules.
- The uppermost layer is in equilibrium with vapour phase.
- In all layers except the first, heat of adsorption is equal to heat of condensation.
- In all layer except the first, evaporation-condensation conditions are identical.
- At saturation vapour pressure, numbers of layers becomes infinity.

The BET isotherm can be represented by the equation 3.26 (adapted from Timmermann, 2003; Time 1998 and Collet *et al.* 2011):

$$V(\varphi) = \frac{W_{mB} C_B \varphi}{(1-\varphi)(1+(C_B-1)\varphi)} \qquad [3.26]$$

Where,

v(φ) = the amount of adsorbate adsorbed by a gram of adsorbant at adsorbate activity or relative humidity φ,

$v_{mB}$ = monolayer value in the same units as v

$$C_B = \text{energy constant} = \frac{a_1 v_2}{a_2 v_1} \exp \frac{q_{1-} q_L}{RT} \qquad [3.27]$$

$a_1, a_2$= constants

$v_1$, $v_1$ = frequencies of molecule oscillations in a direction normal to the surface

R= gas constant

T= temperature

$q_1$ - $q_L$ = differential heat of sorption, $q_1$ being the activation energy of the first layer and $q_L$ being the heat of condensation

In practice, the following simplified form of equation is used:

$$C_B = exp\ \frac{q_1 - q_L}{RT} \qquad [3.28]$$

BET equation is linearized to determine the value of the two constants, $C_B$ and $V_{mB}$. The linearization for BET equation is expressed as the following function:

$$F(\mathrm{BET}) \equiv \frac{\varphi}{(1-\varphi)\mathrm{V}(\varphi)} = \frac{1}{C_B V_{mB}} + \frac{C_B - 1}{C_B V_{mB}}\varphi \qquad [3.29]$$

***3.3.9.3 The Guggenheim/ Andersen/ de Boer isotherm***

The Guggenheim/ Andersen/ de Boer (GAB) isotherm is based on further modification of BET isotherm. Like the BET formulation, the GAB formulation also assumes that adsorbate molecules beyond the first layer are similar. However, according to the GAB model, the states of the other adsorbate layers are different at pure liquid state. For this reason, the GAB equation introduces an additional parameter namely K that determines the state of the adsorbed molecules beyond the first layer (Timmermann, 2003). The equation for GAB isotherm is:

$$V(\varphi) = \frac{W_{mG} C_G K \varphi}{(1 - K\varphi)(1 + (C_G - 1)K\varphi)} \qquad [3.30]$$

Where,

$C_G$ = energy constant related to the difference of free enthalpy of water molecules in the liquid state and in the monolayer

$W_{mG}$ = monolayer value in the same unit as W.

K= the third parameter, characterizing the state of the adsorbed molecules beyond the first layer.

It can be noticed that if K=1, then there is no difference between the BET equation and the GAB equation.

The linearized function of GAB isotherm is:

$$F(\mathrm{GAB}) \equiv \frac{\varphi}{(1-\mathrm{K}\varphi)\mathrm{W}(\varphi)} = \frac{1}{C_G K W_{mG}} = \frac{1}{C_G K W_{mG}} + \frac{C_G - 1}{C_G W_{mG}}\varphi \qquad [3.31]$$

#### *3.3.9.4 Hailwood and Horrobin model*

Hailwood and Horrobin (HH) model is based on the solution-hydration model and is widely used in wood science. According to this model, adsorbed water partly forms hydrate with the adsorbent and partly forms a solid solution in the cell wall.

It has been shown that the equation for determining GAB isotherm is equivalent to the equation of HH model (Boquet, Chirife and Iglesias, 1980 cited in Timmermann, 2003). Time (1998) observed that the equations used in GAB model were based on the following equation initially derived in the HH model:

$$W = \frac{\varphi}{A + B.\varphi - C.\varphi^2} \qquad [3.32]$$

Where,

A, B, C= constant, Φ= relative humidity, W= moisture content.

Similar to the GAB model, determination of the value of three constants is also required in HH model.

## 3.4 Moisture buffering

### *3.4 1. Introduction*

Moisture buffering capacity is a property of hygroscopic materials. Hygroscopic materials in touch with surrounding air adsorb and desorb moisture to create equilibrium with the relative humidity of the surrounding space. Moisture buffering capacity is most effective when air change rate is very low. Increased rate of air change can create humidity equilibrium with external air undermining the adsorption-desorption capacity of the hygroscopic surface materials and furniture.

### *3.4.2 Application of moisture buffering capacity of materials*

Moisture buffering capacity can be used for moderating the humidity fluctuations in an internal space. Sustained steady relative humidity near the interior surfaces can mitigate the risk of surface condensation and surface mould growth. Moisture buffering can specially be useful in archives where internal relative humidity has to be maintained to a certain level to protect old manuscripts and other related items. In terms of roof and attic applications, moisture buffering capacity of thermal insulations can potentially lessen the risk and frequency of occurrence of condensation in the roof provided that the insulation surfaces are open to the internal air of the attic.

### *3.4.3 Levels of moisture buffering*

Moisture buffering capacity has been divided in three levels according to the scale of moisture interaction by Rode (2005) and Svennberg (2006), as shown in Figure 3.9. These three levels are:

- Material level
- System level
- Room level

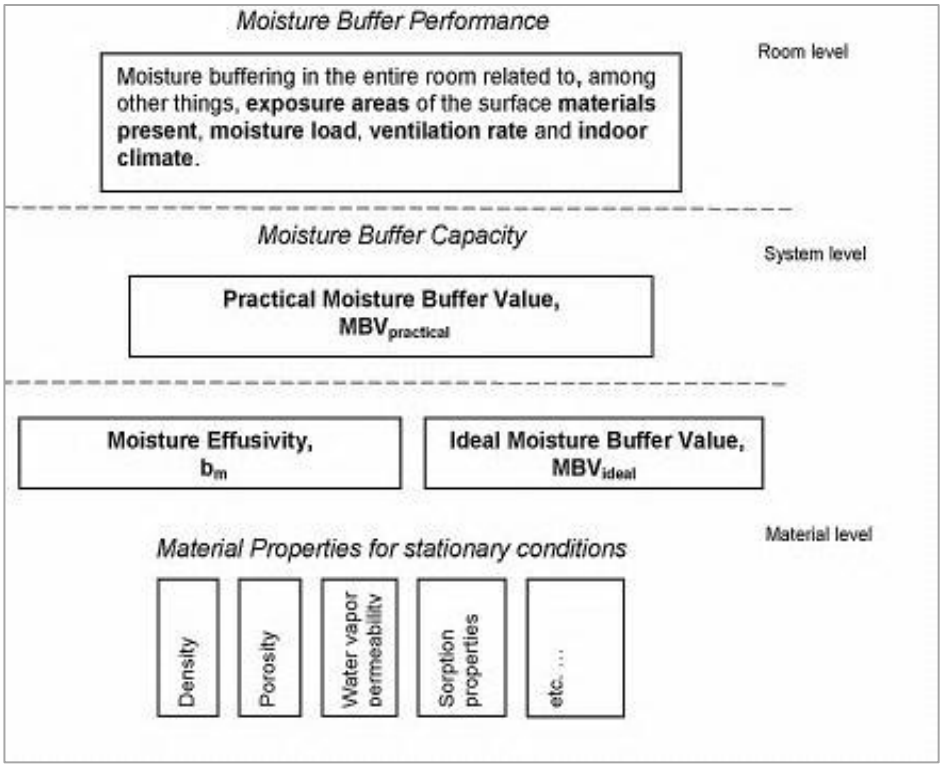


**Figure 3.9: Three levels of moisture buffering (Rode, 2005).**

At material level, properties of the material are considered, not the boundary conditions such as surrounding air layer. At system level, a material system is considered with the convective boundary air layer; material system can contain a single homogenous material or a composite of materials. At room level, all hygroscopic materials exposed to the interior air is considered and all internal climatic conditions as well as moisture load and ventilation rates are taken into account.

### *3.4.4 Moisture penetration depth*

Moisture penetration depth is a key consideration in determining moisture buffer performance. The concept of penetration depth comes from electromagnetism, which means how deep an electromagnetic wave can penetrate into a material. It is usually defined as the depth at which the intensity of the radiation falls to 1/e (27%) of its original value, where e is the Euler's number. While determining moisture buffer value, moisture penetration depth is measured in relation to the amplitude of relative humidity variation at a certain depth compared to the amplitude of relative humidity variation at the surface of the material. Figure 3.10 shows the penetration depths of 1/e and 1% in a hypothetical material.

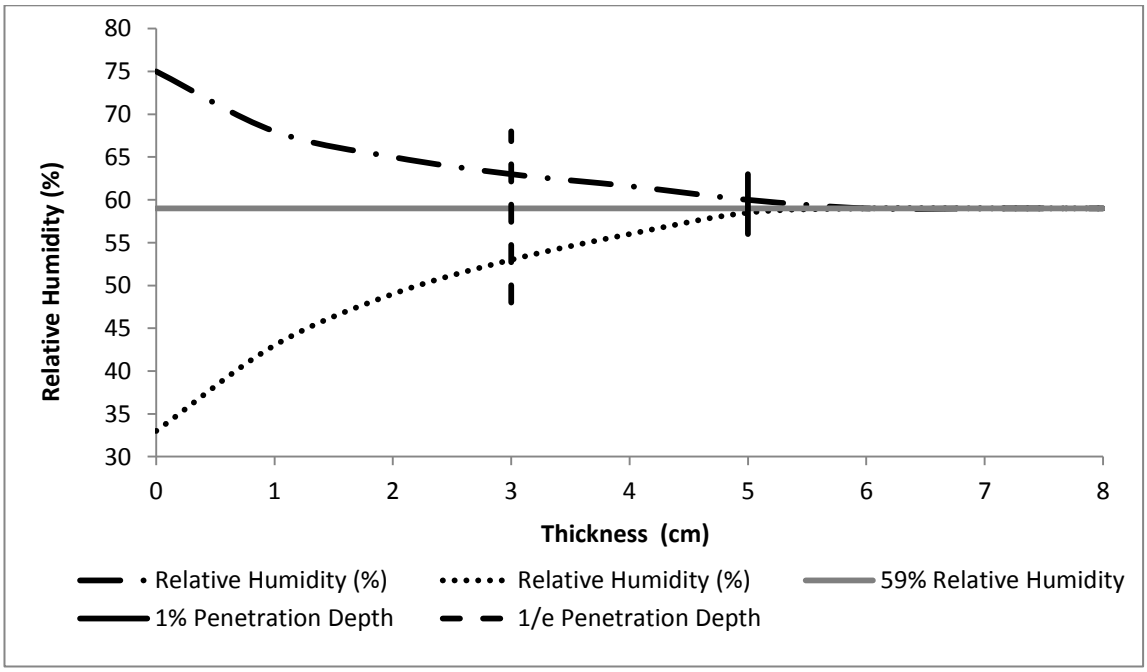


**Figure 3.10: Moisture penetration depth (Time, 1998).**

In the Nordtest method, moisture penetration depth of 1% or less is taken as the material thickness. An approximation of this penetration depth is possible through the following equation:

$$d_p 1\% = 4.6 \sqrt{\frac{D_w . t_p}{\pi}} \qquad [3.33]$$

Where, $D_w$ is moisture effusivity of the material [kg/ ($m^2$. Pa. $s^{1/2}$ )], $t_p$ is the cycle time, $d_{p,1\%}$ is the thickness of the material at 1% penetration depth. Equation 3.33, applicable to semi-infinite materials, is an approximation since it is derived from sinusoidal periodic variations rather than from stepwise periodic variations.

### *3.4.5 The methods and units of moisture buffering capacity*

Several quantitative methods and the corresponding units are available to determine and represent the moisture buffering capacity. The Nordtest method explains three different ways and units of representing the moisture buffering capacity. Different methods of measuring moisture buffering values are also adopted by Japanese Industrial Standard (JIS, 2002) ISO 24353 (2008) and Padfield and Jensen (2009). ISO 24353 is similar to the Japanese method except for the cycle time of relative humidity exposure. The other methods are briefly described in the following subsection.

#### *3.4.5.1 Nordtest units*

The three ways of representing moisture buffering capacity described by Nordtest method are explained below:

***Moisture Effussivity:***

Moisture effusivity ($b_m$ ) is the measure of the ability of the material to exchange moisture with its surroundings when the surface of the material is exposed to sudden change in humidity. The equation for moisture effusivity is:

$$b_m = \sqrt{\frac{\delta_p . \rho_0 . \frac{\partial u}{\partial \varphi}}{P_s}} \qquad [3.34]$$

Where, $b_m$ is moisture effusivity [kg/($m^2$. Pa. $s^{1/2}$ )], $\delta_p$ is water vapour permeability [kg/(m.s.Pa)], $\rho_o$ is the dry density of the material [Kg/$m^3$], u is moisture content (kg/kg), $\phi$ is relative humidity [-], $P_s$ is saturation vapour pressure [Pa].

***Ideal Moisture Buffer Value***

Relative humidity in an interior space can sometimes change as a harmonic oscillation, and in some instances, as a step function. Sudden flux of vapour in the air by a boiling kettle is a widely used example of the step change in relative humidity.

The most common step change function for moisture buffering is to expose the surface to 75% Relative Humidity for 8 hours and to 33% Relative humidity for 16 hours in each cycle. Through Fourier analysis it is possible to predict the surface moisture flux in relation to time. The equation for the relation is:

$$G(t) = \int_0^t G(t)dt = b_m.\Delta \mathrm{P}.h(\alpha)\sqrt{\frac{t_p}{\pi}} \qquad [3.35]$$

Where

*G(t)* is accumulated moisture uptake [kg/m$^2$] and the corresponding moisture release during a time period $t_p$ , *g(t)* is moisture flux over the surface at time *t*, and *h(α)* can be expressed by the following equation:

$$h(\alpha) = \frac{2}{\pi}\sum_{n=1}^{\infty}\frac{Sin^2(n\pi\alpha)}{n^{3/2}} \approx 2.252[\alpha(1-\alpha)]^{0.535} \qquad [3.36]$$

where

α is the fraction of the time period when moisture load is high. In this case the value of h=1/3 and *h(α)* = 1.007 and therefore, the equation 3.35 becomes:

$$G(t) \approx 0.568\,.\,b_m.P_{s.}\sqrt{t_p} \qquad [3.37]$$

The ideal moisture buffer value is measures in [kg/(m$^2$.%ΔRH). The value is determined by normalizing the equation 3.37, by dividing it by the change in relative humidity. Consequently, the ideal moisture buffer value can be expresses as,

$$MBV_{ideal} \approx \frac{G(t)}{\Delta RH} = 0.568\,.\,b_m.P_{s.}\sqrt{t_p} \qquad [3.38]$$

***Practical Moisture Buffer Value***

Practical moisture buffer value $MBV_{practical}$ is defined as the amount of moisture content that passes through the unit open surface of the material during a certain period of time when the material is exposed to variation in relative humidity of the surrounding air. Direction of the moisture transport (in or out of the material) will depend of the humidity potential. The unit of $MBV_{practical}$ is [kg/$m^2$-%ΔRH] when moisture exchange is reported for unit surface area and unit % relative humidity variation.

Practical moisture buffer value ($MBV_{practical}$) is determined through an experimental method where the sample is exposed to cyclic square waves of relative humidity of 75% (high relative humidity) and 33% (low relative humidity). The material is exposed to the high value for 8 hours and to the low value for 16 hours in a 24-hour cycle. The moisture buffer value is calculated as the mass change per unit area for unit difference of relative humidity (total difference of relative humidity being 42%) during the last eight hour period of adsorption. Therefore the unit is kg/($m^2$.%ΔRH).

According to the Nordtest method, the thickness of the material should be less than 1% penetration depth for daily humidity variations.

Practical Moisture Buffer value can be equal to Ideal Moisture Buffer Value if the material is homogeneous and the thickness of the material is equal to or greater than the moisture penetration depth of the material.

***3.4.5.2 'Buf' value***

Padfield and Jensen (2009) proposed a new unit for measuring moisture buffering capacity in terms of moisture buffering equivalent air volume. The unit is called 'Buf' (B) and is expressed in meter. According to this method, the area of the upper and lower surfaces of the volume will always be kept as an unit area (1 $m^2$ ) and any change in buffer value will be reflected along the height of the volume (equivalent air column). The basic concept is, the amount of moisture that is releases or taken up by the buffer material during a step change can be expresses in terms of a volume of air that can hold the similar amount of moisture for a given temperature, relative humidity cycle and waveform. Therefore, In terms of expression, it is analogous to how vapour diffusion

resistance is expressed as vapour diffusion equivalent air layer thickness where meter is used as the unit.

According to this definition, a material with high buffer value will absorb more water in a given relative humidity and therefore it will have higher equivalent air column. If the temperature changes, the height of the air column will also change (Figure 3.11). For example, if temperature decreases in the air, less water will be required for similar relative humidity whereas the buffer material due to sorption properties will still absorb a certain fixed amount of water (equilibrium moisture content). Moisture buffering capacity does not need to be related to the exposed surface area of the buffering material, it can also be linked to small holes or grills in a wall (like a ventilator) linked to another buffering source. It this kind of situation the present model of buffering will be a better representation of the state rather than expressing buffering buffer value in terms of per square meter area.

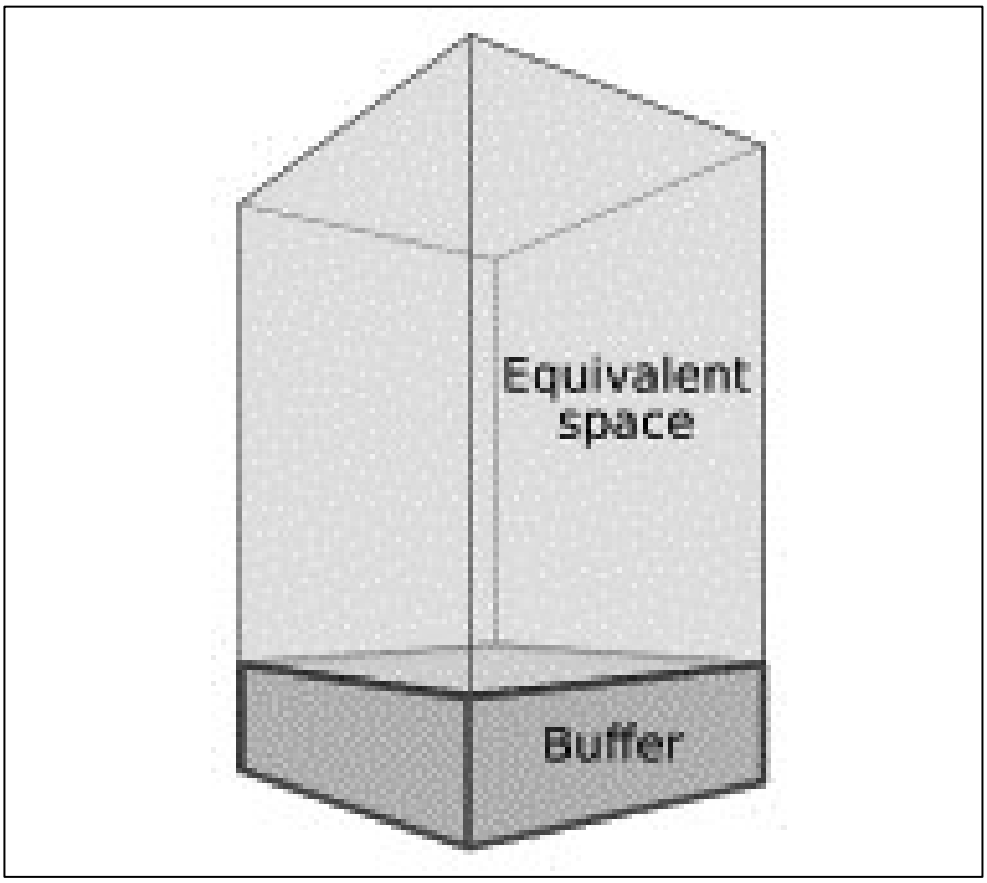


**Figure 3.11: Moisture buffering Equivalent volume (Padfield and Jensen, 2009).**

### *3.4.6 The Japanese Standard and the Nordtest method*

The Japanese Industrial Standard (JIS) is in many ways similar to the Nordtest protocol and is the first protocol to be published as a standard. The main difference between these two methods lies in the details like the selection of depth of the samples, creating distinction between step signal and square wave signal, selecting the period, peak and trough of humidity cycles and also in the way surface film moisture resistance is controlled during the experiment.

In Japanese method, a material is exposed to high humidity for 24 hours and low humidity for 24 hours in each 48-hour cycle. There are three levels of high-low humidity considered: 33%-43%, 53%-75%, 75%-93%. The depth of the sample is equal to the depth of the available product.

A sensitivity analysis has been carried out by Roels and Janssen (2006) to find how these variations affect the result of moisture buffer value in the two broadly similar techniques. Both tests were carried out through numerical simulations for wood fibreboard (WFB), plywood (PW), gypsum plaster (GP) and aerated cellular concrete (ACC). These materials had varying moisture penetration depth. It was found that 1/e (27%) penetration depth was more suitable and feasible for the test than 1% (as recommended by Nordtest). It was also found that the buffering values obtained by JIS were higher than the buffering values obtained by Nordtest method by factor of 1.5. Exceptions were observed when moisture penetration depth was less than 1/e (observed for ACC and GP) and similar MBVs were found during both the tests. Both materials reached their EMC in both testes and therefore provided similar results.

JIS recommended a surface film resistance of $4.8*10^7$ ± 10% m²sPa/kg during the test, meaning that the velocity of air around the surface has to be adjusted to this value. The Nordtest tests method recommends normal interior air velocity of 0.1 ± 0.05 m/s around the specimen surface that corresponds to a surface film resistance of $5.0*10^7$ m²sPa/kg. Roels and Janssen (2006) have found that variation of MBV value between materials can change when the surface film resistance of the materials are changed. They also observed that since both methods for buffering engage long periods of high and low relative humidity exposures, Nordtest method using relatively shorter cycle, the results do not

necessarily represent the real life situation where relative humidity can vary within a shorter period.

### *3.5* Water absorption coefficient

Mass transfer in a porous material at more than 95% relative humidity is governed by liquid transport. When a porous material is in direct contact with liquid water, water will be absorbed by the free water surface into the material by capillary forces. When the contact is removed, water can be redistributed in the material. The amount of water absorbed is proportionate to the square root of time. The water absorption coefficient or 'A' value is thus expressed as the ratio of water flux through the free water surface and the square root of time and is determined by a one-directional free water intake test.

In the absence of any further standardised methods for liquid absorption and redistribution, the 'A' value is presently indicative of the liquid transport performance of a porous material. Materials with higher water absorption coefficient can effectively manage liquid water in situations such as direct exposure to driving rain, surface diffusion, etc.

### *3.6* Vapour permeability and vapour diffusion resistance factor

Moisture transfer occurs through porous materials when there is vapour pressure differential between two opposite surfaces. Fick's law (Hens, 2007) expresses isothermal moisture transfer through the following equation:

$$g_v = -\delta . \nabla \rho_v \qquad [3.39]$$

Where, $g_v$ = vapour/ moisture flux (kg/m$^2$.s), δ =Vapour permeability of the porous system in the material (Kg/m.s.Pa), $\rho_v$ = Water vapour partial pressure (Pa).

Vapour diffusion resistance factor is introduced by Krischer (Hens, 2007) as an alternative for determining diffusion characteristic of a porous material on the basis that vapour flow rate through a unit surface of air is always higher than that through a unit surface of a porous material. The equation for this is expressed as:

$$\mu = \frac{\delta_a}{\delta} \qquad [3.40]$$

Where, μ = Vapour diffusion resistance factor (-), $\delta_a$ =Vapour permeability of air (Kg/m.s.Pa).

In hygroscopic materials, vapour diffusion is friction diffusion or Knudsen diffusion rather than pure diffusion. The diffusion equation is expressed in terms of vapour diffusion resistance factor as follows:

$$g_v = \frac{\delta_a}{\mu} . \nabla \rho_v \qquad [3.41]$$

Vapour transmission property is also expressed in terms of the thickness of a motionless air layer, which has the same water vapour resistance as the test specimen and expressed as the water vapour diffusion equivalent air-layer thickness ($S_d$ Value). $S_d$ is expressed in meters by the following equation:

$$S_d = \mu . d \qquad [3.42]$$

Where d is the thickness of the sample (m).

Vapour diffusion resistance factors of materials depends on the following characteristics of the pore system (Hens, 2007):

- Open pore area for each unit surface of the material. Increasing open pore area decreases vapour resistance factor and vice versa.
- The path length or the average distance the diffusing molecules have to travel in the pores compared to the thickness of the layer.
- Relative humidity of the pores in hygroscopic building materials.
- At high relative humidity, water transfer in the adsorbed water layers and pores filled with capillary water can influence vapour diffusion.
- Diffusion length can be shortened at high relative humidity as moisture travels from water islet to water islet.

Vapour diffusion resistance factor is also expressed as the ratio between tortuosity or the deviousness of the pore system (Figure 3.12) and total open porosity as show in equation 3.43.

$$\mu = \frac{\psi_1}{\psi_0} \qquad [3.43]$$

Where $\psi_1$ (-) is tortuosity of the material and $\psi_o$ (-) is open porosity.

The fibre orientation in the insulation matrix is stochastic, resulting in varying path length, tortuosity and local porosity. For this reason, large standard deviations can occur during measuring vapour diffusion resistance factor of fibrous insulation, which is shown in chapter six.

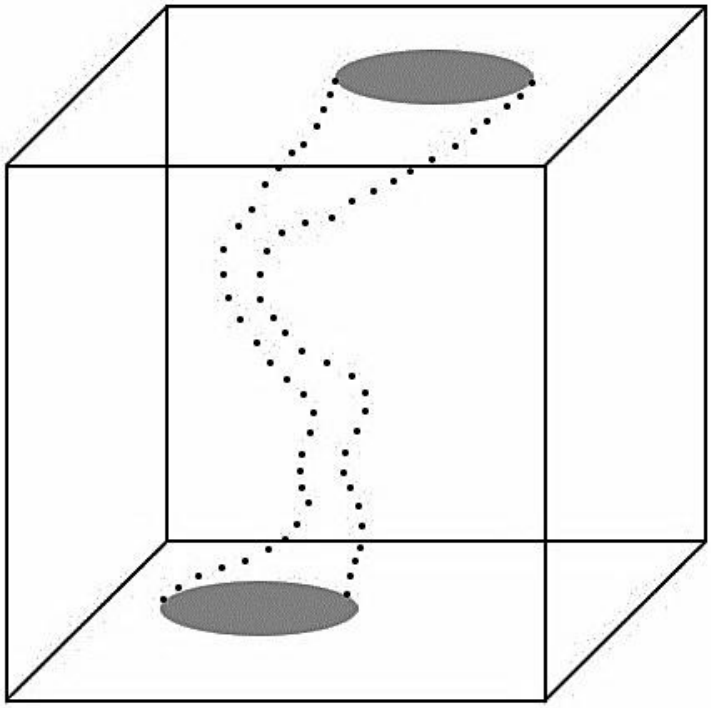

**Figure 3.12: Tortuosity (Hens, 2007).**

### 3.7 Prediction of mould growth

The likelihood of germination and the growth of mould and other microorganisms on a surface depends on the combination of temperature, moisture, substrate type, exposure time and the type of species (Viitanen *et al*., 2010). Among the parametric models, IEA-Annex 14 (1991) provides a simplified approach to predicting mould spore germination where conditions on the surface of a material meet certain relative humidity-exposure time criteria, as shown in Table 3.1.

**Table 3.1: Mould spore germination conditions in IEA-Annex 14.**

| Relative humidity | Exposure time (day) |
|---|---|
| 99% | 1 |
| 89% | 7 |
| 80% | 30 |

Isopleths are developed based on stationary laboratory experiments. Simplified isopleth curves take only temperature and relative humidity into account such as the one developed by Hens (Vereecken and Roels, 2012). The comprehensive isopleth curves can include all the following variables: temperature, relative humidity, exposure time and substrate type such as the one developed by Sedlbauer (Sedlbauer, Krus, and Breuer, 2003). Figure 3.13 shows the germination isopleths developed by Sedlbauer incorporating the 'Lowest Isopleth for Mould' for substrate class 1 or biodegradable substrates (LIM I).

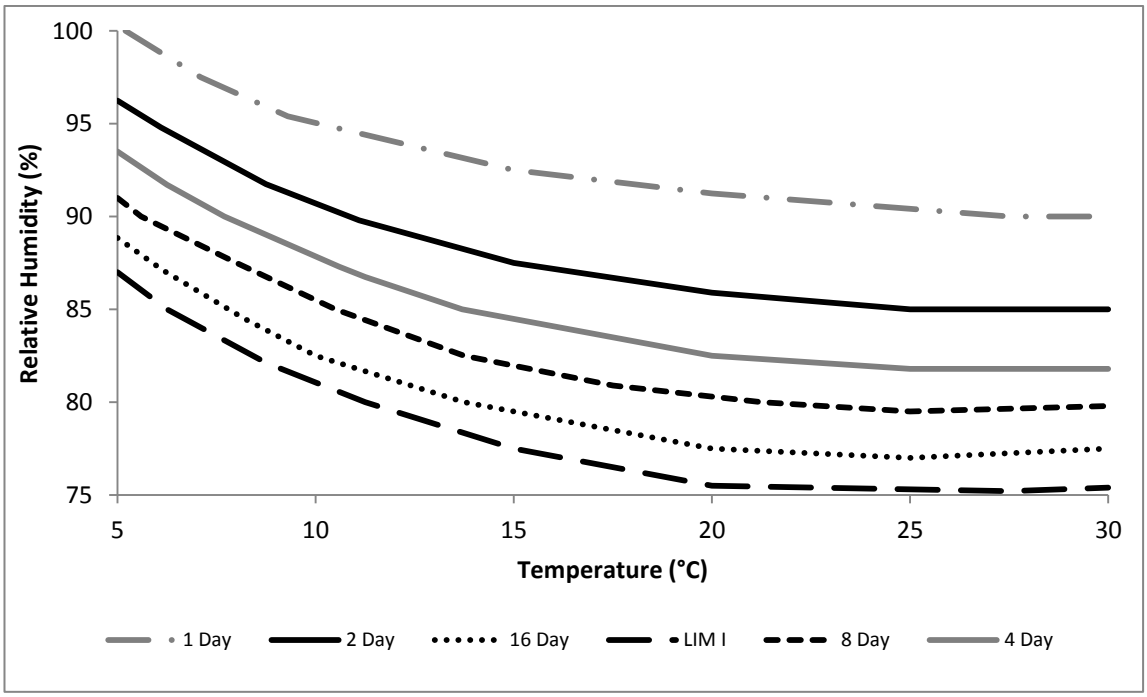


**Figure 3.13: Sedlbauer's isopleth system for substrate class I (Vereecken, 2012).**

The 'Lowest Isopleth for Mould' (LIM) curves are developed by analysing the combined growth conditions of all fungal species and thus represent worst-case scenario for mould spore germination. Mould growth is plausible when the

hygrothermal condition of a bio-based material is above the LIM 1 isopleth. As for the other isopleth lines, to predict mould growth, the hygrothermal conditions have to sustain for the period of time designated to those isopleth lines.

WUFI-Bio is a biohygrothermal modelling tool for predicting spore germination and mould growth rate based on relative humidity, temperature, exposure time and substrate type (Sedlbauer, Krus, and Breuer, 2003). Both spore germination isopleth and mould growth isopleths are used for predictions. Relevant data can be imported from WUFI results as input for WUFI-Bio. The result is presented in terms of mould growth rate. When mould growth rate is below 50 mm/year, a green signal light is provided representing an acceptable condition. When growth rate is between 50 mm/year and 200 mm/year, yellow signal light is shown to represent a situation where further assessment is required for acceptability. When the growth rate is more than 200 mm/year, a red signal is shown to represent a usually unacceptable condition.

### 3.8 Chapter summary

Theoretical aspects of thermal conductivity, adsorption-desorption, moisture buffering and mould growth have been discussed in this chapter. The steady state measurement method for moisture dependent thermal conductivity does not seem to be fully reliable. Due to the strong adsorption capacity of bio-based insulations, heat flux is also influenced by the heat of wetting and the phase of water at various EMCs, therefore experimental and in situ measurements are required to develop a better understanding of the heat flux through bio-based insulations like hemp. The adsorption-desorption capacity and the rate of adsorption-desorption contribute to the moisture buffering capacity of hygroscopic materials. Bio-insulations have unique capabilities of adsorbing moisture through hydroxyl bonding by cellulose, hemicellulose and pectin up to certain humidity ranges. At those ranges, conventional approach to moisture dependent conductivity may not be fully valid. As far as in situ determination of thermal transmittance and thermal conductivity of hemp insulations are concerned a gap of knowledge exists which needs addressing.

Since adsorption-desorption are measured in the laboratory at few number of humidity points or EMCs, one or more of the experimentally developed isotherm equations are required to find the intermediate ranges. For bio-insulations, GAB

and Hailwood and Horrobin models seem to be most the representative among the isotherm equations.

Moisture buffering capacities of bio-insulations are most important in lessening the occurrence of surface and interstitial condensations and maintaining a steady humidity in the interior. However, no published work is available on the moisture buffering values of hemp insulations. There is therefore a clear need of experimental assessment of moisture buffering values of hemp insulations.

Mould growth is a very important concern with bio-based insulations. Bio-based insulations like hemp contain nutrients for fungi. Experimental and numerical studies are required to study the germination of spore and growth of mould in the bio-based insulations like hemp. Sedlbauer's isopleth and WUFI-Bio are two important parametric and numerical tools in this respect.

# Chapter 4

# Research Methodology: Materials, Equipment, Test Methods and Numerical Simulation Software

## 4.1 Introduction

This chapter provides a description of the selected thermal insulation materials and an outline of the methods used in this thesis to determine the hygrothermal properties of the selected insulation materials. The following definitions of research methodology and research method are used in this chapter:

**Research methodology:** A research methodology is usually a guideline system for solving a problem, with specific components such as phases, tasks, methods, techniques and tools (Berg, 2009). Research methodologies are broadly classified as qualitative and quantitative (Nyame-Asiamah and Patel, 2009).

**Research method:** A research method is a technique for collecting data (Bryman, 2008). Some examples of research methods for quantitative research are experimental method, field experiment and numerical modelling.

In line with the aforementioned definitions, the main methodology for the present research is a quantitative one. The only exception in the present research is the qualitative judgement during the comparison of the moisture content of two hemp insulations in chapter 7. The research methods used for data collection and analysis are described in section 4.3 while section 4.4 provides a brief description of the material properties of the insulation materials used during the course of the present research.

## 4.2 The methodological philosophy

The objectives of the research are to determine the heat and moisture management capacity of hemp insulations and to compare the findings with those of conventional thermal insulation materials. By achieving these

objectives, the hygrothermal performance of hemp insulations can be put in the broader context of the hygrothermal performance of the mainstream thermal insulation materials.

To achieve the aforementioned research objectives, the following two research methods have been applied: experimental research and numerical simulation. Experimental research included laboratory based experiments and in situ experiments. Laboratory based experiments are essential to conduct standard steady state tests to determine the steady state hygric and thermal properties of hemp insulation at material level. Steady state tests serve two purposes. Firstly, the results for different materials are comparable in terms of steady state hygrothermal boundary conditions and secondly, the material data are required as input for numerical hygrothermal simulations using a piece of software. However, steady state tests do not necessarily represent the hygric and thermal response of insulations in dynamic boundary conditions for materials with variable heat and moisture management capacities. Consequently, laboratory based experiments also include experiments conducted in dynamic and quasi steady state hygrothermal boundary conditions.

The difference between the predicted and monitored performance of a building in terms of energy use is a widely discussed issue. Energy use in buildings designed with similar thermal comfort criteria can vary due to the hygrothermal performance of the building materials and the energy efficiency of the building service equipment. The discrepancy between the predicted and measured energy use in a building may imply that the hygrothermal performance of thermal insulation materials determined by laboratory tests may not always reflect the hygrothermal performance of the insulations during service conditions. For this reason, despite laboratory based experiments providing valuable data on the hygothermal properties of the insulations at material level, in situ experiments are useful in terms of determining the hygrothermal behaviour of the insulation as system level in service conditions. In the present research, in situ experiments have been carried out on timber frame wall panels incorporating hemp and stone wool insulations.

Numerical simulation has also been used in this research as it was not possible to carry out laboratory based or in situ experiments of various building

envelopes due to the constraint of time and resources. It is important to determine the long-term hygrothermal performance of the insulation materials as it influences the whole life energy use of the buildings. With this aim, initial simulations have been carried out to study the hygrothermal performance of the insulations for a 10-year period. However, it is not necessary to analyse 10-year data if equilibrium is reached earlier in terms of the hygrothermal response of the building envelope. It was found that this equilibrium was reached during the third year in most of the cases. For this reason, the third year data are analysed during the majority of the numerical simulations.

The data obtained through laboratory based experiments, in situ experiments and numerical simulations complement each other in terms of acquiring comprehensive knowledge of the hygrothermal performance of hemp insulation and thus provide more confidence in the research findings and the characterisation of such performance. Figure 4.1 shows the aforesaid research methods and their relationship to the broader research findings.

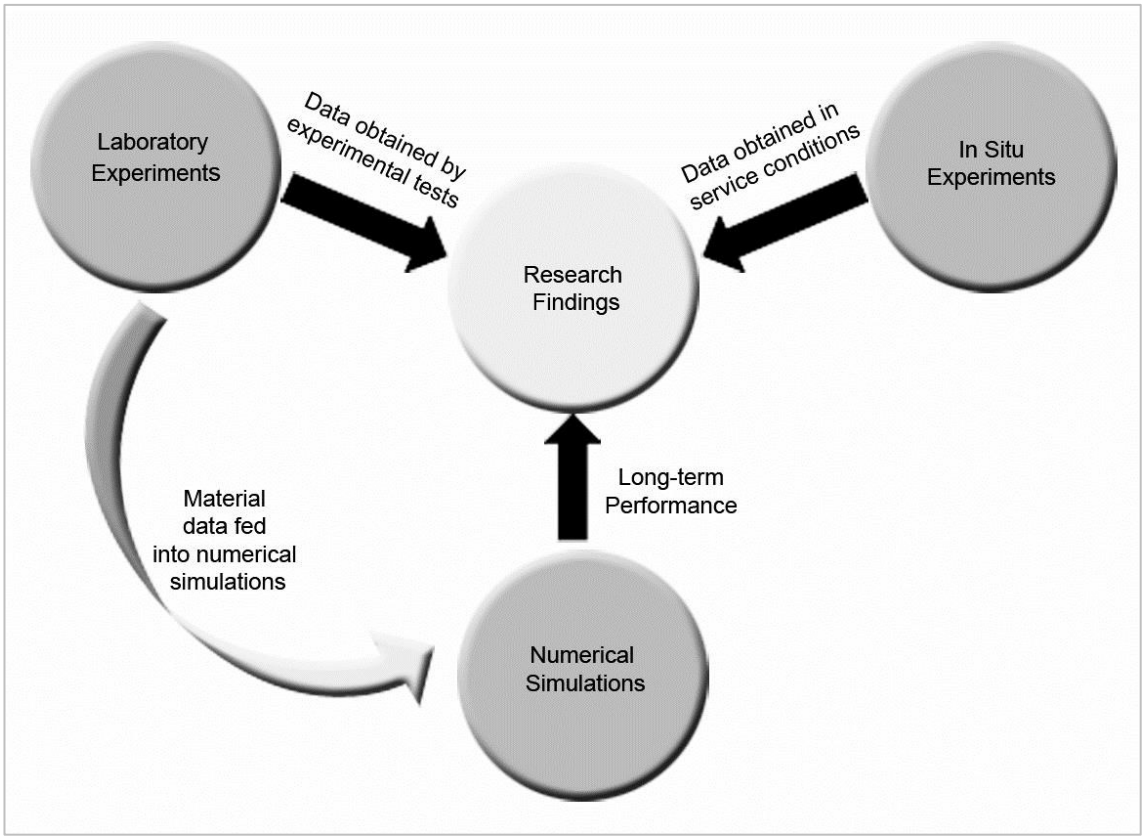


**Figure 4.1: The research methods and their relationship.**

## 4.3 Outline of the research methods

The methodological approach to the present research is quantitative one. The research methods used to obtain data are experimental and numerical methods. These methods are selected to support the objectives of determining the heat, moisture and mould management capacities of hemp insulations, as outlined in section 1.3 of chapter one.

The quantitative assessments of hygrothermal properties of the selected insulations are carried out at two levels: material level and system level. In this thesis, the material level and the system level in relation to the selected thermal insulations are described as follows:

**Material level:** At the material level, the experimental test is conducted on the insulation material at a given boundary condition. The insulation material is characterised in terms of hygric and thermal properties.

**System level:** At the system level, the insulation material is part of the thermal envelope of the building or part of a system representing the thermal envelope in the laboratory. The hygric and thermal properties of any thermal insulation material for any given boundary condition are determined thorough experimental and numerical methods.

Different quantitative methods have been used for the determination of different steady state and dynamic hygrothermal properties of the selected insulations. Data are analysed following the guidelines provided by the British Standards, and ISOs for the respective methods. The Statistical Package for the Social Sciences (SPSS) has been used as the statistical analysis tool to determine standard deviations and Microsoft Excel has been used to determine regressions and correlations. In this chapter a brief outline of the employed methods is presented. The experimental and numerical methods are described in detail in the corresponding chapters on experimental tests and numerical simulations.

### *4.3.1 The material level and the research methods*

Assessments of hygrothermal properties at material level are done by laboratory-based experiments. Most of the steady state experimental methods are described in the British Standards. Material data derived from the

experiments are used in two ways. Firstly, the data of the hygric and thermal properties of selected materials are individually analysed and compared to rank their performances. Secondly, these data are used as input data in numerical hygrothermal simulation software to determine the combined impact of the hygrothermal properties, represented by these data, on the insulation materials in dynamic hygrothermal conditions at system level. The determination of the following hygrothermal properties is carried out:

- Adsorption-desorption isotherm
- Vapour diffusion resistance factor (μ Value)
- Water absorption coefficient (A value)
- Moisture buffer value
- Thermal conductivity: Isomet heat transfer analyser
- Thermal conductivity: Fox 600 hot plate

The individual methods for aforementioned experimental tests are described in chapter five and Appendices A, B and I.

### *4.3.2 The system level and the research methods*

System level assessments are done by laboratory-based experiments, in situ experiments and computer based numerical hygrothermal simulations. The followings system level tests were carried out:

- Dynamic experiments
- Quasi steady state experiments
- In situ experiments
- Numerical simulations

The methods for the system level tests are elaborated on in chapters five, six, seven and eight. Figure 4.2 shows the schematic diagram of the research methodology.

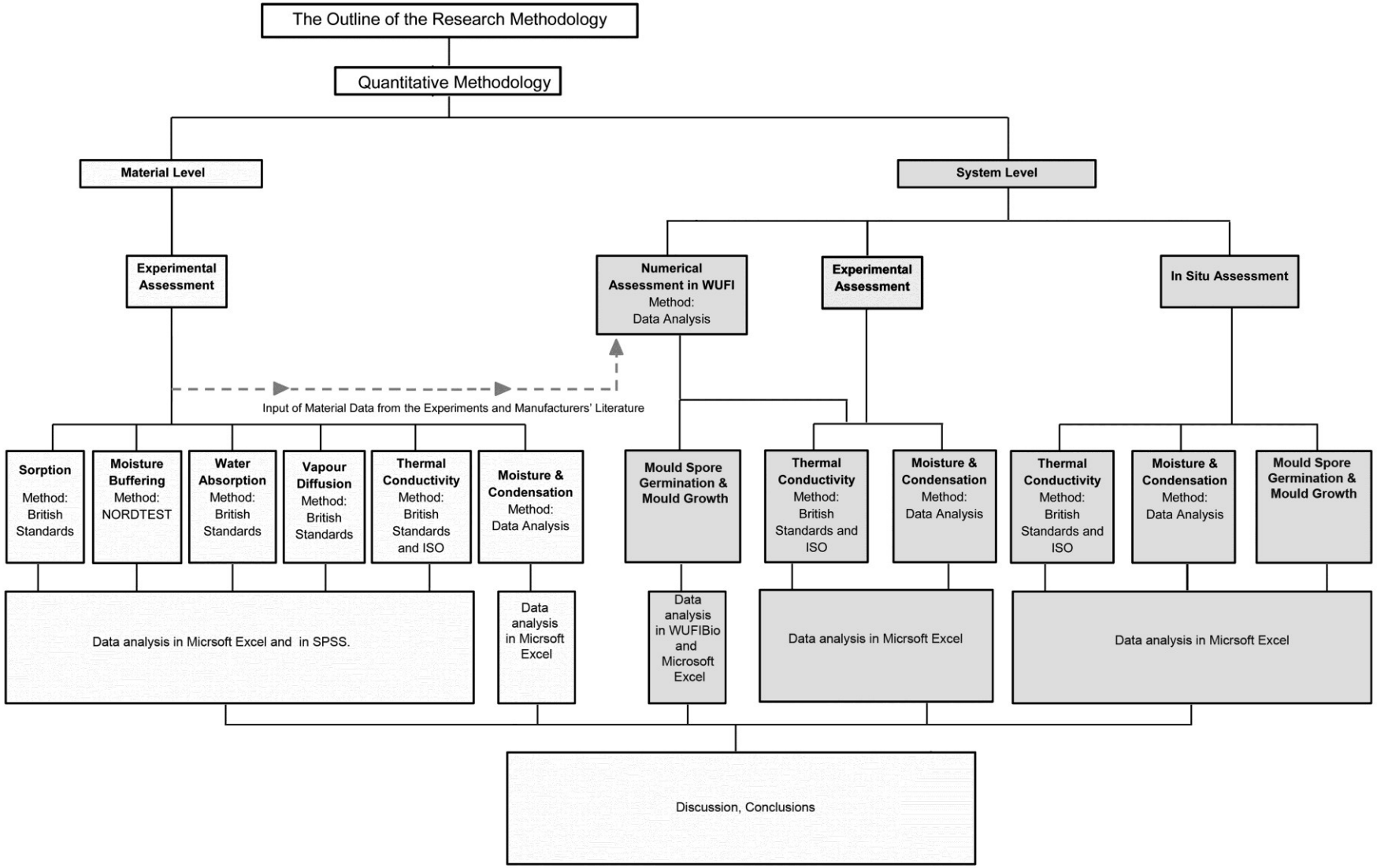


**Figure 4.2: Schematic diagram of the research methodology.**

## 4.4 Material selection

Based on the background and objectives of this research as described in chapter one and the literature review in chapter two, it is apparent that the investigations on the hygrothermal potential of bio-insulations in the UK need particular focus on the fibrous hemp insulations. This is due to the lack of adequate experimental and in situ research based knowledge of the hygrothermal performance of hemp insulations despite the enormous agricultural and manufacturing potential of this unique renewable non-food crop in the UK. Hemp insulations from five different manufacturers have been sourced from the UK market. The commercial names are replaced by the following names: hemp-1, hemp-2, hemp-3, hemp-4 and hemp-5 and their physical structure is shown in figure 4.4.

Figure 4.3 shows the material assessment pyramid which links the experiments to the insulations used. It can be noticed that fewer types of insulations have been used in system level test than in material level test.

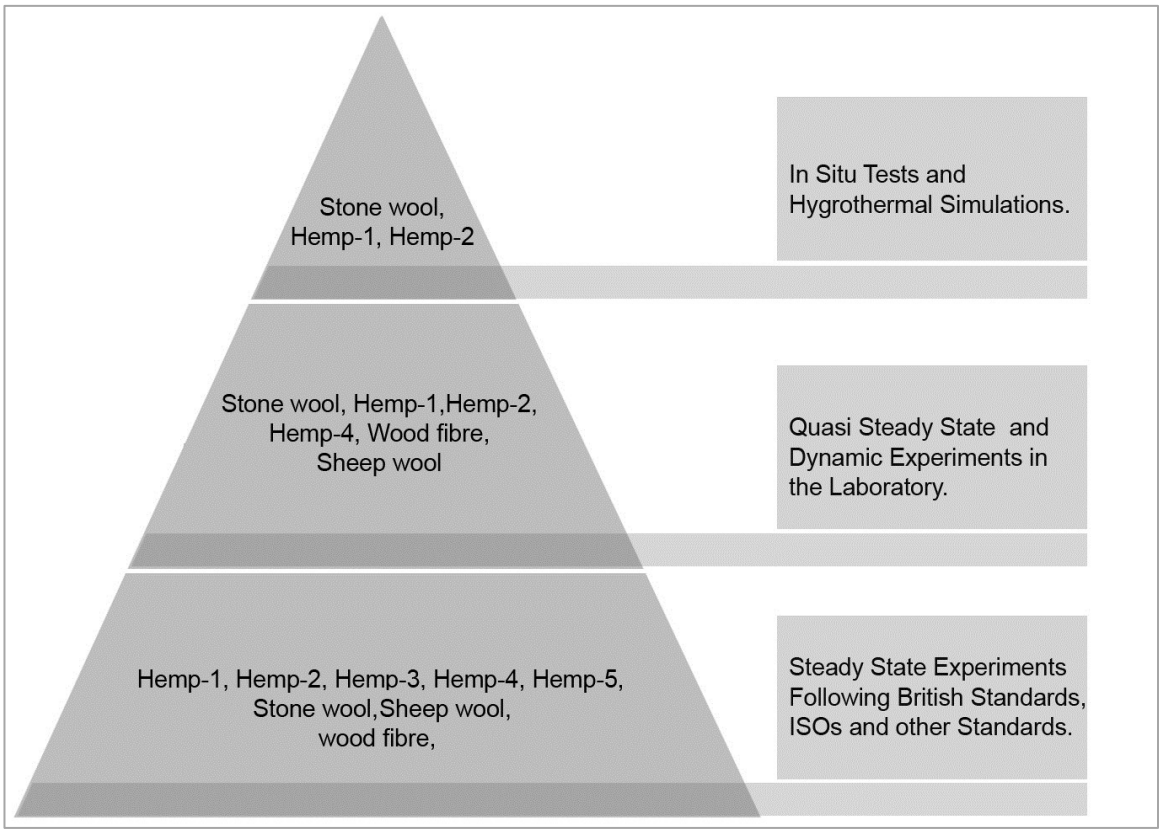


**Figure 4.3: Material assessment pyramid.**

The key reasons for using fewer types of insulations during the system level tests are:

- The system level tests are time and resource engaging
- In situ system level tests are particularly resource engaging in terms of installation of construction materials and monitoring devices
- Given the constraint of time, it is more useful to gather reasonably adequate data on fewer number of materials for a longer time than gathering very limited data on more materials for a shorter time
- One of the key reasons for using more materials during the material level test is to use the material data as input into hygrothermal simulation software. When the data were examined, it was clear that among the hemp insulations, hemp-1, hemp-2 and hemp-4 could reasonably represent most of the hemp insulations. These insulations were selected for system level tests on the basis of their hygric and physical properties and their thermal conductivity values were nearly similar. In terms of physical structure, this selection included insulations with higher and lower hemp content and density. In terms of hygric properties, this selection included insulations with higher and lower moisture adsorption capacity and vapour diffusion resistance factor.

- It is assumed that selecting the insulations on the basis of the higher and lower extremes of their structural and hygric properties will provide the full range of their hygrothermal performance

Thus, hemp-1, hemp-2 hemp-4 insulations were selected for system level tests, in relation to laboratory-based experiments. Hemp-1 and hemp-2 was selected for in situ experiments and hemp-4 was not suitable for vertical installation during in situ tests. While particular attention is given to hemp insulations, the following insulations are also included at different stages of the research: stone wool, wood fibre and sheep wool insulations (Figures 4.5 to 4.7). This is to place the performance potential of hemp insulation within the broader context of the fibrous thermal insulations:

Figures 4.8 to 4.23 show the microscopic images of the selected insulations in order to visually compare the structure of the insulations. It can be noticed that, hemp fibres and wood fibres are mostly curvilinear shaped with uneven surfaces and the fibres have different diameters. This is because hemp and wood fibres contain fibres and fractions of shives and woody core. Hemp fibres

are also mixed with other fibres such as cotton. Additionally, these hygroscopic fibres exist as technical fibres (bundle of fibres) which may have different diameters.

On the contrary, stone wool fibres are with straight geometry compared to the natural fibres and the fibre diameters are uniform and consistent. The non-hygroscopic surfaces of stone wool fibres are also smoother than the surfaces of natural fibres. It can be observed in Figures 4.18 and 4.19 that the diameter of stone wool is about one-fourth of the diameter of hemp fibres as shown in Figures 4.8-4.17. Stone wool and glass fibres are considered respirable as the diameter of these fibres are less than 5 μm, with an aspect ratio of at least 3:1. For this reason, the National Toxicology Program (NTP) of USA considered these man-made fibres (MMF) as carcinogenic (NTP, 2010). Compared to glass and stone fibres, the diameter of hemp fibres ranges from 18 μm to 25 μm (Bocsa and Karus, 1998) and the diameter is much larger when fibres exist in fibre bundles. Thus, hemp fibres are not respirable.

A brief description of the selected insulation materials are provided in the following sub sections.

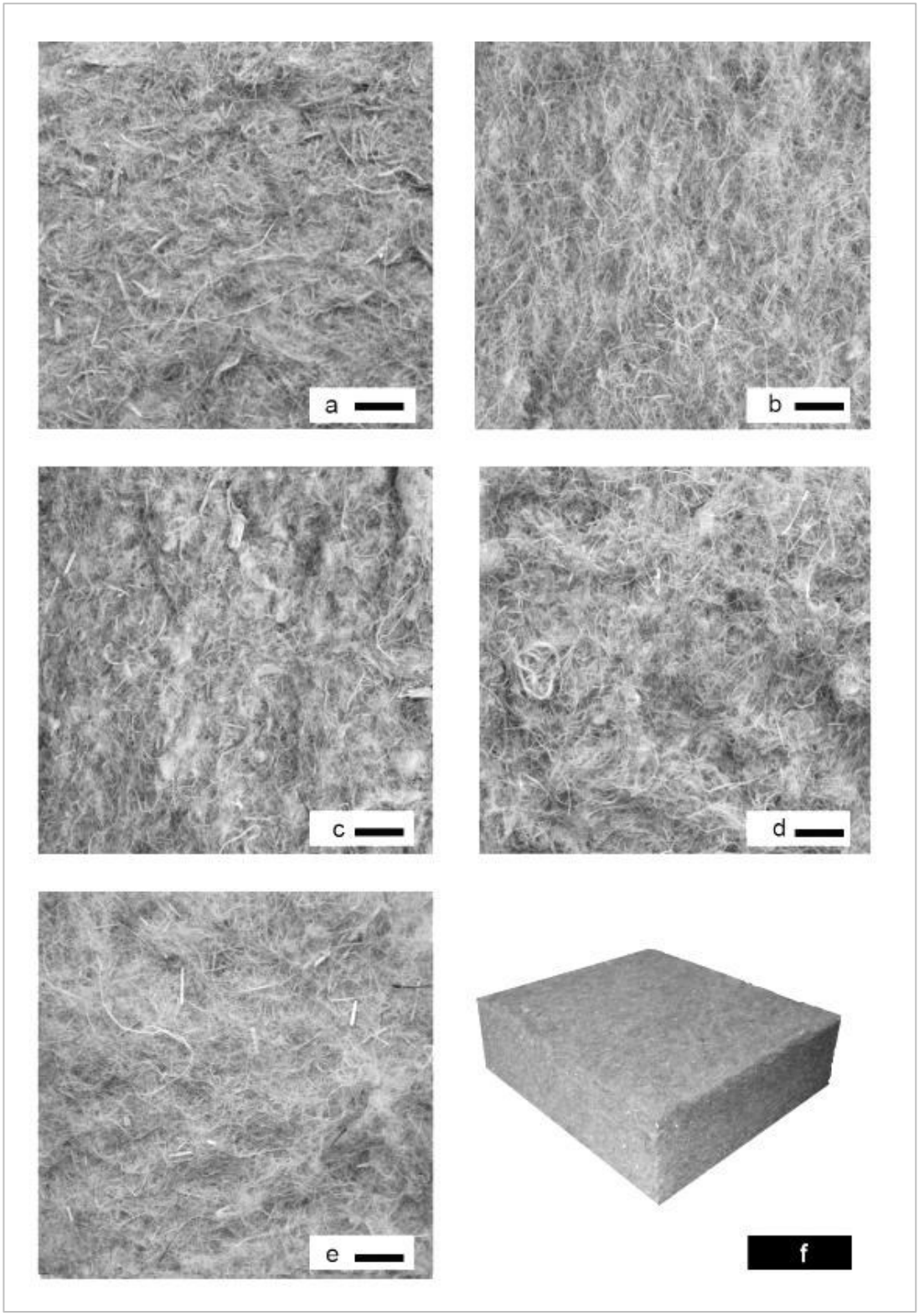


**Figure 4.4: Illustrations of hemp samples, (a) hemp-1, (b) hemp-2, (c) hemp-3, (d) hemp-4, (e) hemp-5, (f) perspective image of hemp-2. Scale bar: 1 cm.**

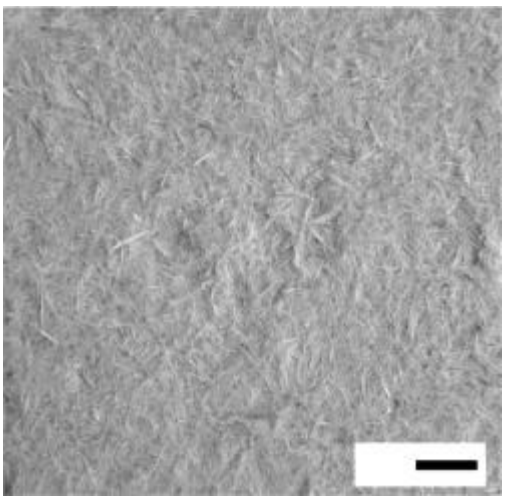

**Figure 4.5: Illustration of wood fibre insulation sample. Scale bar: 1 cm.**

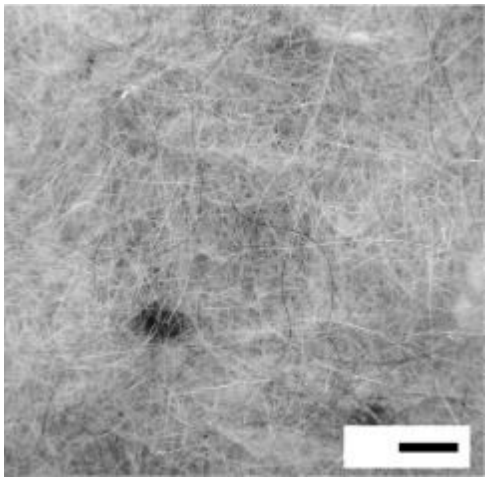

**Figure 4.6: Illustration of sheep wool insulation sample. Scale bar: 1 cm.**

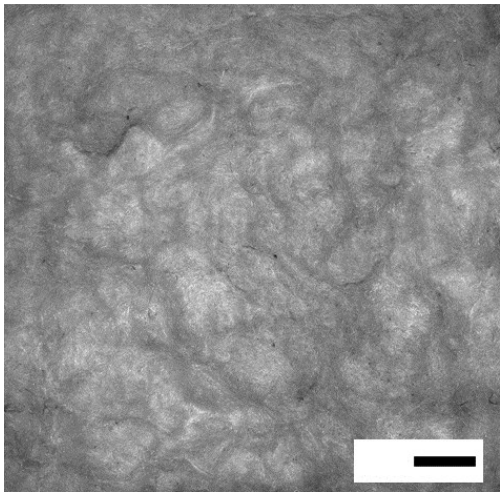

**Figure 4.7: Illustration of stone wool insulation sample. Scale bar: 1 cm.**

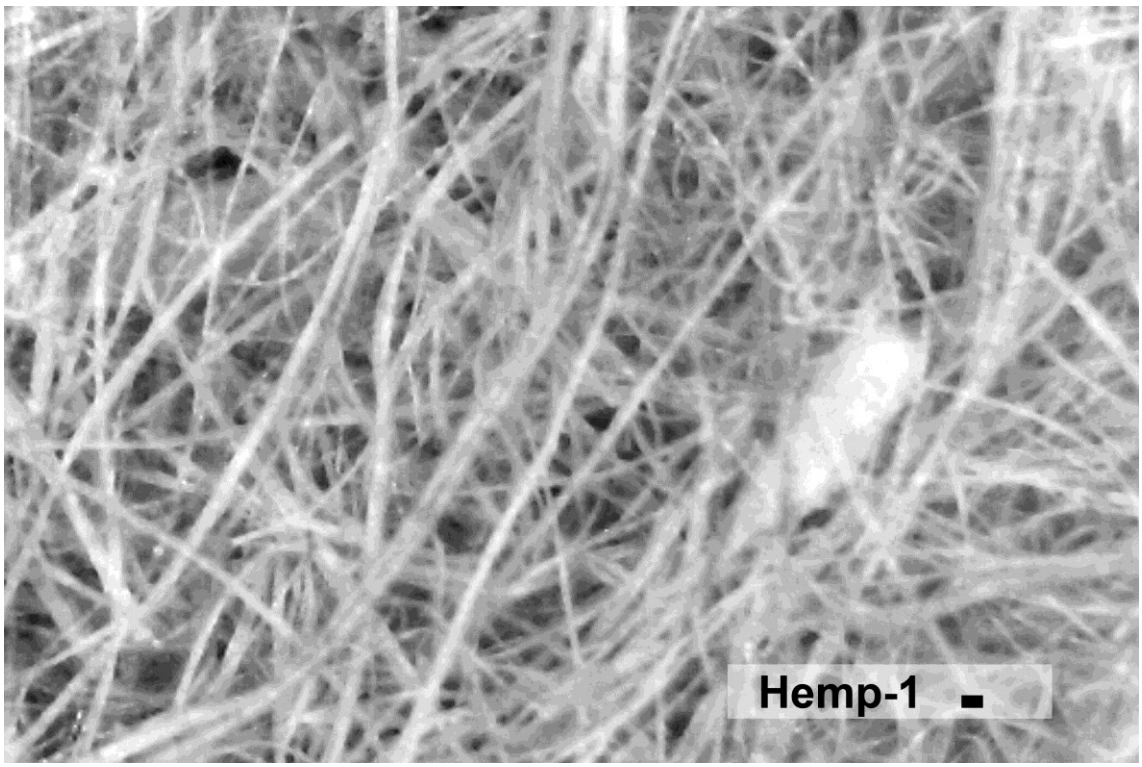


**Figure 4.8: Microscopic image of the sample of the hemp-1 insulation. Scale bar: 100 µm.**

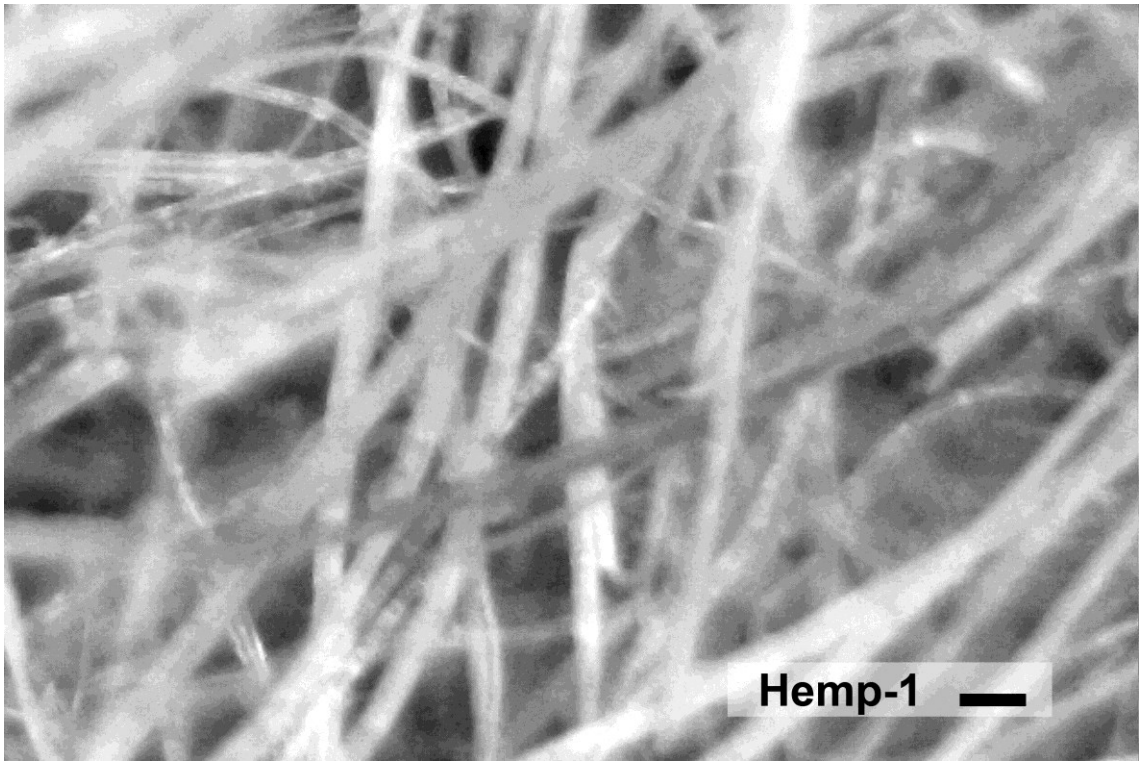


**Figure 4.9: Microscopic image of the sample of the hemp-1 insulation. Scale bar: 100 µm.**

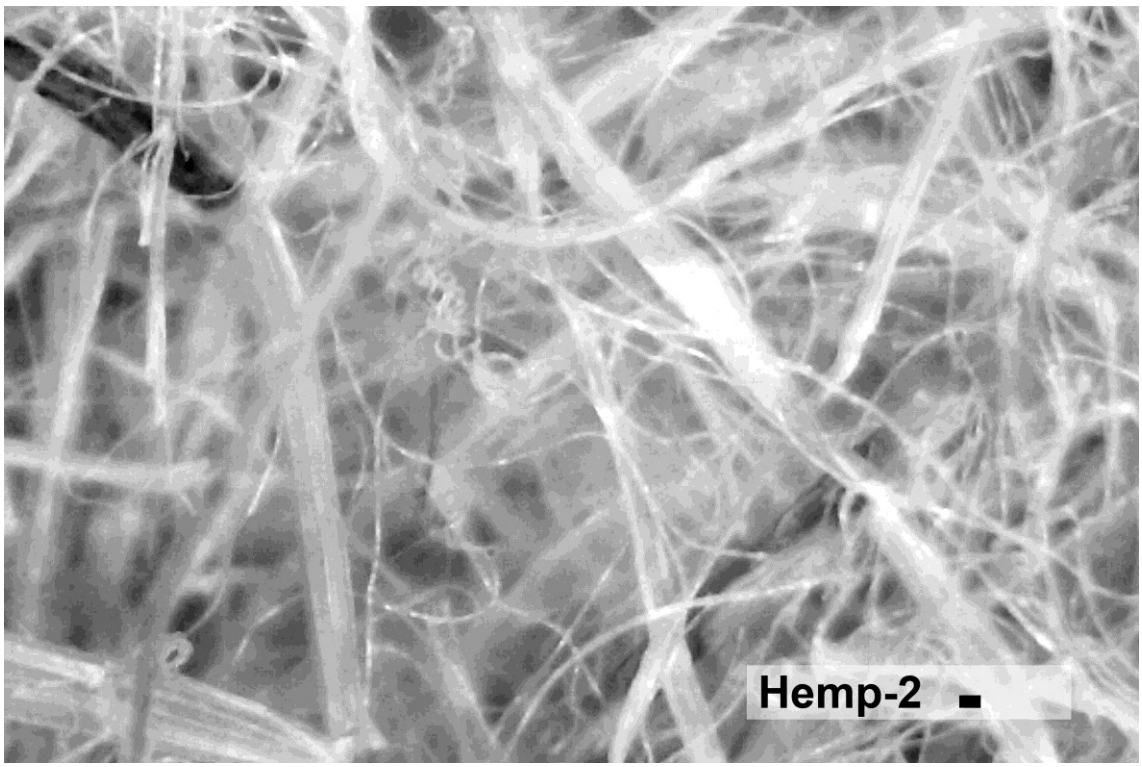


**Figure 4.10: Microscopic image of the sample of the hemp-2 insulation. Scale bar: 100 µm.**

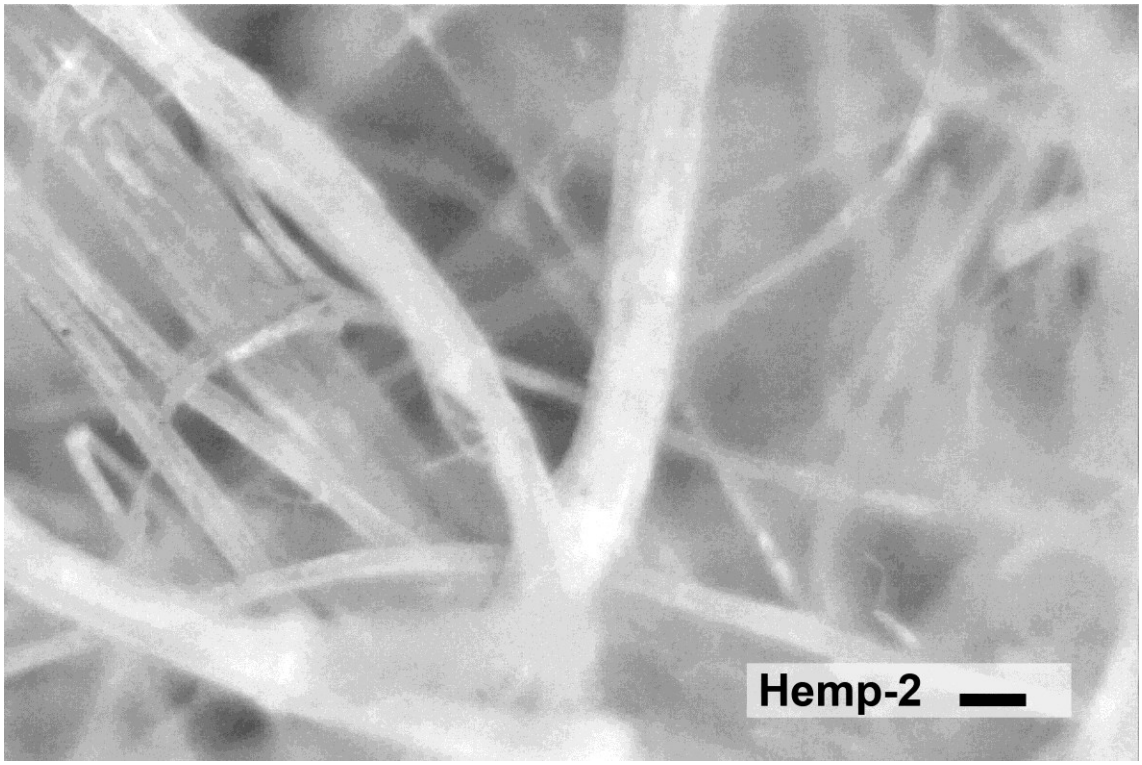


**Figure 4.11: Microscopic image of the sample of the hemp-2 insulation. Scale bar: 100 µm.**

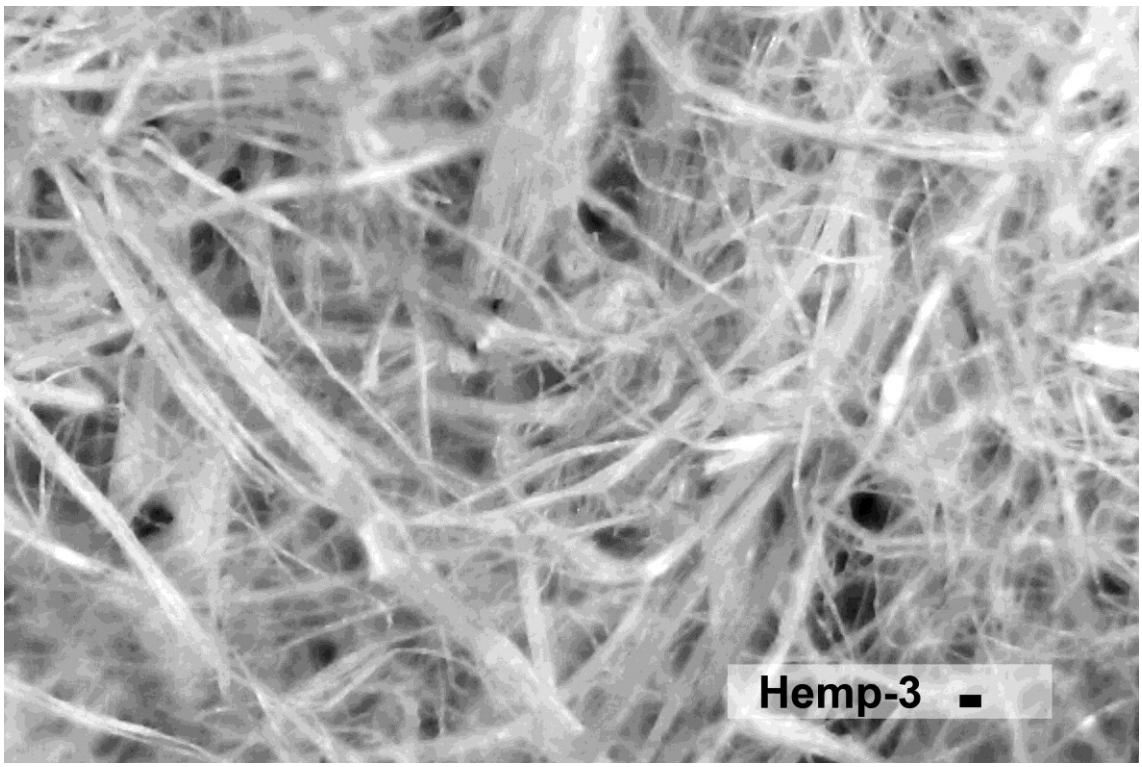


**Figure 4.12: Microscopic image of the sample of the hemp-3 insulation. Scale bar: 100 µm.**

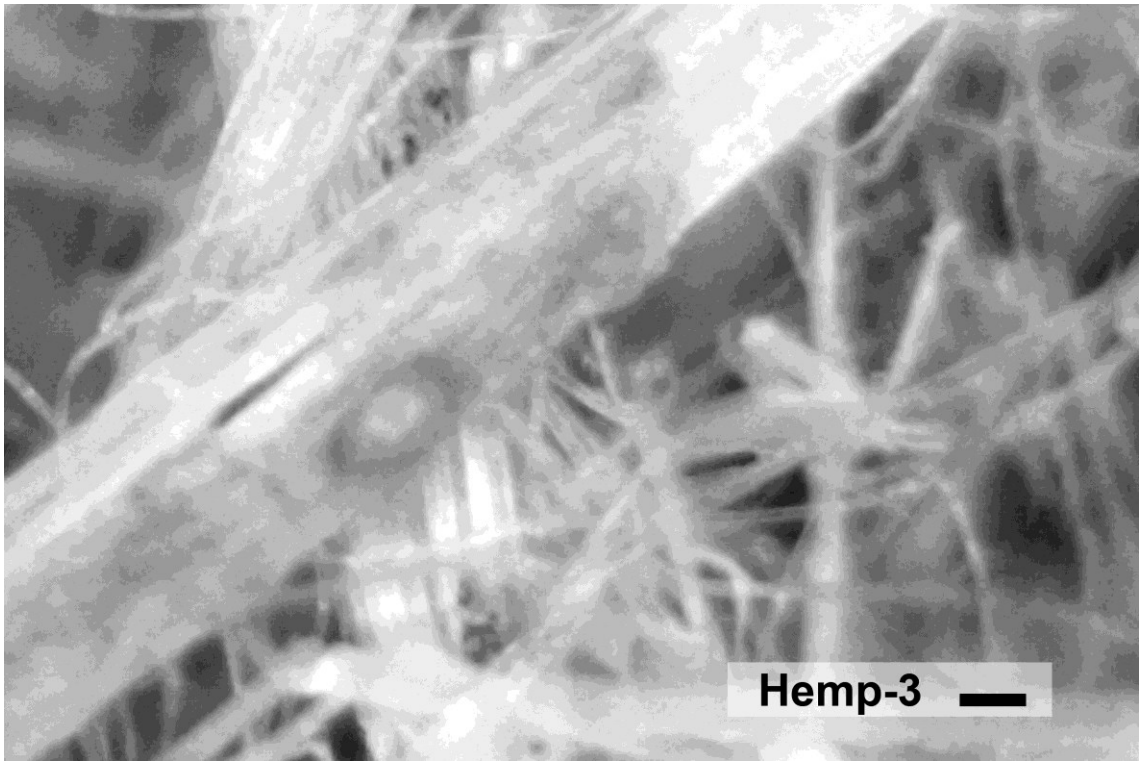


**Figure 4.13: Microscopic image of the sample of the hemp-3 insulation. Scale bar: 100 µm.**


**Figure 4.14: Microscopic image of the sample of the hemp-4 insulation. Scale bar: 100 µm.**

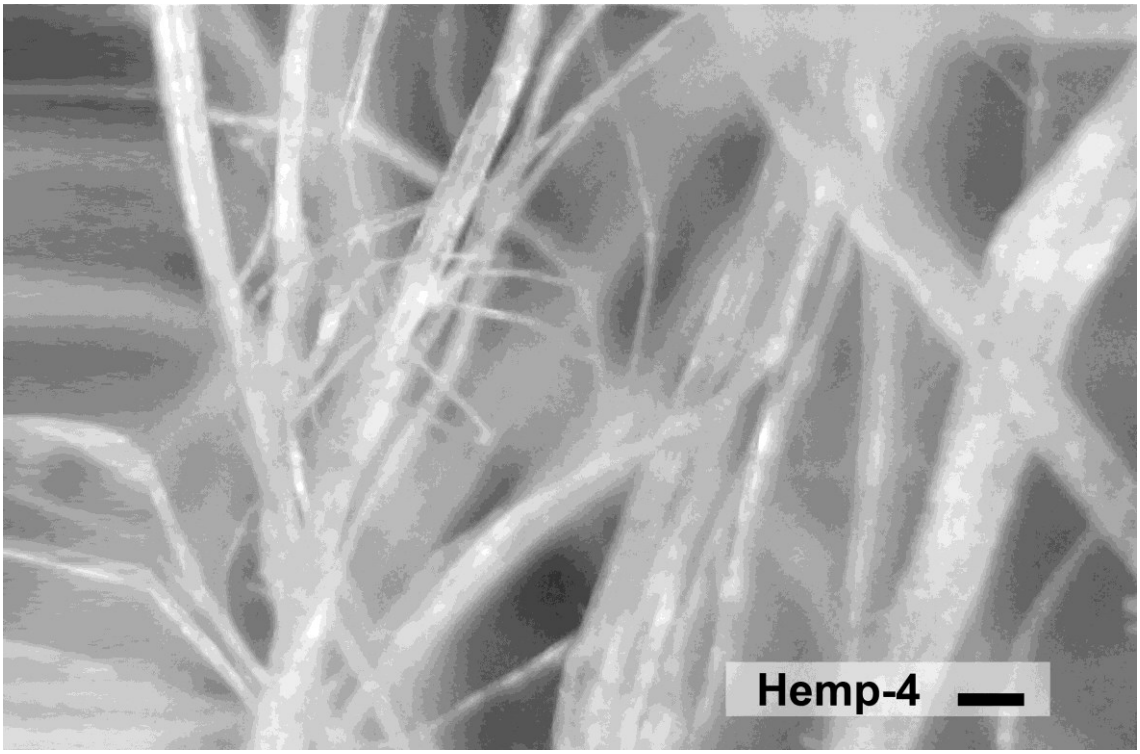


**Figure 4.15: Microscopic image of the sample of the hemp-4 insulation. Scale bar: 100 µm.**

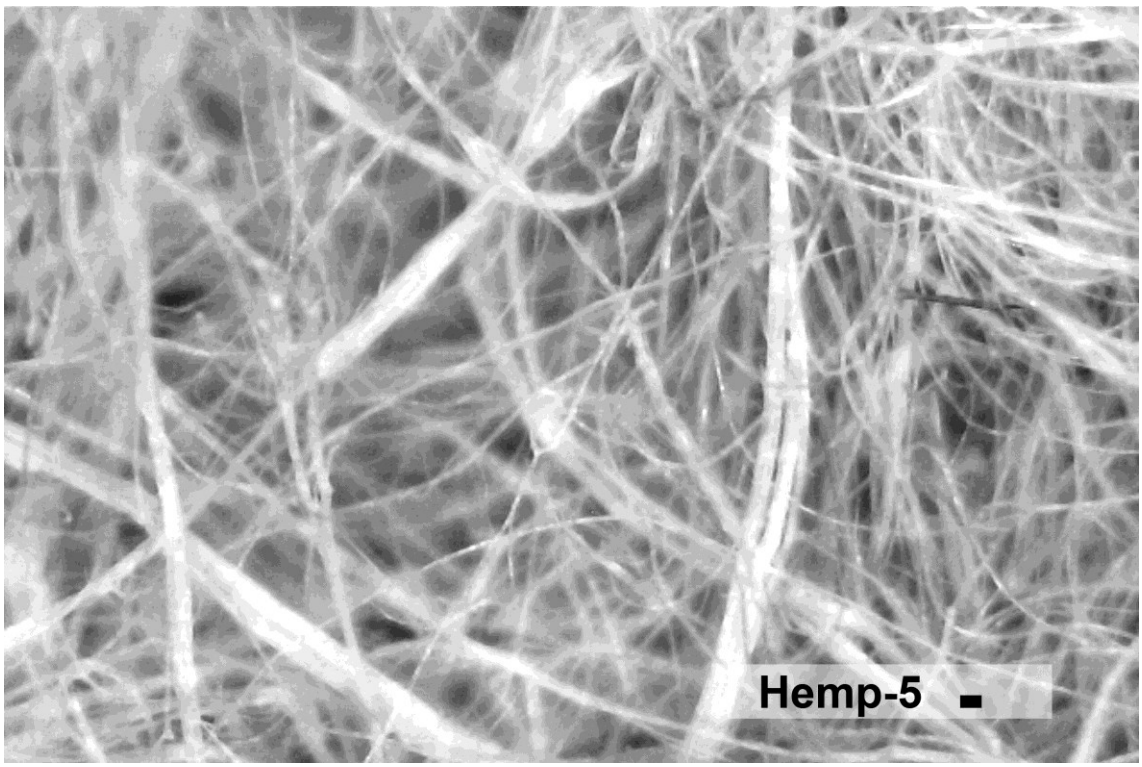


**Figure 4.16: Microscopic image of the sample of the hemp-5 insulation. Scale bar: 100 µm.**

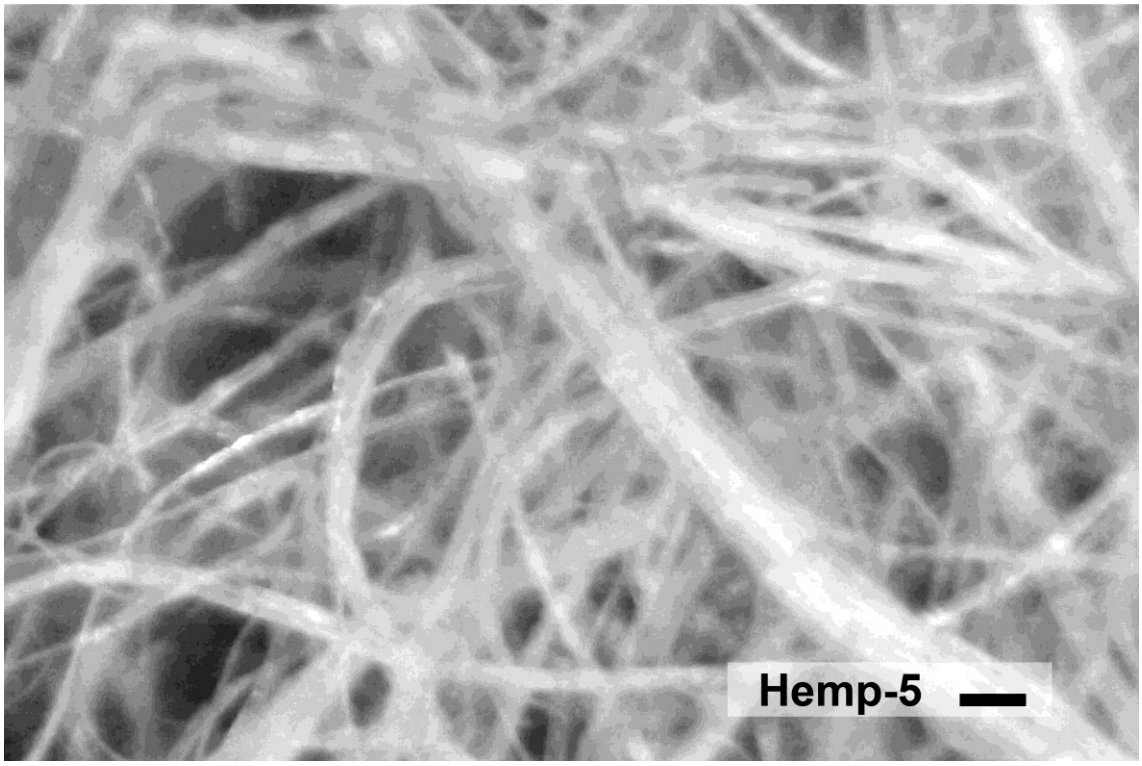


**Figure 4.17: Microscopic image of the sample of the hemp-5 insulation. Scale bar: 100 µm.**

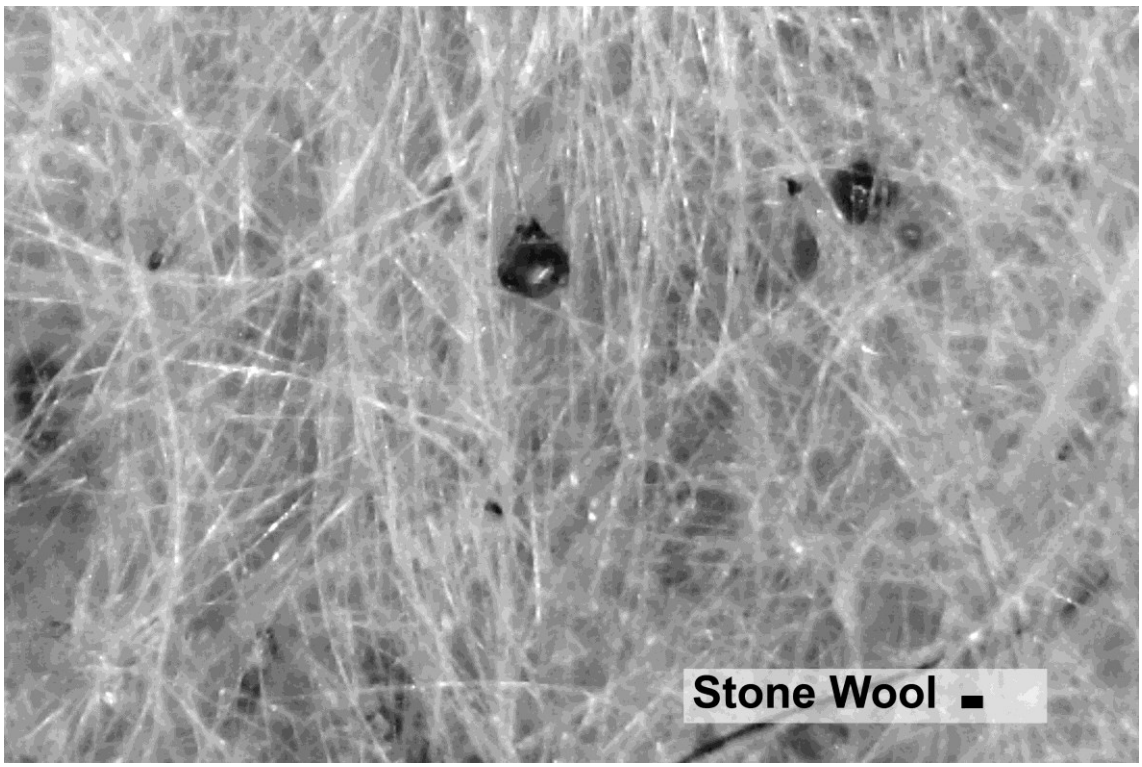


**Figure 4.18: Microscopic image of the sample of the stone wool insulation. Scale bar: 100 µm.**

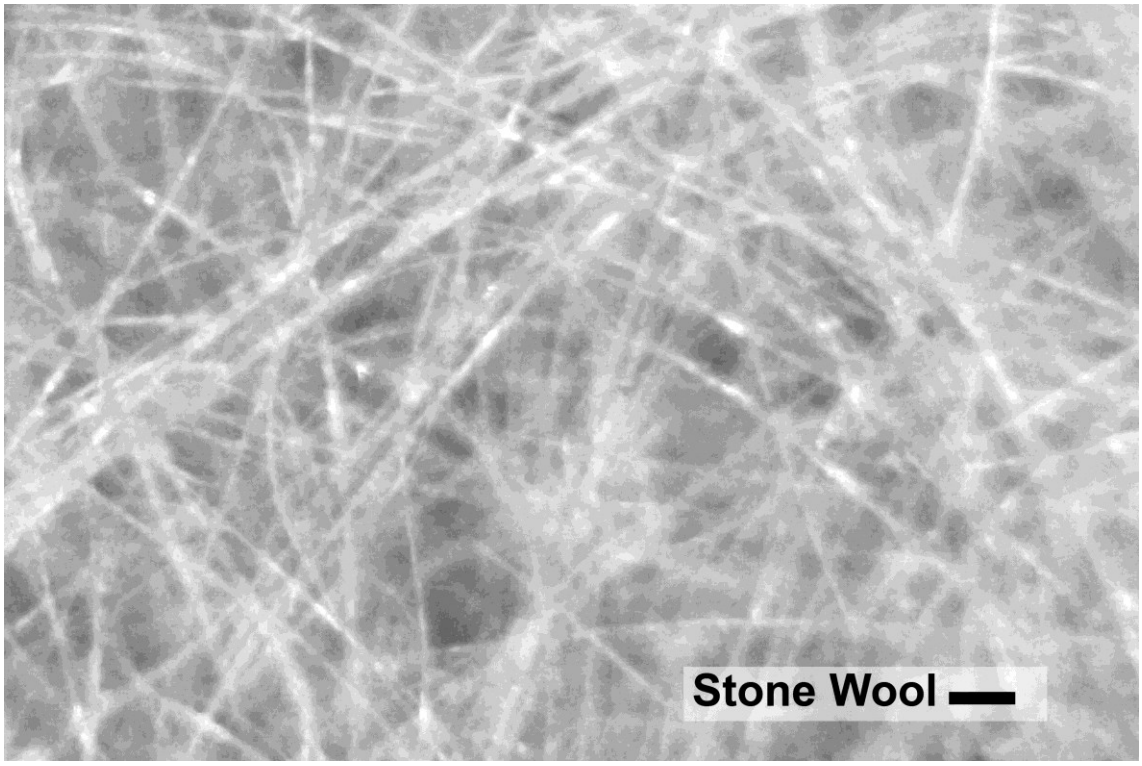


**Figure 4.19: Microscopic image of the sample of the stone wool insulation. Scale bar: 100 µm.**

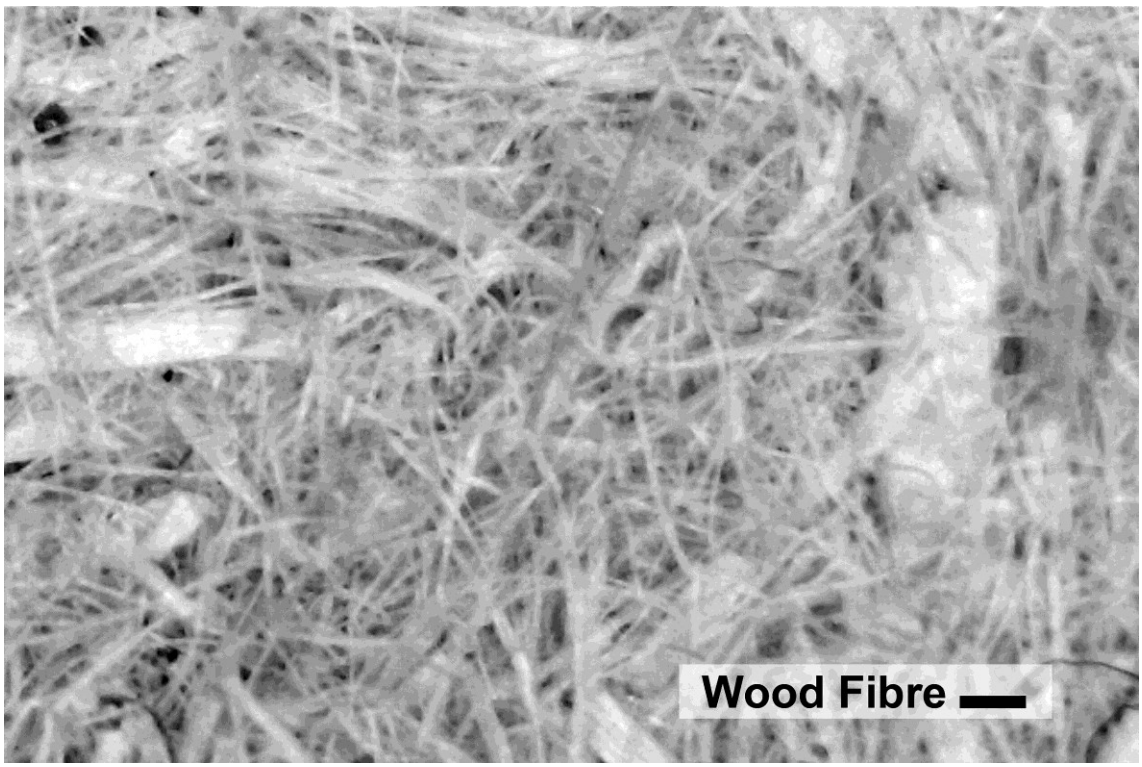


**Figure 4.20: Microscopic image of the sample of the wood fibre insulation. Scale bar: 100 µm.**

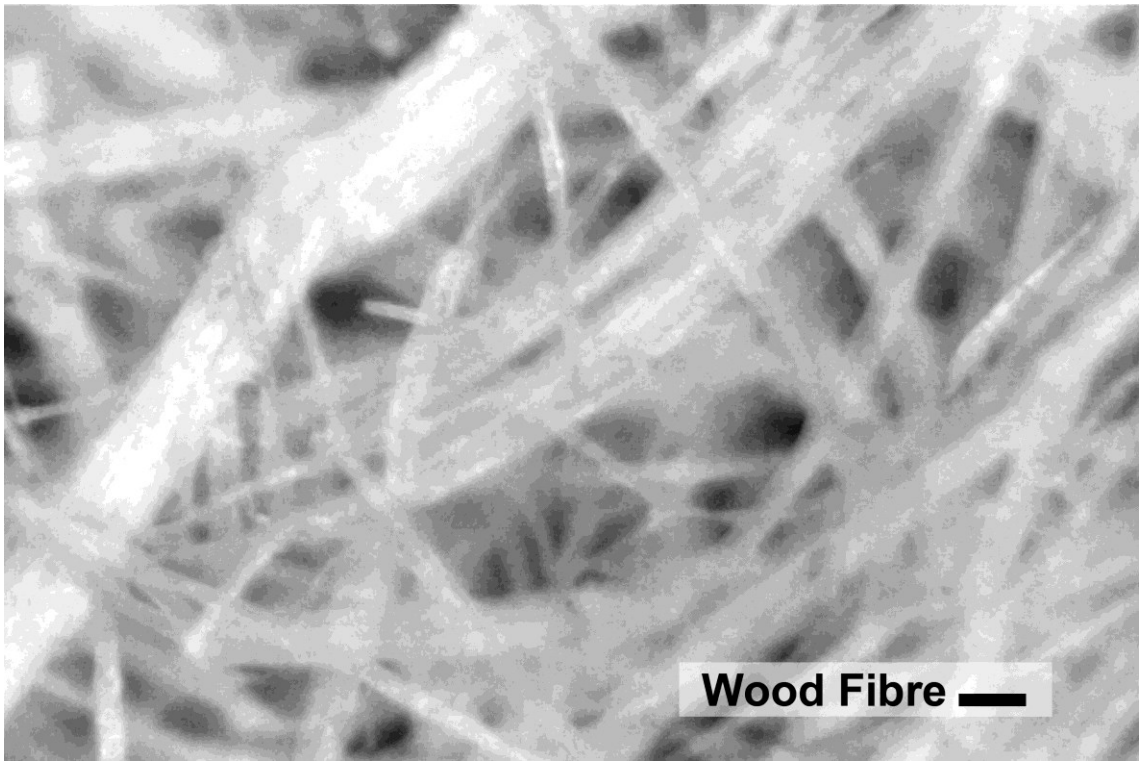


**Figure 4.21: Microscopic image of the sample of the wood fibre insulation. Scale bar: 100 µm.**

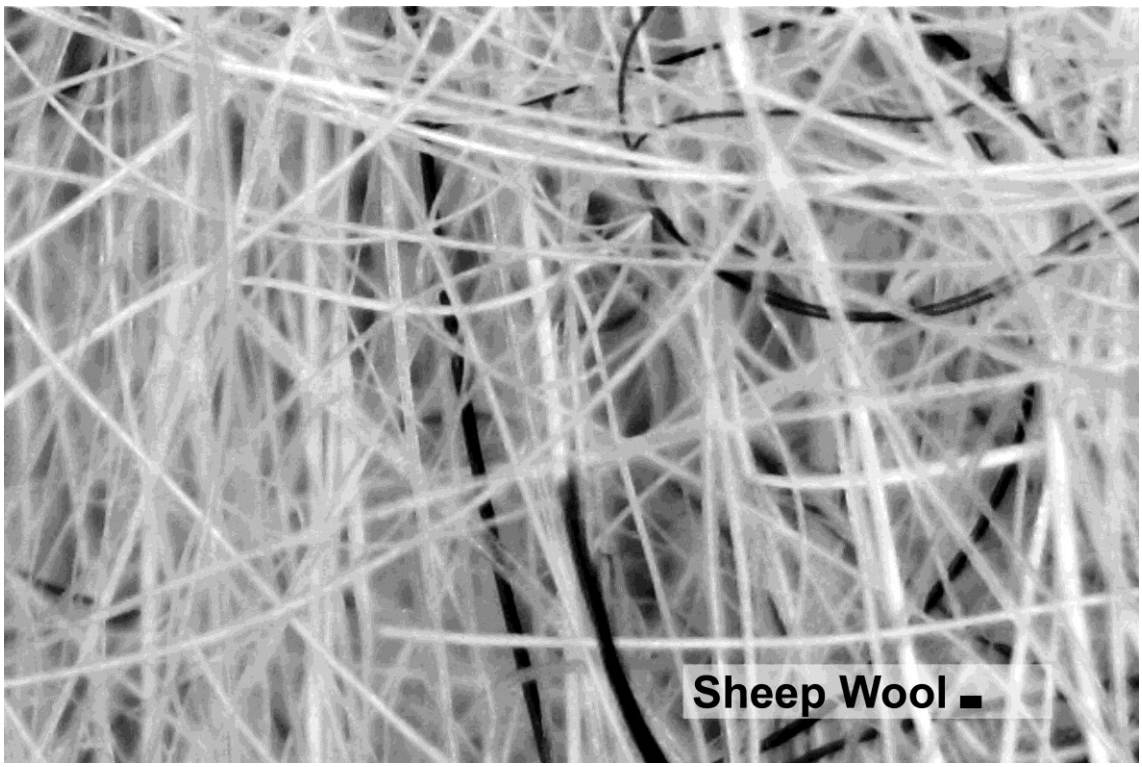


**Figure 4.22: Microscopic image of the sample of the sheep wool insulation. Scale bar: 100 µm.**

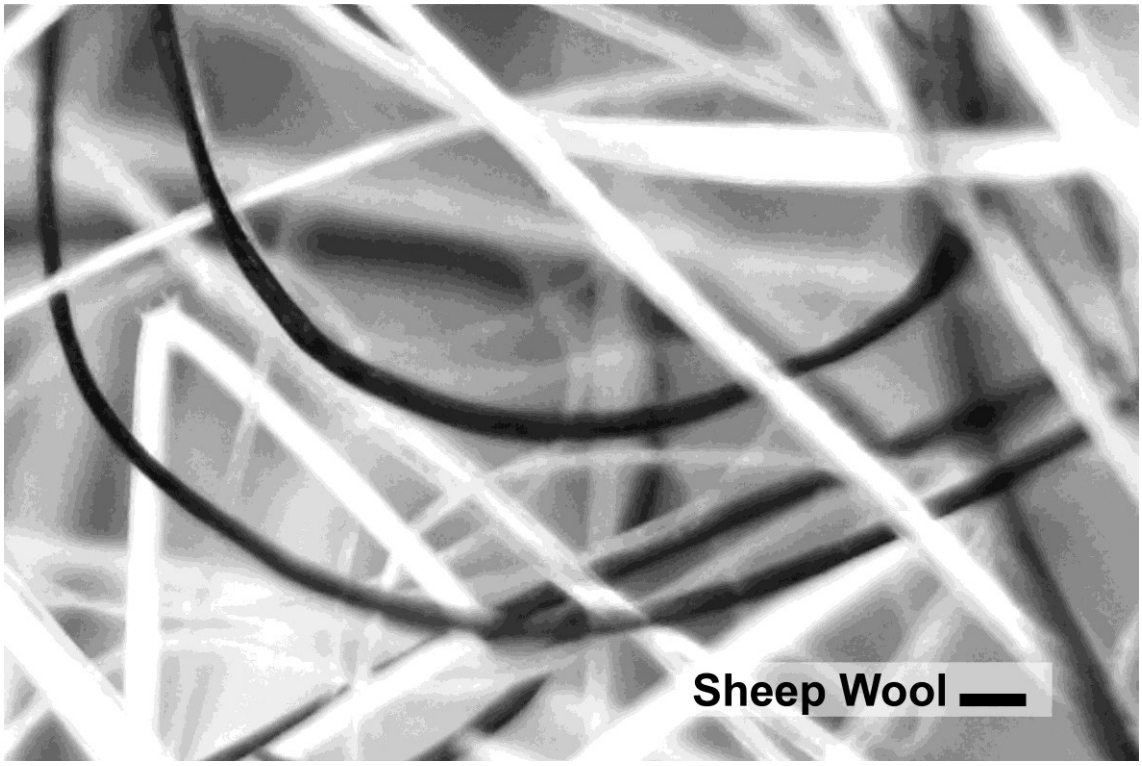


**Figure 4.23: Microscopic image of the sample of the sheep wool insulation. Scale bar: 100 µm.**

### *4.4.1 Hemp insulation*

Hemp is one of the oldest non-food fibre crops worldwide (Schultes, 1970 cited in Struik *et al*, 2000). The stem of hemp consists of wood and bast tissues. Bast tissue, the plant's transport system, forms the exterior layer of the stalk. In bast tissue, groups of fibre cells (bast fibres) are formed whose outer cell walls are strengthened with cellulose. The main purpose of this fibre cells is providing tensile strength and break and torque resistance to the stalk (Bocsa and Karus, 1998). Fibre cells are hold together in bundles mainly by pectin. This bond is broken down during fibre processing by biological, mechanical or chemical processes. These bast fibres are used as raw materials for thermal insulations.

Almost all types of hemp insulations available in the UK market, with different amount of hemp fibres in the fibre matrix, are selected for this study. The commercial names are replaced by the following names: hemp-1, hemp-2, hemp-3, hemp-4 and hemp-5. The basic material properties of these insulations are summarised in Table 4.1. The supplier has not provided the proportions of the constituent materials of hemp-3 insulation.

**Table 4.1: Summary of the properties of the hemp insulations.**

| Material | Density ($kg/m^3$) | Thickness (mm) | Declared specific heat capacity (J/kgK) | Constituents | Declared thermal conductivity (w/mk) |
|---|---|---|---|---|---|
| Hemp-1 | 55 | 48 | 1700 | 30% hemp fibre, 60% wood fibre, and 10% polyester | 0.038 |
| Hemp-2 | 50 | 55 | 1600 | 85% hemp fibres, 10-12% bi-component fibres and 3-5% soda | 0.038 |
| Hemp-3 | 60 | 47 | 1700 | Hemp fibres, ammonium phosphate, polyolefin fibres | 0.043 |
| Hemp-4 | 39 | 45 | 1700 | 95% hemp fibres 5% combination recycled adhesive binder | 0.039 |
| Hemp-5 | 45 | 57 | 1700 | 35% hemp fibre, 35% recovered waste cotton fibre, 15% bi-component polyester fibre and 15% fire retardant | 0.039 |

### *4.4.2 Stone wool insulation*

Stone wool is the most important thermal insulation in terms of its commercial implications as it accounts for 35% of the European market (Karamanos, Hadiarakou and Papadopoulos, 2008). The key ingredient of stone wool is amphibolite which is mixed with 6% lime stone and up to 9% calcium oxide. The mixture is heated in a blast furnace at 1450 °C to 1520 °C temperature. To produce stone fibres, the melted raw materials are drawn through the microscopic holes of a rotating spinner. The fibres are injected with small amount of resin and given shape by mechanical compression. Table 4.2 provides the summary of the properties of stone wool insulations used in the present research.

**Table 4.2: Summary of the properties of stone wool insulation.**

| Material | Density ($Kg/m^3$) | Thickness (mm) | Specific Heat Capacity (J/KgK) | Constituents | Declared Thermal Conductivity (W/mK) |
|---|---|---|---|---|---|
| Stone Wool | 23 | 100-110 | 850 | Amphibolite, about 6% lime stone, about 9% calcium oxide, resin | 0.038 |

### *4.4.3 Sheep wool insulation*

Sheep wool insulation is produced from 95% natural fibre and 5% adhesive. The sheep wool used in the insulation is categorised as a waste by-product while the main function of sheep farming is designated as meat production. Table 4.3 shows the properties of the sheep wool insulation used in the present research.

**Table 4.3: Summary of the properties of the sheep wool insulation.**

| Material | Density ($Kg/m^3$) | Thickness (mm) | Specific Heat Capacity (J/KgK) | Constituents | Declared Thermal Conductivity (W/mK) |
|---|---|---|---|---|---|
| Sheep Wool | 19 | 100 | 1700 | 95% natural wool fibre, 5% combination recycled adhesive binder | 0.039 |

### *4.4.4 Wood fibre insulation*

The raw materials for wood fibre insulations consist of splinters and wood chips of softwoods which are the by-products in sawmills. In the selected sample, the natural lignin of wood is used as the binder. However, some manufacturers also use synthetic resin as binder. At the end of life, wood fibre can be recycled, composted or used to produce heat energy. The summary of the properties of the wood fibre insulation is shown in the Table 4.4.

**Table 4.4: Summary of the properties of the wood fibre insulation.**

| | Density ($Kg/m^3$) | Thickness (mm) | Specific Heat Capacity (J/KgK) | Constituents | Declared Thermal Conductivity (W/mK) |
|---|---|---|---|---|---|
| Wood fibre | 170 | 100 | 2100 | Splinters and chips of soft woods, binder. | 0.042 |

## 4.5 Use of equipment

This section briefly describes the equipment used during the course of the research.

### *4.5.1 Standard equipment*

The standard equipment is used directly without any addition or modification. The standard equipment in relation to the present research is discussed in the following sub sections.

#### *4.5.1.1 The TAS climate chamber*

The Temperature Applied Sciences climate chamber (TAS) is used during the laboratory based experiments for exposing the insulations to steady or dynamic hygrothermal conditions (Figure 4.24). The external and the internal dimensions of the climate chamber are given in Table 4.5. The range and accuracy of relative humidity and temperature simulation in the climate chamber are provided in Table 4.6.

**Table 4.5: Dimensions of the TAS climate chamber.**

| | Height (mm) | Width (mm) | Depth (mm) |
|---|---|---|---|
| Total Climate Chamber | 2065 | 700 | 800 |
| Hot/ Cold Chamber | 2000 | 700 | 800 |

**Table 4.6: Range and accuracy of conditioning of the TAS climate chamber.**

| | Range | Accuracy |
|---|---|---|
| Temperature | -65 °C to 150 °C | ≤± 1 °C |
| Relative Humidity | 10% to 98% | 10% to 98% |


**Figure 4.24: The TAS climate chamber.**

### *4.5.1.2 The Feutron climate chamber*

The Feutron climate chamber consists of two conditioning chambers (Figure 4.25). The external and the internal dimensions of the climate chamber are given in the Table 4.7. The range and accuracy of relative humidity and temperature simulation is given in Table 4.8. As long as the minimum temperature is more than or equal to 5 °C, any of the chambers can be treated as cold or hot chamber. Sample building materials can be attached to the partition screen between the two chambers.

**Table 4.7: Dimensions of the Feutron dual climate chamber.**

| | Height (mm) | Width (mm) | Depth (mm) |
|---|---|---|---|
| Total climate chamber | 2360 | 2700 | 1600 |
| Cold chamber | 1020 | 770 | 745 |
| Hot chamber | 1020 | 770 | 745 |
| Partition frame | 775 | 515 | 210 |

**Table 4.8: Range and accuracy of conditioning of the chambers.**

| | Range | Accuracy |
|---|---|---|
| Temperature (cold chamber) | -40 °C to 100 °C | ≤ ± 0.5 °C |
| Temperature (Hot chamber) | 5 °C to 100 °C | ≤ ± 0.5 °C |
| Relative Humidity | 10% to 95% | ≤ ± 3% |

**Figure 4.25: The Feutron dual climate chamber.**

### *4.5.1.3. Measurement and control module*

A CR1000 measurement and control module (Figure 4.26), by Campbell Scientific, has been used for data acquisition from the temperature, temperature and relative humidity, heat flux sensors and from the water content reflectometer. During some experiments, the CR1000 module has also been used to control the temperature in the hot box. Table 4.9 presents the relevant technical data about this module. Detailed technical information about CR1000 measurement and control module can be found at the website of the Campbell Scientific (Campbell Scientific, 2013).

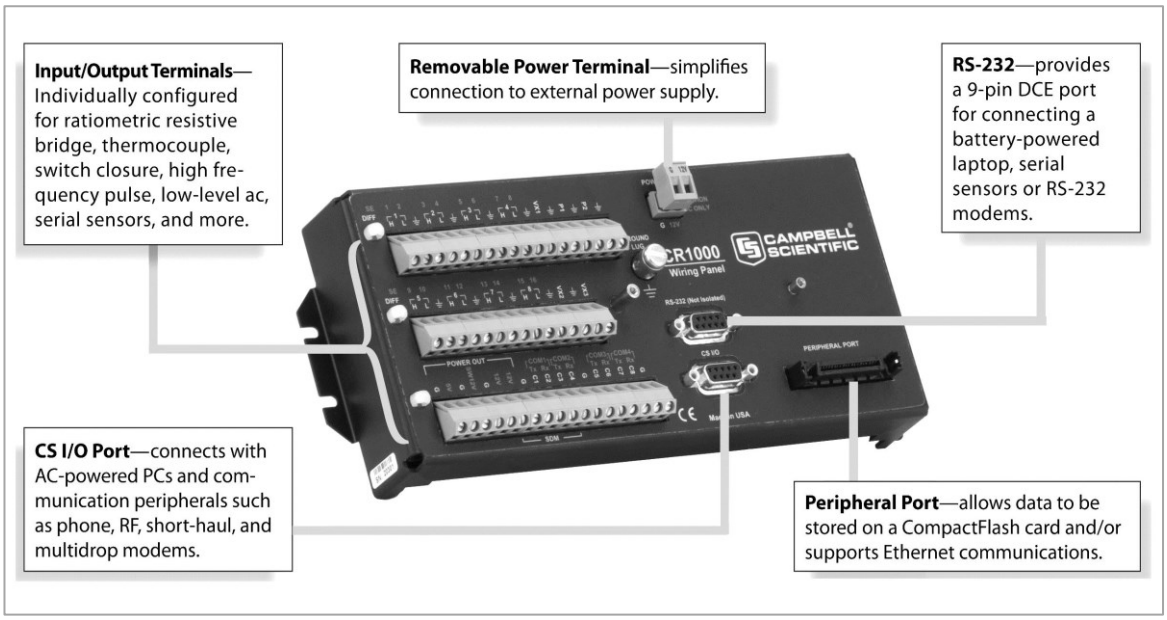


**Figure 4.26: The CR1000 measurement and control module (CR1000: Specifications and Technical Data, 2013).**

**Table 4.9: Technical details of the CR1000 measurement and control module.**

| Analogue input | Analogue Voltage Accuracy | Digital ports | Dimension (cm) |
|---|---|---|---|
| 16 single-ended or 8 differential individually configured | ± (0.06% of reading + offset), 0 °C to 40 °C | 8 ports software selectable, as binary inputs or control outputs | 23.9 x 10.2 x 6.1 |

#### *4.5.1.4. Temperature probes*

A number of 107 thermistor probes (Figure 4.27), manufactured by Campbell Scientific, have been used during some of the laboratory based experiments. The operating temperature of the 107 probe is -55 °C to +70 °C. The typical accuracy of the probe is ± 0.2 °C and the time constant in air is 30 seconds to 60 seconds in a wind speed of 5 m/s. PT100 temperature probes, equipped with platinum resistance thermometers, from Campbell Scientific, have been used to calibrate the 107 thermistor probes. The measurement range of the PT 100 probe is - 200 °C to 650 °C and the accuracy is ±0.1 °C at 0 °C and ± 0.19 °C at 100 °C.

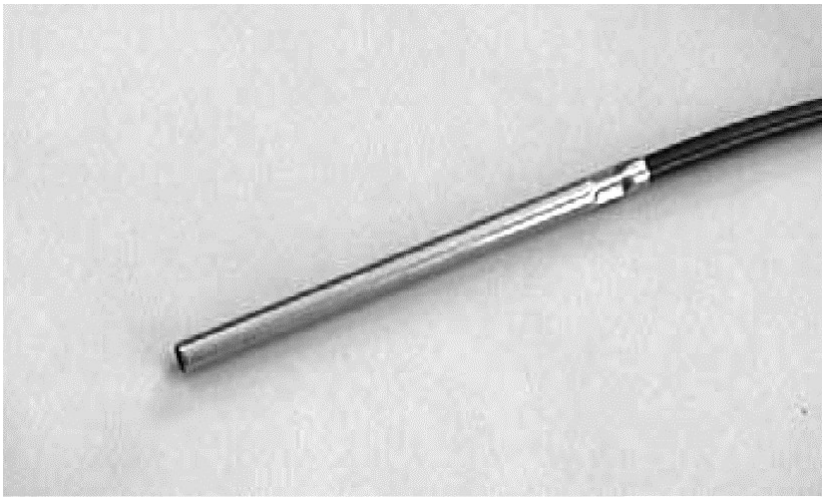

**Figure 4.27: The 107 thermistor probe.**

The calibration of the 107 thermistor probes was done by a third party at different temperatures, between 0 °C and 37 °C. The temperature of 0 °C was achieved by using iced, distilled water. Warm water was added to the iced water to increase the temperature up to 37 °C. Linear regression of the temperature data of each 107 thermistor probe against the temperature data obtained from the PT100 probe provided the regression equations. The equations were used to adjust the temperature data of the 107 thermistor probes inside the data logger programme.

#### *4.5.1.5 Temperature and relative humidity sensors*

CS215 temperature and relative humidity sensors (Figure 4.28) from Campbell Scientific have been used to measure temperature and relative humidity together. The accuracy of the relative humidity measurement is (at 25 °C) ±4% over 0%-100% relative humidity while the accuracy of temperature measurement is ± 0.9 °C over -40 °C to +70 °C. The calibrations of CS215 sensors are traceable to the National Institute of Standards and Technology (NIST), USA and the National Physical Laboratory (NPL), UK. In addition to these sensors, some temperature and relative humidity data loggers (EL-USB-2) by Lascar Electronics have been used. The temperature measurement range for all samples is -35 °C to 80 °C and the accuracy is ± 0.5 °C. The humidity measurement range is 0% to 100% and the accuracy is ±3%. The response time is less than 10 seconds (63% response time in air moving at 1 m/s).

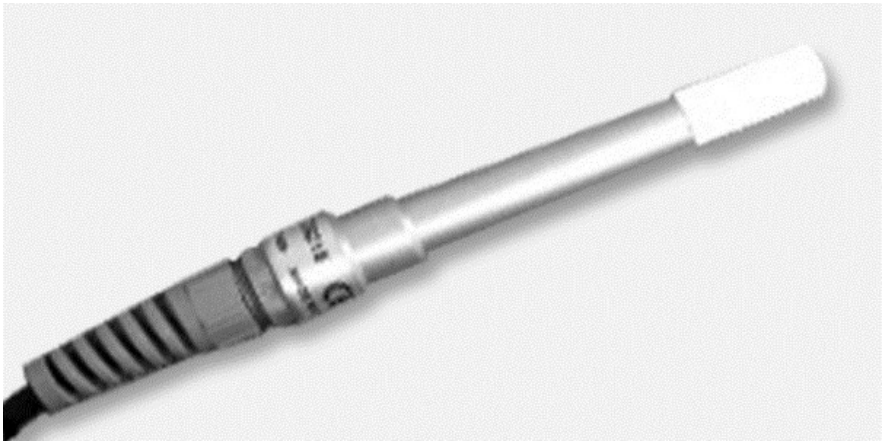

**Figure 4.28: The CS215 temperature and relative humidity sensor.**

#### *4.5.1.6 Heat flux sensors*

HFP01 heat flux sensors (Figure 4.29), by Hukseflux, have been used to measure heat flux through the insulation. The measurement range is between -2000 W/m$^2$ and +2000 W/m$^2$ and the accuracy is ± 5% on walls.


**Figure 4.29: The HFP01 heat flux sensor.**

#### *4.5.1.7 Water content reflectometer*

The CS616 water content reflectometer (Figure 4.30) uses time-domain measurement methods to determine the volumetric water content (VWC) of porous media. Volumetric water content is defined as the ratio of the total volume of the liquid phase and the total volume of the sample. The probe consists of two stainless steel rods that can be inserted from the surface. Table 4.10 shows the technical details of the CS616 water content reflectometer in terms of measuring soil moisture content. Soil moisture content is measured in terms of volumetric water content.

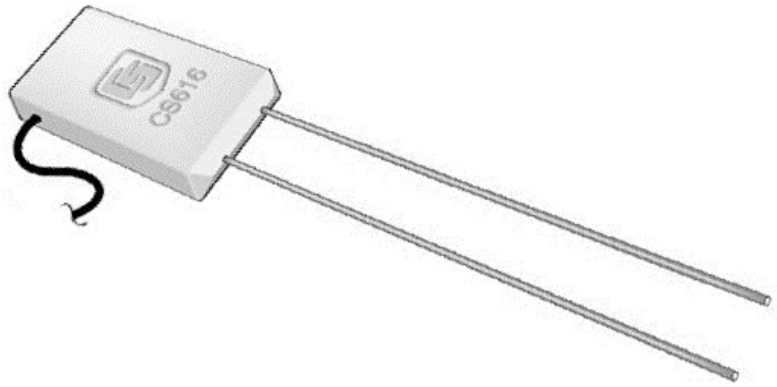


**Figure 4.30: The CS616 water content reflectometer.**

**Table 4.10: Technical details of CS616 water content reflectometer.**

| Accuracy | Precision | Resolution | Dimension |
|---|---|---|---|
| ± 2.5% VWC in the measurement range of 0% to 50% VWC. | 0.05% VWC | 0.1% VWC | Rods: 300 mm long; 3.2 mm diameter; 32 mm spacing, head: (110 x 63 x 20) mm |

#### *4.5.1.8 Isomet heat transfer analyser*

The Isomet heat transfer analyser (Figure 4.31) is used for obtaining the values of thermal conductivity, thermal diffusivity and volume heat capacity of isotropic materials. The aforementioned heat transmission properties are determined by using needle probes (Figure 4.32) for soft materials and surface probes for hard material. The measurement method is standardised by the American Society for Testing and Materials (ASTM) in ASTM D5334 (2008). This dynamic method reduces the measurement time in comparison with steady state measurement methods. Table 4.11 shows the range and accuracy of the measurements.

**Table 4.11: Range and accuracy of conditioning of the chambers.**

| | Range | Accuracy |
|---|---|---|
| Thermal Conductivity | 0.015- 0.7 W/mK | 5 % of reading + 0.001 |
| Volume heat capacity | $4.0.10^4$ - $4.0.10^6$ J/m$^3$K | 15 % of reading + $1.10^3$ J/m$^3$K |
| Temperature | -2° C to 70 °C | 1 °C |

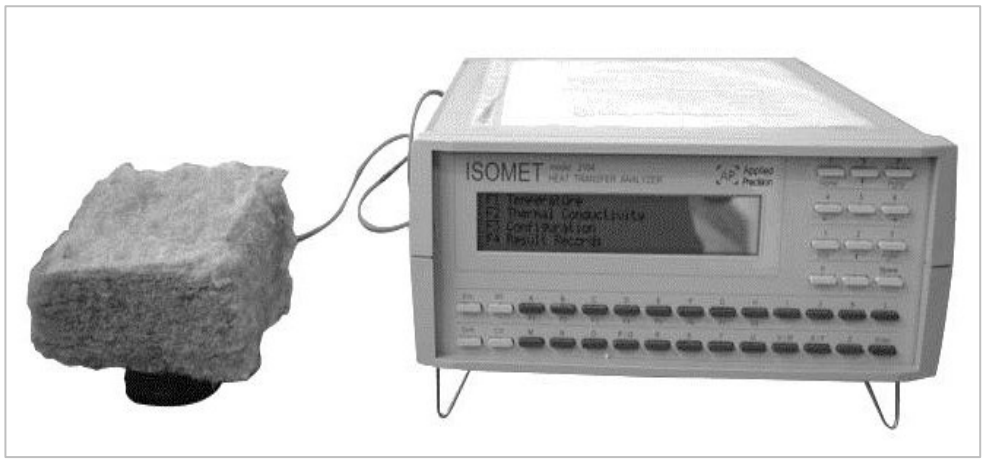


**Figure 4.31: The Isomet heat transfer analyser.**


**Figure 4.32: The surface and needle probes of the Isomet heat transfer analyser.**

#### *4.5.1.9 Precision weighing scales*

The PGW 453e and PGW 4502e (Figure 4.33) precision balances by Adam Equipment have been used for weighing insulations during the experiments. The details of the capapcity and the accuracy of the balances are provided in Table 4.12.

**Table 4.12: Capacity and accuracy of the precision weighing scale.**

| Model | Platform size (mm) | Capacity (g) | Accuracy (g) |
|---|---|---|---|
| PGW 453e | 145 X125 | 450 | 0.001 |
| PGW 4502e | 192X192 | 4500 | 0.01 |


**Figure 4.33: The PGW 4502e precision balance.**

#### *4.5.1.10 Flir i7 thermal imaging camera*

The Flir i7 thermal imaging camera (Figure 4.34) is used during the in situ tests. Filr i7 produces instant thermal images that can be transferred to computers and analysed. The accuracy and resolution of the thermal imaging camera is provided in Table 4.13.

**Table 4.13: Technical details of the Flir i7 thermal imaging camera.**

| Filed of view (°) | Image resolution (pixel) | Sensitivity (°C) | Range (°C) | Accuracy (°C) |
|---|---|---|---|---|
| 29 X 29 | 140 X140 | 0.1 | -20 to 250 | ± (2 or 2%) |


**Figure 4.34: The Flir i7 thermal imaging camera.**

#### *4.5.1.11 Digital microscope*

A HooToo digital microscope (Figure 4.35) has been used to study the insulation at magnified scales. Still and moving images can be viewed through the computer monitors and can be stored in the computer or mobile data storage devices in the Joint Photographic Experts Group (JPEG), bitmap image file (BMP) and Moving Picture Expert Group (MPEG) format. The technical details of the digital microscope are presented in Table 4.14.

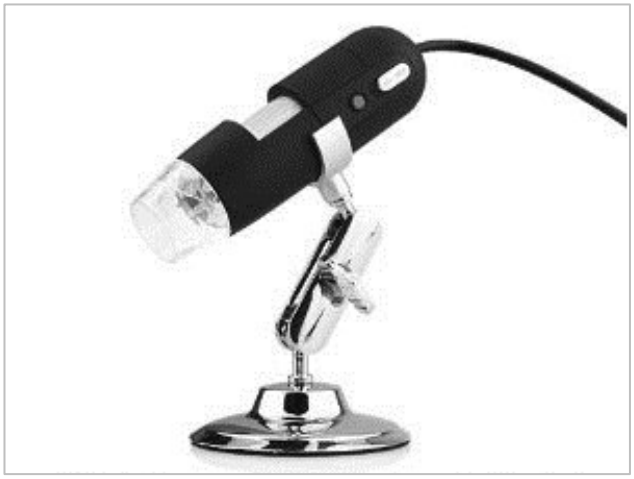

**Figure 4.35: The digital microscope.**

**Table 4.14: Technical details of the HooToo digital microscope.**

| Image sensor (mega pixel) | Highest resolution | Magnification ratio |
|---|---|---|
| 2 | 1600 X 1200 | 20X to 800X |

#### *4.5.1.12 Cirrus 40 fan heater*

The Cirrus 40 fan heaters (Figure 4.36) have been used in some of the laboratory based experiments.

**Figure 4.36: The Cirrus 40 fan heater.**

The Cirrus 40 fan heater incorporates a self regulating heating element and an axial fan. The surface voltage is 12 volt direct current. The Cirrus 40 fan heater can achieve a surface temperature of 35 °C.

#### *4.5.1.13 Fox 600 guarded hot plate*

Thermal conductivity values, determined with Fox 600 hotplate (Figure 4.37), have been used as the third party contribution in the present research. Thermal conductivity is obtained from the values of heat flux through the insulation sample and the temperature gradient between the hot and cold surface of the sample. The technical details of the hot plate are provided in Table 4.15.

**Table 4.15: Technical details of the Fox 600 hot plate.**

| Plate area (mm) | Metering area (mm) | Operating temperature range (°C) | Thickness of sample (mm) | Mode of operation |
|---|---|---|---|---|
| 610 X 610 | 254 X 254 | Room temperature to 250 | ≤ 75 | Single sample |

**Figure 4.37: The Fox 600 hot plate.**

#### *4.5.1.14 Century 4 industrial humidifier*

The Centuray 4 is an evaporative industrial humidifier (Figure 4.38) capable of humidifying an office with volumes of up to 400 m³. The relative humidity can be varied between 0% and 90%.

**Figure 4.38: The Century 4 industrial humidifier.**

#### *4.5.1.15 TH-810H plug-in humidistat*

TH-810H plug-in humidistat (Figure 4.39) has been used in conjunction with the Century 4 industrial humidifier to control relative humidity of the test house during the in situ tests. The relative humidity control range is 10% to 90% and the precision is ± 5%. The temperature operating range is 10 °C to 40 °C. The measurement frequency is 10 second.

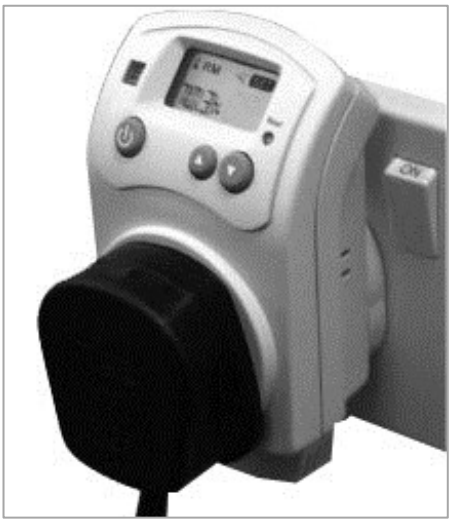


**Figure 4.39: The TH-810H plug-in humidistat.**

### 4.5.2 *Specialist equipment*

#### *4.5.2.1 Data acquisition and temperature control unit*

The data acquisition and temperature control unit is used during the laboratory based experiments. The data acquisition and temperature control unit consists of the CR1000 measurement and control module, 107 thermistor temperature

probes, CS215 temperature and relative humidity probes, HFP01 heat flux sensors and Cirrus 40 fan heaters. Nine thermistor temperature probes, six temperature and relative humidity probes, two heat flux sensors and two fan heaters were connected to the CR1000 measurement and control module for data logging. The fan heaters can be switched on and off based on the temperature set point inside the hot and cold chambers.

#### *4.5.2.2 Data acquisition unit*

Data acquisition unit is used during the in situ tests. The data acquisition unit consists of the CR1000 measurement and control module (data logger), CS215 temperature & relative humidity probes, HFP01 heat flux sensors and CS616 water content reflectometers. Six temperature & relative humidity probes, four heat flux sensors and two water content reflectometers were connected to the CR1000 measurement and control module for data logging.

#### *4.5.2.3 The dynamic hygrothermal hot box*

The dynamic hygrothermal hot box can be used for studying hygrothermal properties of materials both in steady state and dynamic hygrothermal conditions. The dynamic hygrothermal hot box is an assembly of the following individual equipment:

- A hot chamber made of expanded polystyrene (EPS).
- An optional cold chamber made of EPS. The hygrothermal hot box can also operate without this chamber.
- A sample holder made of insulated ply board.
- The TAS climate chamber.

The two chambers were modified from existing experimental equipment, and the sample holder was constructed for the current research. The dynamic hygrothermal hot box, as a system, was designed by the present author.

Both hot and cold chambers are built of 300 mm thick Expanded Polystyrene Insulation (EPS). The external dimension of both chambers is 1460 mm X 1460 mm X 1160 mm and the internal dimension is 860 mm X 860 mm X 860 mm. There is an opening at the front of each chamber with the dimension of 860 mm X 860 mm where insulation sample can be placed for testing. Insulation

samples can also be placed on a 350 mm thick sample holder built of insulated ply board.

Both hot and cold chamber are equipped with Cirrus 40 fan heaters that can create an internal temperature of up to 40 °C. The hot chamber is connected to the TAS climate chamber with an insulated polyvinyl chloride (PVC) pipe of 65 mm diameter so that the temperature and the humidity inside the hot chamber can be reasonably controlled by regulating the temperature in the hot box and the climate chamber and by controlling the relative humidity in the climate chamber. The individual parts and the assembled dynamic hygrothermal hot box are shown in the Figure 4.40.

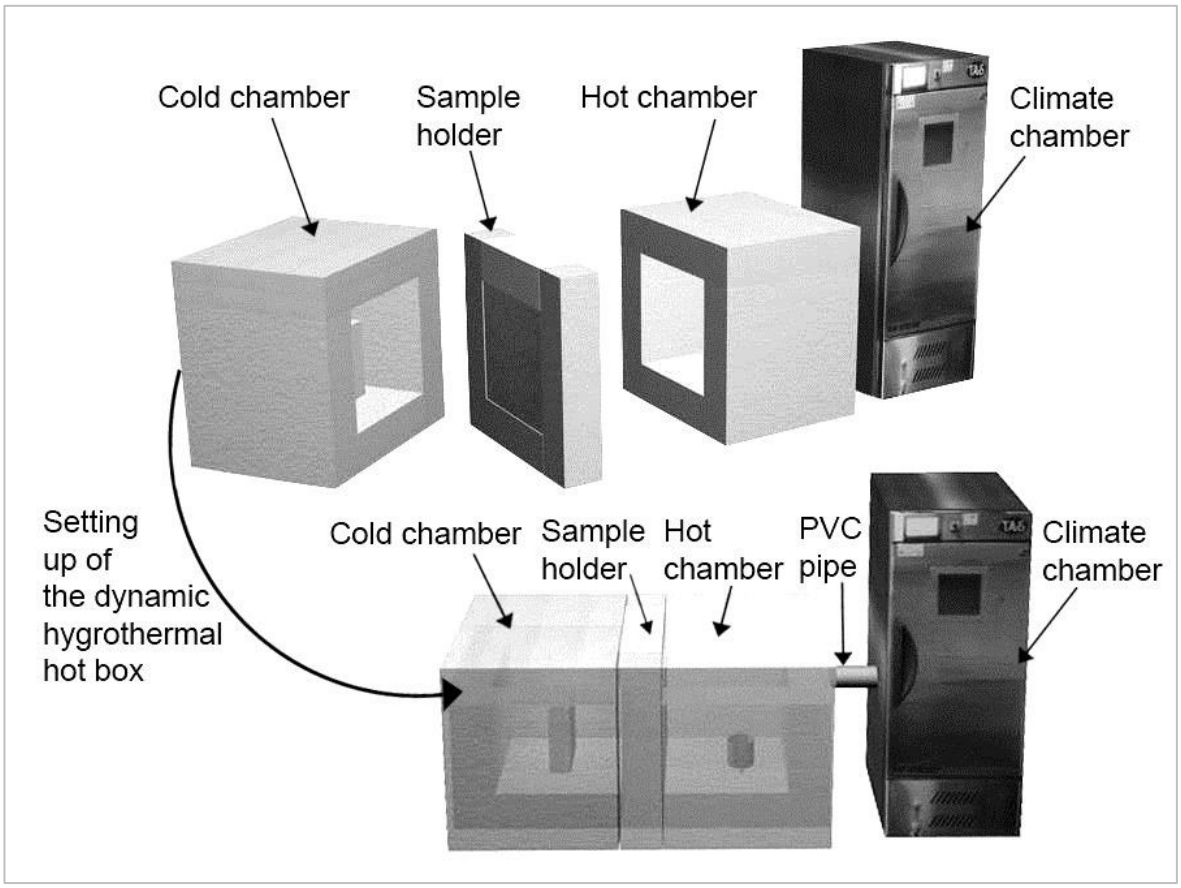


**Figure 4.40: The dynamic hygrothermal hot box.**

### 4.6 Chapter summary

The key objectives of the research are to determine the hygrothermal properties of hemp insulations both in steady state and dynamic hygrothermal conditions. The research methodology is a quantitative one. Assessments of the insulation materials are carried out at two levels: material level and system level. At the material level, both steady state and dynamic assessment methods are applied

in conjunction with numerical hygrothermal simulation in the WUFI software. At the system level, selected building envelopes are tested by laboratory-based experiments, hygrothermal simulations in dynamic and quasi steady state conditions and in situ experiments. Results of the experiments and simulations are mostly assessed with procedures described in the British Standards and in the ISOs. In addition to this, statistical software is also used to assess data in terms of determining standard deviations, regressions and correlations.

Five different makes of hemp insulations are tested in this research. The hemp insulations consist of different amount of hemp fibres in the fibre matrix. Conventional insulations are also selected for the purpose of comparison at various stages of the research such as stone wool insulation, sheep wool insulation and wood fibre insulation.

Both standard and specialist equipment have been used in the laboratory based testing and the situ testing. The dynamic hygrothermal hotbox, as a system, was designed by the author.

# Chapter 5

# Standard Steady State Tests

## 5.1 Introduction

This chapter describes in detail the research methods and findings of the assessment of the hygric properties of hemp, sheep wool, wood fibre and stone wool insulations at material level, as set in the subsection 4.3.1 of chapter four. The hygric properties are determined by using steady state methods according to the corresponding British and international standards. The following moisture transfer properties of the insulation materials are determined experimentally:

- Adsorption-desorption Isotherm
- Moisture buffering capacity
- Vapour diffusion resistance factor
- Water absorption coefficient (A value)

The thermal conductivity of the insulation materials in steady state condition determined by a hotplate is compared with the thermal conductivity results determined by transient methods using a heat transfer analyser in Appendix B. In addition, Appendix C describes some 'rule of thumb' methods developed by the author of this thesis to determine the moisture dependent thermal conductivity values of hemp insulations.

## 5.2 Determination of adsorption-desorption isotherm

### *5.2.1 Method of determination*

The methods for experimentally determining the adsorption-desorption isotherms of thermal insulating materials are outlined in the British Standard BS EN ISO 12571 (2000). At least three samples of a minimum dimension of 200 mm X 200 mm with true thickness are initially dried to reach constant mass. To determine the adsorption isotherm, the samples are consecutively exposed to minimum four approximately evenly distributed increasing relative humidity conditions between 30% to 95% while keeping the temperature constant at 23 (± 0.5) °C in a climate chamber. For determining the desorption isotherm, the

process is carried out in reverse order. During each exposure, the samples have to reach equilibrium moisture content (EMC) according to BS EN 12429 (1998). The test equipment used for this experiment is shown in Figure 5.1.

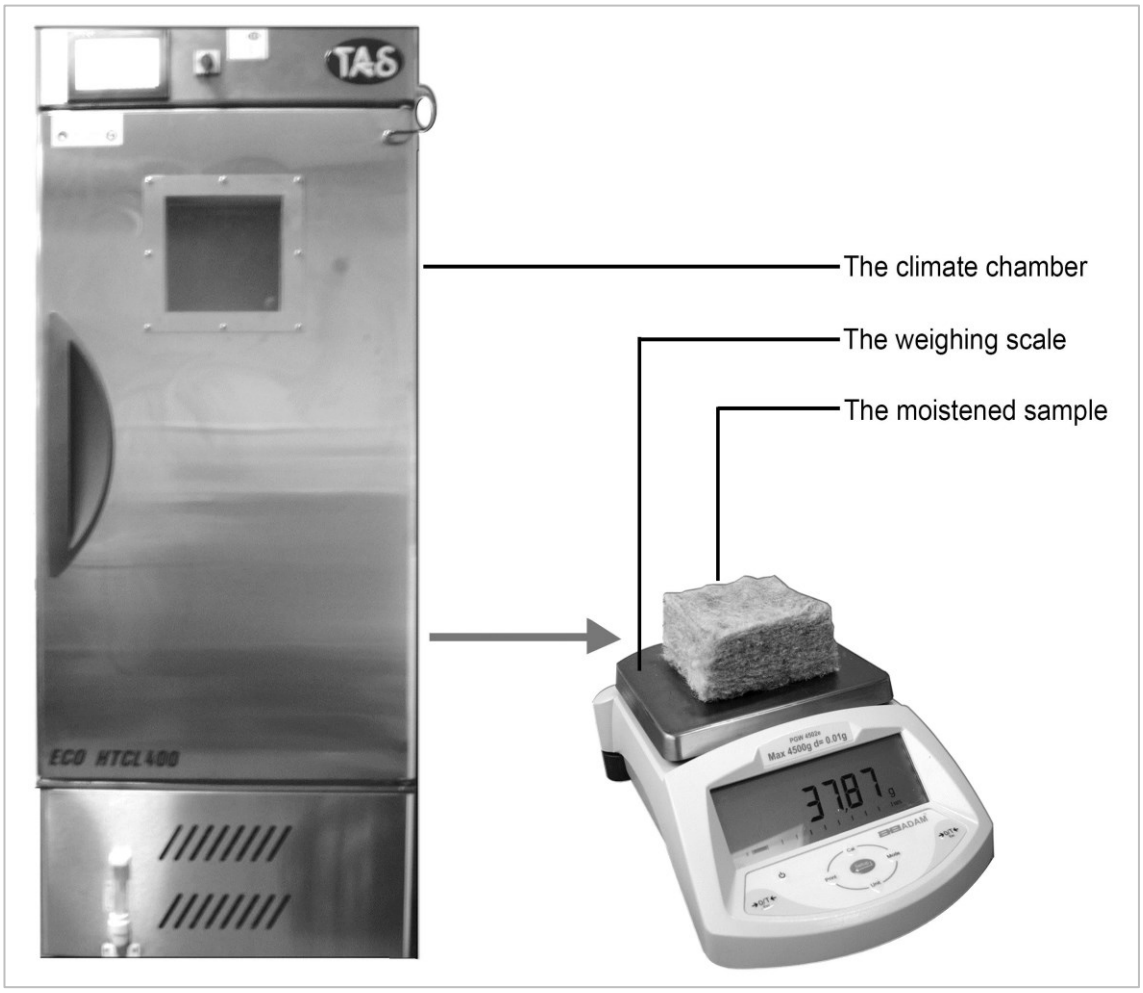


**Figure 5.1: The test equipment for determination of adsorption-desorption isotherm.**

The adsorption/desorption of moisture content by weight U (kg/kg) is calculated as follows:

$$U = (m - m_0)/m_0 \quad [5.1]$$

Where,

$m_0$ is the mass of the material at dry condition and m is the mass of the material at the equilibrium moisture content at any relative humidity.

### *5.2.2 Method of analysis of the adsorption-desorption data*

For bio-based insulation materials, due to their complex microstructures, four or five data of moisture adsorption-desorption at EMC conditions are not always

adequate to develop an isotherm. For this reason, different equations are developed to determine intermediate data points between the experimental data points.

The GAB equation has been selected for the interpretation of the experimental adsorption data. The GAB equation has been chosen for its higher coverage of activity (φ) range for monolayer sorption values ($0.05<\varphi<0.8\text{-}0.9$). Thus, the range of GAB equation is greater than that of the BET equation ($0.05<\varphi<0.3$) (Timmermann, 2003). The GAB isotherm is described in the subsection 3.3.9.3 of chapter three.

Equation 3.30 has been applied to determine the GAB values. The third parameter, K, is determined from the best linearization plot of F (GAB) versus φ, F (GAB) being the linearized function of the GAB isotherm. The other two constants, WmG and CG respectively are then determined from two linear regression coefficients.

Figures 5.2 and 5.3 show the water adsorption capacity of the insulation materials for a range of relative humidity conditions in terms of average moisture content by weight (AMCw) and average moisture content by volume (AMCv), respectively. The adsorption isotherms of selected insulation materials based on the GAB regression, together with the experimental data, are shown in Figures 5.4-5.12.

### *5.2.3 Result and discussion*

It can be noticed that experimental data fits well with GAB model in most of the cases within the range of 80% relative humidity. The GAB regressions of the isotherms start deviating from the experimental data from 80% relative humidity. Exceptions are observed in the case of hemp-2 and hemp-4 where the experimental data agrees closely with the GAB predictions until about 95% relative humidity. However, the predictions have to be treated in conjunction with the fact that GAB equation is accurate up to 90% relative humidity. Overall fit of the experimental data with GAB model confirms the reliability of experimental determination process.

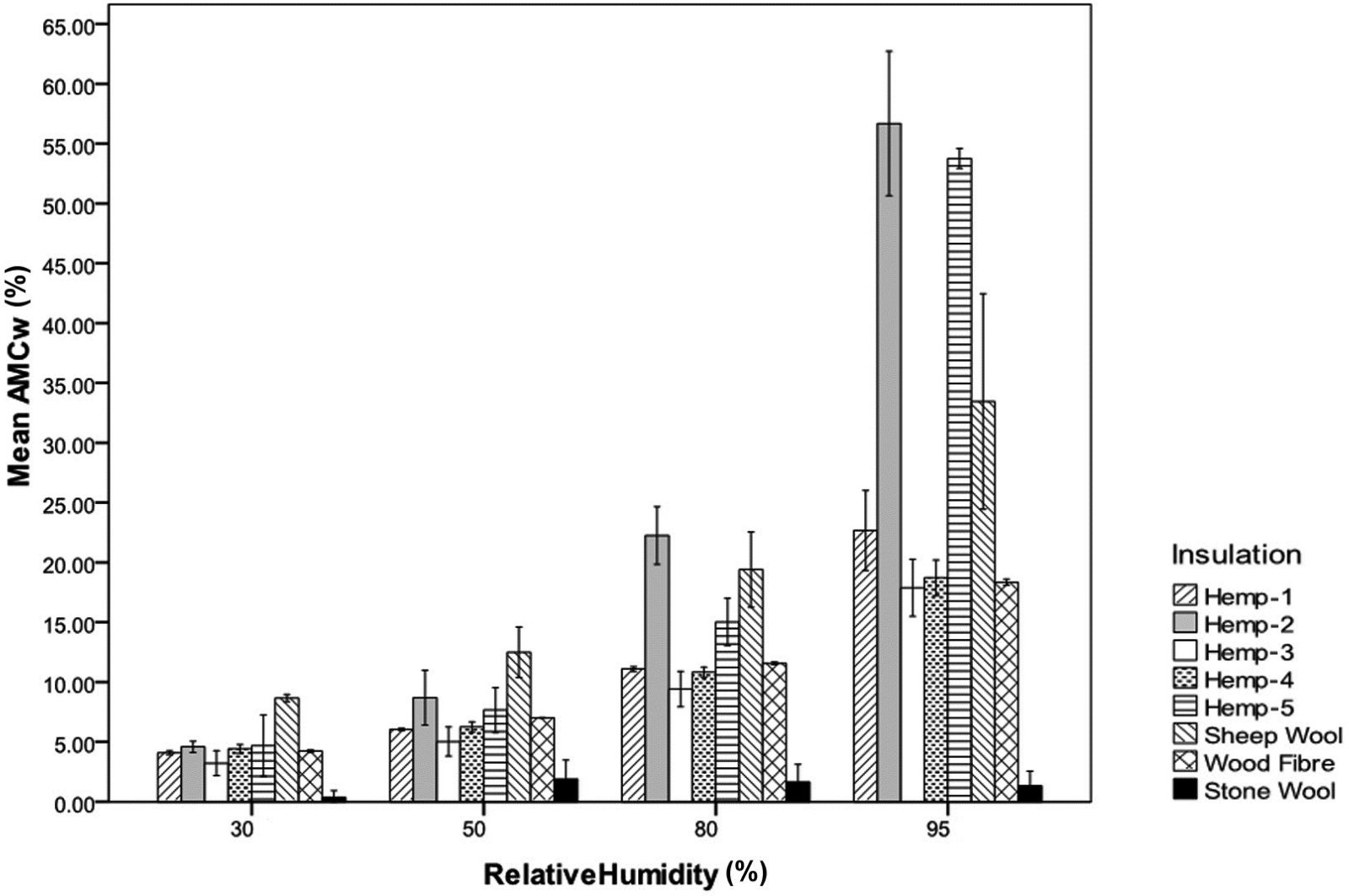


**Figure 5.2: Adsorption of moisture in the insulation materials in terms of average moisture content by weight (AMCw) of each of the insulation types with 1 standard deviation.**

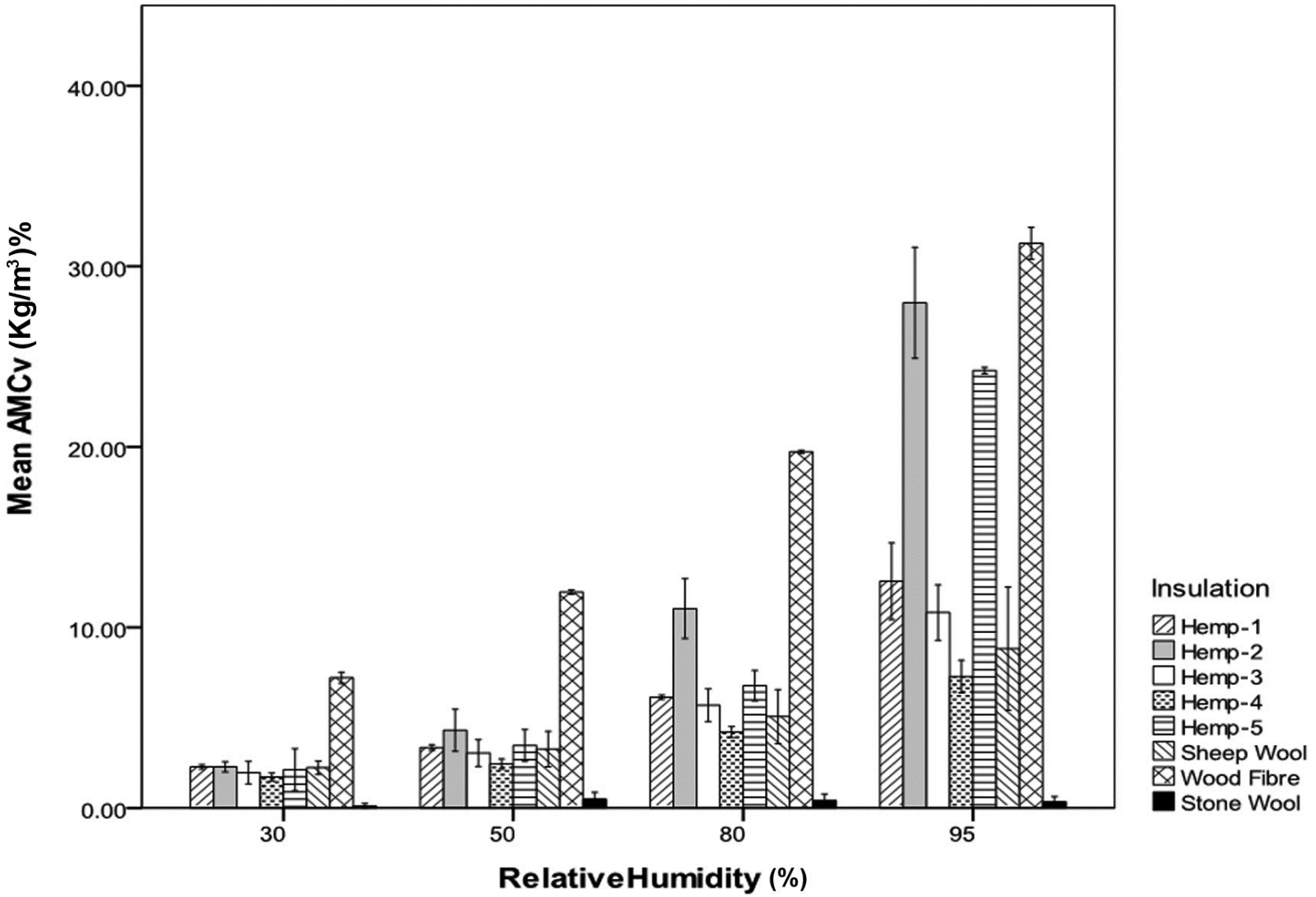


**Figure 5.3: Adsorption of moisture in the insulation materials in terms of average moisture content by volume (AMCv) of each of the insulation types with 1 standard deviation.**

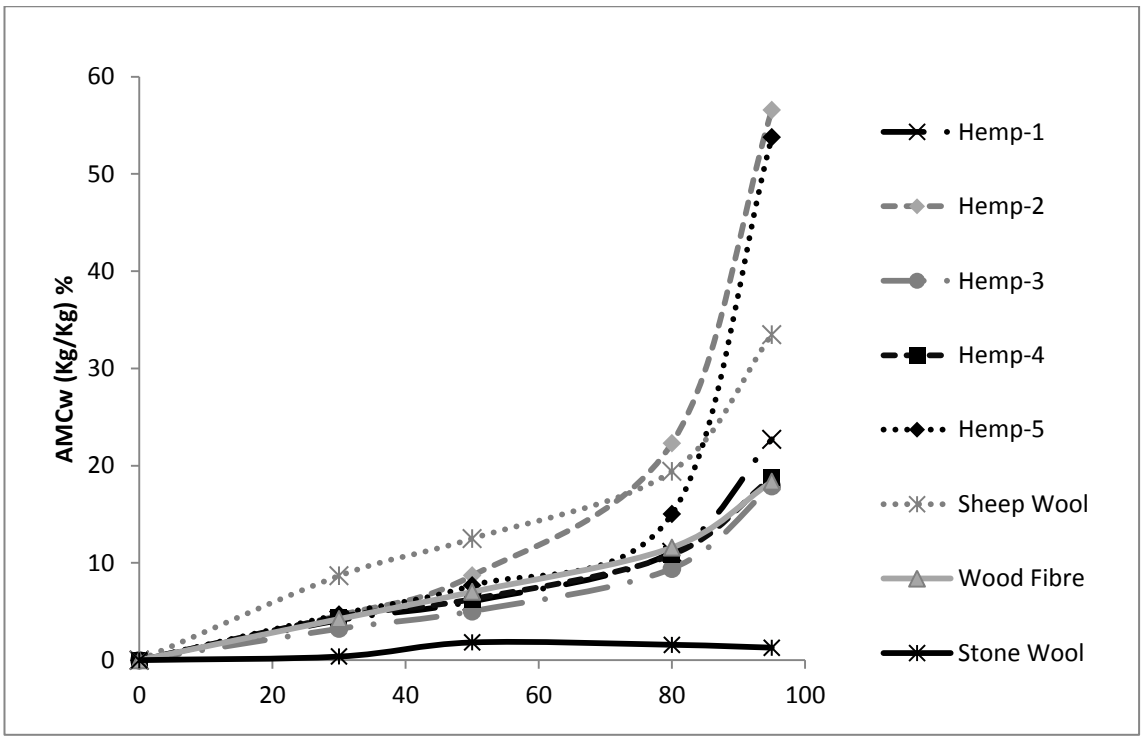


**Figure 5.4: Adsorption isotherms of insulation materials by average moisture content by weight (AMCw).**

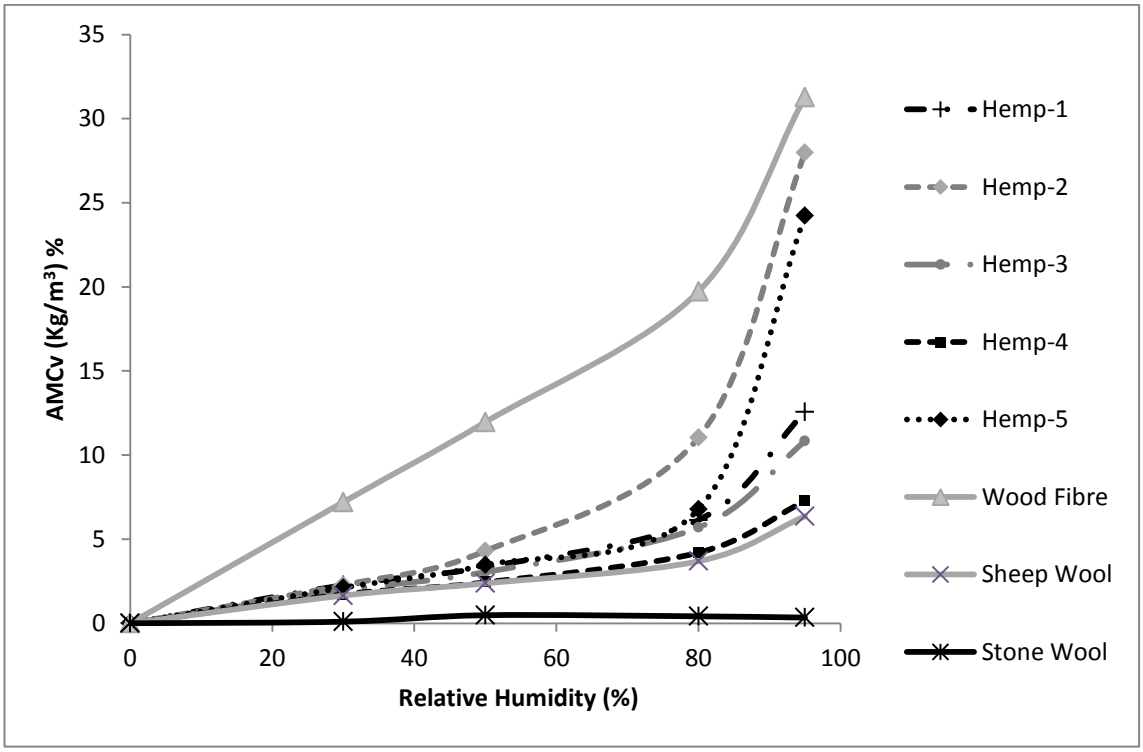


**Figure 5.5: Adsorption isotherms of insulation materials by average moisture content by volume (AMCv).**

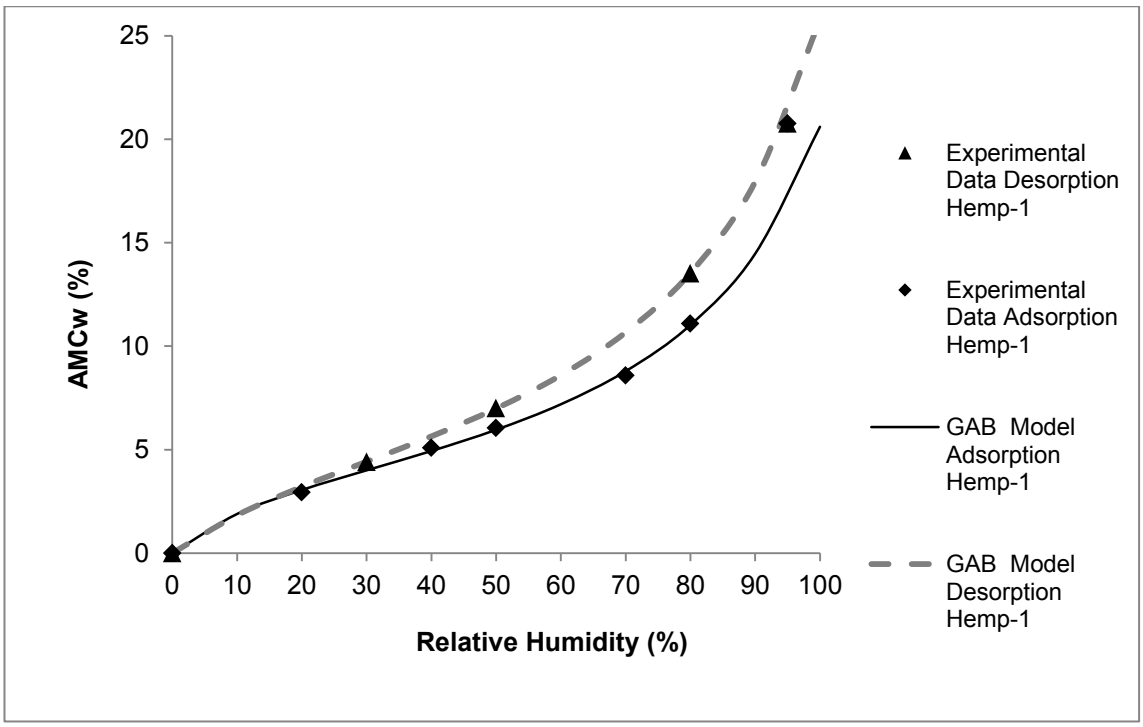


**Figure 5.6: Adsorption-desorption isotherm of hemp-1 with GAB fit in relation to average moisture content by weight (AMCw).**

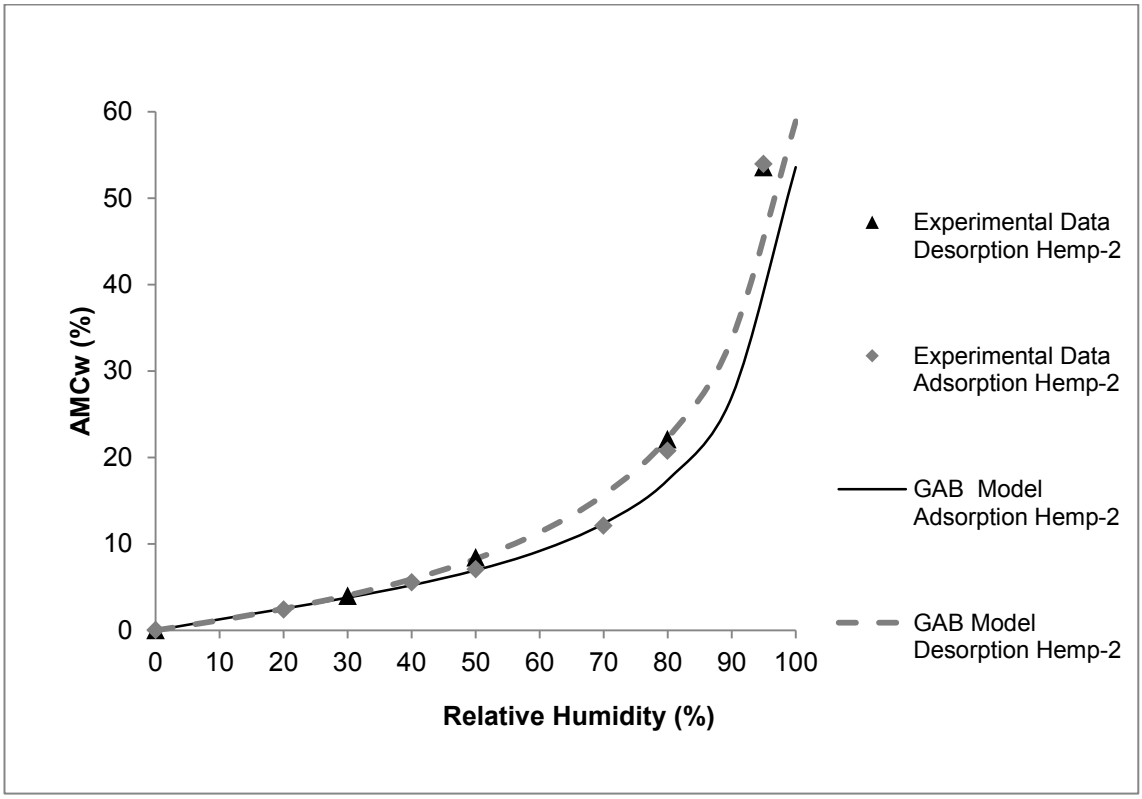


**Figure 5.7: Adsorption-desorption isotherm of hemp-2 with GAB fit in relation to average moisture content by weight (AMCw).**

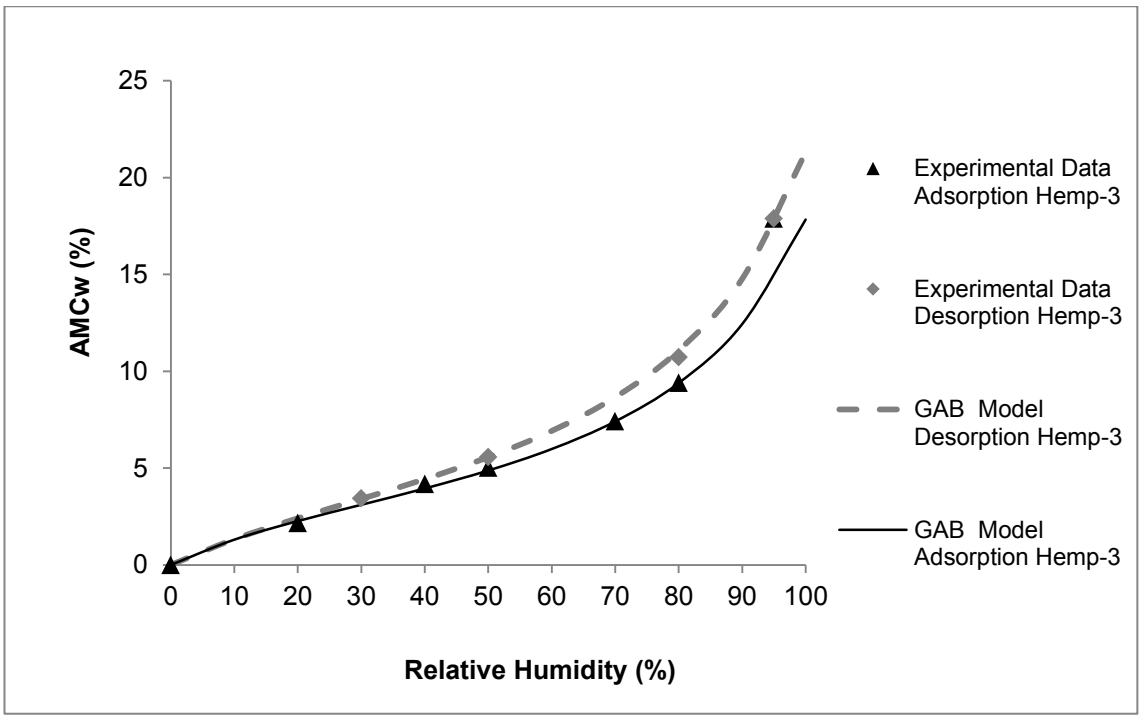


**Figure 5.8: Adsorption-desorption isotherm of hemp-3 with GAB fit in relation to average moisture content by weight (AMCw).**

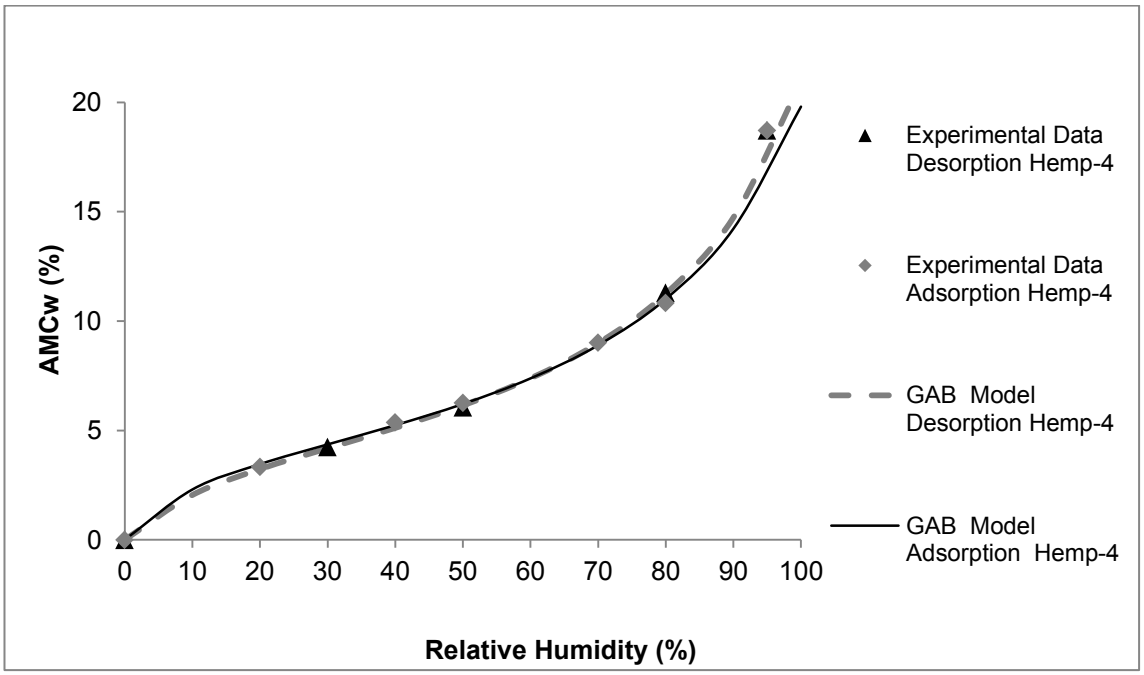


**Figure 5.9: Adsorption-desorption isotherm of hemp-4 with GAB fit in relation to average moisture content by weight (AMCw).**

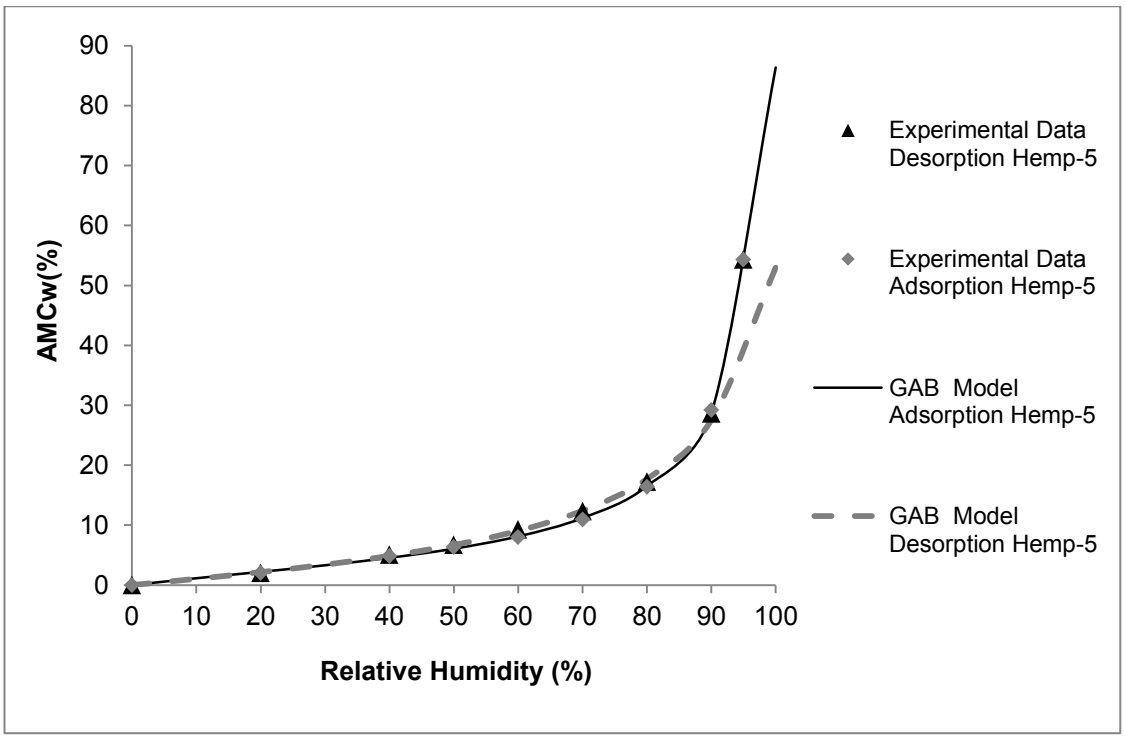


**Figure 5.10: Adsorption-desorption isotherm of hemp-5 with GAB fit in relation to average moisture content by weight (AMCw).**

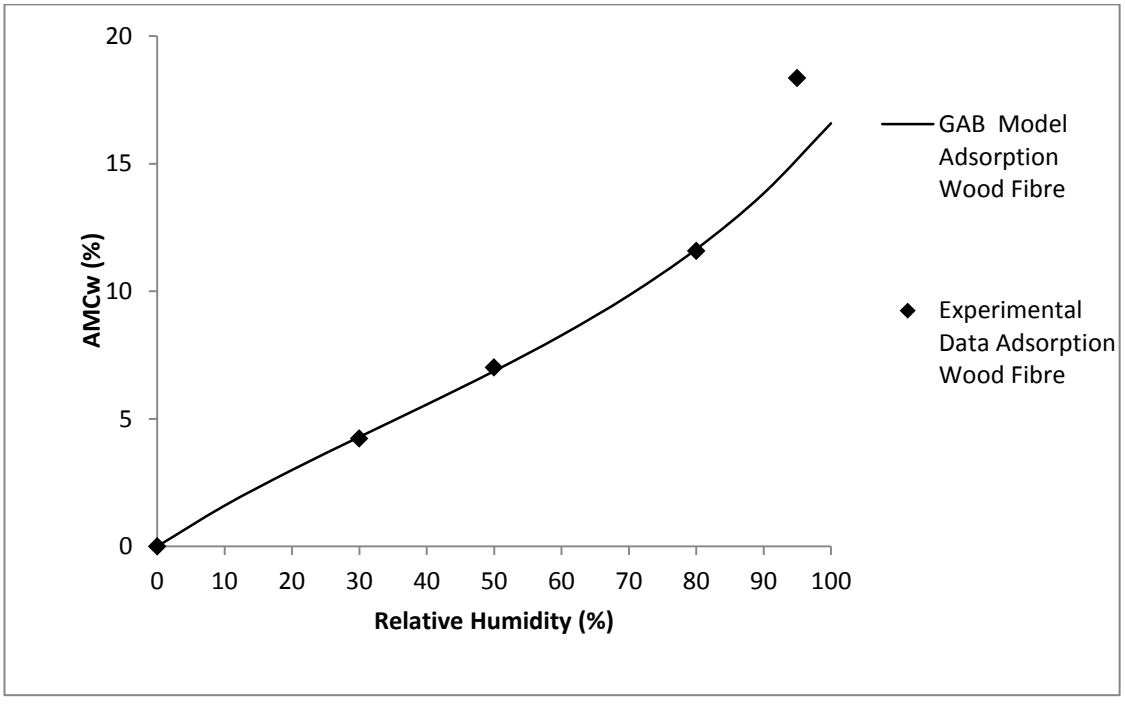


**Figure 5.11: Adsorption-desorption isotherm of wood fibre with GAB fit in relation to average moisture content by weight (AMCw).**

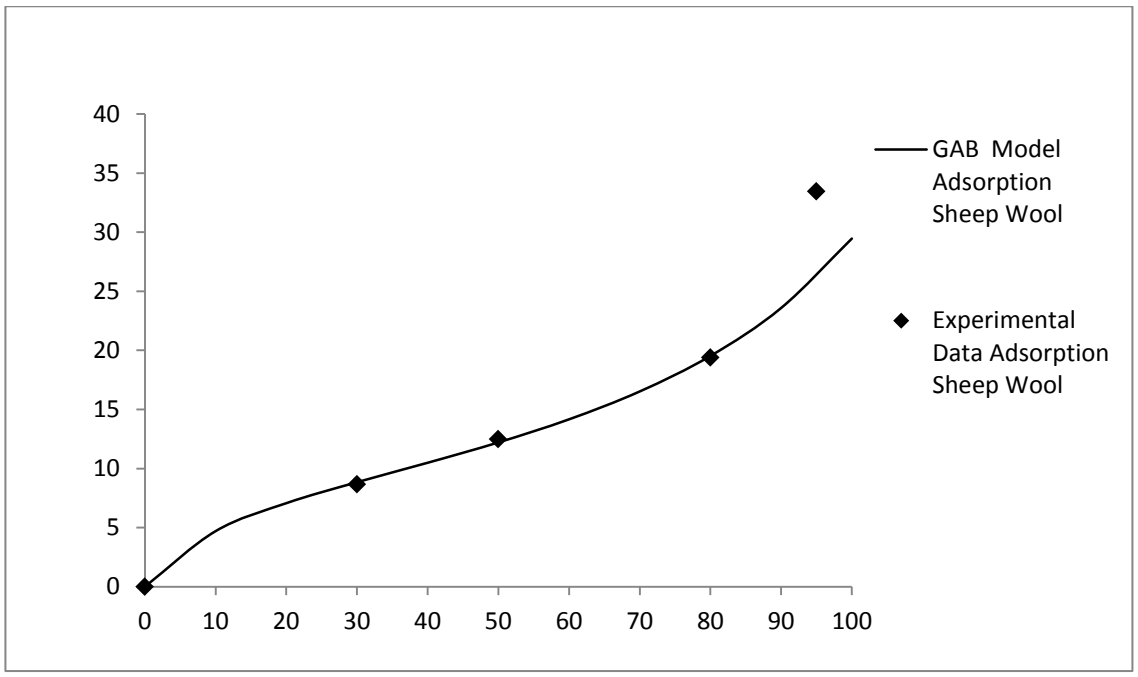


**Figure 5.12: Adsorption-desorption isotherm of sheep wool insulation with GAB fit in relation to average moisture content by weight (AMCw).**

The GAB models of isotherms of products of biological origins are commonly characterised by sigmoidal shapes representing IUPAC type 2 (Blahovec and Yanniotis, 2008; Hill, Norton and Newman, 2008). However, it can be observed that the sorption curves of hemp-2, hemp-3 and hemp-5 are not sigmoidal. This can be explained in terms of the modified classification (Type IIa) of sorption isotherms (Figure 5.13), as proposed by Blahovic and Yanniotis (2008). Similar shapes of sigmoidal and non-sigmoidal regression lines, type IIa and type IIb, were also presented by Collet *et al.* (2011). In their research, they compared two hemp insulation materials using BET and GAB models.

### *5.2.4 Adsorption isotherms in terms of weight and volume*

Figures 5.2 and 5.4 show the comparison of adsorption isotherms between the various insulation materials in terms of mass gain per unit dry mass as a percentage. It can be observed that hemp-2 and hemp-5 are the most hygroscopic materials. All other plant-based insulations are in the middle range in terms of moisture adsorption. This middle range, about 15% to 25% moisture gain, can be assumed as the typical characteristic of most of the hemp fibres as this is the range reported by most of the experimental determination of adsorption isotherms (Collet *et al.*; 2011, Hill, Norton and Newman, 2008; Nilsson, Svennerstedt and Wretfors, 2005). The high adsorption capacity of

hemp-2 and hemp-5 can be advantageous in terms of controlling internal relative humidity and minimising interstitial condensation in an environment with cyclic variations of relative humidity.

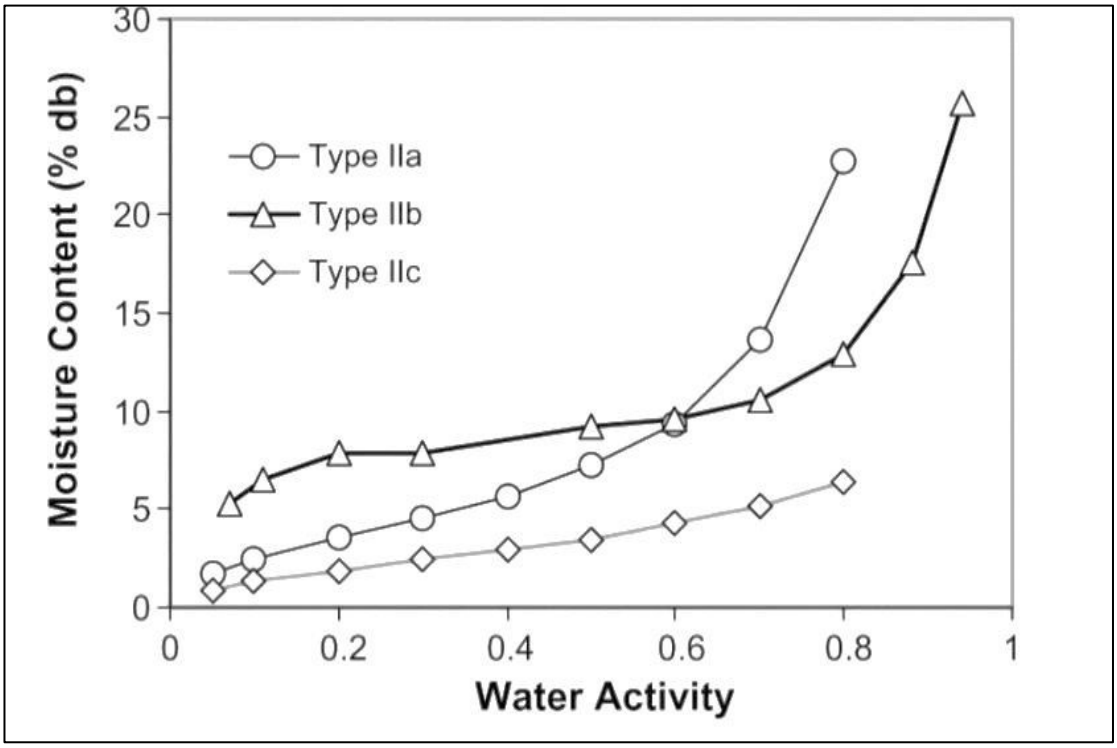


**Figure 5.13: Modified classification of type 2 isotherms (Blahovic and Yanniotis, 2008).**

It can also be observed that in hemp-2 and hemp-4 insulations, both insulations containing higher percentage of hemp fibre, the corresponding adsorption capacities are rapidly increasing at higher water activity ranges, particularly between 70% to 95% relative humidity. It has been mentioned earlier at subsection 3.3.3 of chapter three that at higher water activity, starting from 70% relative humidity, transient micro capillary network is developed in the cellulose and lignocellulosic fibres and capillary condensation becomes increasingly dominant. At the same time, more adsorption sites open up due to the swelling of the cells. There is a likelihood that the observed difference in moisture uptake behaviour of different hemp insulations at higher water activity is due to the different methods of processing of the fibres leading to different mechanical and sorption properties and due to the variations in proportions of the constituent materials in the fibre matrix.

Figures 5.3 and 5.5 compare the insulation materials in terms of weight gain per unit volume. These data are important for building insulation materials, as the insulation materials are produced in various densities. If compared with the data presented in Figure 5.4, it can clearly be noticed that the hierarchy of materials in terms of moisture adsorption capacity is now significantly changed. Wood fibre shows the highest adsorption capacity per unit volume whereas its weight based adsorption capacity was in the middle of the ranges.

Therefore, in practical application, the density of the hygroscopic insulation materials will be a determining factor for their practical hygroscopic capacity. Density can also influence heat capacity and thermal conductivity.

Figure 5.2 and 5.3 show the adsorption capacity of the materials with one standard deviation. The highest standard deviation at higher relative humidity is observed in hemp-2 and sheep wool insulation materials. The lowest standard deviation is observed in wood fibre insulation. It can be assumed that the relatively rigid insulations are more homogenous in nature and show less standard deviation in adsorption capacity, whereas fibrous insulations of relatively lower density and higher flexibility are less homogenous and their adsorption data show higher standard deviations.

### *5.2.5 Hysteresis*

Hysteresis occurs throughout all water activity ranges. In case of hemp insulation materials, hysteresis loop is present between 50% to 95% relative humidity. Figures 5.6 to 5.8 shows hysteresis loops in hemp-1, hemp-2 and hemp-3 insulation materials between 50% to 80% relative humidity, the GAB regression plots confirm the presence of hysteresis loop. The differences between the adsorption and desorption isotherms, as shown in Figures 5.7 and 5.8, reveals that hemp-1 and hemp-3 insulations exhibit higher degree of hysteresis than hemp-2. Both of these insulation materials contain wood fibres. Hemp-4 and hemp-5 show lesser hysteresis. In general, hysteresis is more pronounced where the hemp insulation materials contain wood fibres.

### *5.2.6 Summary of adsorption-desorption isotherm*

Hemp insulations have very high moisture adsorption capacity compared to other fibrous insulations. Hemp insulations obtained from different producers show different moisture adsorption pattern and capacity. This is important in

terms of data input in hygrothermal simulation software. Mineral insulations like stone wool shows negligible hygroscopic capacity. Hysteresis is more pronounced in wood fibre based insulations than in insulations containing higher proportion of hemp fibres. When adsorption capacity is considered in terms of mass per unit dry volume, wood fibre insulation shows higher hygroscopic performance due to its higher density. The role of insulation density is thus important in terms of practical application of the insulation materials.

### *5.3 Determination of moisture buffering capacity*

To determine the practical moisture buffer value ($MBV_{practical}$) of a number of bio-based insulation materials, a moisture buffering experiment was carried out according to the test protocol developed by Nordtest (Rode, 2005). Three samples of each of the following insulation materials were used in the experiment: hemp-1, hemp-2, hemp-3, hemp-4, hemp-5, sheep wool and wood fibre. Since stone wool exhibited negligible capacity for moisture adsorption and desorption, it was excluded from this experiment. Each of the samples had an exposed surface area of 100 mm X 100 mm. The other five surfaces of each sample were sealed with aluminium foil tape, as shown in Figure 5.14. Thickness of each sample was actual product thickness.

The test conditions are shown in Table 5.1. The materials were exposed to cyclic relative humidity conditions. Each 24-hour cycle is a combination of 8 hours' exposure to 75% relative humidity and 16 hours' exposure to 33% relative humidity at 23 °C temperature. As suggested by the Nordtest method, air velocity of about 0.1 ± 0.05 m/s was maintained by two fans with controllers as shown in Figure 5.14.

**Table 5.1: The test conditions of moisture buffering for all the insulation samples.**

| Temperature (°C) | Relative Humidity (%) | Exposure Time (Hours) | Salt Used |
|---|---|---|---|
| 23 ± 0.5 | 33 ± 3 | 16 ± (10 minutes) | $MgCl_2$ |
| 23 ± 0.5 | 75 ± 3 | 8 ± (10 minutes) | NaCl |

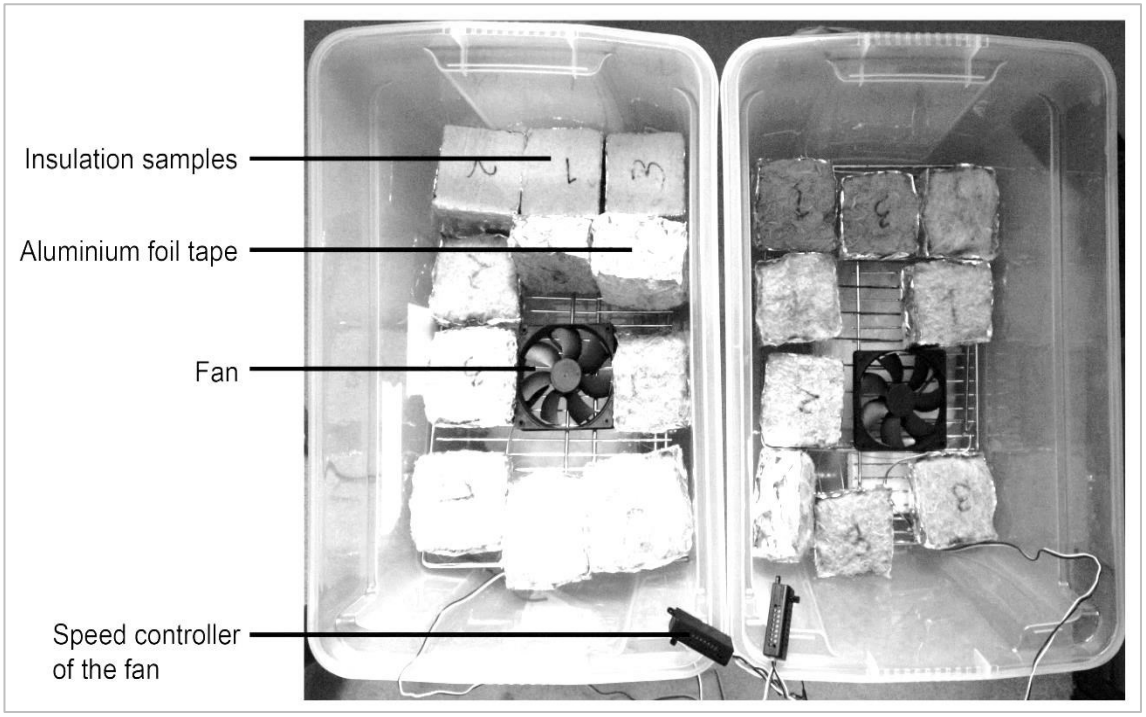


**Figure 5.14: Moisture buffering test setup showing hemp, sheep wool and wood fibre samples.**

At each of the cycles, change of mass of the insulation samples Δm (g) is calculated as the average of the weight gain during adsorption and weight loss during desorption. The experiment is continued until there is not more than 5% variation in 3 consecutive determination of Δm. $MBV_{practical}$ is expressed as weight change per $m^2$ per ΔRH and the unit is g/($m^2$.ΔRH).

The findings of the experiments are shown in the Figure 5.15 and Table 5.2. Figure 5.15 includes 1 standard deviation from the mean value for each of the insulation materials, determined in SPSS. Table 5.3 shows the $MBV_{practical}$ classes (Rode, 2005). Based on these classes, all the insulations show either 'Good' or 'Excellent' $MBV_{practical}$ value. The highest $MBV_{practical}$ is demonstrated by hemp-2 followed by hemp-5.

If the findings are further explored in terms of sorption isotherms, as shown in Figure 5.5, it can be observed that the $MBV_{practical}$ values of the insulation materials are strongly related to their corresponding hygroscopic sorption capacities.

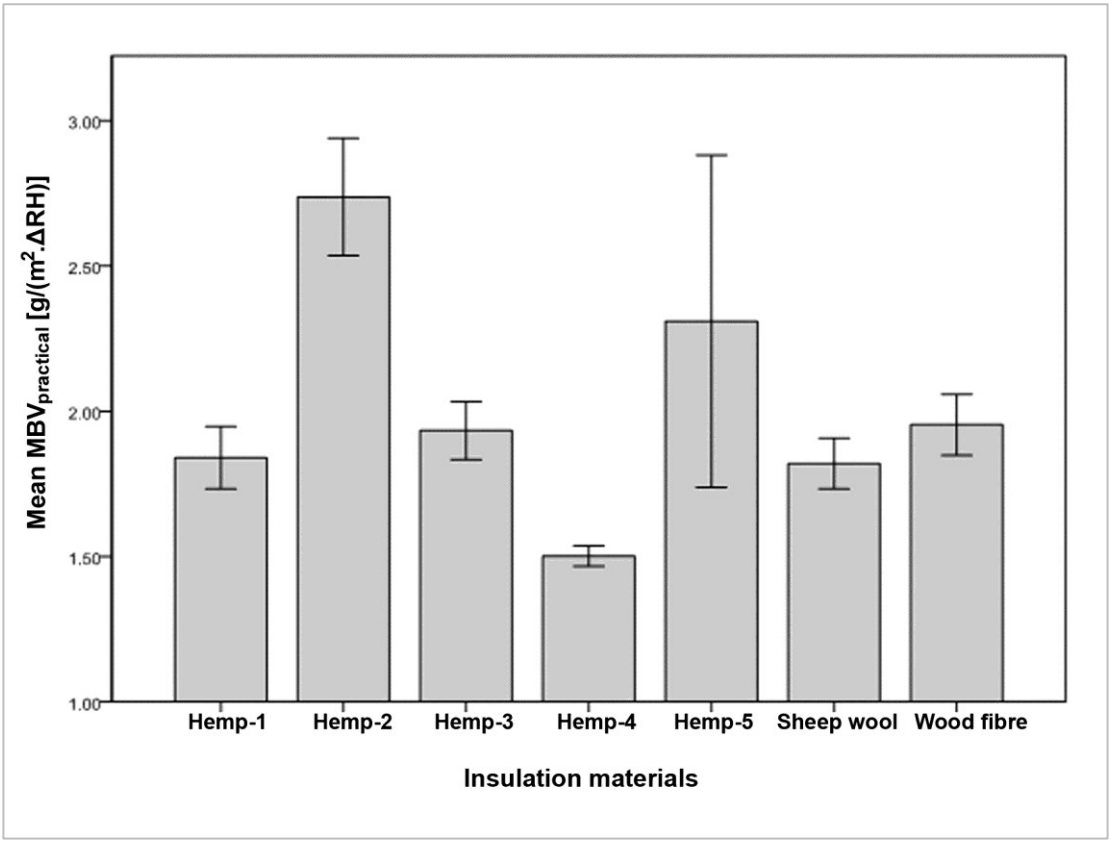


**Figure 5.15: Moisture buffering values with one standard deviation.**

**Table 5.2: Mean practical moisture buffer value of the Hemp insulations.**

| Insulations | $MBV_{practical}$ [g/($m^2$ % RH)] |
|---|---|
| Hemp-1 | 1.84 |
| Hemp-2 | 2.74 |
| Hemp-3 | 1.90 |
| Hemp-4 | 1.50 |
| Hemp-5 | 2.31 |
| Sheep wool | 1.82 |
| Wood fibre | 1.95 |

Figure 5.5 showed that the moisture adsorption capacity of hemp-4 was lowest among the hemp samples, which is also the case in terms of its $MBV_{practical}$ (Figure 5.15 and Table 5.2). Hemp-2 and hemp-5 showed very high moisture adsorption capacity and these findings are also reflected in their respective $MBV_{practical}$ values. Hemp-1, hemp-3, hemp-4 and sheep wool were in the mid-range in terms of hygroscopic capacity, which is also reflected in their performance in terms of $MBV_{practical}$.

**Table 5.3: Ranges for practical Moisture Buffer Value classes (Rode, 2005).**

| $MBV_{practical}$ class | Minimum $MBV_{practical}$ level | Maximum $MBV_{practical}$ level |
|---|---|---|
| | [g/(m$^2$ % RH) @ 8/16h] | |
| Negligible | 0 | 0.2 |
| Limited | 0.2 | 0.5 |
| Moderate | 0.5 | 1.0 |
| Good | 1.0 | 2.0 |
| Excellent | 2.0 | … |

The only difference in this observation is exhibited by wood fibre insulation. Although wood fibre has the highest hygroscopic capacity by volume, its $MBV_{practical}$ is in the mid-range among the samples. One of the key reasons seems to be the difference between the exposed surfaces of wood fibre and the other insulations. While sorption isotherm is determined, all six sides are exposed to the conditioning temperature and relative humidity. Wood fibre insulation, used in the experiment, is consisted of three layers. Each layer is 100 mm thick as shown in Figure 5.16. The layers are adhered to each other with resin. When all the surfaces are open to the environmental conditions during adsorption tests, there will be no difficulty in sorption. However, when only the top surface is exposed for the buffering test and other surfaces are covered with aluminium foils, presumably moisture adsorption and desorption will be influenced by the vapour permeability of those resin based interfaces between the layers. The second reason may be the hysteresis of wood fibre based insulation materials during desorption. Due to considerable hysteresis between sorption and desorption, the desorption part of the cycle can lower the average performance. However, this should not affect much as the difference between sorption and desorption should lessen after a number of cycles.

On the other hand, compared to the layered construction of the wood fibre insulation, hemp and sheep wool insulation materials are homogeneous throughout all the surfaces such as the hemp-2 insulation, comparison between the wood fibre and hemp-2 insulations is shown in Figure 5.16. There is very negligible hysteresis between sorption and desorption of hemp-2 insulation as

shown in figure 5.7. This seems to be the likely reason for their $MBV_{practical}$ values to reflect their corresponding adsorption isotherms.

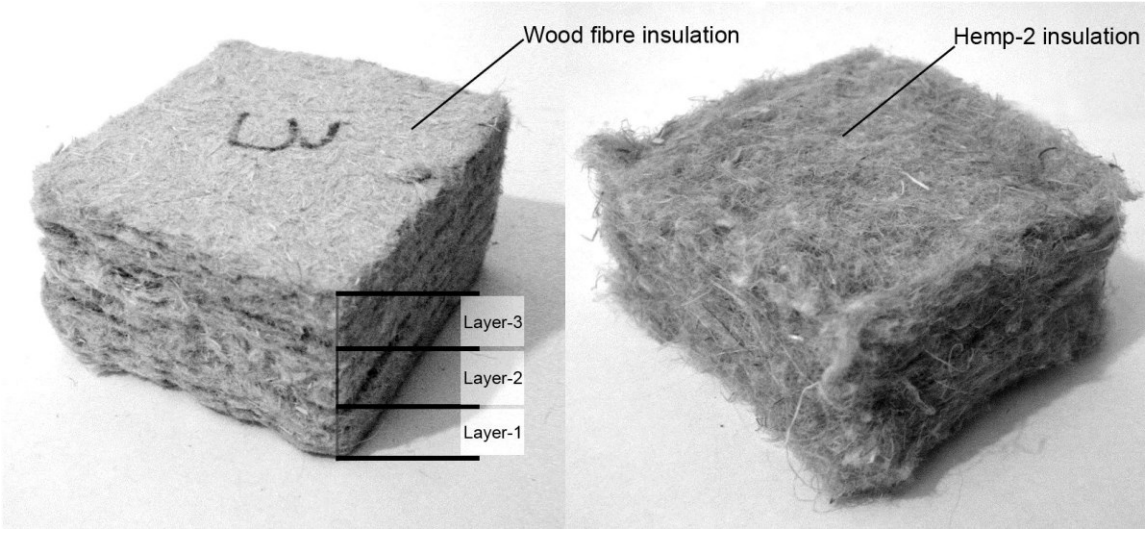


**Figure 5.16: Wood fibre insulation with three layers and hemp-2 insulation.**

### 5.4 Determination of vapour diffusion resistance factor (μ Value)

The vapour diffusion resistance factor, μ, of thermal insulation materials can be determined following the British Standard BS EN 12086 (1997). Five samples of each insulation of a minimum dimension of 50 $cm^2$ and thickness of 40 mm-100 mm are initially conditioned for at least six hours at (23 ± 2) ºC temperature and (50 ± 5) % relative humidity to reach constant mass. Insulation specimens are placed on glass dishes containing desiccants or salt solutions depending on the test type, dry cup or wet cup, respectively. The sides of the insulations are adequately sealed to achieve one directional moisture flow. Thus, the test assembly is the combination of the test specimen, salt solution or desiccant, glass dish and sealant.

For the dry cup test, the relative humidity inside the dishes is 0% and outside the dishes is 50 (±3)%. For the wet cup test, the relative humidity inside the dishes is 93 (±3)% and outside the dishes is 50 (±3)%. The test assembly is initially conditioned in the climate chamber (Figure 5.17) for 1 to 24 hours. The differential of partial vapour pressure between the climate chamber and the test assembly drives the vapour through the specimens. The test assembly is weighed at every 24 hours until five successive determination of change in mass per unit time for each specimen is ± 5% of the mean value.

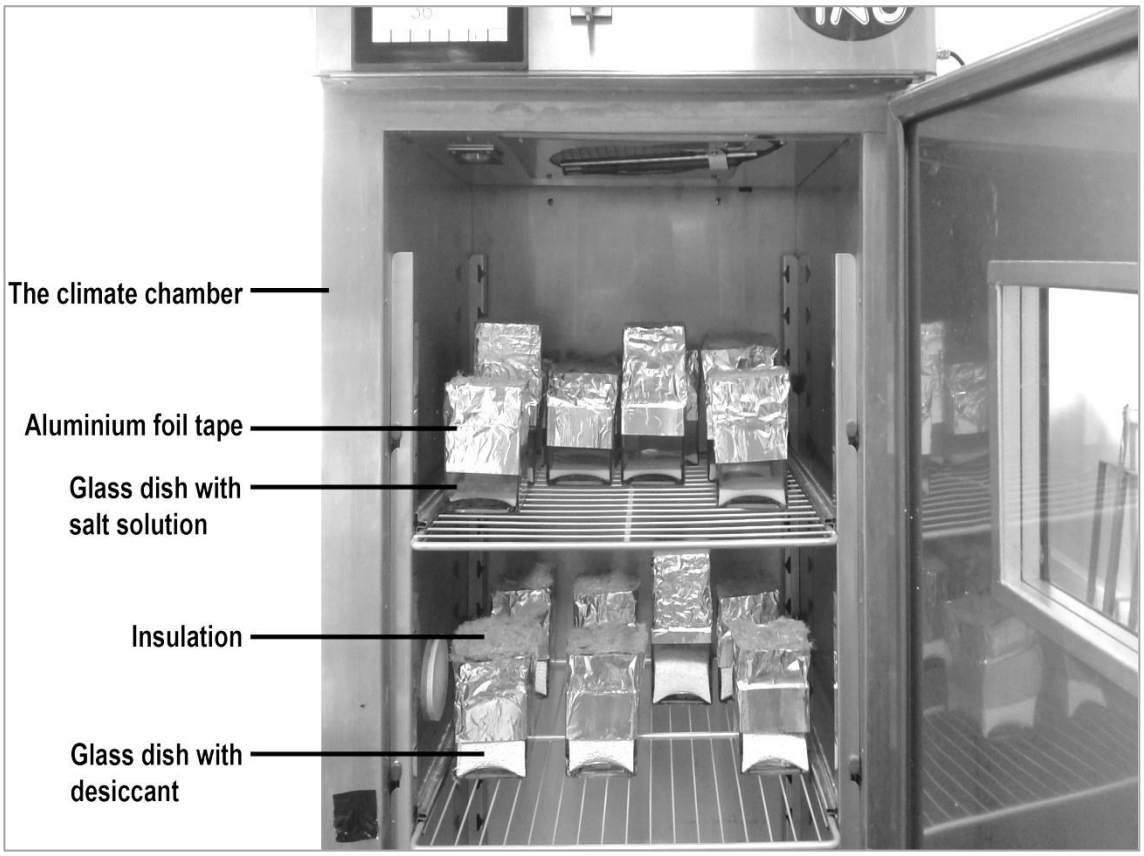


**Figure 5.17: Test setup for assessing vapour diffusion resistance factor.**

The rate of change in mass is calculated from the following equation:

$$G_{1,2} = \frac{(m_2 - m_1)}{(t_2 - t_1)} \qquad [5.1]$$

Where $m_1$ is the mass of the test assembly at time $t_1$ (mg), $m_2$ is the mass of the test assembly at time $t_2$, (mg), $t_1$ and $t_2$ are successive times of weighing (hour), G is the mean of five successive determinations of $G_{1,2}$ (mg/h), where $G_{1,2}$ is within ± 5% of G.

The vapour diffusion resistance factor, μ, is calculated from the following expression:

$$\mu = \frac{\delta_a}{\delta} \qquad [5.2]$$

Where $\delta_{air}$ = Vapour permeability in air and $\delta$ = Vapour permeability of the porous system in the material.

Vapour permeability δ is calculated form the following expression:

$$\delta = W.d \quad [5.3]$$

Where W is water vapour permeance (mg/m$^2$hPa) and d is the test specimen thickness in metres. W is determined from the following expression:

$$W = \frac{G}{(A.\Delta\rho)} \quad [5.4]$$

Where A is the surface area of the specimen in meter squared and Δρ is the pressure difference in Pascal (Pa).

The vapour diffusion equivalent air-layer thickness ($S_d$ Value) is expressed by the following equation:

$$S_d = \mu.d \quad [5.5]$$

Where d is the thickness of the sample (m).

The μ value and $S_d$ value of the insulation samples are shown in Table 5.4, Figure 5.18 and Figure 5.19. Only wet cup test for hemp-5 is performed due to lack of required number of samples. Considerable variations in μ value of the hemp insulation materials are observed. Hemp-5 shows the lowest and hemp-1 shows the highest μ value during the wet cup test. However, the vapour diffusion resistance factor of hemp-5 requires further investigation as the value was less than the value of the vapour diffusion resistance factor of air. During the dry cup test, hemp-4 exhibits the highest and hemp-2 exhibits the lowest μ value among the hemp insulation materials. As shown in Figures 5.18 and 5.19, there are considerable deviations from the mean μ value in hemp-3 and hemp-4 samples during the wet cup and dry cup tests, respectively.

It can be observed in Table 5.4 that the μ value of insulation materials obtained by dry cup tests are always higher than the corresponding μ values obtained by the wet cup tests. This is expected since vapour permeability is moisture dependent and the value of vapour permeability rises with the increase of moisture content of insulation materials.

The non-homogeneity of some of the hemp insulations, as reflected by the high standard deviation from the mean μ value, may make it difficult to predict how the insulations will precisely perform in terms of vapour transmission.

**Table 5.4: μ values and $S_d$ values of the insulations.**

| | μ value (-) | | $S_d$ value (m) | |
|---|---|---|---|---|
| | Dry cup test | Wet cup test | Dry cup test | Wet cup test |
| Hemp-1 | 1.89 | 1.85 | 0.091 | 0.089 |
| Hemp-2 | 1.64 | 1.29 | 0.090 | 0.075 |
| Hemp-3 | 2.54 | 1.43 | 0.119 | 0.059 |
| Hemp-4 | 2.74 | 1.50 | 0.123 | 0.064 |
| Hemp-5 | - | 0.51 | - | 0.029 |
| Sheep wool | 3.01 | 1.15 | 0.127 | 0.031 |
| Wood fibre | 4.16 | 3.04 | 0.405 | 0.31 |

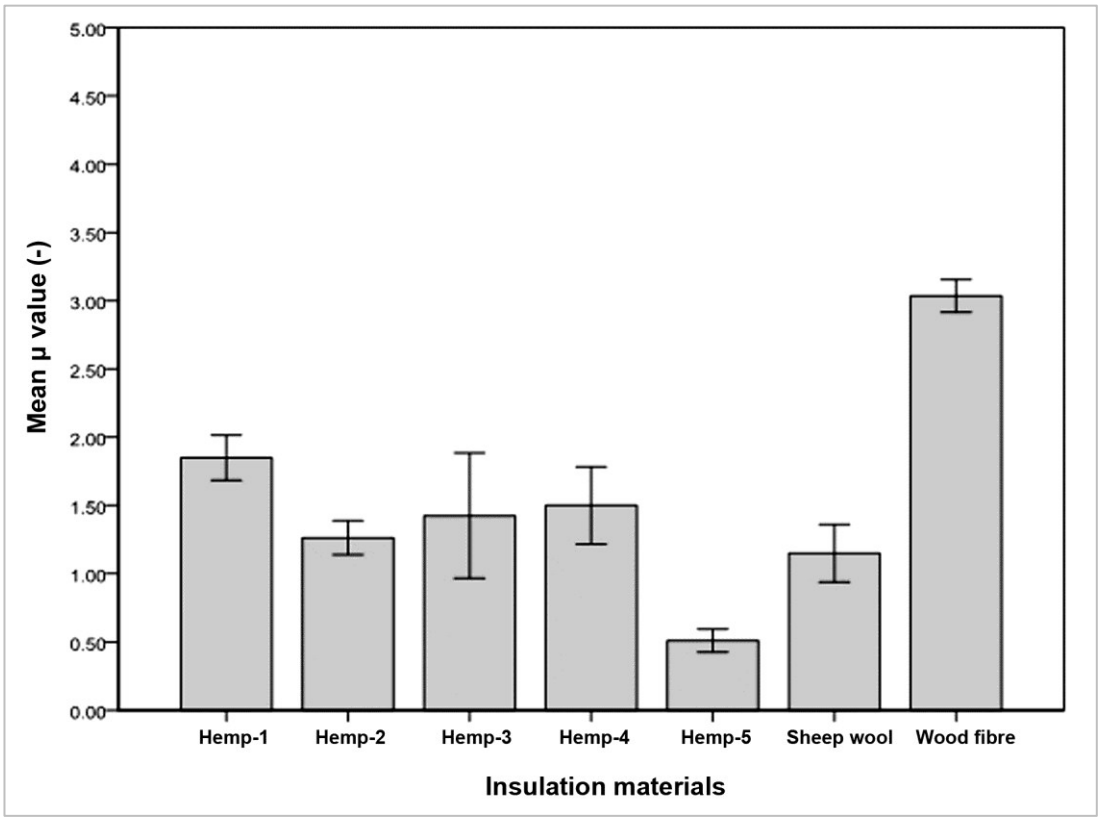


**Figure 5.18: Mean μ value with one standard deviation determined by wet cup tests**.

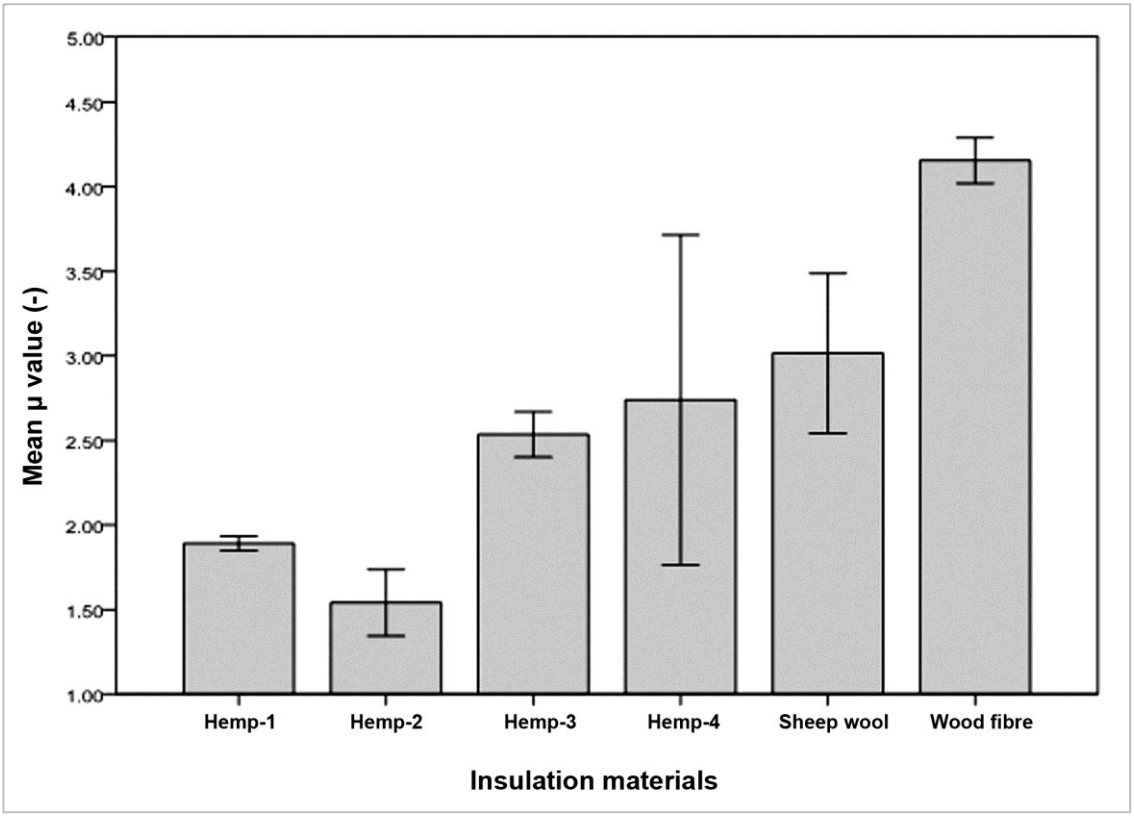


**Figure 5.19: Mean μ value of the insulations determined by dry cup test.**

### 5.5 Determination of water absorption coefficient (A value)

The methods for experimentally determining water absorption coefficient by partial immersion or the A value of building materials are outlined in the British Standard BS EN 15148 (2002). The test specimens are conditioned to the temperature of 18 °C to 28 °C with allowed temperature variation during the tests of ± 2 °C and relative humidity of 40% to 60% with allowed relative humidity variation during tests of ± 5%. Samples are conditioned to the test condition so that the change of mass is 0.1% of total mass when measured over 24-hour intervals. Samples are placed in a tank, resting on point supports so that the bases of the samples do not touch the tank surfaces. The tanks are filled with water so that the water level is (5 ± 2) mm above the highest point of the base of the specimen, as shown in Figure 5.20. The sides of the samples are sealed with water and vapour tight sealant. Samples are weighed at the following times from the beginning: 5 minutes, 20 minutes, 1 hour, 2 hours, 4 hour, 8 hours and another 2 times including one at the 24th hour.

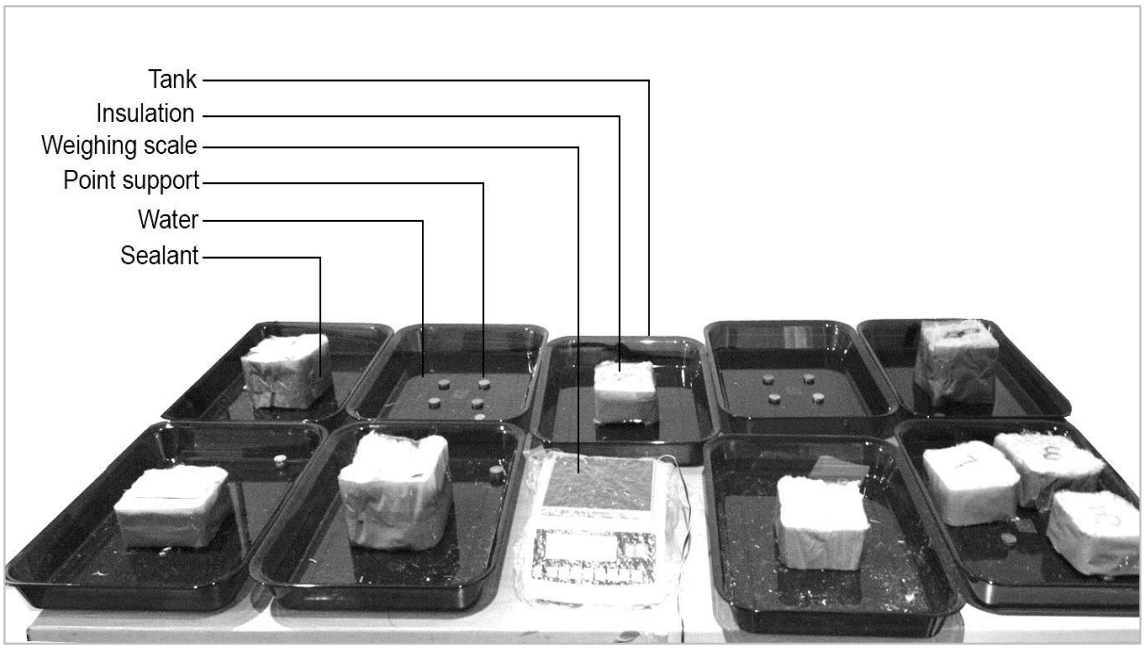


**Figure 5.20: Setup for assessing water absorption coefficient or A-value.**

The difference of mass per area between each weighing and the initial weighing is measured using the following equations:

$$W = \frac{(m_t - m_i)}{a} \quad [5.6]$$

Where $m_t$ = mass at any time of weighing (kg), $m_i$ = mass at initial weighing (Kg) and a = surface area of the sample in contact with water ($m^2$).

According to the British standards, the A value can be expressed as $A_w$, $W_w$, $A_{w,24}$ or $W_{w,24}$. To determine the A value, $\Delta m_t$ is plotted against the square root of the weighing times. When a straight line can be drawn through the values of $\Delta m_t$, the line is extrapolated back to zero time where the value of the intercept is $\Delta m'_0$. Water absorption coefficient $A_w$ can be determined by the following equation:

Either,

$$A_w = \frac{\Delta m'_{tf} - \Delta m'_0}{\sqrt{tf}} \quad [5.7]$$

Or

$$W_w = \frac{\Delta m'_{tf} - \Delta m'_0}{\sqrt{tf}} \quad [5.8]$$

Where $\Delta m'_{tf}$ (kg/m$^2$) is the value of Δm at 'tf' time. The time 'tf' is 1 day expressed in seconds in equation 5.7 and is 1 day expressed in hours in equation 5.8.

When the plot of $\Delta m_t$ against square root of the time does not give a straight line, the equation for A value will be any of the following expressions:

Either,

$$A_{w,24} = \frac{\Delta m'_{tf}}{\sqrt{tf}} = \frac{\Delta m'_{tf}}{\sqrt{86400}} \quad [5.9]$$

Or

$$W_{w,24} = \frac{\Delta m'_{tf}}{\sqrt{tf}} = \frac{\Delta m'_{tf}}{\sqrt{24}} \quad [5.10]$$

Where $\Delta m'_{tf}$ (kg/m$^2$) is the value of Δm at 'tf' time. The time 'tf' is 1 day expressed in seconds in equation 5.9 and is 1 day expressed in hours in equation 5.10.

The A value test was conducted for the following insulations: hemp-1, hemp-2, hemp-3, hemp-4, hemp-5. Three samples of each of these insulations were tested. Wood fibre was also included in the test but the test could not be performed as the bottom layers of wood fibre samples dislodged during the test. Sheep wool is hygrophobic and therefore, is excluded from the test.

Figures 5.21-5.25 show the Δmt versus √s plots for hemp-1, hemp-2, hemp-3, hemp-4 and hemp-5 insulations, respectively. In all the cases, the graph of Δmt against √s does not give a straight line, but curves. In these cases, A value can be determined by applying equation 5.8 or equation 5.9. For the present tests, equation 5.8 has been applied and the A values have been determined in terms of $A_{w,24}$.

Figure 5.26 and Table 5.5 show the $A_{w,24}$ values of hemp-1, hemp-2, hemp-3, hemp-4 and hemp-5. Except hemp-1 insulation, all other hemp insulation materials exhibit about similar $A_{w,24}$ values.

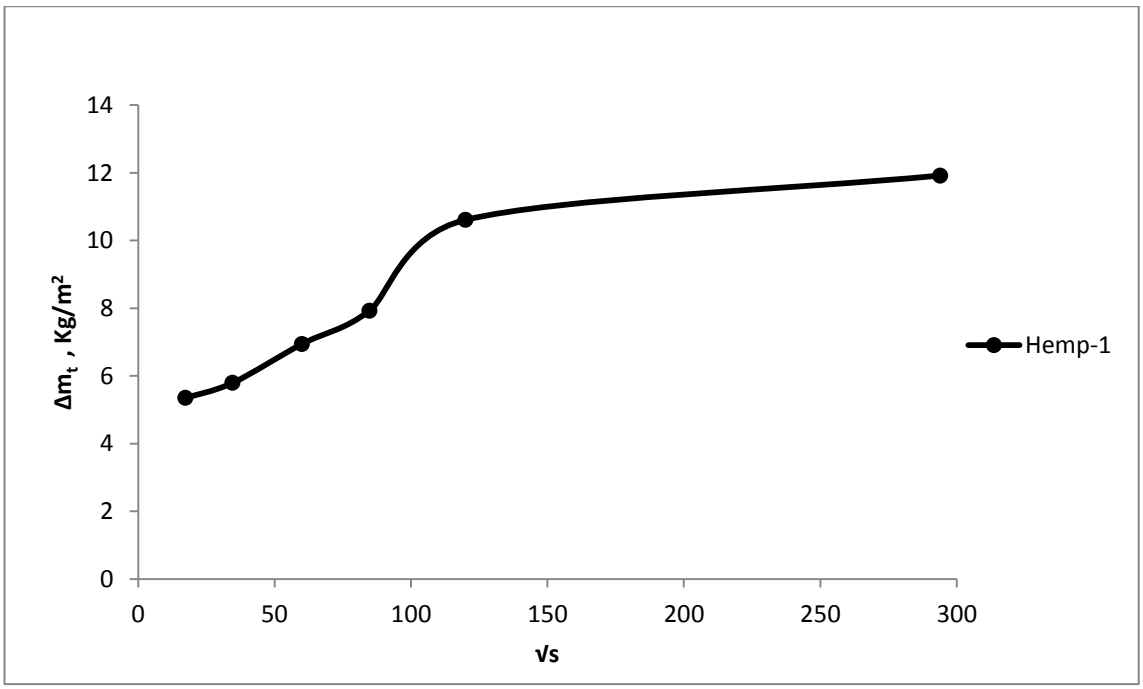


**Figure 5.21: Δmt versus √s plot for hemp-1 insulation, average values of 3 samples.**

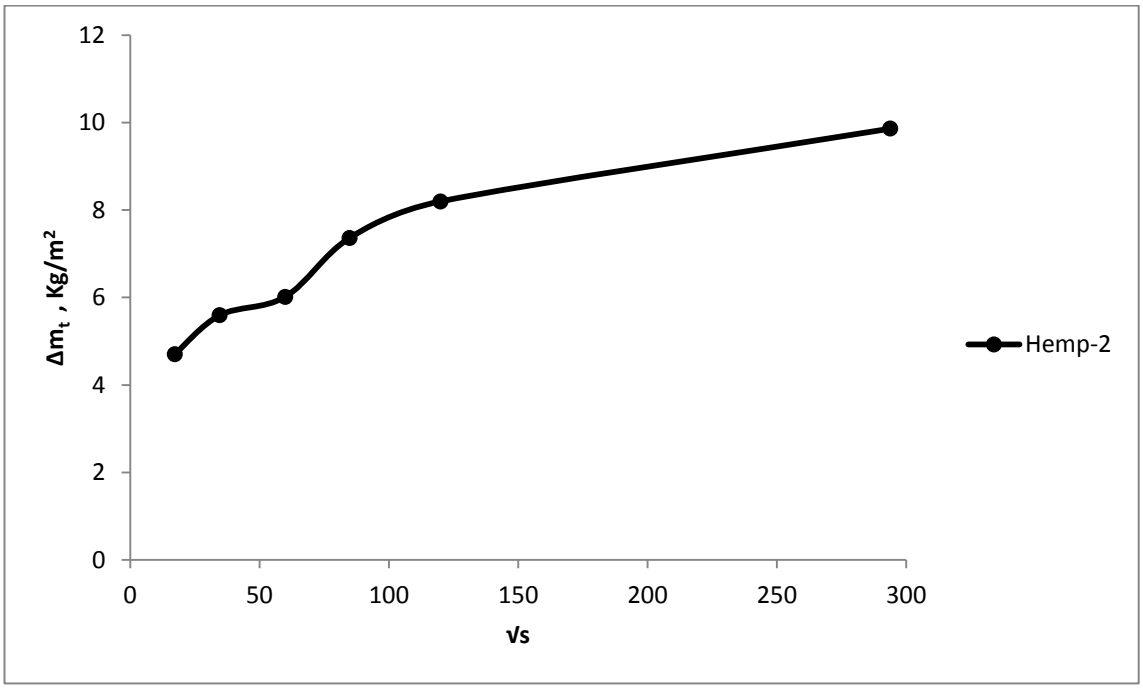


**Figure 5.22: Δmt versus √s plot for hemp-2 insulation, average values of 3 samples.**

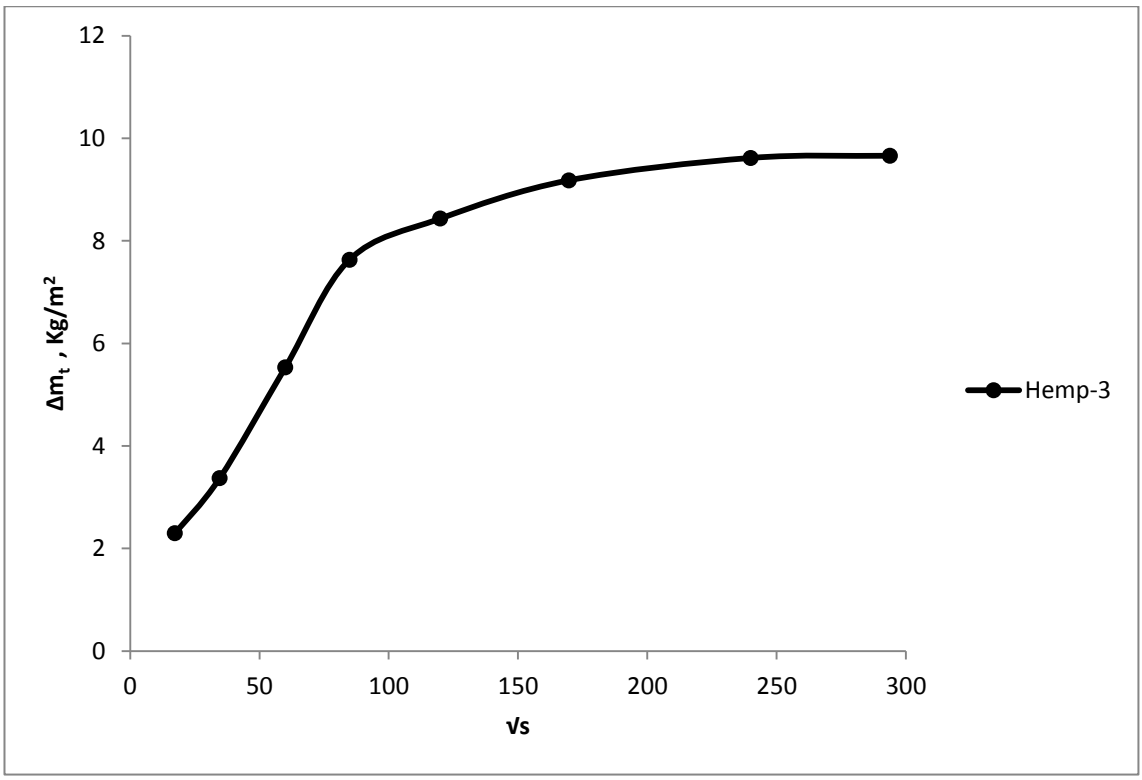


**Figure 5.23: Δmt versus √s plot for hemp-3 insulation, average values of 3 samples.**

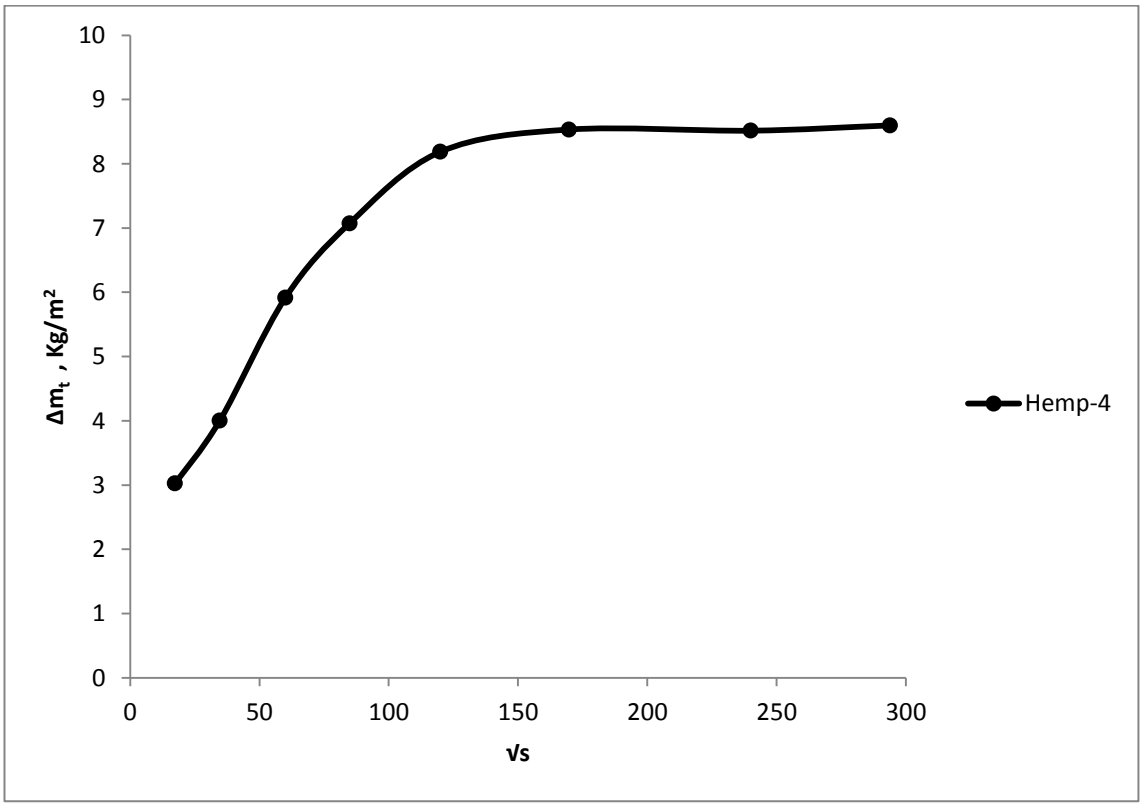


**Figure 5.24: Δmt versus √s plot for hemp-4 insulation, average values of 3 samples.**

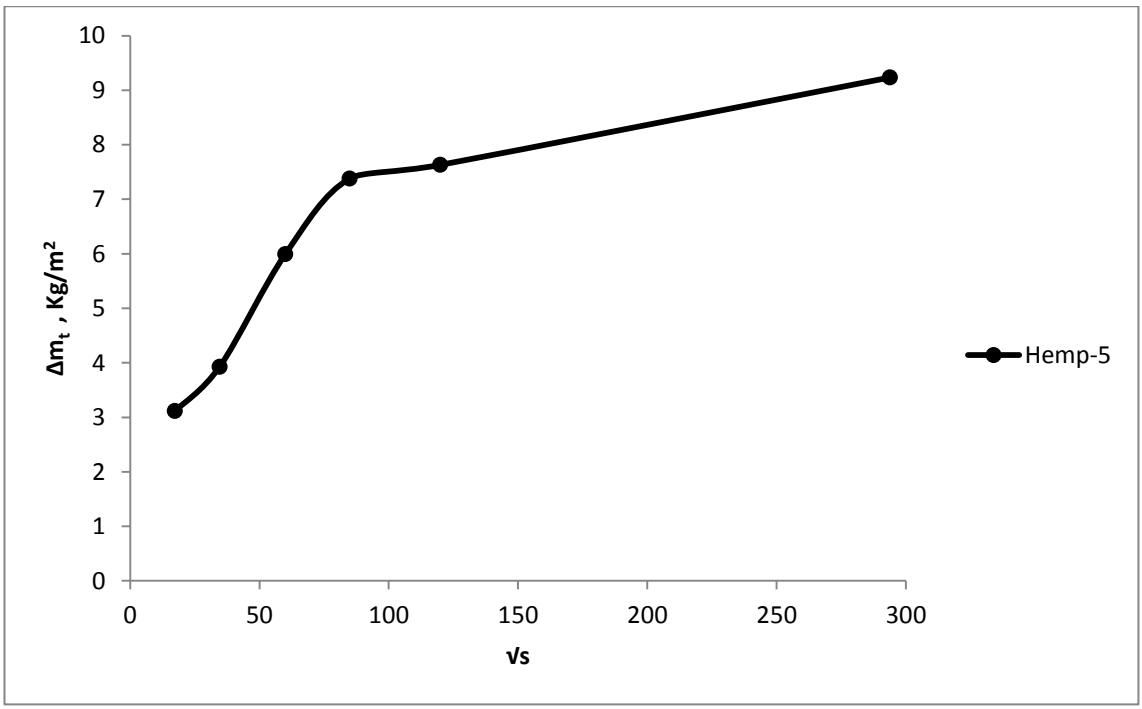


**Figure 5.25: Δmt versus √s plot for hemp-5 insulation, average values of 3 samples.**

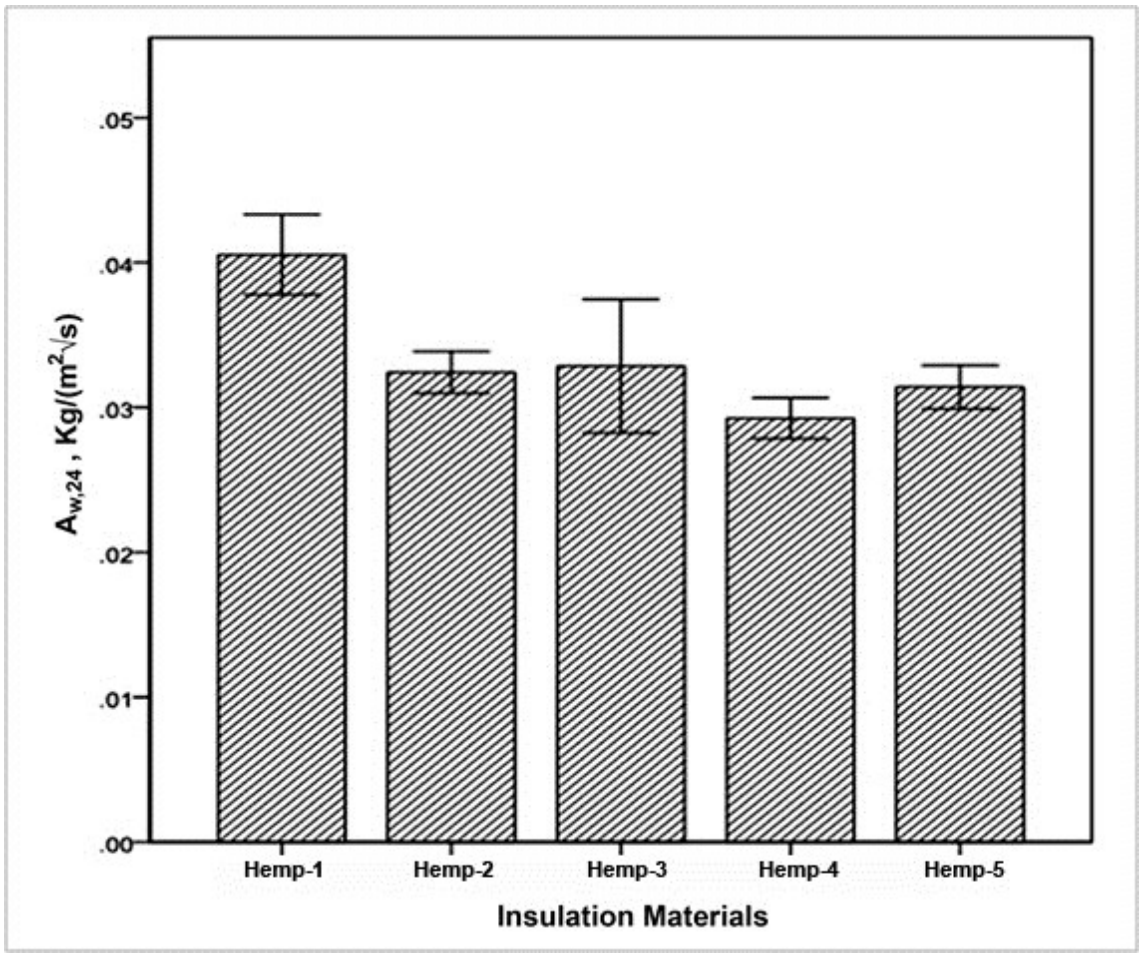


**Figure 5.26: The A value of Hemp insulations with one standard deviation.**

**Table 5.5: Mean $A_{w,24}$ value of the Hemp insulations.**

| Insulations | A Valu ($Kg/m^2\sqrt{s}$) |
|---|---|
| Hemp-1 | 0.041 |
| Hemp-2 | 0.034 |
| Hemp-3 | 0.033 |
| Hemp-4 | 0.029 |
| Hemp-5 | 0.031 |

During the determination of the A values, it was observed that the long-term contact with liquid water could change the structure of the insulation surface that was in contact with water. Fibres were hardened and compacted near the surface and the density near the surface seemed to increase as a result. The implication of this on the thermal conductivity and vapour diffusion may need further studies. In the case of the wood fibre insulation, one of the plies disintegrated during the course of the experiment and the A value was not determined. Structural integrity of the wood fibre insulations, built of multiple layers, when in contact with liquid water for substantial period of time may need further examination.

### 5.6 Chapter summary

The standard steady state tests were used to assess the four important hygric characteristics of the selected insulations, which are: adsorption-desorption isotherms, practical moisture buffer values, vapour diffusion resistance factors and water absorption coefficients (A value). Most of the data, except the moisture buffering value, can be used as input for hygrothermal simulation software.

In relation to adsorption-desorption isotherm, hemp insulation materials exhibited higher moisture adsorption capacity compared to other fibrous insulations. Hemp insulations obtained from different manufacturers showed different moisture adsorption pattern and capacity. At 95% relative humidity, hemp-2 and hemp-5 adsorbed about three times the amount of moisture that

the other hemp insulations adsorbed. Between 0% to 60% relative humidity, sheep wool adsorbed the highest amount of moisture and at 95% relative humidity sheep wool adsorbed about half that of hemp-2. Mineral insulations like stone wool showed negligible hygroscopic capacity. Hysteresis was more pronounced in wood fibre based insulations than in insulations containing higher proportion of hemp fibres. When adsorption capacity was considered in terms of mass per unit dry volume, wood fibre insulation showed higher hygroscopic performance due to its higher density. This is important in terms of practical application of the insulation materials. It can be assumed that the relatively rigid insulations are more homogenous in nature and showed less standard deviation in adsorption capacity, whereas fibrous insulations of relatively lower density and higher flexibility are less homogenous and their adsorption data showed higher standard deviations.

In relation to practical moisture buffer value, hemp-2 and hemp-5 showed 'excellent' moisture buffering capacity. Hemp-1, hemp-3, hemp-4, sheep wool and wood fibre exhibited 'good' moisture buffering capacity. It was observed that the insulation materials with higher moisture adsorption capacity showed higher $MBV_{practical}$ values.

In terms of μ values of the insulations, wood fibre showed the highest μ values, of 4.16, during the dry cup test and 3.04 during the wet cup test. Considerable variations in μ values of the hemp insulation materials were observed. Hemp-5 showed the lowest and hemp-1 showed the highest μ value during the wet cup test. During the dry cup test, hemp-4 exhibited the highest and hemp-2 exhibited the lowest μ value among the hemp insulation materials. There were considerable deviations from the mean μ value in hemp-3 and hemp-4 during the wet cup and dry cup tests respectively. It was observed in Table 5.4 that the μ value of insulation materials obtained by dry cup tests were always higher than the corresponding μ values obtained by the wet cup tests. This is expected since vapour permeability is moisture dependent and the value of vapour permeability rises with the increase of moisture content of insulation materials.

The A values of the insulation materials were determined in terms of $A_{w,24}$. The $A_{w,24}$ values of hemp-2, hemp-3, hemp-4 and hemp-5 insulation materials were equal to the second decimal point, the value being 0.03 kg/($m^2\sqrt{s}$). The $A_{w,24}$

value of hemp-1 was 0.04, which was 33% higher than the $A_{w,24}$ values of other hemp insulations.

During the A value tests, it was observed that long-term contact with liquid water hardened the surface of the hemp insulation and increased the density of that surface. This change in surface structure may have implication on the thermal conductivity and vapour diffusion resistance factor of hemp insulations. The multi-layered wood fibre insulation disintegrated during long-term contact with liquid water. Therefore, structural integrity of multi-layered wood fibre insulations in contact with liquid water may need further examination.

# Chapter 6

# Dynamic and Quasi Steady State Experiments

## 6.1 Introduction to the dynamic and quasi steady state experiments

This chapter addresses the research objectives of determining heat and moisture management capacity of hemp insulations by conducting laboratory based experimental tests. In accordance with the research methods outlined in subsection 4.3.2 of chapter four, the present chapter focuses on system level tests comprising of dynamic and quasi steady state experiments.

Standard tests on building materials to determine their hygrothermal properties provide adequate assessment of their behaviour and performance in steady state conditions. However, dynamic conditions represent more realistic hygrothermal boundary conditions. Building materials may behave differently in those conditions due to their differing thermal and hygric mass. Materials with similar thermal conductivity may have significantly different heat capacity and materials with similar vapour diffusion resistance factor may have significantly different moisture adsorption capacity, which may result in varied hygrothermal behaviour of the materials in dynamic boundary conditions.

In this chapter, a number of tests have been carried out to assess the hygrothermal properties of the insulation materials in dynamic and quasi steady state conditions. For this research, dynamic and quasi steady state conditions are defined below:

**Dynamic condition:** In dynamic conditions, the temperature difference between the two opposite surfaces of an insulation sample or an insulation assembly changes with time. The relative humidity conditions, which the insulation or insulation assembly is exposed to, also change with time. Here, insulation assembly is defined as a combination of an insulation material and any other materials.

**Quasi steady state condition:** In quasi steady state conditions, adopted in this thesis, the temperature difference between the two opposite surfaces of an insulation sample or insulation assembly does not change with time. The relative humidity conditions, which the insulation material or the insulations assembly is exposed to, change as a step function of time as described in test-6.2 below.

Table 6.1 provides a brief overview of the experimental tests described in this chapter.

**Table 6.1: Overview of the experimental tests.**

| Name | Number of experimental runs | Test Materials | Test Type |
|---|---|---|---|
| Test-6.1 | 2 | Hemp-2, stone wool | Dynamic Test |
| Test-6.2 | 1 | Hemp-2, stone wool | Quasi steady state test |
| Test-6.3 | 3 | Hemp-2 | Steady state test |
| Test-6.4 | 1 | Hemp-1, hemp-4, stone wool, sheep wool | Steady state test |

The present chapter describes the following four laboratory based experimental tests:

**Test- 6.1:** Test-6.1 describes the laboratory based experiments to determine the heat and moisture management capacity of hemp-2 and stone wool insulation in dynamic hygrothermal boundary conditions. In relation to moisture management, the experiments particularly focus on interstitial condensation and drying out of the insulations. As a result of this test, the effect of the dynamic hygrothermal boundary conditions on heat and moisture flux through hemp-2 and stone wool insulation can be better understood.

**Test-6.2:** Test-6.2 describes the laboratory based experiment to determine the heat and moisture management capacity of hemp-2 and stone wool insulation materials in quasi steady state conditions. Similar to test-6.1, interstitial condensation and drying out of insulations are given particular focus. In each

time step of 24 hours, insulations are exposed to relative humidity conditions to reach EMC.The insulations are exposed to a constant temperature difference and step changes of relative humidity so that the effect of relative humidity on moisture and heat management of hemp-2 and stone wool insulations can be better understood.

**Test-6.3:** Test-6.3 consists of three experimental runs to study the nature of heat flux and moisture migration along the depth of the insulations. The tests represent the conventional steady state test methods of determining thermal conductivity of moistened insulations that involves covering the insulations with vapour impermeable cling film. The insulation is conditioned in a climate chamber to achieve 80% and 95% EMC before conducting the steady state tests. These tests attempt to show the limitations of the conventional method of measuring thermal conductivity in representing the thermal behaviour of insulations in vapour open walls.

**Test- 6.4:** High relative humidity and condensation in loft space is a concern in many UK buildings. As such, the objective of this experiment was to assess the moisture management capacity of the insulations in a humid loft space. At the same time, the equivalent thermal conductivity values of the insulations can also be determined. The heat and moisture management capacities of hemp-1, hemp-4, sheep wool and stone wool insulations were determined during the experimental runs resembling the hygrothermal conditions of a loft space.

Hemp-2 insulation material was selected for test-6.1 to test-6.3 for the following reasons: Among the hemp insulation materials, hemp-2 and hemp-4 insulation materials contain mostly hemp fibres in the insulation matrix. However, hemp-4 is too flexible for vertical installation. Therefore, hemp-2 insulation, with high hemp content, wass selected for the tests involving vertical installation of the insulation materials.

For test-6.4, hemp-1 and hemp-4 insulations were selected. Hemp-1 and hemp-4 were selected for the following reasons:

- Hemp-1 and hemp-4 insulation materials were selected to study the performance of hemp insulation materials with lower and higher hemp content, respectively.

- Although both hemp-2 and hemp-4 insulations contains higher amount of hemp in the insulation matrix, hemp-4 is particularly selected for the test as it is manufactured for loft applications.

Sheep wool and stone wool insulations were also assessed during test-6.4 for the purpose of comparing the hygrothermal behaviour of hemp-1 and hemp-4 insulations with these insulation materials.

The following notations are developed and used by the author in the present and subsequent chapters in order to explain the experimental tests, in situ tests and the hygrothermal simulation runs:

**(Insulation)-material interface:** the interface between the insulation and the material. The word 'insulation' was replaced by the name of the insulation and the word 'material' was replaced by the name of the next external layer to the insulation.

## 6.2 Dynamic hygrothermal performance of hemp-2 and stone wool insulation materials: test-6.1

### *6.2.1 Introduction*

The aim of this experiment was to assess the moisture management capacity, the likelihood of condensation and the equivalent thermal conductivity of hemp-2 and stone wool insulation materials in a dynamic hygrothermal hotbox setup (Latif, 2011). Both insulation materials were exposed to identical hygrothermal conditions. The moisture management capabilities of the insulation samples were explored and equivalent thermal conductivity values were determined from heat flux, temperature and relative humidity readings. The experimental setup is henceforth referred to as a 'dual-insulation dynamic hygrothermal hotbox setup'.

### *6.2.2 The sample insulation materials*

The measured material properties of the sample insulation materials and manufacturers' declared thermal conductivity values of the insulation materials are provided in Table 4.1 and Table 4.2 of chapter four.

### *6.2.3 The experimental setup*

The experimental setup consists of the following equipment and sensors:

#### *6.2.3.1 The dynamic hygrothermal hot box*

The dynamic hygrothermal hot box has been described in subsection 4.5.2.3 of chapter four. The individual parts and the assembled dynamic hygrothermal hot box are shown in the Figure 4.40 of chapter four. Figure 6.1 shows the cross section of the dynamic hygrothermal hot box.

#### *6.2.3.2 The air conditioner*

A 2.5 KW portable air conditioner was used to lower the temperature in the cold chamber. The temperature control range is between 15° C to 25 °C. A baffle has been placed in front of the air conditioner to reduce nonhomogeneous convective airflow on the acrylic surface.

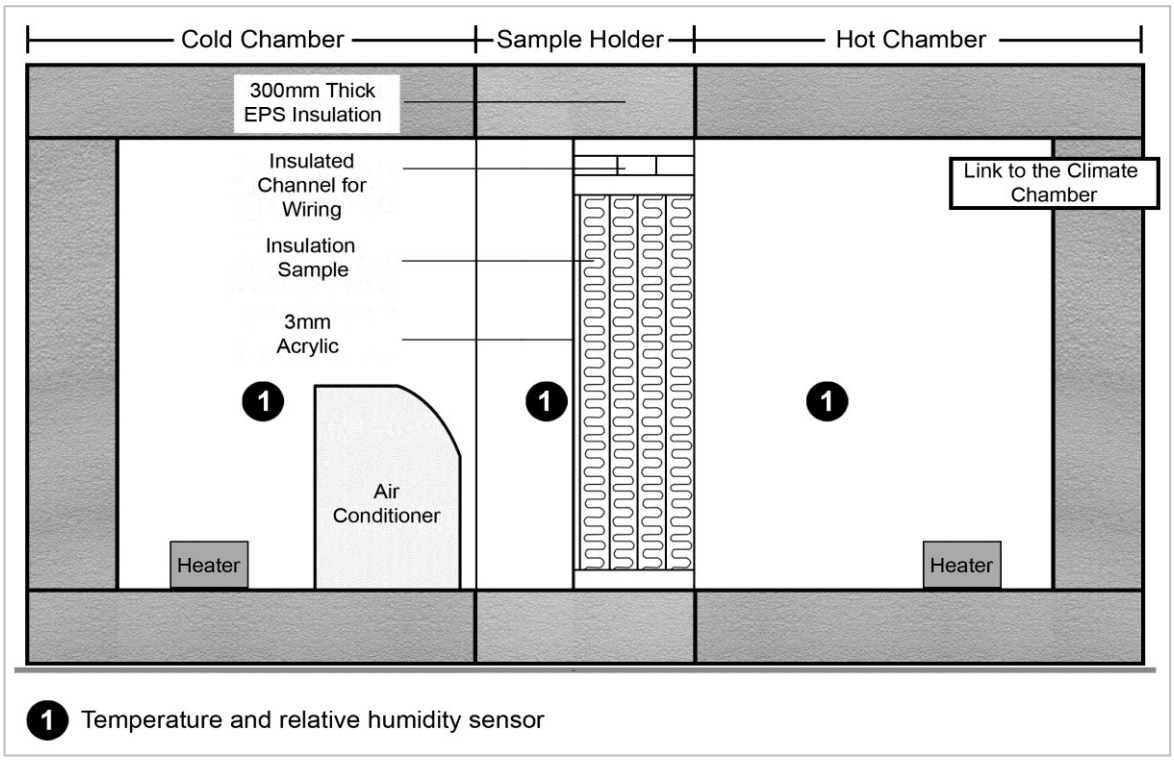


**Figure 6.1: The cross section of the setup showing the dynamic hygrothermal hot box and the air-conditioner.**

#### *6.2.3.3 Temperature and relative humidity sensors*

CS215 temperature and relative humidity sensors were used to measure temperature and relative humidity together. 107 thermistor probes were used to measure temperature. The technical details of 107 thermistor probe and CS215 temperature and relative humidity probe can be found in subsections 4.5.1.4

and 4.5.1.5, respectively, of chapter four. In addition to these sensors, temperature and relative humidity data loggers (EL-USB-2) by Lascar Electronics were used. The temperature measurement range of the EL-USB-2 data logger is -35 °C to 80 °C and accuracy is ± 0.5 °C. The humidity measurement range is 0% to 100% and accuracy is ±3%.

#### *6.2.3.4 Heat flux sensors*

HFP01 heat flux sensors were used to measure the heat flux through the insulation. The technical details of the heat flux sensors can be found in subsection 4.5.1.6 of chapter four.

#### *6.2.3.5 Isomet needle probe*

Isomet needle probes measure thermal conductivity applying transient method. Further details are provided in subsection 4.5.1.8 of chapter four. In this experiment Isomet needle probe was used to measure thermal conductivity randomly during the experiment.

#### *6.2.3.6 CR1000 data logger*

CR1000 data logger was used for gathering data from the sensors and probes. A brief description of CR1000 data logger is provided in subsection 4.5.1.3 of chapter four. The data can be displayed in the computer by using the PC400 software. CR 1000 data logger can also be connected to PC 200w software. CR1000 data logger and the PC400 software were also used to control the temperature profile of the internal heaters of the hygrothermal hot box.

### *6.2.4 Material preparation and instrumentation*

The insulation materials were kept in the laboratory conditions of 50% relative humidity and 23°C temperature for 3 months. The insulation materials were partially sliced and opened up along its depth to accommodate the temperature, relative humidity and heat flux sensors, as shown in Figure 6.2.

Each of the insulation samples was fitted with one heat flux sensor, four temperature and relative humidity sensors, two temperature sensors and one Isomet needle probe. All the sensors are stitched to the insulations with cotton thread. Once the sensors are robustly placed, the partially opened layers are sewn together with cotton threads. Figure 6.3 shows the schematic of the arrangement.

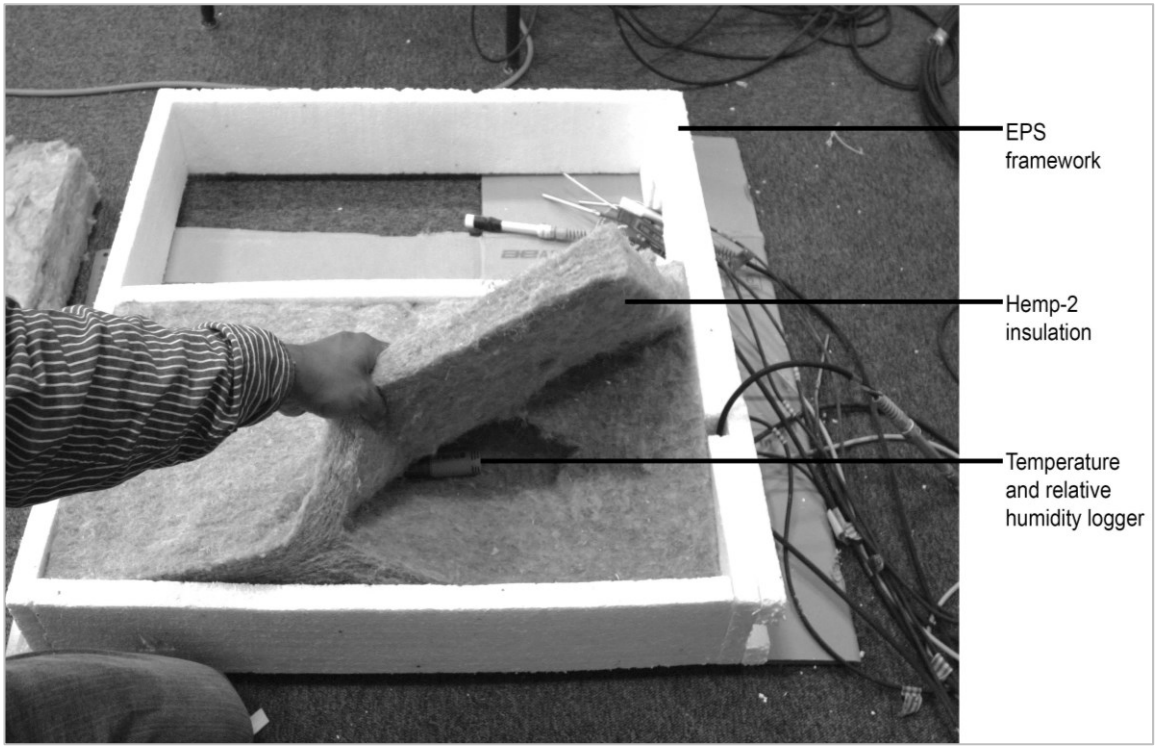


**Figure 6.2: Installation of sensors inside the insulation.**

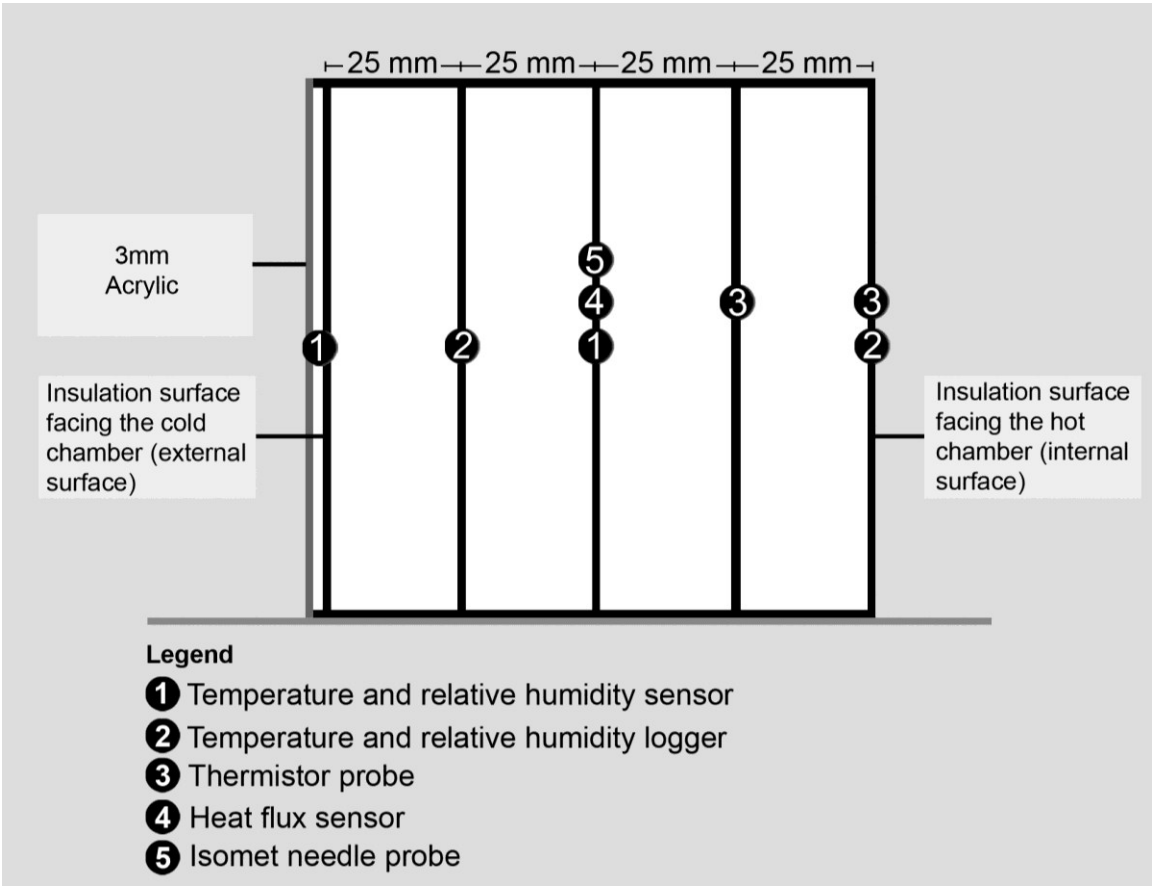


**Figure 6.3: The cross section of the insulation sample showing the position of the sensor and probes.**

The two insulation samples are placed side by side in a 30 mm EPS framework (the dual insulation setup) and the samples are separated by a 30 mm layer of EPS insulation, as shown in Figures 6.4 and 6.5.

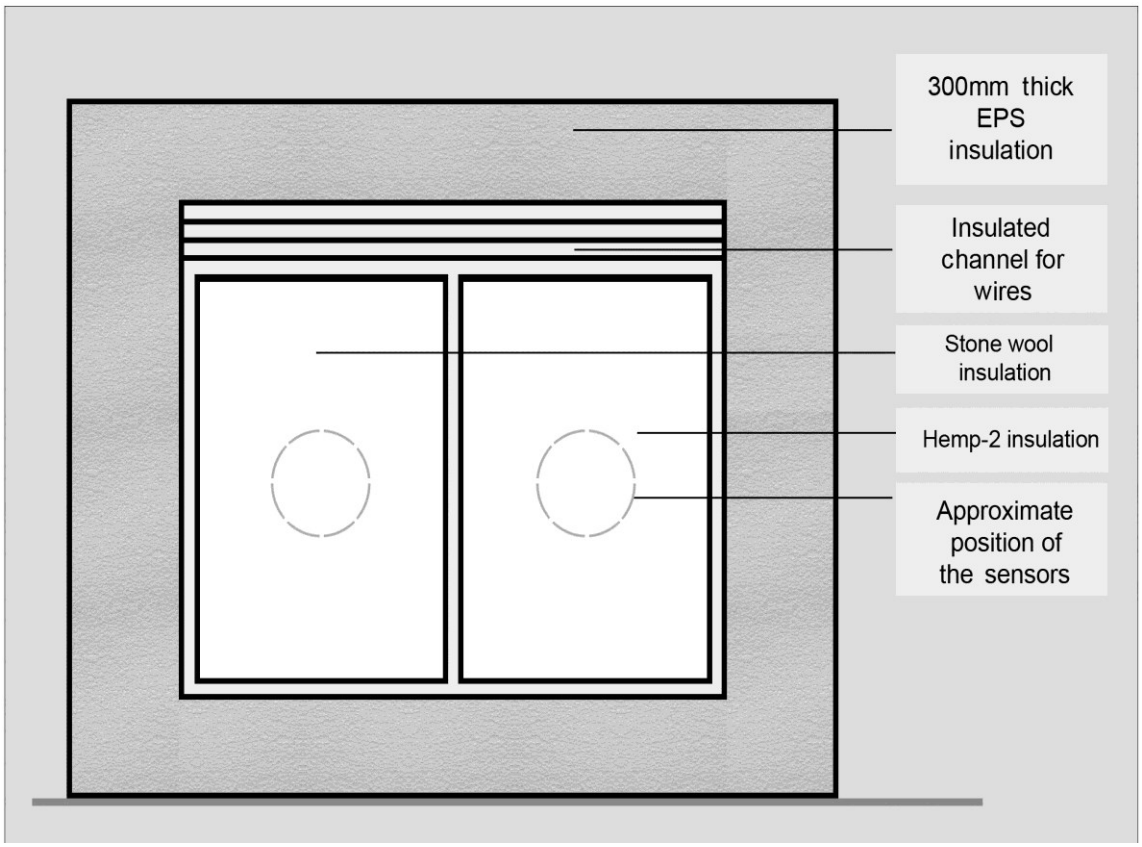


**Figure 6.4: The front elevation of the dual-insulation setup.**

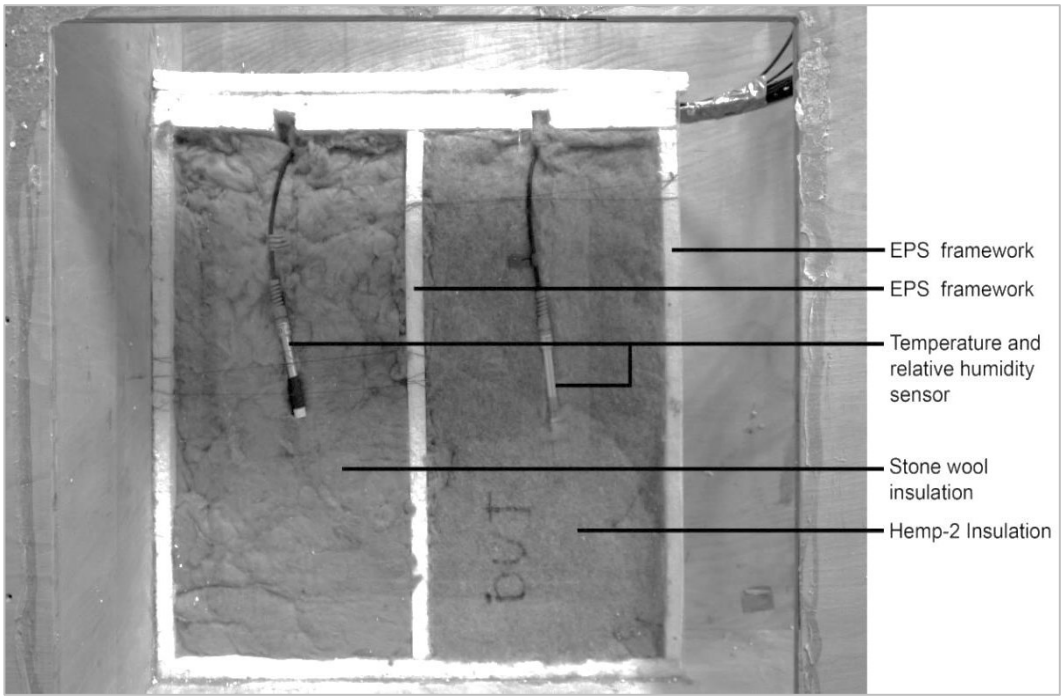


**Figure 6.5: The installed samples.**

During this experiment, one heat flux sensor was placed in each insulation sample. The heat flux sensors were placed in the centre of the insulations in terms of height, width and thickness. This was done for two reasons: firstly, it was easy to keep the heat flux sensors more stable at the centre without any risk of falling off as this could happen if the sensors were placed on the surface of the insulations. Secondly, on placing the heat flux sensors at the centre of the insulation, the risk of error due to the radiant heat from the fan heater placed in the hot chamber was reduced.

Thus, it was assumed that placing the heat flux sensor at mid-thickness of the insulation would provide the typical data of heat flux, uninterrupted by radiant heat and movement of the heat flux sensor, caused by the relative humidity of the hot chamber and the ambient temperature difference between the hot chamber and the exterior. However, the heat flux sensors, placed at the mid-thickness of the insulations, would be unable to register any heat flux due to phase change in the insulation-acrylic interface, which may occur at high relative humidity. This experiment is conducted taking this limitation into account and this limitation is addressed during test-6.2 of this chapter.

The relative humidity sensors were placed at the following locations, from the external surface to the internal surface, of each insulation: 0 mm, 25 mm, 50 mm, (100-110) mm. The relative humidity sensors were also placed at the exterior and interior of the hygrothermal hot box to measure the relative humidity conditions of the ambient air. It is assumed that the relative humidity sensors would provide sufficient data to analyse the moisture management capacity of the insulations. Temperature data are gathered from the following positions of the insulations, from external surface to the internal surface: 0 mm, 25 mm, 50 mm, (100-110) mm. External and internal ambient temperature data was also recorded using 107 thermistor probes.

### *6.2.5 Insulation installation*

The EPS framework containing two insulation materials is placed inside the insulation holder in front of the hot chamber. A temperature and relative humidity sensor is placed inside the hot chamber and a temperature and humidity logger is placed outside the hot chamber. The external surface of the insulation materials are covered by the 3 mm clear acrylic sheet. The acrylic

sheet is glued to the EPS insulation borders of the samples with silicon sealant in such a way that there is no moisture leakage to the exterior and no moisture interaction between the two samples. The wires from all the sensors run through an insulated channel at the upper part of the EPS insulation frame. The wires are linked to the CR1000 data logger. Some of the temperature and humidity loggers (EL-USB-2) are independent and data from those loggers are extracted in the software programme 'EL-WIN-USB Windows Control Software' (2013). The 3 mm clear acrylic outer surfaces of the dual insulations serve two purposes, firstly, it works as an interface surface for assessing the likelihood of interstitial condensation and secondly, it provides the opportunity to record the evidence of condensation visually. Figure 6.6 shows the dynamic hygrothermal hot box setup without the optional cold chamber.

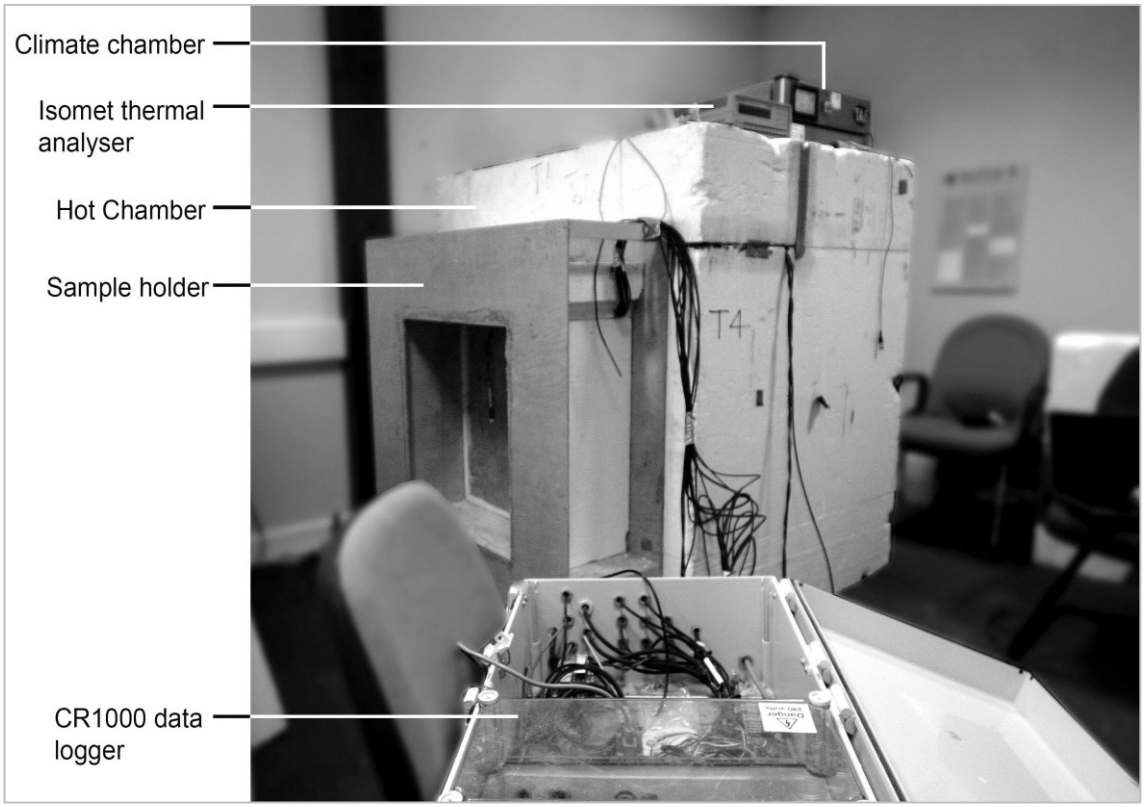


**Figure 6.6: The experimental setup.**

### *6.2.6 Experimental method*

Hemp-2 and stone wool insulation materials were exposed to dynamic relative humidity ranges of the hot chamber varying from 35% to 80%. The internal temperature at the hot chamber was kept at 35 °C and the external temperature was kept at 19 °C with amplitude of 3 °C. The temperature difference between the interior and exterior of the insulation materials was maintained between

10 °C and 15 °C so that unidirectional heat flux could be achieved. Study of relative humidity and heat flux in the insulation materials provided information about the insulation materials' heat flux and moisture management capacities.

Two tests were conducted: test-1 and test-2. During test-1, the relative humidity of the hygrothermal hot box was gradually increased from 45% to 75% in 72 hours and then decreased from 75% to 52% in 24 hours. During test-2, the relative humidity of the hot chamber was raised from 30% to 80% in about 48 hours and then gradually decreased from 80% to 40% in about 216 hours. Test-2 was longer than test-1 in order to study the drying out of the insulation materials.

It was assumed that the moisture and vapour pressure gradient would vary across the depth of the insulation materials, according to the vapour diffusion resistance factors and the sorption isotherms of the insulation materials. With increased temperature and continuing moisture flow from the climate chamber, the vapour pressure inside the hot chamber started increasing. With increased vapour pressure potential between the external surface of the insulation and the hot chamber of the hygrothermal hot box, vapour permeated through the insulation materials. When the relative humidity in the hot chamber was decreased, the relative humidity in the (stone wool)-acrylic and (hemp-2)-acrylic interfaces also decreased at different rates.

The vapour diffusion resistance factor was measured using the dry and wet cup method according to the ISO 12086 (British Standards Institute, 1997) and the sorption isotherm was developed according to the ISO 12571 (British Standards Institute, 2000). Condensation occurs wherever the surface temperature is lower than or equal to the dew point temperature of the moistened air at that point. If condensation occurs in the acrylic-insulation interface, this will easily be visible from outside. Thus, it can also be identified in which insulation the condensation occurs quicker while subjected to similar boundary conditions. Once condensation is observed, the humidity is decreased inside the hygrothermal hotbox to study the drying-out effect of the insulation samples.

Condensation in the insulation-acrylic interfaces and inside the insulation materials was also analysed by plotting the dew point gradient from the relative humidity and temperature data gathered from the different positions of the

sensors, as shown in Figure 6.3, across the depth of the insulation samples. Numerical simulations using the WUFI software were also run to compare the experimental data with numerical predictions and the results are reported in subsection 6.2.7.1.

The equivalent thermal conductivity is measured from the heat flux and the temperature differences based on the following equation:

$$q = -\lambda_{equi} * \nabla T \quad [6.1]$$

Where q is heat transfer rate (W/m$^2$), $\lambda_{eq}$ is the equivalent thermal conductivity (W/mK) and ∇T is the temperature gradient (°C).

Equivalent thermal conductivity values are calculated for the instances where the temperature difference is greater than 10 °C to achieve unidirectional heat flow. Equivalent thermal conductivity data can then be related to average relative humidity in the hot chamber. Equivalent thermal conductivity values of the insulation materials for a range of average relative humidity conditions can thus be calculated.

**Declared value and design value**

BS EN ISO 10456 (British Standards Institute, 2007) describes two different thermal conductivity values for the same material: one being the 'declared value' and other being the 'design value'.

**Declared value ($\lambda_1$):** Declared value is the thermal conductivity value derived from measured data at reference conditions. Usually the samples are either dry or conditioned at 23 °C temperature and 50% relative humidity. Declared value of thermal conductivity of an insulation material is provided by the manufacturer.

**Design value ($\lambda_2$):** Design value is the thermal conductivity value of the building material or product in specific internal and external condition. The concept of design value is developed to get an estimation of the thermal conductivity of an insulation material during service conditions. The design value of thermal conductivity can be determined by using particular equations.

As far as the effect of moisture on conductivity is concerned, the relationship between the declared value of thermal conductivity and the design value of thermal conductivity can be expressed as:

$$\lambda_2 = \lambda_1 * F_m \quad [6.2]$$

$$F_m = e^{f_U(U_2 - U_1)} \quad [6.3]$$

Where, $\lambda_1$ is the declared value of thermal conductivity, λ2 is the design value of thermal conductivity, $f_u$ is the moisture conversion coefficient mass by mass, $u_1$ is the moisture content mass by mass of the first set of conditions, $u_2$ is the moisture content mass by mass of the second set of conditions.

**Dew point temperature and actual vapour pressure**

Condensation can be visually observed on the acrylic surface. Condensation can also be calculated from relative humidity and temperature data of the insulation-acrylic interface air and the inner surface temperature data of the acrylic. If the surface temperature of the acrylic is equal or less than the dew point temperature of the humid interface air, then there is a likelihood of condensation if the air gets in touch with the acrylic surface. Dew point temperature can by determined from actual vapour pressure.

The following equations are used to derive dew point temperature, $T_D$,and actual vapour pressure, e:

$$T_D = \left[ \left(\frac{v}{100}\right)^{\frac{1}{8}} \right] (112 + 0.T9) + 0.T1 - 112 \quad [6.4]$$

$$e = 6.11 * 10^{\frac{(7.5 * T_D)}{(237.7 + T_D)}} \quad [6.5]$$

Where,

$T_D$ = dew point temperature (°C)

v = relative humidity (%)

T = temperature (°C)

e = actual vapour pressure (hPa)

**Operational Errors in heat flux measurement**

ISO 9869 outlines the following likely errors in heat flux measurements:

- 5% error due to the calibration of the heat flux sensor and the temperature sensors.

- 5% error due to the random variation caused by difference in thermal contact between the sensors and the surface when one heat flux sensor is used.
- 2% operational error due to the modification of isotherms by the placement of heat flux sensors.
- 1% error due to low variations in temperature and heat flux over time and when the test wall is not in direct contact with sunlight.

The total error in the heat flux measurements for each panel, following the ISO 9869, will be square root of the sum of square of the individual errors. For the present test, the total error can be estimated as follows:

Total error in heat flux measurement = $\sqrt{5^2 + 5^2 + 2^2 + 1^2}$ = 7.4%

According to ISO 9869, another 5% error is introduced to the thermal transmittance value or U-value measurement due to the temperature variations within the space and difference between air and radiant temperature. Thus, the total error in U-value measurement can be calculated as:

Total error in U-value measurement= $\sqrt{5^2 + 5^2 + 2^2 + 1^2 + 5^2}$ = 8.9%

### *6.2.7 Results and discussion*

#### *6.2.7.1 Relative humidity and interstitial condensation*

It has been observed that the hemp-2 insulation and the stone wool insulation respond to relative humidity and vapour pressure changes in different ways. Humidity and vapour pressure distributions in the insulation materials and in the hot chamber during the experiment show that stone wool responds rapidly to the fluctuation of relative humidity and vapour pressure whereas hemp responds slowly both to the increase and decrease of relative humidity and vapour pressure in the hot chamber. Figures 6.7 and 6.8 show the relative humidity and vapour pressure in the hemp-acrylic interface and in the hot chamber during test-1 and test-2, respectively.

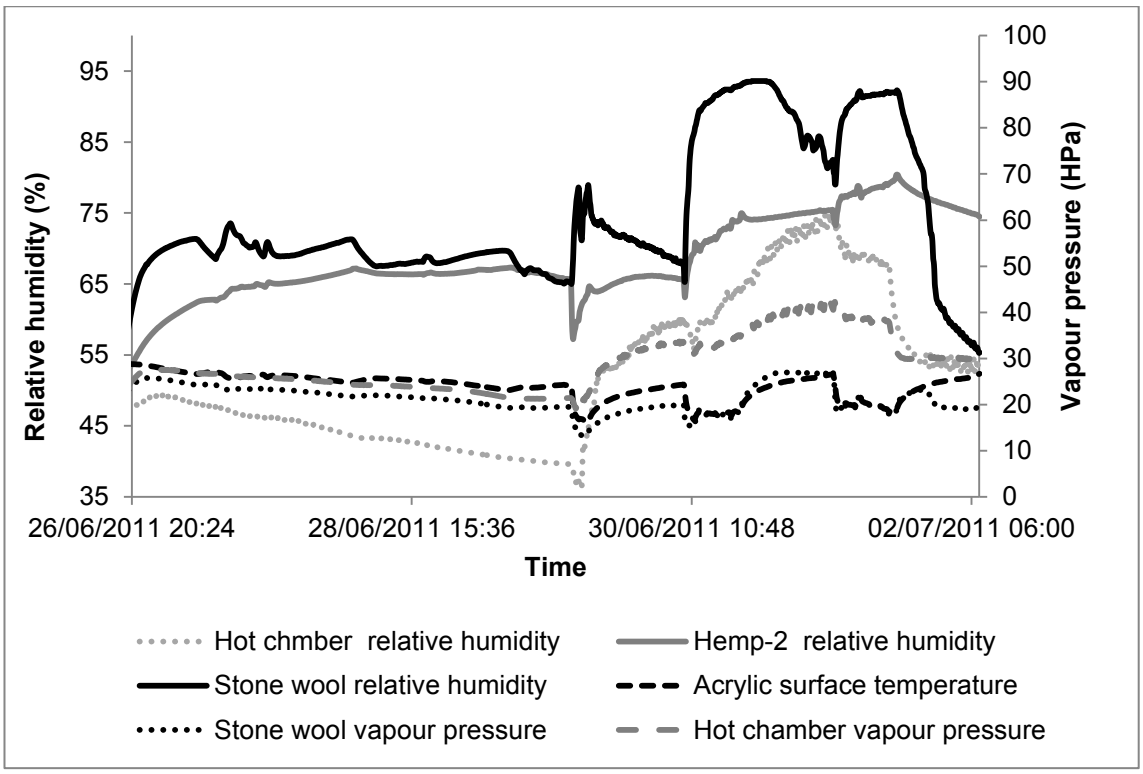


**Figure 6.7: Relative humidity and vapour pressure inside the dynamic hot box and in the insulation external surfaces during test-1.**

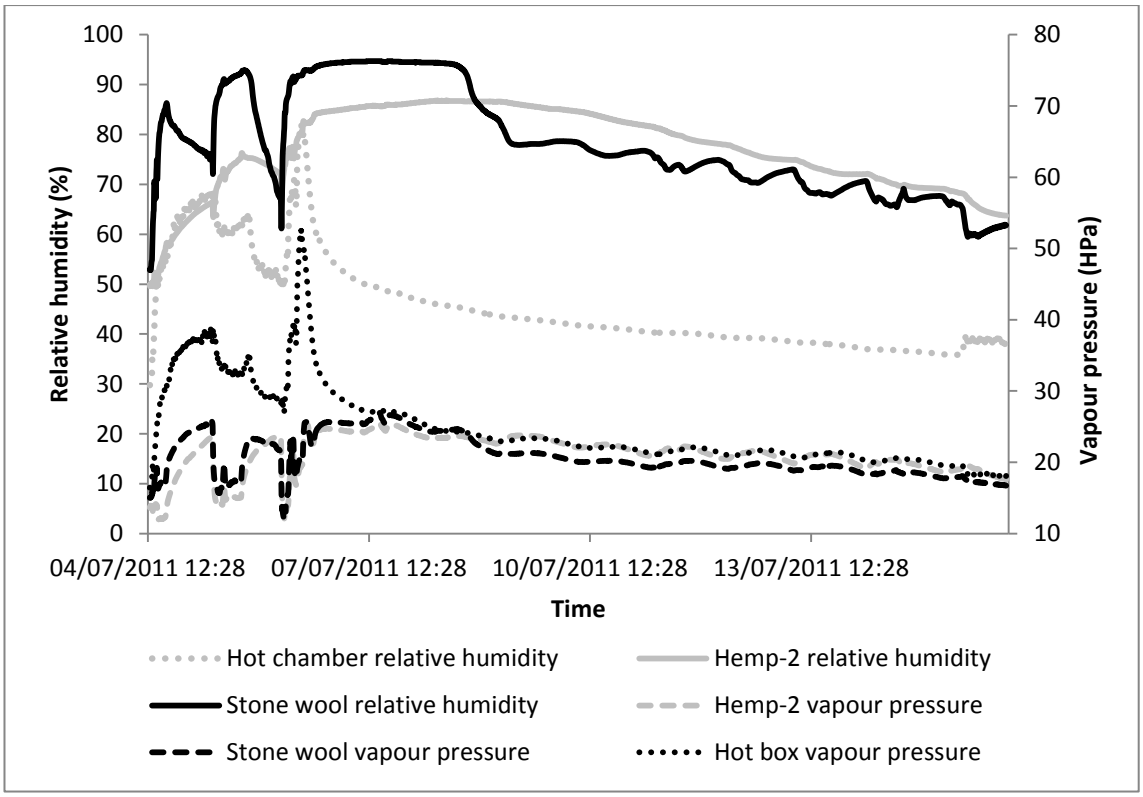


**Figure 6.8: Relative humidity and vapour pressure inside the dynamic hot box and in the insulation external surfaces during test-2.**

During test-1, the relative humidity in the (stone wool)-acrylic interface increased very quickly to about 90% in response to the rise in relative humidity in the hot chamber to about 62%. At the same time relative humidity in the (hemp-2)-acrylic interface increased to about 72%. During test-1, in response to the decrease of relative humidity in the hot chamber, the relative humidity decreased quicker in the stone wool-acrylic interface than in the hemp-2-acrylic interface. Similar observation about the insulations materials' response to changes in relative humidity can also be made from Figure 6.8 during test-2.

During test-1, minor interstitial condensation was visually observed in the (stone wool)-acrylic interface on 30.06.2011, the relative humidity sensor registered about 86% relative humidity in the (stone wool)-acrylic interface during that time.

During test-2, severe condensation in the (stone wool)-acrylic interface was noticed on 06.07.2011, as shown in Figure 6.9. The relative humidity sensor registered about 93% relative humidity at that time.

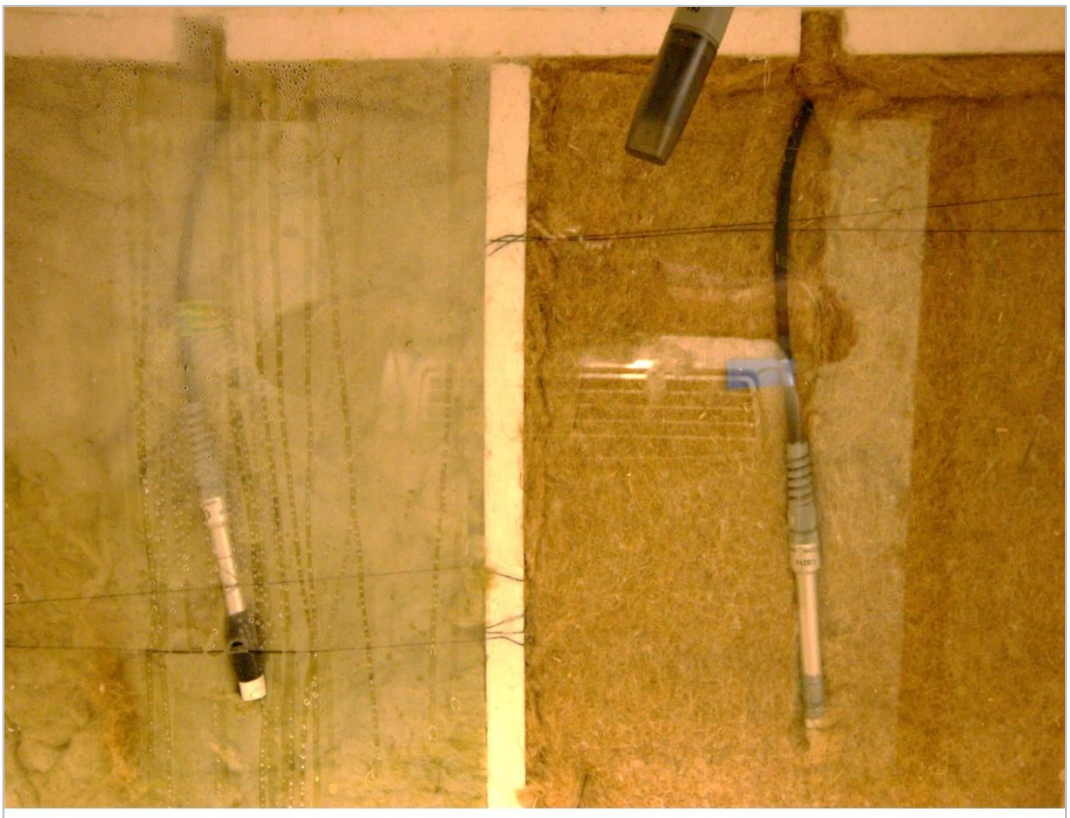

(a) Stone wool insulation (b) Hemp-2 insulation

**Figure 6.9: Test-2: (a) Condensation is observed in (stone wool)–acrylic interface, (b) (hemp-2)-acrylic interface remains dry.**

The relative humidity data from the relative humidity sensors during the periods of condensation clearly show the limitation of the relative humidity sensors to sense actual condensation as they measure the water activity in the air and not on the solid surface. The instances of occurrences of condensation can be identified and explained by determining the vapour pressure gradient along the insulation layers and by determining the dew point temperature gradient from the vapour pressure gradient. Condensation is likely whenever the surface temperature of the acrylic or of any point along the depth of insulation is equal to or lowers than the dew point temperature.

It can be observed in Figure 6.10 that condensation was likely to occur in the (stone wool)-acrylic and (hemp-2)-acrylic interfaces on 29.06.11 at around 6:30 pm as the temperature of the inner surface of acrylic are equal to the dew point temperature of the moist air of the insulation-acrylic interfaces. This numerical estimation could not be verified as the laboratory where the experiment was performed was unmanned after 6.00 pm on that particular day. However, the author noticed condensation on the (stone wool)-acrylic interface on the morning of 30.06.11 while no condensation was noticed on the (hemp-2)-acrylic interface. There is a likelihood that condensation might also have occurred in the (hemp-2)-acrylic interface and the hemp-2 surface had absorbed the condensed water. It can also be noticed in Figure 6.10 that there was a brief period on 01/07/2011 at around 17:25 pm when condensation occurred in the (stone wool)-acrylic interface. However, both of these occurrences of condensations during test-1 were minor. The acrylic surface of (stone wool)-acrylic interface was covered by fog and few drops of water during both of the occasions.

During test-2, condensation was more prominent in the (stone wool)-acrylic interface between 07.07.11 and 08.07.11. In Figure 6.11, it can be observed that condensation started on the (stone wool)-acrylic interface at around 8:30 pm on 06.07.11 and ended on around 8:00 pm on 08.07.11. This is marked by the grey shades between the line of acrylic surface temperature and the line of stone wool dew point temperature. The calculated timing of condensation was confirmed by the visual observation of condensation on the acrylic surface of the (stone wool)-acrylic interface. The photographic image of the condensation during test-2 is already shown in Figure 6.9.

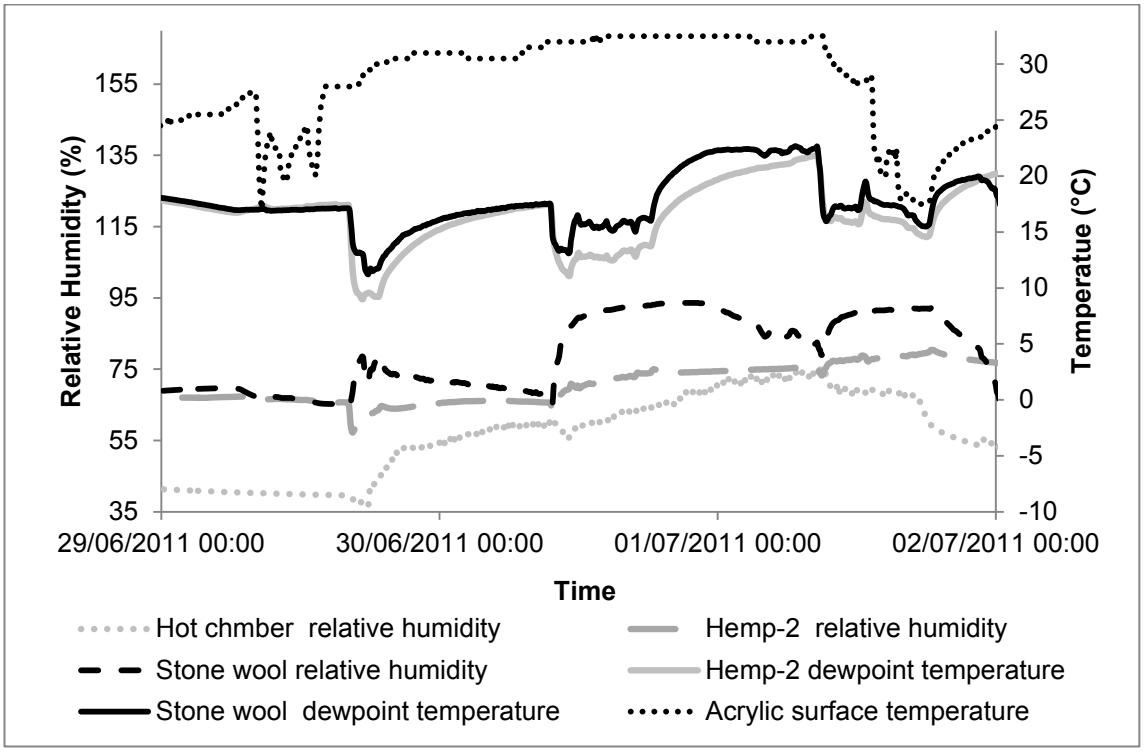


**Figure 6.10: Dew point temperatures of hemp-2 and stone wool and the acrylic surface temperature during condensation (test-1).**

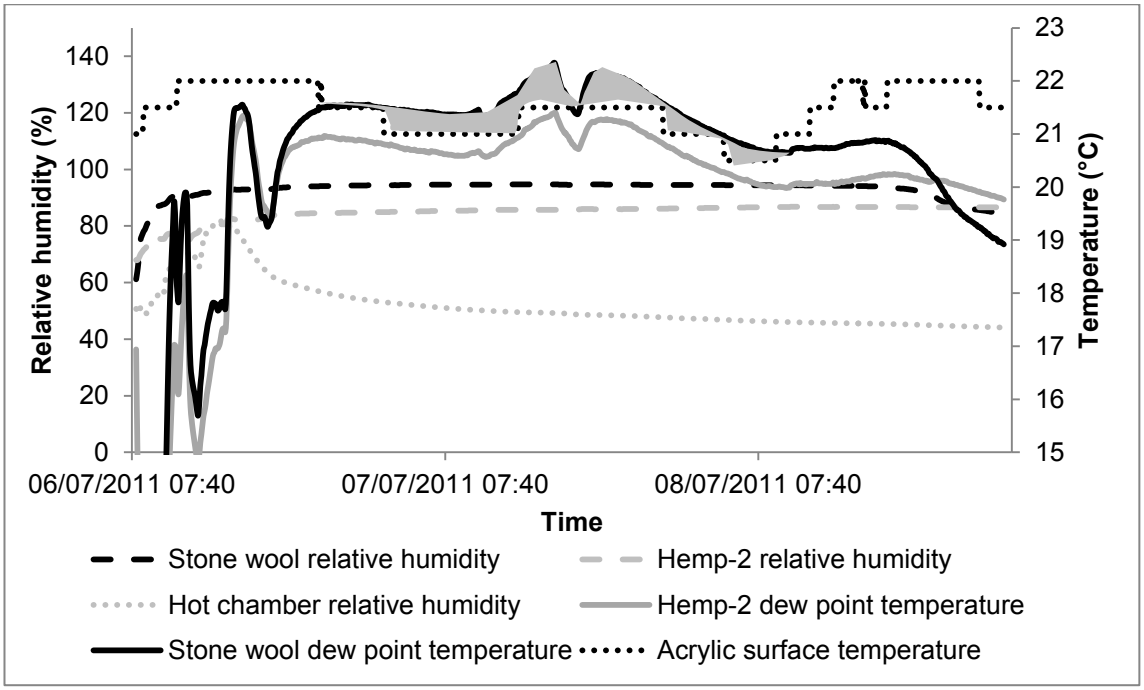


**Figure 6.11: Dew point temperatures of hemp-2 and stone wool and the acrylic surface temperature during condensation (test-2).**

Figure 6.12 shows the calculated dew point temperature and insulation temperature gradient along the depth of stone wool and hemp-2 insulation

materials during one instance of condensation. In this Figure, it can be observed that condensation might have occurred up to 10 mm inside the depth of the stone wool insulation. No condensation was observed on the inner surface of the acrylic behind the hemp insulation during these two tests. This can also be confirmed by the aforementioned dew point temperature analysis.

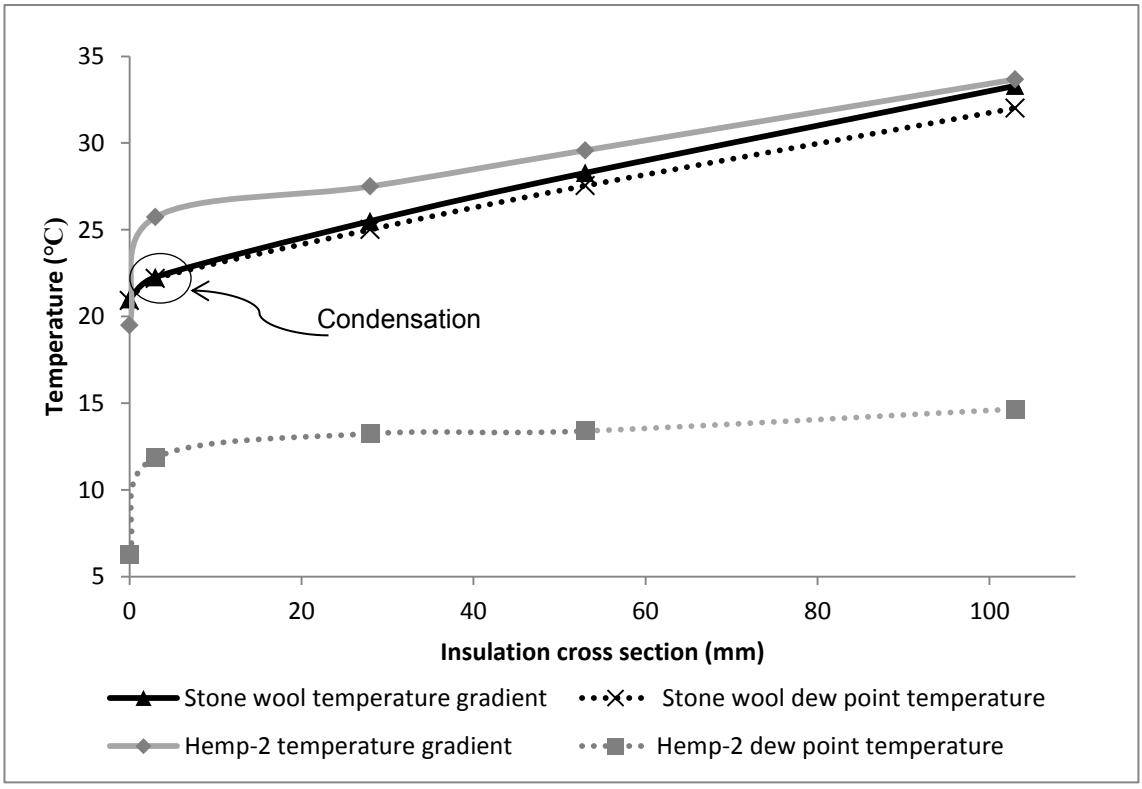


**Figure 6.12: Calculated dew point temperature along the depth of the hemp-2 and stone wool insulations and the surface temperatures at those points.**

When condensation was noticed during test-2, the climate chamber was switched off on 06.07.11 at around 09:00 am so that the relative humidity inside the hot chamber could decrease. This eventually would induce the relative humidity inside the insulation materials to decrease along the vapour pressure gradient. Figure 6.13 shows the relative humidity at different depths of stone wool and hemp insulation materials before, during and after the second occurrence of condensation.

It can also be noticed in Figure 6.13 that peak relative humidity near the external surface of the stone wool insulation is about 8% higher than the peak relative humidity near the external surface of hemp insulation for about 50 hours. Although both insulation materials are exposed to identical external and

internal temperature and humidity boundary conditions, when the climate chamber was switched off, the drop of relative humidity on the external surface of stone wool insulation was rapid, with the gradient of drop being about 68° for about 18 hours. The drop of relative humidity in hemp external surface started almost 15 hours later than in stone wool external surface. The drop of the relative humidity in the external surface of hemp insulation was slow and steady, with the gradient of drop being about 18° for about 144 hours.

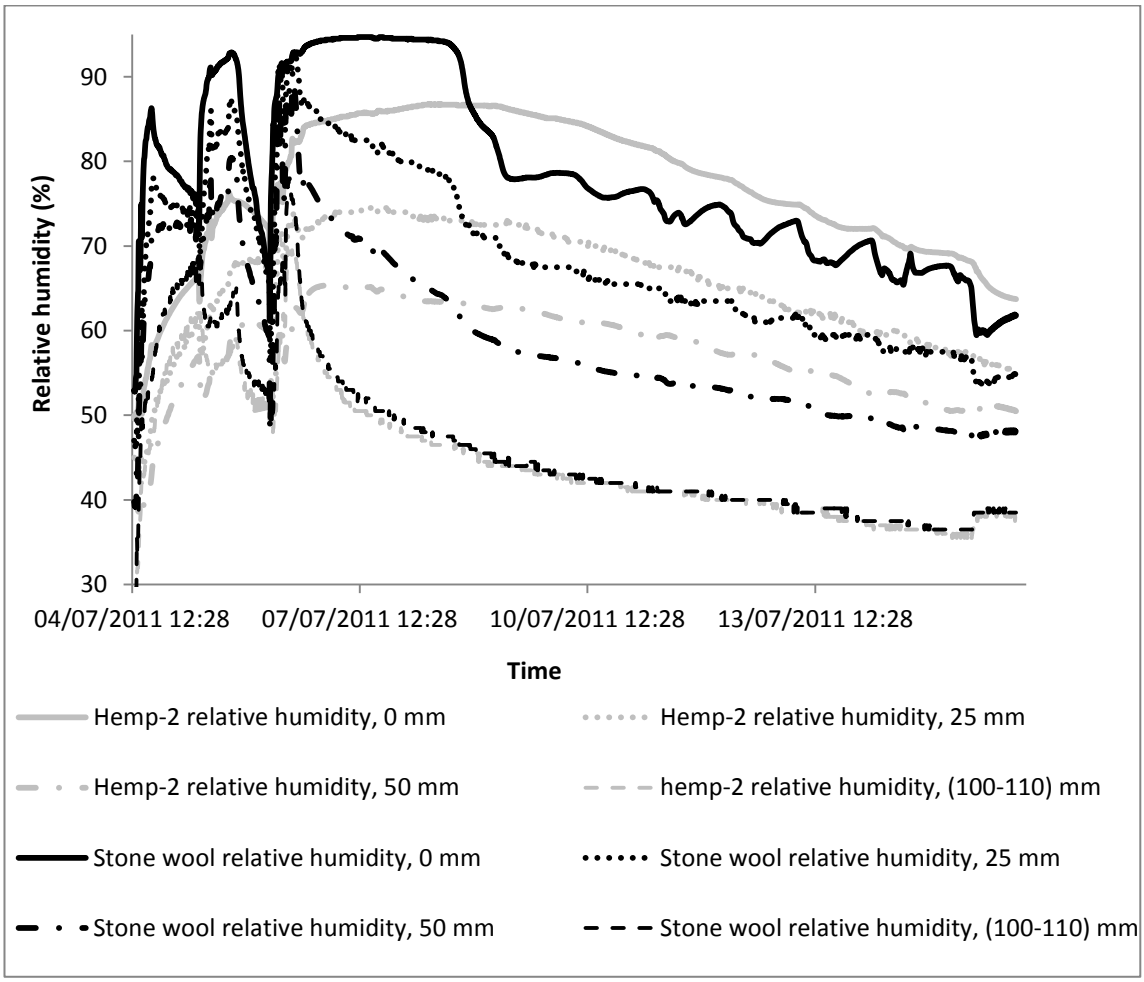


**Figure 6.13: Relative humidity distribution in the insulation materials during test-2.**

While hemp-2 and stone wool insulation materials exhibit about similar vapour diffusion resistance factors (1.29 and 1.36, respectively, in wet cup test), yet visible condensation occurred only in the (stone wool)-acrylic interface. It seems that moisture adsorption, moisture buffering and water absorption capacity of hemp-2 insulation have prevented condensation from happening in the (hemp-2)-acrylic interface. The moisture adsorption and water absorption capacities of hemp-2 insulation are shown in Figures 6.14 and 6.15. In dynamic

conditions, moisture adsorption capacity will be analogous to heat capacity and, similar to the thermal mass, the hemp-2 insulation may perform as the hygric mass. In dynamic conditions, this hygric mass may effectively prevent moisture from passing steadily through the insulation and from contacting the inner surface of the acrylic sheet. Even if condensation occurs, there is a likelihood that water will be absorbed by the hemp insulation due to its water absorption capacity.

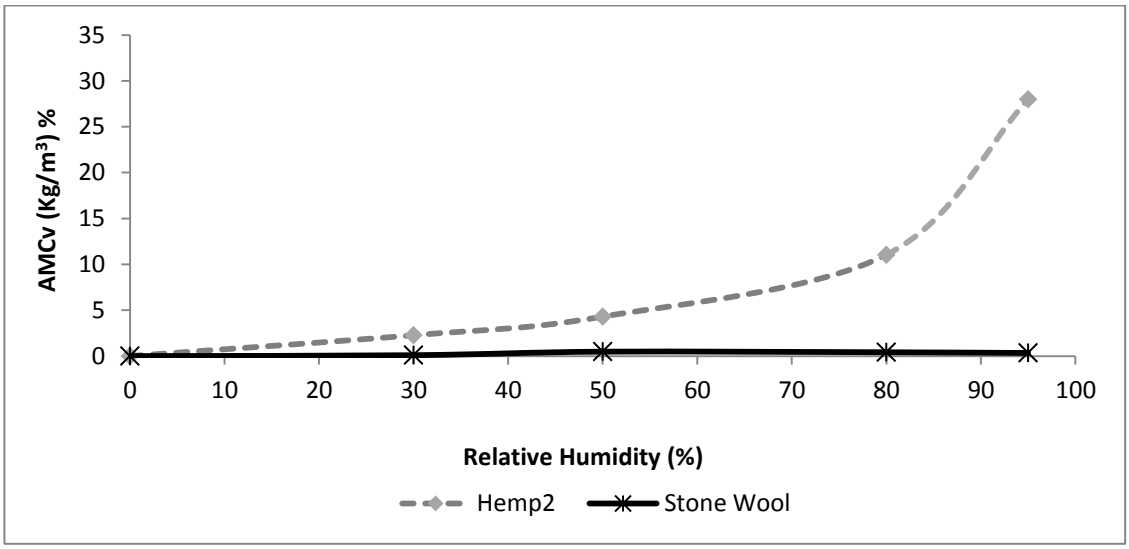


**Figure 6.14: Adsorption isotherms of hemp-2 and stone wool insulation in terms of average moisture content by volume (AMCv).**

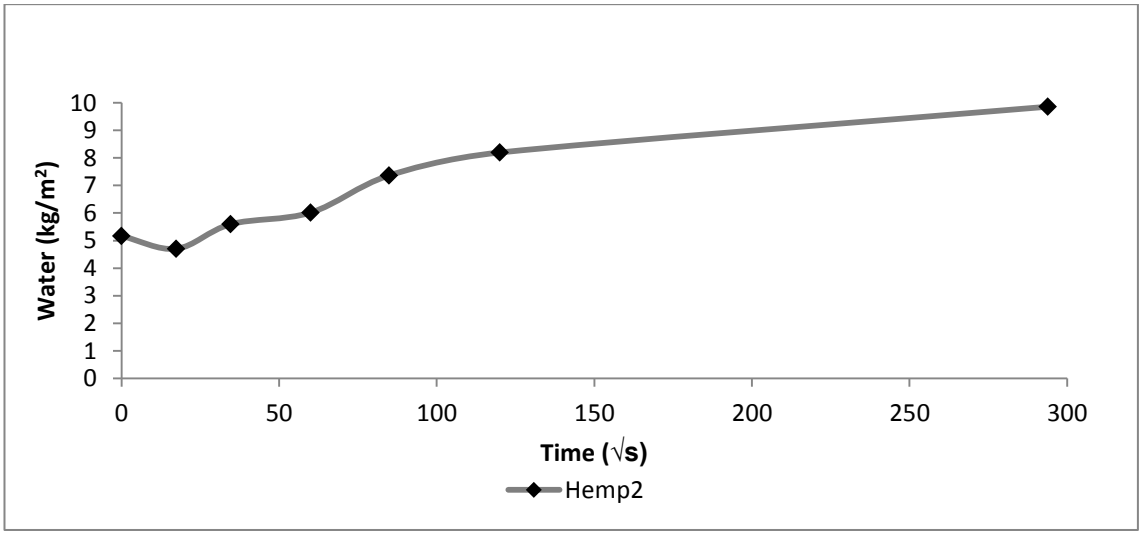


**Figure 6.15: Water absorption of hemp-2 in relation to square root of time.**

Test-2 has been simulated in the WUFI software. Figure 6.16 shows the simulated water content and relative humidity in the insulation-acrylic interfaces along with the experimental data of relative humidity. It can be noticed that

between 01.10.1999 and 04.10.1999 (the default year set by the WUFI programme), the relative humidity in the insulation-acrylic interfaces during the experiment were under-predicted by the WUFI software.

It can be noticed that between 01.10.1999 and 04.10.1999, the WUFI software under-predicted the increase in the relative humidity in the insulation-acrylic interfaces of stone wool and hemp-2 insulation materials. During those times, the WUFI software predicted peak relative humidity values of about 86% and 82% in (stone wool)-acrylic and (hemp-2)-acrylic interfaces, respectively. However, the experimental data of test-2 show the peak relative humidity of 95% and 85 % in the (stone wool)-acrylic and (hemp-2)-acrylic interfaces, respectively during the same period. When it comes to the drying up period, the prediction using the WUFI software closely agrees to the experimental data between 05.10.99 and 07.10.99. After that period, there is a sudden rise in the predicted interface relative humidity both in hemp-2 and stone wool insulation, which is different from the experiment results.

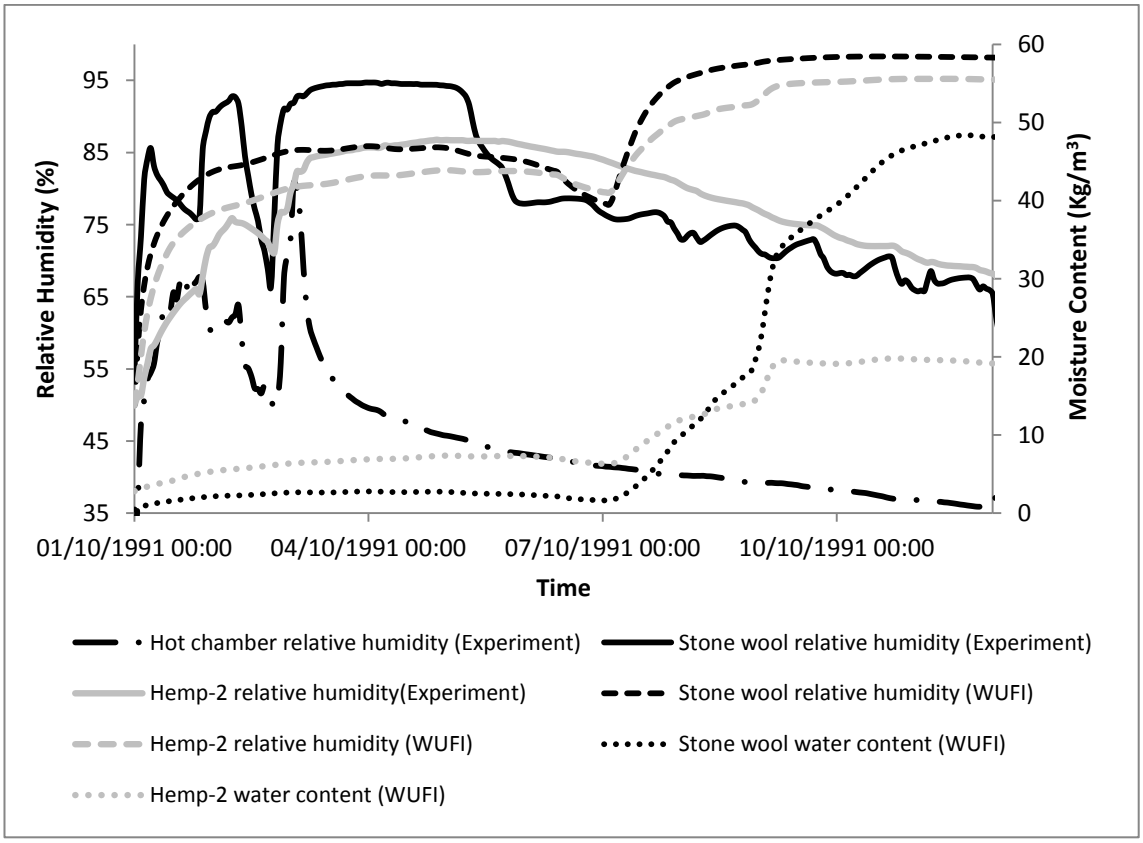


**Figure 6.16: Comparison of the WUFI numerical simulations and experimental results during test-2 in terms of relative humidity and water content in the insulation-acrylic interface.**

Since the internal surface of both stone wool and hemp-2 insulations were exposed to interior conditions of the dynamic hot box, in addition to vapour diffusion, the effect of convection current may have been substantial. Since the WUFI software does not include convection of air in the governing equations, the deviation in prediction can be expected.

#### *6.2.7.2 Heat Flux and thermal conductivity*

The experimental data have been explored to determine the equivalent thermal conductivity of hemp-2 and stone wool insulations for the total period of the experiment and for the following ranges of relative humidity: 50%, 60%, 70% and 80%. Equivalent thermal conductivity values of hemp-2 insulation were also determined for the adsorbed water content for the aforementioned ranges of relative humidity. The data have also been analysed to explore the following bivariate relationships between:

- Heat flux and ambient temperature difference,
- Heat flux and relative humidity,
- Heat flux and vapour pressure difference,
- Equivalent thermal conductivity and ranges of relative humidity,
- Equivalent thermal conductivity and adsorbed water content by the hemp-2 insulation at the considered ranges of relative humidity.

Equivalent thermal conductivity values for test-1 and test-2 are determined from ambient temperature differences, heat flux and thickness of the material according to equation 6.1 and are shown in the Figure 6.17 and Figure 6.18.

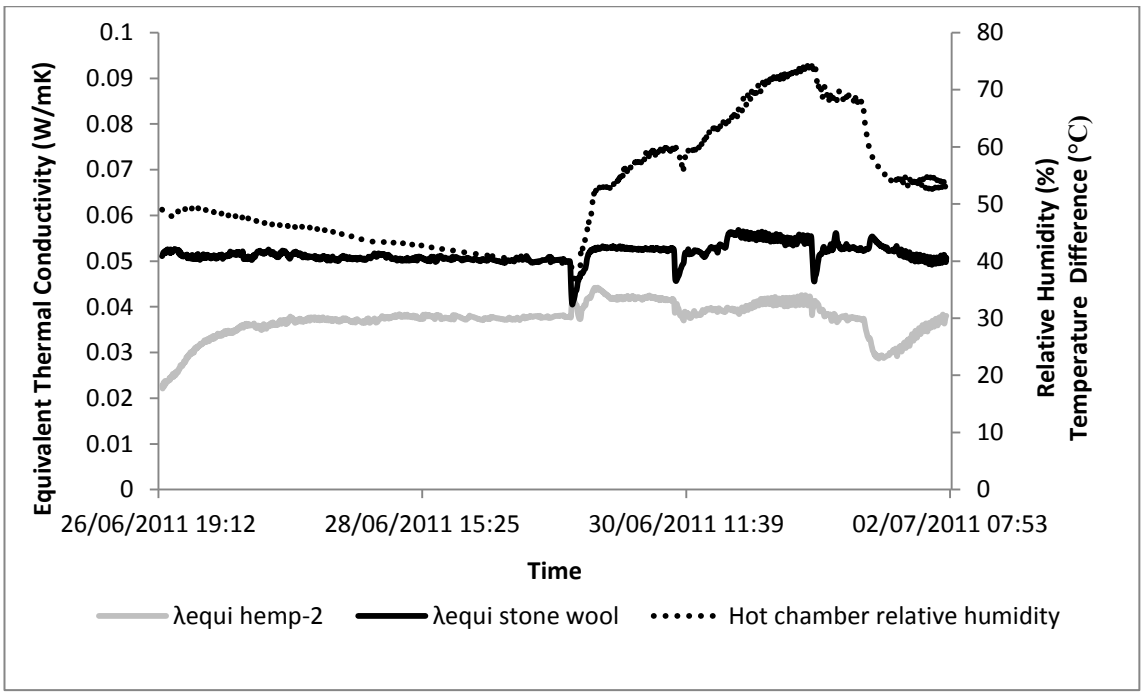


**Figure 6.17: Equivalent thermal conductivity of the hemp-2 and stone wool insulations during test-1.**

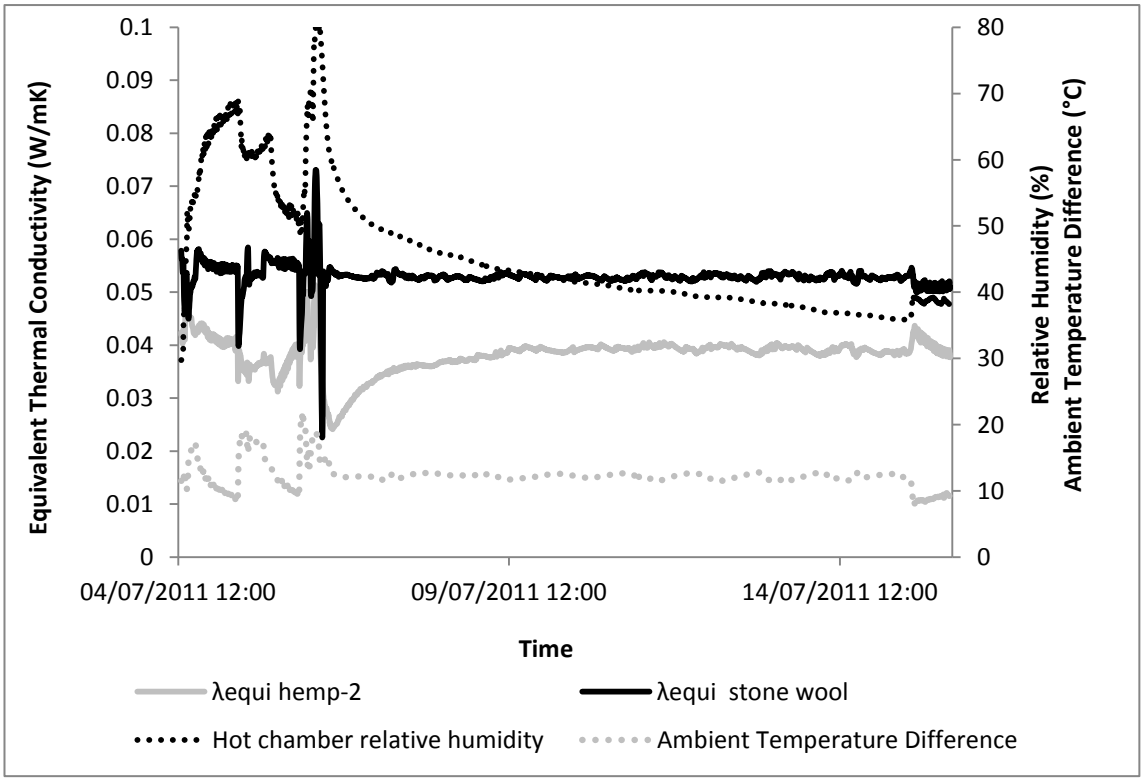


**Figure 6.18: Equivalent thermal conductivity of hemp-2 and stone wool insulations during test-2.**

The average conductivity for any specific range of average internal relative humidity can be statistically determined from the conductivity readings when the insulations are continuously exposed to certain humidity for a continuous

period. However, to transform the relative humidity exposure to adsorbed equilibrium moisture content, a 100 mm thick fibrous insulation requires about 20 hours to reach equilibrium moisture content (EMC) in isothermal condition.

In this experiment the insulation materials are exposed to temperature gradient and, due to the nature of the dynamic conditions, it has not been possible to obtain continuous 20 hours data during the periods of peak relative humidity. Therefore, for peak relative humidity of 70% and 80%, exposure times of 6.7 hours and 2.7 hours are used respectively, as those were the highest continuous exposure period available within the data set.

These equivalent thermal conductivity values are presented in Figure 6.19. It can be noticed that the average equivalent thermal conductivity of hemp-2 insulation at 45% average relative humidity is similar to the manufacturer's declared thermal conductivity of hemp-2 insulation. It apparently implies that if the hemp-2 insulation is exposed to fewer periods of high internal relative humidity compared to the periods of moderate internal relative humidity, then the effect of higher relative humidity on thermal conductivity of hemp-2 insulation is negligible.

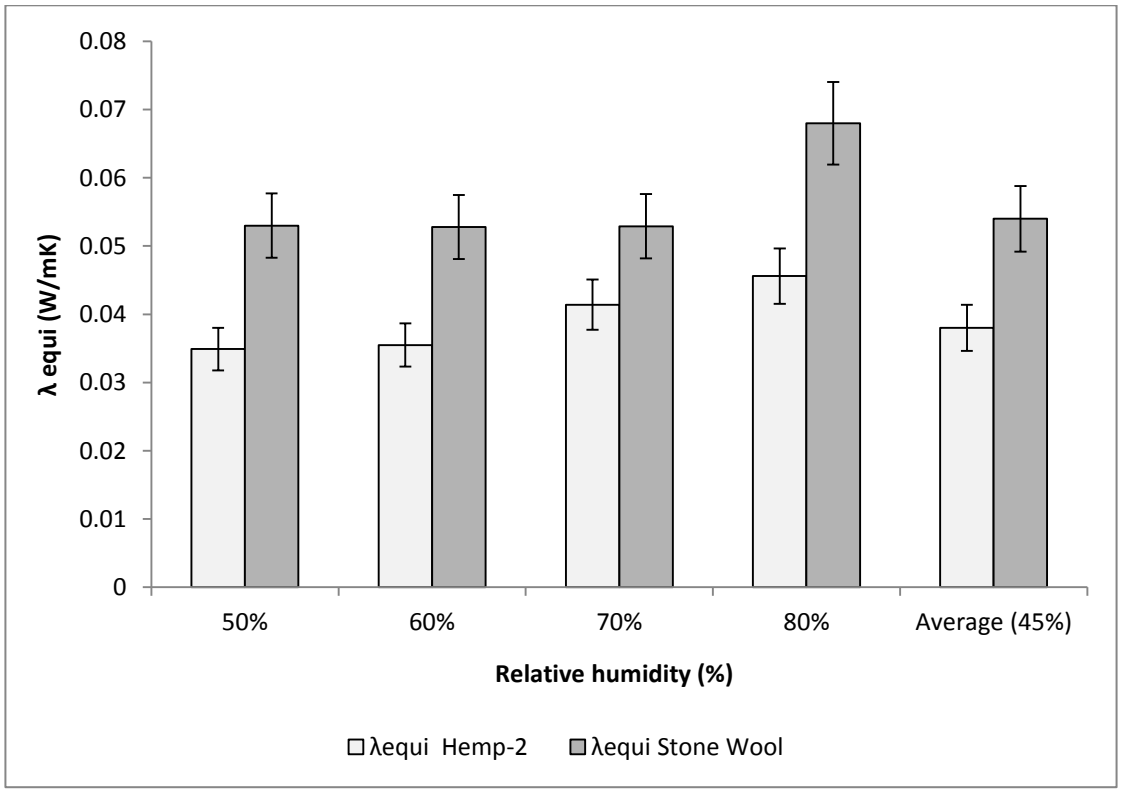


**Figure 6.19: Equivalent thermal conductivity values of hemp-2 and Stone wool Insulations.**

Figure 6.19 also shows the equivalent thermal conductivity values of hemp-2 and stone wool insulation materials at 50%, 60% 70% and 80% relative humidity. For stone wool insulation, the average equivalent thermal conductivity is about 0.054 W/mK, which is about 42% higher than the manufacturer's declared thermal conductivity. It implies that the heat loss through enthalpy flow and phase change may have occurred in stone wool insulation. It is also explicit in Figure 6.19 that the change in equivalent thermal conductivity of the hemp-2 insulation is steady at 50% and 60% relative humidity and deviations start at 70% relative humidity.

A matrix of equivalent thermal conductivity values has been developed from the data related to Figure 6.19. This is presented in Table 6.2 along with the design values of the thermal conductivity of hemp-2 and stone wool insulation materials. The design values have been determined by applying equation 6.2. The average of the entire data shows that the equivalent thermal conductivity of hemp-2 when exposed to an average relative humidity of 45% is 0.038 W/mK. Average relative humidity value was determined from the relative humidity data of the hot chamber. The design value of the thermal conductivity of hemp-2 for a similar relative humidity exposure is 0.039 W/mK. For determining design values of hemp-2 insulation, the moisture conversion coefficient has been taken as equal to that of the cellulose fibre. Moisture content by mass is determined from sorption isotherm. The experimental thermal value of stone wool (0.054 W/m-K) is higher than the design thermal value (0.04 W/m-K)).

It can be also be observed in Table 6.2 that, while there is reasonable agreement between the design values and experimental values of hemp-2 insulation, the experimentally determined thermal conductivity values of hemp-2 insulations at 50% and 60% relative humidity are about 15% lower than the respective design values. For stone wool insulation, there is substantial difference between experimental and design values of thermal conductivity. For stone wool insulation, this is plausible because of the standard method of measuring design value of thermal conductivity. Since stone wool adsorbs negligible quantity of moisture, the value of moisture supplement to determine design value of thermal conductivity is very low. However, in this experiment, increase in heat flux through stone wool insulation may be due to the moisture transmission and phase change rather than due to adsorption. Whereas the

increase in thermal conductivity in hemp-2 during the experiment seems to be more due to increase in moisture content in the insulation by adsorption than moisture transmission and phase change. This is because of the high adsorption capacity of hemp-2 insulation compared to the negligible adsorption capacity of stone wool insulation.

**Table 6.2: Equivalent and design values of thermal conductivity of hemp-2 and stone wool insulation materials.**

| Internal relative humidity (%) | λequi of hemp-2 (W/m-k) | No. of data | Standard deviation | Design value of λ of hemp , (W/m-k) | λequi of stone wool, (W/m-k) | No. of data | Standard deviation | Design value of λ of stone wool, (W/m-k) |
|---|---|---|---|---|---|---|---|---|
| 50% | 0.0349 | 392 | 0.006 | 0.040 | 0.053 | 392 | 0.005 | 0.04 |
| 60% | 0.0355 | 412 | 0.008 | 0.041 | 0.0528 | 412 | 0.006 | 0.04 |
| 70% | 0.0414 | 80 | 0.011 | 0.041 | 0.0529 | 80 | 0.012 | 0.04 |
| 80% | 0.0456 | 32 | 0.009 | 0.044 | 0.068 | 32 | 0.012 | 0.04 |

The relationship between the heat flux and the following variables has been explored in Figure 6.20 to Figure 6.25: temperature difference (Figures 6.20, 6.21), relative humidity (Figures 6.22, 6.23), vapour pressure difference (Figures 6.24, 6.25). There is a significant correlation between the heat flux and the ambient temperature difference, which is reflected by square of the correlation coefficient ($R^2$) values as shown in the Figures 6.20. The $R^2$ value is, however, reduced both for hemp-2 and stone wool insulations during test-2 (Figure 6.21). From figure 6.20 and 6.21, it can be concluded that the linear relationship between heat flux and temperature difference, which is usually observed in dry insulation in steady state condition, is not much affected by the dynamic condition and the exposure to the ranges of relative humidity.

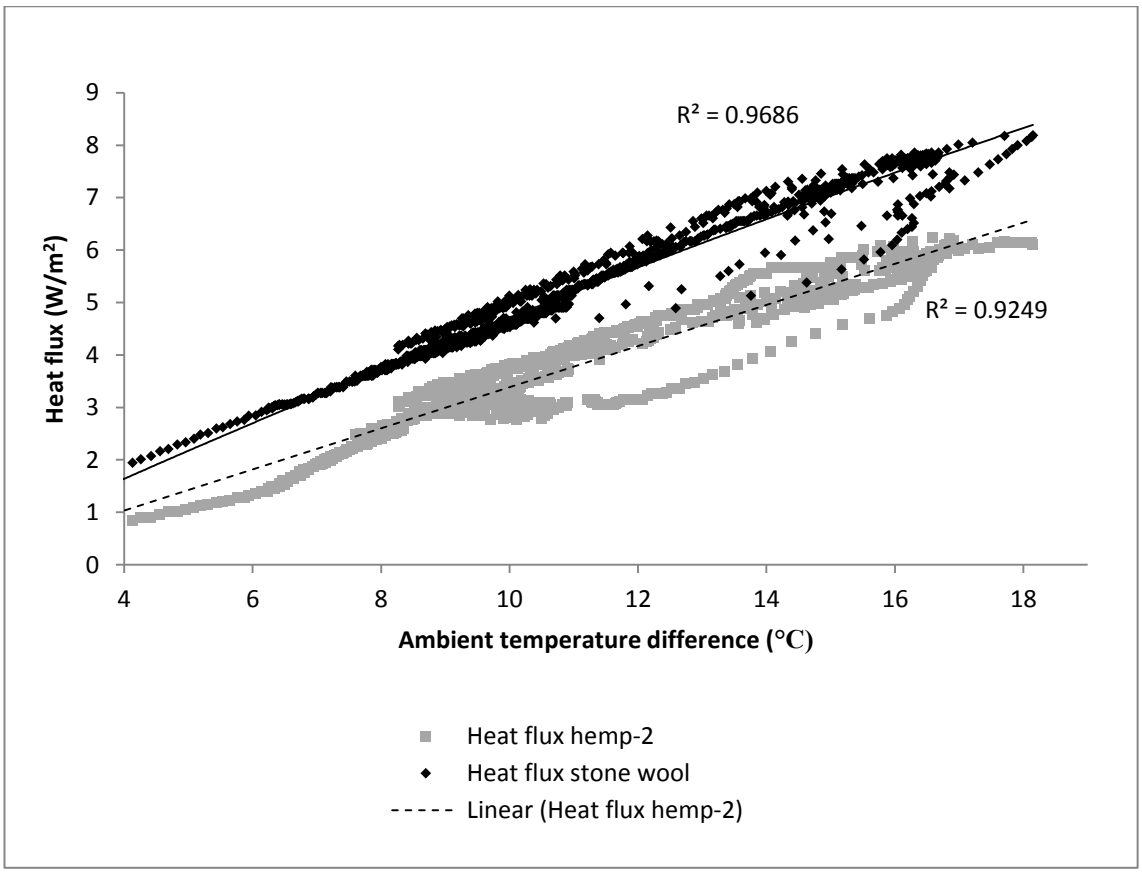


**Figure 6.20: Correlation between ambient temperature difference and heat flux in hemp-2 and stone wool during test-1.**

Figure 6.21 also represents the period (test-2) when significant condensation occurred in the stone wool insulation. Vapour pressure difference was also higher between the external surfaces of the insulations and the hotbox during the test-2 compared to that in test-1 (Figures 6.26 and 6.25). This may imply that the increased vapour pressure difference and resulting moisture movement affected the heat flux. It can be observed in the Figures 6.22 and 6.23 that the relationship between heat flux and relative humidity is nonlinear. Nonlinearity is also observed between heat flux and vapour pressure difference between the external surfaces of the insulations and the dynamic hot box. It implies that temperature difference is the dominant factor in heat flux through the insulations with moisture having a nonlinear influence.

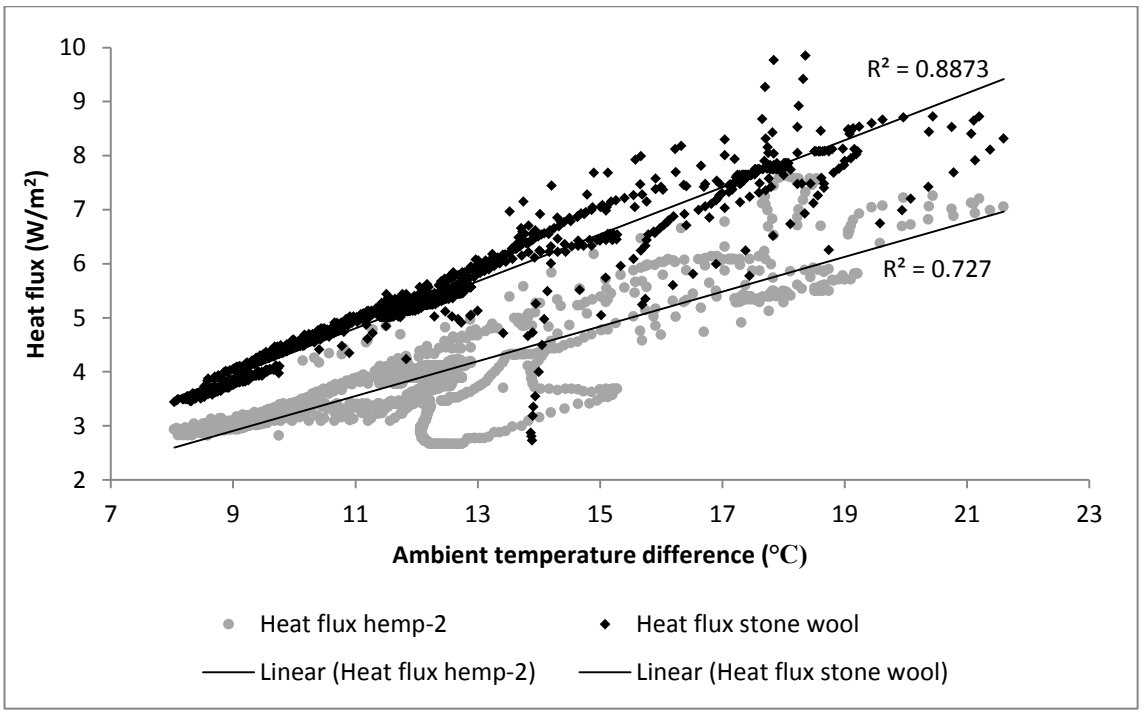


**Figure 6.21: Correlation between the ambient temperature difference and heat flux in hemp-2 and stone wool during test-2.**

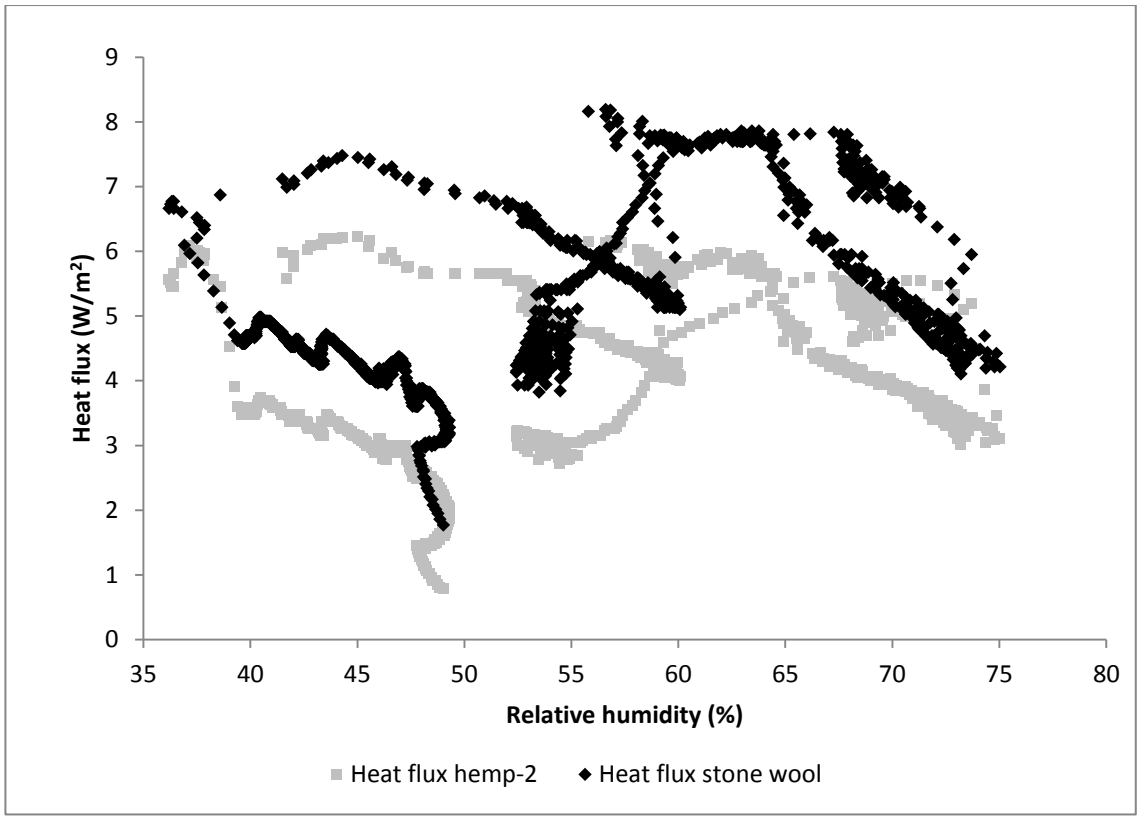


**Figure 6.22: Relative humidity in the hot box and heat flux in hemp-2 and stone wool insulation during test-1.**

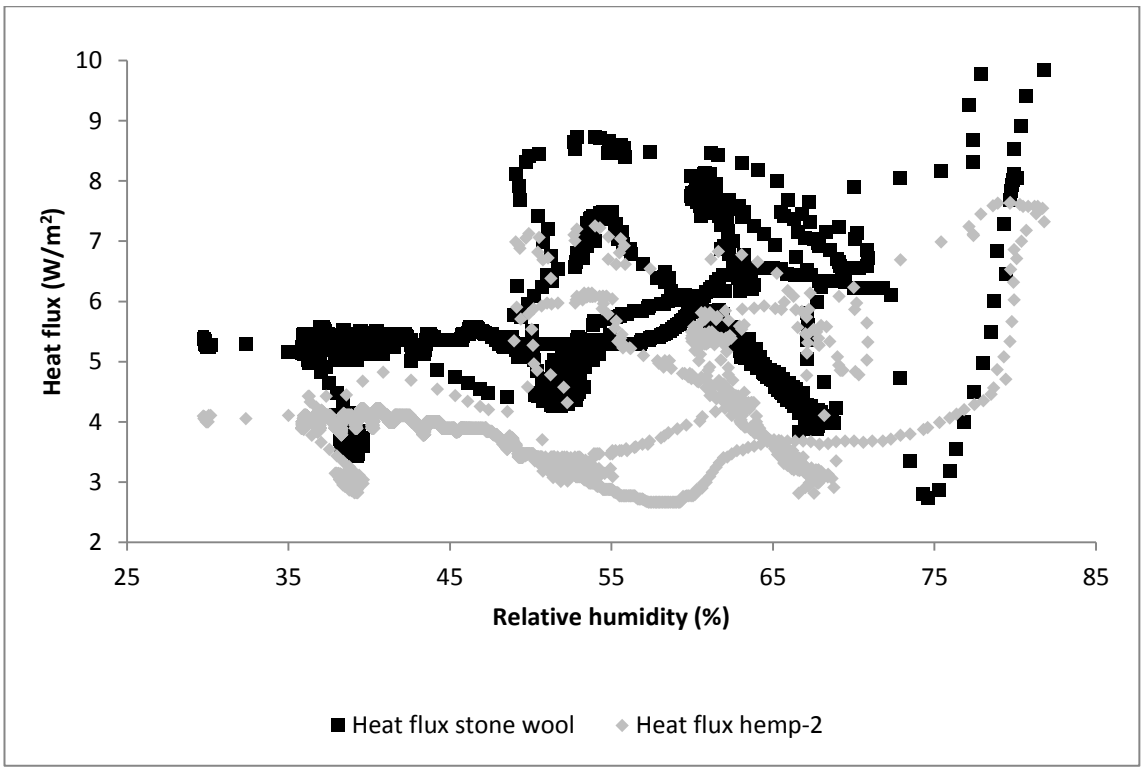


**Figure 6.23: Relative humidity in the hot box and heat flux in hemp-2 and stone wool insulation during test-2.**

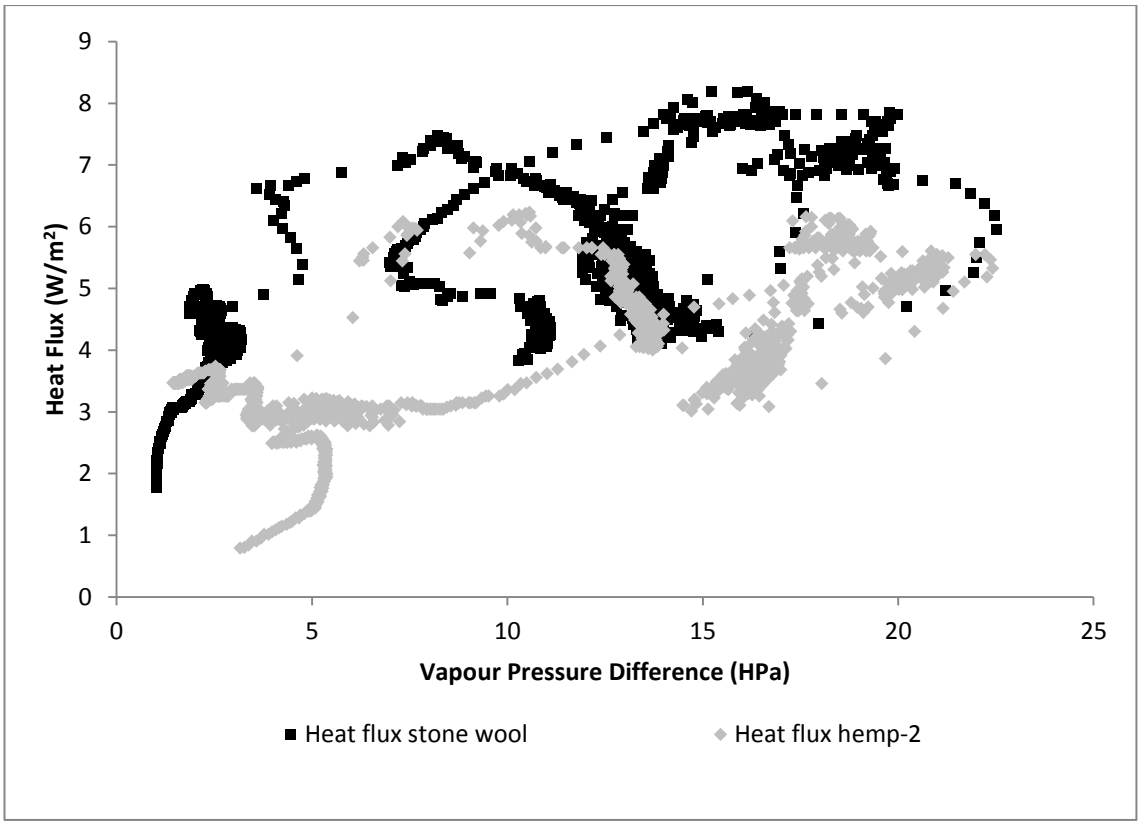


**Figure 6.24: Vapour pressure difference and heat flux in hemp-2 and stone wool insulation during test-1.**

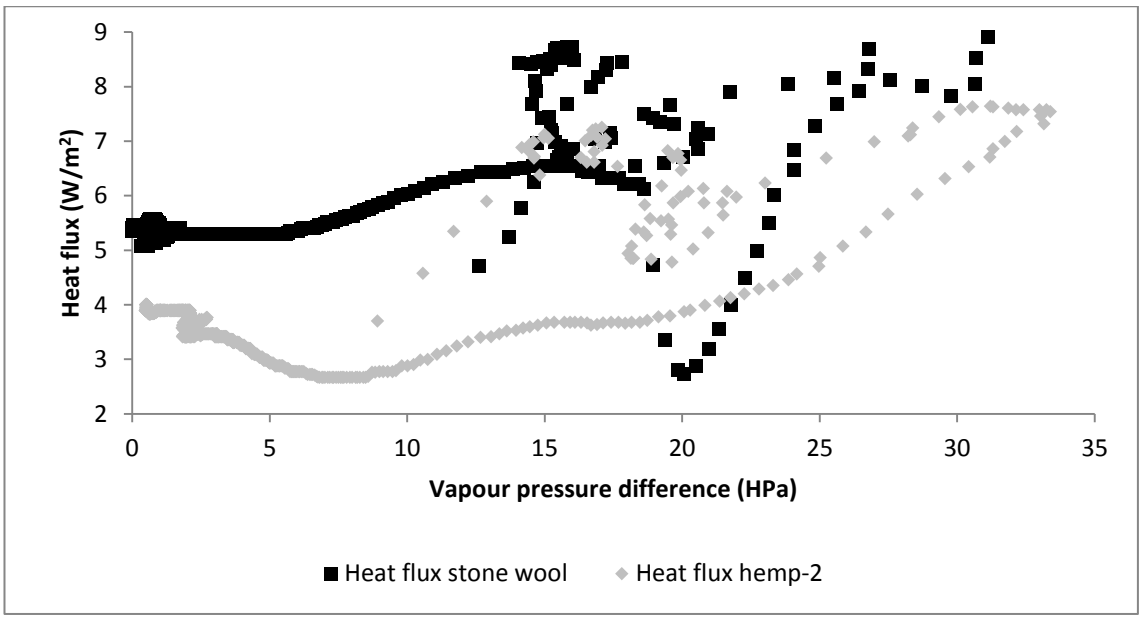


**Figure 6.25: Vapour pressure difference and heat flux in hemp-2 and stone wool insulation during test-2.**

Figure 6.26 shows the numerical heat flux predictions in the WUFI software and the corresponding experimental heat flux data during test-2 for hemp-2 and stone wool insulation materials. The average heat flux values are shown in Table 6.3. It can be noticed in the WUFI data in Table 6.3 that the heat flux in hemp-2 is higher than that in stone wool for most of the time. This may be because the WUFI software accounted for and over predicted the moisture dependent increase of thermal conductivity of hemp-2 insulation, whereas the heat loss through stone wool insulation by convective vapour flow and phase change went unregistered.

**Table 6.3: The average heat flux values of hemp-2 and Stone wool Insulations materials.**

| | Average heat flux in hemp-2 ($W/m^2$) | Average heat flux in stone wool ($W/m^2$) |
|---|---|---|
| Experimental Data | 4.37 | 5.37 |
| WUFI Prediction | 5.1 | 4.96 |

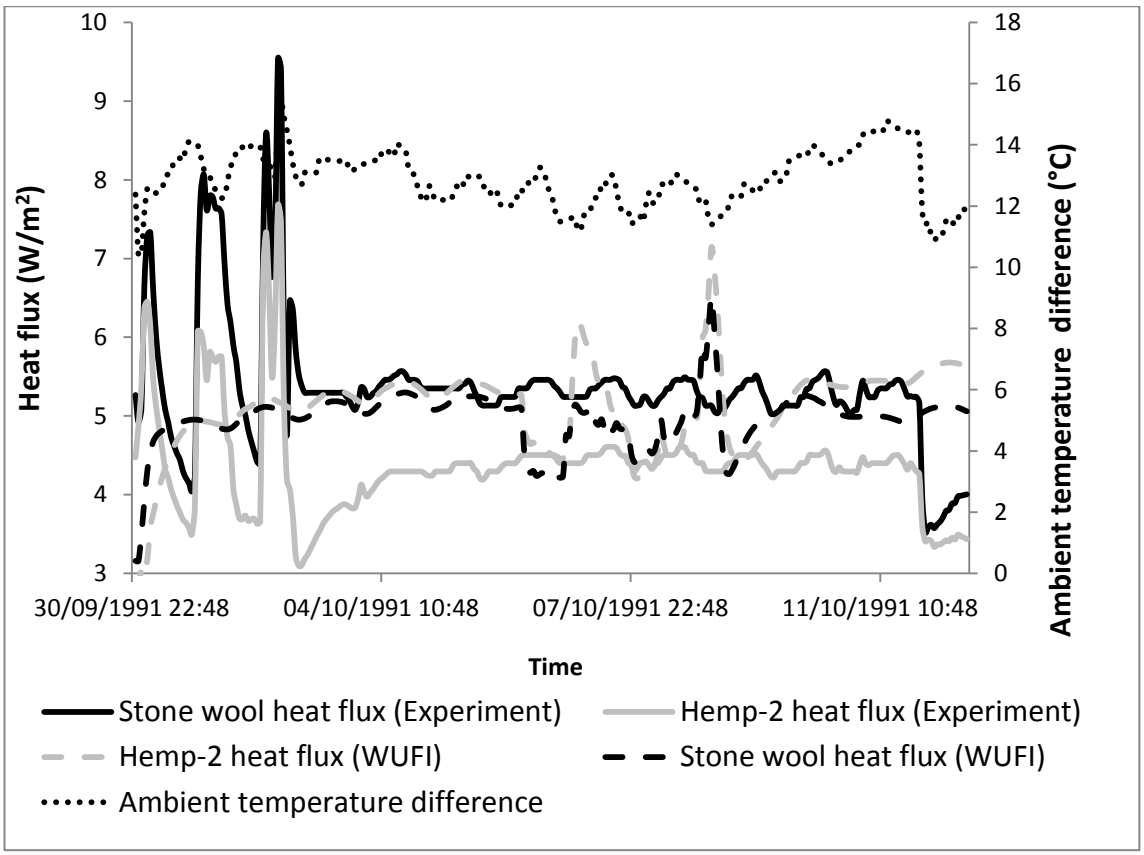


**Figure 6.26: Experimental data and numerical predictions (WUFI) of heat flux during test-2.**

The relationship between the ranges of average interior relative humidity and equivalent thermal conductivity are explored in Table 6.4, Figures 6.27 and 6.28. For hemp-2 insulation, the relationship between heat flux and relative humidity is expected to be nonlinear because of the nonlinear relationship between relative humidity and moisture adsorption capacity of hemp-2 insulation as shown in Figure 5.7 of chapter five. However, figure 6.27 shows a linear fit with a $R^2$ value of 0.93. This may happen due to the fact that, for hemp-2 insulation, EMC was not reached in the dynamic hygrothermal condition. For the stone wool insulation, equivalent thermal conductivity is unchanged from 50% until 80% relative humidity and then a sudden increase in equivalent thermal conductivity is observed at 80% relative humidity. This may indicate the onset of condensation and heat loss due to phase change. Figure 6.29 shows the relationship between equivalent thermal conductivity and the adsorbed moisture contents of hemp-2 insulation. The relationship is reasonably linear with an $R^2$ value of 0.88. It can be observed that if only the first three data points were used for the correlation, the relationship would have been absolutely linear. The EMC data for 80% relative humidity was based on

32 readings compared to the 392 readings for the EMC at 50% relative humidity. The use of more data may have shifted the last data point upward along the Y-axis, resulting in better linear fit. Alternatively, the slight nonlinearity in the relationship may indicate the existence of the 'other' mechanisms of heat flow (namely enthalpy flow, phase change, heat of wetting) in addition to the moisture dependent heat flux.

**Table 6.4: The average interior relative humidity and the corresponding equivalent thermal conductivity values of hemp-2 insulation and the corresponding adsorption water content**.

| Relative Humidity | $\lambda_{equi}$ (W/mK) | Adsorbed Water (from experimental data and GAB equation) (Kg/m$^3$) |
|---|---|---|
| 50% | 0.0349 | 8.69 |
| 60% | 0.0355 | 9.18 |
| 70% | 0.0414 | 12.35 |
| 80% | 0.0456 | 22.32 |

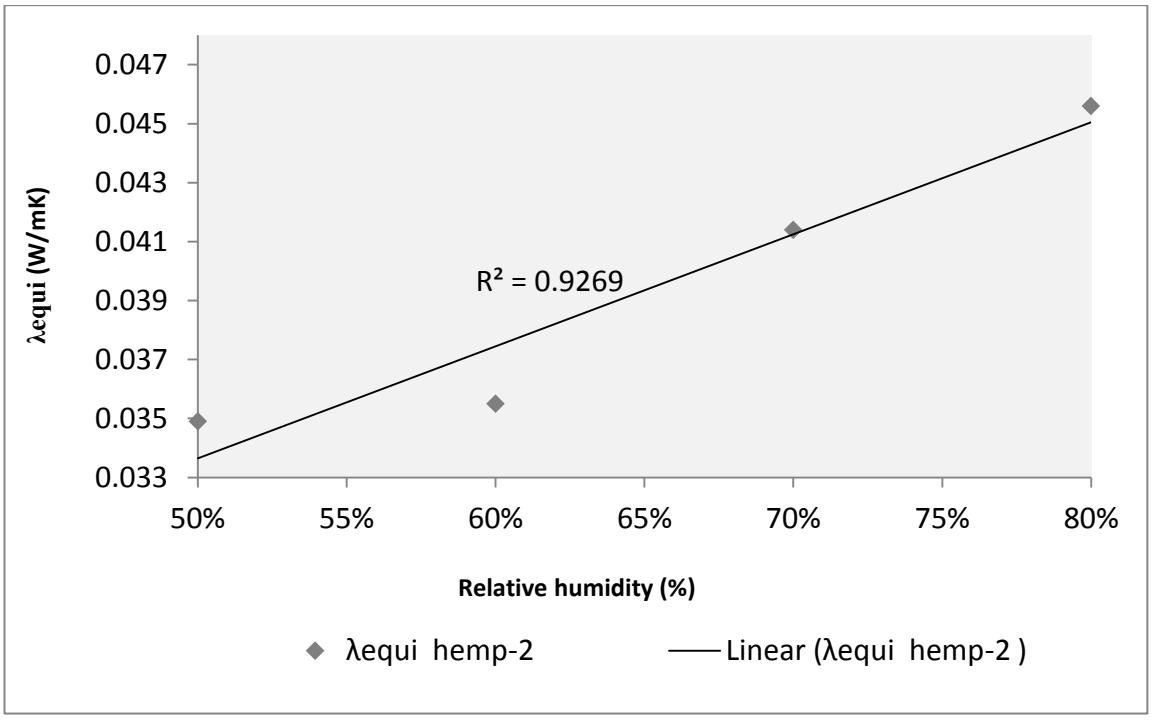


**Figure 6.27: Correlation between ranges of average relative humidity and equivalent thermal conductivity of hemp-2.**

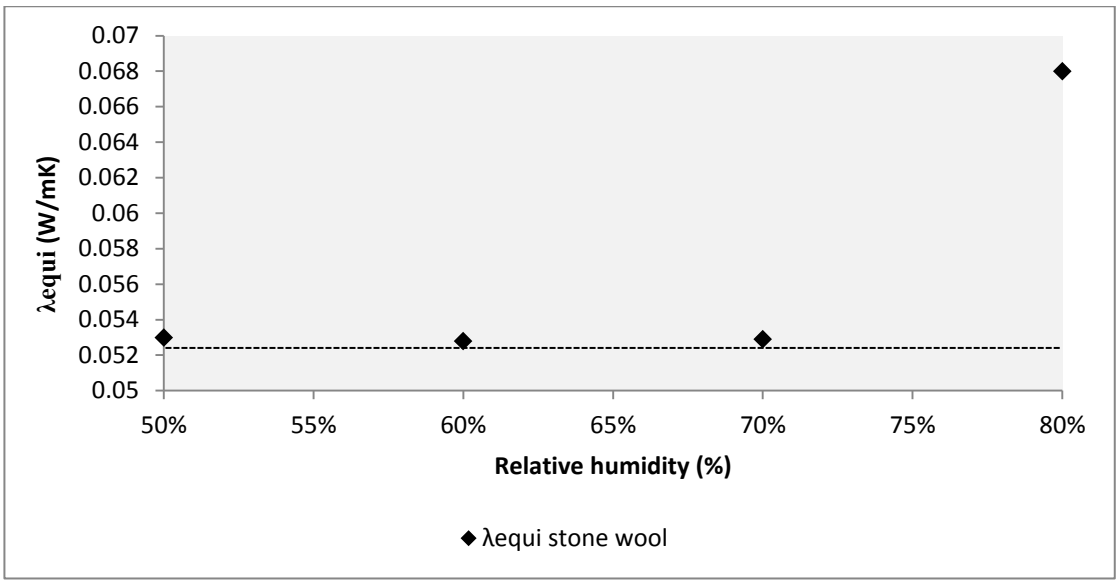


**Figure 6.28: Ranges of average relative humidity and corresponding equivalent thermal conductivity of stone wool.**

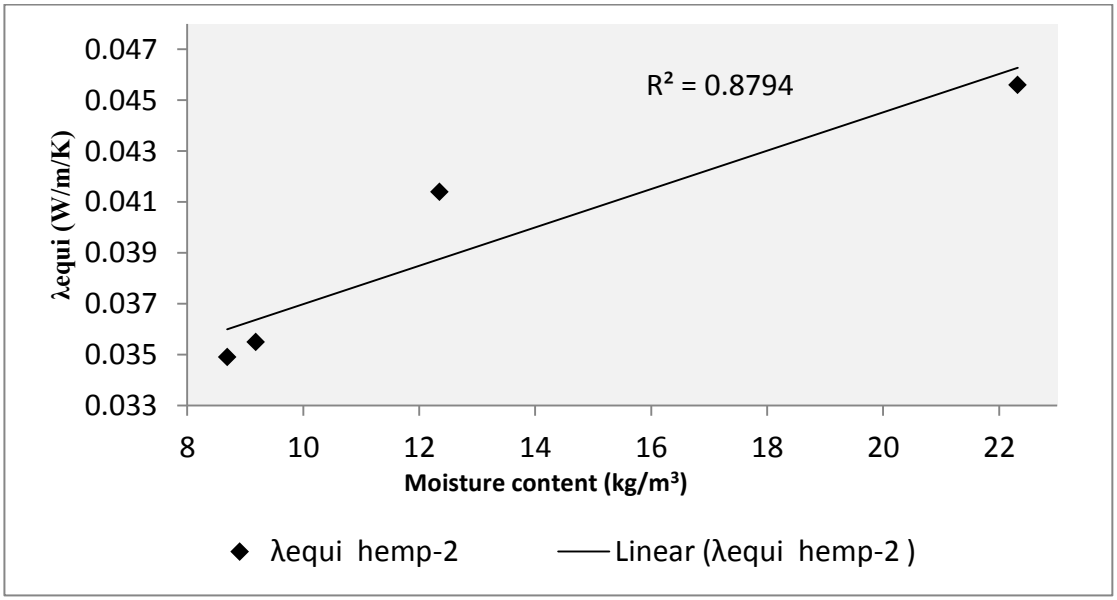


**Figure 6.29: Correlation between ranges of adsorbed moisture content and equivalent thermal conductivity of hemp-2.**

### *6.2.8 Summary of the dynamic experiment*

Samples of commercially available hemp-2 insulation and stone wool insulation were hygrothermally tested in a dual-insulation setup. The main objective of the study was to assess the likelihood of interstitial condensation in the interfaces of insulation materials and to determine the moisture and humidity dependent conductivity in dynamic conditions. The insulations were exposed to similar temperature, relative humidity and vapour pressure boundary conditions for

about 3 weeks' time during test-1 and test-2. It was observed that for the studied insulation samples, condensation could occur much earlier in the moisture barrier interface of stone wool insulation than in hemp-2 insulation if there is a vapour resistive substrate present behind the insulation. It has been observed that, compared to stone wool insulation, the relative humidity in hemp-2 insulation increases and decreases slowly in response to the increase and decrease of relative humidity in the hot chamber. This slow response of hemp insulation has two implications: firstly, in terms of the hygrothermal state of the building envelope, there is lesser likelihood of interstitial condensation in the insulation-OSB interface; secondly, since the rate and capacity of moisture adsorption and desorption is higher in hemp-2 insulation than in stone wool insulation, the amount of moisture adsorbed from and desorbed to the hot chamber will still be significantly higher than that by stone wool insulation. Thus, hemp-2 insulation will potentially function as a moisture buffer.

It was also calculated from the experimental data that condensation could occur as far as 10 mm inside the stone wool insulation during the interface condensation. It was also observed that moisture dependent thermal conductivity of hemp-2 insulation was lower than the moisture dependent thermal conductivity of stone wool insulation in a range of average relative humidity conditions. Another important finding is that the average thermal conductivity value obtained in average humidity for the test periods comprising test-1 and test-2 closely agrees with the result of design thermal conductivity value determined using BS EN 10456 for hemp-2 insulation. These results can be relevant to the conditions where insulations are installed in a roof with vapour barrier at the outer surface, or to a vapour open situation (or a situation with a faulty vapour barrier) where there is a relatively impermeable material on the cold side of the insulation.

### 6.3 Hygrothermal performance of hemp-2 and stone wool insulation materials in quasi steady state hygrothermal conditions

The previous tests in section 6.2 focused on assessing hygrothermal properties of hemp-2 and stone wool insulations in dynamic conditions. Due to the limitations of the setup and the dynamic nature of the hygrothermal conditions, data have been gathered when both the relative humidity and temperature

difference were state variables during test-1 and test-2. Equivalent thermal conductivity values for the peak relative humidity were based on very limited data. The aim of the experiment in this section was to assess the hygrothermal performance of hemp-2 and stone wool insulations materials in hygrothermal conditions where the temperature difference would remain constant and step changes would be made in interior relative humidity. Thus, each step would provide sufficient time for the insulation materials to reach equilibrium moisture content. The hygrothermal boundary conditions are a combination of steady and dynamic conditions (the step changes of interior relative humidity) and are defined here as quasi steady state conditions.

### *6.3.1 The insulation samples*

The material properties of the sample insulation materials and manufacturers' declared thermal conductivity values of the insulation materials are provided in Table 4.1 and Table 4.2 of chapter four.

### 6.3.2 *Instrumentation and experimental setup*

#### *6.3.2.1 Feutron dual climate chamber*

The Feutron duel climate chamber is described in subsection 4.5.1.2 of chapter five.

#### *6.3.2.2 Temperature and relative humidity sensors*

CS215 temperature and relative humidity sensors were used to measure temperature and relative humidity. 107 thermistor probes from Campbell Scientific were used to measure temperature. Further details of 107 thermistor probe and CS215 temperature and relative humidity probe can be found in subsections 4.5.1.4 and 4.5.1.5, respectively, of chapter four of this thesis. In addition to these sensors, temperature and humidity data loggers (EL-USB-2) by Lascar Electronics were used. The temperature measurement range of the EL-USB-2 data logger is -35 °C to 80 °C and the accuracy is ± 0.5 °C. The humidity measurement range is 0% to 100% and accuracy is ±3%.

#### *6.3.2.3 Heat flux sensors*

HFP01 heat flux sensors were used to measure the heat flux through the insulation materials. Further detail of the heat flus sensors can be found in subsection 4.5.1.6 of chapter four.

#### *6.3.2.4 CR1000 data logger*

CR1000 data logger was used for gathering data from the sensors and probes. A brief description of CR1000 data logger is provided in subsection 4.5.1.3 of chapter four. The data can be displayed in the computer by using the PC400 software.

#### *6.3.2.5 Sample installation*

Hemp-2 and stone wool insulation samples were placed inside the extruded polystyrene (XPS) insulation frameworks. The dimensions of the framework, the placement of insulations and the sensors are shown in Figures 6.30 and 6.31.

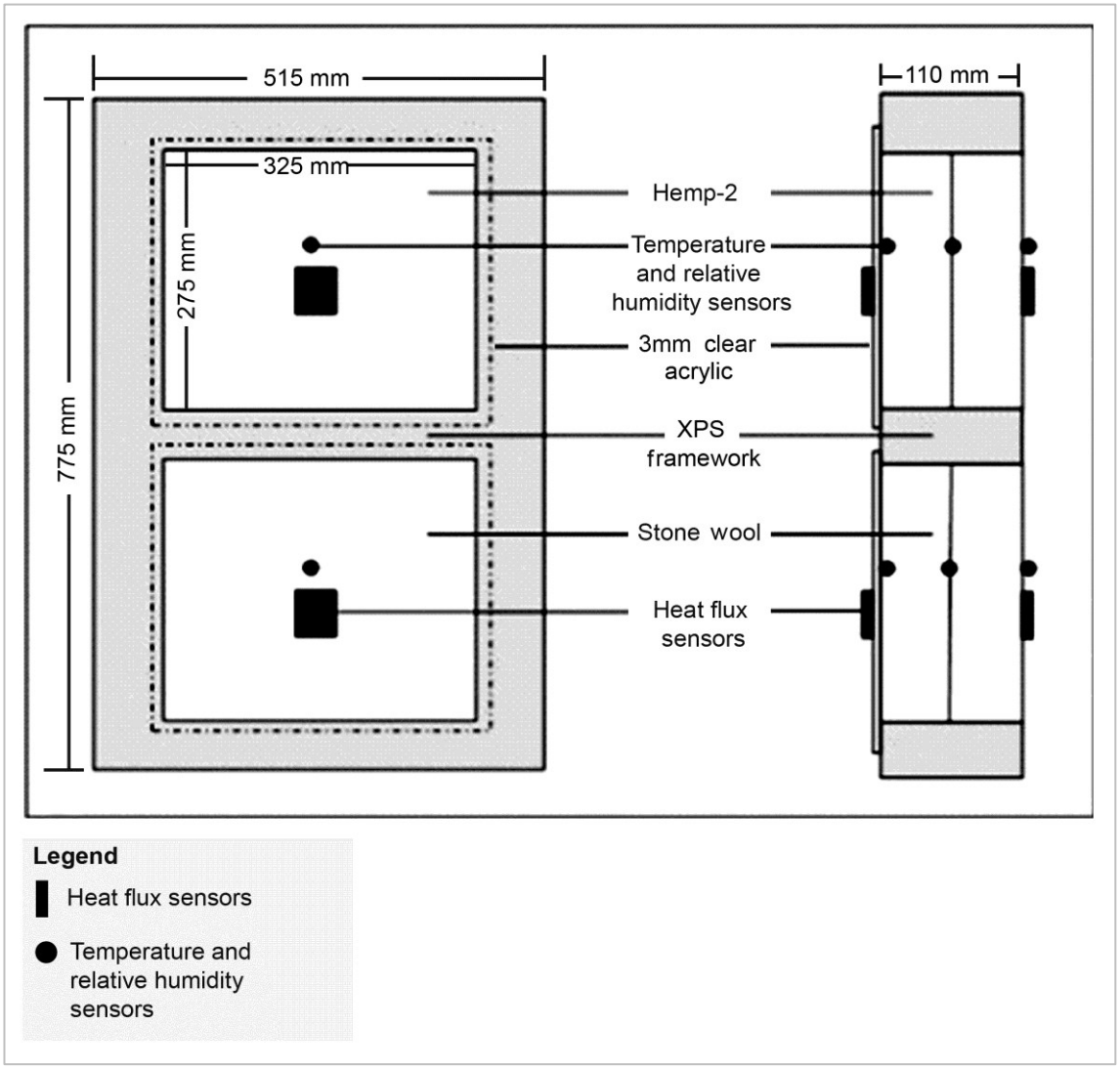


**Figure 6.30: Front elevation and cross section of the insulation setup.**

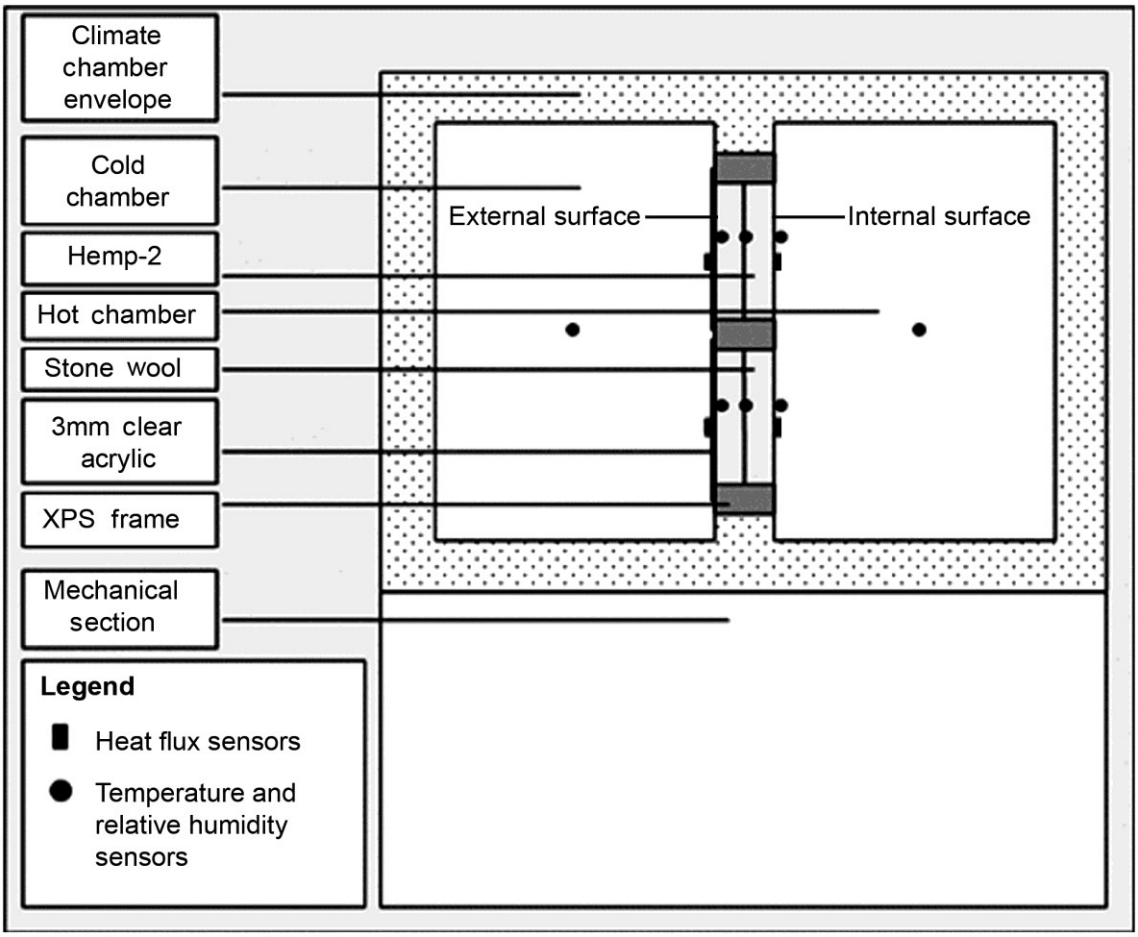


**Figure 6.31: Cross section of the dual climate chamber.**

The XPS frameworks (Figure 6.32) were placed in a steel partition frame as shown in Figure 6.33. The steel partition frame was installed between the hot and cold chamber, as shown in Figures 6.34 and 6.35. Temperature and relative humidity sensors were placed in the mid-thickness, on the cold side surface and on the warm side surface of the insulation materials. Heat flux sensors were placed on the cold and warm side surfaces of the insulation materials.

The cold side of the hemp-2 and stone wool insulation surfaces were covered with 3 mm acrylic sheets. The 3 mm acrylic sheets were integrated with the XPS frameworks, as shown in Figure 6.30, in such a way that there was no moisture related interaction between the cold chamber and the insulation.

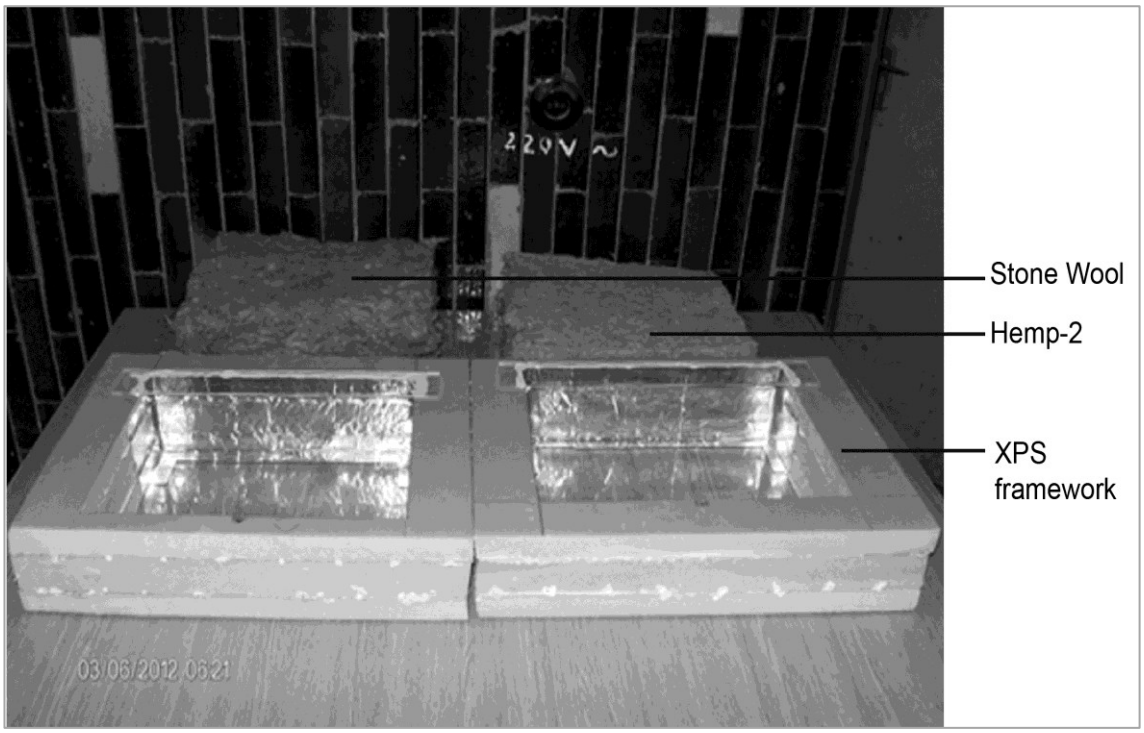


**Figure 6.32: Insulation materials to be placed on the EPS frameworks.**

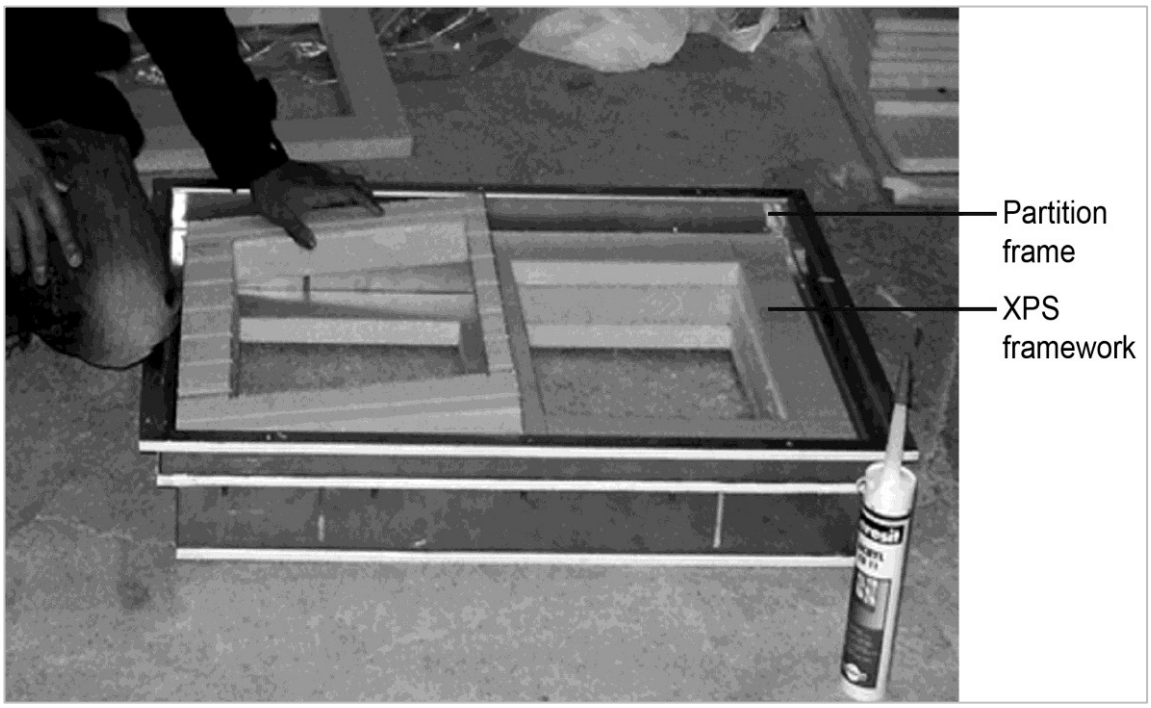


**Figure 6.33: The XPS framework and the partition frame.**

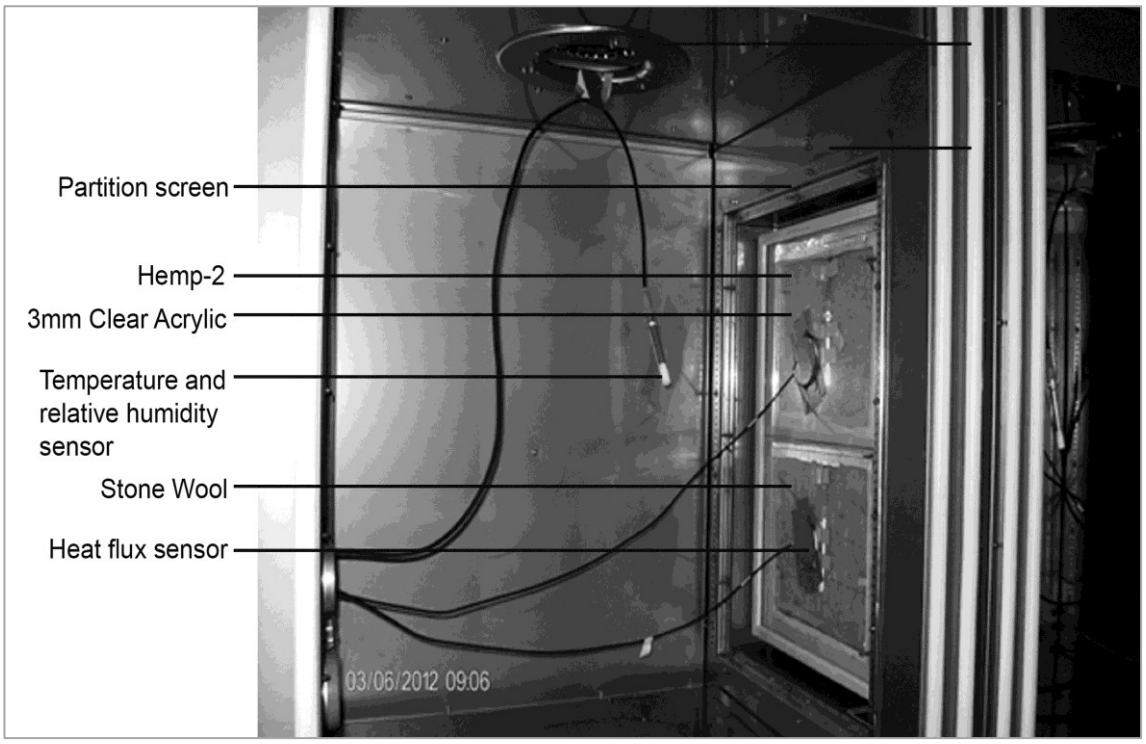


**Figure 6.34: The insulation materials placed between the hot and cold chamber.**


**Figure 6.35: The insulation materials between the hot and cold chamber with all the sensors installed.**

### *6.3.3 Experimental method*

The temperature and relative humidity profile for the laboratory experiment and the WUFI simulation is shown in Table 6.5 and Figure 6.36. Temperature in the hot chamber was set at constant 23 °C and in the cold chamber at constant 7 °C resulting in a constant temperature difference of 16 °C ± 1 °C. The following step changes in relative humidity were made in the hot chamber at every 24 hours: 33%, 55%, 80%, 95%, 55%. However, the duration of the initial step (33%) was 33 hours instead of 24 hours so that the insulation materials were in reasonably dry states. The relative humidity in the cold chamber was kept steady at 55%.The relative humidity in the cold chamber was not interacting with the insulation since the insulation materials were covered with acrylic sheet in the cold side surfaces.

The analysis of the temperature, relative humidity and heat flux data will show how the insulation materials are managing moisture and relative humidity at critical interfaces and how the changes in relative humidity are influencing heat flux through the insulation materials.

**Table 6.5: The temperature and relative humidity profile of the climate chamber.**

| | **Cold Chamber** | | | **Hot Chamber** | | |
|---|---|---|---|---|---|---|
| **Steps** | **Temperature (°C)** | **Relative Humidity (%)** | **Duration (Hours)** | **Temperature (°C)** | **Relative Humidity (%)** | **Duration (Hours)** |
| 1 | 7 | 55 | 33 | 23 | 33 | 33 |
| 2 | 7 | 55 | 24 | 23 | 55 | 24 |
| 3 | 7 | 55 | 24 | 23 | 80 | 24 |
| 4 | 7 | 55 | 24 | 23 | 95 | 24 |
| 5 | 7 | 55 | 24 | 23 | 55 | 24 |

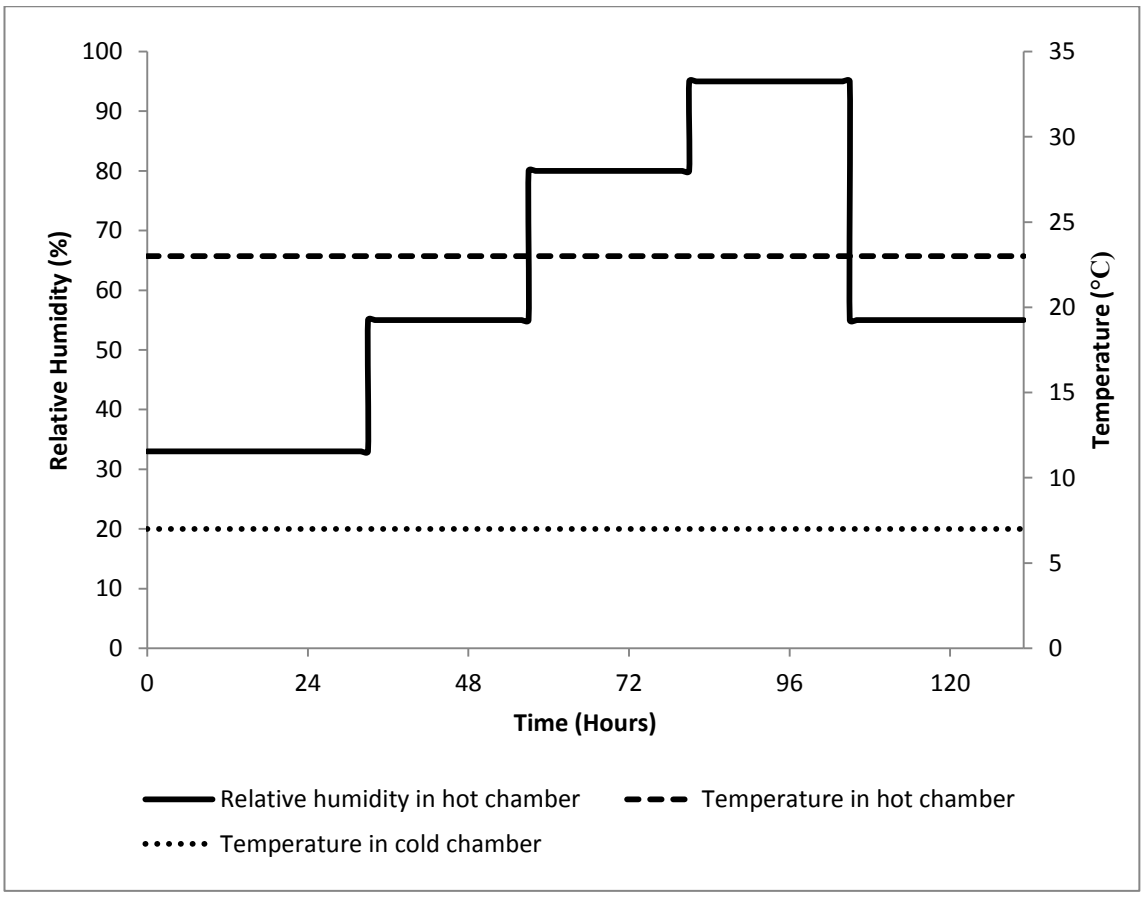


**Figure 6.36: The temperature and Humidity profile of the climate chamber.**

### *6.3.4 Results and discussion*

#### *6.3.4.1 Relative humidity and interstitial condensation*

The relative humidity condition at internal surface, middle and external surfaces of the hemp-2 and stone wool insulation materials are shown in the Figure 6.37 and 6.38. Relative humidity at internal surface, external and in the middle of the stone wool insulation changes immediately in response to the step changes of relative humidity in the hot chamber. On the contrary, the relative humidity in the middle and in the external surface of hemp-2 insulation changes slowly in response to the step changes of relative humidity in the hot chamber.

In Figure 6.39, it can be observed that the relative humidity in the interface of (stone wool)-acrylic rose to about 95% as soon as the relative humidity of the hot chamber changed from 33% to 55%. At the same time, relative humidity of (hemp-2)-acrylic interface gradually increased to 72%. When the relative humidity of the hot chamber increased to 80% after 77 hours from the beginning of the experiment, the relative humidity of (stone wool)-acrylic interface

increased to about 98.4% while relative humidity of (hemp-2)-acrylic interface increased to about 84.3%.

Although the highest relative humidity in the hot chamber was planned as 95%, the relative humidity of the hot chamber actually reached 100% (±3%) as registered by the relative humidity sensors. When the relative humidity of the hot chamber increased from 80% to 100%, relative humidity of the interface of (stone wool)-acrylic went up to 100%, and of (hemp-2)-acrylic went up to 95% (which is equal to the initial response of stone wool interface in response to the 55% relative humidity of the hot chamber). Relative humidity of (hemp-2)-acrylic interface became 100% only after the insulation was exposed to all the increasing step changes of relative humidity (33 hours to 33%, 24 hours to 55%, 24 hours to 80% and 24 hours to 100%) in 105 hours.

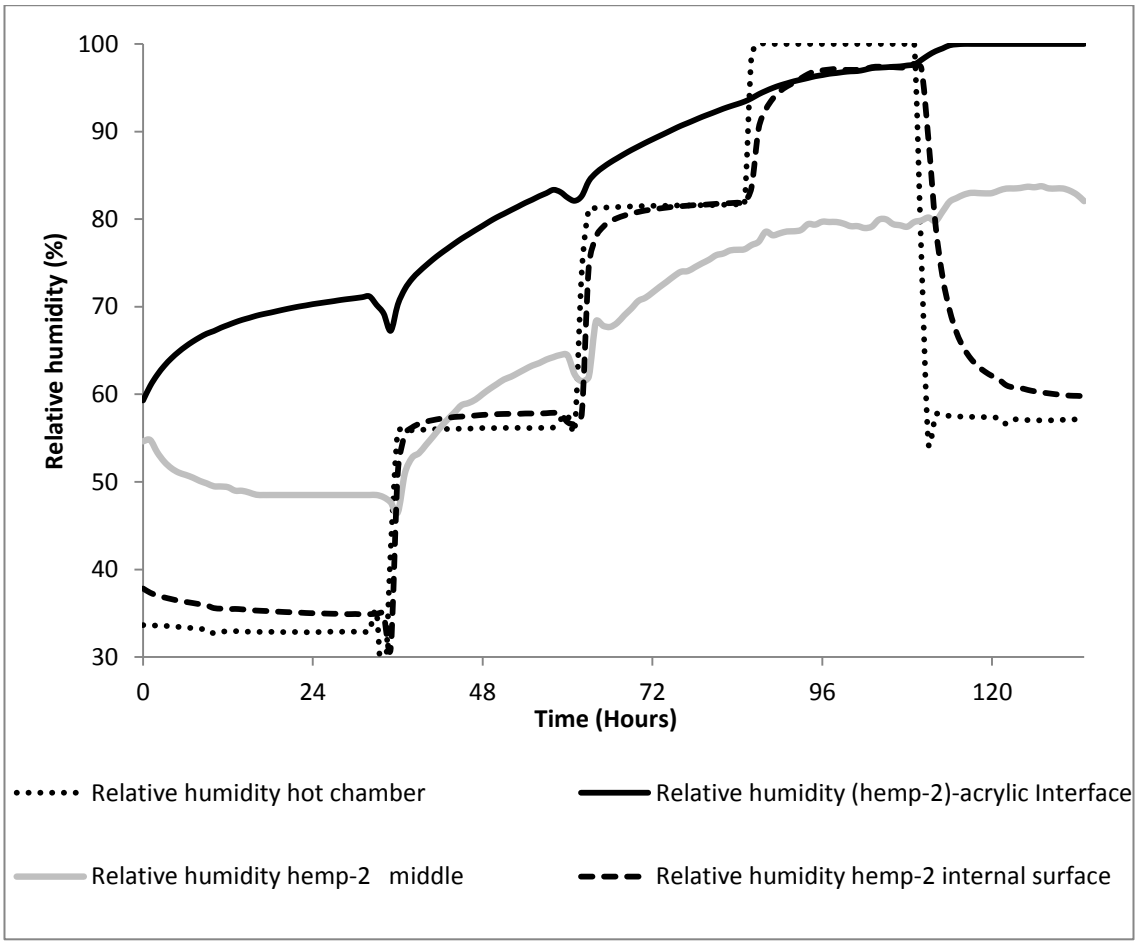


**Figure 6.37: Relative humidity in the middle and in the surface of hemp insulation.**

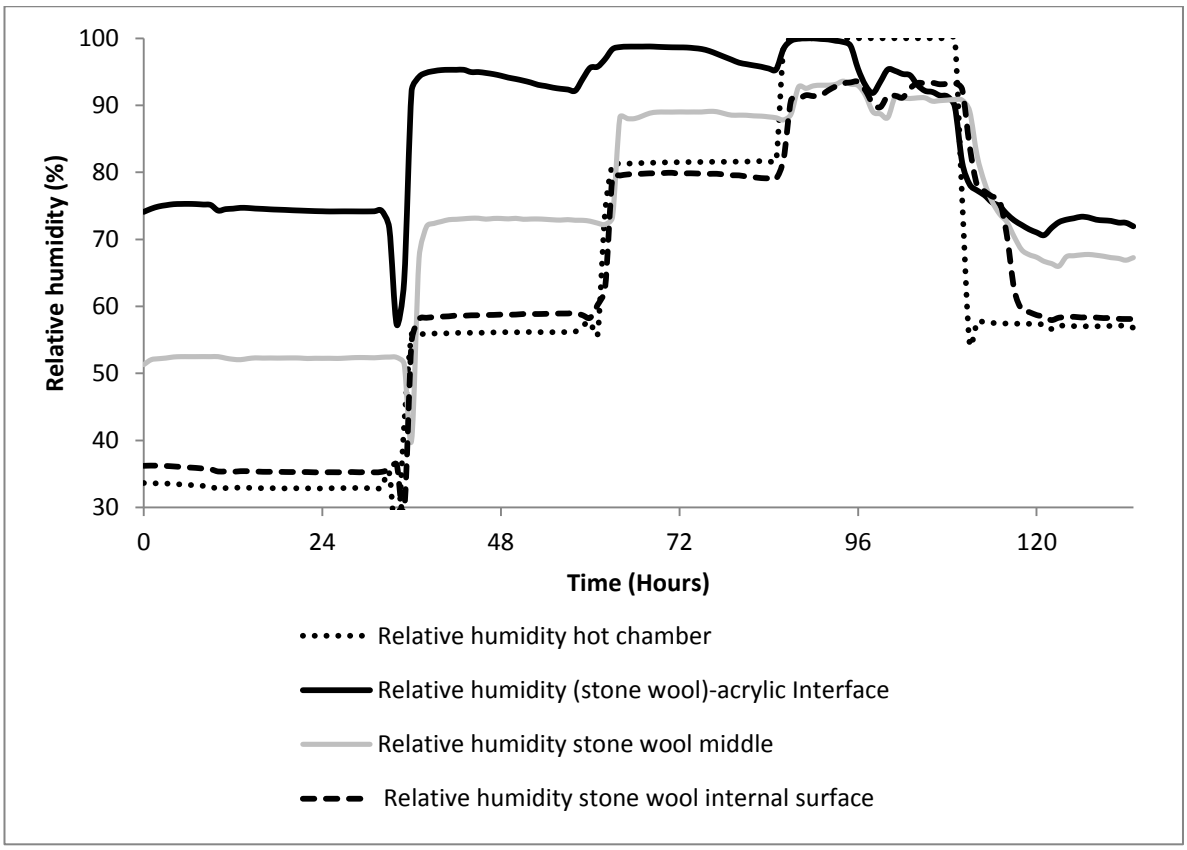


**Figure 6.38: Relative humidity in the middle and in the surface of stone wool insulation**.

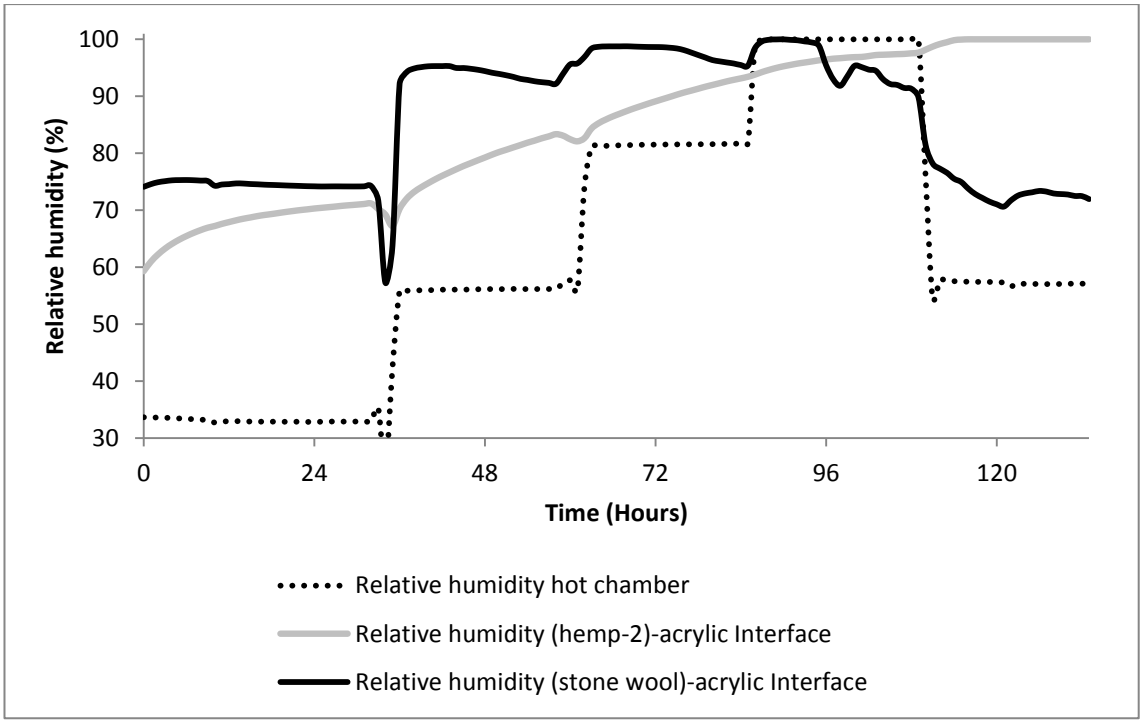


**Figure 6.39: Relative humidity in the insulation-acrylic interface and in the hot chamber.**

Figure 6.40 shows droplets of condensed water on the inner surface of the acrylic in the stone wool setup and foggy deposit of moisture on the acrylic surface of the hemp-2 setup. The photograph was taken at the end of the experiment, as it was not technically possible to open the door of the cold chamber when the experiment was running. When the insulation materials were removed from the framework, water deposits on the lower inner surface of the framework of the stone wool insulation were also noticed, meaning that further condensation had occurred in the stone wool insulation setup during the experiment. From the experiment, it can be assumed that hemp-2 insulation can delay the occurrence and lower the frequency of condensation compared to stone wool insulation.

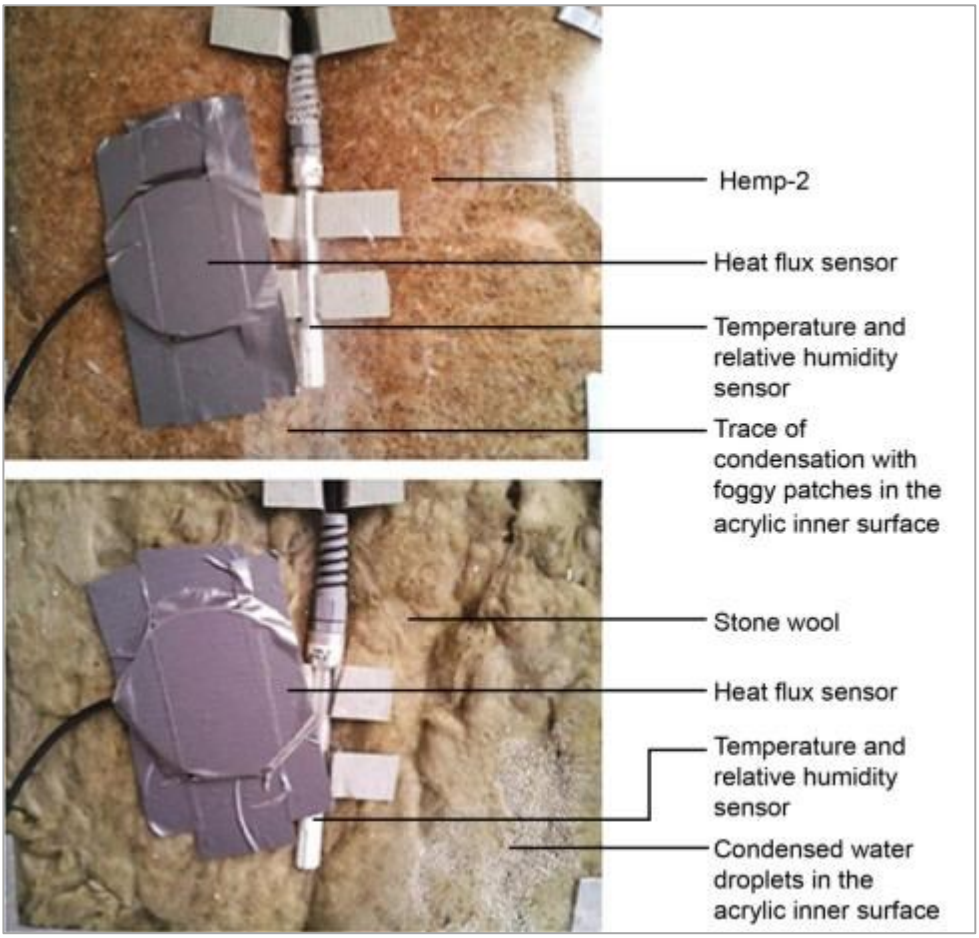


**Figure 6.40: Dew formed in acrylic inner surface of stone wool insulation and foggy patches in acrylic inner surface of hemp-2 insulation.**

Hygrothermal simulation in the WUFI software for the similar setup and similar boundary conditions to those of the experiment was carried out. The result is shown in Figure 6.41 along with the experimental results in relation to the relative humidity conditions in the insulation-acrylic interfaces. For

(hemp-2)-acrylic interface, the initial rise in relative humidity is over predicted and final rise in relative humidity is under predicted compared to the experimental data. Apart from this, the prediction is close to the experimental measurements. Relative humidity sensors have an error range of ±4% and the moisture flow by convection current is not taken into account in WUFI simulation. These factors can also contribute to the difference between the experimental results and WUFI simulation results. The WUFI software prediction for hemp-2 insulation seems to provide reasonable background for taking decisions about the use of insulation during the design stage of a building.

For stone wool-acrylic interface, the humidity rise in WUFI simulation is under predicted most of the times compared to the experimental data. The WUFI software also fails to predict the response of stone wool insulation when relative humidity in the warm chamber suddenly goes down from 100% to 55%.

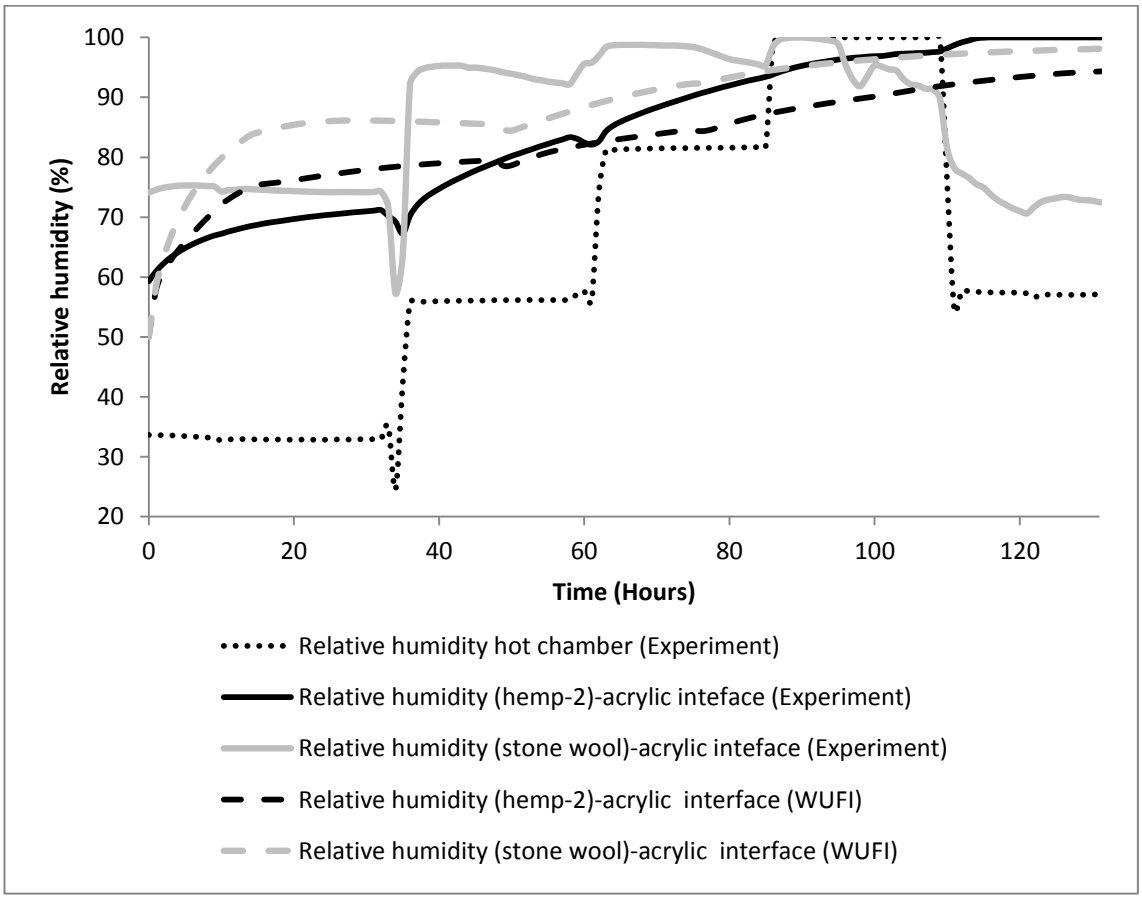


**Figure 6.41: Relative humidity in the insulation-acrylic interface and in the warm chamber during the laboratory experiment and simulation in the WUFI software.**

Figure 6.42 shows the internal surface temperature of the acrylic and the dew point temperature of (hemp-2)-acrylic interface air and (stone wool)-acrylic interface air. Condensation seemed to occur in the acrylic surface of the (stone wool)-acrylic interface as soon as the humidity of hot chamber increased from 33% to 55% and remained at 55% for about next 60 hours. Condensation occurred in the acrylic surface of the (hemp-2)-acrylic interface approximately 36 hours later than it occurred in the (stone wool)-acrylic interface. By that time, hemp-2 was exposed to 33% relative humidity for 33 hours, 55% relative humidity for 24 hours and 82% relative humidity for 8 hours. It is also important to note that hemp responded slowly to the decreasing step change in boundary relative humidity conditions. Figures 6.37 and 6.38 show the relative humidity distribution in the external surface, internal surface and in the middle of the hemp-2 and stone wool insulation materials, respectively. Clearly, the middle of the stone wool insulation is also responding instantly to the changes of relative humidity in the warm chamber whereas the middle of the hemp insulation is showing a dampened response to the relative humidity changes in the warm chamber.

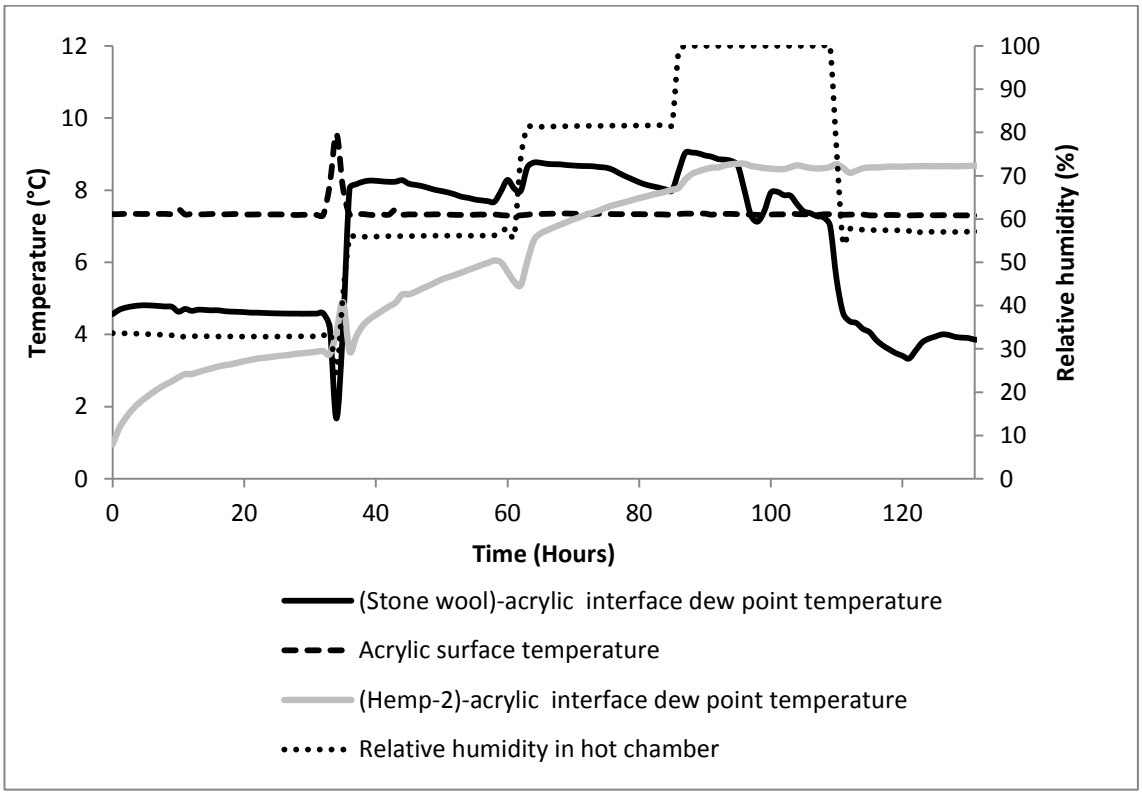


**Figure 6.42: Internal surface temperatures of the acrylic and the insulation-acrylic dew point temperatures.**

So far it has been noted that relative humidity in the middle and in the insulation-acrylic interface of hemp-2 insulation increases very slowly over a time of period of 105 hours while the relative humidity in similar positions for stone wool insulation increases almost instantly in response to its exposure to the increase of external relative humidity. The temperature difference between the warm side and cold side of both insulations remained equal and constant most of the time. The temperature in the insulation-acrylic interfaces also remained nearly the same and unchanged. It can be then stated that the rate of moisture flow in (hemp-2)-acrylic interface was lower than that in (stone wool)-acrylic interface during the experimental run despite the fact that vapour permeability of the particular hemp insulation is higher than that of the particular stone wool insulation. The higher moisture adsorption capacity of hemp-2 seems to be the main reason for this response of hemp-2 insulation.

Figure 6.43 shows the dew point temperature of insulation-acrylic interface air and the actual temperature of the humid air in (stone wool)-acrylic and (hemp-2)-acrylic interfaces. It can be noted that the air temperature in stone wool insulation is nearing the dew point temperature many times. When the relative humidity of the hot chamber increased from 33% to 55%, the actual air temperature in (stone wool)-air interface was 8.83 °C and the dew point temperature was about 8.23 °C. When the hot chamber relative humidity increased from 55 % to 80%, the stone wool-acrylic interface air temperature was 8.97 °C and the dew point temperature was 8.76 °C. Thus, in the case of (stone wool)-air interface, dew may even form in the air at those critical moments without having to touch the acrylic surface. Similar observation can be made about hemp-2 insulation approximately at $112^{th}$ hour of the experiment after the insulation is exposed to 100% relative humidity for 24 hours.

Moisture flow is a function of hygroscopic capacity, vapour permeabilityand rate of air flow. Vapour permeability can also vary in thermal insulation if bulk density changes (Batty *et al.*, 1981). Vapour permeability has been determined according to ISO 12086 (British Standards Institute, 1997). Vapour permeability of the hemp-2 insulation is a little higher than that of the stone wool insulation, the rate of air flow should not be much different as both these fibrous insulation have approximately similar porosity (0.95) and are exposed to similar boundary conditions. Therefore, moisture adsorption capacity plays an important role in

terms of regulating moisture flow through these insulationsin dynamic conditions.

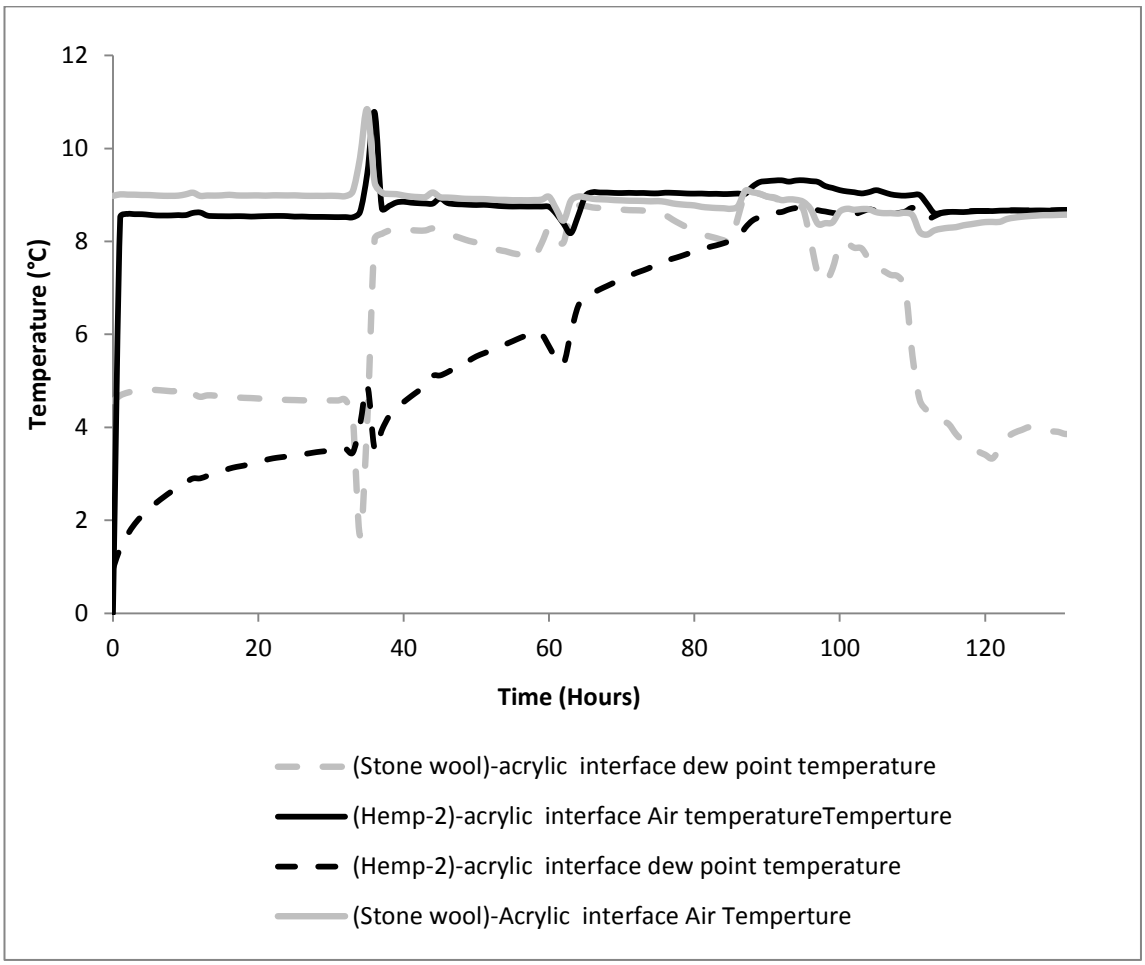


**Figure 6.43: Insulation-acrylic interface air temperature and dew point temperature.**

Figure 6.44 shows the WUFI simulation results for water contents in the insulation materials. It can be observed that the highest amount of moisture content in the hemp-acrylic interface air is 8.5 kg for each unit volume compared to 20 kg in the stone wool-acrylic interface air. This implies higher amount of water will be condensed in stone wool-acrylic interface. The highest moisture content inside the external surface of hemp-2 is about 23 kg, which is within the hygroscopic sorption range. The highest moisture content inside the external surface of stone wool insulation is about 10 kg, which is only possible when there is condensation inside the stone wool insulation surface.

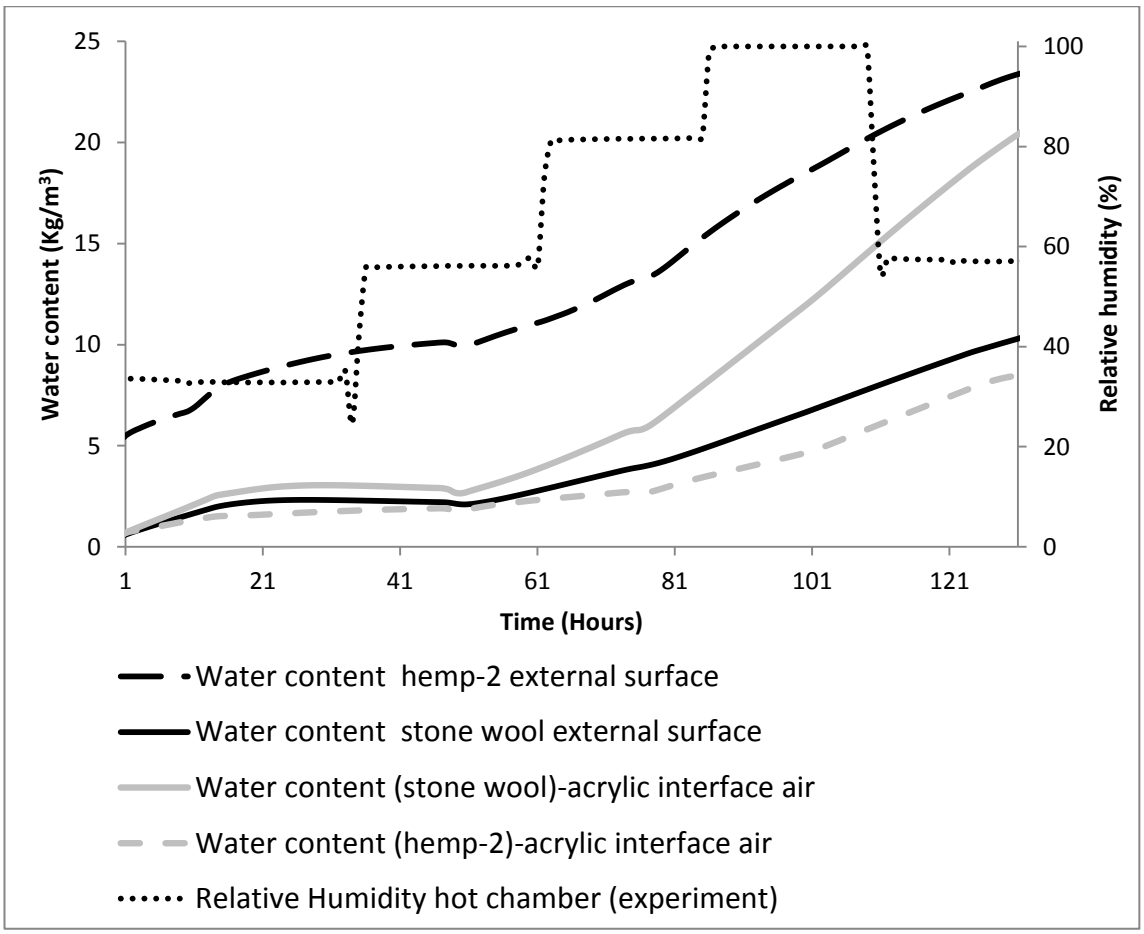


**Figure 6.44: WUFI simulation data of water content in insulation external surfaces and insulation-acrylic interfaces.**

Once condensation occurs in the insulation-acrylic interface, condensed water in touch with the insulation can be absorbed by the insulation. The amount of water that will be left on the surface of the acrylic will depend on the rate of condensation and the coefficient of water absorption. Water absorption coefficient was determined according to BS EN ISO 15148 (British Standards Institute, 2002). Water absorption coefficient of hemp-2 insulation is 0.034 $kg/m^2\sqrt{s}$. Water absorption coefficient of stone wool insulation should be negligible. Therefore, hemp-2 will absorb more water than stone wool insulation when condensed water is in touch with the insulation surfaces. In stone wool insulation, the insulation-acrylic interface contains more water than the external surface of the insulation. In hemp insulation the situation is opposite due to the absorption and adsorption capacity of hemp-2 insulation.

#### *6.3.4.2 Heat flux and equivalent thermal conductivity*

The experimental data were examined to determine the equivalent thermal conductivity values of hemp-2 and stone wool insulation materials for the total

period of the experiment and for the following ranges of relative humidity: 33%, 56%, 81% and 100%. The equivalent thermal conductivity values of hemp-2 insulation were also determined for the adsorbed water content for the aforementioned ranges of relative humidity. The data were also analysed to explore the following bivariate relationships:

- Heat flux and relative humidity,
- Heat flux and vapour pressure difference,
- Equivalent thermal conductivity and ranges of relative humidity,
- Equivalent thermal conductivity and adsorbed water content by the hemp-2 insulation at ranges of relative humidity.

The equivalent thermal conductivity values were determined from ambient temperature differences, heat flux and thickness of the material according to the equation 6.1. These values are shown in Figures 6.45 and 6.46. It can be noticed in Figure 6.45 that the temperature difference between the hot and cold chambers was constant throughout the duration of the experiment. Therefore, changes of equivalent thermal conductivity values of the insulation materials can be assumed to be due to the changes in relative humidity in the hot chamber. It can be observed that the equivalent thermal conductivity of hemp-2 increases with each increasing relative humidity range, which can be explained in terms of the EMC of hemp-2 insulation. However, it can also be noticed that the equivalent thermal conductivity of stone wool insulation started decreasing from the onset of condensation (as calculated) whereas the heat flux was expected to increase due to phase change. One of the reasons for this phenomenon can be the difference in the position of the heat flux sensor and the area of condensation on the acrylic surface. The heat flux sensors, due to its placement, failed to log the heat flux due to phase change. There is also a possibility that the oncoming heat was absorbed by the condensate and thus the heat flux sensor registered lower heat flux.

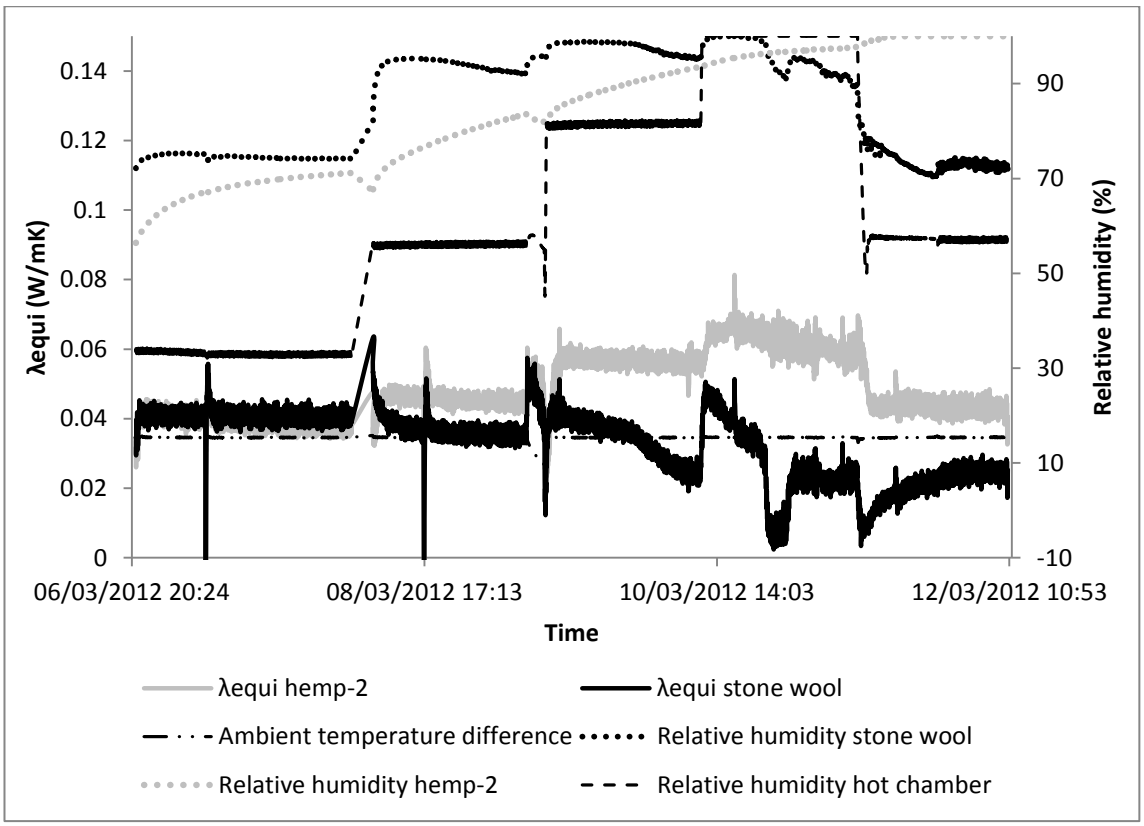


**Figure 6.45: Equivalent thermal conductivity values of hemp-2 and stone wool insulation along with the values of interior and insulation-acrylic interface relative humidity.**

A matrix of equivalent thermal conductivity has been developed from the data shown in Figure 6.46 and is presented in Table 6.6 along with the design values of the thermal conductivity. As the heat flux meters in the cold side were firmly attached to the acrylic throughout the experimental period, heat flux data from that side are used for the analysis and determination of equivalent thermal conductivity values of the insulation materials. In Figure 6.46 and Table 6.6, it can be noticed that the equivalent thermal conductivity value of hemp-2 is gradually increasing and that of stone wool is gradually decreasing with the increase in relative humidity. The design values of thermal conductivity of the insulation materials in Table 6.6 are determined by applying equation 6.2. The average of the whole data in Figure 6.46 shows that the equivalent thermal conductivity of hemp-2 at an average relative humidity of 63% is 0.048 W/mK. The design value of hemp-2 for the similar relative humidity exposure is 0.038 W/mK. The experimental average equivalent thermal conductivity value of stone wool (0.033 W/m-K) is lower than the design thermal value (0.04 W/m-K). It can also be observed that, while the design values and experimental values are

equal in terms of first two decimal places of hemp-2 insulations at 33% and 56% relative humidity, design values of hemp-2 insulations at 81% and 100% relative humidity are about 21% and 24% higher than the corresponding experimentally determined thermal conductivity values. For the stone wool insulation, there is a substantial difference between experimental and design values of thermal conductivity, with design values of thermal conductivity being about 18%, 25% and 54% higher than the experimental values for 56%, 81% and 100% relative humidity, respectively.

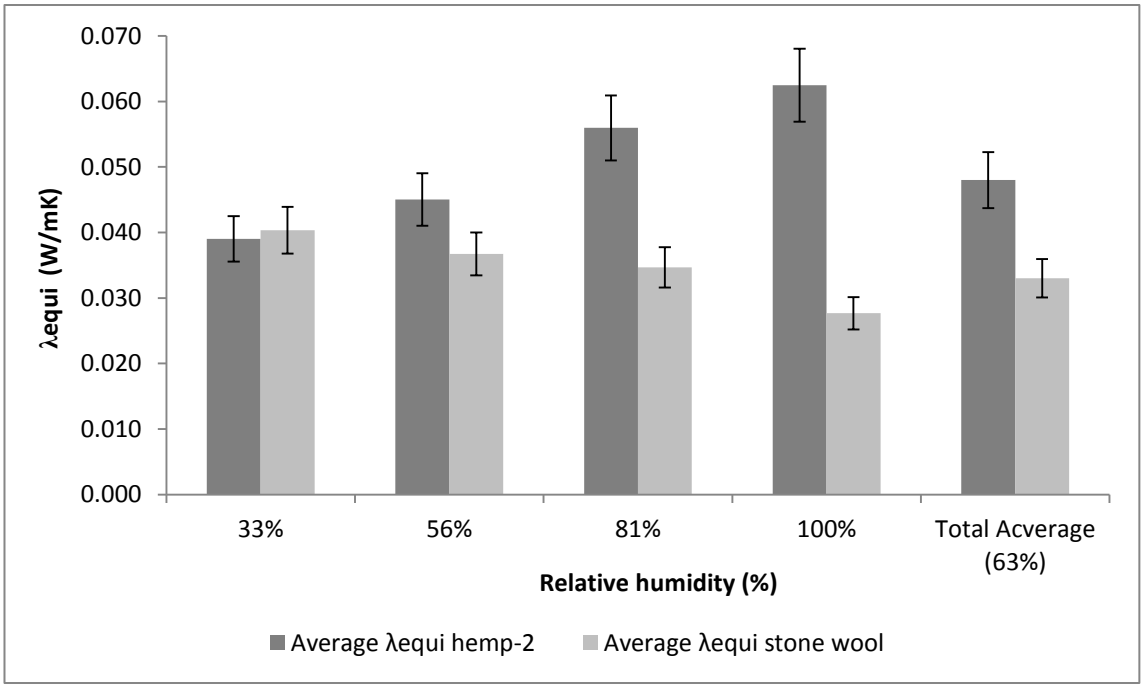


**Figure 6.46: Equivalent thermal conductivity values of hemp-2 and stone wool Insulations.**

**Table 6.6: Experimental and design value of thermal conductivity with standard deviations.**

| No. of data | Average relative humidity, (%) | Standard deviation | Average λequi hemp-2, (w/m-k) | Standard deviation | Design value of λ of hemp, (w/m-k) | Average λequi stone wool, (w/m-k) | Standard deviation | Design value of λ of stone wool, (w/m-k) |
|---|---|---|---|---|---|---|---|---|
| 1900 | 33.03 | 0.453 | 0.039 | 0.003 | 0.038 | 0.037 | 0.003 | 0.040 |
| 1300 | 56.06 | 0.414 | 0.045 | 0.004 | 0.038 | 0.034 | 0.004 | 0.040 |
| 1300 | 81.48 | 0.466 | 0.052 | 0.003 | 0.043 | 0.032 | 0.005 | 0.040 |
| 1300 | 100.00 | 0.026 | 0.062 | 0.003 | 0.050 | 0.026 | 0.011 | 0.040 |

Figures 6.47 and 6.48 show the relationship between the ranges of average relative humidity and the equivalent thermal conductivity values at those ranges for hemp-2 and stone wool insulation materials, respectively. Linear relationship can be noticed for both insulation materials, with hemp-2 showing an $R^2$ value of 0.99 and stone wool showing an $R^2$ value of 0.92. However, the gradient of the trend lines of hemp-2 and stone wool insulations are opposite to each other.

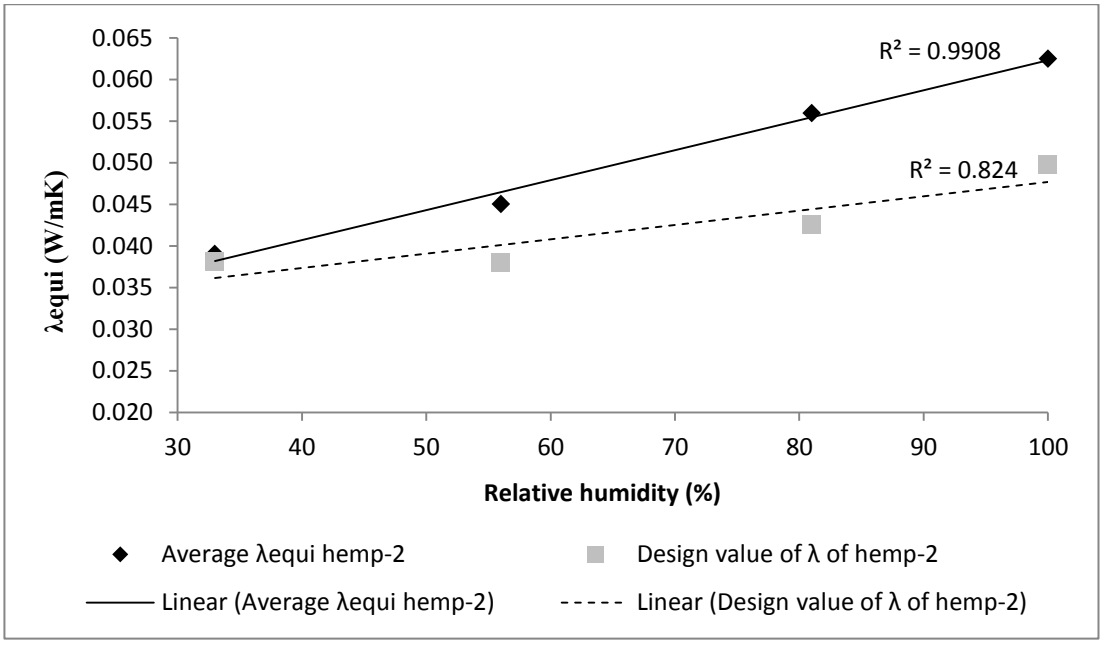


**Figure 6.47: Equivalent thermal conductivity of hemp-2 plotted against relative humidity.**

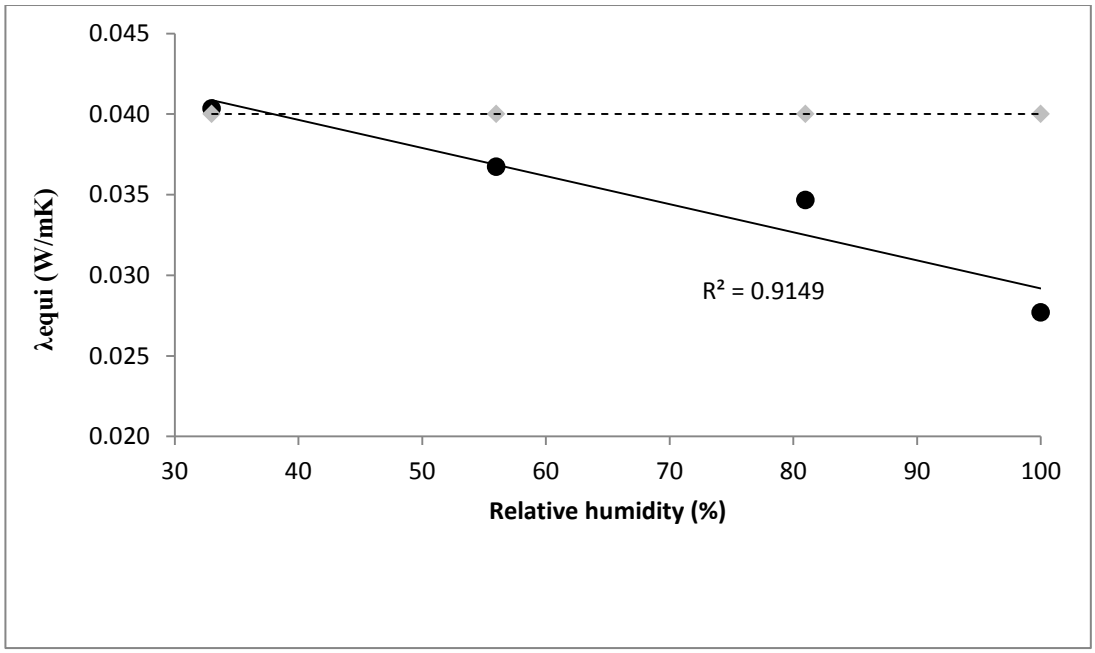


**Figure 6.48: Equivalent thermal conductivity of stone wool plotted against relative humidity.**

Figure 6.49 shows the relation between the equivalent thermal conductivity values of hemp-2 and the corresponding adsorbed moisture content, there is no such graph though for stone wool insulation as it adsorbs negligible amount of moisture. The relationship is reasonably linear with an $R^2$ value of 0.89. However, it can be observed that if only the first three data points were used for the correlation, the relationship would have been more linear. It is plausible that hemp-2 required more exposure time to reach EMC at 95% relative humidity and the higher amount of adsorbed moisture would have shifted the last data point upward. Alternatively, the slight nonlinearity in the relationship may indicate the existence of the 'other' mechanisms of heat flow (namely enthalpy flow, phase change, heat of wetting) in addition to the moisture dependent heat flux.

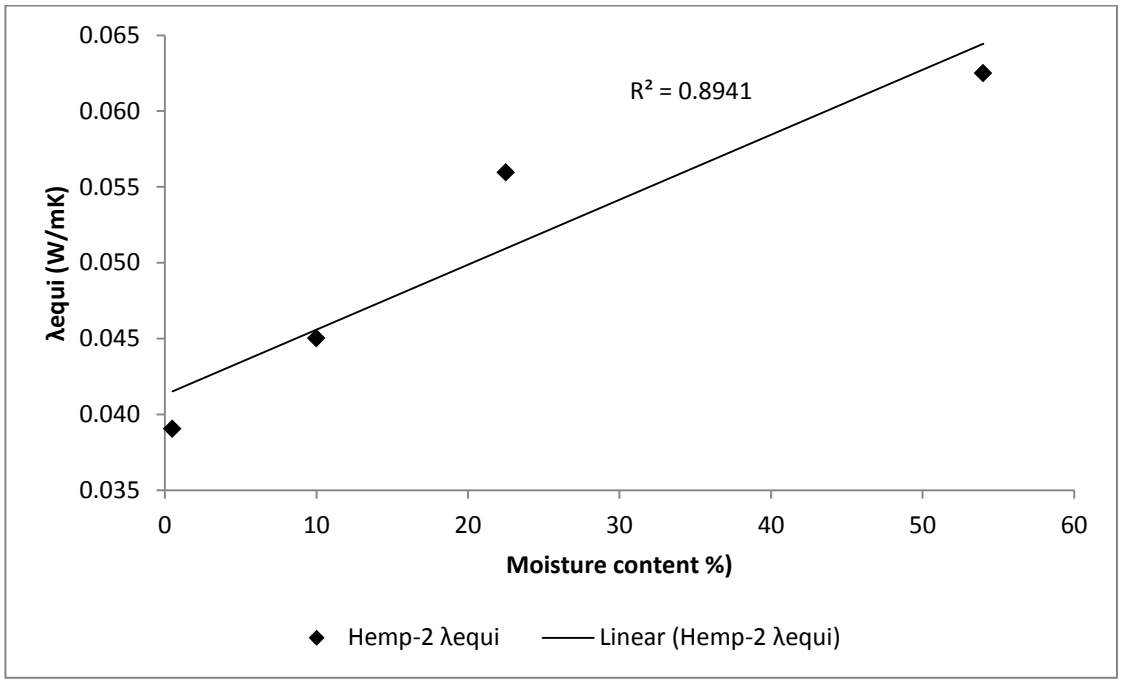


**Figure 6.49 Equivalent thermal conductivity plotted against adsorbed water for hemp-2 insulation.**

Figure 6.50 shows the nonlinear relationship between heat flux in hemp-2 insulation and interior relative humidity, which is expected because of the nonlinear relationship between relative humidity and water adsorption capacity of hemp insulation. Another possible reason for this nonlinearity is the transient nature of the data for heat flux and relative humidity. For stone wool insulation, nonlinearity is more pronounced in the relationship between the interior relative

humidity and the heat flux through stone wool insulation. This is plausibly due to the early condensation in the interior surface of the acrylic.

Similar observations can be made about the relationship between vapour pressure difference and heat flux for these insulations, as shown in Figure 6.51

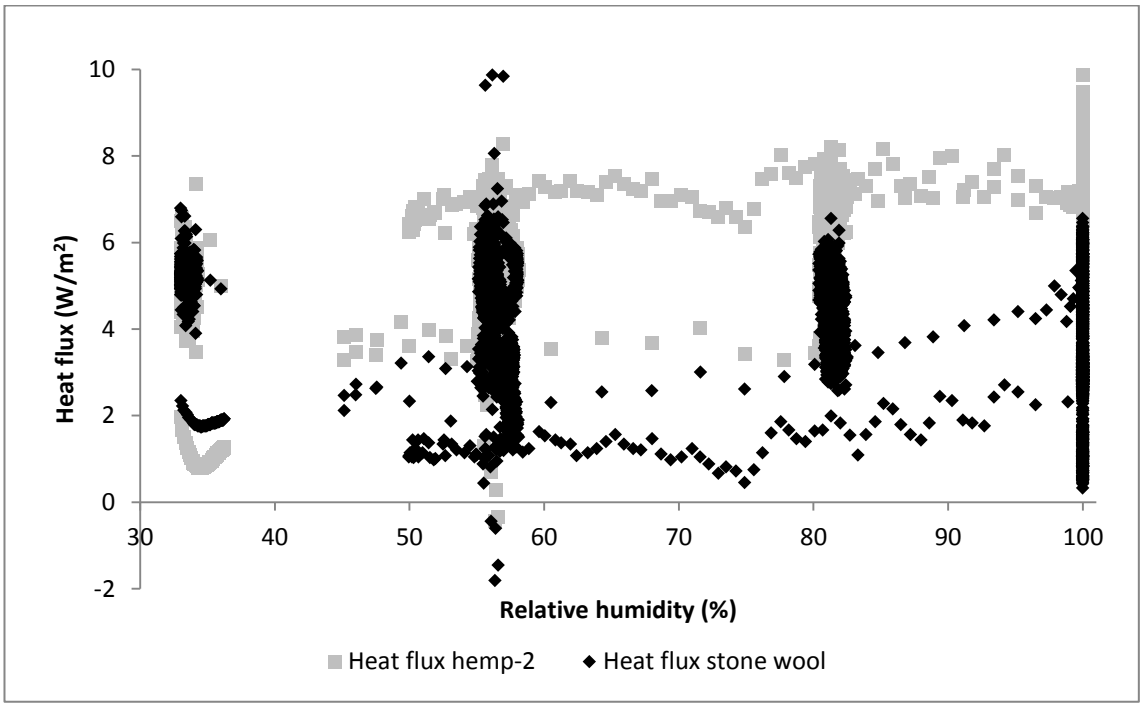


**Figure 6.50: Interior relative humidity and heat flux in hemp-2 and stone wool insulation.**

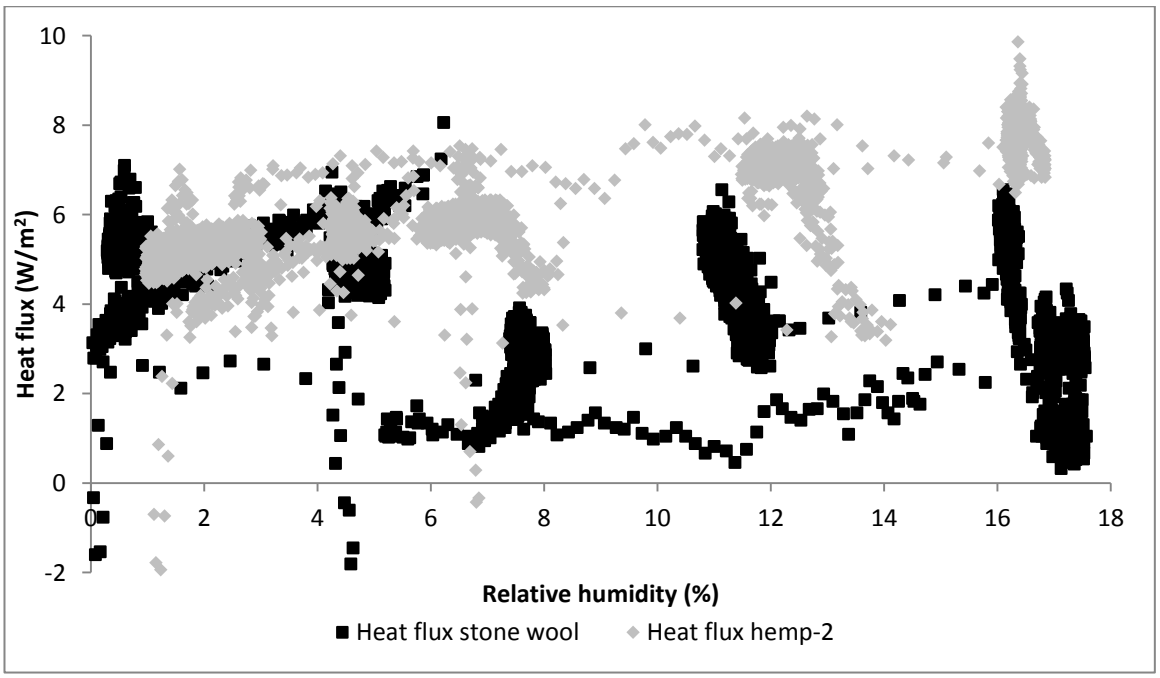


**Figure 6.51: Vapour pressure difference and heat flux in hemp-2 and stone wool insulation.**

Experimental and numerical simulation data of heat flux through warm and cold surface of the insulation samples are shown in Figures 6.52 to 6.53. It can be noted that the data from numerical simulation show a time lag in heat flow response. The most important difference between simulation and experimental data is the increasing heat flux difference as the relative humidity in the interior approaches 100%. This is mostly pronounced in heat flux on the cold side of hemp and stone wool, as shown in Figure 6.52 and Figure 6.53. In Figure 6.52, the difference between experimental and numerical simulation data for the heat flux at 100% relative humidity for stone wool insulation is about 8.5 W/m$^2$ and that for hemp-2 insulation is about 3 W/m$^2$. These values correspond to the approximate thermal conductivity values of 0.069 W/mK and 0.023 W/mK for stone wool and hemp-2 insulation materials, respectively.

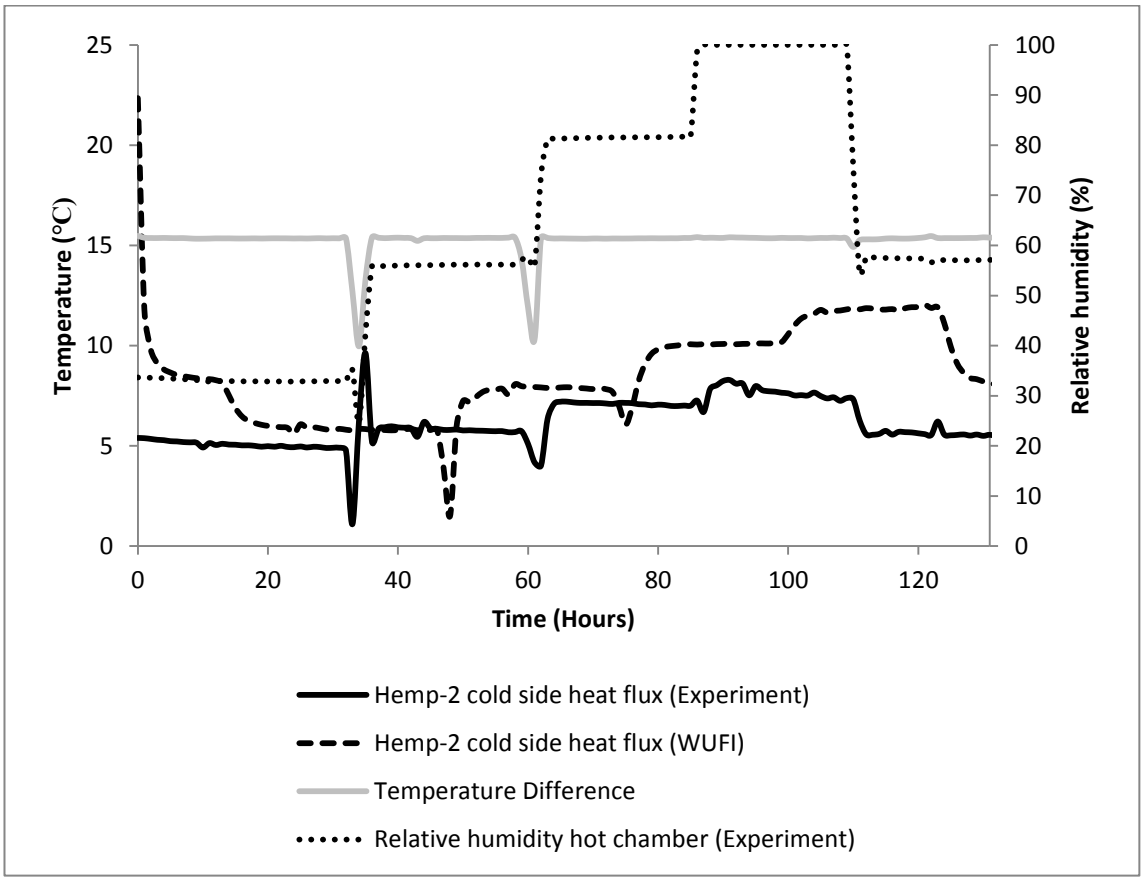


**Figure 6.52: Experimental data and WUFI simulation of heat flux in the cold side of hemp insulation (external surface of the acrylic).**

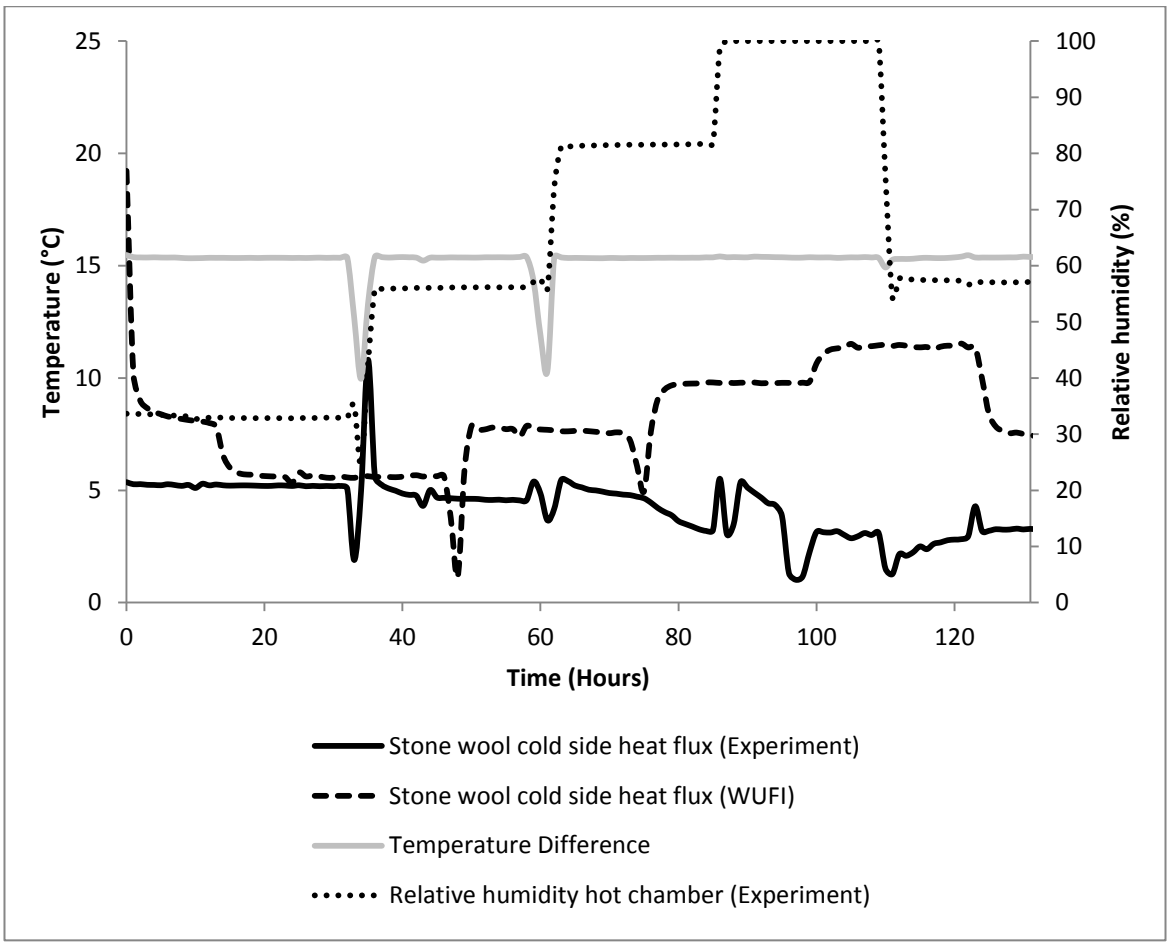


**Figure 6.53: Experimental data and WUFI simulation of heat flux in the cold side of stone wool insulation (external surface of the acrylic).**

Figures 6.54 and 6.55 show the heat flux through the warmer surfaces of hemp-2 and stone wool insulation materials, respectively. For hemp-2 insulation, there is not much difference between numerical and experimental heat flux data as the average difference of experimental and the numerical heat flux values corresponds to the equivalent thermal conductivity value of only 0.003 W/mK. For stone wool insulation, there is a sudden drop of the experimental heat flux at around 97th hour. The heat flux sensor that was attached to the warm side surface of the stone wool insulation was loosened during that time which can be the cause of this sudden drop. There is no such drop of heat flux in hemp-2 insulation.

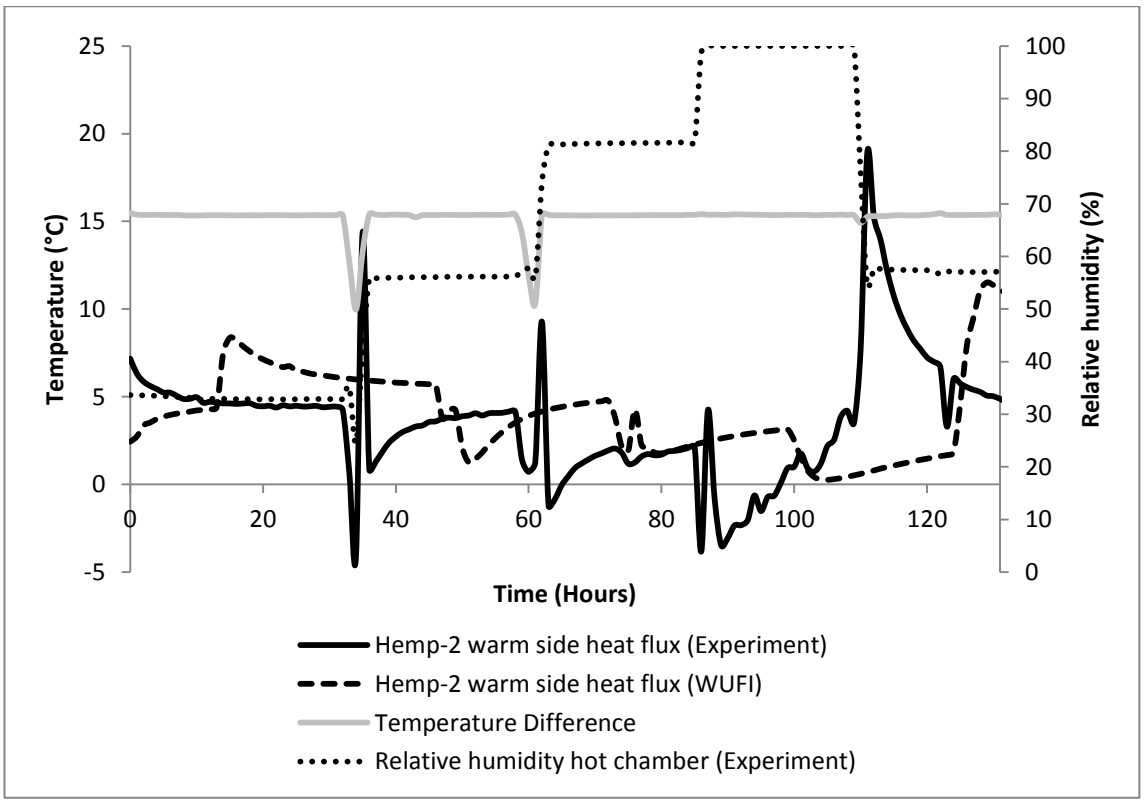


**Figure 6.54: Experimental data and WUFI simulation of heat flux in the warm side surface of hemp insulation.**

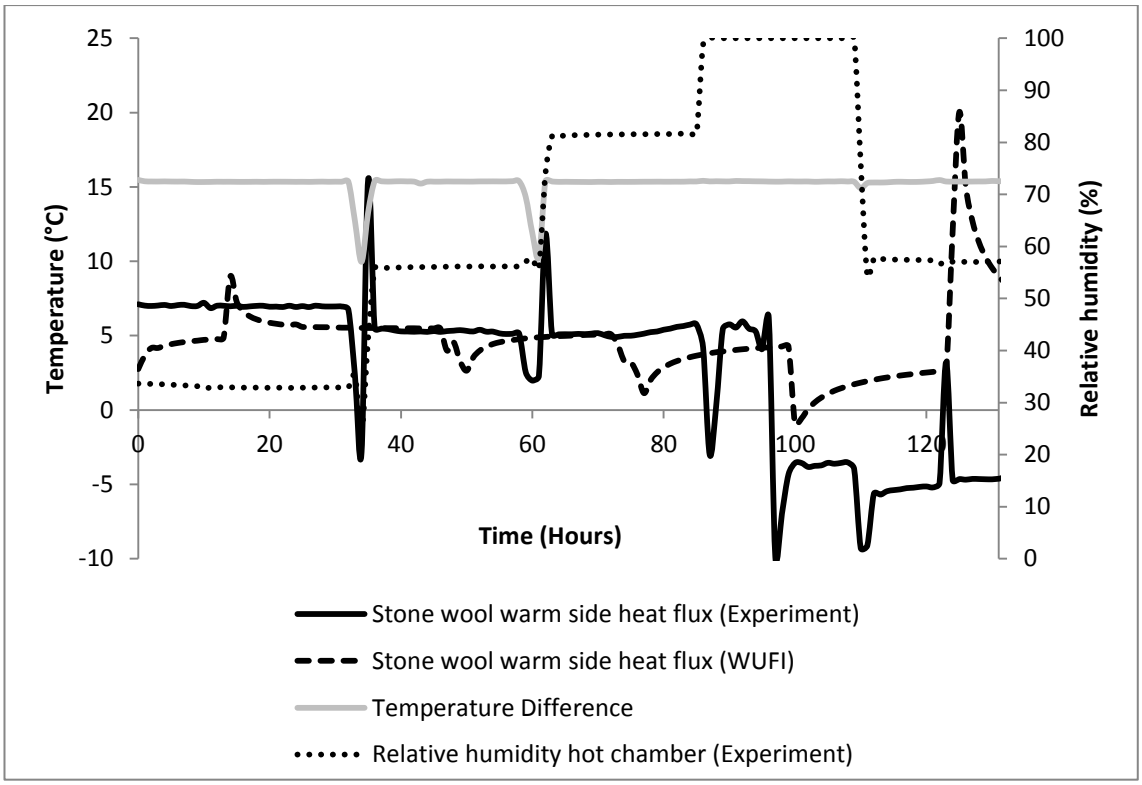


**Figure 6.55: Experimental data and WUFI simulation of heat flux in the warm side surface of stone wool insulation.**

On the basis of this difference, a deduction can be made that even if condensation occurs and heat is released, the released heat does not necessarily move towards the colder side. The initial heat can be scattered into different directions. Once substantial amount of condensation occurs on the acrylic, the condensed water, due to its specific heat capacity, can rather absorb further oncoming heat and reduce heat flux. In transient condition thermal diffusivity, defined as the ratio of thermal conductivity and specific heat capacity, can be low. Gravitational force may also act upon condensed water making heat absorption and heat flux pattern rather random. Hence, in this case, depending on how condensed water is managed on the surface, heat flux can sometimes be higher and sometimes be lower. For example, when Hedlin (1988) conducted his experiment on a glass fibre insulated flat roof, he assumed that in cold temperature frost could even form on the outer surface of the insulation, which contributed to higher heat flux than what would have been if ice were formed.

In hemp-2 insulation, heat flow by mass diffusion and phase change is less dominant when the moisture content in the insulation is within hygroscopic range. However, as sorption is very high in hemp insulation, there may be some effect of heat of wetting which has been discussed in subsection 2.1.4 of chapter two.

### *6.3.5 Summary of the quasi steady state tests*

Hemp-2 and stone wool insulation samples were subjected to the similar hygrothermal boundary conditions in a dual climate chamber. The temperature difference between hot chamber and cold chamber was kept constant and humidity in the hot chamber was increased in steps. The experiment was also simulated in a hygrothermal simulation software, namely the WUFI software.

In terms of moisture management, hemp performs better than stone wool insulation in two ways. Firstly, by utilising the better moisture adsorption capacity of hemp-2 insulation and secondly, by utilising the better water absorption coefficient of hemp-2 insulation. It has been observed that interstitial condensation occurs earlier in (stone wool)-acrylic insulation interface than in (hemp-2)-acrylic insulation interface. This is due to the moisture absorption capacity of hemp-2, which can absorb condensed water better than stone wool

insulation. In the case of stone wool insulation, the condensed water stays at the acrylic surface and some of the droplets slides down due to gravity.

Two types of thermal conductivity values have been studied: equivalent thermal conductivity based on experimental data and moisture dependent thermal conductivity based on the design values. Moisture dependent thermal conductivity takes into account the effect of adsorbed moisture while equivalent conductivity additionally takes into account the effect of enthalpy of moisture flow and effect of phase change during condensation.

It has been found that the average equivalent thermal conductivity of hemp-2 insulation at average relative humidity of 63% is 0.048 W/mK and average equivalent thermal conductivity of stone wool insulation at 63% relative humidity is 0.033 W/mK. It can be also observed that, the design values and experimental values of hemp-2 insulations at 33% and 56% relative humidity are equal in terms of the first two decimal places. However the design values of hemp-2 insulations at 81% and 100% relative humidity are about 21% and 24% higher than the corresponding experimentally determined thermal conductivity values. For the stone wool insulation, there is substantial difference between experimental and design values of thermal conductivity, with design values of thermal conductivity being about 18%, 25% and 54% higher than the experimental values for 56%, 81% and 100% relative humidity, respectively.

It is assumed that the decrease in the equivalent thermal conductivity of stone wool is due to the placement of the heat flux sensor in a position where condensation did not occur and phase change was unregistered. Another possible reason for decrease in the heat flux in the stone wool could be the heat capacity of the water droplets on the acrylic surface. Stone wool adsorbs very limited amount of moisture, which is why moisture dependent conductivity is not significant. However, equivalent thermal conductivity (conductivity change due to vapour diffusion and condensation) of stone wool insulation can be very high or very low depending on the enthalpy of the moisture content, direction of the released heat from phase change and location of the condensed droplets. This is why the experiments in section 6.2 showed higher equivalent thermal conductivity and the present experiment showed lower equivalent thermal conductivity of stone wool.

For hemp-2 insulation, the moisture dependent thermal conductivity value should not be much different from the equivalent thermal conductivity, as it seems that the increase in the thermal conductivity of hemp-2 insulation is mostly due to moisture adsorption. It has been found that the calculated equivalent conductivity values of hemp significantly agree with the design thermal values.

## 6.4 Test-6.4: An experimental assessment of the conventional method of measuring thermal conductivity of moist insulations

### *6.4.1 Introduction*

During the measurement of the thermal conductivity of moist insulations in a hot plate or in a hot box, moisture migration and resulting moisture gradient along the depth of the insulation can influence the heat flux. The aim of this experiment is to examine the change of thermal conductivity values of moistened hemp-2 insulation during a hot box test in relation to the change of thermal conductivity of a non-hygroscopic reference insulation material, namely expanded polystyrene (EPS). This experiment also aims to determine the amount of moisture removed from the insulations by moisture migration and phase change during the determination of thermal conductivity.

### *6.4.2 Method*

This method utilises a combination of experimental setup and an in-situ calculation method to measure thermal conductivity of moistened hemp-2 insulation. The EPS insulation, the reference material with constant thermal conductivity, is used as a control specimen.

In a quasi-steady state experimental situation, temperature and relative humidity in the boundaries are not absolutely steady. Due to this quasi-steady nature of the boundary conditions, the in-situ measurement approach can be applied in accordance with ISO 9869.

The EPS insulation is used as a control or reference insulation in the dual insulation setup to serve the following purposes:

- Determination of thermal conductivity from the control sample will provide confidence to the testing method.

- The pattern of fluctuation in heat flux in moist insulation can be checked against the pattern of fluctuation of heat flux in the reference insulation material. As EPS, the reference material, is vapour and water closed, if a similar fluctuation pattern is visible in EPS, it can be concluded that the pattern is not due to the moisture in the test material (hemp-2). However, the variation in magnitude of the pattern may reflect the influence of moisture.

The following three experimental tests were carried out:

**Test-6.4.1:** During test-6.4.1, thermal conductivity of hemp-2 insulation was determined when the insulation was in EMC with 80% relative humidity at 23 °C temperature. Insulation was wrapped with cling film during the determination of thermal conductivity so that there could not be any air movement through the insulation and no moisture could escape outside the cling film. The duration of test-6.4.1 was 40 hours.

**Test-6.4.2:** During test-6.4.2, thermal conductivity of hemp-2 insulation was determined when the insulation was in EMC with 95% relative humidity at 23 °C temperature. Insulation was wrapped with cling film during the determination of thermal conductivity so that there could not be any air movement through the insulation and no moisture could escape outside the cling film. The duration of test-6.4.2 was 24 hours.

**Test-6.4.3:** EMC at 95% relative humidity is a condition where adsorbed moisture content in hemp-2 insulation is about 3 times higher than that when hemp-2 is at EMC with 80% relative humidity. In this context, EMC at 95% relative humidity is a critical condition for hemp-2 insulation. The aim of the test-6.4.3 is to repeat the test-6.4.2 to examine and verify the results of test-6.4.2. During test-6.4.3, thermal conductivity of hemp-2 insulation was determined when the insulation was in EMC with 95% relative humidity at 23 °C temperature. Insulation was wrapped with cling film during the determination of thermal conductivity so that there could not be any air movement through the insulation and no moisture could escape outside the cling film. The duration of test-6.4.3 was 40 hours.

Thermal conductivity of the reference EPS insulation material is initially measured with Isomet needle probe. Since EPS insulation is an isotropic

material, the Isomet needle probe provided accurate thermal conductivity value of the EPS insulation. The value of thermal conductivity of the EPS insulation obtained by using the Isomet needle probe was used to compare with the thermal conductivity value obtained by using the experimental method.

### *6.4.3 Conditioning and preparation of the insulations*

Hemp-2 and EPS insulation samples have been conditioned in the TAS climate chamber at following equilibrium moisture contents: 23 °C temperature and 80% relative humidity for test-6.4.1; 23 °C temperature and 95% relative humidity for test-6.4.2 and test-6.4.3. The moistened insulation materials are wrapped with cling film to avoid moisture loss and air flow through the insulation materials during the tests.

### *6.4.4 Setup and instrumentation*

The setup is similar to the setup used in the experiment in section 6.2, as shown in Figures 6.56 and 6.57. The difference is that in this test the hot box is not linked to the climate chamber and the heat flux sensors are installed on the inner surfaces of the acrylic sheets. As already mentioned in subsection 6.4.2, insulation materials are wrapped with cling film to achieve air and water tightness. Hemp-2 insulation has two layers. Each of the layers is 55 mm thick. Layer-1 faces the hot chamber and layer-2 faces the exterior.

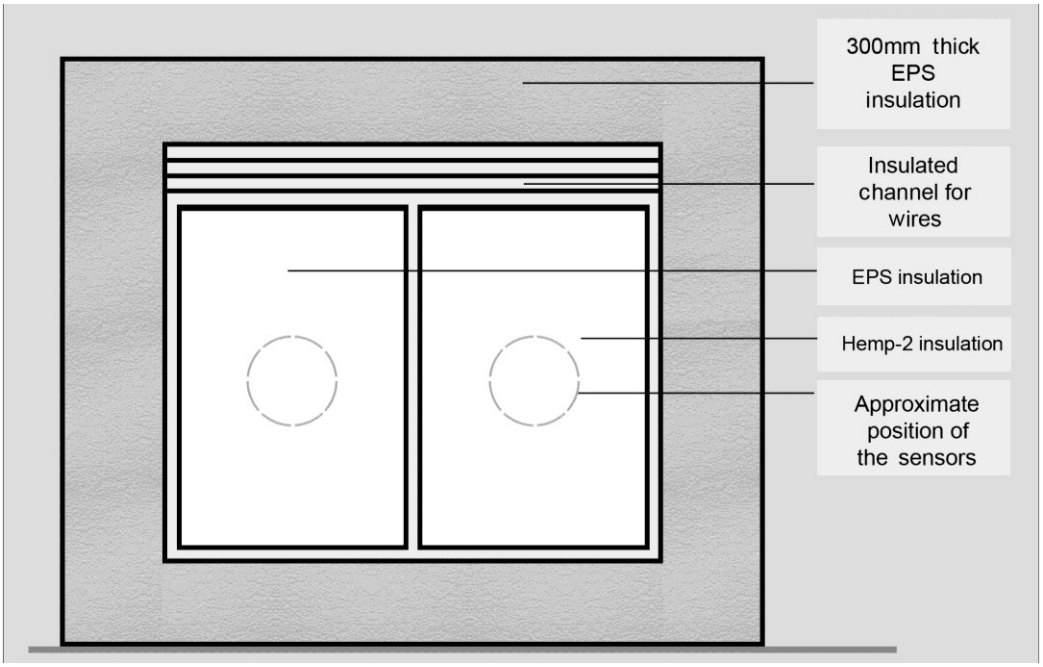


**Figure 6.56: The front elevation of the dual-insulation setup.**

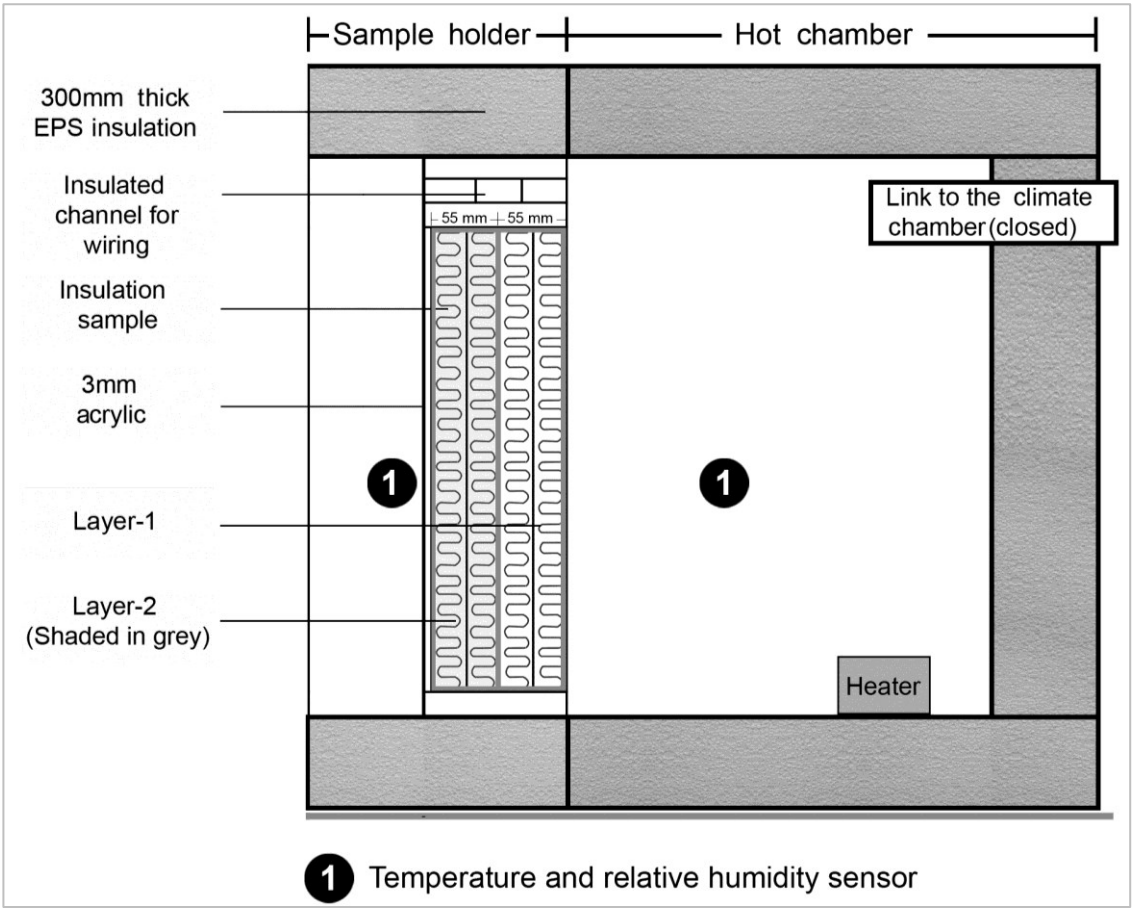


**Figure 6.57: The cross section of the dual-insulation setup.**

### *6.4.5 Measurement of thermal conductivity*

The in-situ method, described in ISO 9869, was developed to measure thermal conductivity in situations where constant temperature difference and steady heat flux were difficult to attain. During the current test, it was difficult to attain a constant temperature difference, as the exterior temperature was the temperature of the laboratory. As the insulation materials were moistened, moisture migration and phase change seemed to influence heat flux. In this situation, it is relevant to measure thermal conductivity using the in situ method. In this method, thermal transmittance is determined by dividing the mean heat flux by mean temperature difference when the average has been taken over longer period. According to this method, the U-value can be expressed using the following equation:

$$U = \frac{\sum_{j=1}^{n}(q_j)}{\sum_{j=1}^{n}(T_{ij} - T_{ej})} \quad [6.5]$$

Where,

U is thermal transmittance ($W/m^2K$), J is the number of individual measurements, $q_j$ is total density of heat flow ($W/m^2$), $T_{ij}$ is total internal temperature (°C) and $T_{ej}$ is total external temperature (°C).

If the system under investigation is a composite one, then the thermal resistance (R) value can be expressed as:

$$R = R_i + R_1 + R_2 + \ldots + R_x \ldots\ldots + R_n + R_o \quad [6.6]$$

Where $R_i$ is the internal surface resistance ($m^2K/W$), $R_o$ is the external surface resistance ($m^2K/W$), and $R_1$ to $R_n$ are the thermal resistance values ($m^2K/W$) of the material 1 to material n.

When $R_x$ is the only unknown parameter of material X, the value of $R_x$ will be:

$$R_x = R - R_i - (R_1 + R_2 + \ldots\ldots + R_n) - R_o \quad [6.7]$$

$$U_x = 1/R_x \quad [6.8]$$

Where $U_x$ is the thermal transmittance value or U-value ($W/m^2K$) of material X.

If $U_x$ is the thermal transmittance value of a homogenous material and moisture distribution is homogenous, the conductivity can be determined using the following equation:

$$\lambda_x = U_x * d \quad [6.9]$$

Where $\lambda_x$ is the thermal conductivity (W/mK) and d is the thickness of the material X.

In this experiment, thermal conductivity of moist insulation is expressed by the following symbol: λ*, and continuous running average is expressed as ‘RA’.

### *6.4.6 Results and discussion*

Three tests have been carried out. Test-6.4.1 was with hemp-2 and EPS insulation materials at 80 EMC; test-6.4.2 and test-6.4.3 were with hemp-2 and EPS insulation materials at 95 EMC. The results of the tests are shown in Figures 6.58, 6.59 and 6.60 with running averages of the thermal conductivity data.

In Figure 6.58, it can be noticed that similar changes occurred in the thermal conductivity curves of hemp-2 and EPS insulation during the course of the experiment. Had the EPS not been present as a control specimen, the change in the conductivity curve in hemp-2 could likely be attributed to the moisture related heat flux properties of hemp-2 insulation. The slope of the thermal conductivity curve of hemp-2 insulation during the test at 80 EMC is approximately horizontal, indicating a steady condition compared to the slope of the curves at 95 EMC (Figures 6.59 and 6.60).

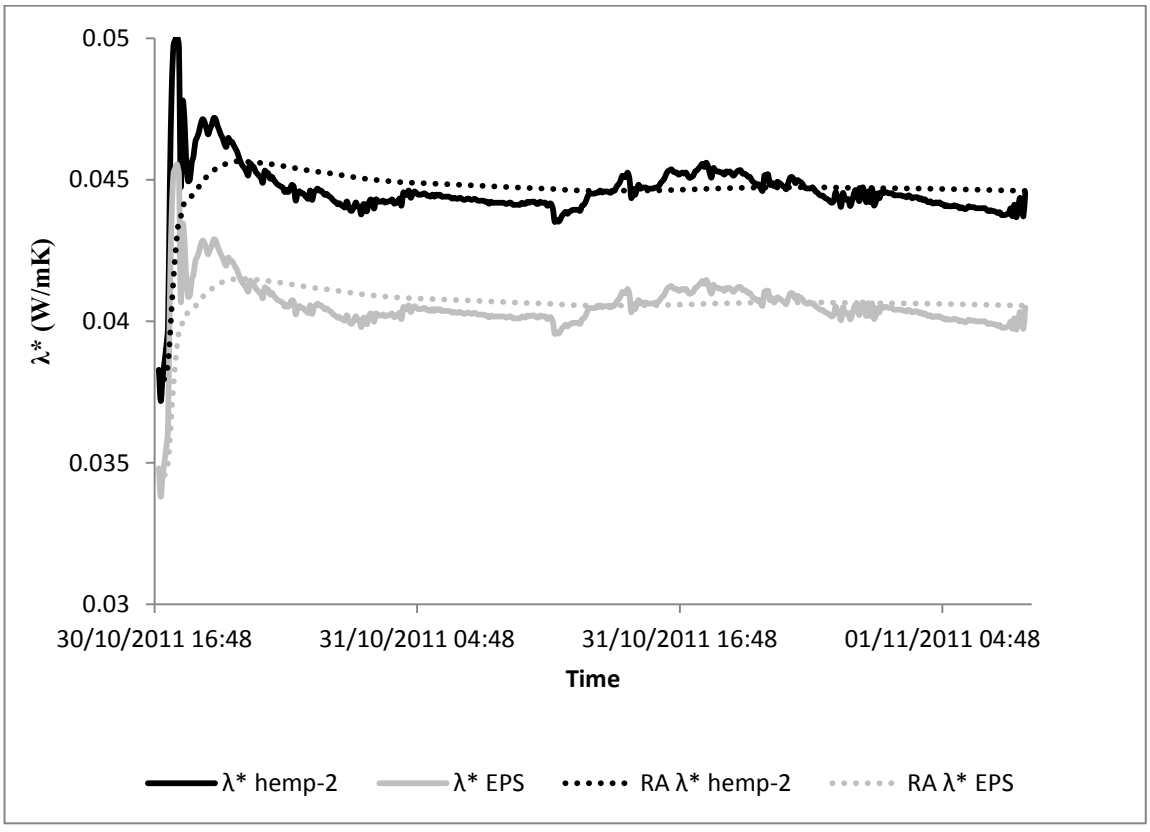


**Figure 6.58: Thermal conductivity measurement of hemp-2 at 80 EMC with EPS insulation as a control (40 hours).**

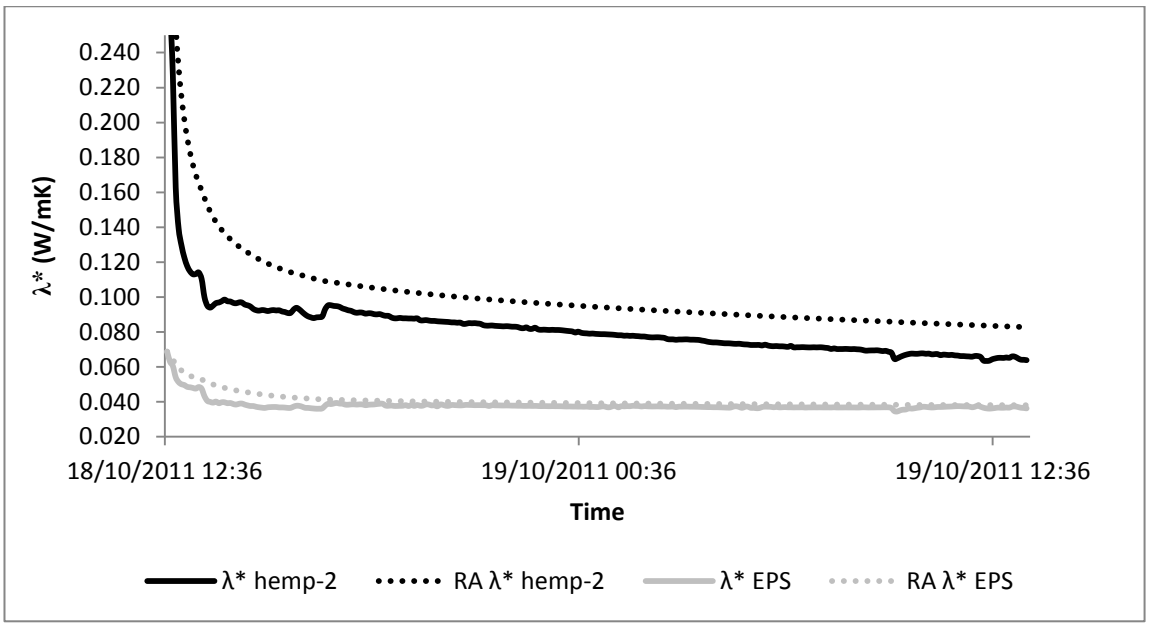


**Figure 6.59: Thermal conductivity measurement of hemp-2 at 95 EMC with EPS insulation as a control (24 hours measurement).**

It seems that during measuring thermal conductivity at 95 EMC, the moisture migration and phase change keep occurring at a decaying rate and the value of thermal conductivity keeps decreasing. Obviously, at some point, the EMC of the insulation will be low and the conductivity value will reflect that. This is a possible reason for registering lower thermal conductivity values of moistened insulations during standard tests in a hot box or hot plate.

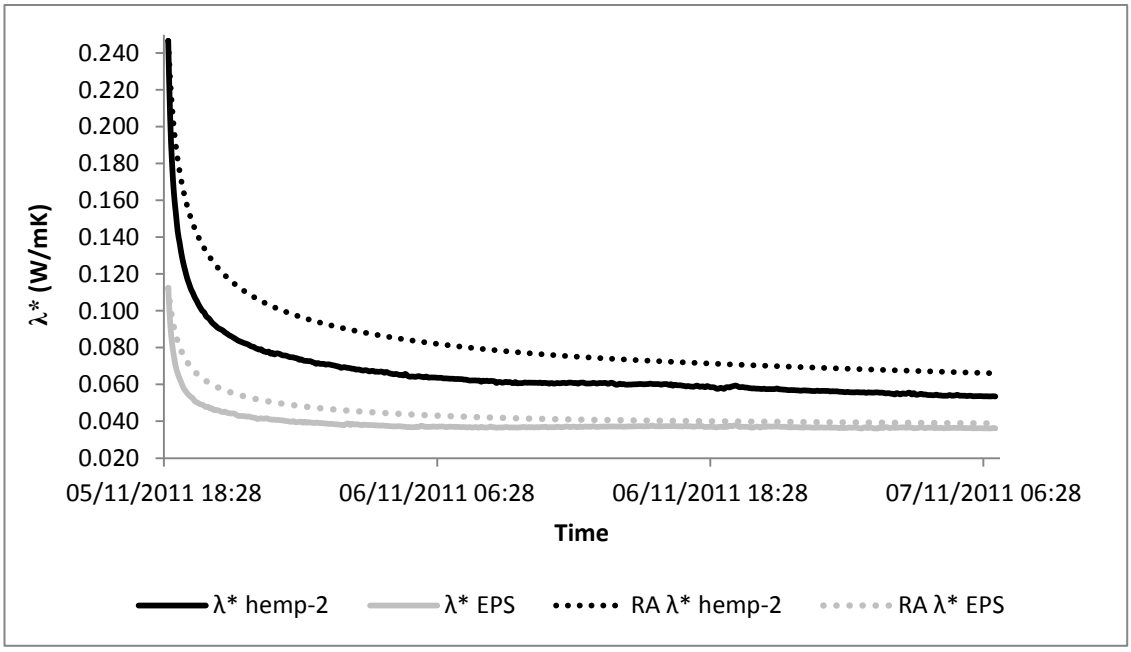


**Figure 6.60: Thermal conductivity measurement of hemp-2 at 95 EMC with EPS insulation as a control specimen (40 hours measurement).**

During these three tests, the assessed average thermal conductivity values of EPS are 0.040, 0.038 and 0.039 W/mK, which are excellent fits of the manufacturers' declared thermal conductivity (0.038 W/mK) of the EPS insulation. Measurement of the thermal conductivity of EPS with Isomet heat transfer analyzer provided a thermal conductivity value of 0.038W/mK. This implies that the test method is reasonably accurate for measuring dry thermal conductivity. However, the moisture dependent thermal conductivity of hemp-2 insulation seems to be continuously decreasing due to moisture movement and gradual drying out of hemp-2 insulation.

The amount of moisture that migrates from the layer-1 at the hot side to the layer-2 at the cold side of hemp-2 insulation during the tests has been measured. The results are shown in the Table 6.7 and Table 6.8. About 48% and 36.7% moisture moved from the inner layer-1 to the outer layer-2 during the test at 80 EMC (test-1) and 95 EMC (test-2), respectively. About 6% and 5% moisture were unaccounted for during the test with 80 EMC (test-1) and 95 (test-2) EMC, respectively. The likely cause is the phase change at the boundary surfaces of the insulation. Due to technical problems, moisture migration during test-3 could not be measured.

**Table 6.7: Moisture migration during conductivity measurements of hemp-2 at 80 EMC during test-6.4.1.**

| Hemp-2 | Dry mass (gm) | Emc mass (gm) | End mass (gm) | Moisture loss (gm) | Moisture loss (%) | Moisture gain (gm) | Moisture gain (%) | Moisture not accounted for (gm) |
|---|---|---|---|---|---|---|---|---|
| Layer-1 | 526 | 605.2 | 567.0 | 38.2 | 48.2 | | | |
| Layer-2 | 522 | 598.3 | 627.2 | | | 28.9 | 37.9 | 9.3 |
| Total | 1048 | 1203.5 | 1194.3 | | | | | |

**Table 6.8: Moisture migration during conductivity measurements of hemp-2 at 95 EMC during test-6.4.2.**

| Hemp-2 | Dry mass (gm) | EMC mass (gm) | End mass (gm) | Moisture Loss (gm) | Moisture Loss (%) | Moisture Gain (gm) | Moisture Gain (%) | Moisture not accounted for (gm) |
|---|---|---|---|---|---|---|---|---|
| Layer-1 | 526 | 635.1 | 595.1 | 40.0 | 36.7 | | | 11.7 |
| Layer-2 | 522 | 652.1 | 680.3 | | | | 21.7 | |
| Total | 1048 | 1287.2 | 1275.4 | | | 28.2 | | |

At 80 EMC, the thermal conductivity of hemp-2 insulation is found to be 0.044 W/m-K. Aat 95 EMC, the thermal conductivity values of hemp-2 are 0.083 and 0.067 in test-6.4.2 and test-6.4.3 respectively. These values can be compared with the design values, thermal conductivity values derived from hot plate and the Isomet heat transfer analyser measurements, as shown in Table 6.9.

It can be noticed that at 80 EMC there is a good agreement between the results of thermal conductivity values obtained by the present experimental method and those obtained by hot plate measurements. However, transient measurement in the Isomet heat transfer analyser registered higher value. At 95 EMC, two different values of thermal conductivity of hemp-2 insulation were determined during test-6.4.2 and test-6.4.3. In Figures 6.59 and 6.60, it can be noticed that the duration of the test-2 was about 24 hours whereas the duration of the test-6.4.3 was about 40 hours. If the test-6.4.3 is analysed for 24 hours from the beginning of the test, the thermal conductivity of hemp-2 becomes 0.073. It implies that the value of thermal conductivity of a moistened insulation is also function of the measurement period because of the moisture movement due to temperature gradient and phase change.

**Table 6.9: Different values of thermal conductivity.**

| | Hemp-2 λ* Exp. | Hemp-2 λ* Hot Plate | Hemp-2 λ* Isomet | Design Value of Hemp λ | EPS λ* Exp. | EPS λ* Hot Plate | EPS λ* Isomet | Design Value of EPS λ |
|---|---|---|---|---|---|---|---|---|
| 80 EMC | 0.044 | 0.044 | 0.066 | 0.043 | 0.041 | 0.035 | 0.037 | 0.038 |
| 95 EMC | 0.083 | | 0.096 | 0.050 | 0.039 | | 0.037 | 0.038 |
| 95 EMC | 0.067 | | 0.096 | 0.050 | 0.038 | | 0.037 | 0.038 |

### *6.4.7 Summary of the assessment*

The assessment described in section 6.4 highlights the limitations of the conventional method of measuring thermal conductivity of moist insulation materials. The assessment shows that at 80 EMC, as much as 37% moisture can migrate from the insulation layer facing the hot chamber to the insulation layer facing the exterior while 10% moisture presumably moved out of the insulation layer and changed phase. For 95 EMC, 37% moisture migrated from the insulation layer facing the hot chamber. It can be assumed that by the time steady state heat flux is achieved through the insulation, the insulation will be near to dry condition. Thus, the thermal conductivity value obtained from the conventional tests will not represent the true thermal conductivity value of the moist insulation. The conventional method of measuring thermal conductivity of moist insulations will also not represent the thermal conductivity of insulations in vapour open walls as the insulation will always be in interaction with the boundary relative humidity.

## 6.5 Insulation in lofts: experimental simulation of moisture management and thermal conductivity

### *6.5.1 Introduction*

There are ‘problem lofts’ in the UK where relative humidity is very high and, as a result, interstitial condensation is frequently likely to develop in the loft envelope. This problem is well recognised in the building industry. It has been identified in the literature review that the high relative humidity in the loft is

mostly due to the infiltration of moist air from the rooms under the loft through the cracks and gaps in the plasterboards of the ceiling and insufficient ventilation.

Some of the previously described experiments in this thesis have identified the excellent adsorption and moisture buffering capacity of the bio-insulations. It can be assumed that bio-insulations, like hemp and sheep wool, compared to conventional insulations like stone wool, are more efficient in managing moisture in the loft and thus reducing the frequency of the occurrence of intestinal condensation in the insulation and in the loft envelope.

While the experiments described in sections 6.2 to 6.4 focused on wall sections, the present experiment focuses on the hygrothermal performance of insulation materials in a simulated loft space. The present experiment examines the following hygrothermal properties of the bio-insulation materials compared to that of stone wool insulation:

- The moisture management capacity of the insulation materials in the loft space.
- The equivalent thermal conductivity values of the insulation materials in the experimental boundary conditions of the loft space.

### *6.5.2 Material selection*

Hemp-1, hemp-4, sheep wool and stone wool insulation materials have been selected for the present experiment. The properties of these insulation materials are shown in Tables 4.1 to 4.3 of chapter four. Hemp-1 is higher in wood fibre content and hemp-4 is higher in hemp fibre content. Sheep wool is an animal-based bio-insulation.

### *6.5.3 Experimental method*

The experimental method is developed from the case study of a ‘problem loft’. In the studied ‘problem loft’ (Ceri and Newman, 2011) stone wool insulation was installed and a dehumidifier was used to remove excessive moisture. The temperature and relative humidity data of the loft was logged for 52 days. The dehumidifier was not used during the period of data logging. Temperature and relative humidity and data loggers were placed in the following locations:

- Externally
- Under the loft hatch (near the bathroom on the first floor)
- In the loft above the insulation
- At the bottom of the insulation
- In the middle of the insulation
- On the top of the insulation

The typical hygrothermal conditions in and around the 'problem loft' over 72 hours period is shown in Figure 6.61.

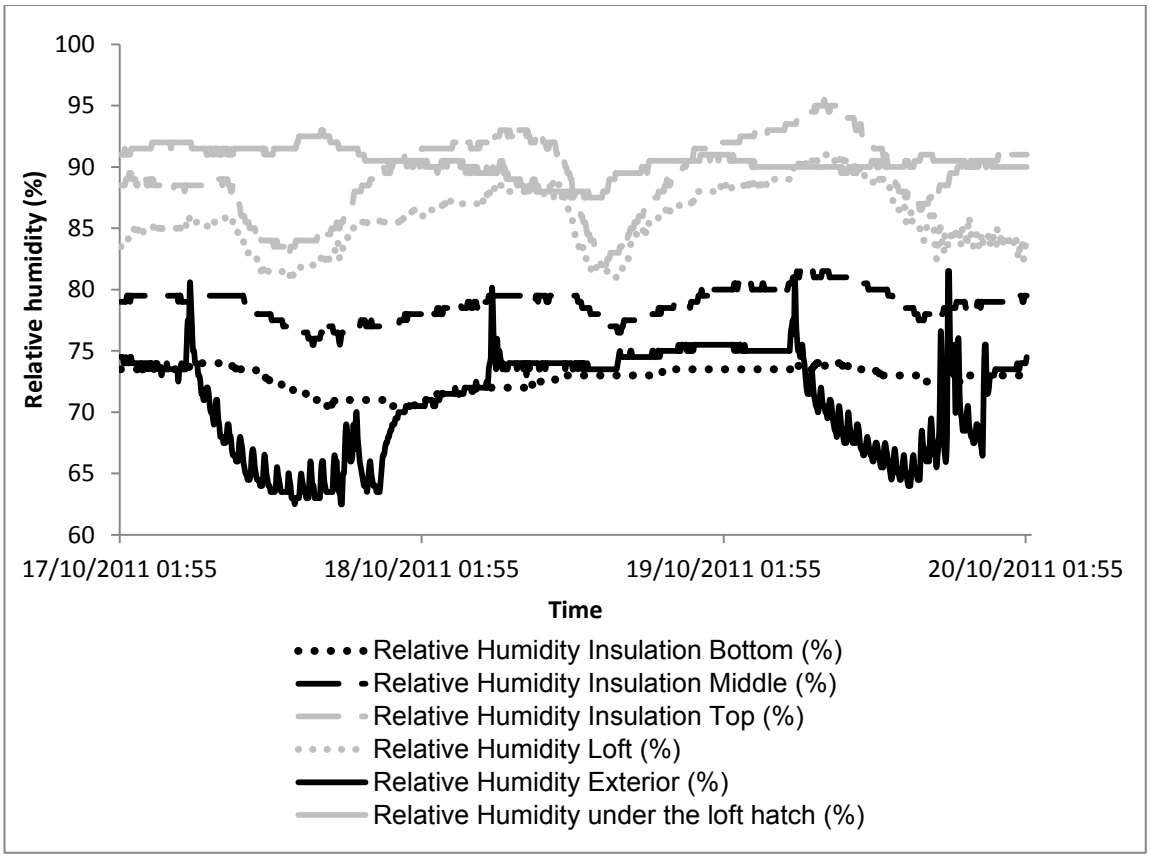


**Figure 6.61: The typical hygrothermal condition in the 'problem loft'.**

The relative humidity of the loft fluctuated between 80% and 90%. The relative humidity under the hatch near the bathroom remained between 87% and 92%. The external relative humidity varied between 63% and 75% with some infrequent peaks. The relative humidity from the bottom to the top of the insulation gradually increased because of the falling temperature gradient from the bottom to the top of the insulation. The relative humidity at the top of the

insulation varied between 82%-95% and was consistently higher than the loft relative humidity.

The temperature and relative humidity data are analysed in order to reproduce the hygrothermal condition of the loft in the experimental setup. Table 6.10 shows the data chosen as representative data from the loft from the whole data set based on the frequency of occurrence. The initial experiments in the climate chamber were designed to simulate this representative data. The corresponding values for the initial experimental work are also shown in Table 6.10.

**Table 6.10: Representative data for experimental simulation of the loft hygrothermal conditions.**

| | Field data | Initial experimental data |
|---|---|---|
| Loft temperature (°C) | 20 | 23 |
| Hatch temperature (°C) | 14 | 17 |
| Loft relative humidity (%) | 80-90 | 95 |
| Hatch relative humidity (%) | 90 | 85-90 |

Some preliminary laboratory based tests were carried out using stone wool, with the objective of setting the climate chamber to run at the conditions shown in Table 6.10 for a fixed period and monitoring the relative humidity and temperature conditions in the insulation and in the loft. The initial laboratory based experiments could not reproduce the high relative humidity that was observed on the upper surface of the insulation during the case study. The setup was further scrutinised and it was found that there were two differences between the laboratory-based experimental set up and the conditions of the 'problem loft' of the case study. Firstly, in the 'problem loft' there were cracks and gaps around the loft hatch and presumably in other parts of the ceiling acting as paths of vapour flow. Secondly, the exterior air was also vented through the 'problem loft', which could influence the moisture concentration in the loft space. Based on this observation, it was decided that some infiltration through the plasterboard would replicate the reality. In addition, simulating winter condition in the loft with lower temperature was assumed to be more

practical in terms of obtaining useful laboratory based experimental results. Figure 6.62 shows the conceptual diagram of the laboratory-based experiment.

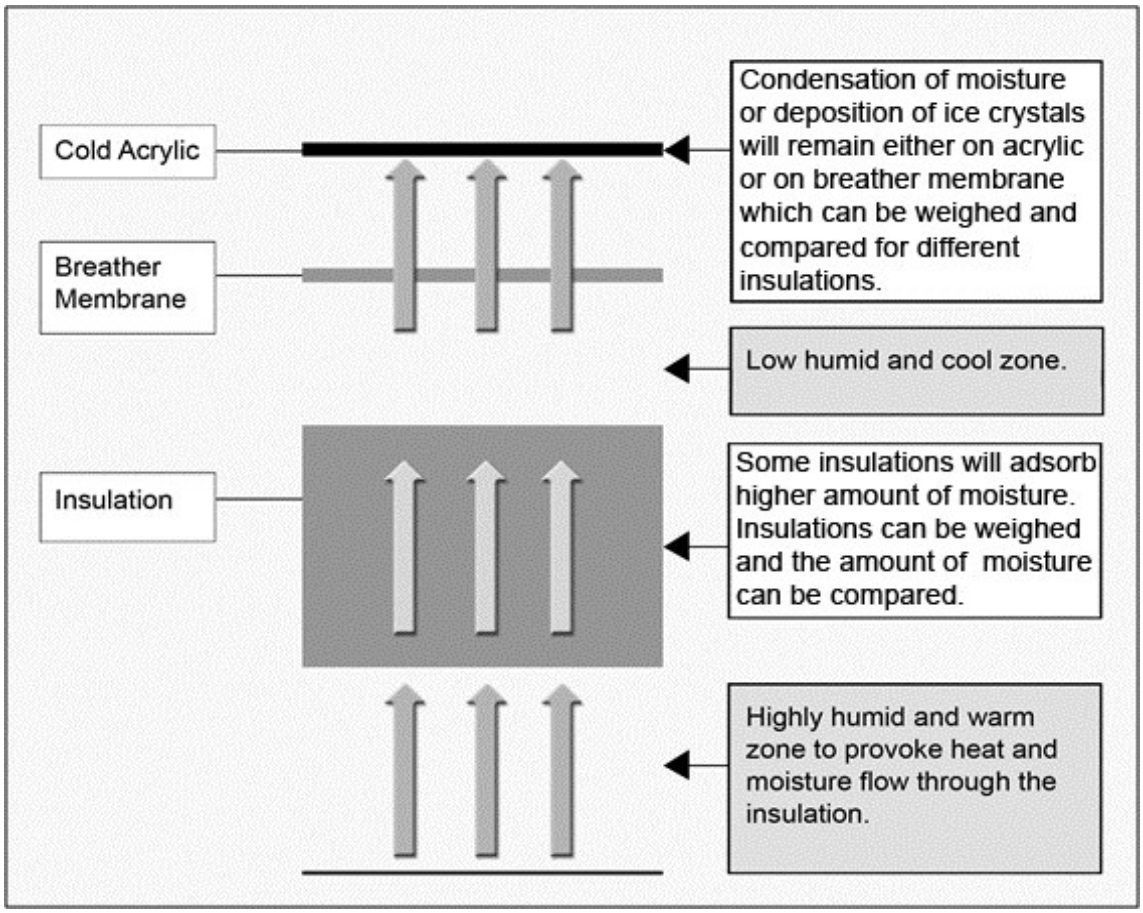


**Figure 6.62: The conceptual diagram of the lab-based experiment.**

The plasterboard of the laboratory based experimental setup was modified by drilling 4 holes of 4 mm diameter to represent cracks and gaps in the ceiling. The temperature above the insulation was set to a three-day profile, ranging from 8 °C to 1 °C to represent a winter condition when condensation is more likely. The temperature and relative humidity conditions below the plasterboard were kept close to the in situ condition observed below the hatch near the bathroom. Figure 6.63 shows the cross section and Figure 6.64 shows the the completed laboratory-based experimental setup. Figure 6.65 shows the plan view of the experimental setup. The various stages of installation of the experimental setup are shown in Figures 6.66 to 6.68.

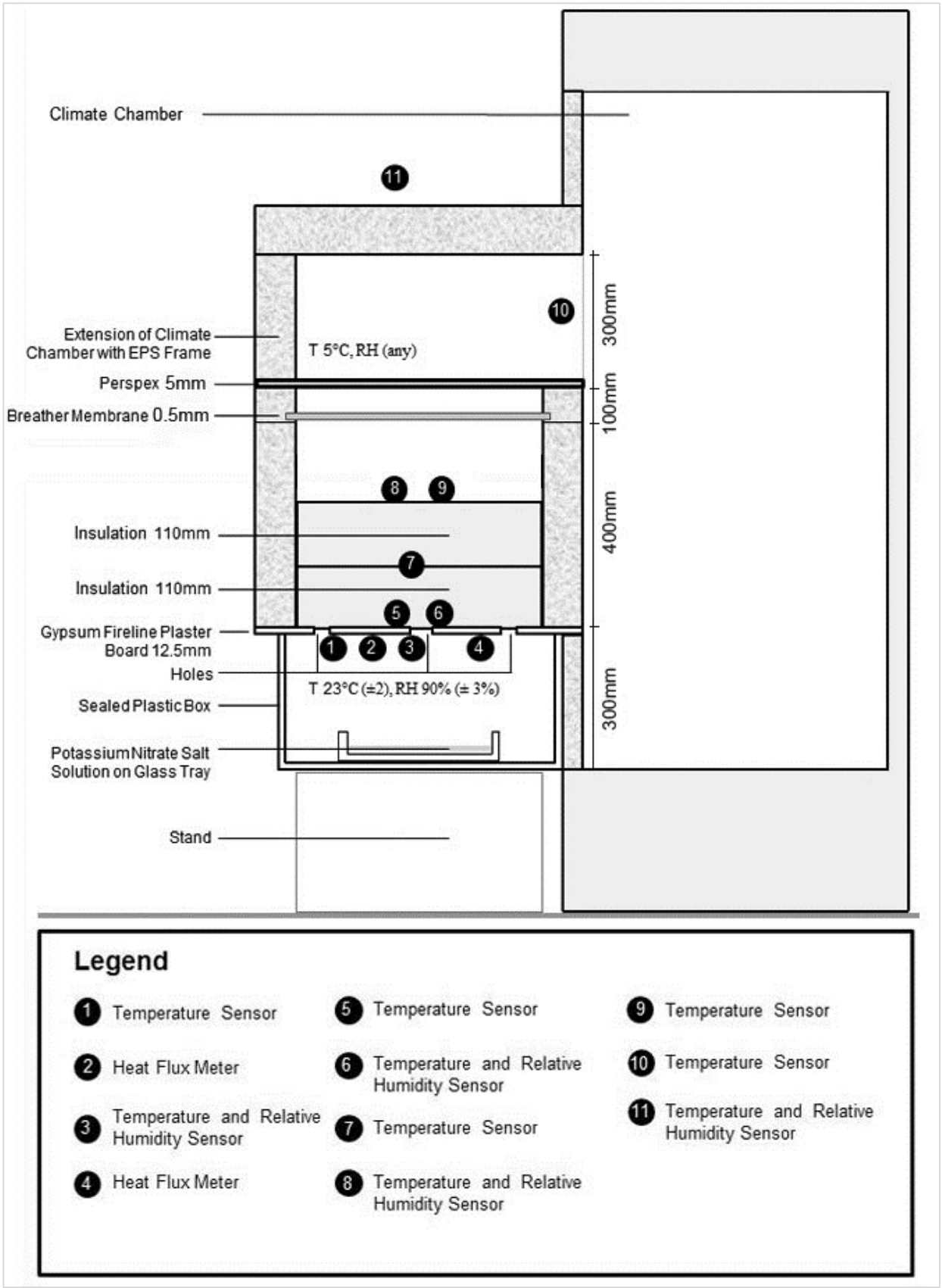


**Figure 6.63: The cross section of the experimental set up.**

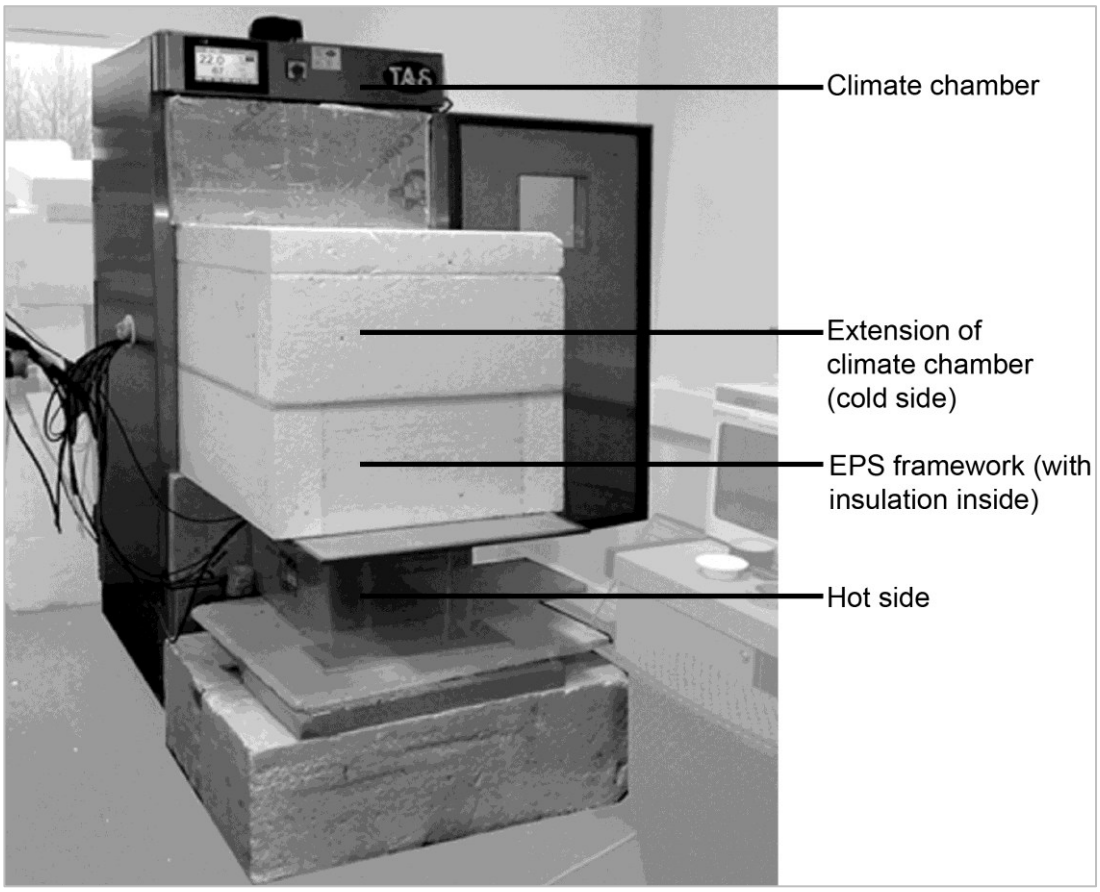


**Figure 6.64: Completed installation of the experimental setup.**

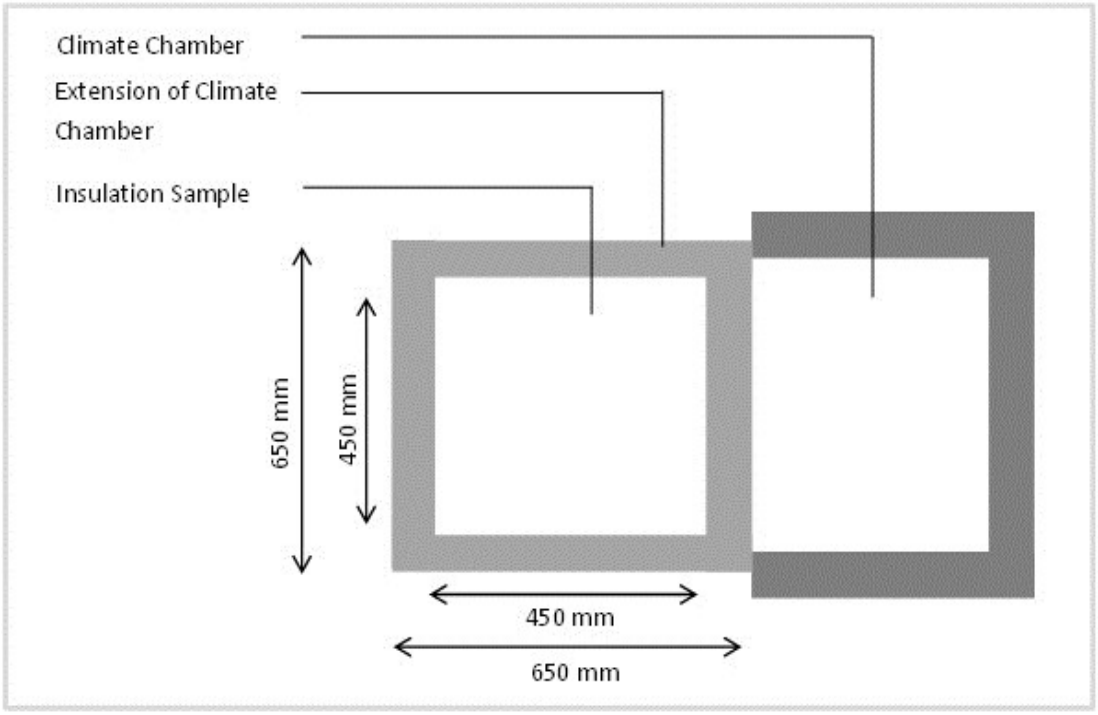


**Figure 6.65: The plan view of the experimental setup.**

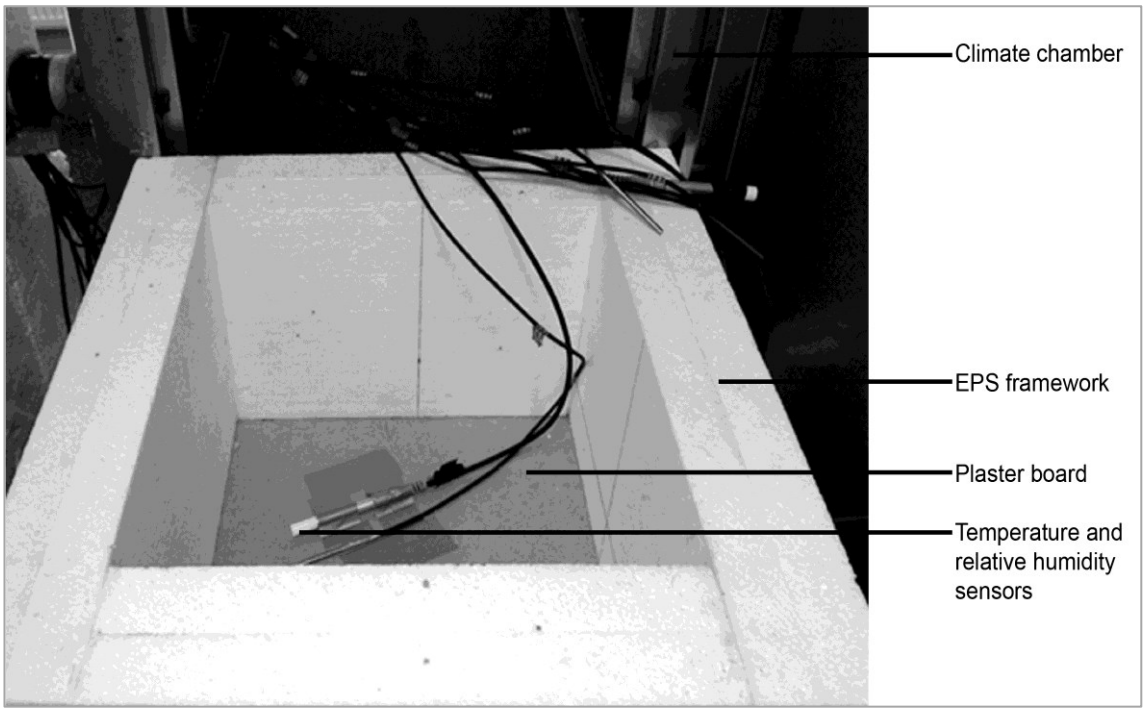


**Figure 6.66: Installation process of the sensors.**

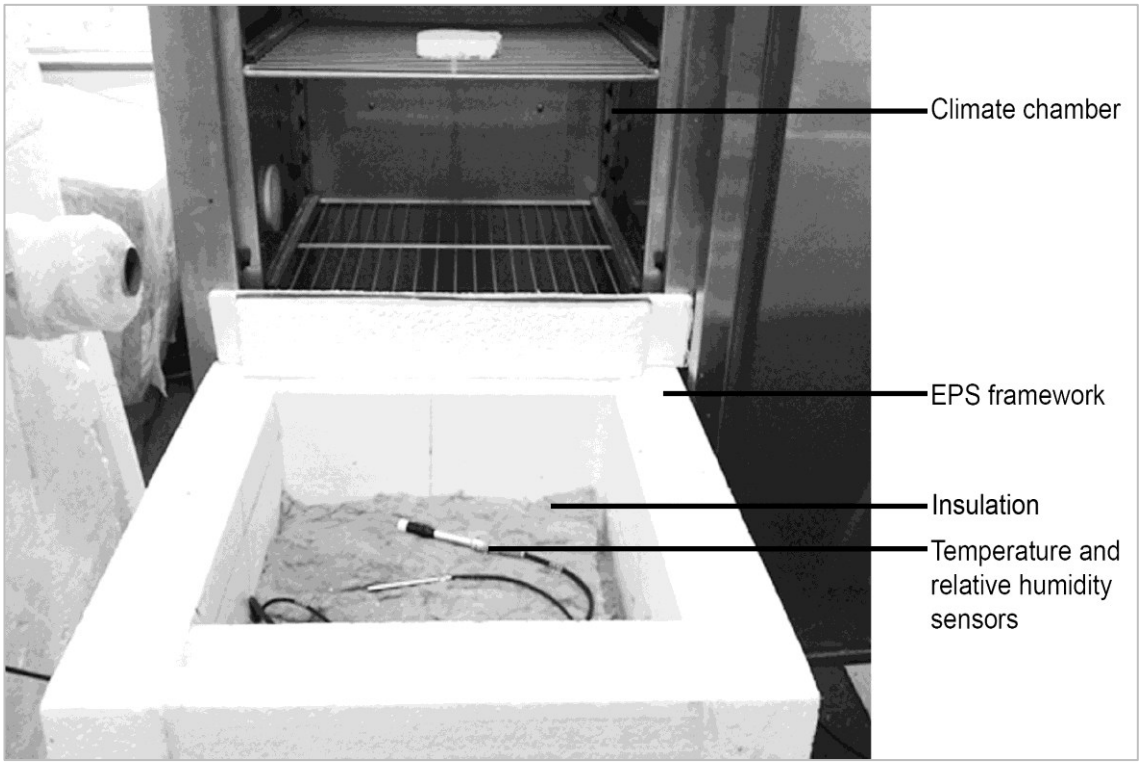


**Figure 6.67: Installation of insulation and temperature and relative humidity sensors.**

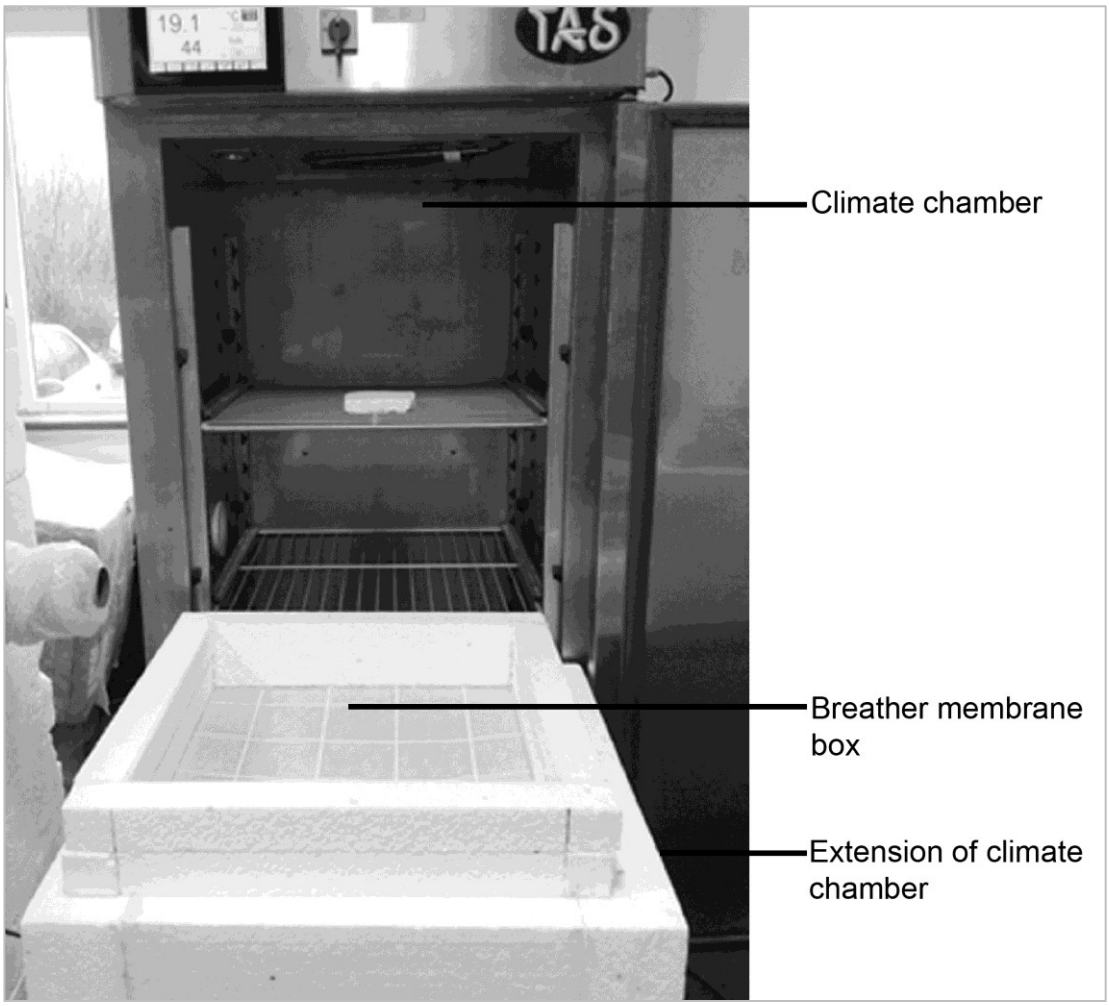


**Figure 6.68: Installation of the breather membrane box.**

A quantitative comparison of moisture management capacities of the hemp-1, hemp-4, sheep wool and stone wool insulation materials was done by measuring the weights of these insulation materials, the 'breather membrane box' and the acrylic sheet during the laboratory based experimental runs. The insulation materials were weighed to assess their moisture management capability by adsorption. The relative humidity sensors on the top and bottom surfaces of the insulation would indicate the relative humidity conditions on the respective surfaces during the experiment. The 'breather membrane box' was weighed to measure the amount of moisture that passed through the insulation, condensed on the acrylic surface and dripped down on the breather membrane. The measurement of the weight of the acrylic surface quantified the amount of moisture that passed through the insulation and condensed or deposited on the acrylic.

### *6.5.4 The experimental protocol*

The experimental protocol is shown in the Table 6.11. A step change has been made in the cold side temperature from 8 (±3) °C to 1 (±3) °C while the hot side temperature has been maintained at 23 (±3) °C. The relative humidity in the hot side has been maintained at 90(±3) % while the cold side does not have any relative humidity interaction other than what is induced by the moisture coming from the cold side.

**Table 6.11: The experimental protocol.**

| | Step 1 | Duration (Hours) | Step 2 | Duration (Hours) |
|---|---|---|---|---|
| Cold side temperature (°C) | 8±3 | 24 | 1±3 | 48 |
| Hot side temperature (°C) | 23±3 | | 23±3 | |
| Cold side relative humidity (%) | No Interaction | | No interaction | |
| Hot side relative humidity (%) | 90±3 | | 90±3 | |

### *6.5.5 Results and discussion*

#### *6.5.5.1 Likelihood of condensation*

Figures 6.69 and 6.70 show the moisture accumulation on the inner surface of the acrylic, immediately after the end of the laboratory based test with stone wool insulation. Moisture has accumulated during tests with all the insulation samples. However, there has been substantial variation in the amount of accumulated moisture, depending on the insulation used for testing.

Table 6.12 shows the change in weight in the insulation materials, in the breather membrane box and in the acrylic during the experimental runs with stone wool, sheep wool, hemp-1 and hemp-4 insulation materials. The changes in mass of the breather membrane box and the acrylic are added together and presented in Figure 6.71 along with the changes in mass of the insulation materials.

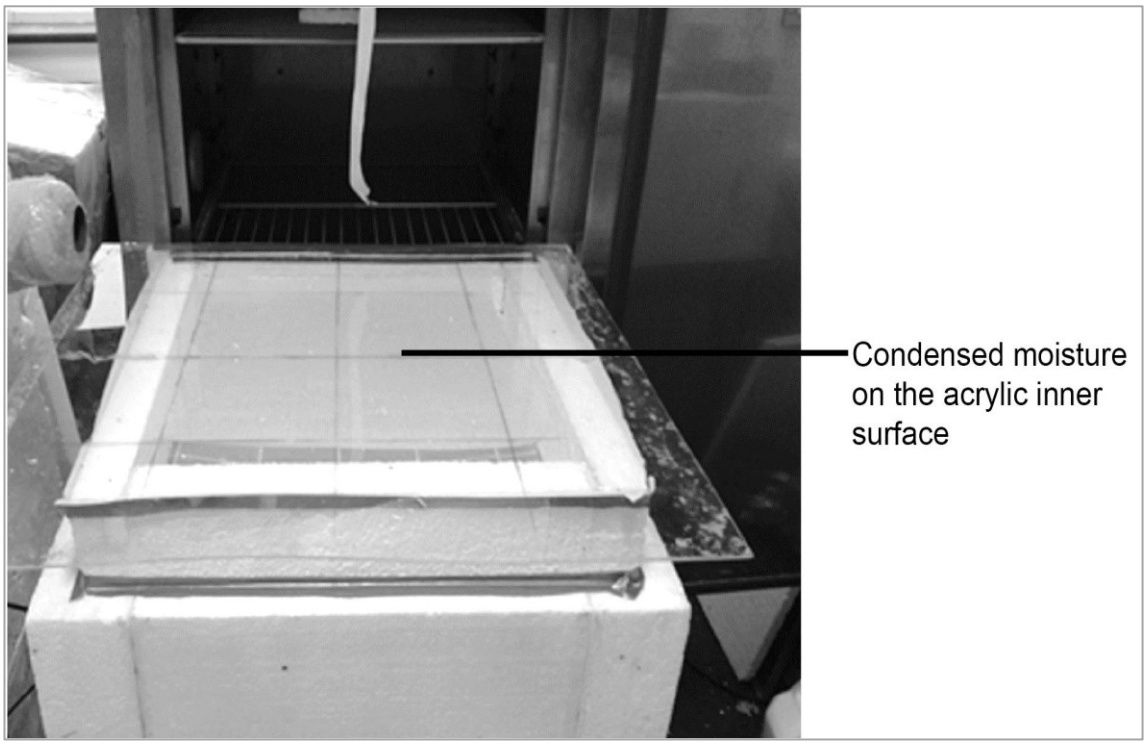


**Figure 6.69: Condensed moisture on the acrylic inner surface after the experiment with stone wool.**

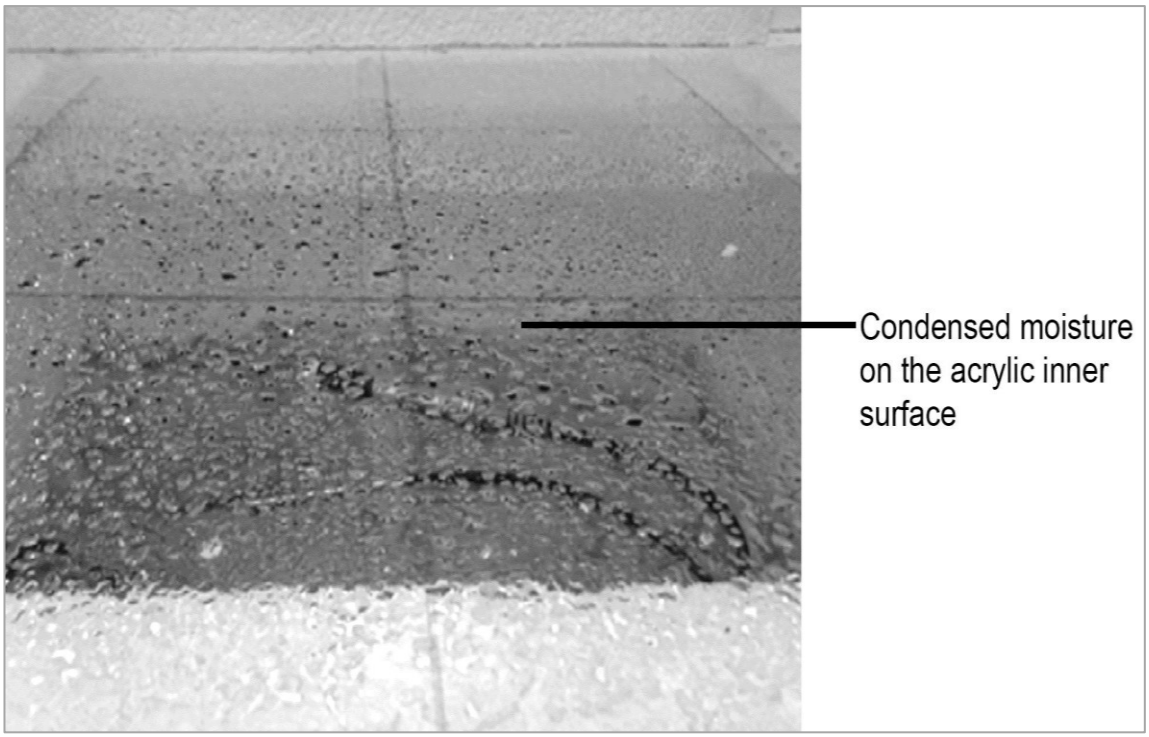


**Figure 6.70: Close-up image of condensed moisture on the acrylic inner surface after the experiment with stone wool.**

In terms of water content in the breather membrane box and acrylic, the amount of water accumulated during the experiment with stone wool insulation is three

times higher than that with hemp-1 and hemp-4 insulation and two times higher than that with sheep wool insulation. In a real life situation, the higher the amount of moisture in the loft space, the greater is the likelihood of condensation when the moisture is in touch with a cooler surface of the roof envelope. Eventually, in real life situation, some of the condensed water can drip back to the insulation surface. In this respect, loft space insulated with stone wool has higher risk for condensation.

In terms of moisture content in insulations, hemp-4 has adsorbed about 86%, hemp-1 about 79%, sheep wool about 71% and stone wool about 3% of the total moisture that propagated through the plasterboard during the successive experiments. Thus, hemp-1, hemp-4 and sheep wool insulation materials are buffering excessive moisture while stone wool shows almost negligible buffering performance. Additionally, for hemp and sheep wool insulation, the enthalpy of moisture will mostly remain in the insulation while for the stone wool the enthalpy of moisture will potentially be transmitted to the exterior while the moisture is in touch with the roof envelope.

**Table 6.12: Moisture accumulation in the acrylic, in the breather membrane box and in the insulation materials.**

| | Stone wool | Sheep wool | Hemp-1 | Hemp-4 |
|---|---|---|---|---|
| Change of mass In acrylic (gm) | 29.11 | 14.13 | 9.685 | 9.96 |
| Change of mass in breather membrane box (gm) | 1.51 | 0.81 | 0.28 | 0.04 |
| Change of mass In insulation (gm) | 0.84 | 35.9 | 37.28 | 60.47 |

Figures 6.72 to 6.75 show the relative humidity in upper surface, lower surface and underneath the plasterboard for stone wool, sheep wool, and hemp-1 and hemp-4 insulation. It can be noticed that the relative humidity in the upper surface of stone wool becomes equal to the relative humidity underneath the plasterboard within 5 hours of the beginning of the experiment. On the contrary, the relative humidity in the upper surface of sheep wool becomes equal to the

relative humidity underneath the plasterboard in about 72 hours. Relative humidity values in upper surfaces of hemp-1 and hemp-4 insulation materials are always lower than the relative humidity underneath the plasterboard. It implies that bio-insulation materials delay the propagation of moisture from the interior of the dwelling to the loft space by utilising their moisture adsorption and buffering capacity which is not the case for stone wool insulation.

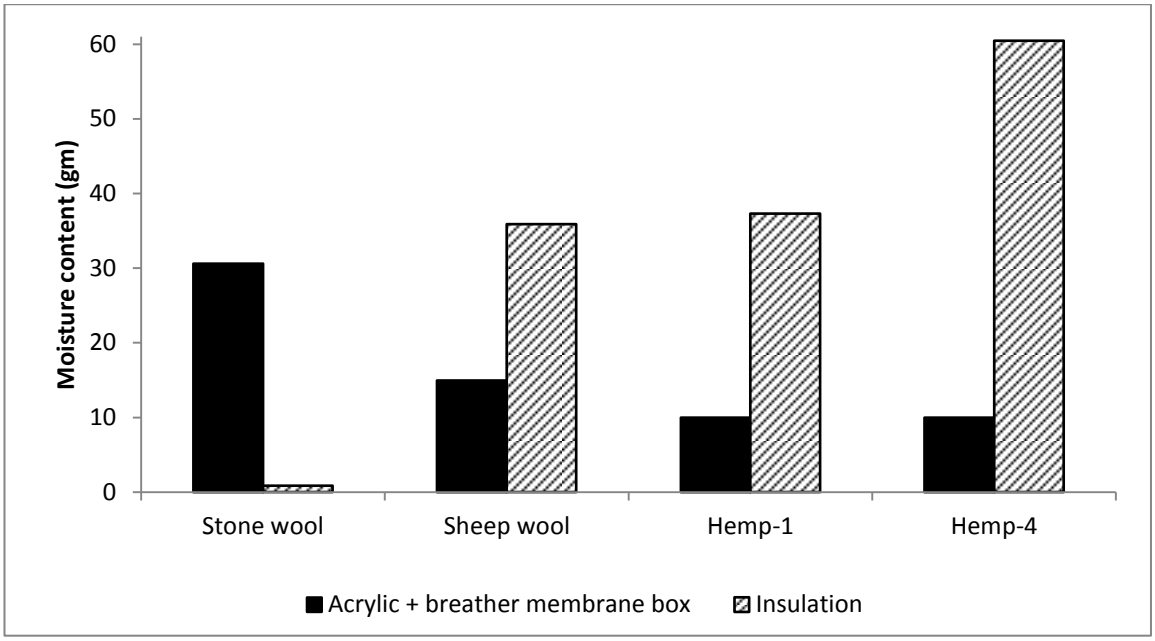


**Figure 6.71: Mass change in the experimental setups for the insulation materials.**

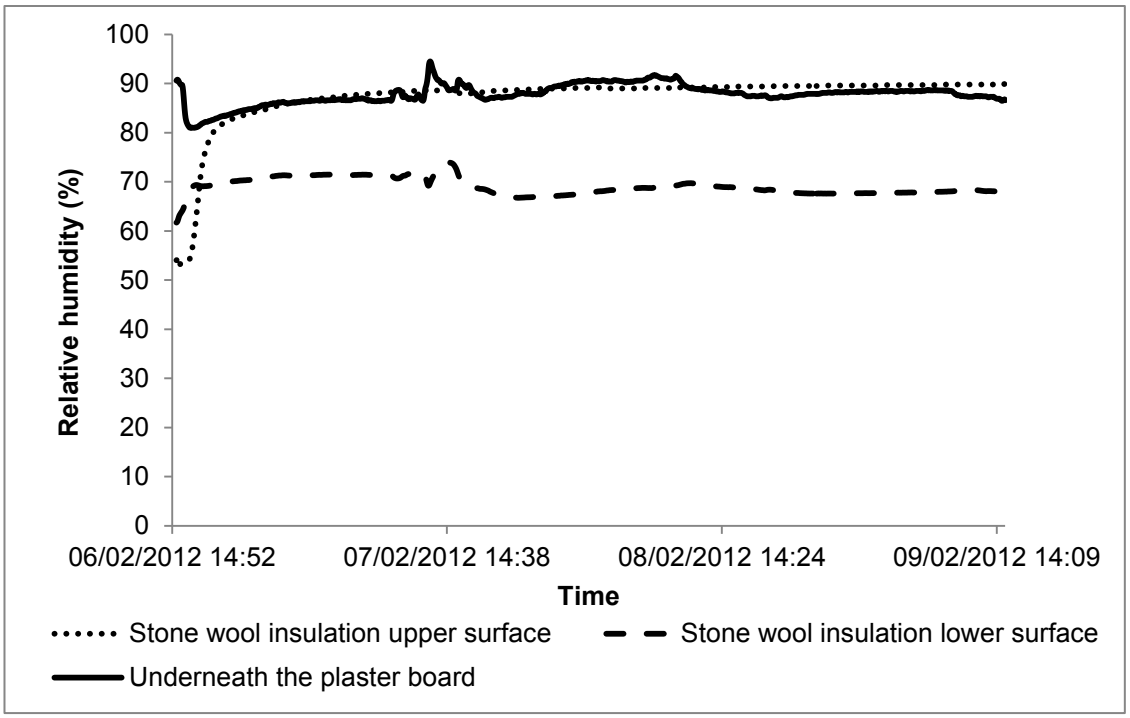


**Figure 6.72: Relative humidity distribution during the stone wool test.**

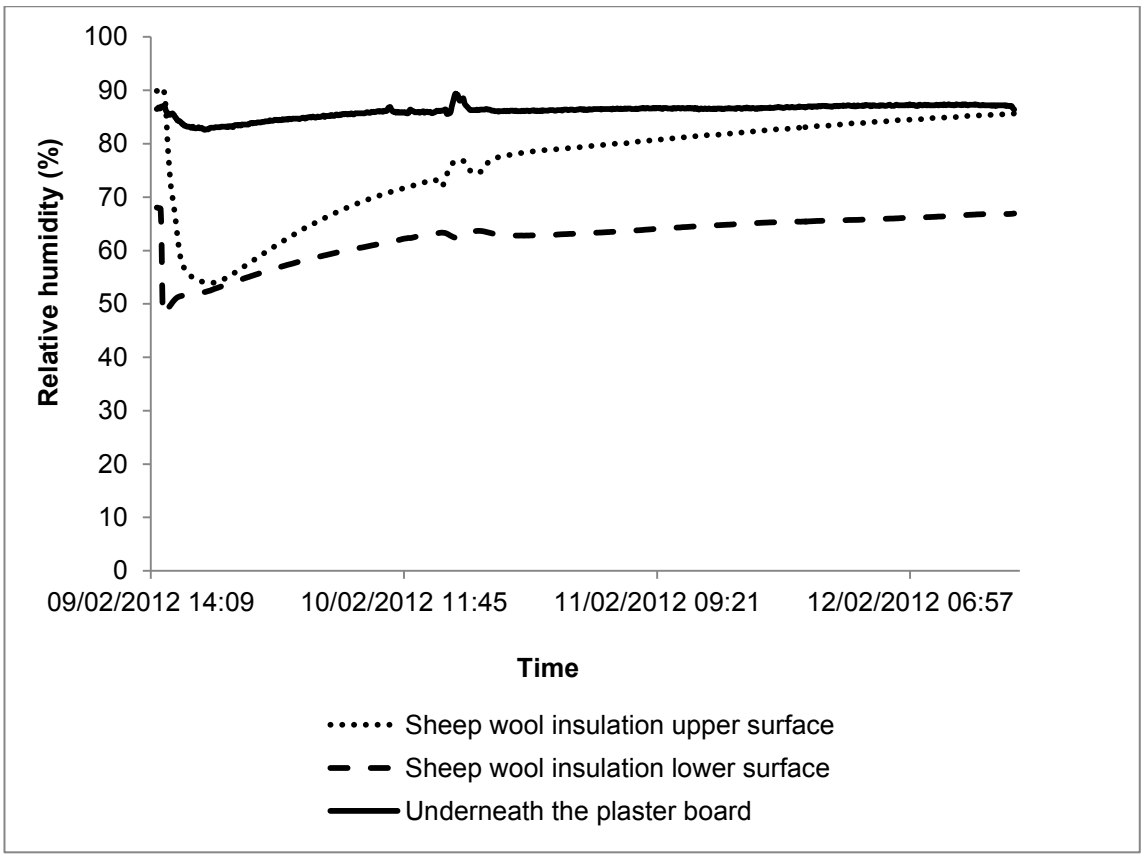


**Figure 6.73: Relative humidity distribution during the sheep wool test.**

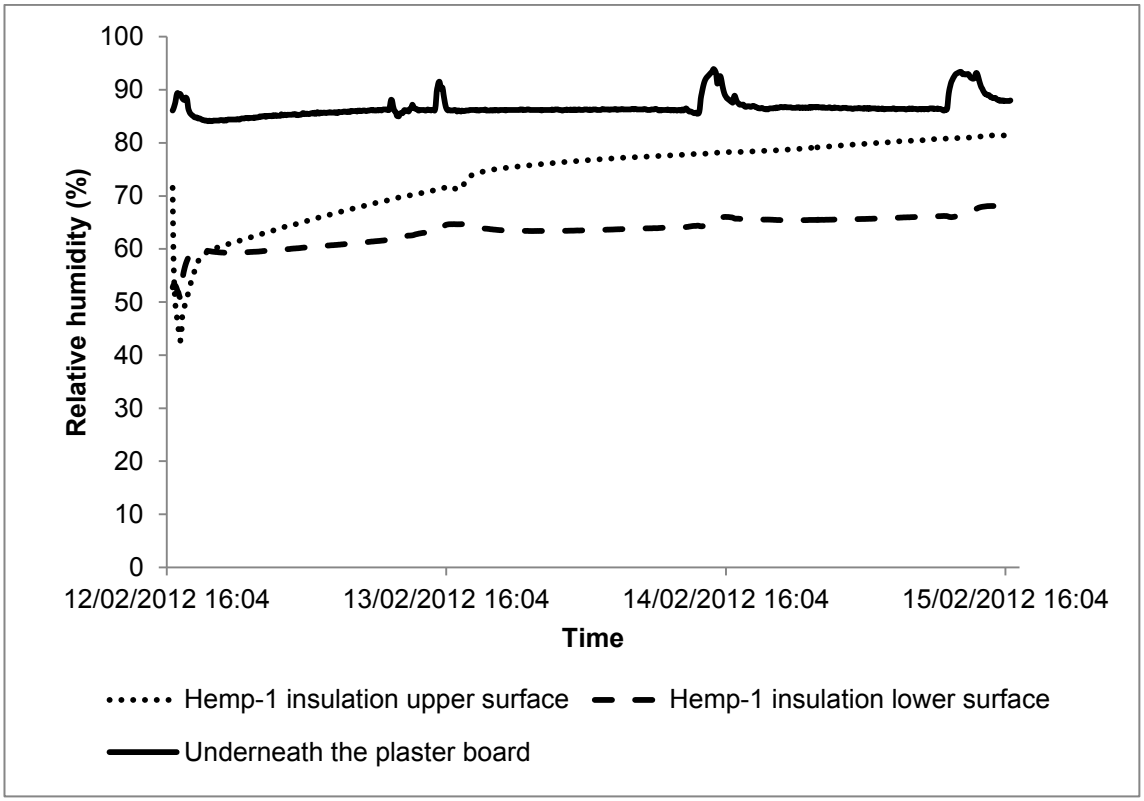


**Figure 6.74: Relative humidity distribution during the hemp-1 test.**

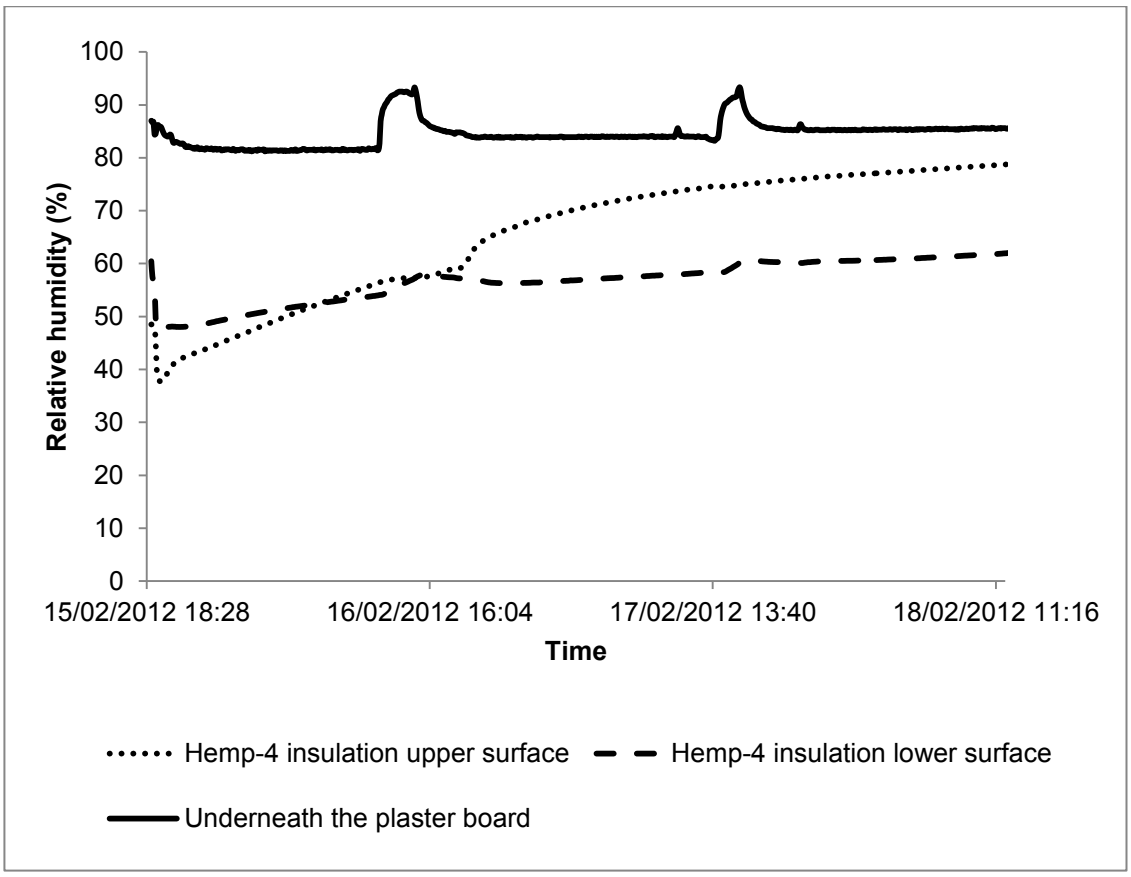


**Figure 6.75: Relative humidity distribution during the Hemp-4 test.**

### *6.5.5.2 Equivalent thermal conductivity*

The equivalent thermal conductivity values of the insulation materials were obtained from the temperature difference between the hot and cold side of the insulation materials and the corresponding heat flux data. They are shown in Table 6.13 and Figure 6.76. The operational error in thermal conductivity is 8.9%, as shown in subsection 6.2.6. The equivalent thermal conductivity of stone wool insulation was obtained as 0.052 W/mK, which is close the equivalent thermal conductivity value (0.054 W/mK) of stone wool insulation obtained during the experiment described in section 6.2. The equivalent thermal conductivity of stone wool insulation was 27% higher than the manufacturers' declared value of thermal conductivity. The equivalent thermal conductivity of hemp-1 was 0.028, hemp-2 was 0.034, and sheep wool was 0.033 W/mK, which were 26%, 13% and 15% lower than the manufacturers' declared values of thermal conductivity of the corresponding insulation materials.

Figure 6.77 shows that, when the temperature difference decreases, the heat flux in hemp-4 insulation also decreases. Heat also flows in the opposite

direction in the hemp-4 insulation setup due to its considerable heat capacity. In stone wool insulation, the response of heat flux to the temperature drop is not as intense as in hemp insulation, since the heat capacity of stone wool insulation is half of the heat capacity of hemp-4 insulation.

**Table 6.13: The equivalent thermal conductivity of the insulations.**

| Insulation | Thermal Conductivity (W/m-K) |
|---|---|
| Stone wool | 0.052 |
| Sheep wool | 0.033 |
| Hemp-1 | 0.028 |
| Hemp-4 | 0.034 |

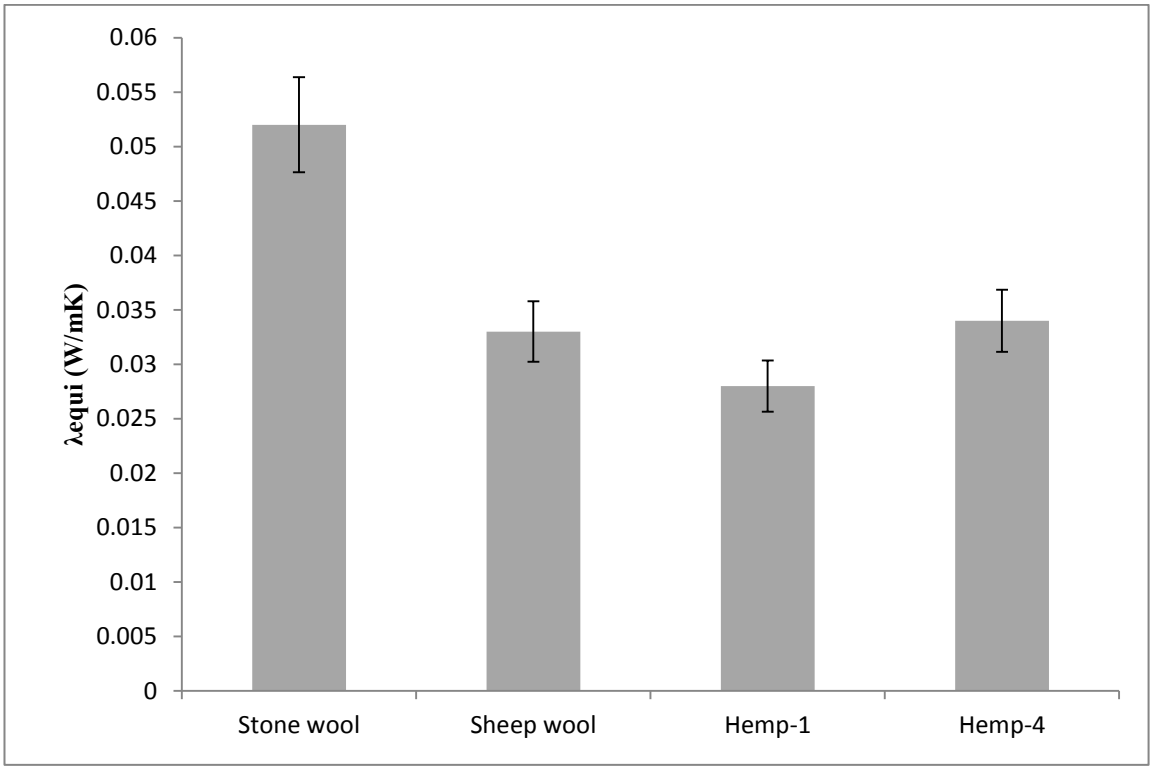


**Figure 6.76: Equivalent thermal conductivity of the insulations with error bar.**

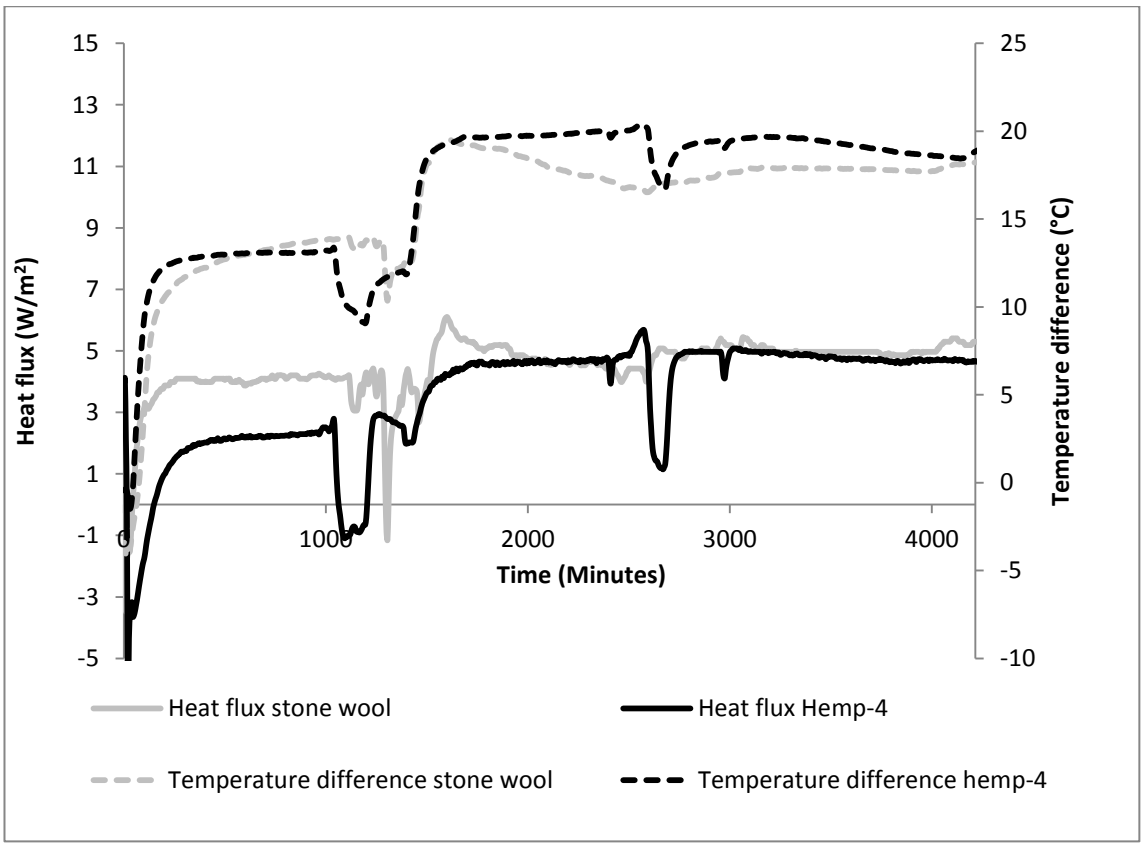


**Figure 6.77: Heat flux and temperature difference in stone wool and hemp-4.**

### *6.5.6 Summary of the loft experiment*

The laboratory based experiment aimed to examine the moisture and heat flux management capacity of hemp-1, hemp-4, sheep wool and stone wool insulation materials in loft space. The experimental hygrothermal boundary conditions of the loft space were derived from the hygrothermal data of a case study of a loft space that was prone to high relative humidity and condensation.

In terms of moisture management capacity, it was found that the amount of moisture content above the stone wool insulation could be three time higher than that in hemp-1, hemp-4 and sheep wool insulation materials. It implies that the likelihood and frequency of high relative humidity and condensation will be three times higher in stone wool insulation than in the hemp-1, hemp-2 or sheep wool insulation in the simulated loft space.

In terms of equivalent thermal conductivity, it was found that the thermal conductivity values of hemp-1, hemp-2 and sheep wool insulation materials were 26%, 13% and 15% lower than the manufacturers' declared values for the

thermal conductivity of the corresponding insulation materials. On the contrary, the equivalent thermal conductivity of the stone wool insulation was 27% higher than the manufacturer's declared value.

### 6.6 Chapter summary

This chapter describes four laboratory-based experiments to examine the heat and moisture management capacity of insulation materials in dynamic and quasi steady state hygrothermal boundary conditions.

The experiments described in sections 6.2, 6.3 and 6.5 establish that hemp-1, hemp-2 and hemp-4 insulation materials can reduce the likelihood and frequency of condensation in the insulation interfaces and in loft spaces by utilising their moisture buffering capacity. On the contrary, there is higher likelihood of condensation in walls and loft spaces when stone wool insulation is used. During the experiments described in subsection 6.2 and 6.3, it was observed that during the drying out period the relative humidity in the (hemp-2)-acrylic interface reduces slowly compared to that in the (stone wool)-acrylic interface. It implies that the critical period for mould growth may stay longer in the hemp-2 interface during the drying out periods. This issue is further studied during the in situ tests, as described in chapter seven.

It was observed that the equivalent thermal conductivity of insulation materials, when exposed to the relative humidity of the interior, depends on how the insulation materials manage moisture. Equivalent thermal conductivity of the insulation materials also depends on the test methods employed.

For the stone wool insulation, condensation occurred in the (stone wool)-acrylic interfaces during the tests described in sections 6.2 and 6.3. The equivalent thermal conductivity of stone wool at 45% average relative humidity, during the test described in section 6.2, was 0.054 W/mK. The average equivalent thermal conductivity of stone wool at 63% average relative humidity during the test described in section 6.3 was 0.033 W/mK. The variations in the equivalent thermal conductivity seemed to occur due to two reasons. Firstly, when condensation occurred in the insulation-acrylic interface, it is plausible that some of the heat went back to the insulation. Secondly, the heat flux sensor could not possibly register the heat loss by condensation as the placement of

heat flux sensor and the area of condensation did not coincide. However, during the test described in section 6.5 it was found that the average equivalent thermal conductivity of stone wool insulation was 0.052 W/mK.

For hemp-2 insulation, the equivalent thermal conductivity at 45% average relative humidity, during the test described in section 6.2, was 0.038 W/mK. The equvalent thermal conductivity at 65% average relative humidity, during the test described in section 6.3, was 0.048 W/mK. Hemp-2 is a highly adsorptive insulation material. During the second test, insulation materials were exposed to each of the relative humidity ranges for at least 24 hours. Hence, the moisture dependent increase of thermal conductivity at 65% average relative humidity was likely. During the test described in section 6.5, the equivalent thermal conductivity values of hemp-1 and hemp-4 insulation materials were measured as 0.028 W/mK and 0.034 W/mK, respectively. Since the experiment described in section 6.5 simulated the service condition and plasterboard was used in the inner surface, it seemed that the in situ test results of equivalent thermal conductivity of hemp insulation materials would produce similar results. The in situ experiments are described in chapter eight.

The test described in section 6.4 attempted to explore the phenomenon of moisture migration across the depth of hemp-2 insulation when the conventional method of measuring moisture dependent thermal conductivity was applied. It was found that 48% and 37% moisture was lost from the warmer first layer of hemp-2 insulation during the determination of thermal conductivity at 80 EMC and 95 EMC, respectively. When substantial amount of moisture as such migrates through the depth of any insulation material during the determination of thermal conductivity at a certain EMC, the results do not reflect the thermal conductivity of that insulation at that particular EMC.

# Chapter 7

# In Situ Tests to Determine the Hygrothermal Properties of Insulation Materials in Service Conditions

## 7.1 Introduction

This chapter addresses the research objectives of determining the heat and moisture management capacity of hemp insulations by conducting in situ experimental tests in accordance with the research methods outlined in section 4.3 of chapter four. The present chapter focuses on system level tests, where the insulation material is part of the thermal envelope of the test building.

The hygrothermal behaviour of hemp insulation in steady state, non-steady state and quasi-steady state boundary conditions has been assessed through a number of laboratory-based experiments in chapters five and six. The present chapter concentrates on the in situ assessment of the hygrothermal behaviour of hemp insulation in a timber frame wall.

Although the hygrothermal properties of the insulation materials assessed by experimental methods provide valuable information about their heat and moisture management capability, the hygrothermal behaviour of the insulation materials can be different in service conditions from that in experimental conditions. This can happen for the following reasons:

- In service conditions, the hygrothermal properties are determined when the insulation materials are placed in the real wall. In addition to the insulation materials, the walls may include plasterboard, oriented strand boards and brick. The hygrothermal behaviour of these materials may influence the hygrothermal behaviour of the insulation materials. Except for the experiment described in section 6.4 of chapter six, all experiments were performed on a hypothetical wall system composed of acrylic sheet and insulation. The hygrothermal data derived from those experiments may provide information about the hygrothermal behaviour of the insulation materials, but not necessarily about

the hygrothermal behaviour of the insulation materials as a part of the real wall assembly.

- It is often difficult to simulate long-term real life hygrothermal boundary conditions in laboratory-based experiments because of limitations of research time and equipment performance.
- The results obtained on the equivalent thermal conductivity of the insulation materials by laboratory based tests were not fully conclusive. In situ determination of equivalent thermal conductivity of the insulation materials is therefore necessary.
- In situ tests are important to study the likelihood of mould spore germination in the insulation interfaces.
- There is lack of hygrothermal data in relation to the study of the situ hygrothermal properties and the likelihood of mould spore germination in hemp insulations.

## 7.2 Outline of the in situ tests

This chapter describes three in situ tests. Although the tests primarily focus on the heat and moisture management capacity of hemp insulations, the tests vary in terms of the setup of the timber frame wall panels and the types of insulations tested. A brief outline of the tests is provided below:

### *7.2.1 Test-1*

Test-1 assesses the difference in hygrothermal performance of hemp-1 insulation in timber frame wall panels with and without vapour barrier. Test-1 serves two purposes. Firstly, the apparent thermal conductivity values of hemp-1 insulations in timber frame wall panels with and without vapour barrier are determined and compared. Secondly, moisture conditions and likelihood of mould spore germinations in the insulation-OSB interfaces of the panels with and without vapour barrier are assessed. As a result of test-1, the potential of vapour open timber frame wall assembly incorporating bio-insulations can be better understood.

### *7.2.2 Test-2*

Test-2 compares the hygrothermal performance of hemp-1 and hemp-2 insulations in vapour open wall panels. The hemp content in hemp-1 is 30% and

in hemp-2 is 85%. The findings of the test-2 represent the limit of the heat and moisture management capacity of the hemp insulations in terms of low and high hemp content, respectively, in the insulation matrix. However, interpretation of the findings of the insulation with low hemp content (hemp-1) needs to take into account the effect of the rest of the constituents in the insulation. The secondary aim of the test-2 is to assess the effect of the position of the heat flux meter in the wall panels on the equivalent thermal conductivity values of the insulations.

### *7.2.3 Test-3*

Test-3 compares the hygrothermal performance of hemp and stone wool insulations in vapour open wall panels. This test shows how hemp-2 insulation performs compared to conventional mineral wool insulation in terms of heat and moisture management in vapour open timber frame wall panels. The secondary aim of test-3 is to assess the effect of the position of the heat flux meter in the wall panels on the values of equivalent thermal conductivity of the insulations.

## 7.3 The test building and the test panels

### *7.3.1 The test building*

The timber frame test building (Figure 7.1) was constructed from scratch by the author of this thesis near the Centre for Alternative Technology in Wales.

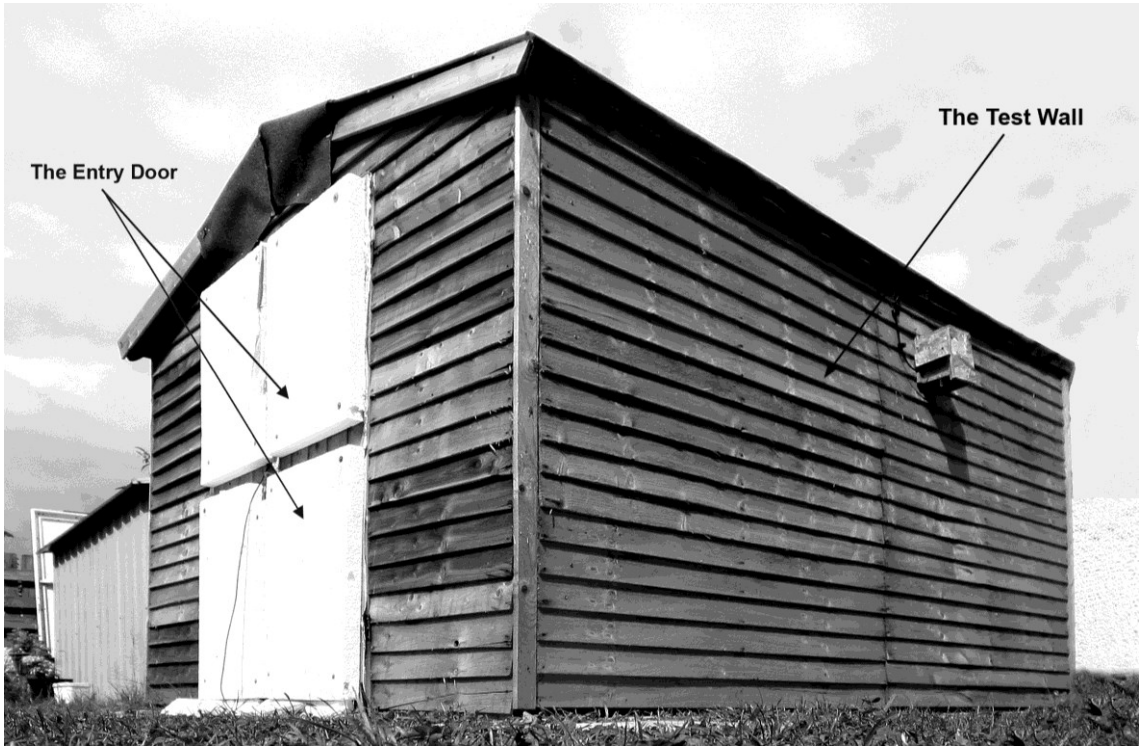


**Figure 7.1: The test building showing the test wall.**

The test building was 3 metres long and 2.4 metres wide (Figure 7.2). The height of the test building was 2 metres along the eaves and 2.4 metres along the ridge. The test building incorporated two test wall panels in the eastern wall to accommodate the insulation samples. Except for the test wall panels, all other walls, floor and roof of the test building were insulated with 100 mm expanded polystyrene (EPS) insulation providing an approximate wall U-value of 0.3 W/m$^2$K (Figure 7.3).

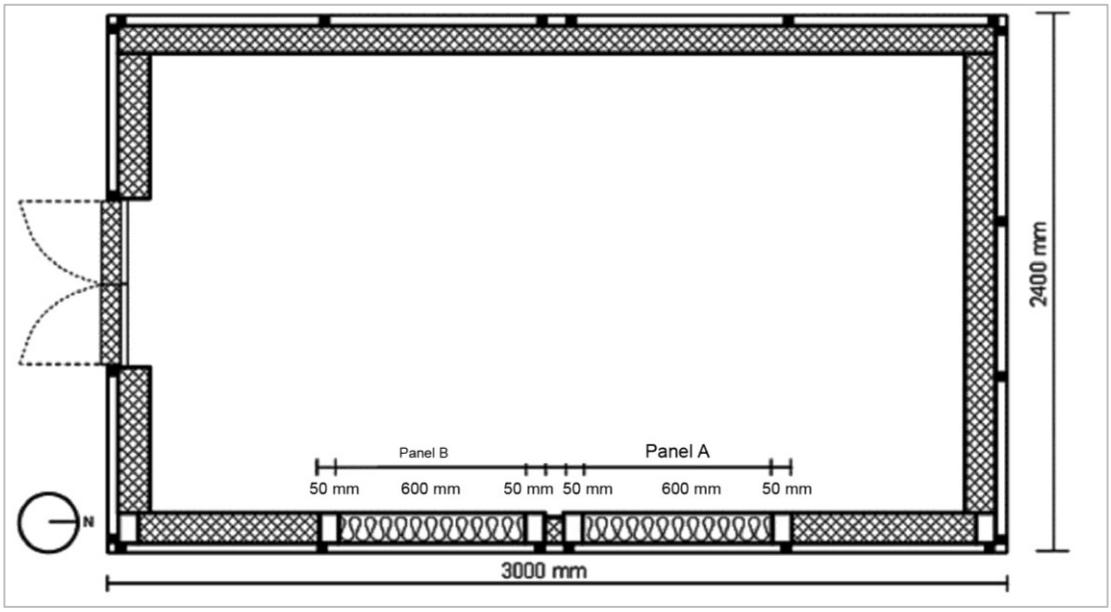


**Figure 7.2: Plan of the test building.**

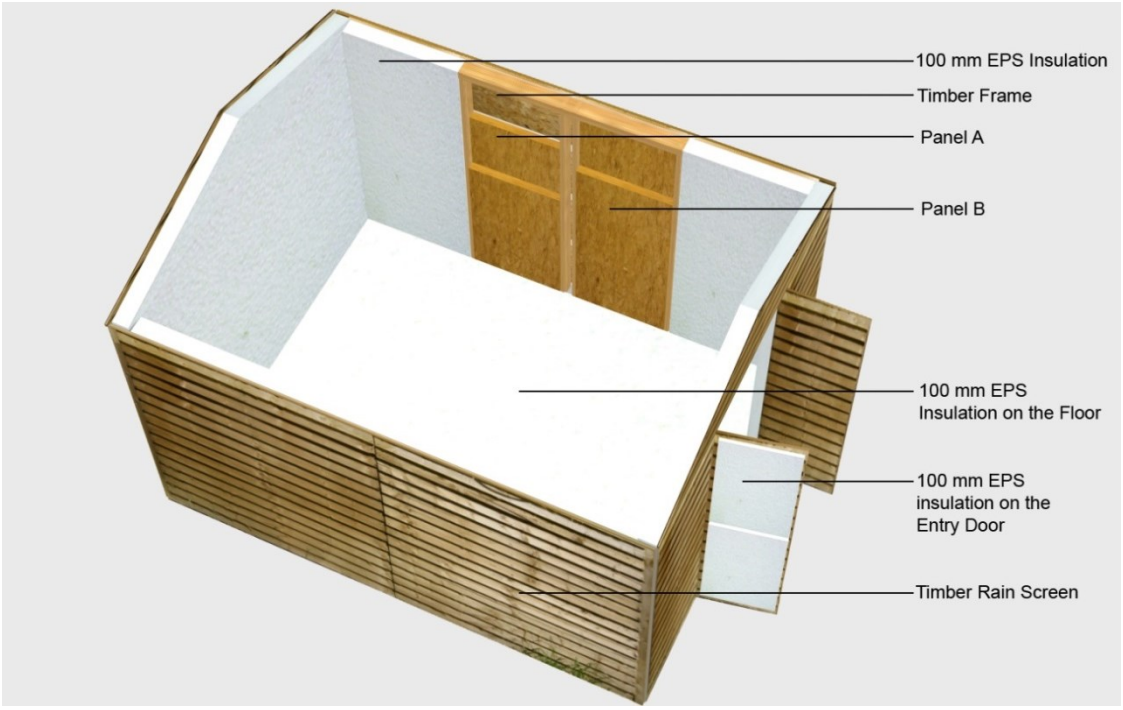


**Figure 7.3: Three dimensional computer image of the test building with the roof removed**

The key stages of the construction process of the test building are outlined below:

**Construction Stage 1:** The outer layer of the wall of the test building was constructed of timber frame and timber rain screen. The structure of the roof was constructed of timber frame, covered by 6 mm exterior grade plywood (Figure 7.4). The plywood is externally covered with roofing felt for weather protection.

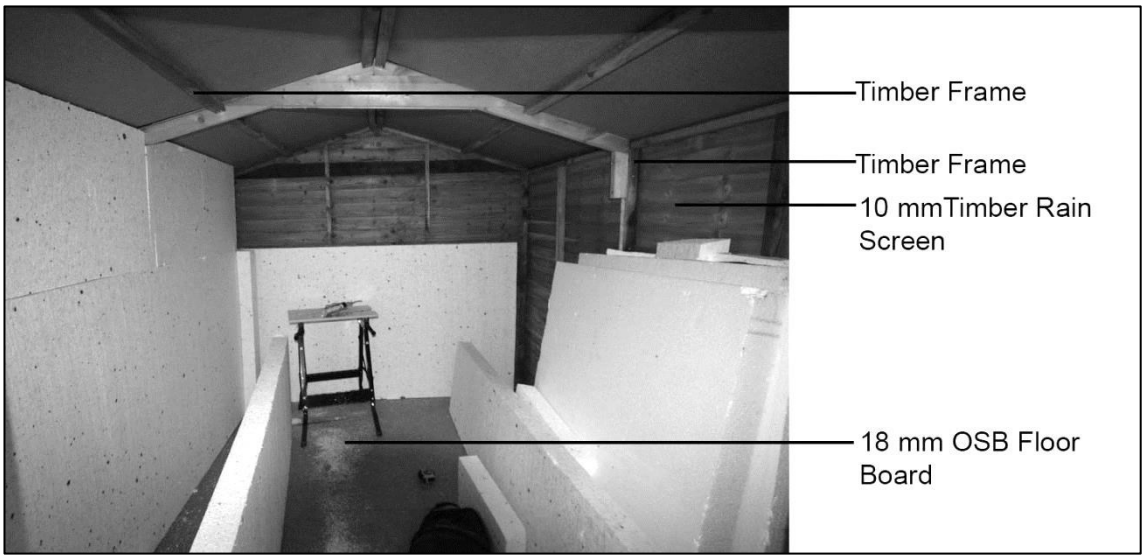


**Figure 7.4: Construction of the outer layer of the test building.**

**Construction stage 2:** Except for the eastern wall, the walls, ceiling and floor were internally covered with 100 mm EPS insulation. Breather membrane was installed on the timber frame in the entire eastern wall from inside (Figure 7.5).

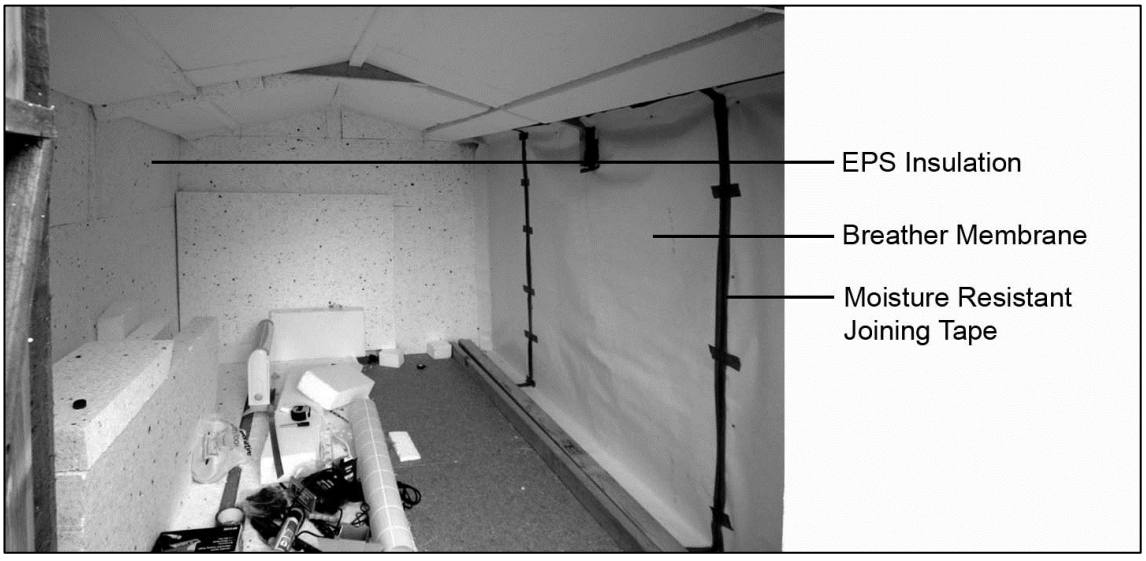


**Figure 7.5: Installation of the EPS insulation and breather membrane.**

**Construction stage 3:** Oriented strand boards **(**OSB) were installed behind the breather membrane from inside. Spaces for two timber frame test panels (panel A and panel B) were constructed in the eastern wall (Figure 7.6 and 7.7). The details of the test panels are provided in section 7.3.

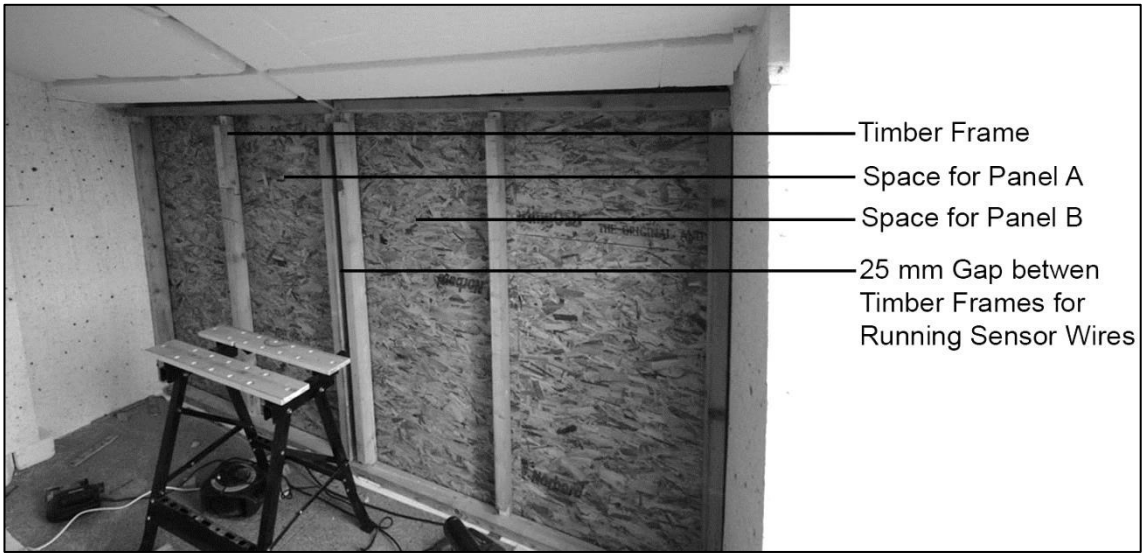


**Figure 7.6: Installation of the OSB boards and timber frames for wall panels.**

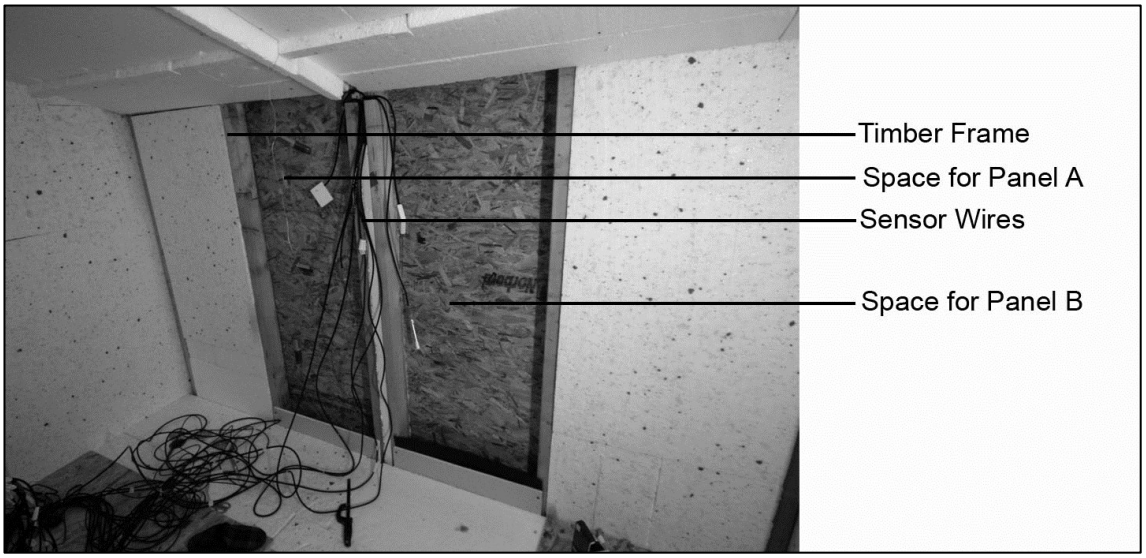


**Figure 7.7: Installation of the EPS insulation in the eastern wall.**

The east façade of the test building is completely shaded by other nearby buildings during the winter and 90% of the daytime during the summer. For this reason the temperature of and the heat flux through the eastern wall are not affected by any incident solar radiation. Hence, thermal conductivity can be determined from the temperature difference of the ambient air and thus, the eastern wall is suitable for testing in situ thermal properties of the wall. The

relative humidity and temperature in the test building can be set at any required level by a shielded convective heater with thermostat and an evaporative industrial humidifier with hygrostat. The thermographic images of the test building during insulation installation are provided in Appendix D. The image of the buildings that provide shadow over the eastern wall of the test building is also attached in Appendix D.

The tests were conducted during the months of January, February, July and August 2012, in order to put the result into the context of the UK winter and summer climatic conditions. The averages of the maximum temperature, minimum temperature and mean temperature of the UK and Wales between 1910 and 2011 for the test months (Met Office, 2012) are shown in Table 7.1. The temperature condition in Wales is not significantly different from the mean temperature conditions in the UK and thus can be considered as representative of the UK climate. Although it is common knowledge that rainfall in Wales and Scotland is highest in the UK, this was not relevant for the tests as the rain screen was used.

**Table: 7.1 Average external temperatures (temp) in the UK and Wales during January, February, July and August.**

| | Maximum temp in the UK (°C) | Maximum temp in Wales (°C) | Mean temp in the UK (°C) | Mean temp in Wales (°C) | Minimum temp in the UK (°C) | Minimum temp in Wales (°C) |
|---|---|---|---|---|---|---|
| January | 5.9 | 6.4 | 3.24 | 3.8 | 0.6 | 1.2 |
| February | 6.3 | 6.5 | 3.4 | 3.8 | 0.5 | 1.0 |
| July | 18.6 | 18.4 | 14.4 | 14.5 | 10.3 | 10.6 |
| August | 18.5 | 18.4 | 14.4 | 14.5 | 10.3 | 10.7 |

### *7.3.2 The test panels*

Two test panels were incorporated in the eastern wall of the test building. The 600 mm X 1800 mm test wall panels (panel A and panel B) consist of a number of layers. From inside to outside, these layers are: 12.5 mm plasterboard (PB) in test-1.1 and 11 mm OSB in test-1.2, vapour barrier (with or without), 100 mm insulation, 11 mm OSB, 0.5 mm breather membrane, 25 mm air gap,

10 mm X 100 mm timber rain screen with 30 mm overlaps. During test-1, panel A was vapour open (without vapour barrier) and panel B was with vapour barrier. During test-2 and test-3, both panels were vapour open. The test panels were assembled either as assembly-1 or as assembly-2, as described below:

**Assembly-1**: For test 1, the test panels are organised as assembly-1 as shown in figure 7.8. In assembly-1, vapour barrier is installed between the plaster board and the insulation in panel B.

In assembly-1, temperature and relative humidity sensors were installed at the following positions in panel A and panel B: one sensor at the insulation-OSB interface, one at the middle of the insulation, one on the outer surface of the PB or OSB inner lining. Two heat flux sensors were installed on the outer surface of the PB or OSB inner lining of each panel, one sensor at the centre of the panel and the other sensor at 300 mm above the centre of the panel, vertically.

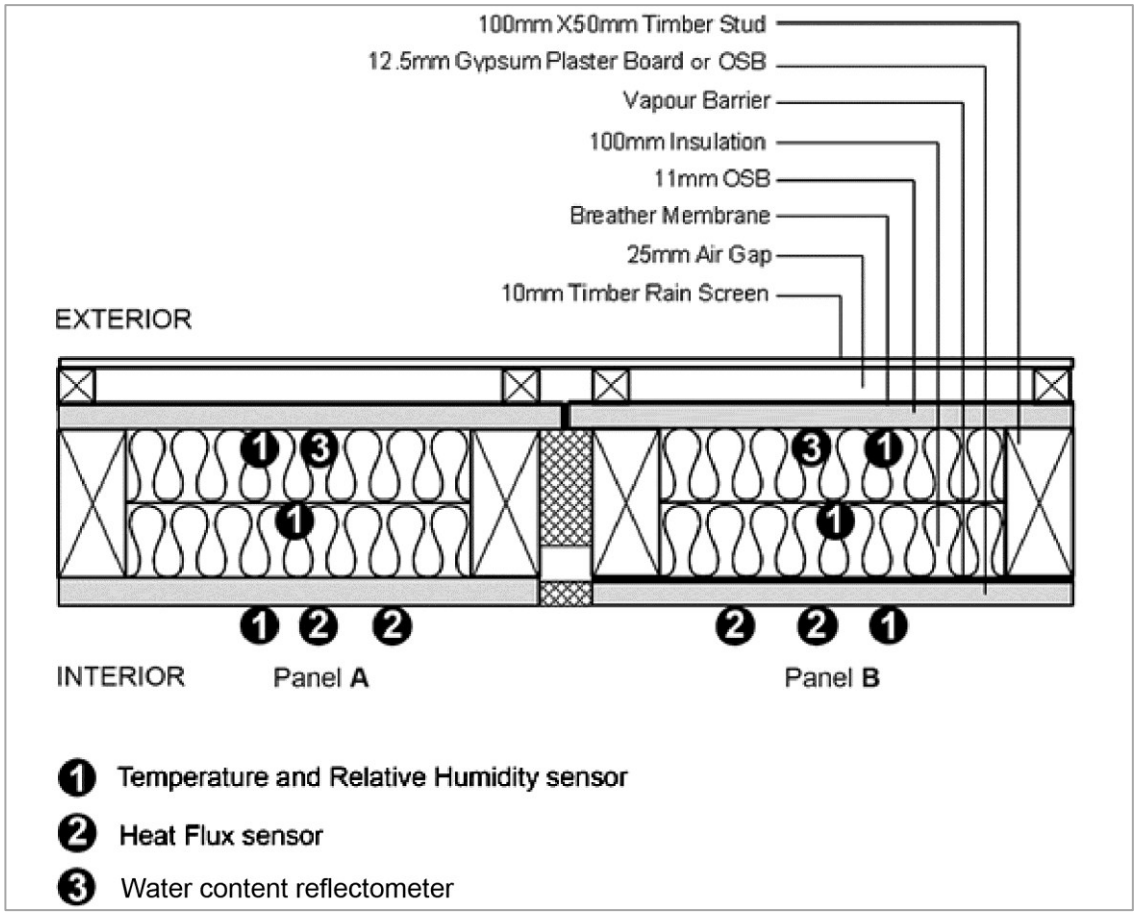


**Figure 7.8: Horizontal cross section showing panel A and panel B and sensor locations in assembly-1.**

A water content reflectometer was placed between the OSB and the insulation in each of the wall panels to assess the moisture content in the insulation in the insulation-OSB interface. Since the water content reflectometer used for testing measures data in terms of soil moisture content, the data gathered from the water content reflectometer was used for qualitative comparison of presence of moisture content between the insulations.

**Assembly-2**: For test-2 and test-3, the panels were organised as assembly-2 (Figure 7.9). In assembly-2, both panels were without a vapour barrier. Assembly-2 also differs from assembly-1 in terms of the placement of the heat flux sensors. In assembly-1, both heat flux sensors were placed on the PB or OSB surface of the panels facing the interior of the test house. In assembly-2, one of the heat flux sensors was placed between the insulation and the OSB board to assess the effect of moisture migration on heat flux. This setup was not used in assembly-1 as one of the panels included a vapour barrier which stopped moisture migration in the panel from the interior.

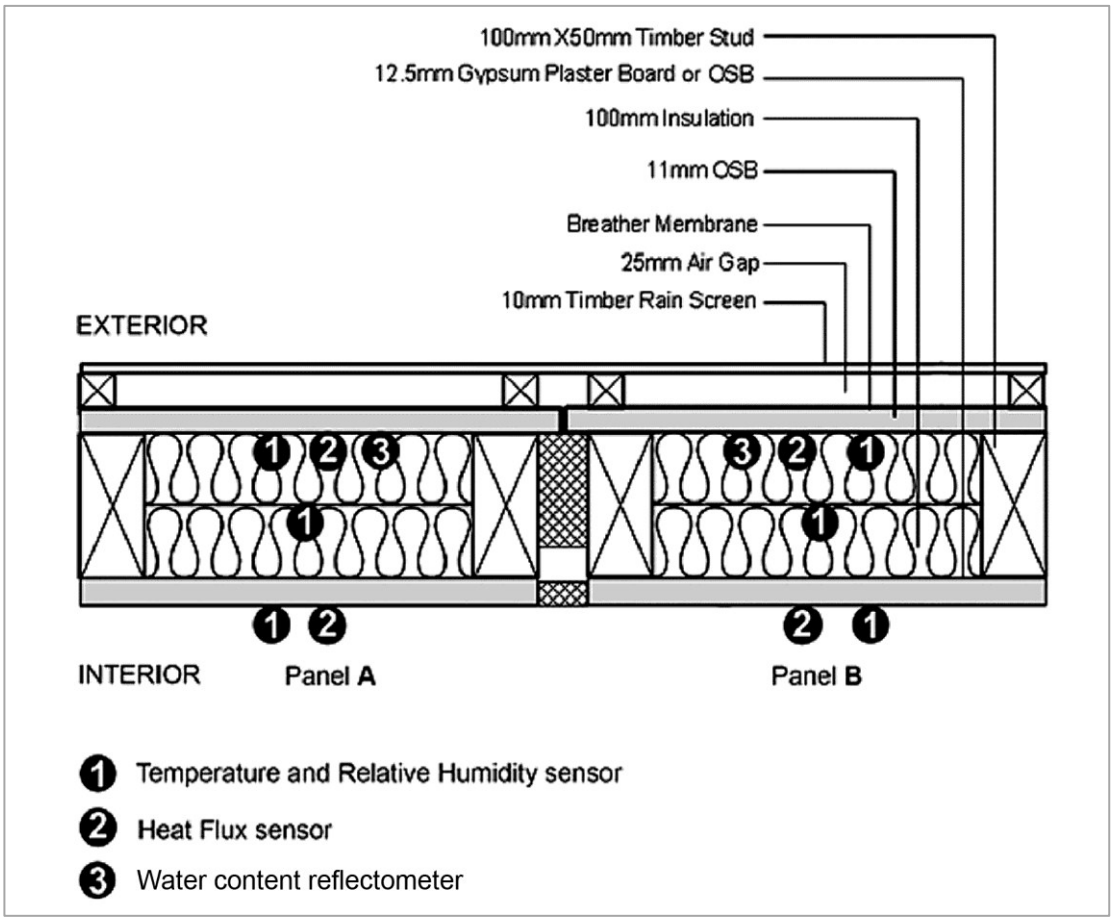


**Figure 7.9: Horizontal cross section showing panel A and panel B and sensor locations in assembly-2.**

In assembly-2, temperature and relative humidity sensors were installed at the following positions in panel A and panel B: one sensor at the insulation-OSB interface, one at the middle of the insulation, one on the outer surface of the PB inner lining. One heat flux sensor was installed on the centre of the outer surface of the PB inner lining of each of the panel. The other heat flux sensor was placed between the outer surface of the insulation and the inner surface of the outer OSB board. The second heat flux sensor was also positioned at the centre of the OSB board. The water content reflectometers were placed in the same location as in assembly-1.

## 7.4 Theory on thermal conductivity and mould spore germination

This section briefly describes the methods for determining equivalent thermal conductivity and the likelihood of mould spore germination in relation to the insulations used during the tests in this chapter.

### *7.4.1 Thermal Properties*

ISO 9869 describes the method for in-situ measurement of U-value of the building elements. U-value can be obtained by dividing the mean density of heat flow rate by the mean temperature difference if the average is taken over a long period of time, i.e. at least more than 72 hours for heavy weight structure and at least three nights' data in case of a light weight structure. The thermal transmittance value (U-value) is determined from the following equation:

$$U = \frac{\sum_{j=1}^{n} q_j}{\sum_{j=1}^{n} (T_{ij} - T_{ej})} \qquad [7.1]$$

Where,

U is thermal transmittance ($W/m^2K$), J is the number of individual measurements, $q_j$ is total density of heat flow ($W/m^2$), $T_{ij}$ is total internal temperature (°C) and $T_{ej}$ is total external temperature (°C).

$$\lambda equi = d/R \qquad [7.2]$$

Where, λequi is equivalent thermal conductivity (W/mK), d is insulation thickness, R is thermal resistance of hemp insulation.

R can be determined by subtracting the thermal resistance values of the individual elements (including surface resistance) from the total thermal resistance of the panel.

### *7.4.2 Mould spore germination: hygrothermal conditions*

The likelihood of germination and growth of mould and other microorganisms on a surface depends on the combination of temperature, moisture, substrate type, exposure time and the type of species. The relationship between temperature, relative humidity, exposure time and substrate type in relation to the risk of spore germination and mould growth is often expressed by isopleth curves. Figure 7.10 shows the germination isopleths developed by Sedlbauer incorporating the lowest isopleth for mould for substrate class 1 or biodegradable substrates (LIM I). The lowest isopleth for mould (LIM) curves are developed by analysing the combined growth conditions of all fungal species and thus represent the worst-case scenario for mould spore germination. A detailed discussion on determining the mould spore germination potential can be found in section 3.7 of chapter three.

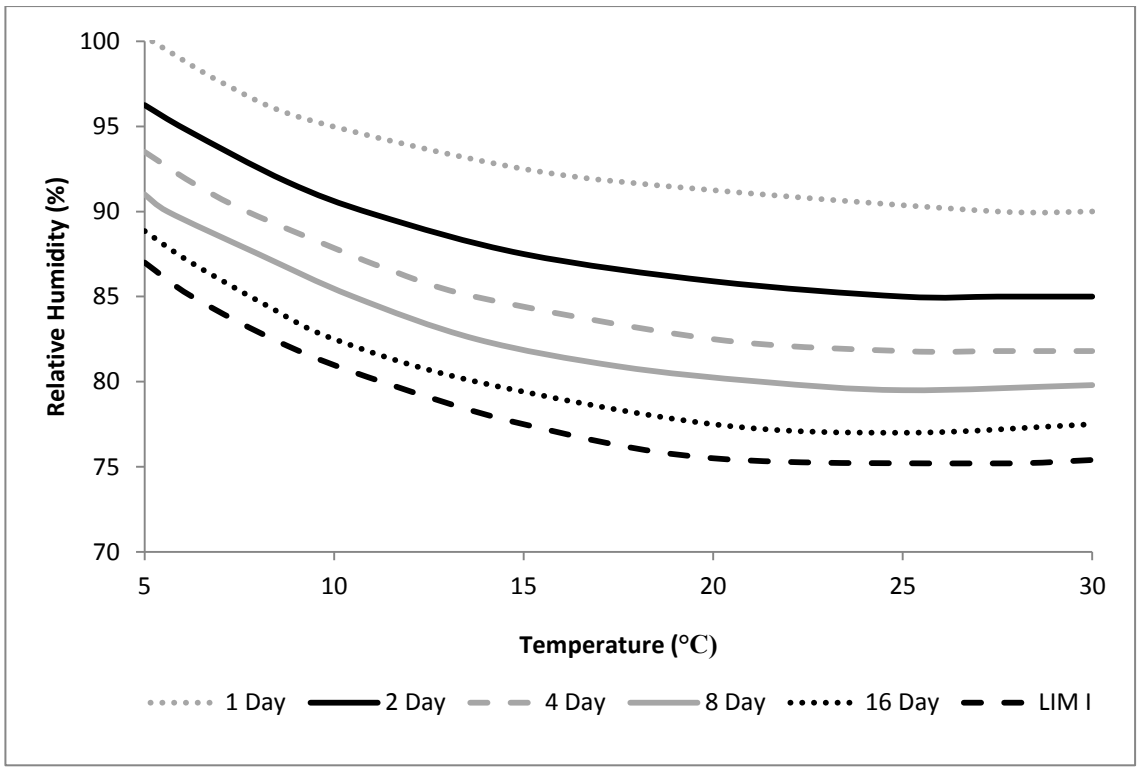


**Figure 7.10: Sedlbauer's isopleth system for substrate class I.**

## 7.5 Operational errors in heat flux measurement

### *7.5.1 Operational errors in heat flux measurement in assembly-1*

The operational errors of the heat flux sensors in assembly-1 can be calculated according to ISO 9869. The ISO 9869 outlines the following likely errors in in-situ heat flux measurements:

- The error due to the calibration of the heat flux sensor and the temperature sensors is about 5%.
- Random variation caused by difference in thermal contact between the sensors and the surface they are applied on, the corresponding error is about 5%. The error reduces when more than one heat flux sensors are used. In the present test, two heat flux sensors were used on the interior surface of each panel; therefore the error is less than 5%. For the present test, the error is assumed as 4%.
- 2% to 3% operational error due to the modification of isotherms by the placement of heat flux sensors. For the present test, the error is assumed as 2%.
- Errors due to the variations in temperature and heat flux over time. The error can be as much as 10% but can be reduced by taking data for a long period of time, keeping the variations in internal temperature low etc. When the test wall is not in direct contact with sunlight and internal variation in temperature is low, the error can be 1%. Since the test wall was not in direct contact with sunlight and internal variations of temperature was low, it can be assumed that the error was about 1%.

The total error of heat flux for each panel, following the ISO 9869, will be square root of the sum of square of the individual errors. For the present test, the total error can be estimated as follows:

Total error in heat flux = $\sqrt{5^2 + 4^2 + 2^2 + 1^2}$ = 6.8%

In addition to the errors in heat flux measurement, according to the ISO 9869, another 5% error is introduced to U-value measurement due to the temperature variations within the space and difference between air and radiant temperature. Thus the total error in U-value measurement will be:

Total error in U-value = $\sqrt{5^2 + 4^2 + 2^2 + 1^2 + 5^2}$ = 8.4%

### *7.5.2 Operational errors in heat flux measurement in assembly-2*

The total error of heat flux for each panel, following the ISO 9869, will be the square root of the sum of square of the individual errors. For assembly-2 heat flux sensors were not placed in the same surface and thermal conductivity values were determined separately for each heat flux data. Therefore, there is no reduction in random error and the total error can be estimated as follows:

Total error in heat flux = $\sqrt{5^2 + 5^2 + 2^2 + 1^2}$ = 7.4%

In addition to the errors in heat flux measurement, according to the ISO 9869, another 5% error is introduced to U-value measurement due to the temperature variations within the space and difference between air and radiant temperature. Thus, the total error in U-value measurement is:

Total error in U-value = $\sqrt{5^2 + 5^2 + 2^2 + 1^2 + 5^2}$ = 8.9%

## 7.6 In situ Test-1: Hygrothermal performance of hemp-1 insulation in timber frame structures with and without vapour barrier

### *7.6.1 Introduction*

Hygrothermal conditions of hemp-1 insulation installed in wall panels with and without vapour barrier were investigated at full scale in the test building described in subsection 7.3.1. In this study, thermal transmittance, relative humidity, moisture conditions, and mould growth potential of hemp insulations were determined in timber frame wall panels with and without vapour barrier in internal boundary conditions incorporating very high interior relative humidity (90%), normal interior relative humidity (50% to 60%) and low interior relative humidity (less than 40%). These particular relative humidity conditions were selected as they are commonly encountered in buildings.

As part of test-1, the following two tests have been carried out: test-1.1 and test-1.2. Table 7.2 shows the brief details of each setup and duration of each test.

**Table 7.2: The test setup and duration.**

| Tests | Wall panel A | Wall panel B | Inner lining in the panels | Dates of test | Test duration |
|---|---|---|---|---|---|
| Test- 1.1 | Without vapour barrier | With vapour barrier | Gypsum plasterboard (PB) | 21.01.12-06.02.12 | 16 days |
| Test- 1.2 | Without vapour barrier | With vapour barrier | Oriented strained board (OSB) | 11.02.12-27.02.12 | 16 days |

### *7.6.2 Test Materials and test panels*

#### *7.6.2.1 The test materials*

The hemp-1 insulation selected for the test contains about 30% hemp fibres, about 60% wood fibres, and about 10% polyester. The insulation has a density of about 55 Kg/m$^3$ and the manufacturer's declared thermal conductivity at dry condition is 0.038 W/m-K. The insulation is conditioned at 25 ± 2 °C temperature and 50% relative humidity before installation as this level of hygrothermal exposure is very common when insulations are stored in the construction sites. The built-in water content in the insulation due to the conditioning is about 3.3 Kg/m$^3$.

#### *7.6.2.2 The Test panels*

The test panels were assembled as assembly-2, as described in section 7.3. Both Panel A and Panel B contained the hemp-1 insulation.

### *7.6.3 Research Method*

#### *7.6.3.1 Experimental protocol*

The tests were carried out in a timber frame test building, as described in subsection 7.3.1. The eastern wall of the test building contained the wall panel A without vapour barrier and the wall panel B with vapour barrier. The panels were insulated with hemp-1 insulation. The interior temperature in the test building was maintained at 25 ± 3 °C. The relative humidity in the interior was

kept at 90 ± 5% for about two days (48 hours) then decreased to 55 ± 5% for about 4 days (96 hours). The relative humidity values of 50% to 60% were chosen by a number of researchers during in situ tests and these values are also recommended for standard hygric tests, as shown in chapter two and chapter five, respectively. In addition, it can be deduced from the discussion in subsection 2.2.1 of chapter two that the relative humidity value of 55 ± 5% can occur frequently in the interior many of the UK houses. On the other hand, it has also been shown in subsection 2.2.1 of chapter two that 90% relative humidity can occur in and adjacent to the bathroom and kitchen areas. The ratio between the exposure times for relative humidity is based on the Nordtest (2005) method where the drying out time is twice the wetting time during exposure to relative humidity conditions. In addition, another 8 to 10 days' exposure to interior humidity of less than 40% is included in the test to assess the effect of lessening the relative humidity on the drying of the insulation-OSB interfaces. The exterior boundary condition was the winter weather condition on the site during January and February of 2012.

The tests were carried out as comparative tests. Emphasis was given on examining how identical hemp-1 insulation materials in different wall panels performed in response to similar hygrothermal boundary conditions at the same time. The performances were compared in terms of thermal transmittance, equivalent thermal conductivity, moisture conditions in the insulation and likelihood of mould spore germination.

The exterior of the test building was exposed to the external weather conditions during the test period. Temperature and relative humidity of the interior, exterior and the wall panels were logged at every minute during the whole test period.

Wall panels with and without vapour barriers were compared in both test-1.1 and test-1.2. A typical installation sequence of insulation materials and the installation of various sensors in the wall panels are shown in Figures 7.11 to 7.14.

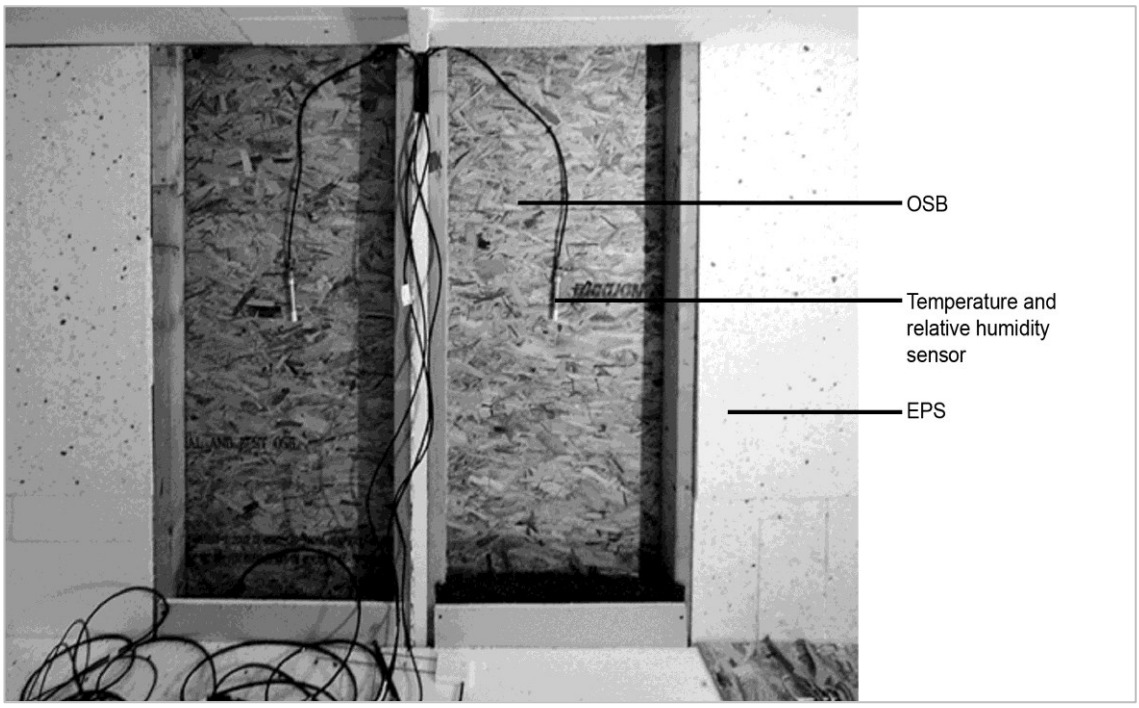


**Figure 7.11: The setup process showing the inner OSB linings and the temperature and relative humidity sensors.**

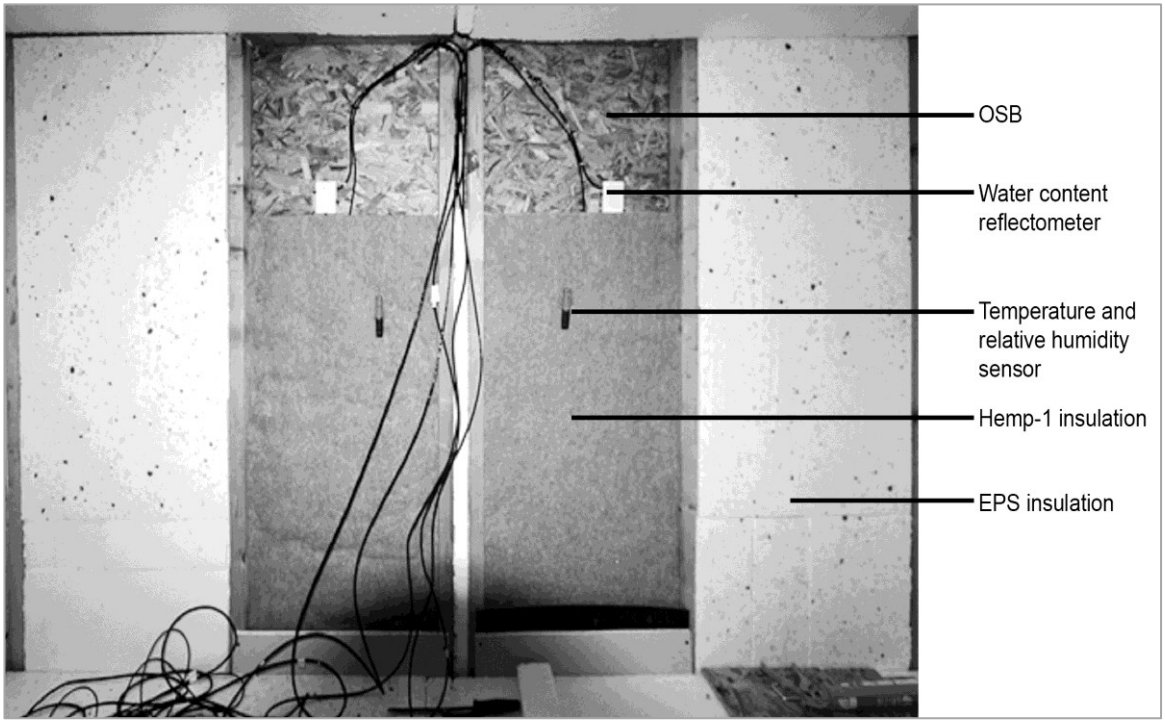


**Figure 7.12: The installation of the inner layer of the insulation with the sensors.**


**Figure 7.13: The installation of the outer layer of the insulation.**

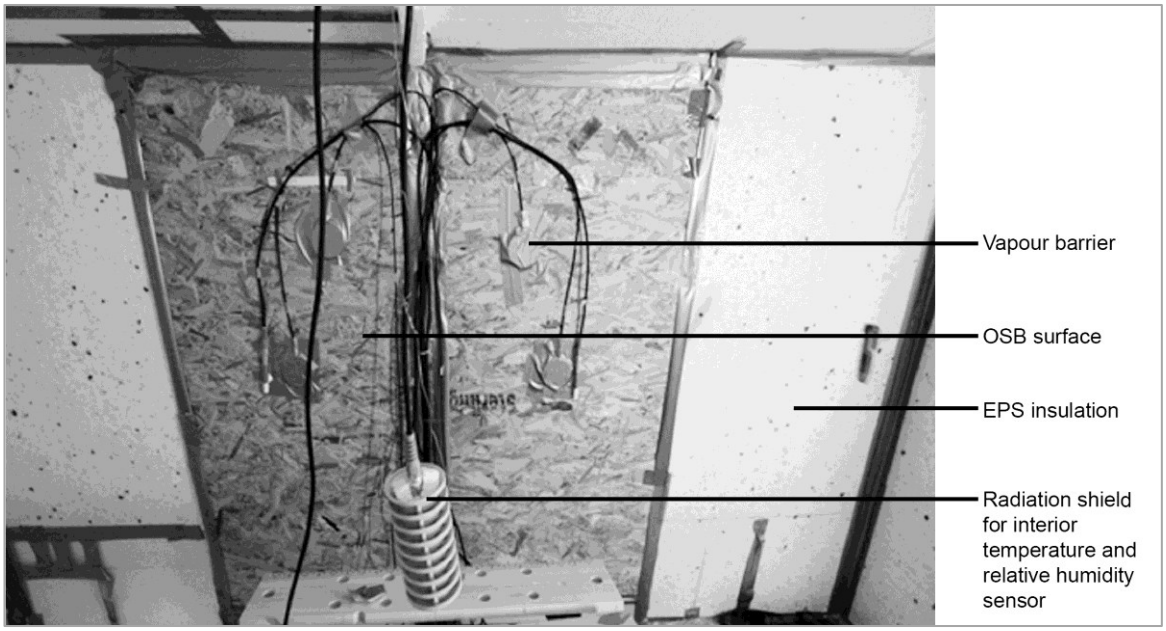


**Figure 7.14: The installation of the surface lining and the sensors.**

### *7.6.3.2 Assessment of thermal performance and mould growth conditions*

The U-values of the insulation materials can be calculated from the recorded experimental data using the average method according to ISO 9869 using equation 7.1 and λequi value can be calculated using equation 7.2, as described in subsection 7.4.1. Mould growth condition is assessed in terms of parametric studies. For parametric studies, the temperature-relative humidity

relationships are plotted from the collected data and compared with the conditions set in Sedlbauer's germination isopleths, as described in section 7.4.2.

### *7.6.4 Results of test-1.1 and test-1.2*

#### *7.6.4.1 Temperature and relative humidity*

A thermographic snapshot of the temperature distribution on the OSB surfaces of panel A and Panel B is shown in Figure 7.15. The infrared image shows that the temperature distribution in the two panels follows a similar pattern with the upper part having about 0.5 °C higher temperature than the lower part. The interior and exterior temperature and relative humidity conditions for test-1 and test-2, as running averages of every one hour for 16 days, are shown in Figure 7.16 and 7.17, respectively.

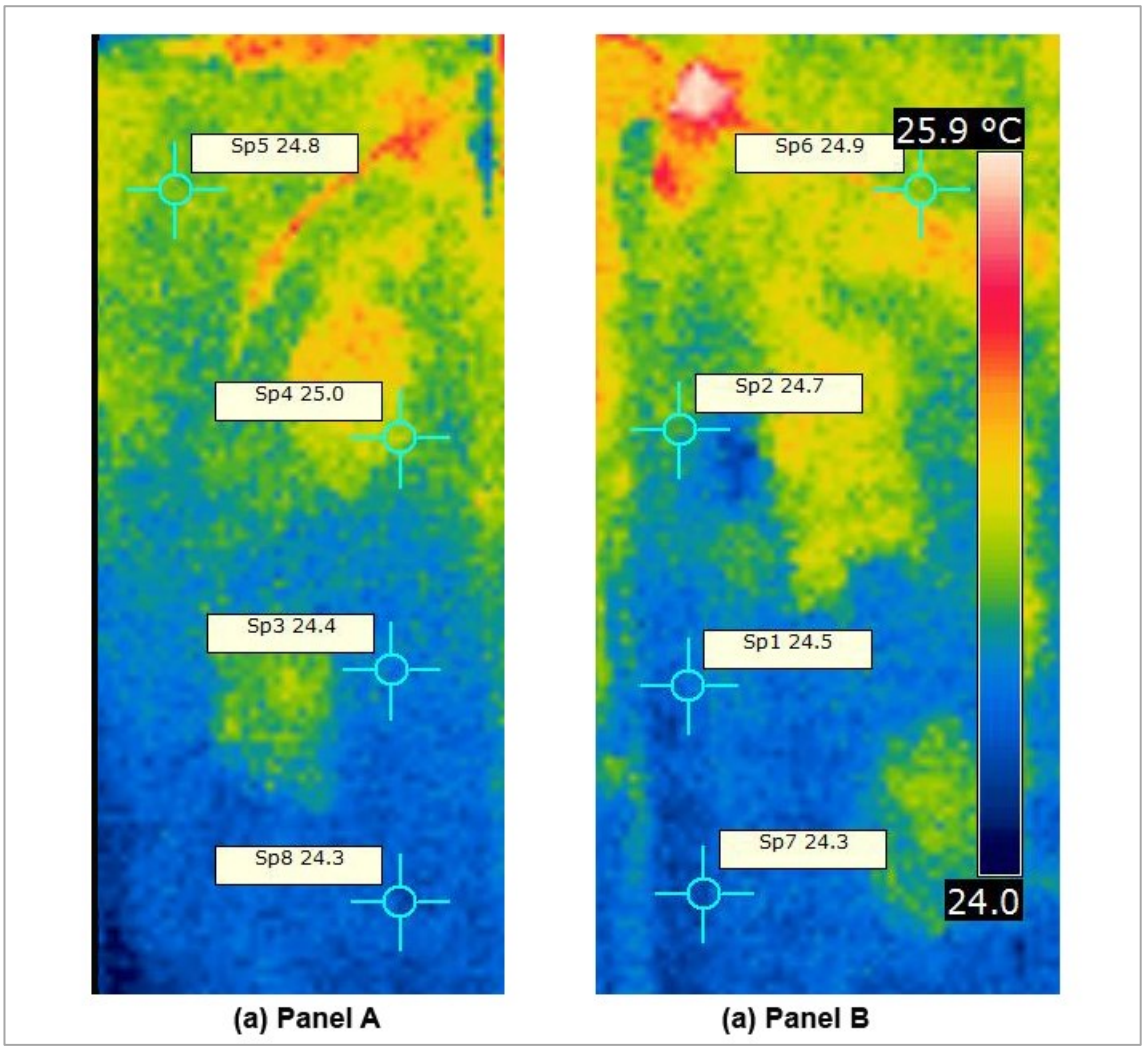


**Figure 7.15: Surface temperatures in OSB inner lining, (a) panel A and (b) panel B.**

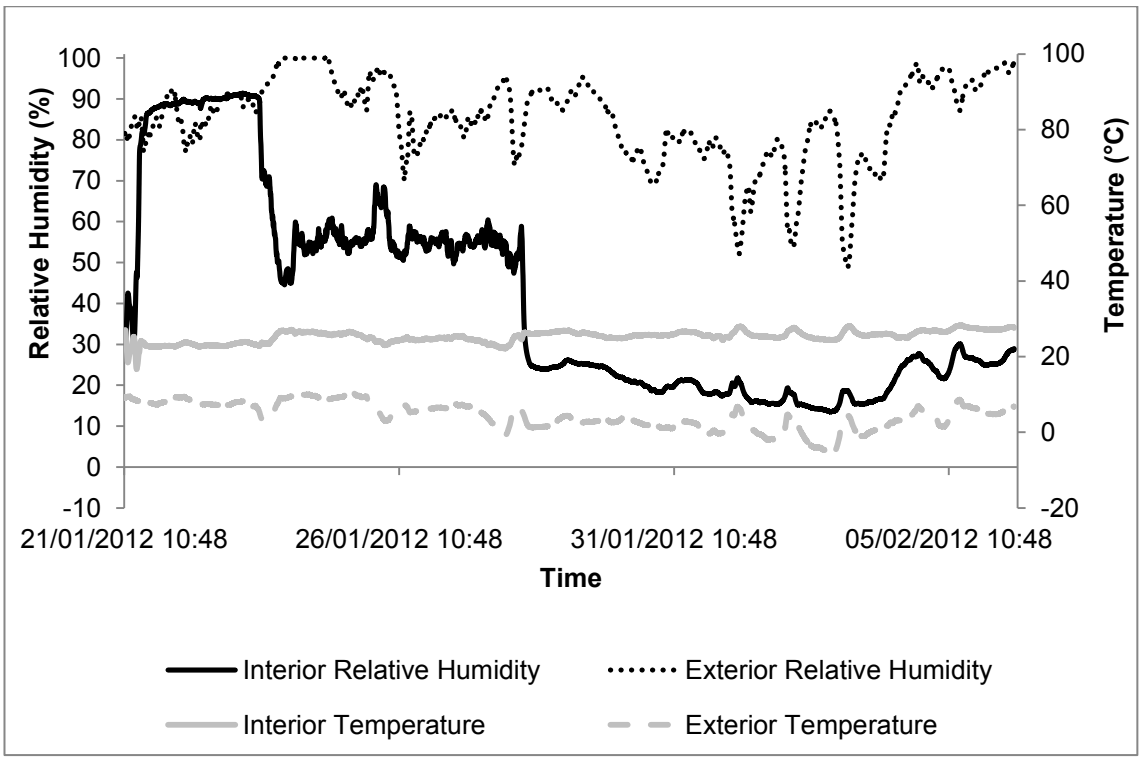


**Figure 7.16: Temperature and relative humidity during test-1.1.**

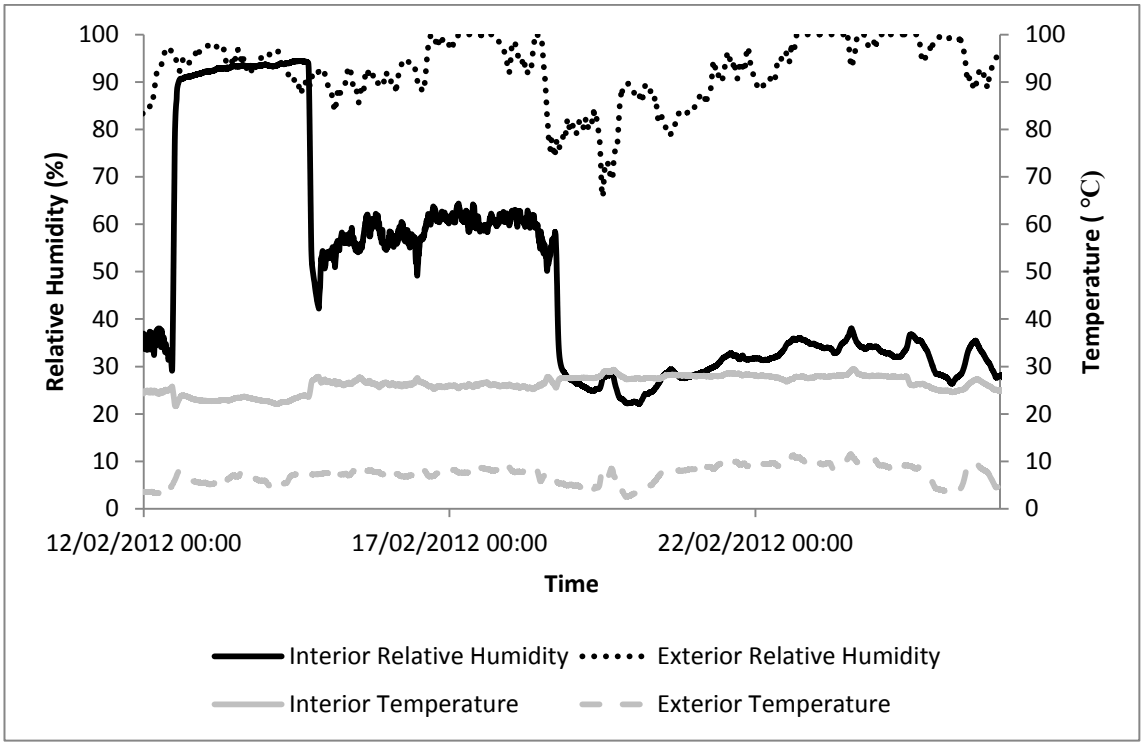


**Figure 7.17: Temperature and relative humidity during test-1.2.**

### *7.6.4.2 Heat flux, U-value and thermal conductivity*

Figures 7.18 and 7.19 show the temperature differences between internal and external ambient temperature of the test house and the heat flux through the

construction panels, with and without vapour barrier, during test-1.1 and test-1.2, respectively.

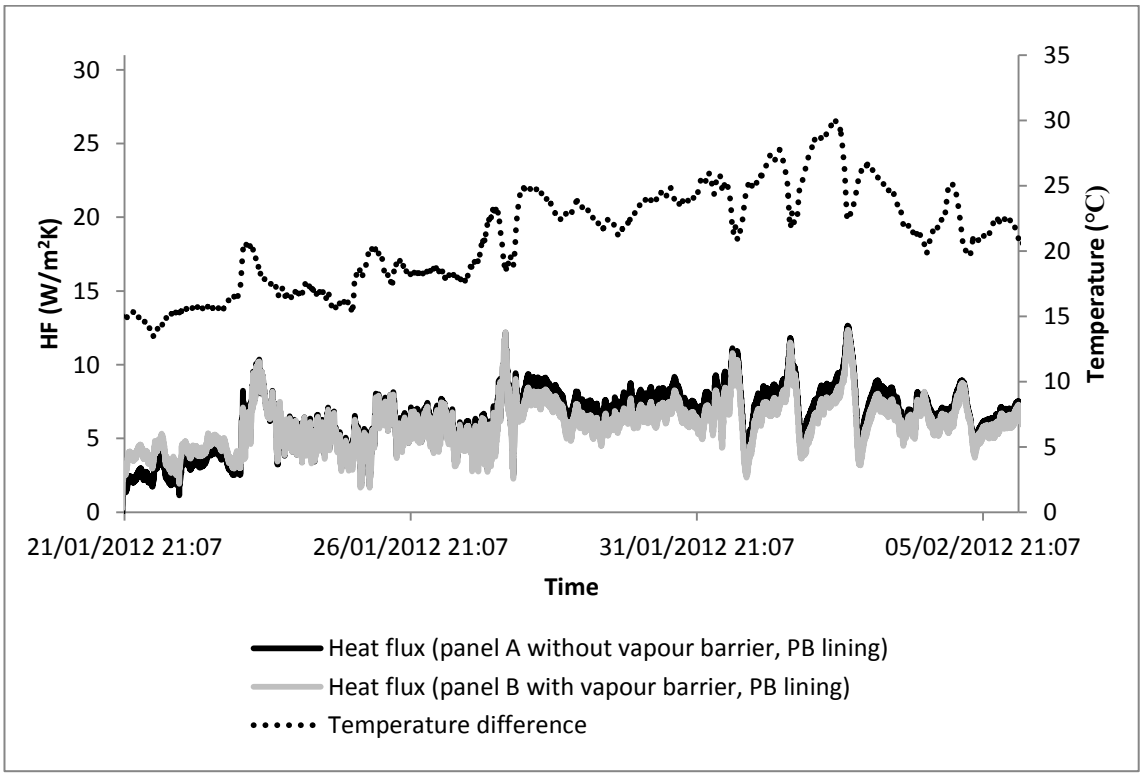


**Figure 7.18: Heat flux in panels with plasterboard lining during test-1.1.**

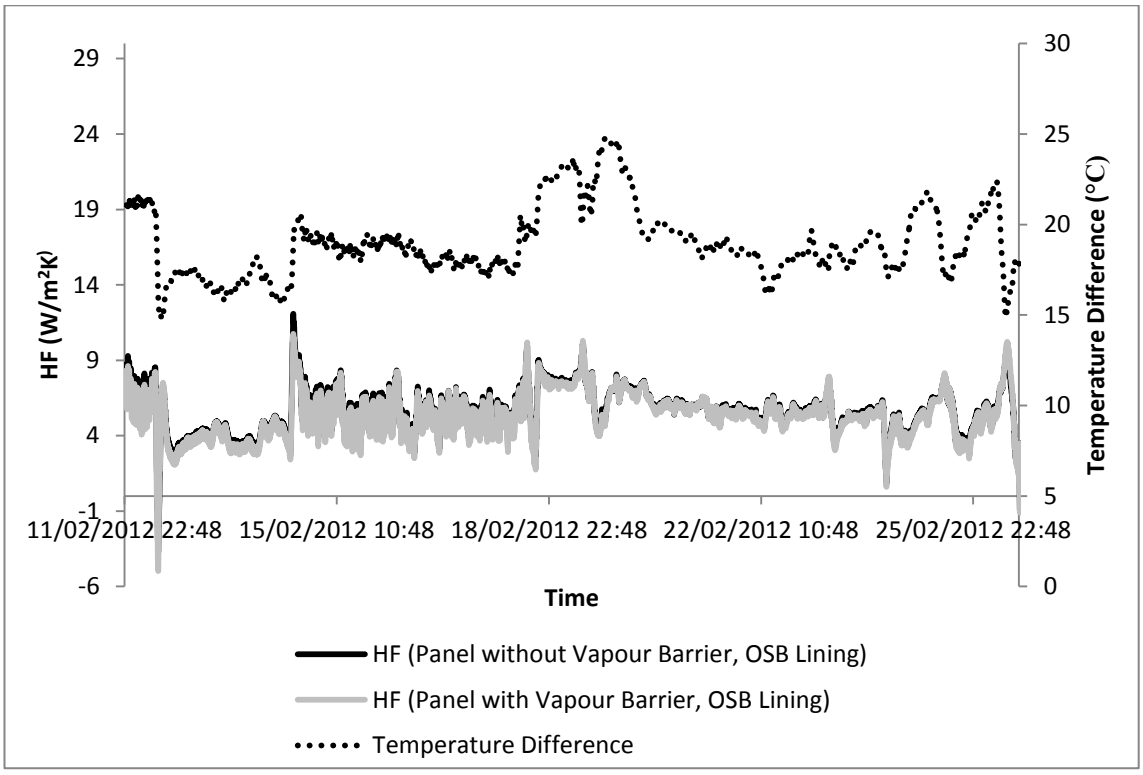


**Figure 7.19: Heat flux in panels with plasterboard lining during test-1.2.**

The U-value of the wall panels and λequi value of hemp insulations with and without vapour barrier are shown in the Table 7.3.

**Table 7.3: U-value of the wall panel A and panel B and equivalent thermal conductivity of hemp-1 insulation.**

| | U-value (panel A without vapour barrier), ($W/m^2K$) | U-value (panel B with vapour barrier), ($W/m^2K$) | λequi hemp-1 (panel A without vapour barrier), (W/mK) | λequi hemp-1 (panel B with vapour barrier), (W/mk |
|---|---|---|---|---|
| Wall panels with PB Inner Lining (Test-1.1) | 0.295 | 0.281 | 0.0374 | 0.0352 |
| Wall panels with OSB Inner Lining (Test-1.2) | 0.292 | 0.281 | 0.0372 | 0.0355 |

### *7.6.4.3 Hygric conditions*

Figures 7.20 and 7.21 show the relative humidity in the (hemp-1)-OSB interfaces in wall panels with PB and OSB inner linings, respectively. In all the cases, the relative humidity in the insulation-OSB interface is more than 85% during most of the time.

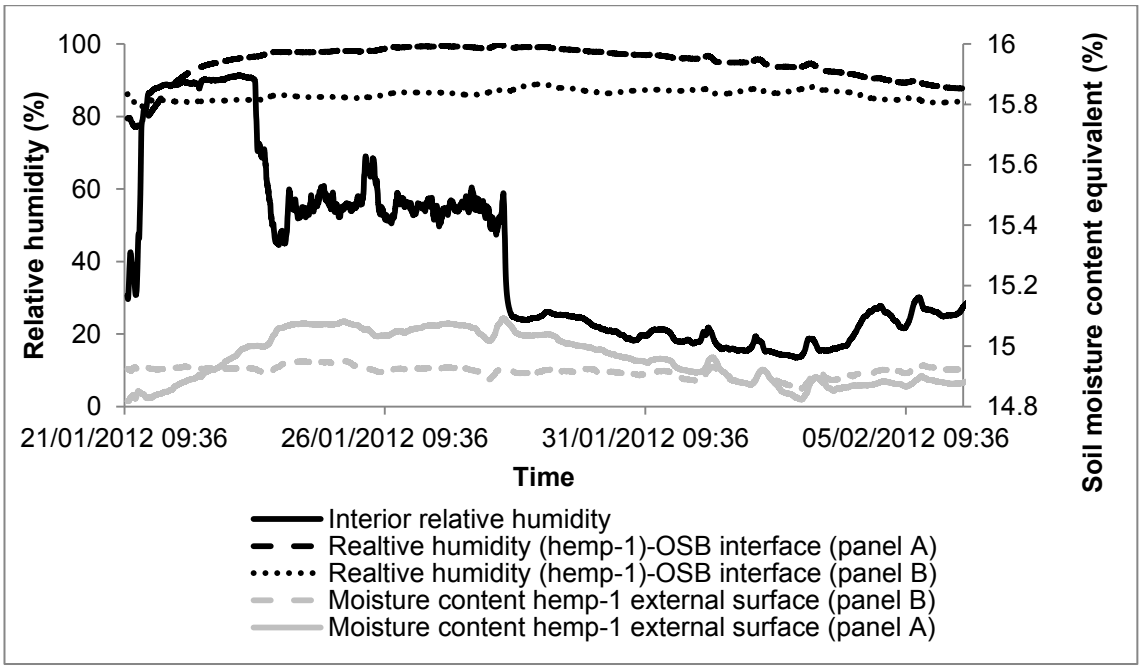


**Figure 7.20: Relative humidity and soil moisture content equivalent in hemp-PB interfaces and interior relative humidity during test-1.1.**

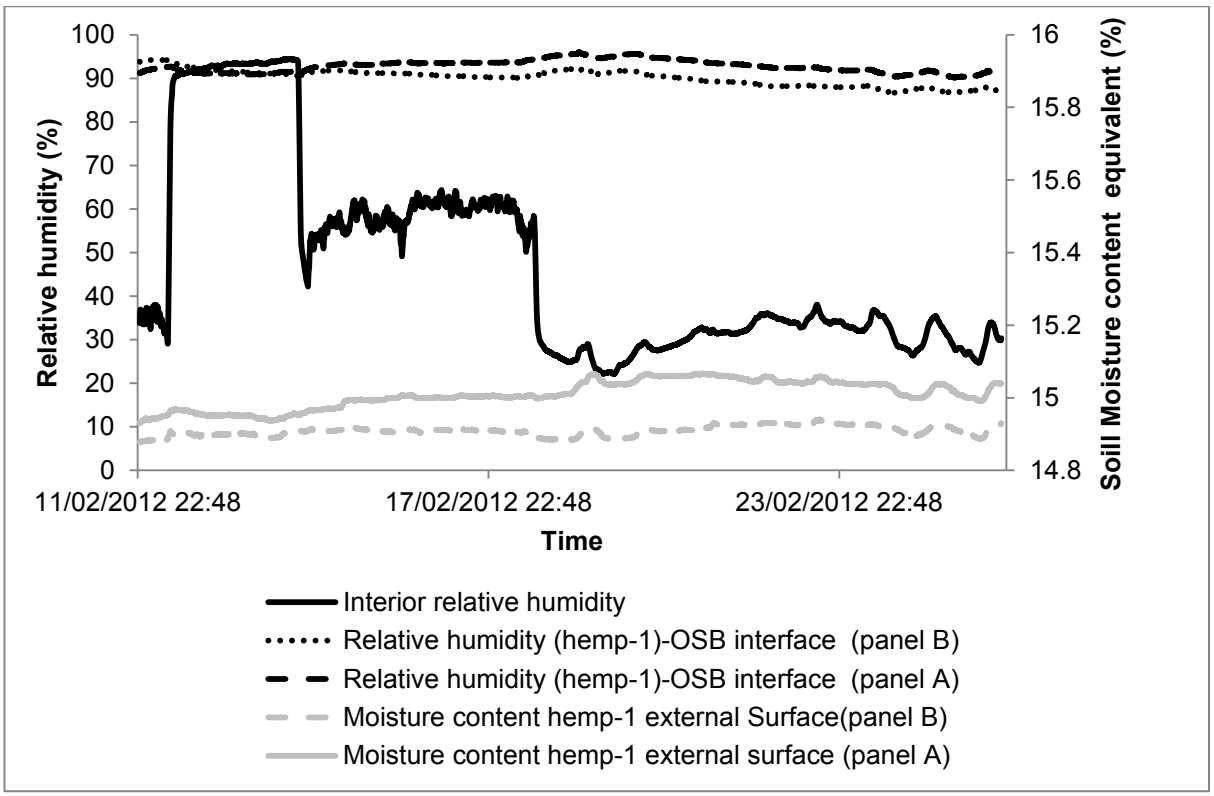


**Figure 7.21: Relative humidity and soil moisture content equivalent in hemp-PB interfaces and interior relative humidity during test-1.2.**

### *7.6.5 Discussion*

#### *7.6.5.1 Thermal properties*

One of the objectives of the study was to determine in situ U-value of the wall panels insulated with fibrous hemp-1 and to assess the difference in the U-value when vapour barrier is used and when it is not used. At the same time, it is possible to compare the equivalent thermal conductivity (λequi) values of the insulation materials incorporated in panel A and panel B. The equivalent thermal conductivity values of hemp-1 insulation at a range of relative humidity and average relative humidity conditions determined during test-1.1 and test-1.2 are shown in Figures 7.22 and 7.23, respectively. Figure 7.24 focuses on average equivalent thermal conductivity of hemp-1 insulation during test-1.1 and test-1.2.

During test-1.1 in winter with internal lining of PB, U-value of the vapour open panel is 5% higher than that of the panel with vapour barrier, λequi value of hemp-1 insulation is 6.3% higher in the vapour open panel than in the panel with vapour barrier. During test-1.2 in winter with internal lining of OSB, U-value

of the vapour open panel is 3.9% higher than the panel with vapour barrier, λequi value of hemp-1 insulation is 4.8 % higher in the vapour open panel than in the panel with vapour barrier.

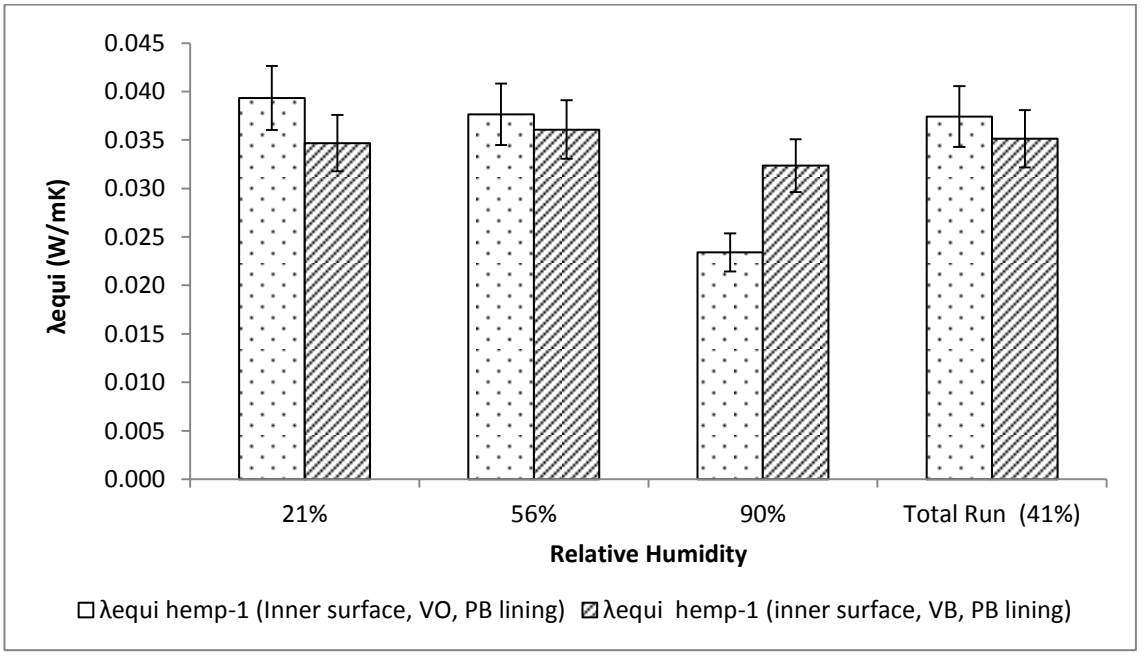


**Figure 7.22: Equivalent thermal conductivity values (λequi) with error bar during test-1.1.**

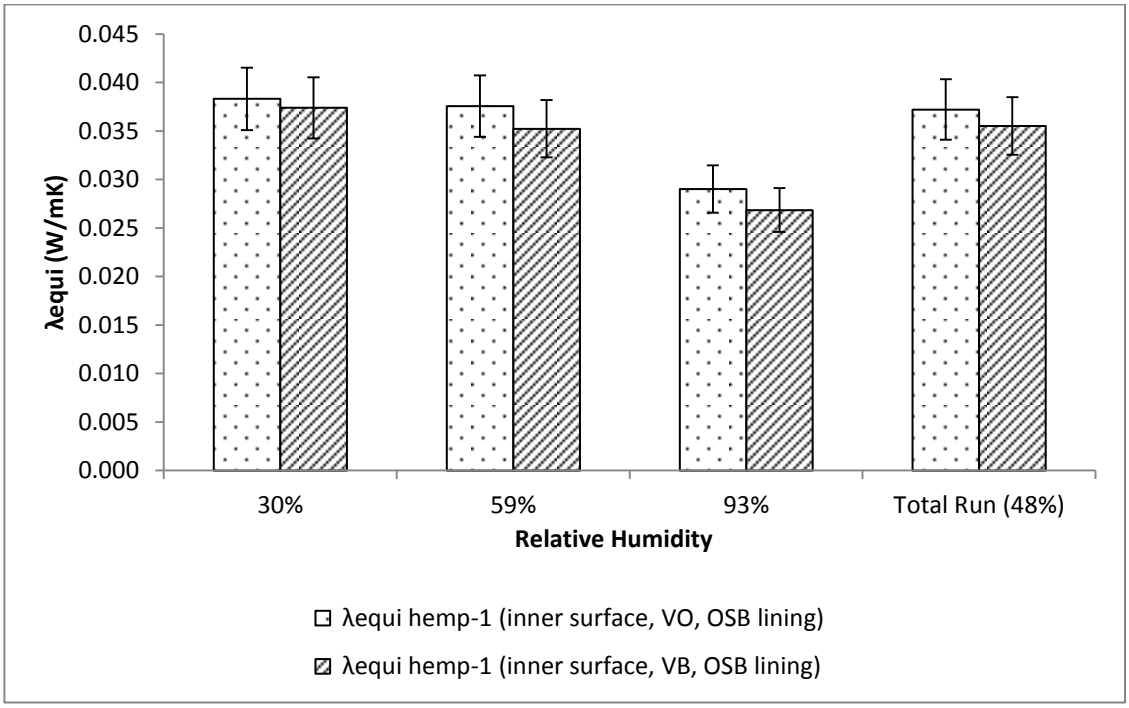


**Figure 7.23: Equivalent thermal conductivity values (λequi) with error bar during test-1.2.**

The variation in average U-value for panels with and without vapour barrier in the abovementioned cases is 2.8% which is not significant in terms of its effect on heat loss. The significance seems further lessened when the 8.4% error, as shown in subsection 7.5.1, in the U-value measurement is considered.

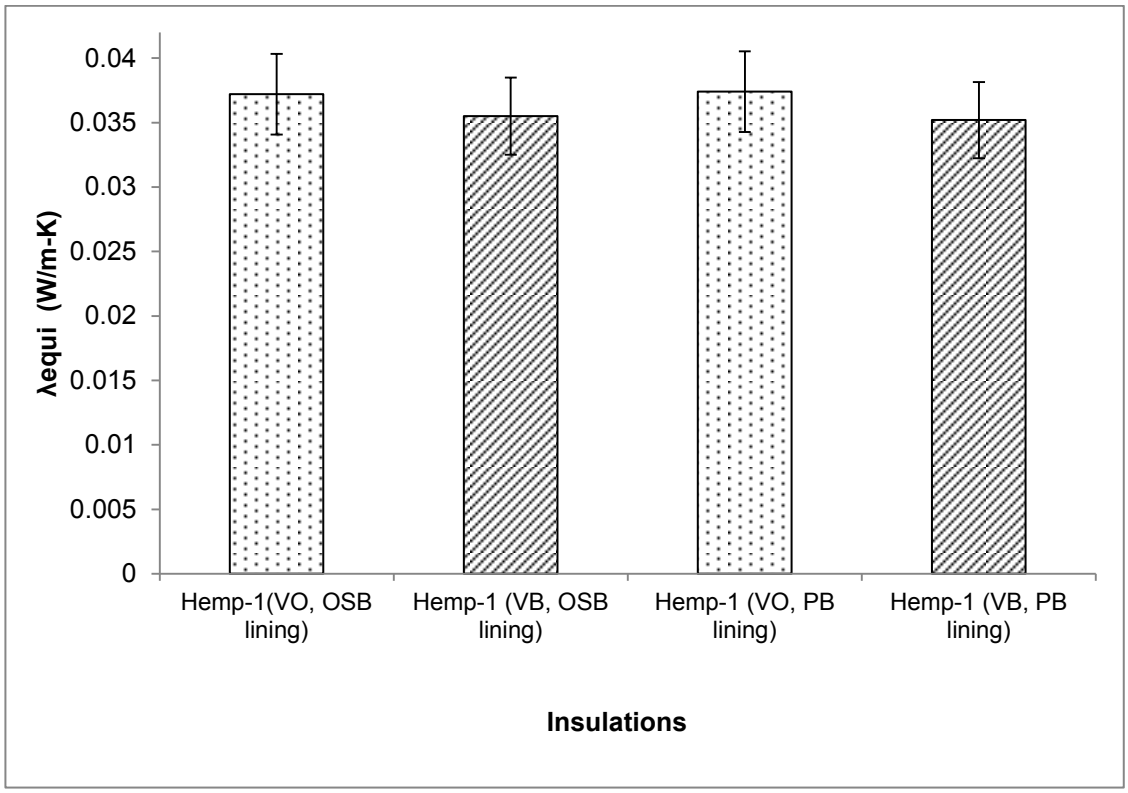


**Figure 7.24: Average equivalent thermal conductivity values (λequi) with error bar during test-1.1 and test-1.2.**

The manufacturer's declared thermal conductivity of hemp-1 insulation is 0.038 W/m-K. The measured λequi values are close to the declared thermal conductivity value in all the cases, as shown in Figure 7.24. These findings reflect Nicolajsen's (2005) findings on cellulose insulation where there was negligible difference in U-value in wall panels with and without vapour retarder.

#### *7.6.5.2 Relative humidity and prediction of mould growth*

Figures 7.25 to 7.27 present the temperature and relative humidity conditions in the insulation-OSB interfaces of panel A and panel B in conjunction with Sedlbauer's isopleths for substrate class1 during test-1.1 and test-1.2.

In terms of LIM I isopleth, Figures 7.25 and 7.27 show that the hygrothermal conditions in the insulation-OSB interface above 5 °C temperature (Sedlbauer's germination isopleths have not included temperatures below 5 °C) in both of the

panel A and panel B during test-1.1 and test-1.2 are above the LIM I isopleth. This implies that, in terms of LIM I isopleth the insulation is susceptible to mould spore germination in both panel A and panel B.

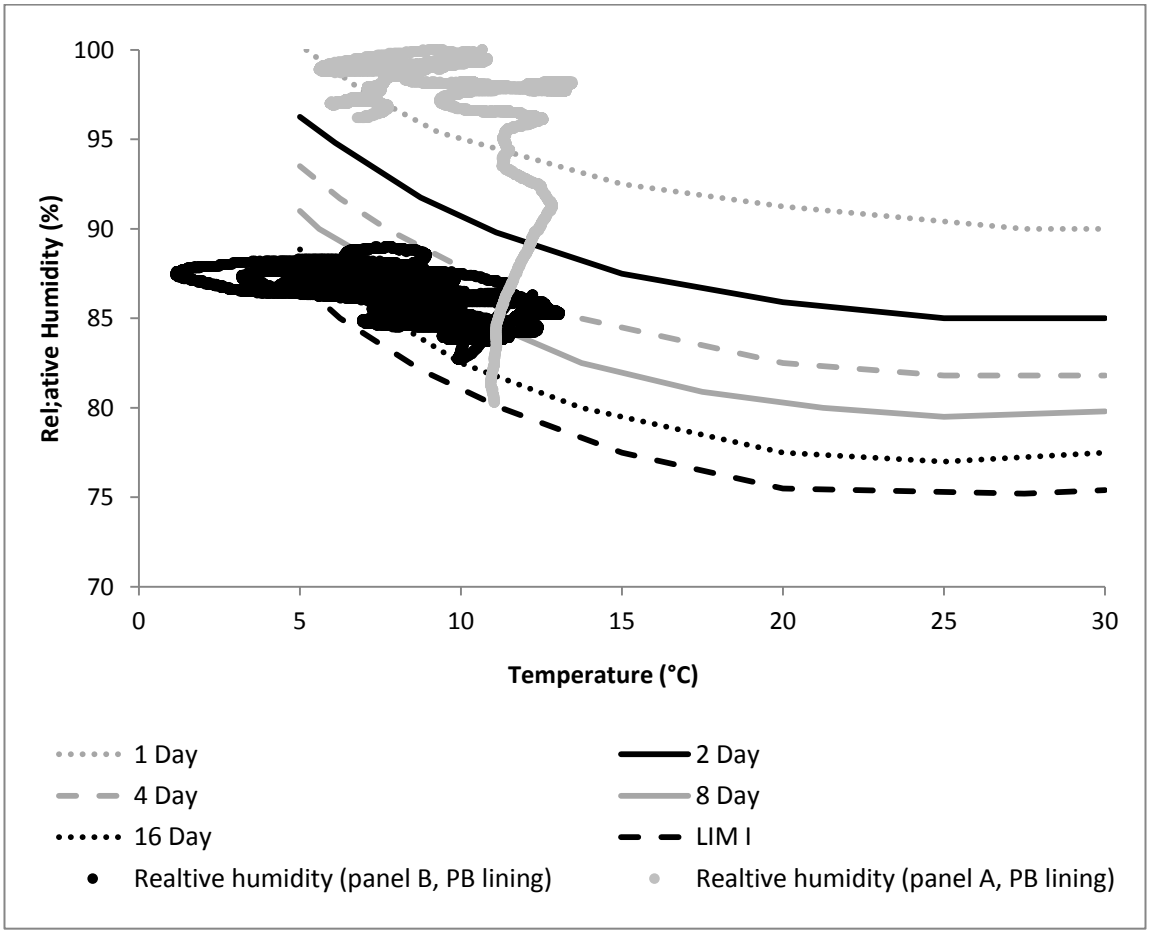


**Figure 7.25: (Hemp-1)-OSB interface conditions against the Sedlbauer's isopleth during the test-1.1.**

From Figure 7.25 it is also apparent that hygrothermal conditions (the plot of temperature versus relative humidity) in panel A (without vapour barrier) is mostly concentrated on the upper part of the graph during test-1.1. This is further analysed and presented in the Figure 7.26. Figure 7.26 shows the continuous 11 days' hygrothermal conditions in (hemp-1)-OSB interface in the panel A (without vapour barrier) and with PB inner lining during test-1.1. Based on the Sedlbauer's germination isopleth for 8-day exposure, germination of mould spores seems plausible as the hygrothermal condition exceeded 8 days.

Figure 7.27 shows the hygrothermal conditions in the insulation-OSB interfaces during test-1.2 in panel A (without vapour barrier) and panel B (with vapour barrier). Hygrothermal conditions in the insulation-OSB interface in panel A is

always over the 4-day isopleth and the hygrothermal conditions in insulation-OSB interface in panel B is most of the time over the 8-day isopleth. The duration of the test was 16 days, exceeding 4 and 8 days, respectively. Hence, hygrothermal conditions in both cases are favourable to mould spore germination. However, the mould spore germination in the insulation–OSB interface of panel A is predicted to occur earlier than in the insulation–OSB interface of panel B since the hygrtothermal conditions in the insulation–OSB interface of panel A were over the 2-day isopleth in 92% of the exposure time (Figure 7.25) whereas the hygrothermal conditions in the insulation–OSB interface of panel B were always under the 2-day isopleth during test 1.1.

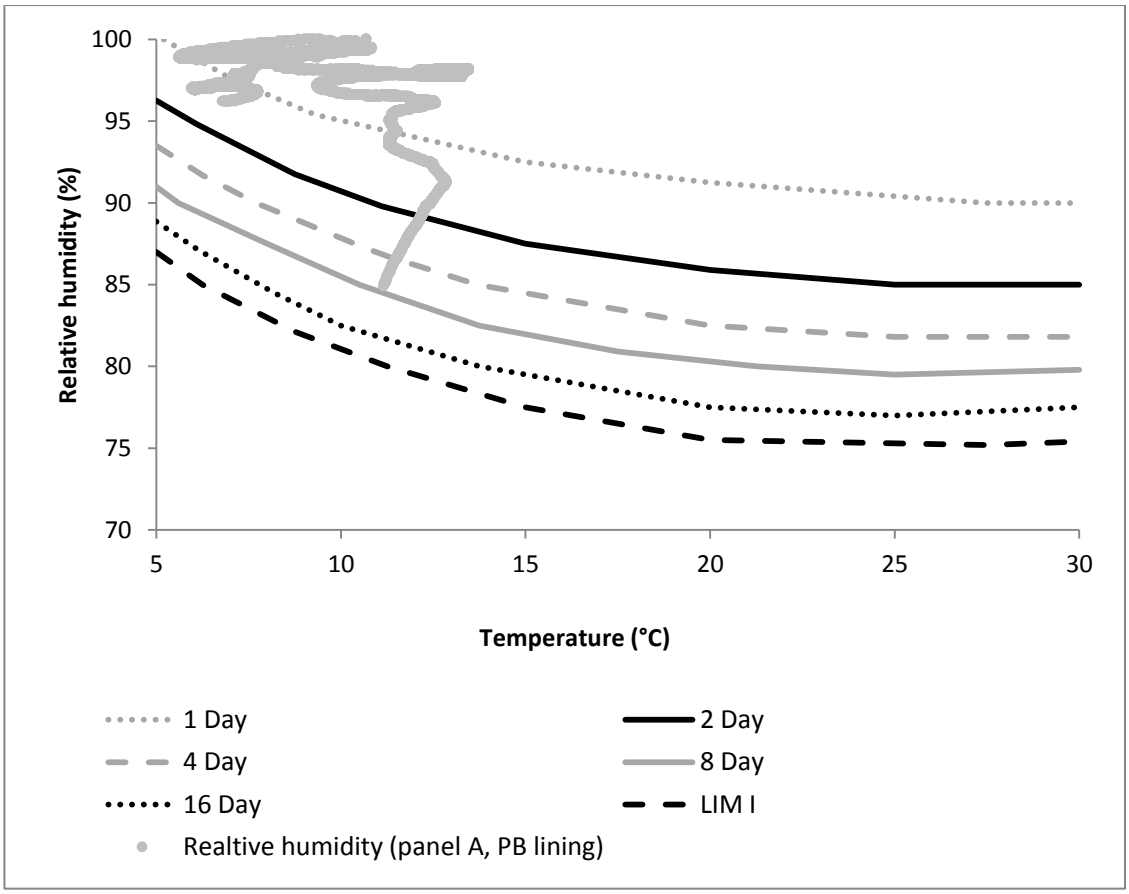


**Figure 7.26: 11 days' conditions of (hemp-1)-OSB interface condition against Sedlbauer's 8-day isopleth line during test-1.1.**

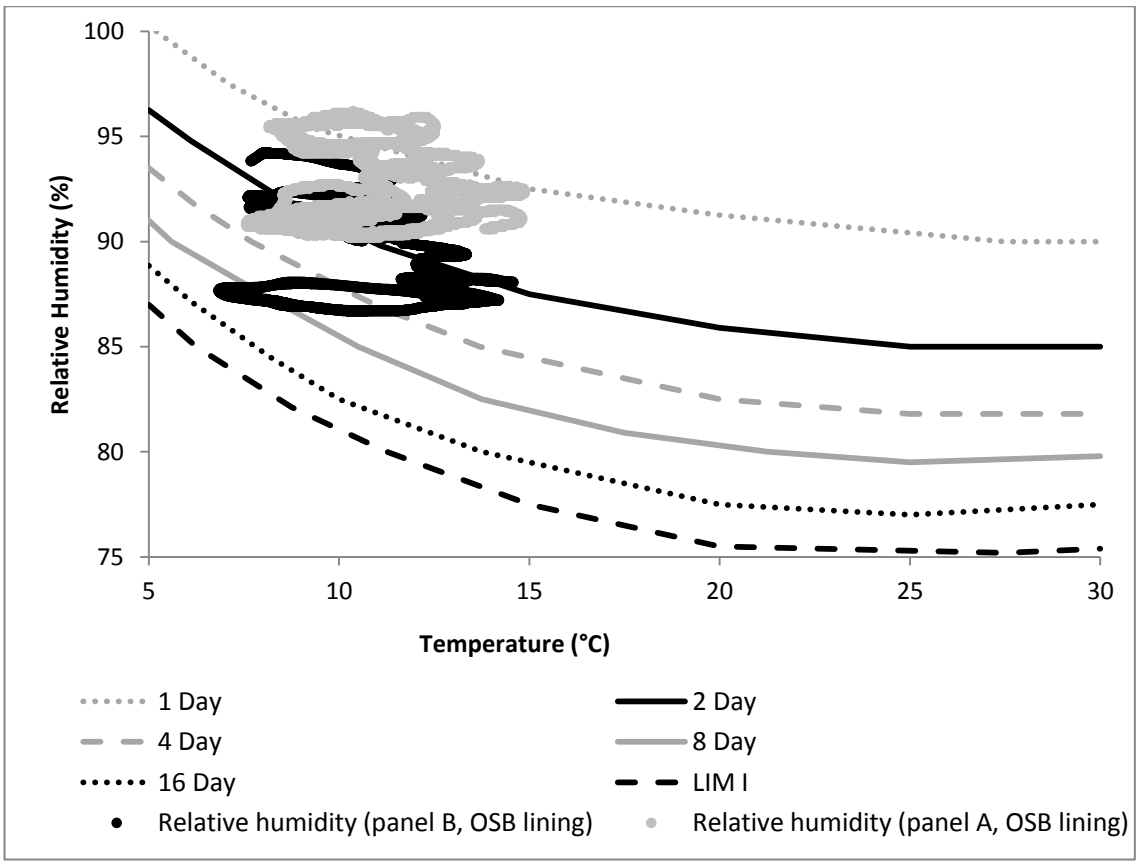


**Figure 7.27: (Hemp-1)-OSB interface condition against Sedlbauer's isopleth during test-1.2.**

In the panel A (without vapour barrier) during test-1.2, relative humidity in the insulation-OSB interface increased to 99%, which is a near saturation condition. However, condensation occurs when the adjacent surface temperature is equal to or is lower than the dew point temperature of the moist air. The wall panels were reasonably airtight and therefore moisture movement inside the insulation may have been caused by vapour diffusion and temperature gradient along the wall sections rather than by any convective flow due to leakage of room air to the external OSB wind barrier. On the other hand, if condensation occurs at a rate lower than the water absorption coefficients of either the insulation or the OSB, the water will be absorbed by the insulation or the OSB. When the insulation samples were dismantled, on visual observation, no trace of wetness was found on the insulation or on the OSB surface. Either no condensation occurred or the condensed water was absorbed by the insulation or the OSB.

## 7.7 In situ Test-2: Hygrothermal performances of two hemp insulations in a vapour open timber frame structure

### *7.7.1 Introduction*

In this test hygrothermal performances of two hemp insulation materials were compared in a vapour open timber frame structure. Hemp-1 contains 30% hemp fibre and hemp-2 contains 85% hemp fibre. These two insulation materials represent two opposite extremes of composite hemp insulation materials in terms of the amount of hemp content included in the insulation matrix. Therefore, it can be argued that comparison of their hygrothermal performance will provide a representative view of the boundary of hygrothermal performance potential of the hemp insulation materials available in the UK market. The properties of hemp-1 and hemp-2 insulation materials are provided in Table 4.1 of chapter four. Table 7.4 shows the brief detail of setup and duration of test-2.

**Table 7.4: The setup and duration of test-2.**

| Tests | Wall panel A | Wall panel B | Inner lining in the panels | Dates of test | Test duration |
|---|---|---|---|---|---|
| Test-2 | Hemp-1 | Hemp-2 | Gypsum plaster board (PB) | 18.05.12-31.05.12 | 12 days |

For test-2, the panels are organised as assembly-2, as shown in figure 7.9. The difference of test-2 from test-1 in terms of measuring heat flux is the positioning of the heat flux sensors. In the test-1, both heat flux sensors were installed on the inner surface of the wall panels. However, in test-2, a further assumption has been made and tested. It is assumed that since vapour barriers are not used in the wall panels, there will be increased vapour diffusion through the wall panels, especially during high internal moisture load. This diffusion of vapour will increase the heat flux by enthalpy flow and phase change through the wall panels. Increased moisture content in the insulation by adsorption may also increase heat flux through the panels. It is assumed that if a heat flux sensor is installed on the interface of the exterior-facing surface of the insulation and the OSB, it will register the added heat flux caused by phase change and enthalpy flow, which may not be registered by the heat flux sensor installed on the inner surface. As a result, there will be a variation in the measurement of the

equivalent thermal conductivity of the insulation materials based on the heat flux data. Figure 7.28 shows the vertical section of the wall panels and the potential heat flux through the wall panels.

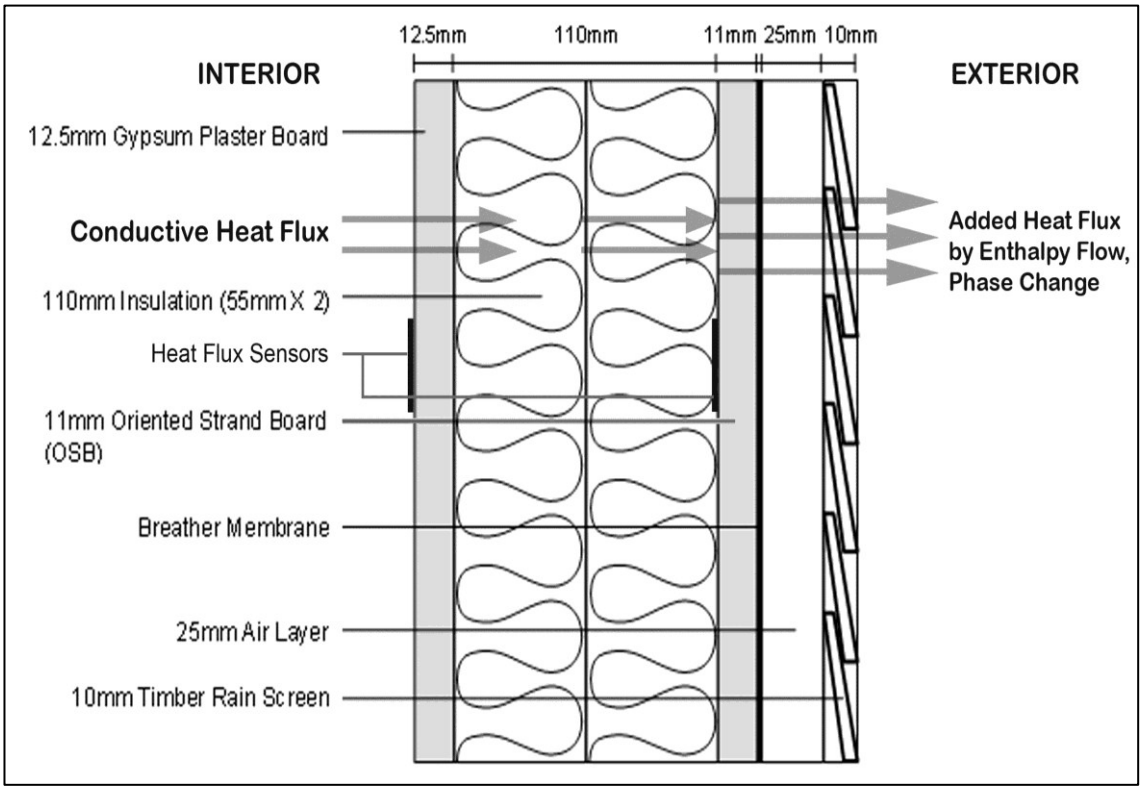


**Figure 7.28: Vertical cross section of the wall panel.**

### *7.7.2 Test materials and experimental setup*

#### *7.7.2.1 Test materials*

Two different makes of semi-rigid composite hemp insulation batts, hemp-1 and hemp-2, have been sourced from the UK market based on their constituent materials and are shown in Figure 7.29. The properties of hemp-1 and hemp-2 are provided in table 4.1 of chapter four.

Hemp-1 and hemp-2 insulations are conditioned at 25 ± 2 °C temperature and 50% relative humidity before installation. This level of hygrothermal exposure is very common when insulations are stored in the construction site. The adsorbed water contents in hemp-1 and hemp-2 for this exposure are about 3.3 Kg/m$^3$ and about 3.5 Kg/m$^3$, respectively. The values of water content were determined from Figures 4.6 and 4.7 of chapter four.


**Figure 7.29: Hemp-1 and hemp-2 insulation materials.**

#### *7.7.2.2 The test panels*

The 600 mm X 1800 mm test wall panels (panel A and panel B) were installed on the eastern wall as assembly-2, as shown in figure 7.9. Wall panel A contained the hemp-1 insulation and wall panel B contained the hemp-2 insulation.

### *7.7.3 Research method*

#### *7.7.3.1 Experimental protocol*

The test-2 attempted to examine how hemp-1 and hemp-2 insulation materials, installed in wall panel A and wall panel B, respectively, performed in response to similar hygrothermal boundary conditions at the same time. The performances are compared in terms of thermal transmittance, equivalent thermal conductivity and likelihood of mould growth.

The interior temperature in the test building was maintained at 25 ± 3 °C. The relative humidity in the interior was kept at 90 ± 5% for two days (48 hours) then changed to 55 ± 5% for 6 days (144 hours) and 40 ± 5% for two days (48 hours). The exterior of the test building is exposed to the external weather conditions during May, 2012. Temperature and relative humidity in the interior, exterior and of the panels were logged at every minute during the testing period.

#### *7.7.3.2 Assessment of thermal performance and mould growth condition*

The thermal transmittance (U-value) was calculated from the recorded experimental data using the average method according to ISO 9869 using equation 7.1 and the equivalent thermal conductivity (λequi) value was calculated using equation 7.2. Mould growth condition was assessed in terms of parametric studies. For parametric studies, the temperature-relative humidity relationships are plotted from the collected data and compared with the conditions set in Sedlbauer's germination isopleths, as described in subsection 7.4.2.

### *7.7.4 Results of the in situ experiment*

#### *7.7.4.1 Temperature and relative humidity*

The internal and external temperature and relative humidity conditions for the test-2, as running averages of every one hour for 12 days, are shown in Figure 7.30.

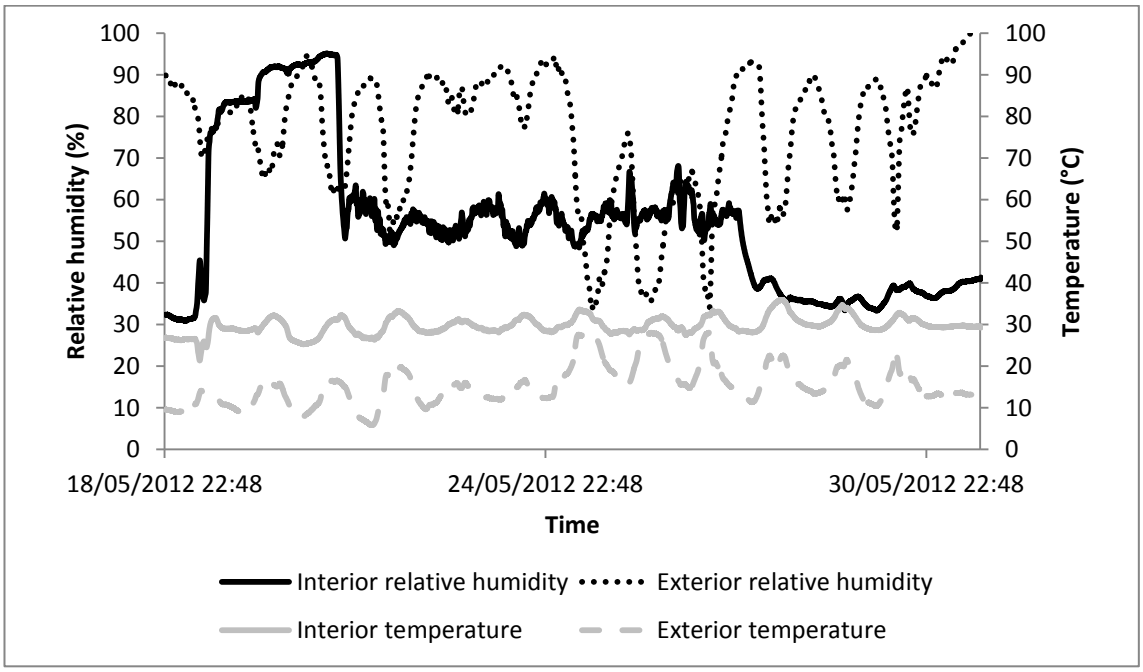


**Figure 7.30: The temperature and relative humidity boundary conditions during the experiment.**

#### *7.7.4.2 Heat Flux, U-value and equivalent thermal conductivity*

Figures 7.31 and 7.32 show the heat flux and temperature differences (between internal and external ambient temperature) in the construction panels with hemp-1 and hemp-2 insulation materials.

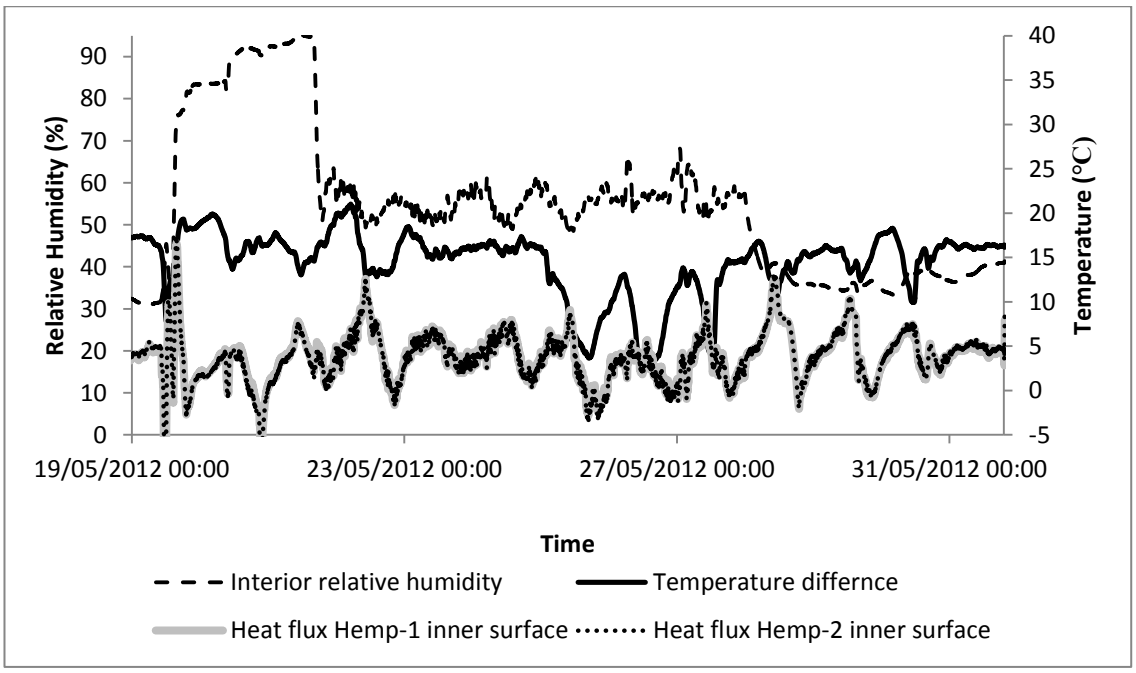


**Figure 7.31: Heat Flux data gathered from the surface of the plasterboards during test-2.**

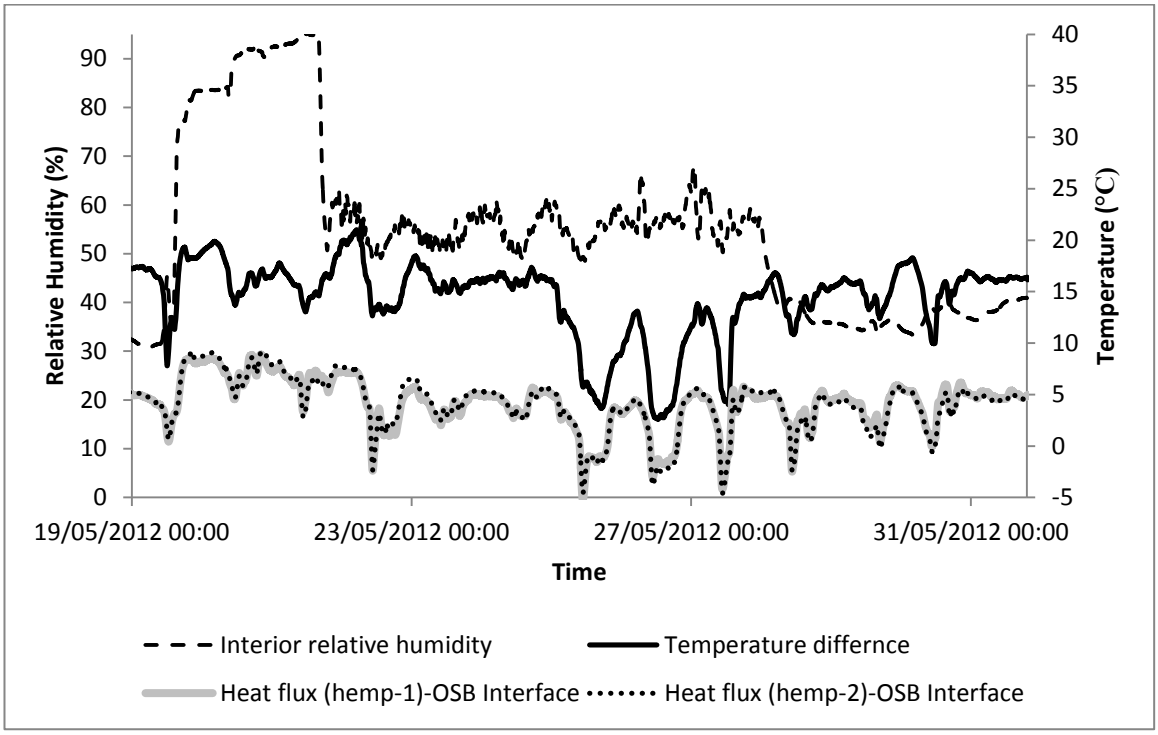


**Figure 7.32: Heat flux data gathered from insulation-OSB interfaces during test-2.**

The U-values of the wall panels A and B and λequi values of hemp-1 and hemp-2 insulation materials are shown in the Table 7.5.

**Table 7.5: U-value of the wall panel A and panel B and equivalent thermal conductivity of the hemp insulation measured according to the ISO 9869.**

| | U-value Panel A, ($W/m^2K$) | U-value Panel B, ($W/m^2K$) | λequi hemp-1, (W/mK) | λequi hemp-2, (W/mK) |
|---|---|---|---|---|
| Using heat flux sensors on the plasterboard inner surface | 0.263 | 0.261 | 0.033 | 0.032 |
| Using heat f lux sensors on the insulation-osb interface | 0.288 | 0.288 | 0.036 | 0.036 |

### *7.7.4.3 Hygric conditions*

Figure 7.33 shows the relative humidity in the insultion-OSB interfaces in wall panels A and B. After initial 24 hours, the relative humidity values in the insulation-OSB interfaces are always more than 75%.

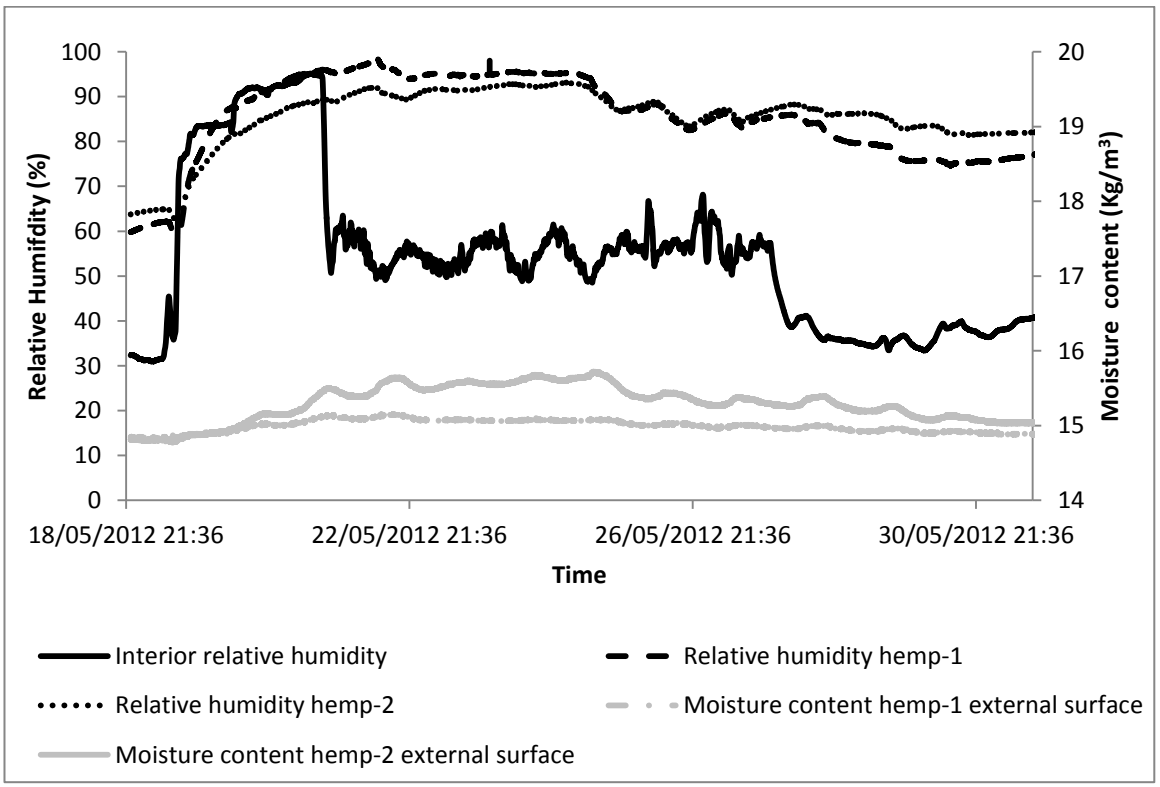


**Figure 7.33: Relative humidity and moisture content in the insulation-OSB interface during test-2.**

### *7.7.5 Discussion*

#### *7.7.5.1 Thermal properties*

In terms of thermal properties, this particular study focused on assessing the difference in thermal conductivity values of two significantly different hemp insulation materials in vapour open wall panels. The study also focused on assessing the variations of equivalent thermal conductivity values based on the placement of heat flux sensors. It was assumed that when there was very high relative humidity in the interior, equivalent thermal conductivity values would be higher if the heat flux values were derived from the heat flux sensors installed in the hemp-OSB interfaces than when the heat flux values were derived from the heat flux sensor installed on the plasterboard inner surfaces.

It was found that the above assumption was correct. Figure 7.34 shows the equivalent thermal conductivity values of hemp-1 and hemp-2 insulation materials at different relative humidity ranges. In terms of thermal conductivity values derived from the total period of the experiment at an average internal relative humidity of 55%, thermal conductivity value derived from the (hemp-1)-OSB interface is higher than that derived from hemp-1 inner surface by 11.6 % and thermal conductivity value derived from the (hemp-2)-OSB interface is higher than that derived from hemp-2 inner surface by 12.9 %.

In terms of thermal conductivity values derived during the average interior relative humidity of 37%, the thermal conductivity value derived from hemp-1 inner surface is higher than that derived from (hemp-1)-OSB interface by 2.6 % and the thermal conductivity value derived from the hemp-2 inner surface is higher than that derived from (hemp-2)-OSB interface by 24.1 %.

In terms of equivalent thermal conductivity values derived during the average interior relative humidity of 56%, the equivalent thermal conductivity value derived from the hemp-1 inner surface is higher than that derived from (hemp-1)-OSB interface by 17.1 % and equivalent thermal conductivity value derived from the hemp-2 inner surface is higher than that derived from (hemp-2)-OSB interface by 6.6 %.

In terms of thermal conductivity values derived during the average interior relative humidity of 92%, the thermal conductivity value derived from the

(hemp-1)-OSB interface is higher than that derived from hemp-1 inner surface by 288.1 % and the thermal conductivity value derived from the (hemp-2)-OSB interface is higher than that derived from hemp-2 inner surface by 436.8 %.

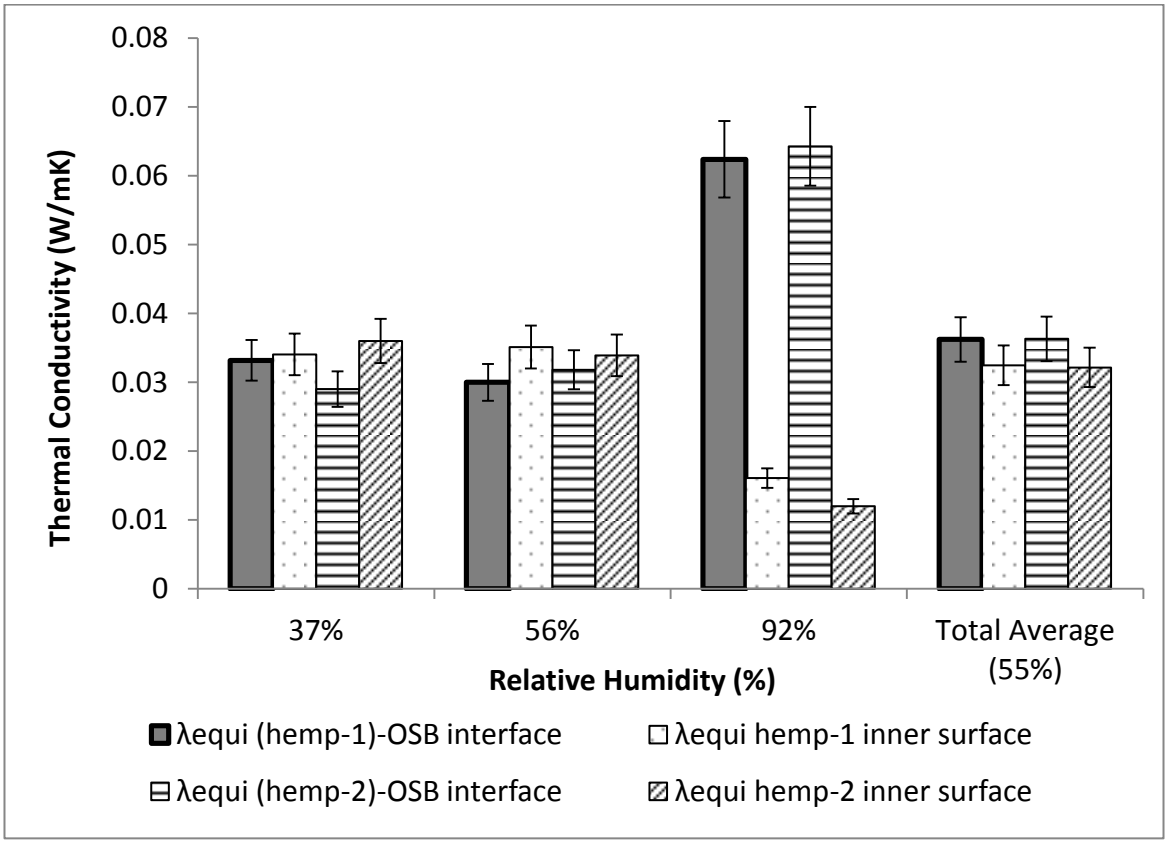


**Figure 7.34: Equivalent thermal conductivity values with error bar.**

### *7.7.5.2 Relative humidity and prediction of mould growth*

Relative humidity values in hemp-1 and hemp-2 insulation materials are always over 75% after initial 24 hours. In terms of relative humidity in the insulation-OSB interfaces, hemp-1 responded to the changing interior relative humidity quicker and in higher magnitude than hemp-2 insulation.

However, in reference to the moisture content in the external surfaces of the insulations in the insulation-OSB interfaces, hemp-2 adsorbed more moisture than hemp-1 which can be explained in terms of their respective moisture adsorption capacities, as shown in Figure 7.35. It can be noticed in Figure 7.35 that, when exposed to over 90% relative humidity, hemp-2 adsorbs more than twice the amount of moisture content that hemp-1 adsorbs for each unit volume of dry mass.

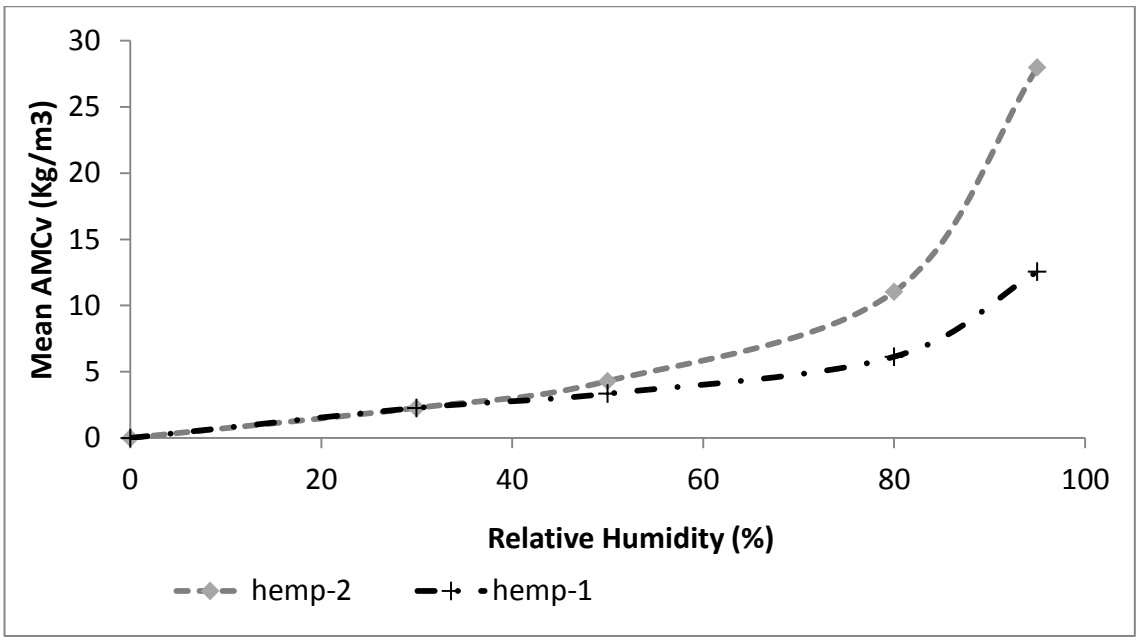


**Figure 7.35: Adsorption isotherms of hemp-1 and hemp-2.**

Figure 7.33 also shows that relative humidity in both (hemp-1)-OSB and (hemp-2)-OSB remained more than 90% for about 5 days with occasional rise of humidity to more than 95%. This is a near condensation condition. However, no condensation was visually observed on the insulation-OSB interfaces at the end of experimental run.

Figure 7.36 presents the temperature and relative humidity conditions in the insulation-OSB interfaces of panel A and panel B in conjunction with the Sedblauer's isotherms during test-2. Figure 7.36 shows that the hygrothermal conditions in the insulation-OSB interface in both panel A and panel B during the 12-day long experiment are always above the 8-day isopleth. This implies that in terms of 8-day isopleth, the insulation materials are susceptible to mould spore germination in both panel A and panel B. However, when the insulation materials were dismantled at the end of the test run, no mould growth was visually observed either on the insulation surface or on the OSB surface of the insulation-OSB interfaces.

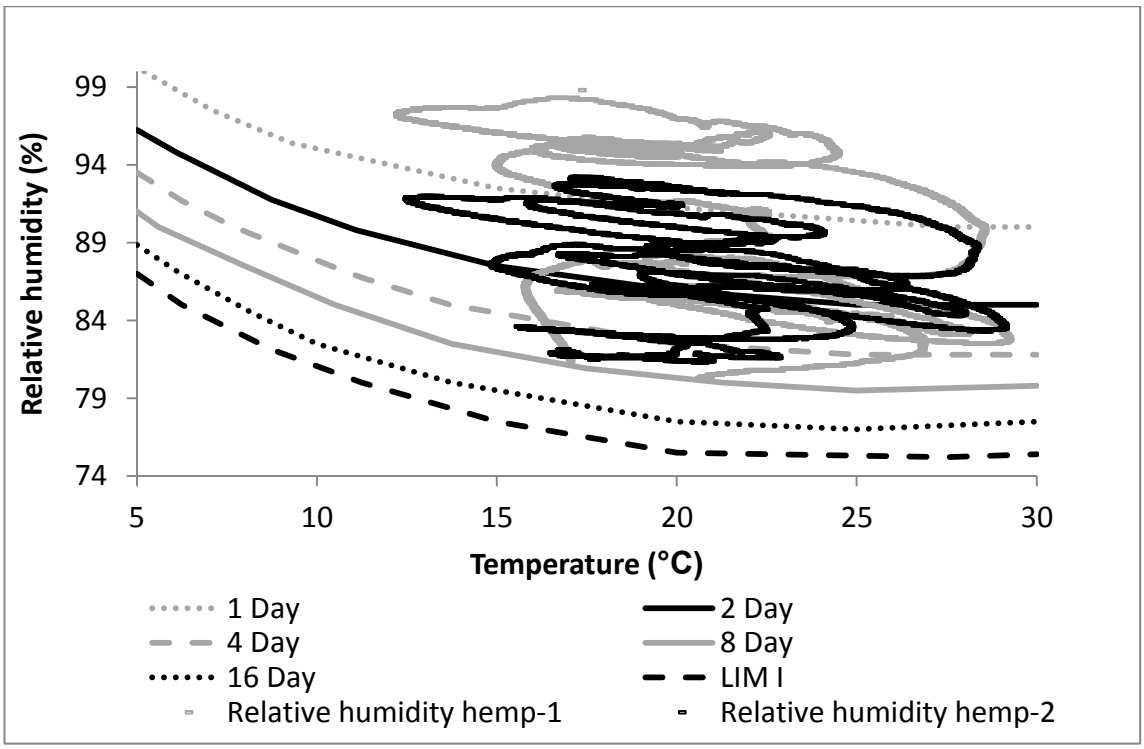


**Figure 7.36: Hygrothermal conditions in the insulation-OSB interface in conjunction with spore germination isopleths**.

## 7.8 In situ Test 3: Hygrothermal performance of hemp-2 and stone wool insulation materials

### *7.8.1 Introduction*

In the experimental tests described in chapter six, it was found that the equivalent thermal conductivity of hemp insulations at 95% relative could be as high as 0.064 W/mK and the average equivalent thermal conductivity in a range of relative humidity conditions could be around 0.04 W/mK (Figure 6.32 in chapter six). It was also found that the equivalent thermal conductivity of stone wool insulation at 80% relative humidity could be as high as 0.068 W/mK (Figure 6.20 in chapter six). However, the results for the equivalent thermal conductivity of stone wool insulation at high relative humidity varied between the experiments.

In all the experiments, it was also found that stone wool responded very quickly to the changing relative humidity boundary conditions and there was a higher likelihood of interstitial condensation in stone wool insulation than in hemp insulation.

The first objective of the current test was to compare the hygrothermal performance of hemp-2 and stone wool insulation materials in vapour open construction as an extension of the experimental tests and to assess their respective thermal conductivity values at a range of interior relative humidity conditions. The second objective of the in situ test was to assess whether the likelihood of interstitial condensation was lower in hemp insulation than in stone wool insulation as had been found in the experimental works.

Since significant difference in heat flux reading based on the placement of heat flux sensors was observed in test-2, the similar installation schedule was followed in the current experiment. Table 7.6 shows the test set up and the duration of the test.

**Table 7.6: The test setup and duration.**

| Tests | Wall panel A | Wall panel B | Inner lining in the panels | Dates of test | Test duration |
|---|---|---|---|---|---|
| Test-3 | Stone wool | Hemp-2 | Gypsum plasterboard (PB) | 19.07.12-27.08.12 | 41 days |

### *7.8.2 Test materials and experimental set-up*

#### *7.8.2.1 Test materials*

Hemp-2 and stone wool insulation materials were sourced from the UK market based on their constituents. The properties of the insulations are shown in Table 4.1 and Table 4.2 of chapter four. Both Hemp-2 and stone wool insulation materials were conditioned at 25 ± 2 °C temperature and 50% relative humidity before installation as this level of hygrothermal exposure is commonly encountered when insulations are stored in the construction site. The adsorbed water contents in hemp-2 and stone wool for this exposure are 4.3 Kg/m$^3$ and 0.5 Kg/m$^3$ respectively as shown in Figure 5.5 of chapter Five.

#### *7.8.2.2 The test panels, instrumentation*

The wall panel construction and instrumentation followed the assembly-2, as described in subsection 7.3.2.

### *7.8.3 Research method*

#### *7.8.3.1 Experimental protocol*

The test was carried out in a timber frame test building, as described in subsection 7.3.1. The eastern wall of the test building contained wall panel A and wall panel B as assembly-2, as described in subsection 7.3. Both panels are without a vapour barrier. The panel A was insulated with stone wool and the panel B was insulated with hemp-2 insulation. The interior temperature in the test building was maintained at 25 ± 3 °C. The duration of the test was about 39 days. The test period was longer than the previous tests due to its different hygrothermal protocol. In the current test, an attempt was made to find out the effect of repeated exposure to high, low and medium interior relative humidity on the hygrothermal conditions of the insulations. There was a continuous 13 days' period of exposure to about 60% interior relative humidity during the test to determine the impact of this common interior relative humidity conditions on the insulation materials. The test protocol is shown in Table 7.7.

**Table 7.7: The relative humidity protocol.**

| Relative humidity (±5%) | From | To | Days |
|---|---|---|---|
| 35% | 19/07/2012 10:00 | 21/07/2012 10:00 | 2 |
| 60% | 21/07/2012 10:00 | 22/07/2012 10:00 | 1 |
| 90% | 22/07/2012 10:00 | 24/07/2012 10:00 | 2 |
| 60% | 24/07/2012 10:00 | 25/07/2012 10:00 | 1 |
| 35% | 25/07/2012 10:00 | 28/07/2012 10:00 | 3 |
| 60% | 28/07/2012 10:00 | 10/08/2012 10:00 | 13 |
| 85% | 10/08/2012 10:00 | 11/08/2012 10:00 | 1 |
| 55% | 11/08/2012 10:00 | 17/08/2012 10:00 | 6 |
| 90% | 17/08/2012 10:00 | 18/08/2012 10:00 | 1 |
| 60% | 18/08/2012 10:00 | 21/08/2012 10:00 | 3 |
| 90% | 21/08/2012 10:00 | 23/08/2012 10:00 | 2 |
| 55% | 23/08/2012 10:00 | 27/08/2012 10:00 | 4 |

The exterior of the test building was exposed to the external weather conditions during July and August, 2012. Temperature and relative humidity of the interior, exterior and the wall panels were logged at every minute during the testing period.

#### *7.8.3.2 Assessment of thermal performance and mould growth conditions*

The U-values were calculated from the recorded experimental data using average method according to ISO 9869, as shown in equation 7.1 and λequi value was calculated using equation 7.2. Mould growth condition was assessed in terms of parametric studies. For parametric studies, the temperature-relative humidity relationships were plotted from the collected data and compared with the conditions set in Sedlbauer's germination isopleths.

### *7.8.4 Results*

#### *7.8.4.1 Temperature and relative Humidity*

Internal and external temperature and relative humidity conditions for test-3, as running averages of every one hour for 39 days, are shown in Figure 7.37.

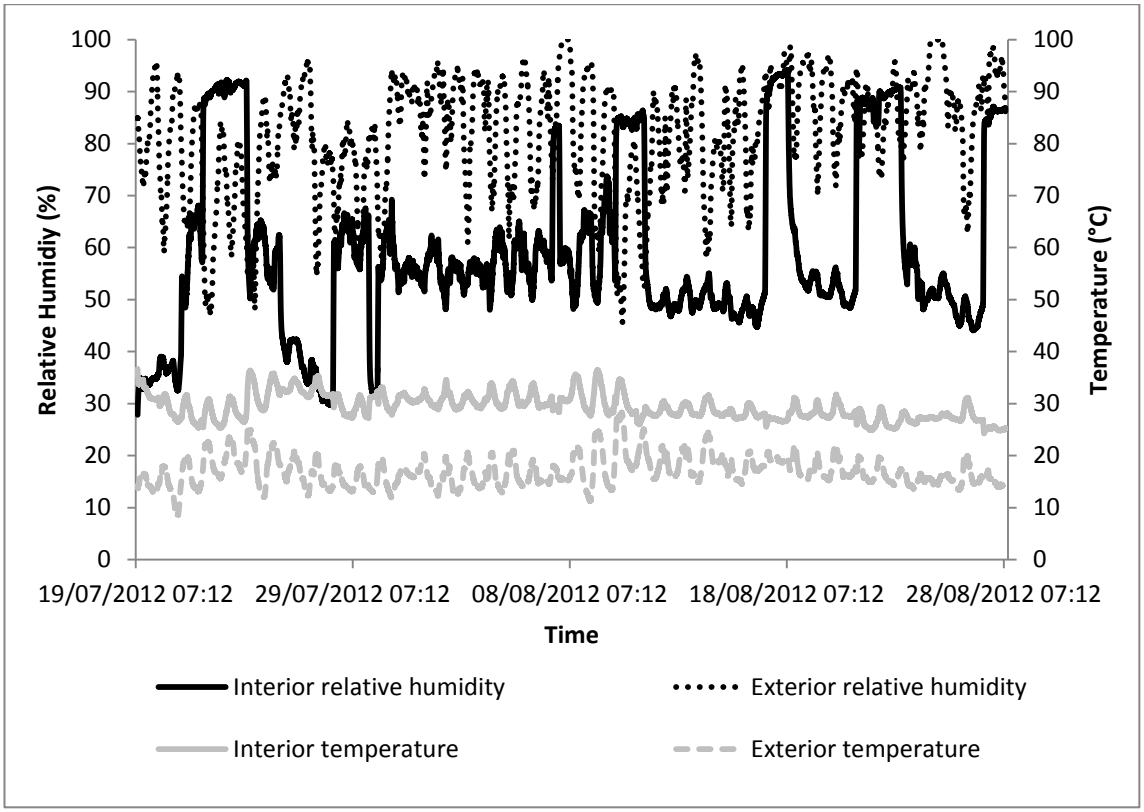


**Figure 7.37: The hygrothermal boundary conditions**.

### *7.8.4.2 Heat Flux, U-value and thermal conductivity*

Figures 7.38 and 7.39 show the heat flux and the differences between internal and external ambient temperature in the construction panels A and B during test-3. U-values of the wall panels A and B and λequi values of stone wool and hemp-2 insulation materials are shown in the Table 7.8.

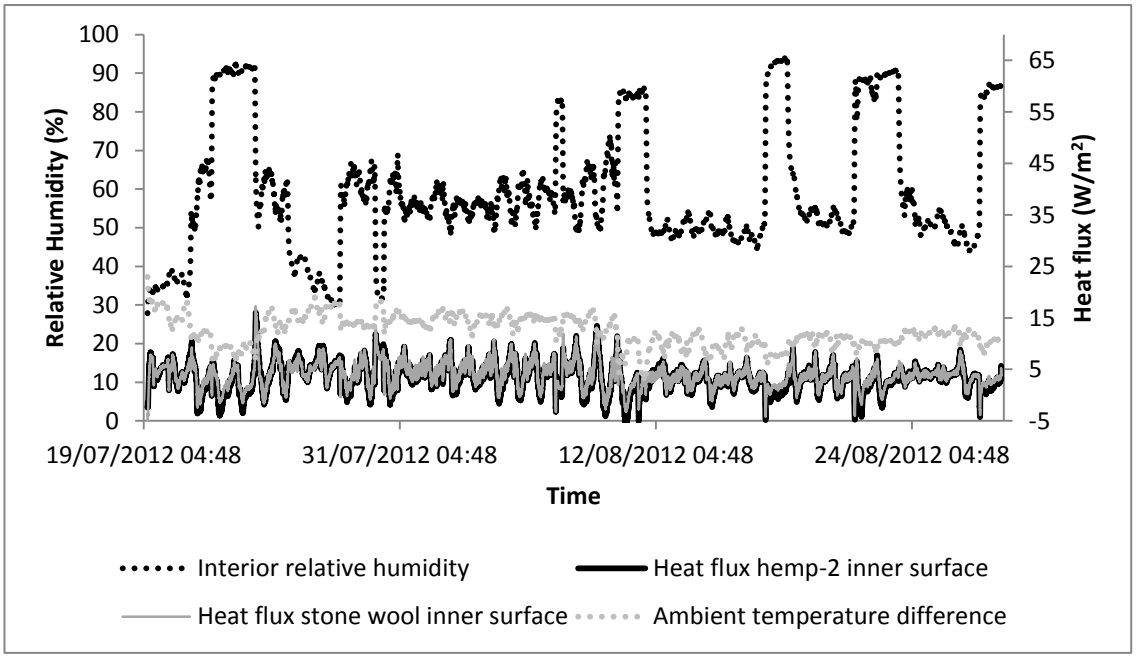


**Figure 7.38: Heat flux in panel A (hemp-2) and panel B (stone wool) based on the heat flux sensors located on the inner plasterboard surfaces.**

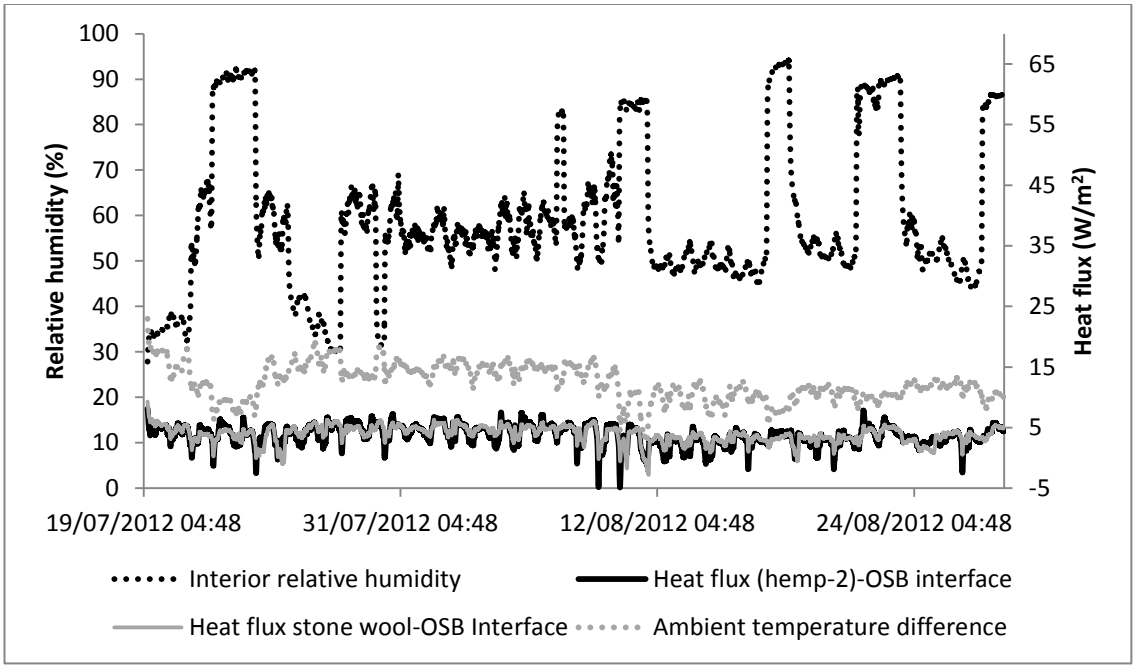


**Figure 7.39: Heat flux in panel A (hemp-2) and panel B (stone wool) based on the heat flux sensors located in the insulation-OSB interfaces.**

**Table 7.8: U-values of the wall panel A (hemp-1) and panel B (stone wool) and λequi values of hemp-2 and stone wool insulation materials.**

| | U-value panel A (stone wool), ($W/m^2K$) | U-value panel B, (hemp-2), ($W/m^2K$) | λequi stone wool, (W/mK ) | λequi hemp-2, (W/mK) |
|---|---|---|---|---|
| Using heat flux sensors on the inner surface | 0.313 | 0.285 | 0.040 | 0.036 |
| Using heat flux sensors on the insulation-OSB interface | 0.309 | 0.300 | 0.040 | 0.038 |

### *7.8.5 Discussion*

#### *7.8.5.1 Thermal properties*

Figure 7.40 shows the equivalent thermal conductivity values of the insulation materials during test-3. In terms of equivalent thermal conductivity values derived from the total period of the experiment at an average internal relative humidity of about 59%, the equivalent thermal conductivity value derived from the (hemp-2)-OSB interface was higher than that derived from hemp-2 inner surface by 6.7 %. Equivalent thermal conductivity value derived from (stone wool)-OSB interface was lower than that derived from stone wool inner surface by 1.7 %.

In terms of equivalent thermal conductivity values assessed during the average interior relative humidity of 57%, the equivalent thermal conductivity value derived from (hemp-2)-OSB interface was higher than that derived from hemp-2 inner surface by 8% and equivalent thermal conductivity value derived from stone wool inner surface was higher than that derived from (stone wool)-OSB interface by 2.2 %.

In terms of equivalent thermal conductivity values assessed during the average interior relative humidity of 90%, the equivalent thermal conductivity value derived from (hemp-2)-OSB interface was higher than that derived from hemp-2 inner surface by 241.6% and the equivalent thermal conductivity value derived from (stone wool)-OSB interface was higher than that derived from stone wool inner surface by 94 %.

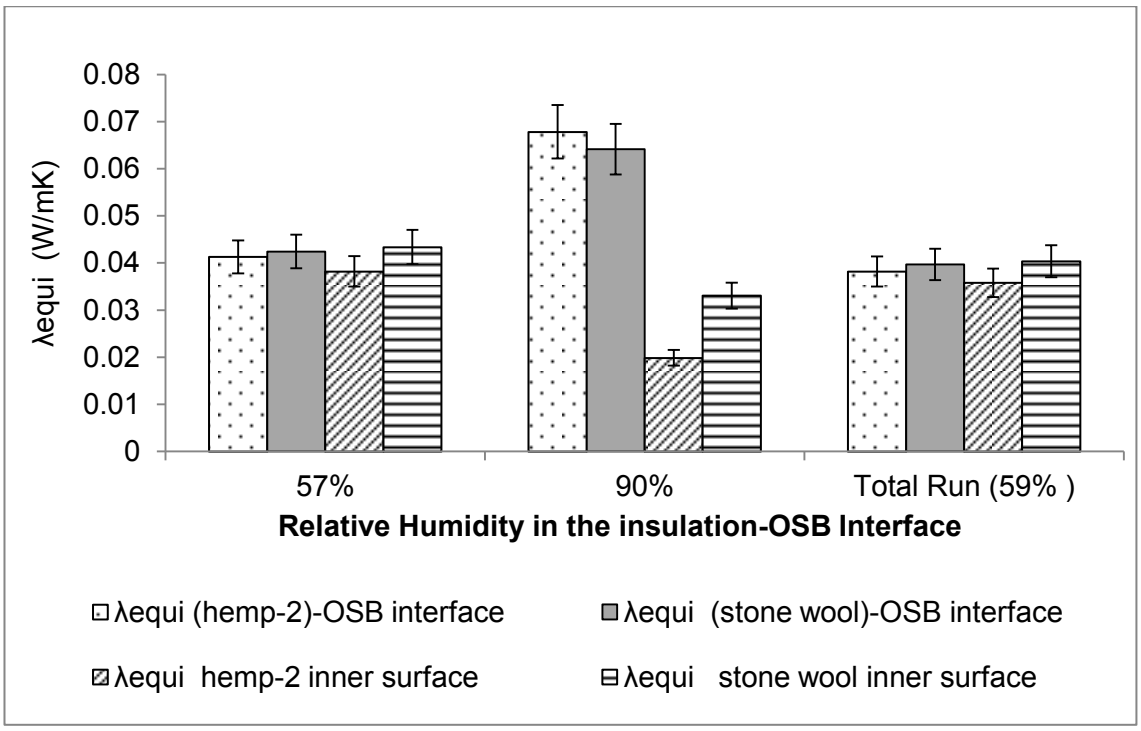


**Figure 7.40: The equivalent thermal conductivity values of the insulations.**

### *7.8.5.2 Relative humidity and prediction of mould spore germination*

Figure 7.41 shows the relative humidity conditions in the insulation-OSB interfaces in wall panel A (stone wool) and panel B (hemp-2) along with the interior relative humidity for the total duration of the test-3.

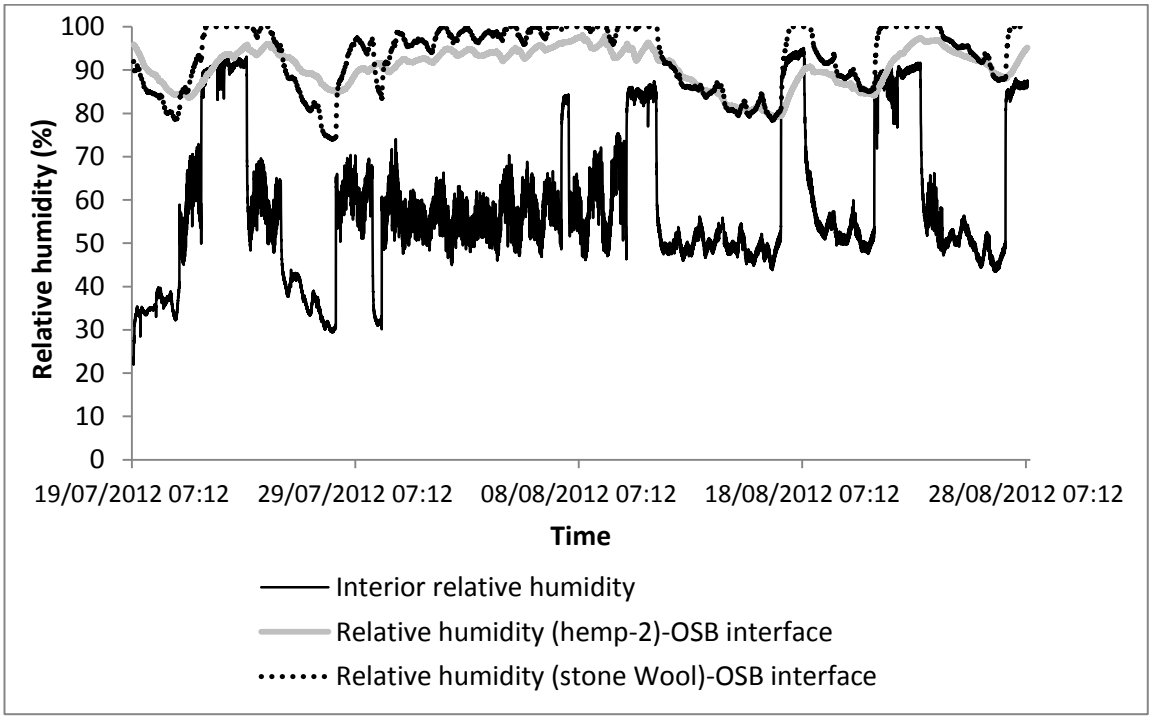


**Figure 7.41: The relative humidity conditions at insulation-OSB interfaces.**

Except for between 27 and 28 July 2012, relative humidity values in the insulation-OSB interfaces were always more than 80%. The key difference between hemp-2 and stone wool insulation in terms of hygric response was that the interface between stone wool and OSB frequently reached 100% relative humidity value while the 100% relative humidity never occurred in the (hemp-2)-OSB interface.

Figure 7.42 shows the details of the insulation-OSB interface hygric conditions of hemp-2 and stone wool insulation materials between 19 and 25 July 2012. It can be observed that when interior relative humidity increased from 60% to 90%, the relative humidity in (stone wool)-OSB interface immediately rose up to 100%, while the relative humidity in (hemp-2)-OSB interface increased to 78%. During the whole duration of the interior relative humidity of 90%, the (stone wool)-OSB interface relative humidity always stayed at 100% while the (hemp-2)-OSB interface relative humidity slowly increased to 95%. It can be further noticed from Figure 7.43 that the likelihood of both the frequency and duration of condensation is higher in (stone wool)-OSB interface than in (hemp-2)-OSB interface.

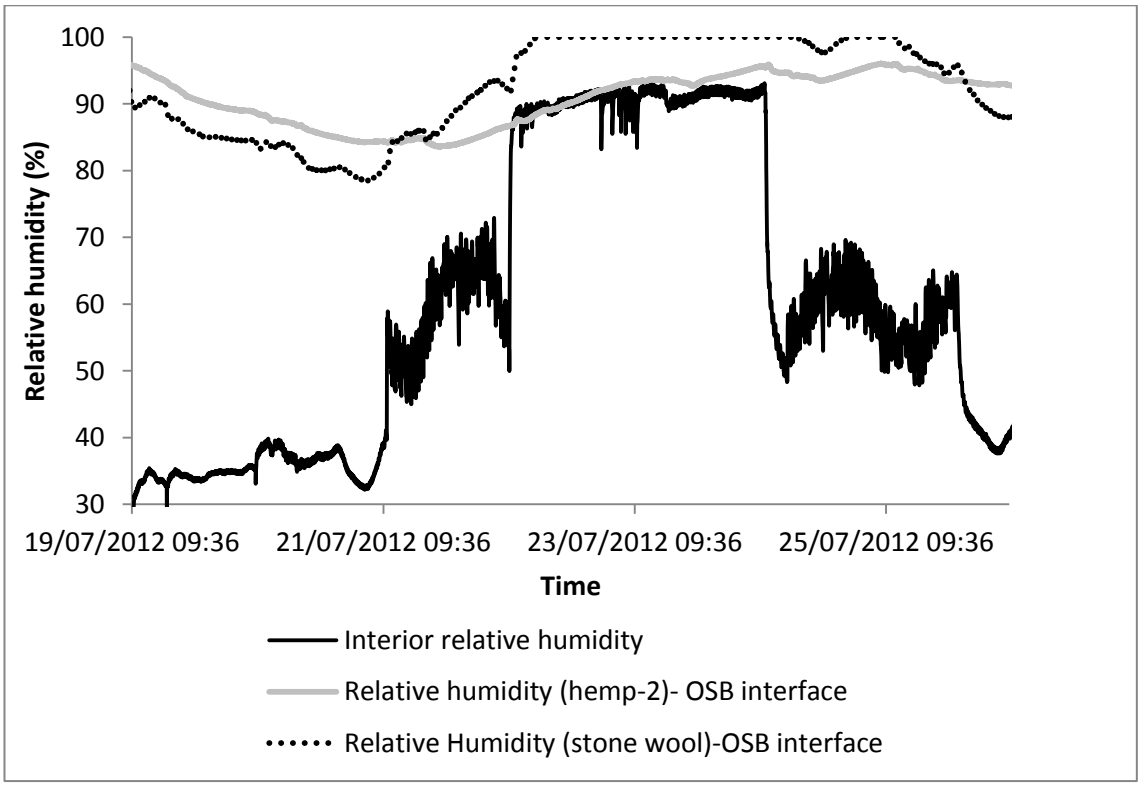


**Figure 7.42: The insulation-OSB interface hygric conditions.**

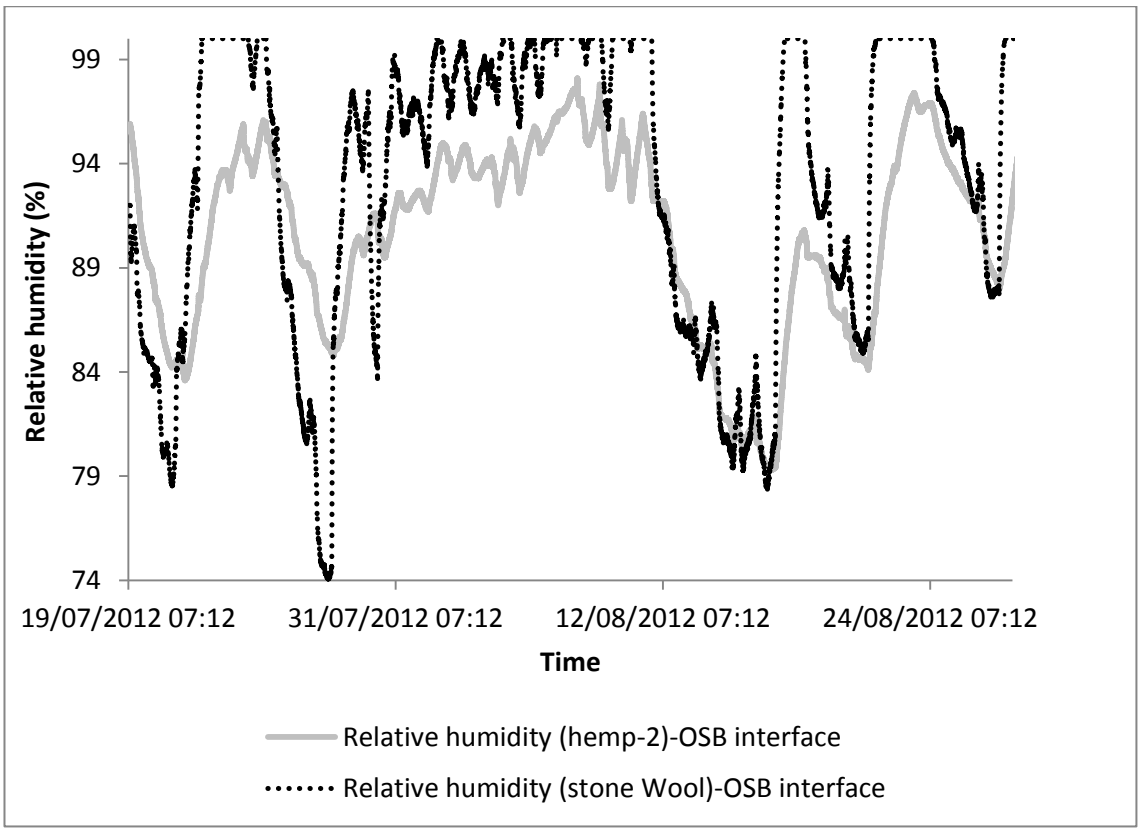


**Figure 7.43: The insulation-OSB interface hygric conditions.**

Figure 7.44 presents the temperature and relative humidity conditions in the (stone wool)-OSB interface of panel A in conjunction with the Sedlbauer's isopleth for substrate class I during test-3. The hygrothermal conditions in the (stone wool)-OSB interface in the panel A during the 39-day long experiment were most of the time above the LIM I isopleth. Figure 7.45 shows the graph of continuous 11 days when the hygrothermal conditions were well above the 1-day isopleth. Germination of mould spore was highly likely during those 11 days.

Figure 7.46 shows the temperature and relative humidity conditions in the (hemp-2)-OSB interface of panel B with reference to the Sedlbauer's isotpleth for substrate class I during test-3. The hygrothermal conditions are above the 8-day isopleth most of the time. Figure 7.47 shows continuous 11 days' hygrothermal conditions in the (hemp-2)-OSB interface. The hygrothermal conditions are mostly above the 1-day isopleth meaning that germination of mould spore is highly likely.

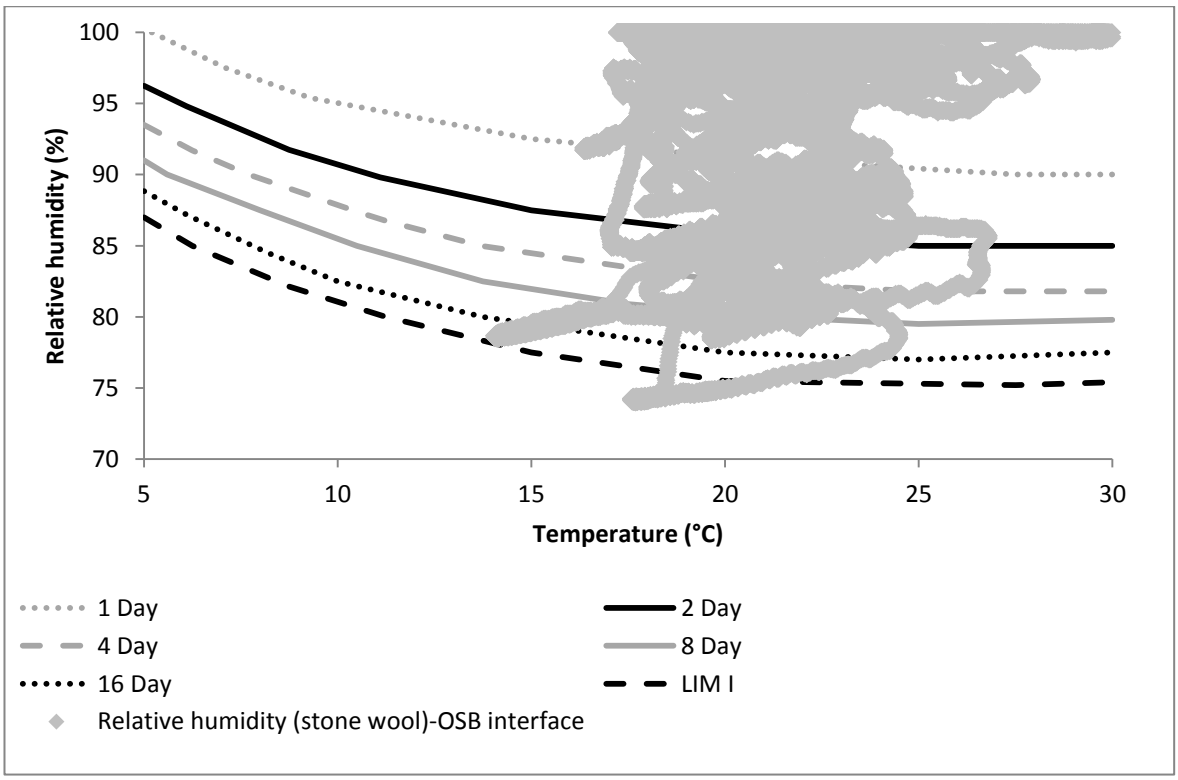


**Figure 7.44: 39 days' hygrothermal conditions in the (stone wool)-OSB Interface**.

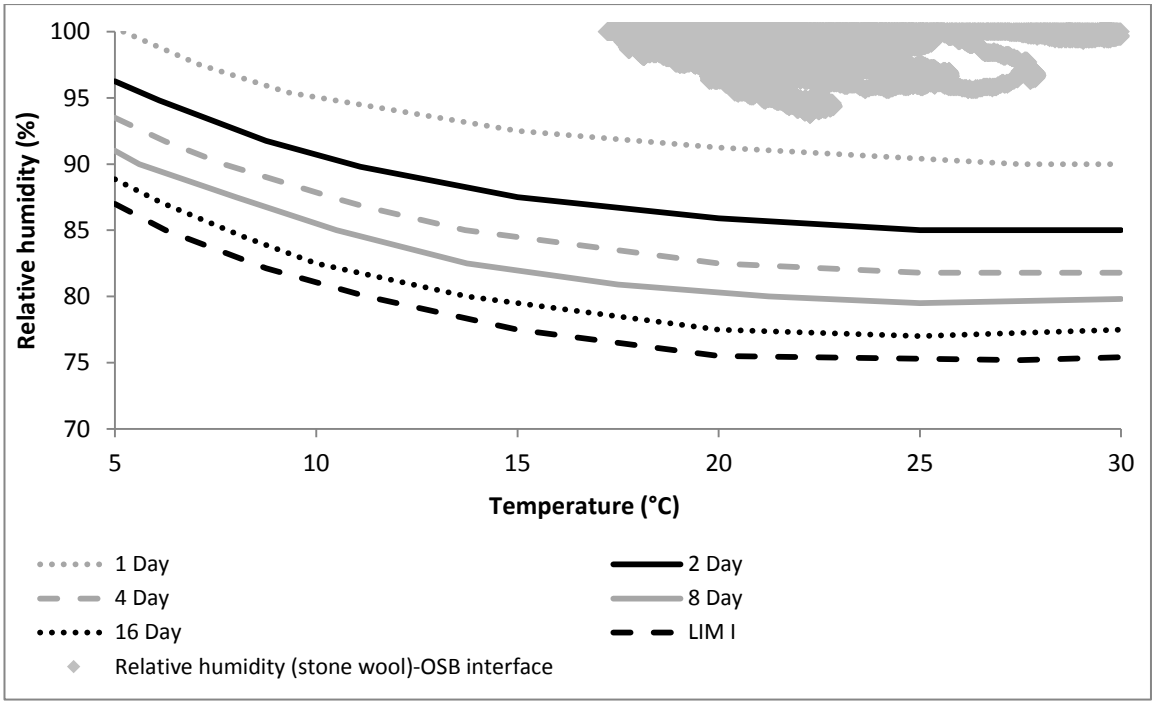


**Figure 7.45: Continuous 11 days hygrothermal condition in (stone wool)-OSB interface.**

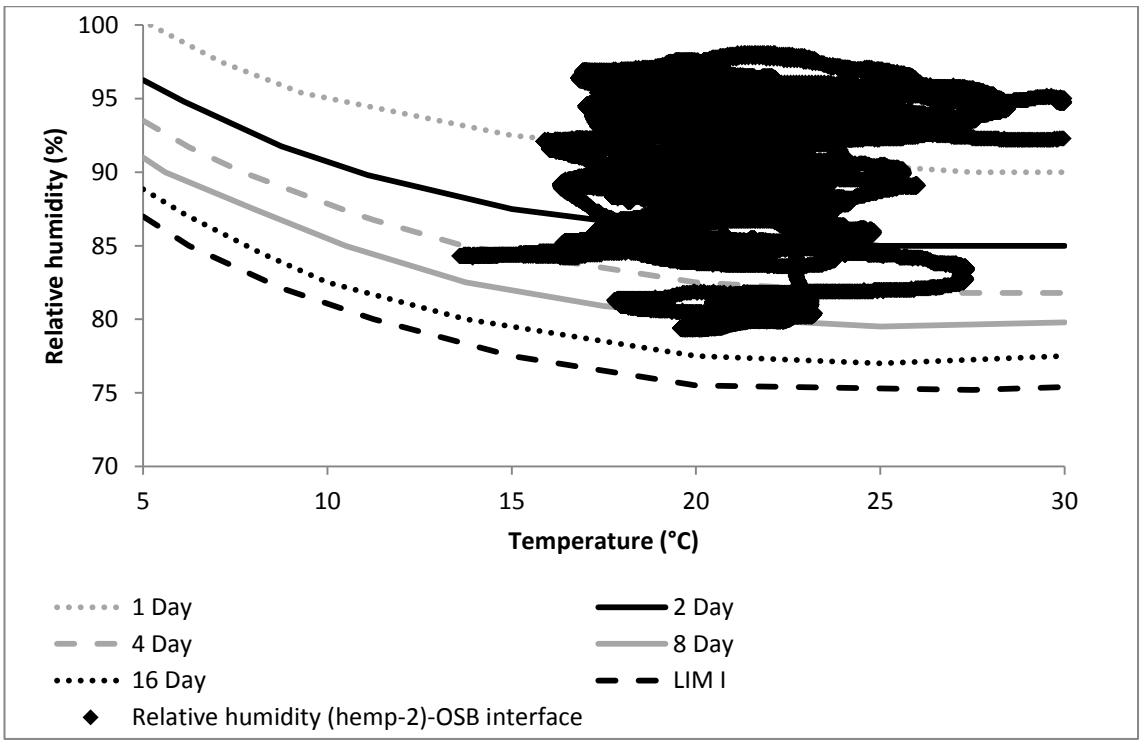


**Figure 7.46: 39 days' hygrothermal condition in (hemp-2)-OSB Interface.**

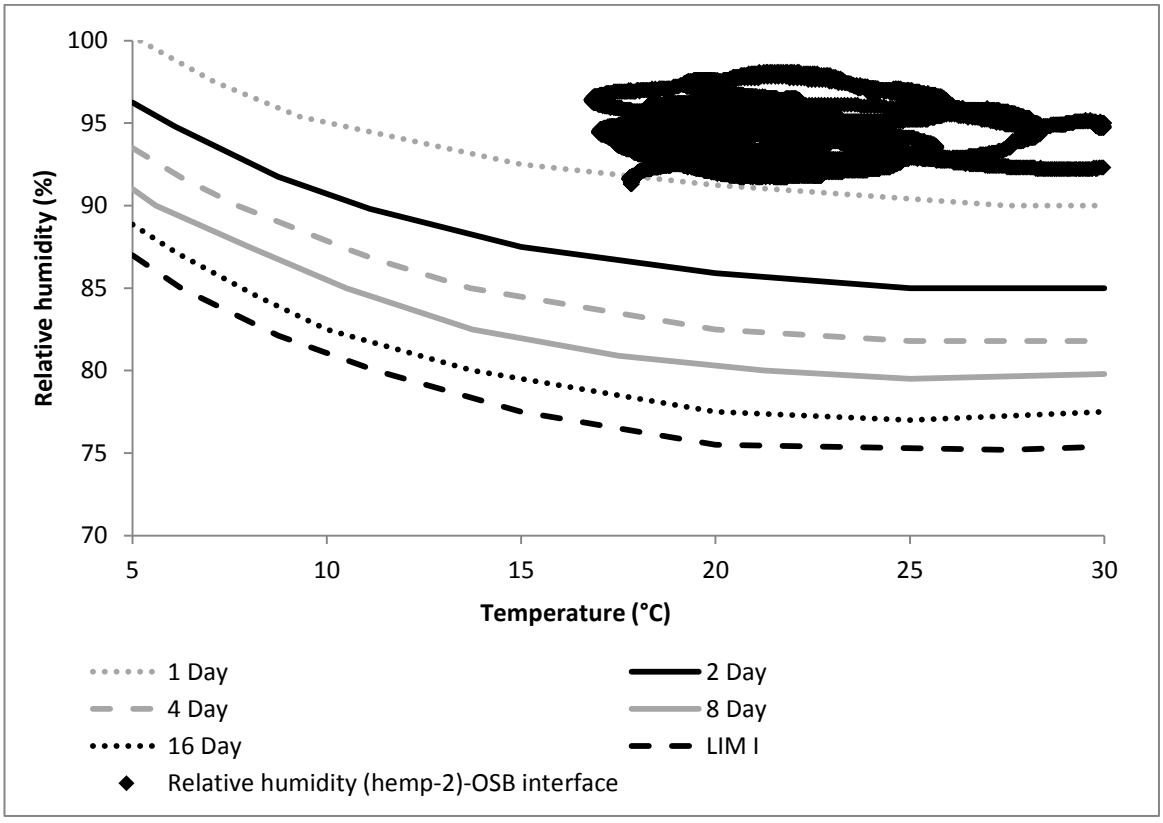


**Figure 7.47: Continuous 11 days' hygrothermal condition in (hemp-2)-OSB interface.**

Despite the predictions of mould spore germination, no visible evidence of mould growth was observed in the external faces of insulations when the

insulations were dismantled. Nevertheless, further observation with a digital microscope revealed some possible traces of mould on one of the OSB panels, but the sample has not been cultured for further confirmation.

When the insulation materials were dismantled at the end of the test-3, condensation was observed only on the impermeable surface of the water content reflectometer in the (stone wool)-OSB interface. Therefore, it may be possible that some condensation might have occurred on the OSB surface of the (stone wool)-OSB interface and the condensate might have been readily absorbed by the OSB. No condensation or wet surface was observed in the (hemp-2)-OSB interface.

### 7.9 Chapter summary

During test-1 (test-1.1 and test-1.2), wall panels with and without vapour barrier were compared for hemp-1 insulation. Heat flux through the wall panels with and without vapour barrier was assessed and then compared in terms of U-value and equivalent thermal conductivity of the insulation materials. The U-value of the wall panels varied between 0.281 and 0.292 W/m$^2$K. The equivalent thermal conductivity values varied between 0.035 and 0.037 W/m-K while the manufacturers' declared conductivity was 0.038 W/mK. Equivalent conductivity of insulation in vapour open panel was higher than equivalent thermal conductivity of insulation in wall panels with vapour barrier by 6.3% and 4.8% for PB and OSB inner lining respectively. Installing a vapour barrier did not ensure a hygrothermal condition that deterred the spore germination although the likelihood was higher in the construction panel without vapour barrier. Therefore, as far as the computational prediction of mould spore germination was concerned, antifungal treatment of hemp-1 insulation might be needed.

During the second test (test-2), the hygrothermal performances of hemp-1 and hemp-2 insulation materials in vapour open timber frame construction were compared. It was found that, in terms of equivalent thermal conductivity, both hemp-1 and hemp-2 insulation materials showed reasonably similar performance. However, in terms of mould spore germination, hemp-1 (with lower hemp content) seemed to be more susceptible than hemp-2 (with higher hemp content). One important observation is that at higher interior relative

humidity (92%), equivalent thermal conductivity value could be significantly higher when the heat flux reading was taken from the insulation-OSB interface than when the reading was taken from the interior surface of the wall panels. It is plausible that the heat flux meter in the insulation-OSB interface registered higher moisture flux due to moisture migration and phase change at the interface.

The third test (test-3) focused on the comparative in situ hygrothermal performance of hemp-2 and stone wool insulation materials. It was observed that, in terms of equivalent thermal conductivity, there was no significant difference between hemp-2 and stone wool insulation materials, with both insulation materials showing thermal conductivity values close to the manufacturers' declared values. However, in terms of mould spore germination, while hygrothermal condition in the insulation-OSB interfaces of both hemp-2 and stone wool insulation materials seemed to favour mould spore germination, stone wool seemed to be more susceptible. Another important observation during test-3 was that the relative humidity in the (stone wool)-OSB interface frequently rose to nearly 100% meaning that there was a likelihood of frequent condensation in the (stone wool)-OSB interface. Compared to stone wool, the frequency and likelihood of occurrence of condensation were less in (hemp-2)-OSB interface.

# Chapter 8

# Hygrothermal Simulations Using Test Reference Year Data of Two UK Sites

## 8.1 Introduction

Due to the constraints of time and equipment, it is not always possible to assess the long-term hygrothermal performance of building envelopes by means of laboratory experiments and field monitoring only. It is also helpful to get an indicative idea of the performance of building envelopes for specific boundary conditions during the design stage. In these situations, hygrothermal simulation tools prove suitable. In this chapter, long-term hygrothermal performances of hemp insulation materials are assessed for both timber frame walls and solid brick walls by using the WUFI software. The mould growth index and the rate of mould growth in the selected location of the insulations are determined by using the WUFI-Bio software. The scopes of the WUFI and WUFI-Bio software are discussed in subsection 3.1.3 and section 3.7, respectively, of chapter three. Numerical simulations are also conducted for stone wool insulation in order to assess the performance of hemp insulations in relation to that of stone wool insulation. It is possible to determine the effect of using different insulation materials on the building energy use by using energy simulation software. The energy simulation is not included in this chapter. It was carried out during the initial simulation runs using the Integrated Environmental Solution (IES) software and showed that moistened insulation had limited effect on space conditioning sensible energy load (Appendix E). The IES virtual environment is a software package consisting of a number of energy related simulation tools to address dynamic thermal properties, air flow, lighting, lifecycle analysis, computational fluid dynamics, etc., in relation to buildings. The IES uses the transient heat balance equations in its algorithm. Further details of the governing equation can be found on the website of IES (2013).

## 8.2 Validation of WUFI software and parameter sensitivity analysis

### *8.2.1 Validation of the WUFI software*

WUFI hygrothermal simulation tool has been validated by the developer of the software in accordance with European Standard EN 15026 ((2007). EN 15026 provides the benchmark example for validating any hygrothermal simulation software in terms of the capability of the software to produce results that are correct within a specified tolerance. The benchmark example focuses on determining the heat and moisture adsorption of a semi-infinite slab of material. The material is initially in equilibrium with the boundary condition of 20°C temperature and 50% relative humidity. The material is then subjected to the new hygrothermal boundary condition of 30°C temperature and 95% relative humidity. Increase in temperature and relative humidity will cause heat and moisture to flow into the material. The temperature and moisture profile in the material have to be calculated for 7, 30 and 365 days (Benchmark Test of EN 15026, 2012). The maximum allowable deviance of the results from the reference result should not be more than 2.5%. The WUFI validation test results for moisture and temperature distribution in the semi infinite slab are shown in Figures 8.1 and 8.2, respectively. The results confirm that the moisture and temperature distribution are identical to the reference solutions. Thus the compliance of the WUFI software with the requirements of EN 15026 was established.

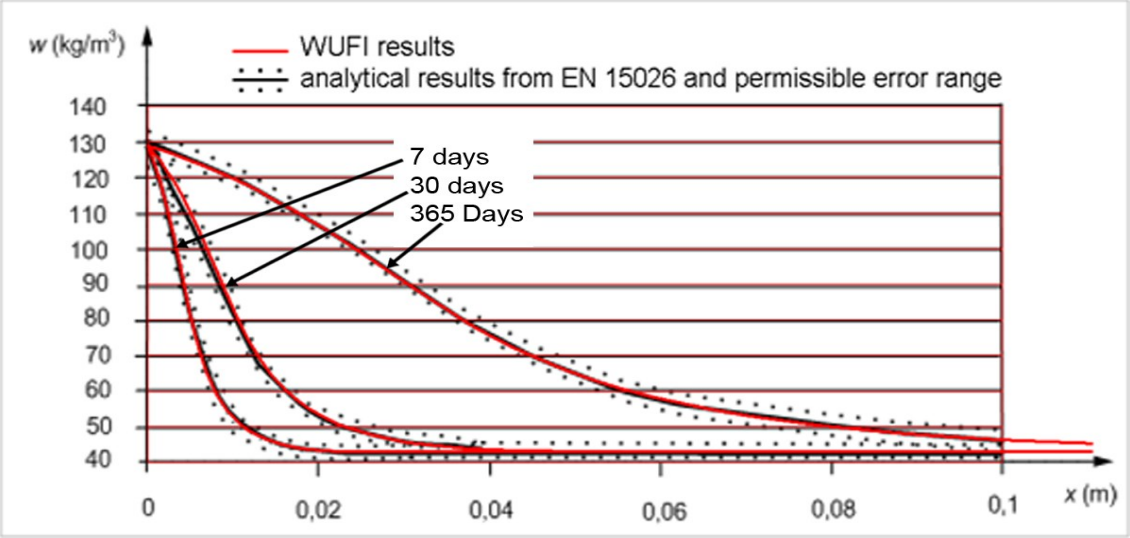


**Figure 8.1: Moisture distribution in the slab in 7 days, 30 days and 365 days (Benchmark Test of EN 15026, 2012).**

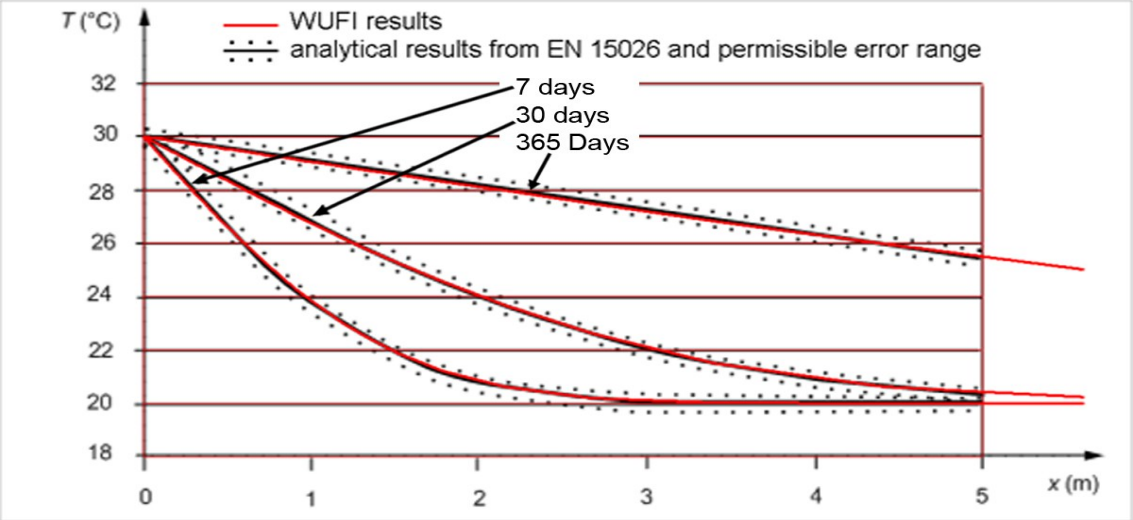


**Figure 8.2: Temperature distribution in the slab in 7 days, 30 days and 365 days (Benchmark Test of EN 15026, 2012).**

WUFI software has been also validated repeatedly by comparison with experimental data (Holm and Kunzel, 1999). Additinally, the WUFI simulations described in section 6.2 and 6.3 of chapter six show reasonable agreement with the related experimental data.

### *8.2.2 Parameter sensitivity analysis*

Sensitivity analysis is used to determine the sensitivities of the predictions or outcomes to the changes in the value of the input parameters of any parametric model where the outputs are a function of the input parameters. Based on Hamby (1994), Holm (2001), Spitz *et al.* (2012), and Tian (2013), sensitivity analysis can be useful for the following purposes:

- To build confidence in the model by assessing the impact of the uncertainties of the individual input parameters of the model.
- To determine the level of accuracy that the parameters need to have to make a model valid by reducing output uncertainty.
- To determine which input parameters are highly correlated with the output.
- To identify the parameters those are most important by assessing their impact on the predictions. The important parameters may require higher accuracy whereas estimated values of the less important parameters can be used.

Thus, sensitivity analysis is critical to model validation. The details of the types of sensitivity analyses used in different modelling situations can be found in Hamby (1994). For the present research, a one-at-a-time parameter sensitivity analysis has been carried out to assess the relative importance of the input parameters of the hygrothermal properties of hemp insulation in the WUFI software. The one-at-a-time sensitivity analysis is a simplified approach and is less time consuming. However, in many cases, the results obtained from simplified sensitivity analusis methods are comparable to the comprehensive methods (Hamby, 1995).

**Method of sensitivity analysis**

A base case model has been selected as shown in Figure 8.9 and an initial simulation with a certain set of input parameters is run in the WUFI software for the base case. Afterwards, a number of simulations are run having changed the value of one input parameter at a time to see how the change in an individual input parameter causes changes in the hygrothermal behaviour of the base case model. Hemp-2 insulation has been selected for the sensitivity analysis as it was used in most of the laboratory and in situ experiments.

The base case simulation was run using the mean value of the following seven parameters: adsorption isotherm, vapour diffusion resistance factor (μ value), water absorption coefficient (A value), density, porosity, heat capacity and moisture dependent thermal conductivity (MTC). The mean values of the aforementioned parameters, except porosity and heat capacity, were determined from the experimental detrminations of the values of those parameters from more than or equal to three samples. The value of heat capacity was taken from the manyfacturer's data and the value of porosity was taken from the WUFI database of fibrous insulations. In the subsequent forty simulation runs, the value of each parameter was changed by the following percentages: ±5%, ±10%, ±20%. However, for porosity, 10% and 20% increase was not possible as the new values would exceed the maximum porosity value of 1.

Relative humidity and water content are selected as the key output measures since condensation and high relative humidity in the hemp insulations are key concerns to explore in the hygrothermal simulations.

The results are shown in Figures 8.3 to 8.9. For moisture content in the hemp-2 insulation, the most sensitive parameter is adsorption isotherm. It can be noticed that ±5% to ±20% changes of adsorption isotherm results in ±5% to ±20% changes of moisture content in hemp-2 insulation. Changes of ±20% of moisture dependent thermal conductivity result in the changes of ±2% of insulation moisture content. The changes in moisture content in response to the changes in the values of other parameters between ±5% to ±20% is less than 1%.

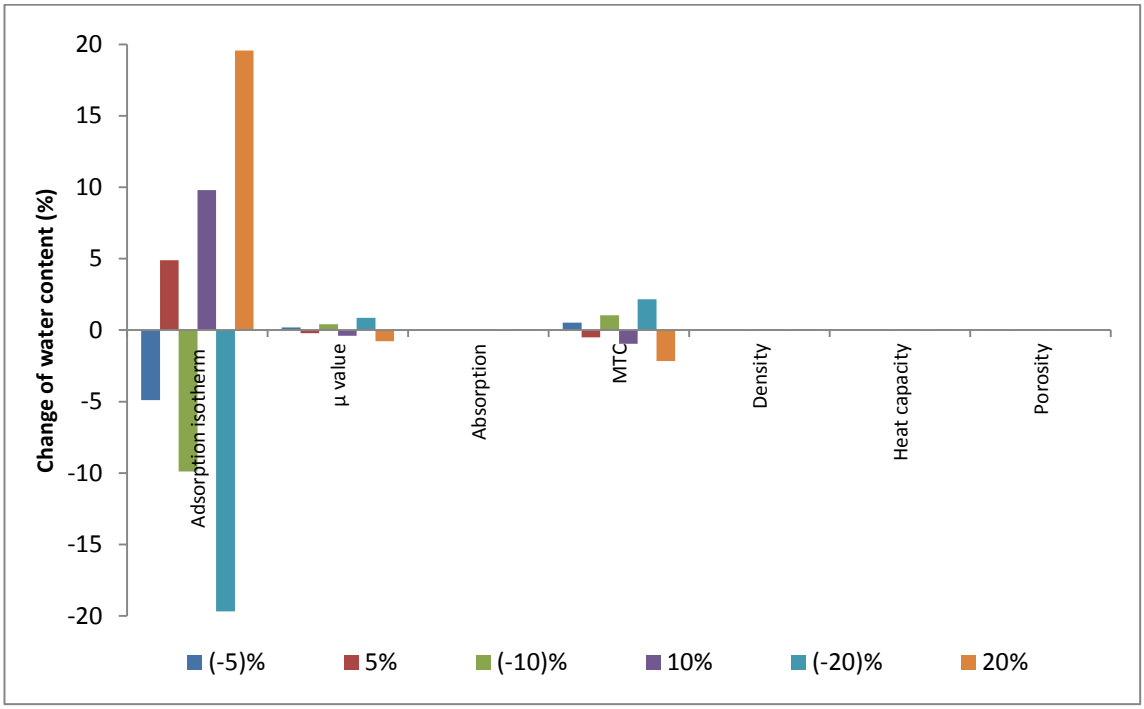


**Figure 8.3: Effect of (%) change of parameters on (%) change of water content in hemp-2 from base case.**

For moisture content in (hemp-2)-OSB interface, similar observation can be made about the sensitivity of adsorption isotherm. Changes of ±20% of moisture dependent thermal conductivity result in changes of ±5% of insulation moisture content. Change of 20% of vapour diffusion resistance factor causes a change of 2.5% of water content in the (hemp-2)-OSB interface. A 20% change of the values of other parameters from the base case values causes less than 1% change in moisture content in (Hemp-2)-OSB interface.

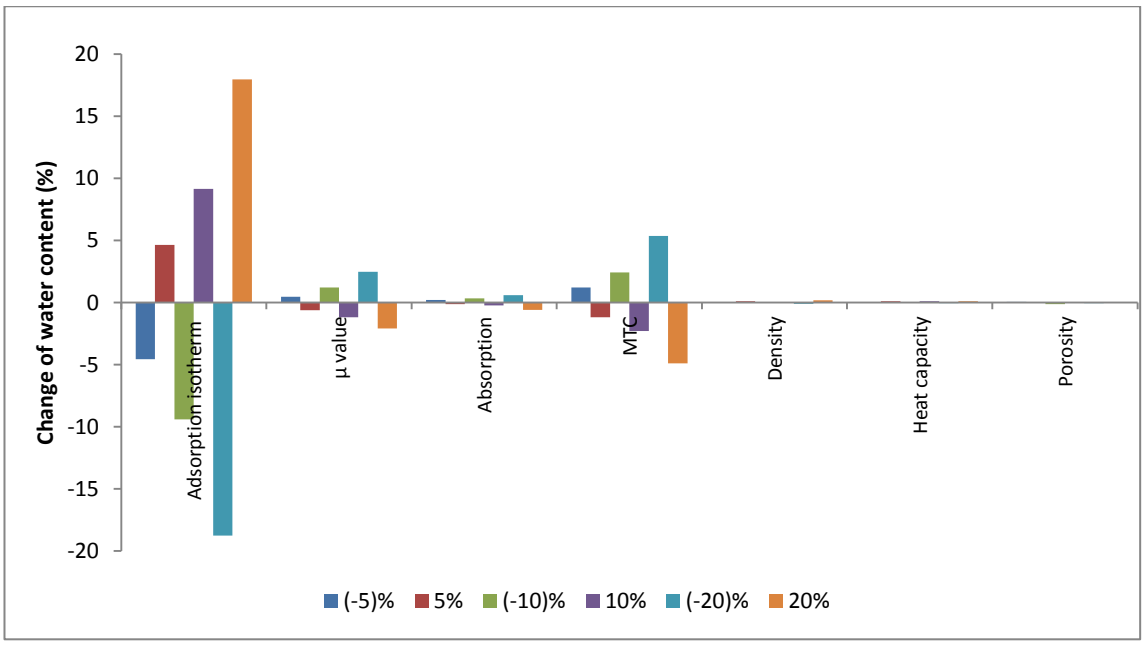


**Figure 8.4: Effect of (%) change of parameters on (%) change of water content in (hemp-2)-OSB interface from base case.**

In terms of relative humidity in the (hemp-2)-OSB interface, 20% change of the values of the input parameters from the base case causes less than 1% change in relative humidity as shown in figure 8.5. Figure 8.6 shows the similar data in narrower range of relative humidity for the purpose of clarity.

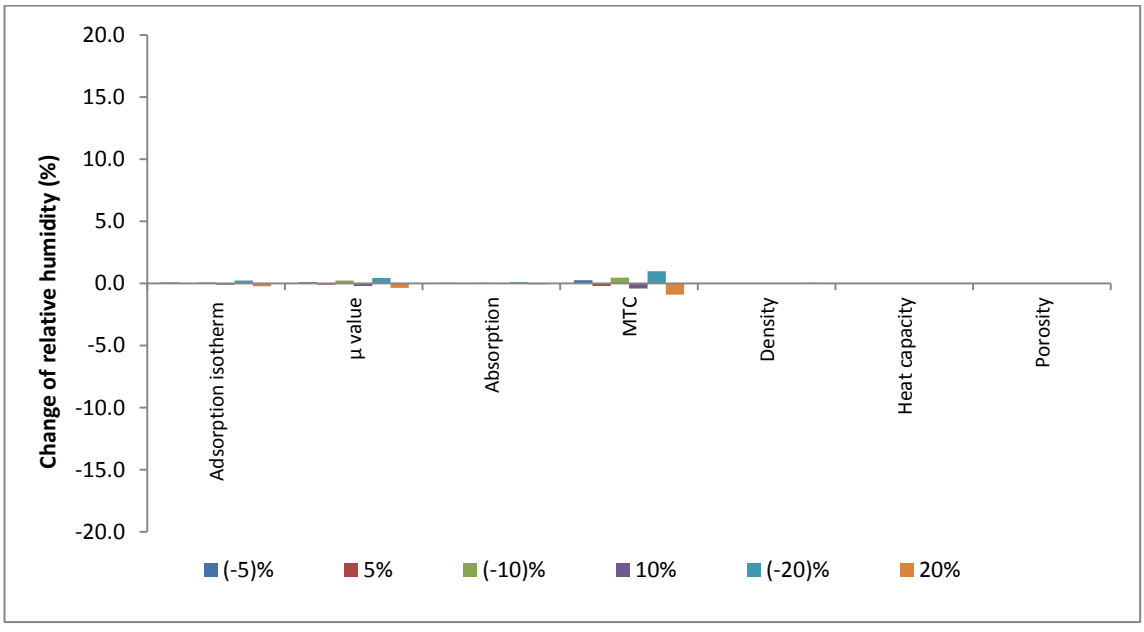


**Figure 8.5: Effect of (%) changes of parameters on (%) changes of relative humidity in (hemp-2)-OSB interface from base case.**


**Figure 8.6: Effect of (%) changes of parameters on (%) changes of relative humidity in (hemp-2)-OSB interface from base case (ranges of y axis narrowed down to ±1%).**

Similar observation can be made about the sensitivity of the parameters on insulation temperature, as shown in figure 8.7. Figure 8.8 presents the similar data in narrower range of temperature.

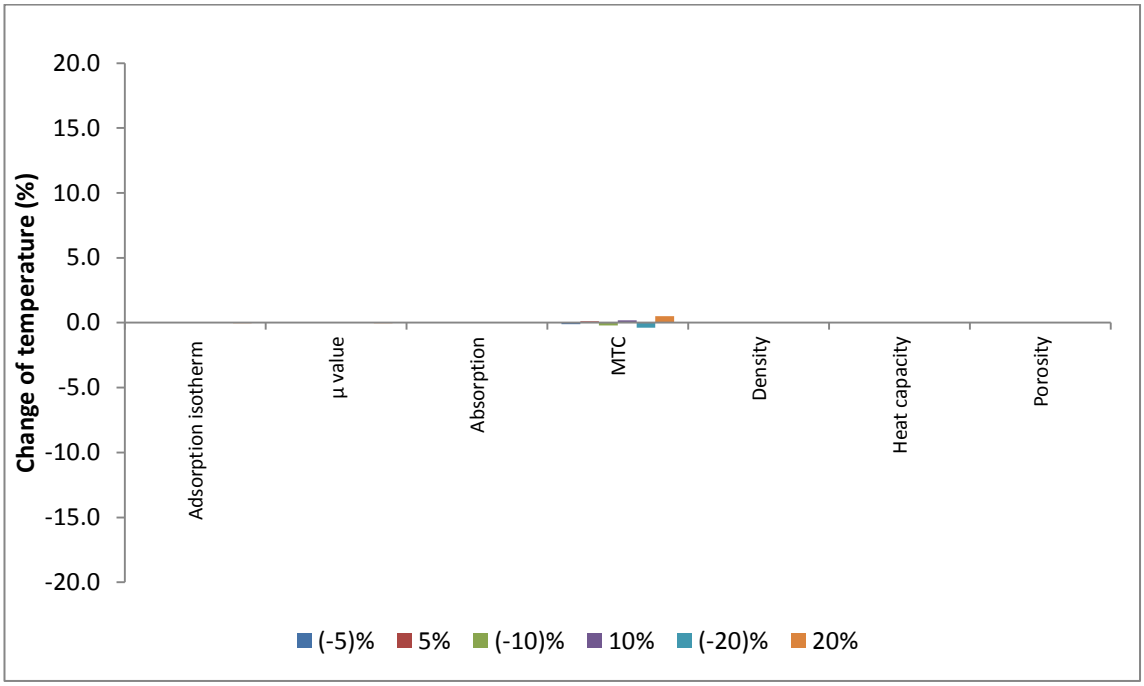


**Figure 8.7: Effect of (%) change of parameters on (%) change of temperature in hemp-2 from base case.**

From the sensitivity analysis it is apparent that adsorption isotherm is the most sensitive parameter, followed by moisture dependent thermal conductivity and vapour diffusion resistance factor. Data for these parameters were robustly measured during the experiments. The complete set of results of the sensitivity analysis can be found in Appendix F.

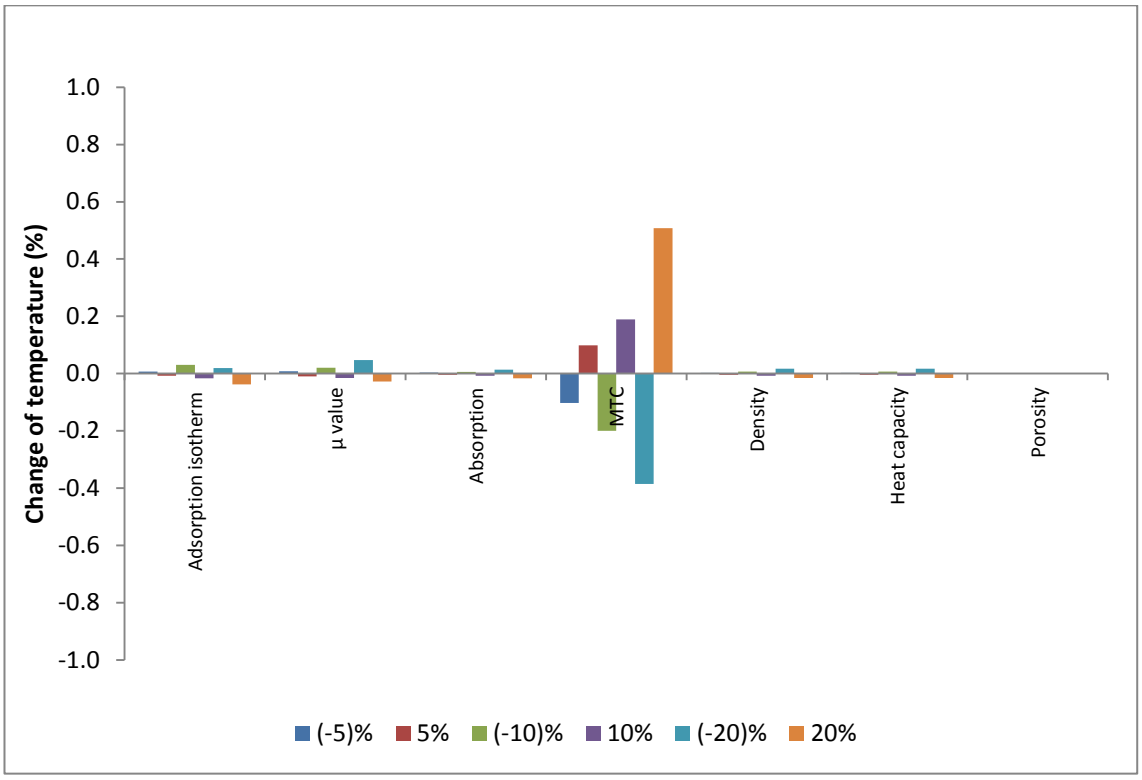


**Figure 8.8: Effect of (%) change of parameters on (%) change of temperature in hemp-2 from base case (ranges of y axis narrowed down to ±1%).**

## 8.3 Material selection and wall types

### *8.3.1 Materials*

Hemp-1, hemp-2 and stone wool insulation materials have been selected for the numerical simulations. Hemp-1 is higher in wood content and hemp-2 is higher in hemp content. All three insulation materials are already used in the in situ testing. The properties of these insulation materials can be found in Table 4.1 and Table 4.2 of chapter four.

### *8.3.2 Wall types*

The wall types assessed in the hygrothermal simulations are described in subsections 8.3.2.1 and 8.3.2.2.

### *8.3.2.1 Timber frame wall*

The selected timber frame wall panels for the current tests are shown in Figures 8.9 and 8.10. Figure 8.9 represents one of the common environmental practices for vapour open timber frame walls (Woolley, 2012). From interior to exterior, the wall is comprised of the following layers: gypsum plasterboard, insulation, oriented strand board, breather membrane, air layer and rain screen. The timber frame wall in Figure 8.10 differs from that in Figure 8.9 in its use of vapour barrier. The use of vapour barrier is a conventional practice for timber frame walls. The timber frame walls in Figures 8.9 and 8.10 will be referred to as 'wall-1' and 'wall-2', respectively.

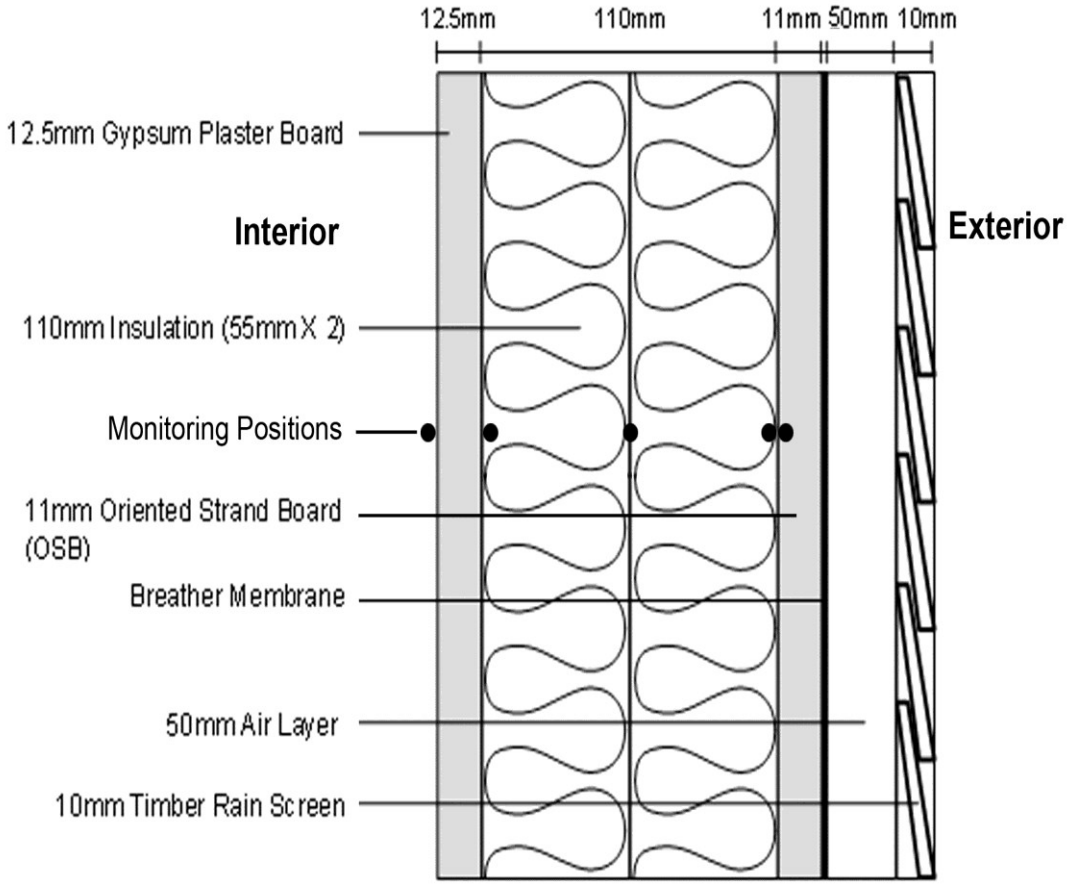


**Figure 8.9: The vertical cross section of the timber frame wall assembly without vapour barrier (wall-1).**

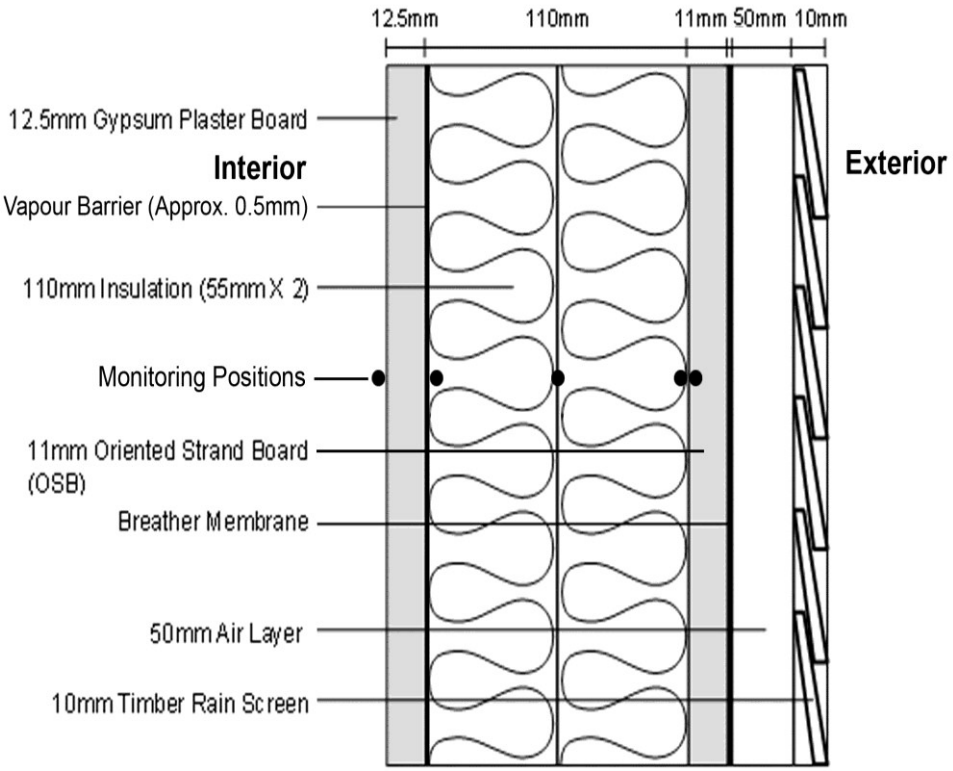


**Figure 8.10: The vertical cross section of the timber frame wall assembly with vapour barrier (wall-2).**

### *8.3.2.2 Solid brick wall with internal insulation*

Solid brick walls can be thermally refurbished by applying internal or external insulations. Applications of external insulations can be limited when it interferes with the external appearance of a building, in particular when the building is part of a block of individually owned buildings. There can also be problems with rainwater leakage and freeze-thaw cycle. In these situations, internal insulation is a preferable option. The key concerns associated with internally insulating a solid brick wall are condensation and mould growth in the interface of the insulation and the solid wall. To solve this problem, application of highly absorbent plaster between the solid wall and the insulation has been tested for stone wool insulation and claimed to be successful by Pavlik and Cerny (2009). Using a ventilated air gap over the insulation is a common practice in roofs and may be relevant to wall applications. In line with these concepts of using highly absorbent plaster and providing air gap between the insulation and the next layer of material, three types of internal applications of insulations on solid brick wall have been assessed in this chapter. Long-term hygrothermal performance is tested by using the WUFI software for the following types of brick wall assemblies in relation to the absence or presence of vapour barriers:

- Direct application of insulation materials on solid walls, as shown in Figures 8.11 and 8.12. The walls shown in Figures 8.11 and 8.12 will be referred to as ‘wall-3’ and ‘wall-4’, respectively.

- Application of air layer between the insulation and the solid wall, as shown in Figures 8.13 and 8.14. The walls shown in Figures 8.13 and 8.14 will be referred to as ‘wall-5’ and ‘wall-6’, respectively. However, the air layer is treated as ‘stagnant’ in the WUFI software as the WUFI software does not simulate the effect of ventilation.

- Application of lime plaster as a highly absorbent material between the insulation and the solid wall, as shown in Figures 8.15 and 8.16. The walls shown in Figures 8.15 and 8.16 will be referred to as ‘wall-7’ and ‘wall-8’, respectively.

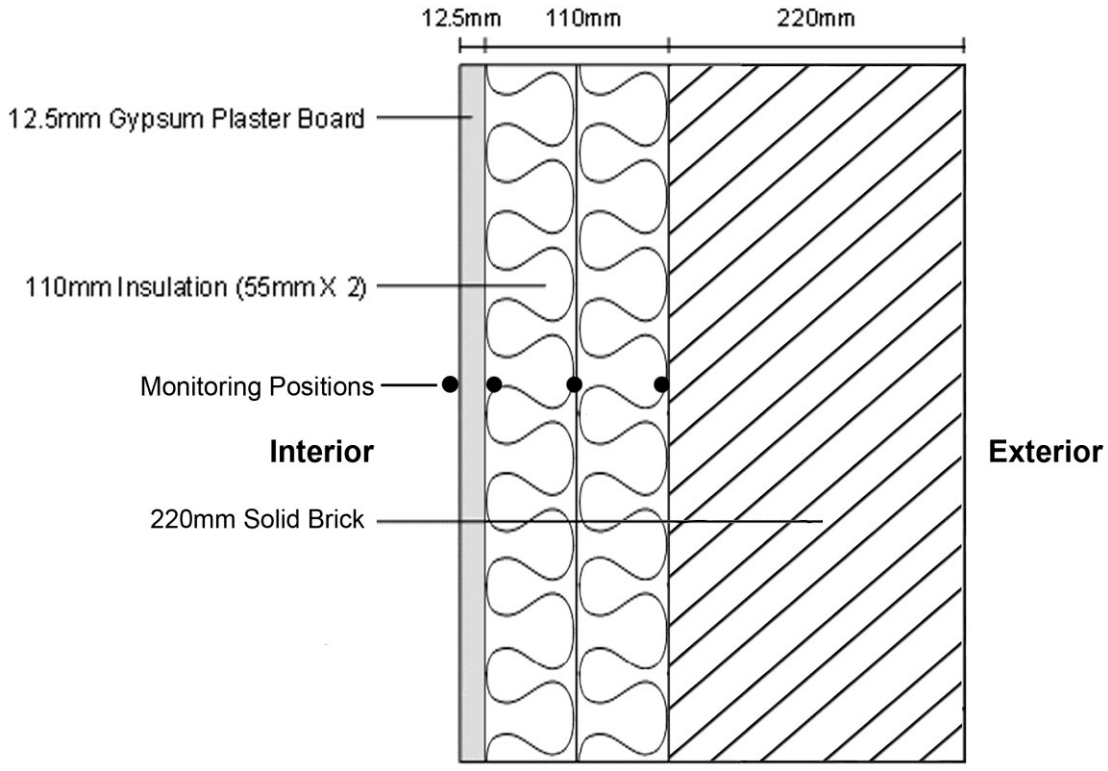


**Figure 8.11: The vertical cross section of the solid brick wall assembly without vapour barrier (wall-3).**

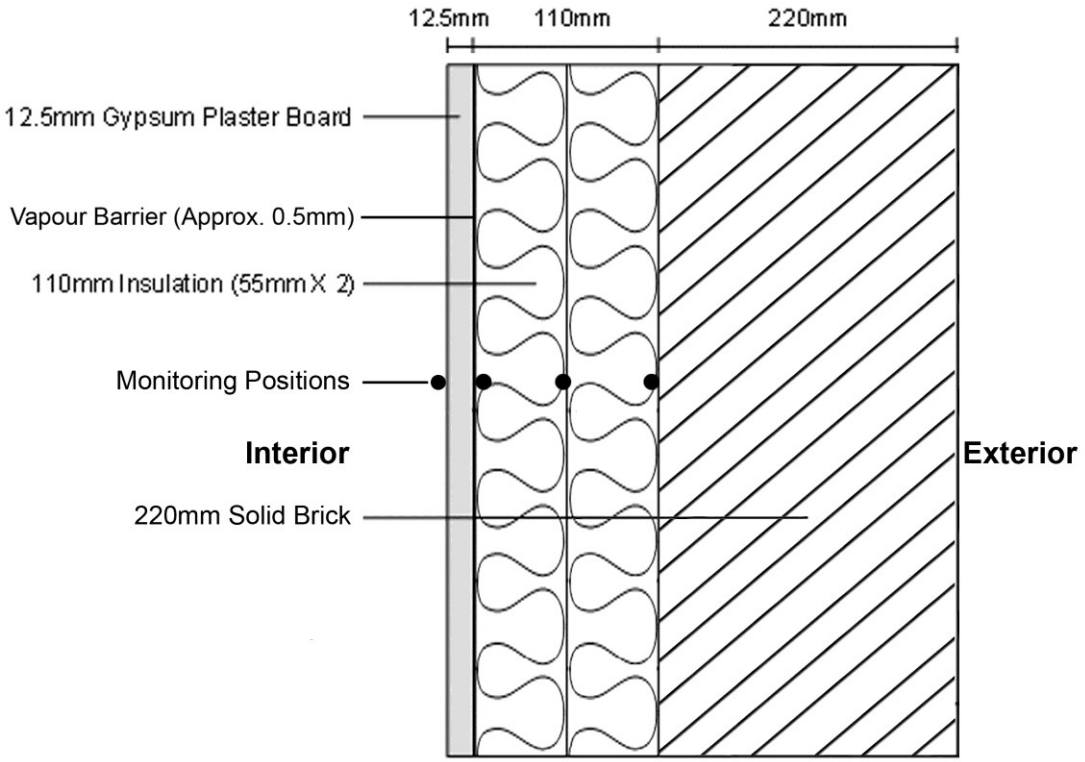


**Figure 8.12: The vertical cross section of the solid brick wall assembly with vapour barrier (wall-4).**

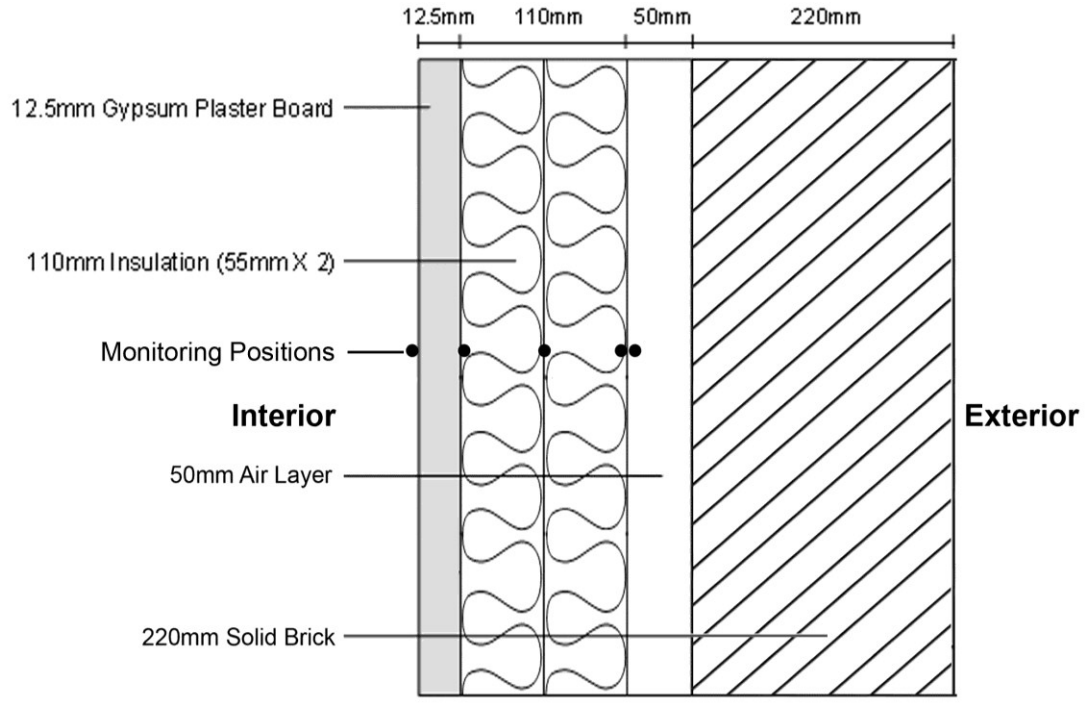


**Figure 8.13: The vertical cross section of the solid brick wall assembly (with air gap) without vapour barrier (wall-5).**

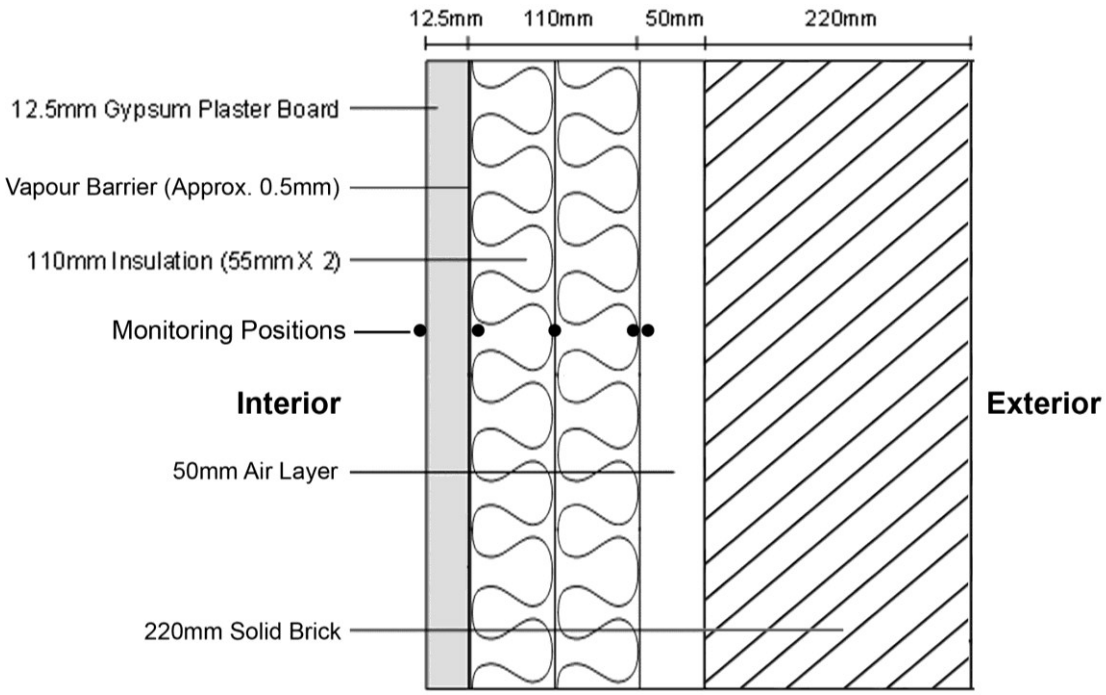


**Figure 8.14: The vertical cross section of the solid brick wall assembly (with air gap) assembly with vapour barrier (wall-6).**

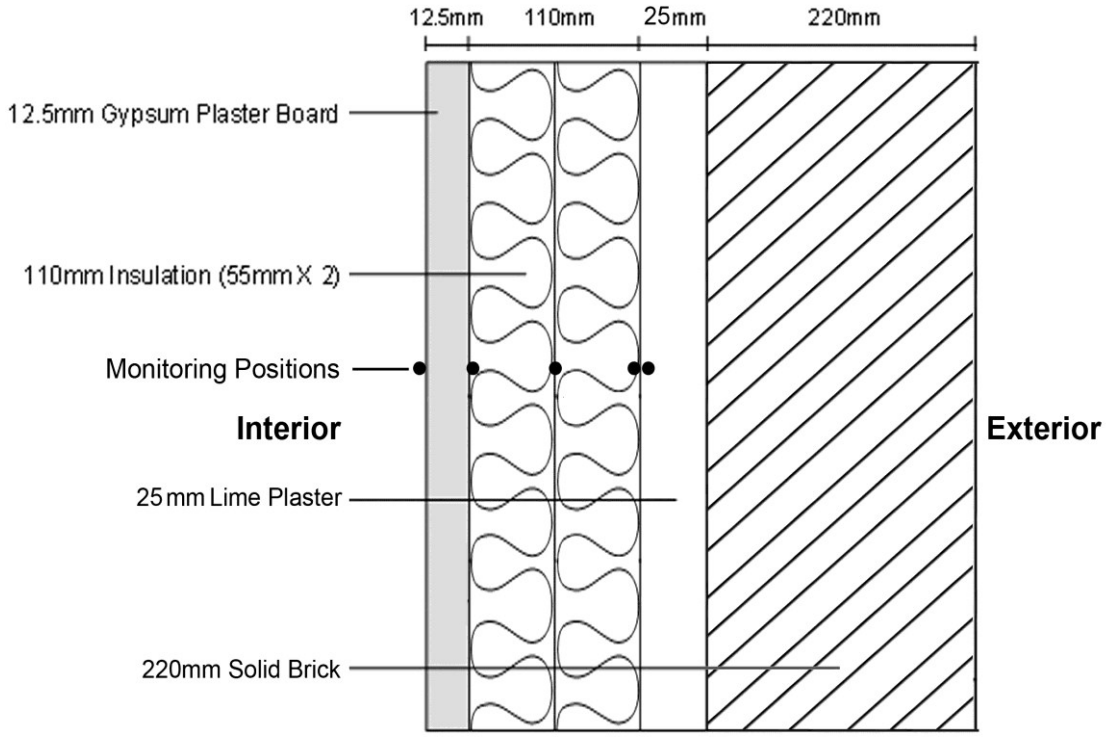


**Figure 8.15: The vertical cross section of the solid brick wall assembly (with lime plaster) without vapour barrier (wall-7).**

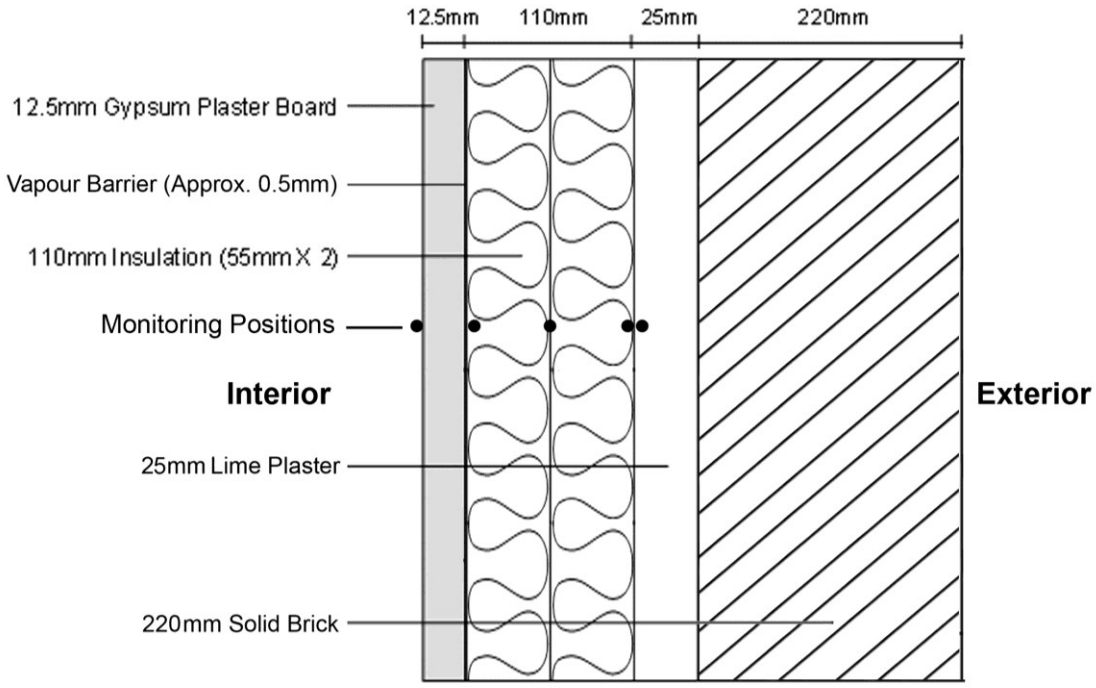


**Figure 8.16: The vertical cross section of the solid brick wall assembly (with lime plaster) with vapour barrier (wall-8).**

## 8.4 Boundary conditions

### *8.4.1 Interior temperature and relative Humidity*

Hygrothermal simulations using the WUFI software were carried out for high interior moisture load. The moisture loads were estimated by the WUFI software by following EN 15026 (2007) which is the European standard for assessing moisture transfer through building components and building elements by numerical simulation. In EN 15026, the internal temperature and the internal relative humidity can be determined from the external temperature and the external relative humidity.

### *8.4.2 Weather data*

The Test Reference Year (TRY) data of Edinburgh and Birmingham developed by the Chartered Institute of Building Services Engineers (CIBSE, 2012) were used as weather data. The TRY weather data includes the following weather parameters: dry bulb temperature, wet bulb temperature, mean sea level pressure, wind direction, wind speed, global radiation, and diffuse radiation. However, the TRY data do not contain rain data which is required for hygrothermal simulations. Rain data for Edinburgh and Birmingham were

collected from a global meteorological database, namely Meteonorm (Meteonorm, 2012) and were added to the existing TRY weather data.

Edinburgh was selected as a representative city of Scotland. Scotland is the coldest and wettest country in the UK (Met Office, 2013). On the contrary, Birmingham represents a mild temperate climate (Met Office, 2013). The numerical simulations in the WUFI software in one extreme and in one mild climatic condition helped to examine the hygrothermal performances of the thermal insulation materials in a wider climatic context.

## 8.5 Method of hygrothermal simulation

### *8.5.1: Material data*

The material data were obtained from a number of laboratory-based experiments, as described in chapter five, chapter six and chapter seven. Some of the material properties of stone wool insulation were available in the WUFI software. The following material properties were used: thermal conductivity, moisture adsorption, density, porosity, vapour diffusion resistance factor and water absorption coefficient. These data were used as inputs data to the WUFI software. In the WUFI material database, most of the fibrous insulation materials have the porosity value of 0.95. In the sensitivity analysis, it is shown that any error upto ±20% in porosity value will have negligible effect on the outcome of the hygrothermal simulation tests. Thereby, the porosity value of the selected fibrous insulation materials was assumed as 0.95.

### *8.5.2 Simulation period*

Prior to the final numerical simulations in the WUFI software, some trial simulations were run. During the trial simulation runs it was observed that for the hygrothermal interaction in the building envelope to come to an equilibrium condition, it took two years for a timber frame assembly and between two and three years for a brick masonry wall, depending on the configuration of the wall system. An example is shown in Figure 8.17 with the following configuration (from internal to external): 12.5 mm plaster board, 100 mm hemp-2 insulation and 220 mm solid brick wall. Simulation was run for six years in external weather condition of London and in high internal moisture load, as specified by the WUFI software. It can be observed for the particular configuration of the solid brick wall that equilibrium of water content and relative humidity was

reached in the second year. However, there were cases with solid brick walls where hygrothermal equilibrium was reached in three years. Consequently, the final simulation period for timber frame assemblies and for masonry walls were set as three years. Longer hygrothermal simulation runs were also performed when it was observed that the hygrothermal equilibrium was not reached in the walls within the stated period.

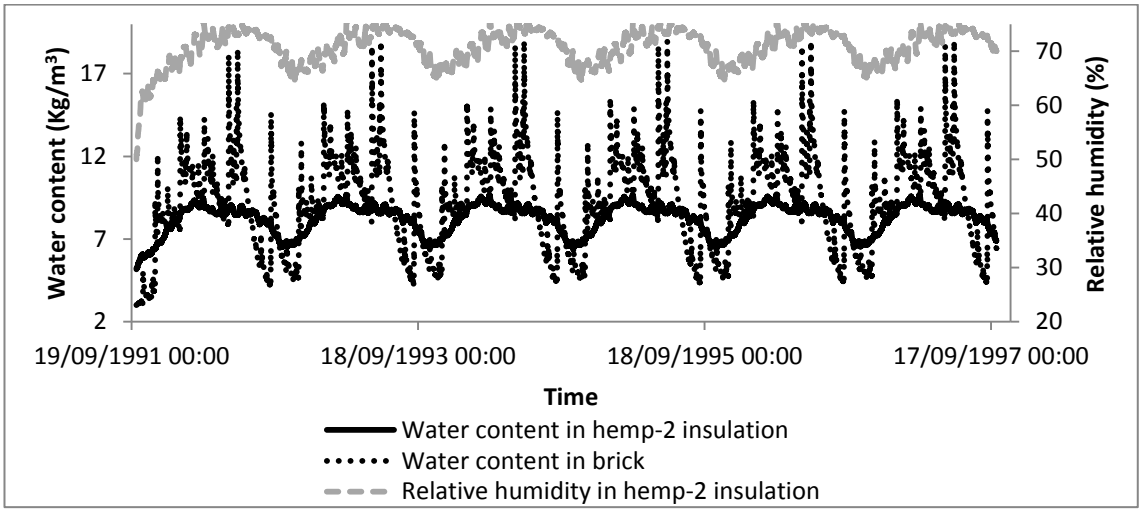


**Figure 8.17: The study of an insulated solid brick wall to explore the time required to reach hygrotheral equilibrium.**

### *8.5.3 Data analysis and comparison*

During the laboratory based experiments and the in situ tests, the following hygrothermal properties and conditions were assessed and compared: relative humidity, likelihood of condensation and mould spore germination in the interface between the external surface of the insulation and the layer next to it, thermal conductivity of the insulation materials during service conditions. The same hygrothermal properties and conditions were assessed and compared using the output data from WUFI simulations. The WUFI-Bio software was used to determine mould index and amount of mould growth. For each of the insulation installations, thermal conductivity was determined twice based on the heat flux measurements at the following two different locations: one at the inner surface of the wall and the other at the insulation-OSB or insulation-brick interface. The external temperature was determined from the CIBSE weather data of Birmingham and Edinburgh. The interior temperature was determined from the temperature of the air layer adjacent to the inner surface of the wall obtained from the WUFI simulation data. Thus thermal conductivity was determined from the heat flux, the temperature difference and the thickness of

the insulation materials using equations 7.1 and 7.2, as described in chapter seven.

## 8.6 Results and discussion

This section describes the results of the numerical hygrothermal simulations of timber frame and solid brick walls. One year only of the total simulation period was considered for data analysis, when the hygrothermal conditions were in equilibrium.

### *8.6.1 Timber frame wall in Edinburgh*

#### *8.6.1.1 Relative humidity conditions*

The relative Humidity conditions (RH) in the insulation-OSB interfaces of wall-1 and wall-2 for hemp-1, hemp-2 and stone wool insulation materials are shown in Figures 8.18 to 8.20.

In terms of relative humidity in the insulation-OSB interface of hemp-1 insulation, between wall-1 and wall-2, a maximum difference of 42% relative humidity can be observed during the month of March 1993 and a minimum difference of 9% relative humidity can be observed during the month of September 1992. During the whole period, the relative humidity is higher in wall-1 than in wall-2 as shown in Figure 8.18.

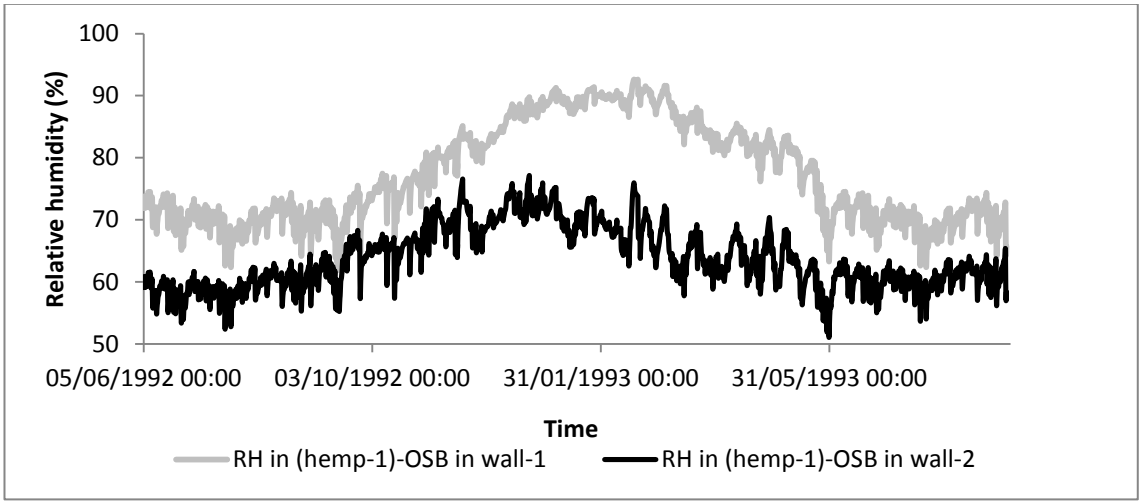


**Figure 8.18: Relative humidity conditions in the (hemp-1)-OSB interfaces in wall-1 and wall-2 in Edinburgh.**

In hemp-2 insulation, between wall-1 and wall-2, the maximum difference of 43% relative humidity in the insulation-OSB interface of hemp-2 insulation can be observed during the month of March 1993 and minimum difference of about

6% can be observed during the month of September 1992. In all the cases, the relative humidity is higher in wall-1 than in wall-2, as shown in Figure 8.19.

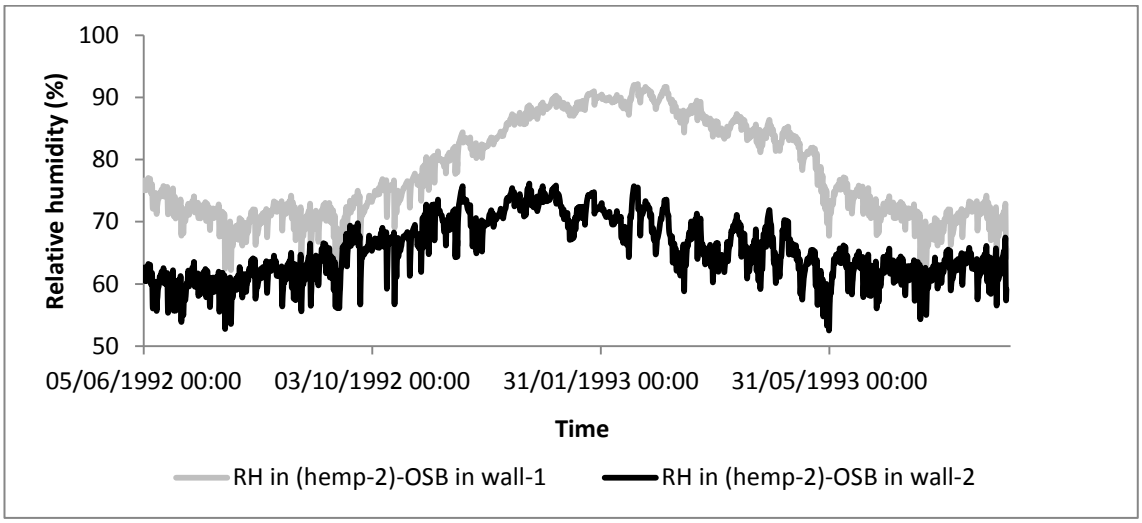


**Figure 8.19: Relative humidity conditions in the (hemp-2)-OSB interfaces in wall-1 and Wall-2 in Edinburgh.**

In stone wool insulation, between wall-1 and wall-2, the maximum difference of about 35% relative humidity in the insulation-OSB interface of hemp-1 insulation can be observed during the month of March 1993 and minimum difference of about 1% relative humidity can be observed during the month of September 1992. The relative humidity is always higher in the wall-1 than in wall-2, except during the period of minimum difference of relative humidity, when the relative humidity is lower in wall-1.

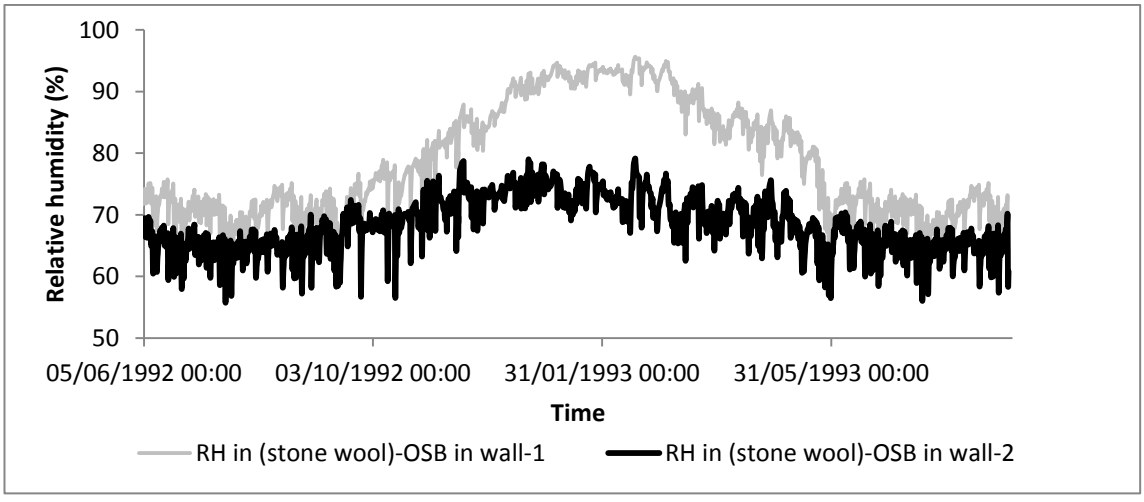


**Figure 8.20: Relative humidity conditions in the (stone wool)-OSB interfaces in wall-1 and wall-2 in Edinburgh.**

Figure 8.21 collates the data related to the Figures 8.18 to 8.20. It shows that the relative humidity values in the (stone wool)-OSB interfaces are about 3%

higher than the relative humidity values in (hemp-1)-OSB and (hemp-2)-OSB interfaces in the weather conditions of Edinburgh during high internal moisture loads. In low temperature conditions, 3% increase in relative humidity may cause interstitial condensation.

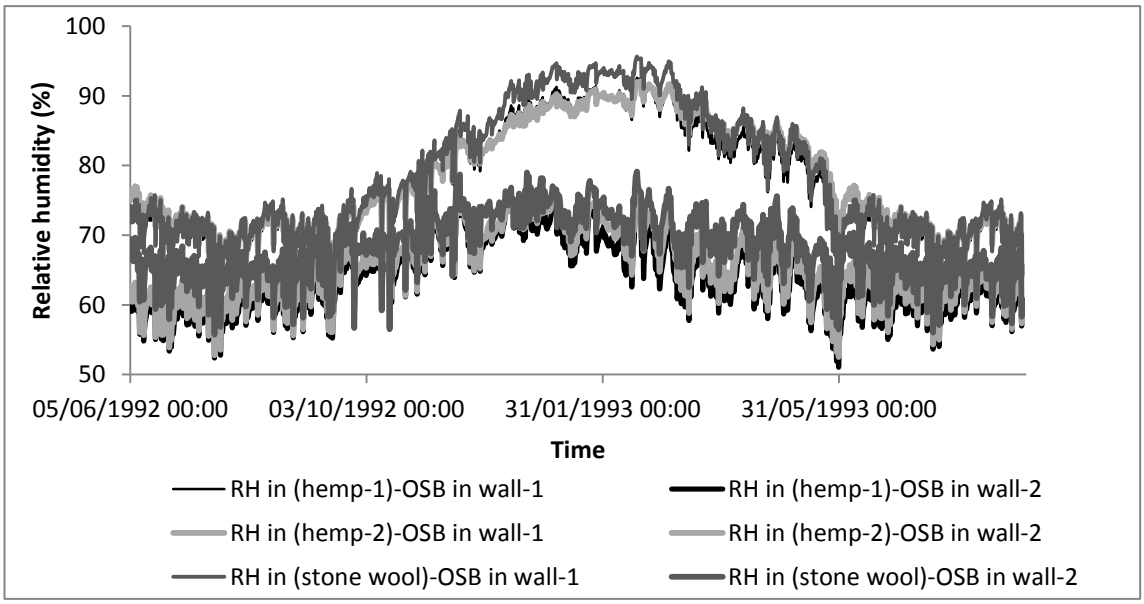


**Figure 8.21: The relative humidity conditions in the insulation-OSB interfaces in wall-1 and wall-2 in Edinburgh.**

The relative Humidity conditions in the inner surfaces of the insulation materials in wall-1 and wall-2 are shown in Figures 8.22 to 8.24. Since in all the cases relative humidity is less than 70% for more than 99% of the total period, there is no potential risk of condensation or mould growth on the inner surfaces of the insulation materials.

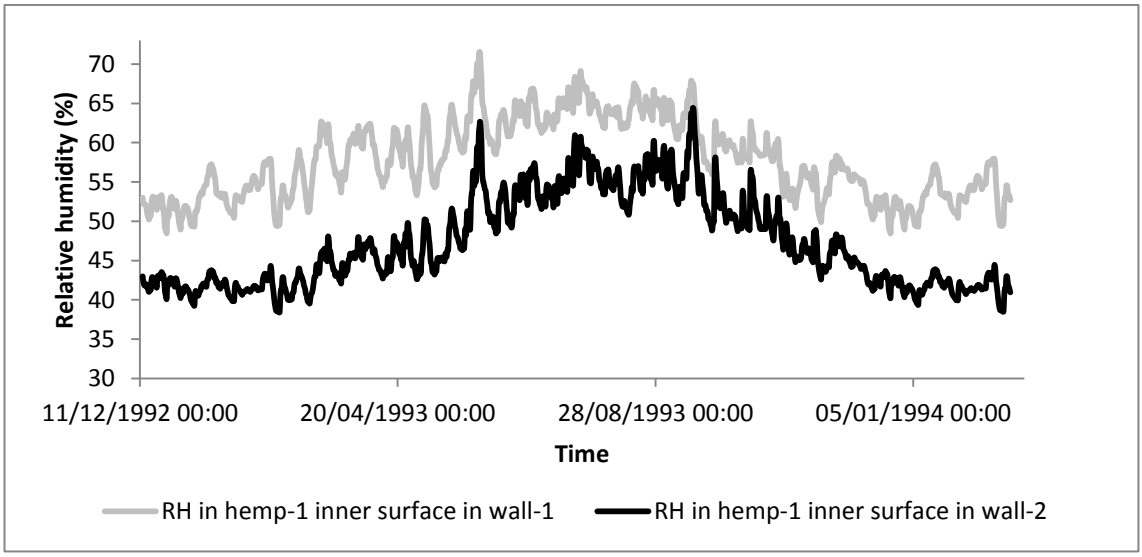


**Figure 8.22: The relative humidity conditions in the inner surfaces of the hemp-1 insulations in wall-1 and wall-2 in Edinburgh.**

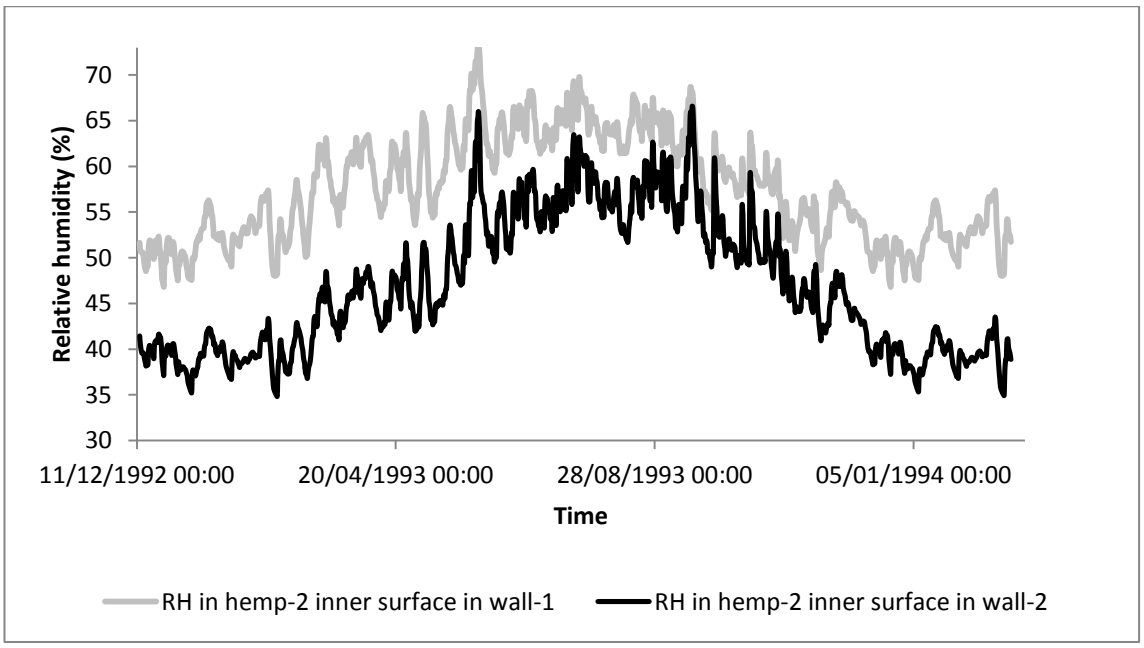


**Figure 8.23: The relative humidity conditions in the inner surfaces of the hemp-2 insulations in wall-1 and wall-2 in Edinburgh.**

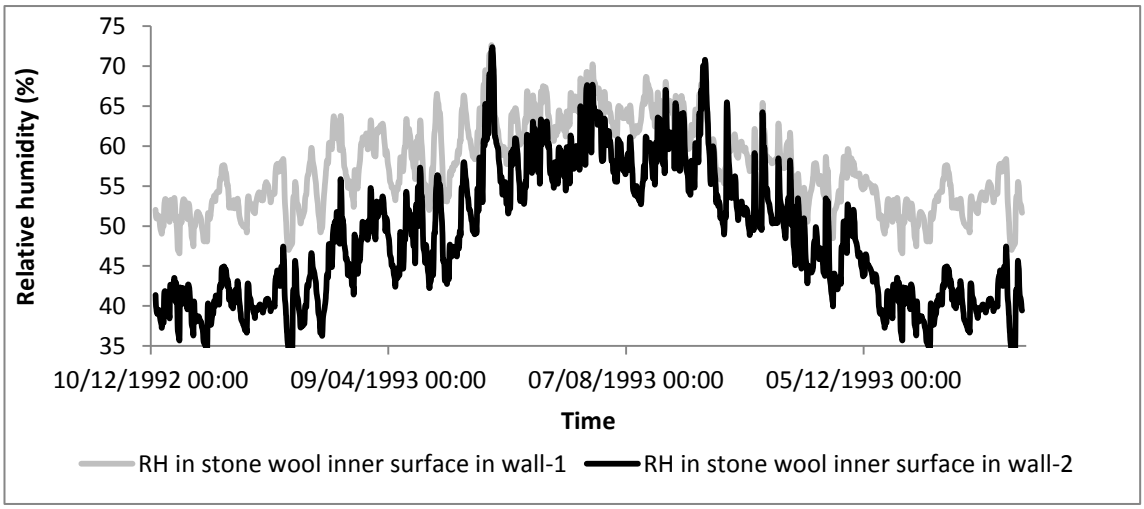


**Figure 8.24: The relative humidity conditions in the inner surfaces of the stone wool insulations in wall-1 and wall-2 in Edinburgh.**

### *8.6.1.2 Water content*

Water content in the OSB surfaces of the insulation-OSB interfaces are shown in Figures 8.25-8.27. In relation to the water content in the OSB surfaces, the highest differences between wall-1 and wall-2 are 39%, 40% and 50% for hemp-1, hemp-2 and stone wool insulation materials, respectively, with higher water content noted in wall-1 than in wall-2.

Figure 8.28 shows that the highest amount of water among the OSB surfaces of the walls analysed is in wall-1 incorporating stone wool insulation. Additionally,

the peak water content in stone wool is about 15% higher than that in hemp-1 and hemp-2 insulation materials during the same period.

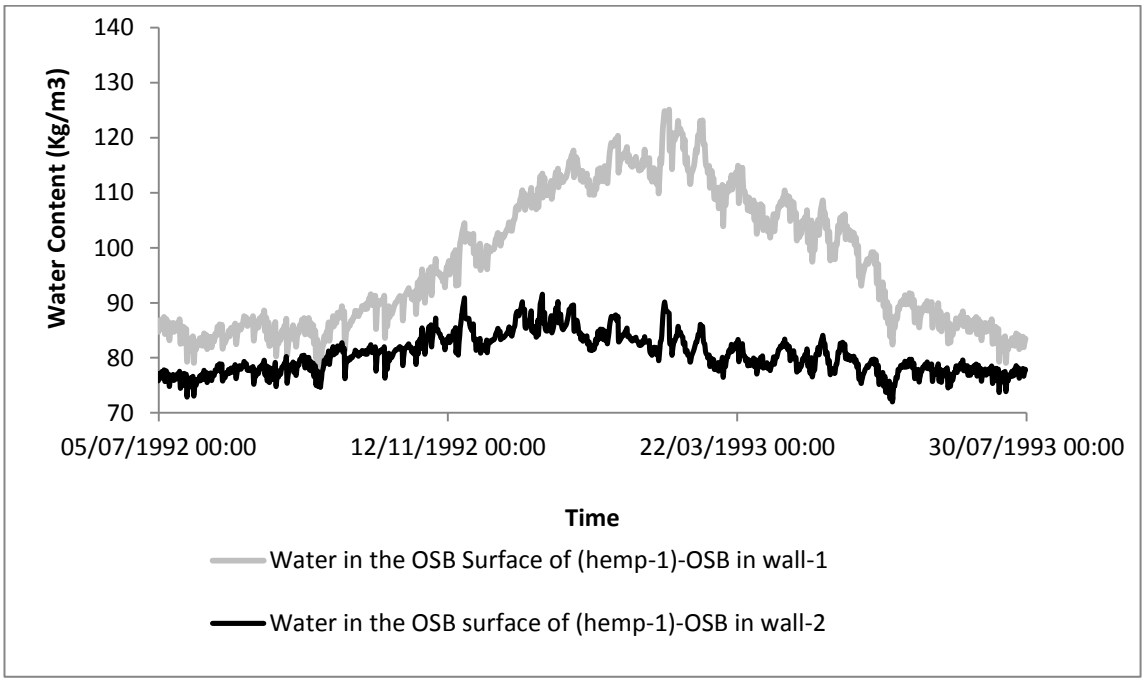


**Figure 8.25: Water content in the (hemp-1)-OSB interfaces of wall-1 and wall-2 in Edinburgh.**

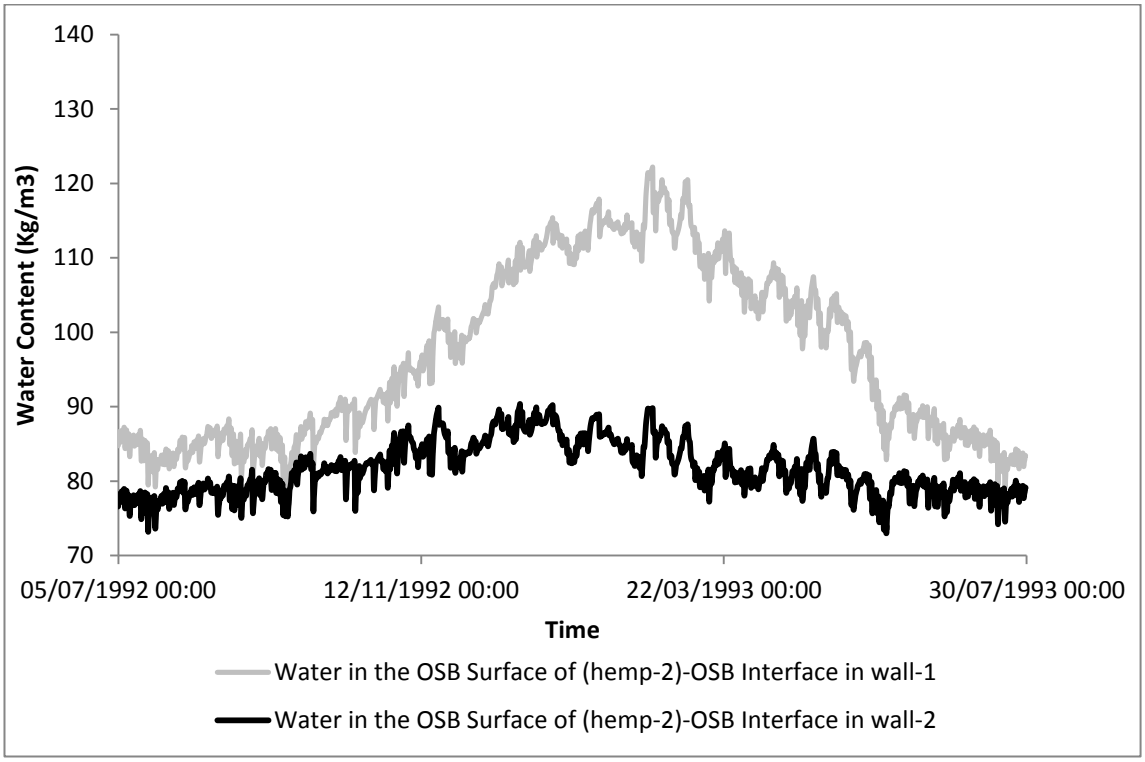


**Figure 8.26: Water content in the (hemp-2)-OSB interfaces of wall-1 and wall-2 in Edinburgh.**

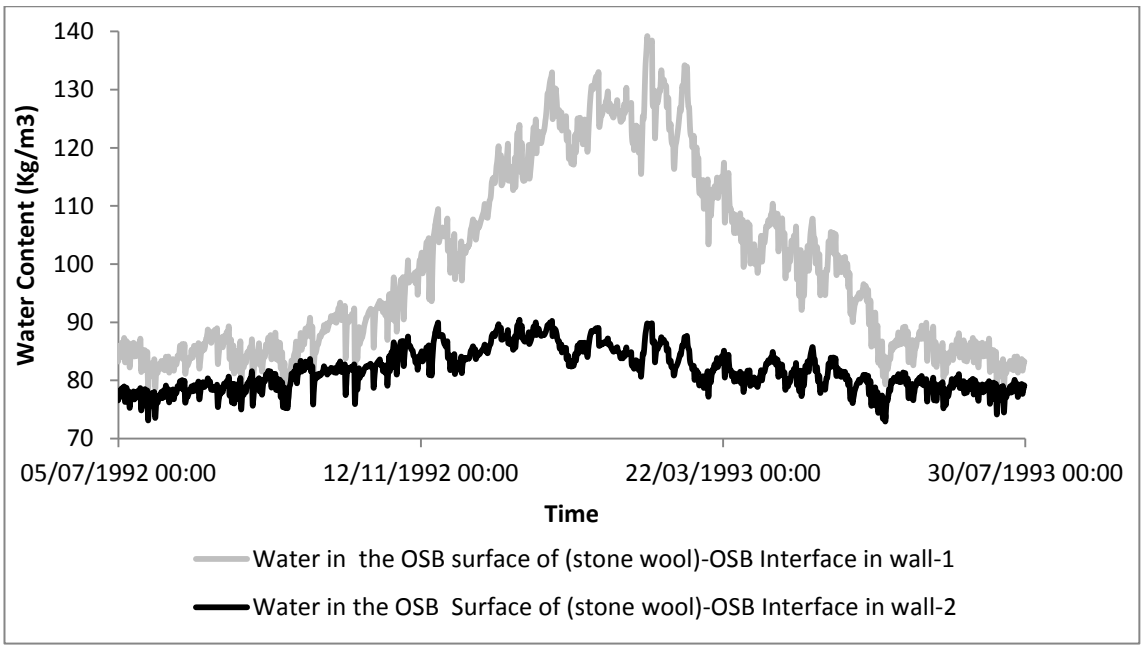


**Figure 8.27: Water content in the (stone wool)-OSB interfaces of wall-1 and wall-2 in Edinburgh.**

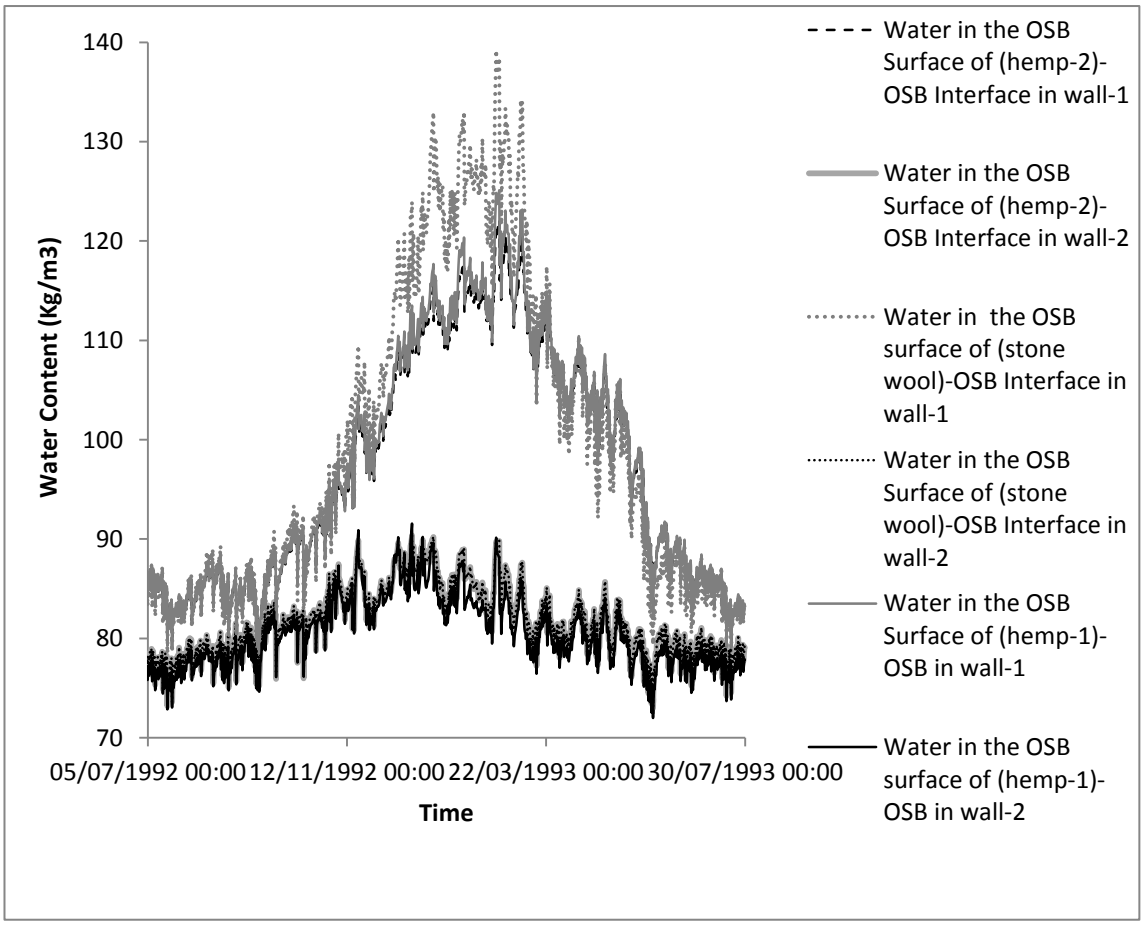


**Figure 8.28: Water content in the insulation-OSB interfaces of wall-1 and wall-2 in Edinburgh.**

#### *8.6.1.3 Mould spore germination and mould growth*

***Wall-1***

The water content in the mould spore in relation to the critical water content for spore germination is shown in Figures 8.29 to 8.34. The hygrothermal conditions in the insulation-OSB interfaces in relation to the Sedlbauer's isopleth are shown in the Figures 8.35 to 8.40. Figures 8.29, 8.31 and 8.33, in relation to the wall-1, show that for hemp-1, hemp-2 and stone wool insulation materials, the water content in the spores are higher than the critical water content for mould spore germination. It implies that mould spore germination is likely to occur in the insulation materials installed in the timber frame walls without vapour barrier. The increased water content remains in the insulation interfaces for 54%, 59% and 59% time of one year in hemp-1, hemp-2 and stone wool insulation materials, respectively.

As for hygrothermal conditions in wall-1, as shown in Figures 8.35, 8.37 and 8.39, there are occurrences when the hygrothermal conditions (the plots of relative humidity versus temperature) are between the LIM isopleth and the 2-day isopleth for hemp-1 and hemp-2 insulation materials. For stone wool insulation in wall-1, there are occurrences when the hygrothermal conditions are between the LIM isopleth and the 1-day isopleth.

***Wall-2***

In wall-2, the water content in the mould spores is always below the critical water content for all three insulation materials, as shown in Figures 8.30, 8.32 and 8.34. The hygrothermal conditions in the insulation-OSB interfaces of all three insulation materials are always below the LIM isopleth, as shown in Figures 8.36, 8.38 and 8.40.

Therefore, according to the analysis of the output data of the numerical simulations, mould growth is unlikely in timber frame walls with vapour barrier.

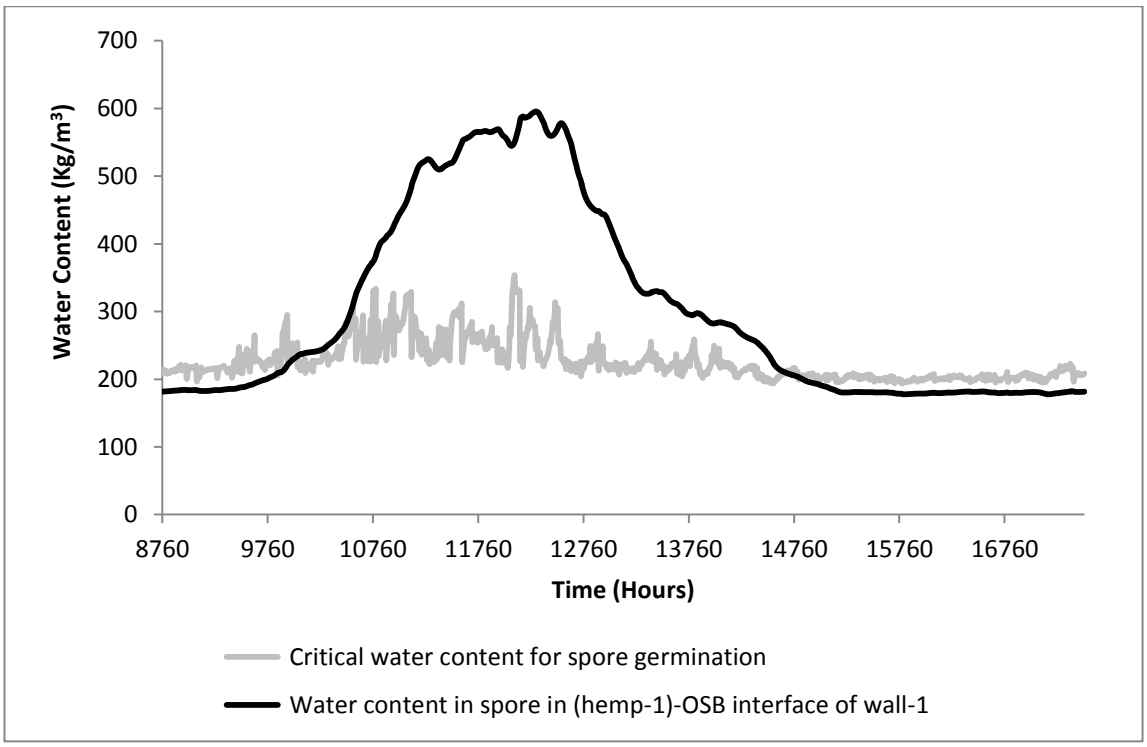


**Figure 8.29: Estimated and critical water content in the mould spore in the (hemp-1)-OSB interface of the timber frame walls without vapour barrier (wall-1) in Edinburgh.**

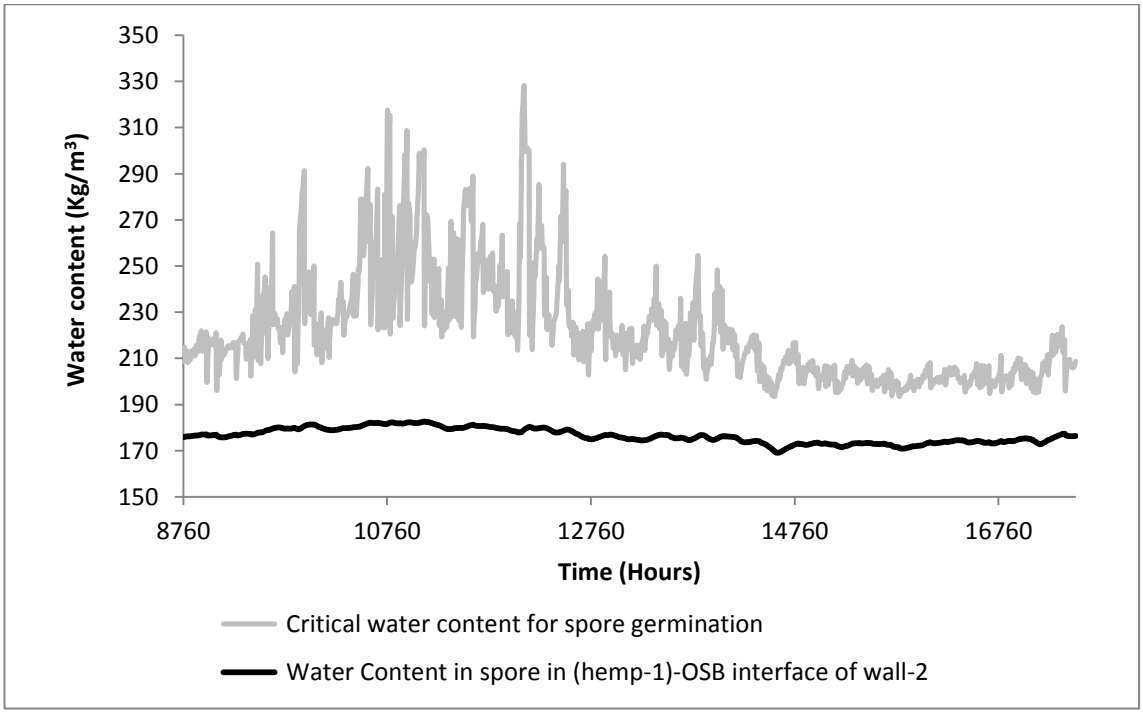


**Figure 8.30: Estimated and critical water content in the mould spore in the (hemp-1)-OSB interface of the timber frame walls with vapour barrier (wall-2) in Edinburgh.**

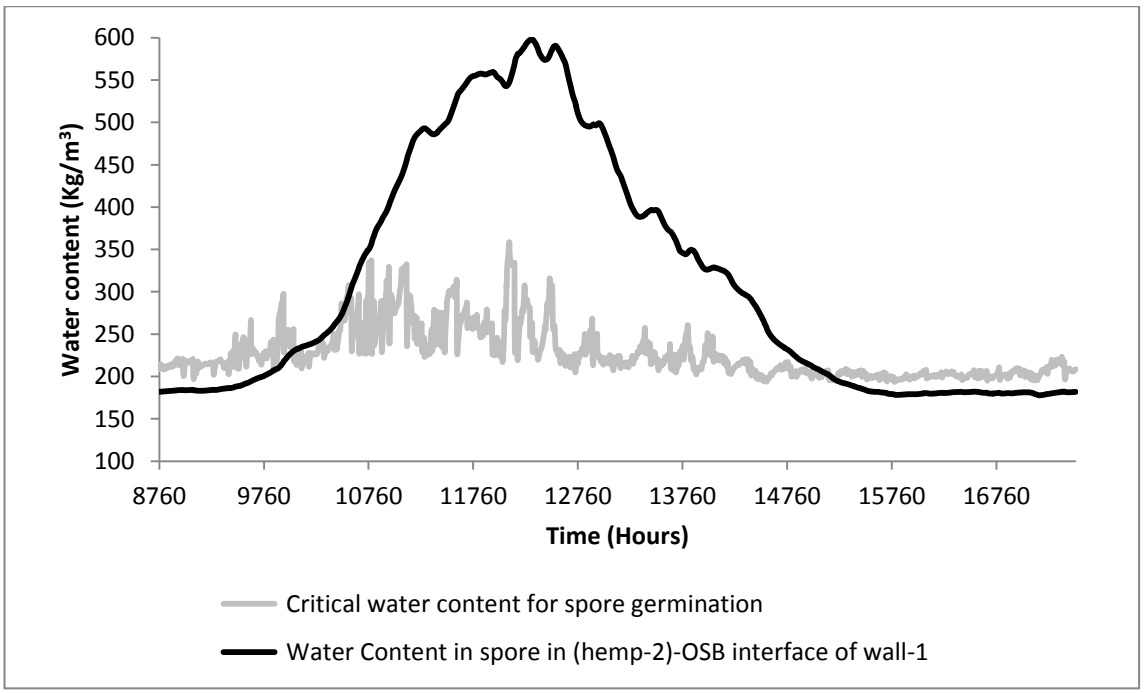


**Figure 8.31: Estimated and critical water content in the mould spore in the (hemp-2)-OSB interface of the timber frame walls without vapour barrier (wall-1) in Edinburgh.**

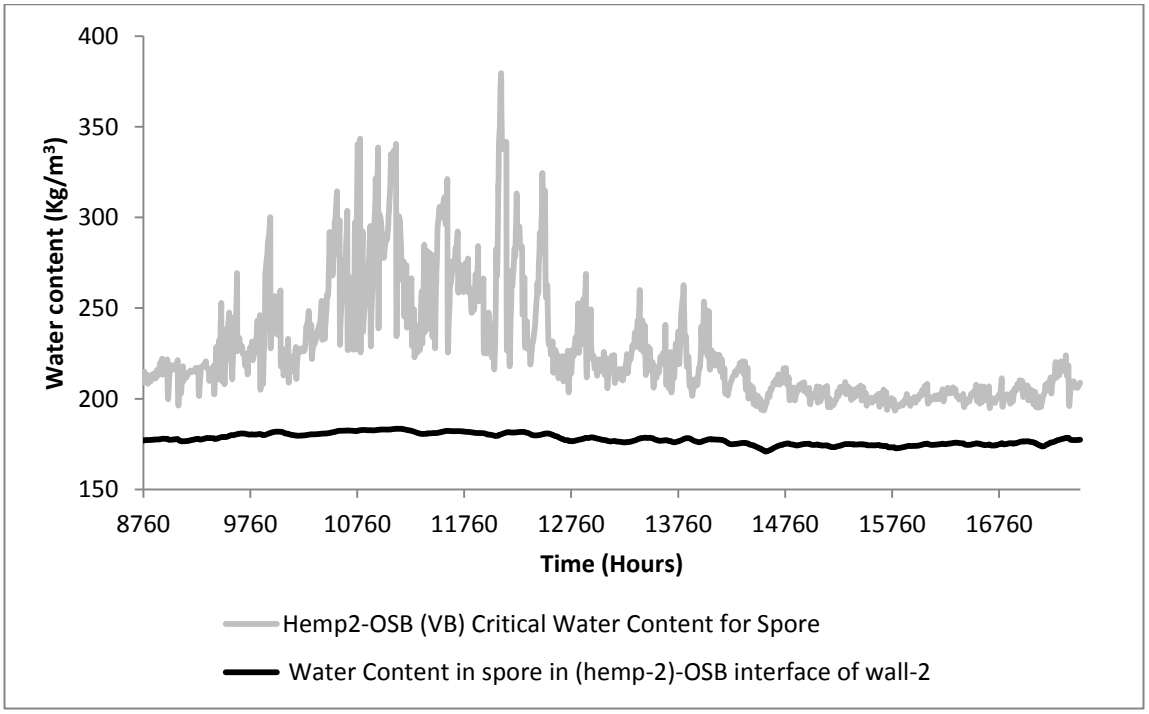


**Figure 8.32: Estimated and critical water content in the mould spore in the (hemp-2)-OSB interface of the timber frame walls with vapour barrier (wall-2) in Edinburgh.**

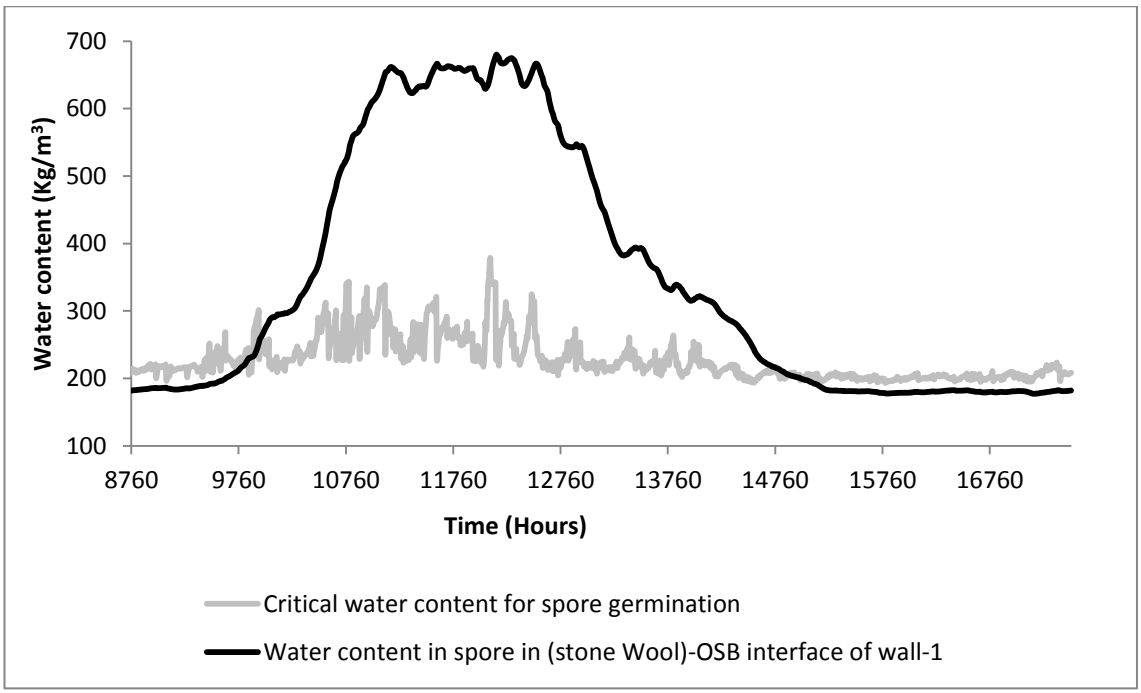


**Figure 8.33: Estimated and critical water content in the mould spore in the (stone wool)-OSB interface of the timber frame walls without vapour barrier (wall-1) in Edinburgh.**

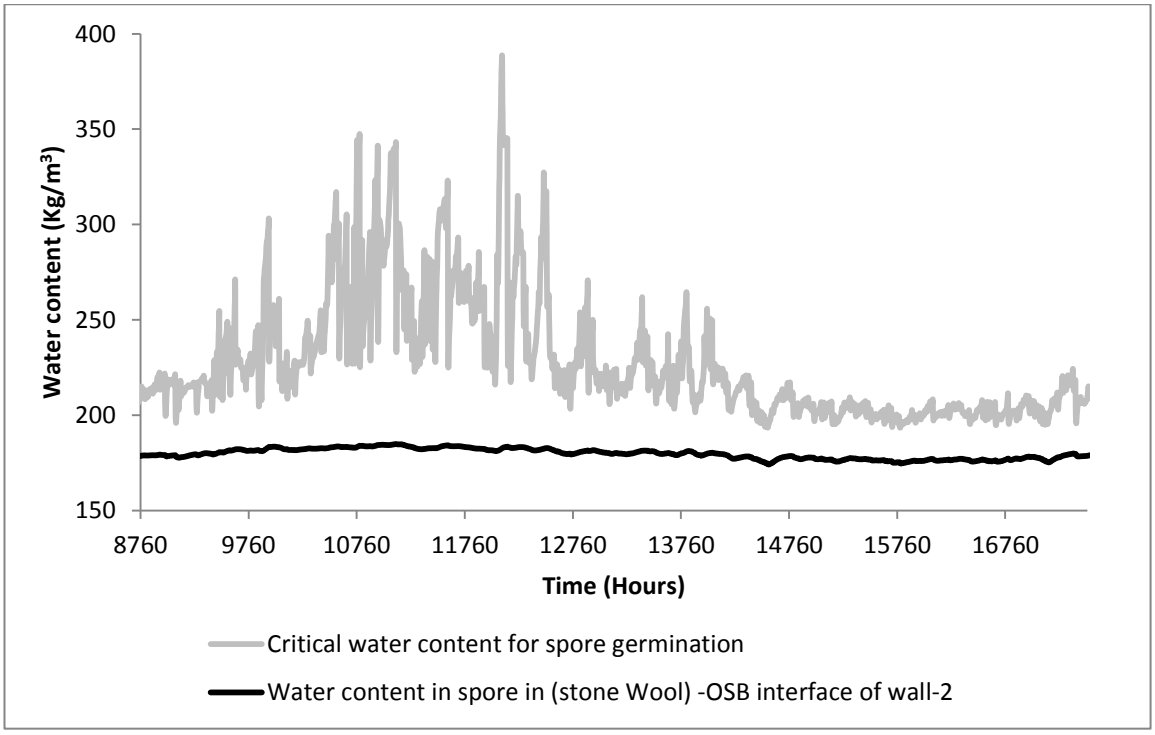


**Figure 8.34: Estimated and critical water content in the mould spore in the (stone wool)-OSB interface of the timber frame wall with vapour barrier (wall-2) in Edinburgh.**

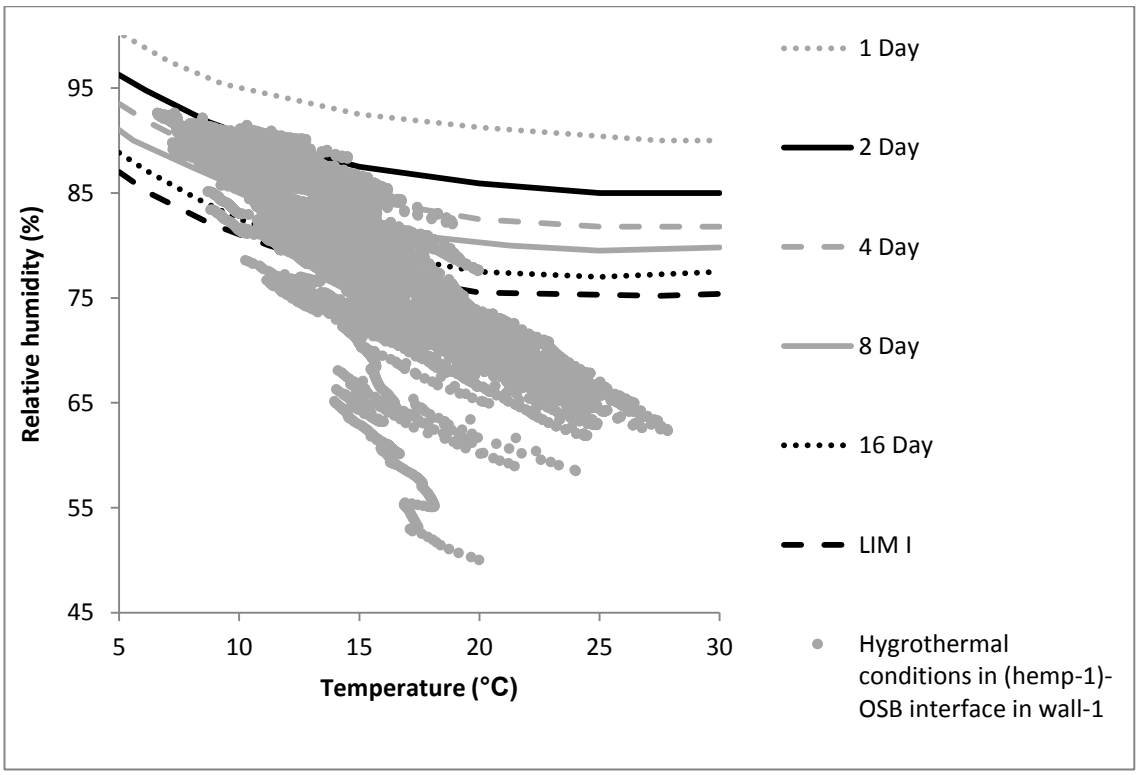


**Figure 8.35: Hygrothermal condition in the (hemp-1)-OSB interface of timber frame wall without vapour barrier (wall-1) in Edinburgh.**

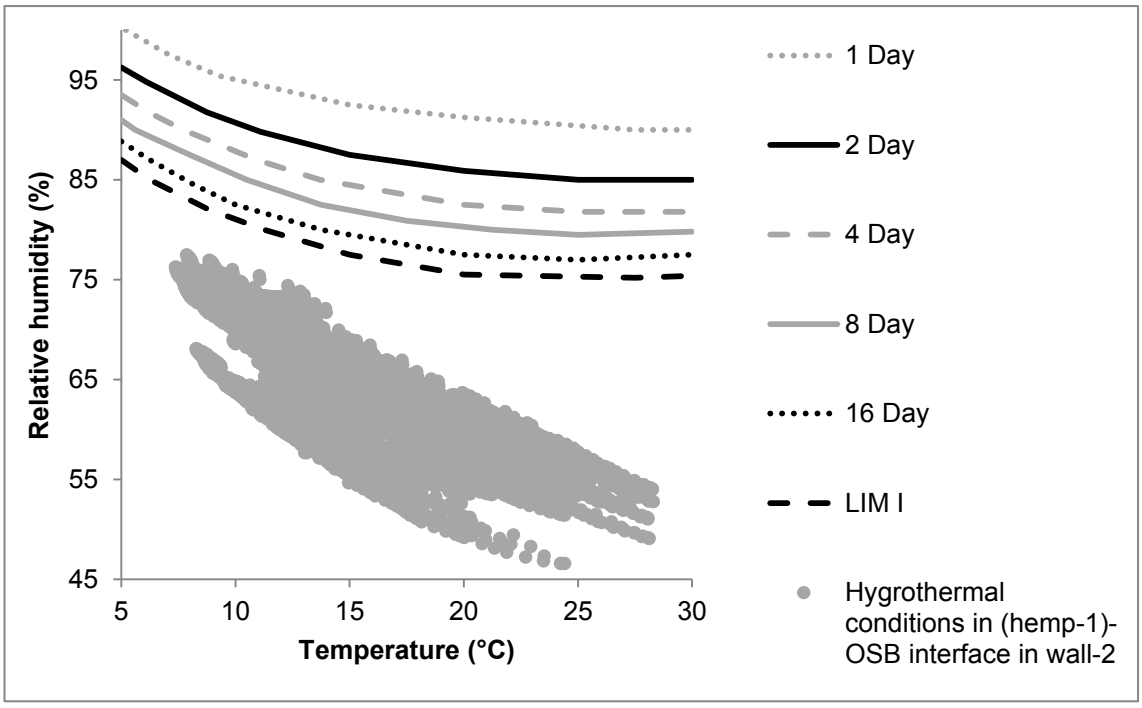


**Figure 8.36: Hygrothermal condition in the (hemp-1)-OSB interface of timber frame wall with vapour barrier (wall-2) in Edinburgh**.

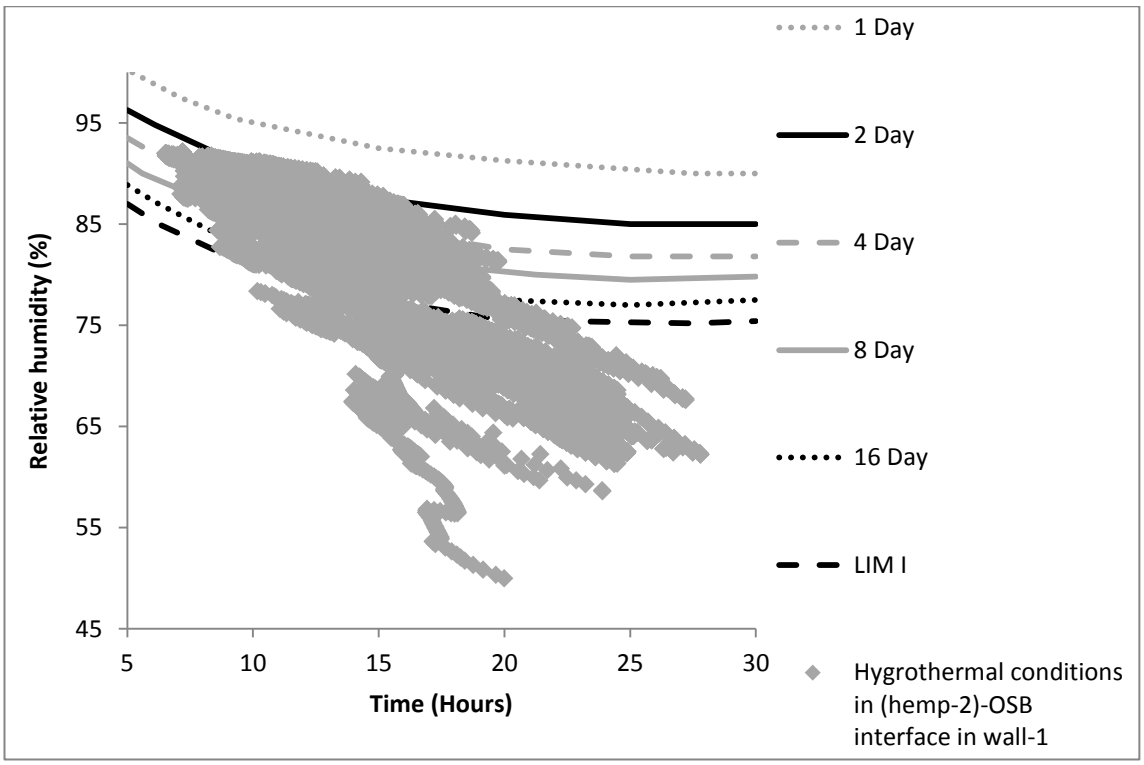


**Figure 8.37: Hygrothermal condition in the (hemp-2)-OSB interface of timber frame wall without vapour barrier (wall-1) in Edinburgh.**

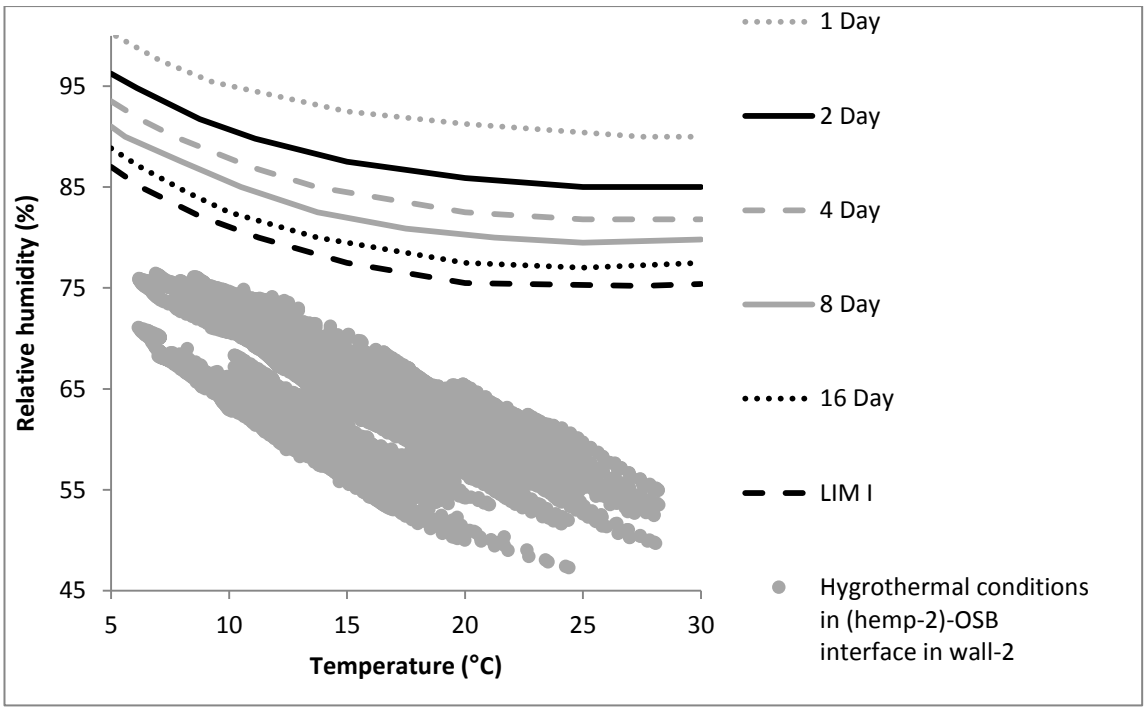


**Figure 8.38: Hygrothermal condition in the (hemp-2)-OSB interface of timber frame wall with vapour barrier (wall-2) in Edinburgh.**

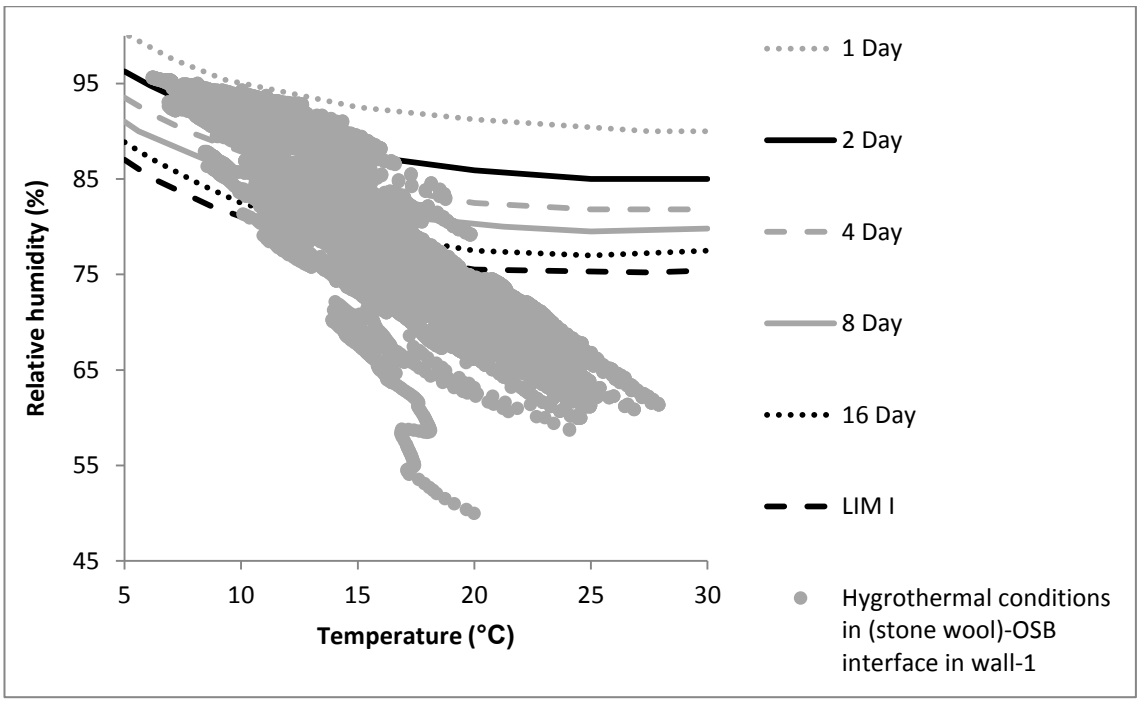


**Figure 8.39: Hygrothermal condition in the (stone wool-OSB) interface of timber frame wall without vapour barrier (wall-1) in Edinburgh.**

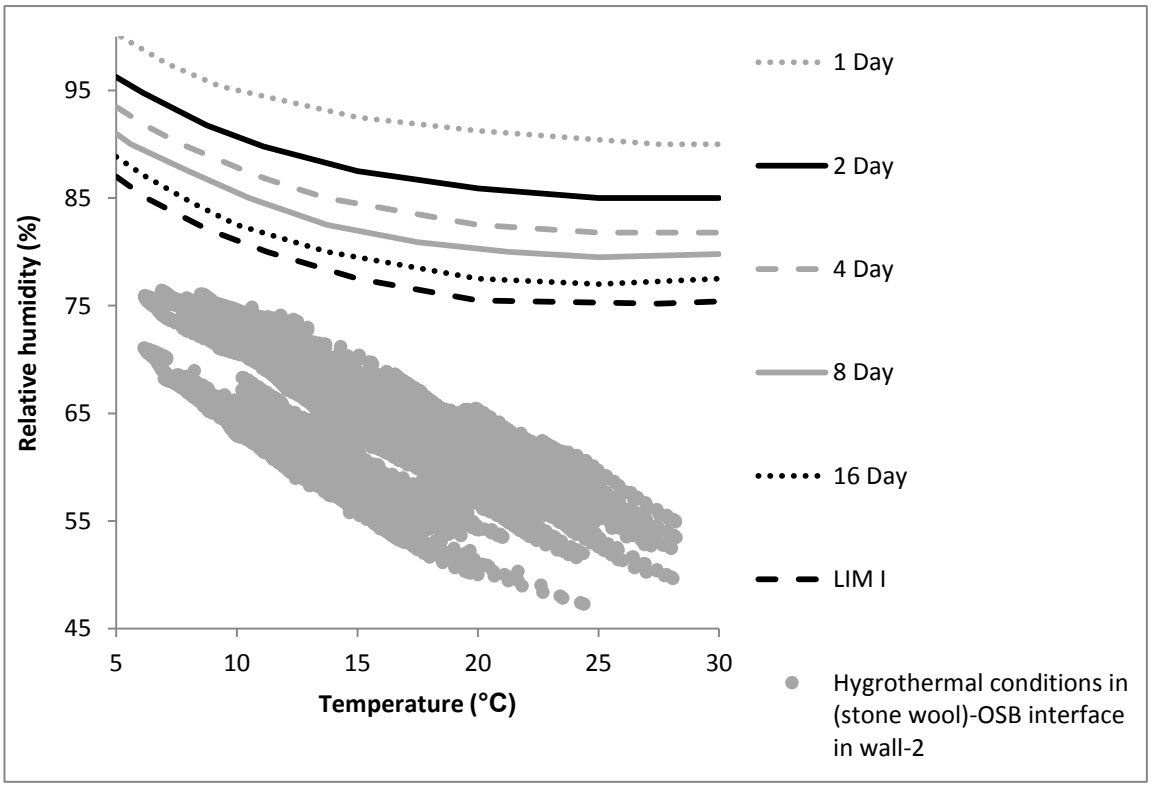


**Figure 8.40: Hygrothermal condition in the (stone wool)-OSB interface of timber frame wall with vapour barrier (wall-2) in Edinburgh.**

#### *8.6.1.4 Mould index and mould growth*

Figures 8.41 and 8.42 show the mould index and rate of mould growth, respectively, in the insulation-OSB interfaces of the timber frame walls incorporating hemp-1, hemp-2 and stone wool. For wall-2, both mould index and rate of mould growth is zero in all the insulation-OSB interfaces.

For wall-1, the rate of mould growth in stone wool insulation is about 60% and 44% higher than in hemp-1 and hemp-2 insulations, respectively, during the second year. In Figure 8.41, it can be noted that the mould growth index of stone wool insulation is about 60% and 44% higher than the mould growth index for hemp-1 and hemp-2 insulations, respectively. However, beyond the threshold of 570 mm of mould growth, mould index is always 6. For this reason, during the third year, Figure 8.41 shows equal mould index for all the insulations irrespective of the varying rate of mould growth in hemp-1, hemp-2 and stone wool insulation.

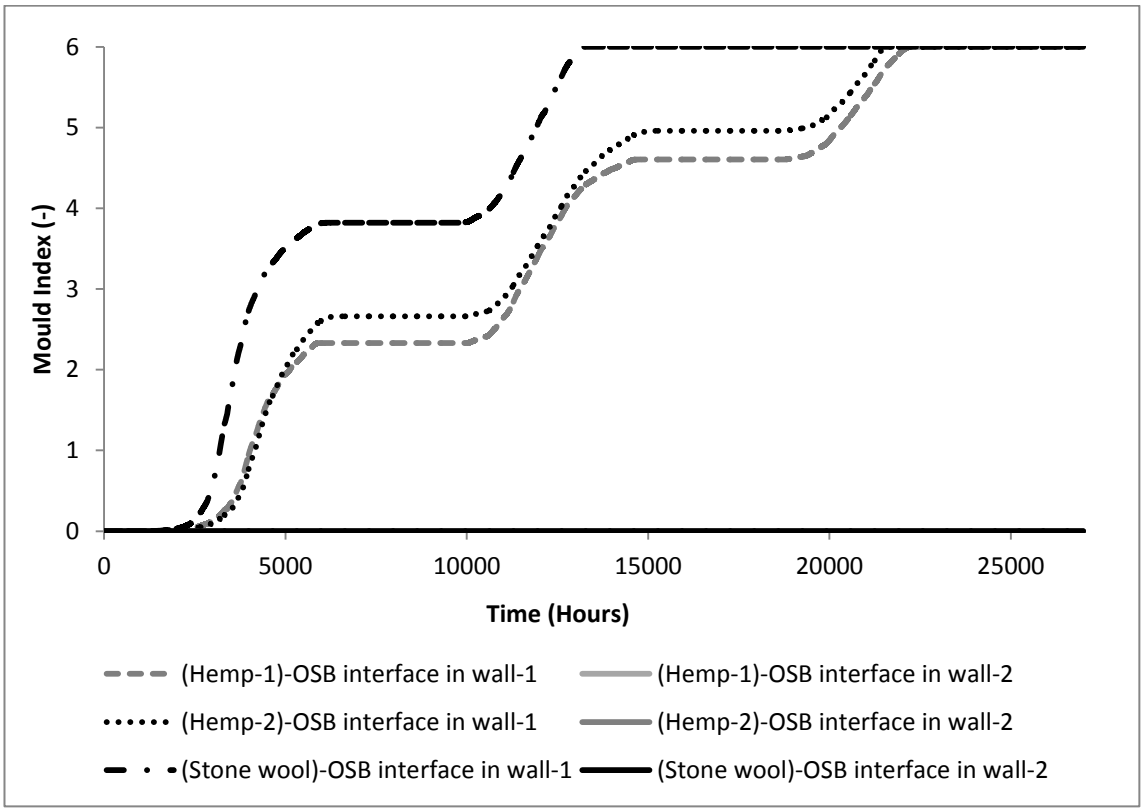


**Figure 8.41: Mould index in insulation-OSB interfaces for different insulations in Edinburgh.**

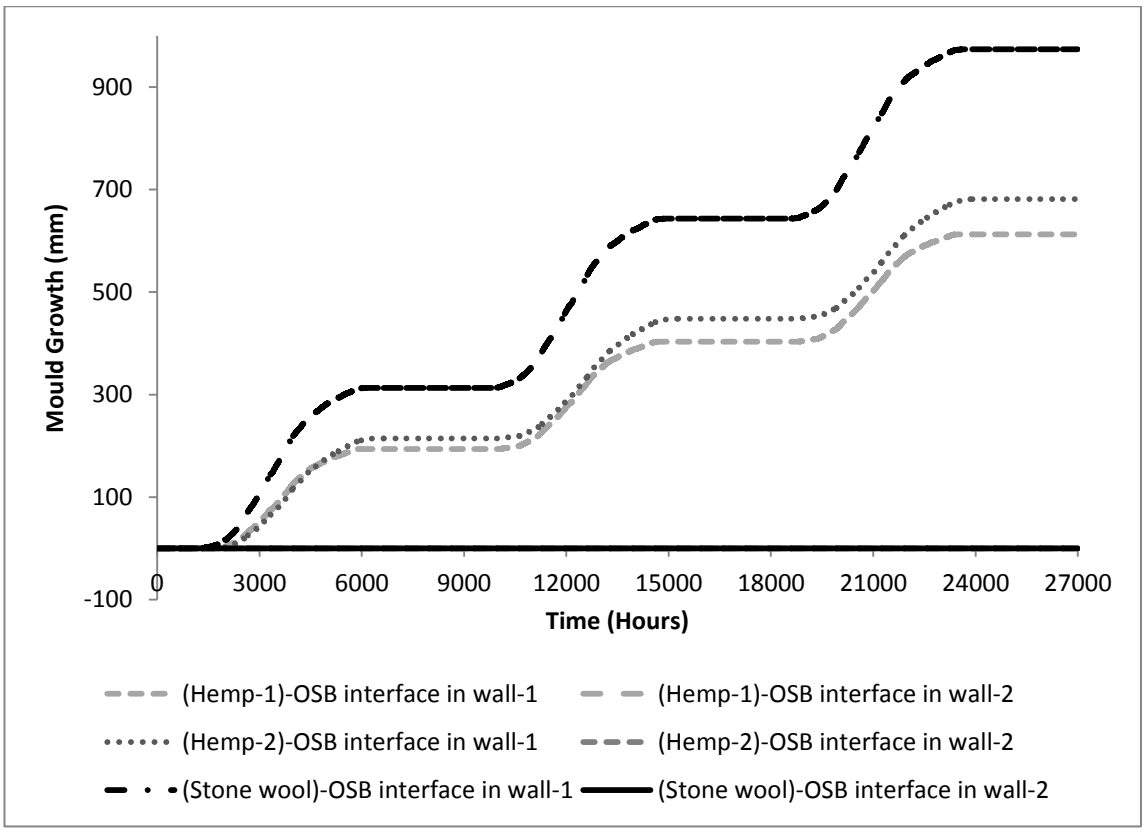


**Figure 8.42: Mould growth in insulation-OSB interfaces for different insulations in Edinburgh**

#### *8.6.1.5 Thermal conductivity of the insulations*

Figure 8.43 shows the equivalent thermal conductivity values of the insulation materials in wall-1 and wall-2. The lowest equivalent thermal conductivity values are observed in hemp-2 and stone wool insulation materials. The lowest equivalent thermal conductivity values of hemp-2 are 0.022 W/mK and 0.021 W/mK for wall-1 and wall-2, respectively and of stone wool are 0,021 and 0.020 W/mK for wall-1 and wall-2, respectively. All the abovementioned values are in relation to the heat flux measured on the inner surface. The highest equivalent thermal conductivity values are observed in hemp-1 in wall-1. These values are 0.038 W/mK when heat flux is measured in the hemp-1-OSB interface and 0.032 W/mK when heat flux is measured in the inner surface.

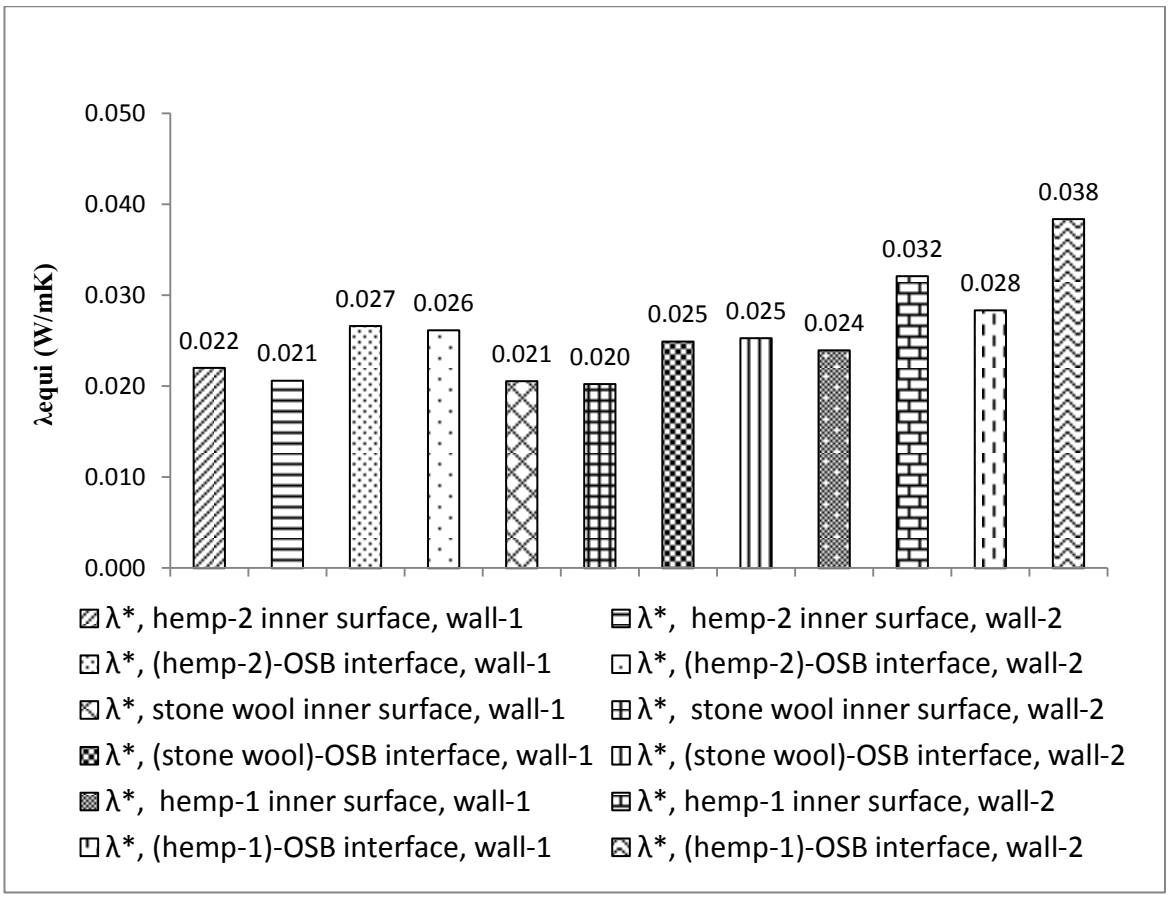


**Figure 8.43: Equivalent thermal conductivity values of the insulations in Edinburgh.**

It can be observed that thermal conductivity values determined from the heat flux readings in the insulation-OSB interfaces are always higher than the thermal conductivity values determined from the heat flux readings in the inner plasterboard surfaces, irrespective of the wall types. In all the cases, except for the value determined for hemp-1 insulation from the heat flux in (hemp-1)-OSB interface in wall-2, the equivalent thermal conductivity values are below the manufacturers' declared thermal conductivity values. The equivalent thermal conductivity of hemp-1 in wall-2, determined from the heat flux in (hemp-1)-OSB interface, is equal to the manufacturer's declared value.

### *8.6.2 Timber frame walls in Birmingham*

#### *8.6.2.1 Relative humidity*

The relative Humidity conditions in the insulation-OSB interfaces in wall-1 and wall-2 for hemp-1, hemp-2 and stone wool insulation materials are shown in the Figures 8.44 to 8.46.

It can be observed that, between wall-1 and wall-2, there is a maximum difference of about 29% relative humidity in the (hemp-1)-OSB interfaces during the month of March 1993 and a minimum difference of about 6% relative humidity during the month of September 1992. Relative humidity is always higher in wall-1 than in wall-2.

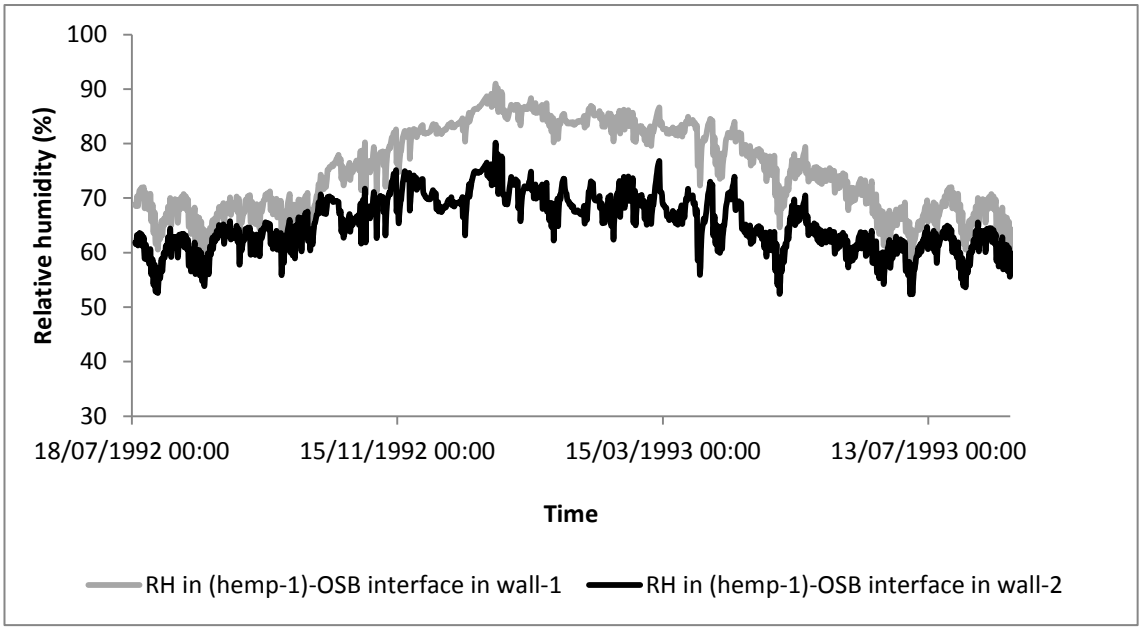


**Figure 8.44: Relative humidity conditions in the (hemp-1)-OSB interfaces for timber frame walls with and without vapour barrier in Birmingham.**

In Hemp-2 insulation, the relative humidity in the (hemp-2)-OSB interface can be 60% higher in wall-1 than in wall-2 during the month of March 1993 and can be 18% lower in wall-1 than in wall-2 during the month of September 1992. Between the months of September 1992 to June 1993, the relative humidity is higher in the (hemp-2)-OSB interface in wall-1 then in wall-2.

In stone wool insulation, relative humidity in the (stone wool)-OSB interface can be 24% higher in wall-1 than in wall-2 during the month of March 1993 and can be 2% lower in wall-1 than in wall-2 during the month of September 1992.

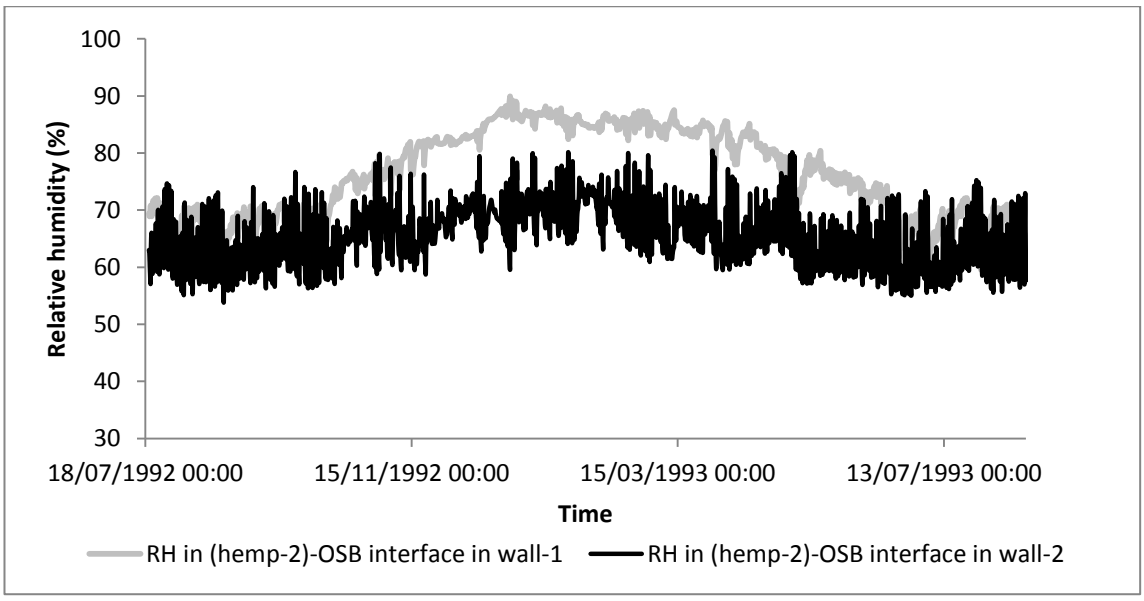


**Figure 8.45: Relative humidity conditions in the (hemp-2)-OSB interfaces for timber frame walls with and without vapour barrier in Birmingham.**

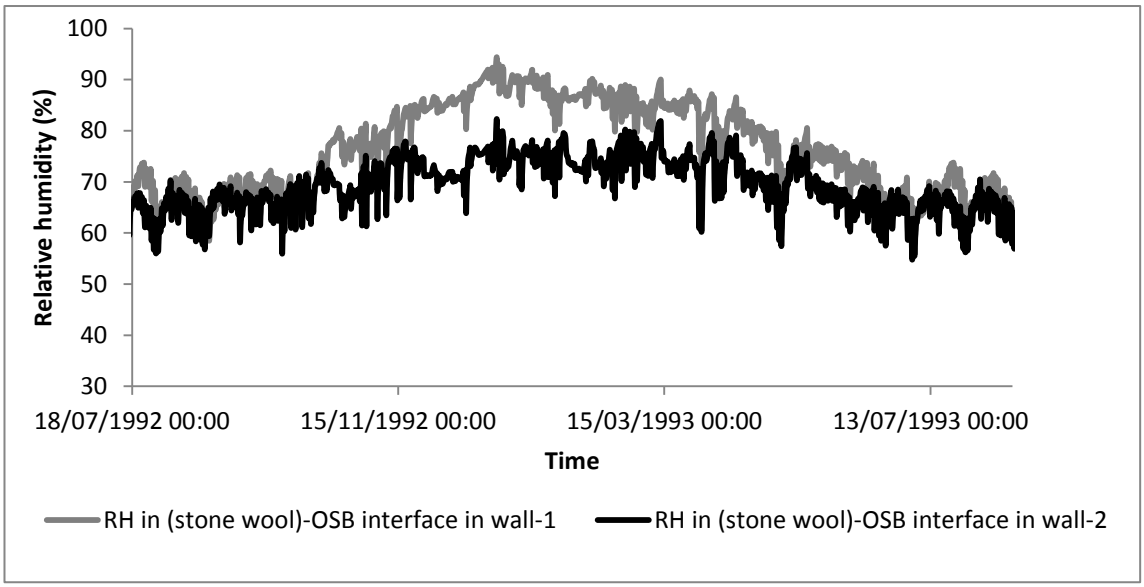


**Figure 8.46: Relative humidity conditions in the (stone wool)-OSB interfaces in wall-1 and wall-2 in Birmingham.**

The relative humidity conditions in the inner surfaces of the insulations in the timber frame walls, with and without vapour barrier, are shown in Figures 8.47 to 8.50. Since in all the cases, the relative humidity is less than 70% for more than 99% of the total period, there is no potential risk of condensation or mould growth on the inner surfaces of the insulation materials.

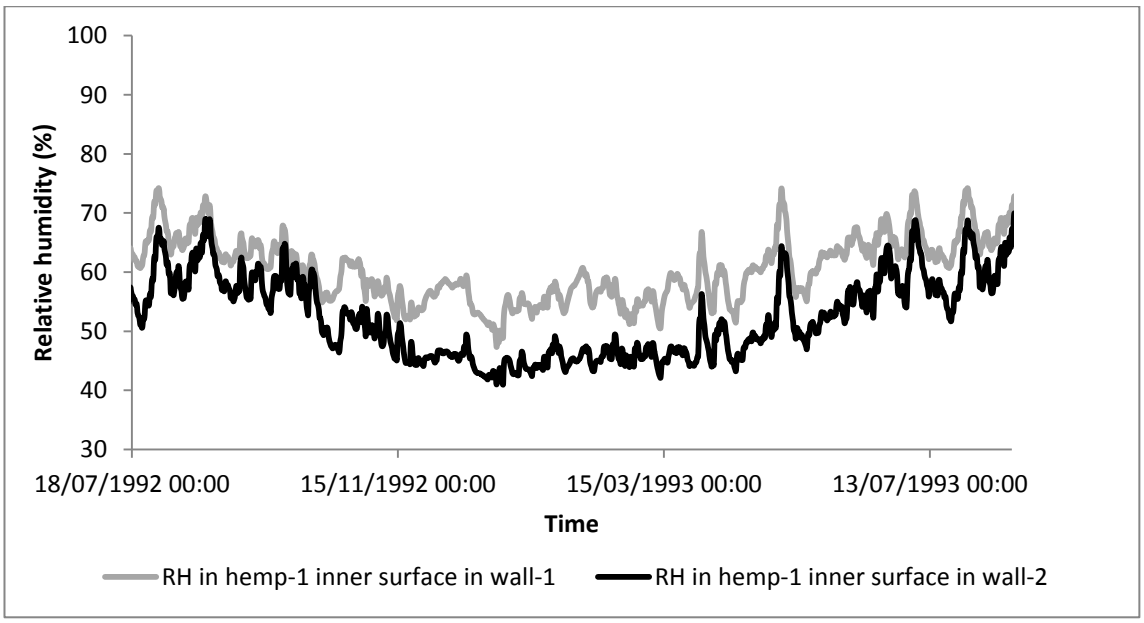


**Figure 8.47: Relative humidity conditions in the inner surfaces of the hemp-1 insulations in wall-1 and wall-2 in Birmingham.**

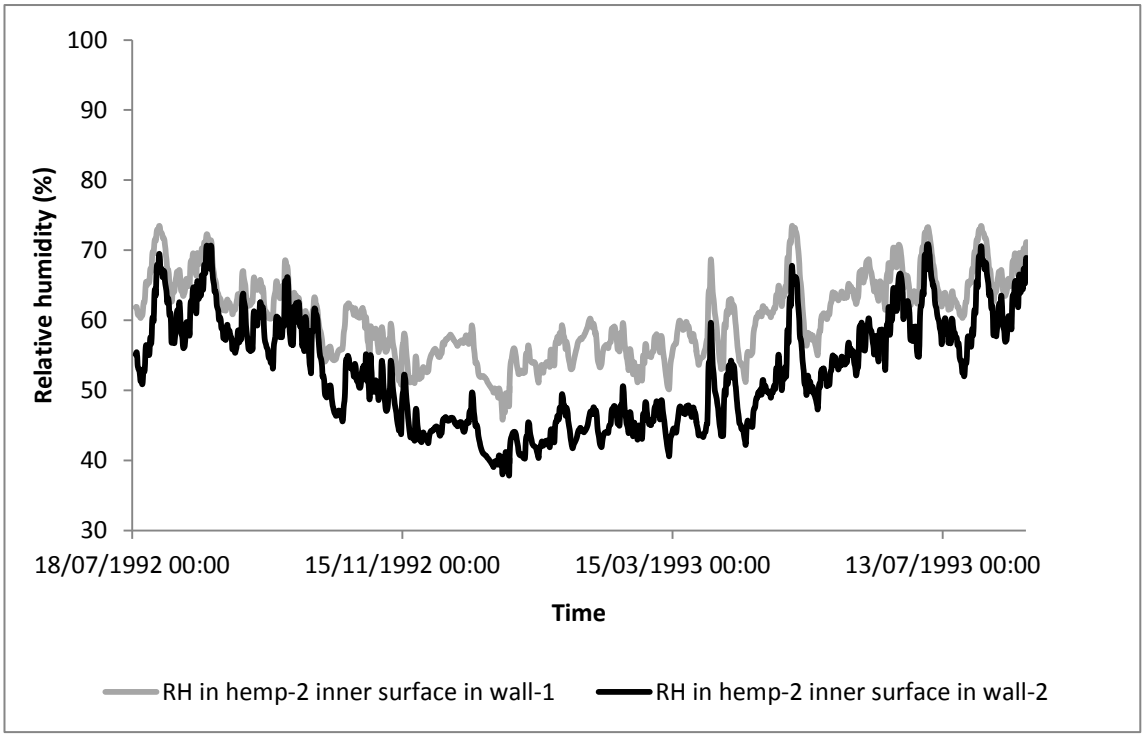


**Figure 8.48: Relative humidity conditions in the inner surfaces of the hemp-2 insulations in wall-1 and wall-2 in Birmingham.**

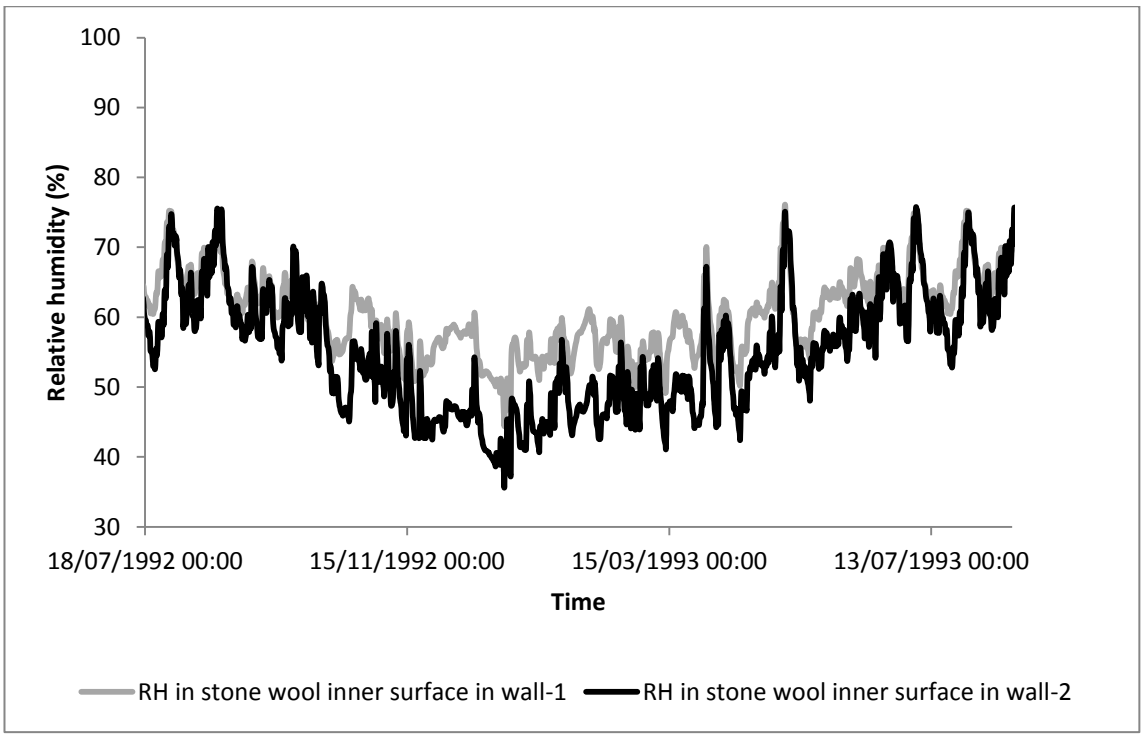


**Figure 8.49: Relative humidity conditions in the inner surfaces of the stone wool insulations in wall-1 and wall-2 in Birmingham.**

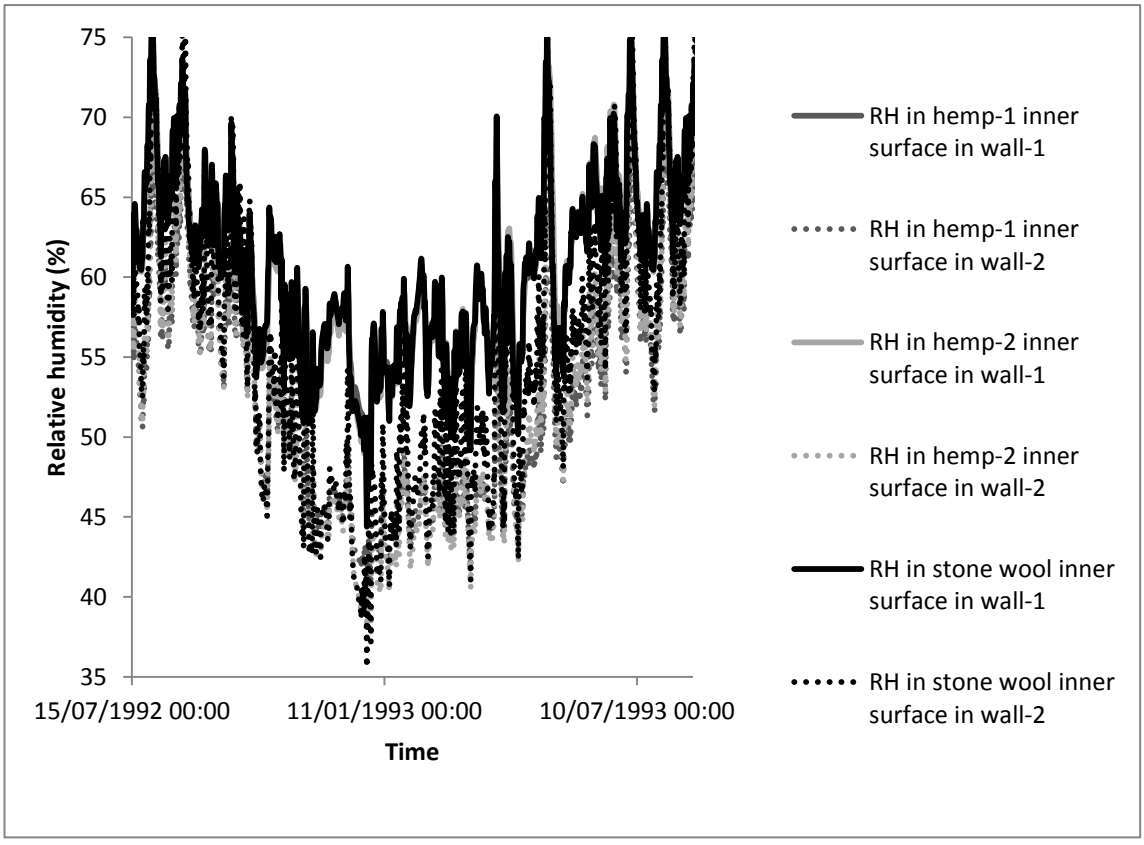


**Figure 8.50: Relative humidity conditions in the inner surfaces of the insulations in wall-1 and wall-2 in Birmingham.**

### *8.6.2.2 Water content*

The water content in the OSB surfaces of the insulation-OSB interfaces is shown in Figures 8.51 to 8.53. In relation to the water content in the OSB surfaces of wall-2, the highest differences between wall-1 and wall-2 are 38%, 11% and 35% for hemp-1, hemp-2 and stone wool Insulation materials, respectively. In hemp-1, hemp-2 and stone wool insulation materials, water content is higher in wall-1 than in wall-2 for 74%, 99% and 52% of the total period of one year. Figures 8.54 and 8.55 present the corresponding collated data for wall-1 and wall-2. Figure 8.54, based on the combined data for wall-1, shows that the type of the insulation does not have much effect in wall-1 in terms of the accumulated water content in the OSB board. However, Figure 8.55, based on the combined data for wall-2, shows that water content is about 4% and 3.8% higher in the OSB board of the (stone wool)-OSB interface than in the OSB boards of the (hemp-1)-OSB and (hemp-2)-OSB interfaces, respectively.

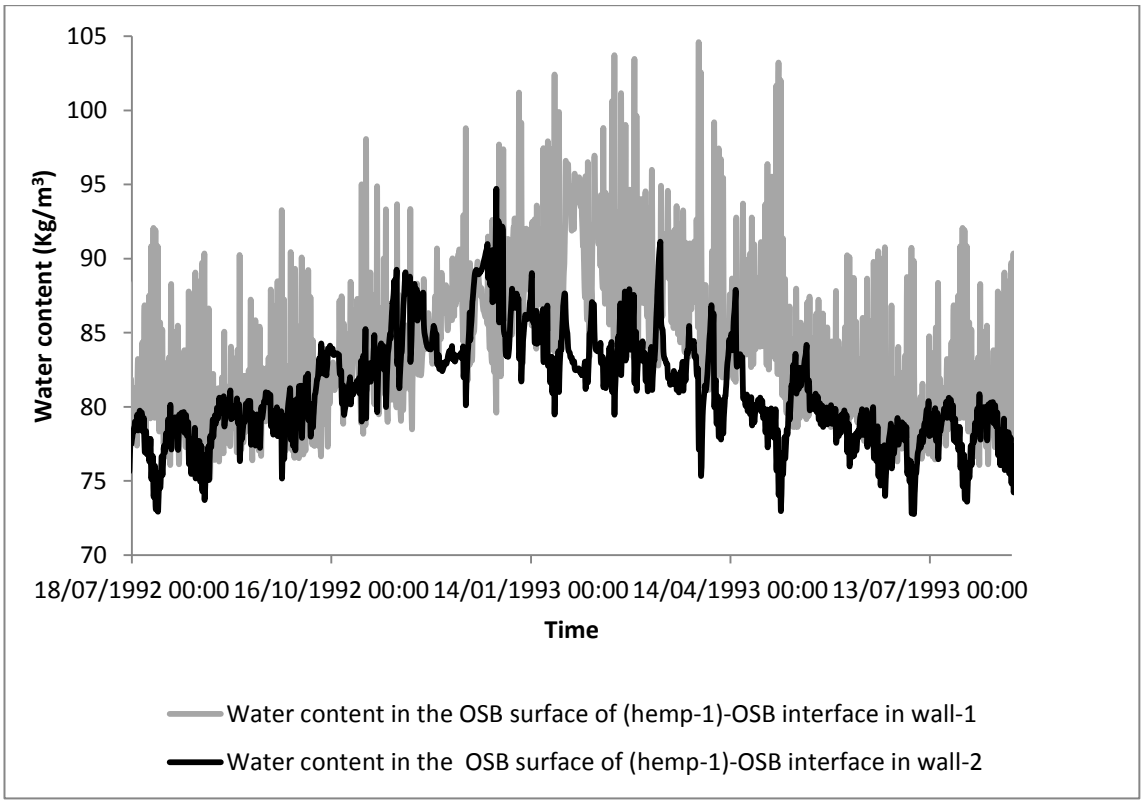


**Figure 8.51: Water content in the (hemp-1)-OSB in wall-1 and wall-2 in Birmingham.**

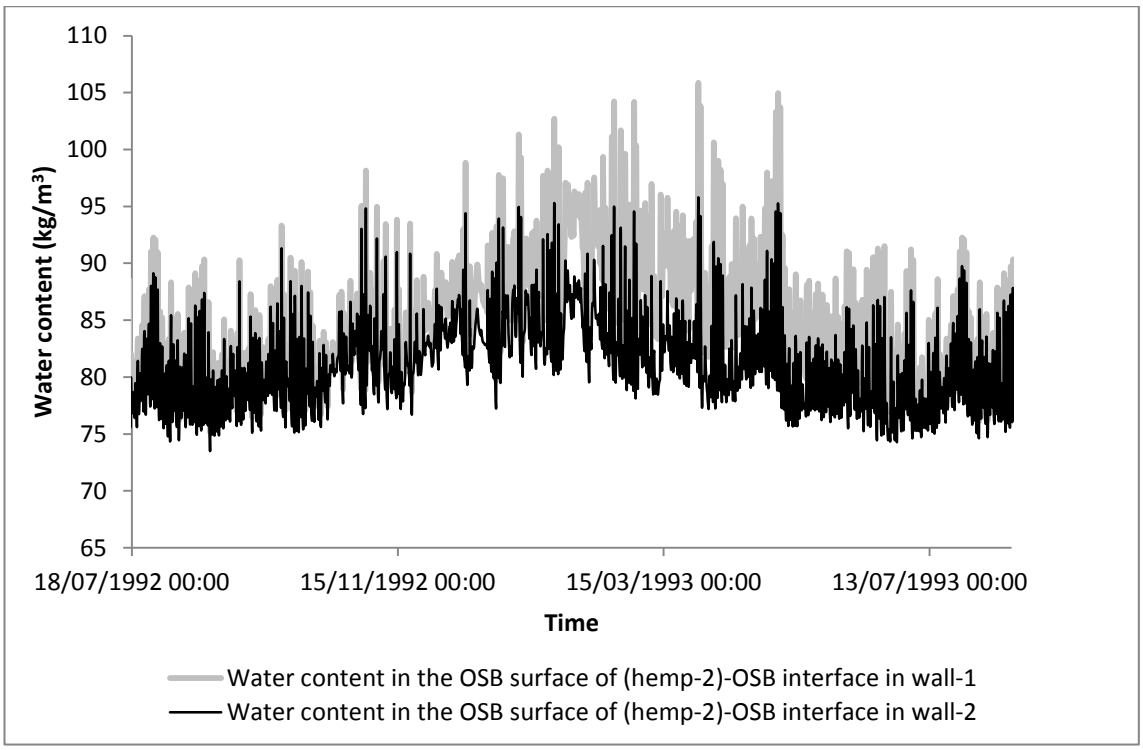


**Figure 8.52: Water content in the (hemp-2)-OSB interfaces in wall-1 and wall-2 in Birmingham.**

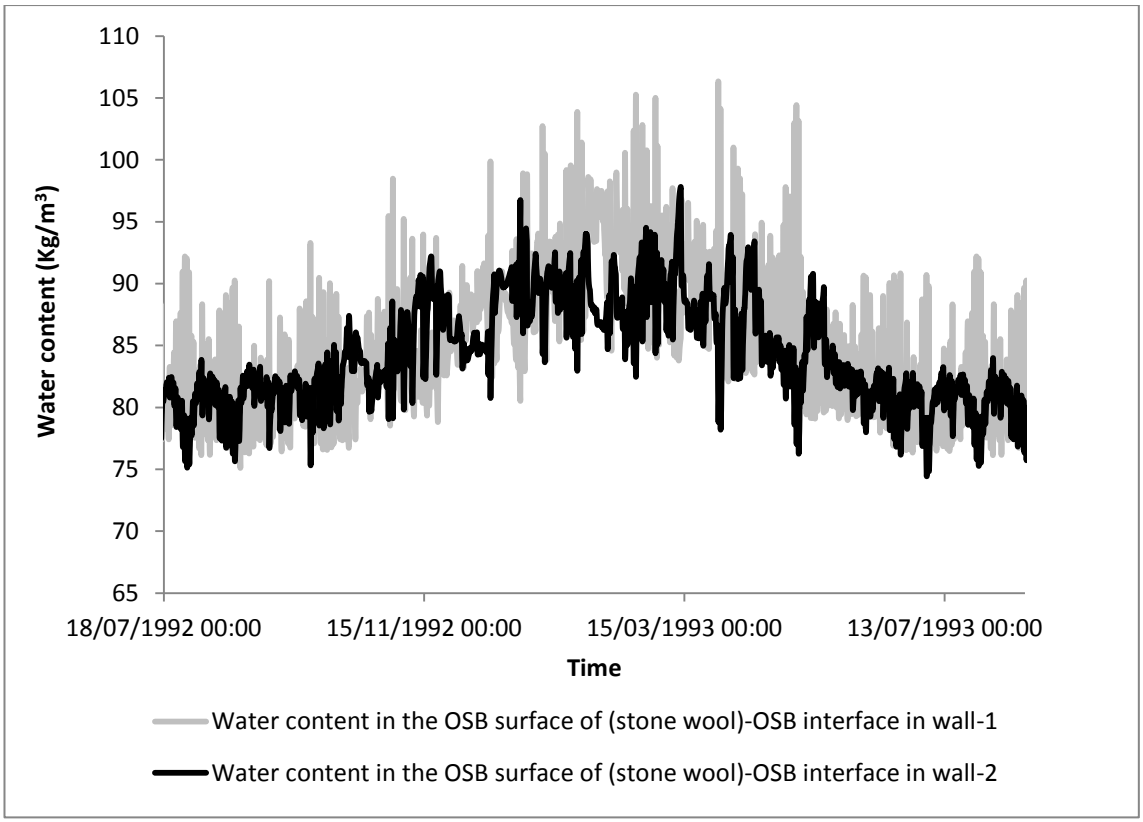


**Figure 8.53: Water content in the (stone wool)-OSB interfaces in wall-1 and wall-2 in Birmingham.**

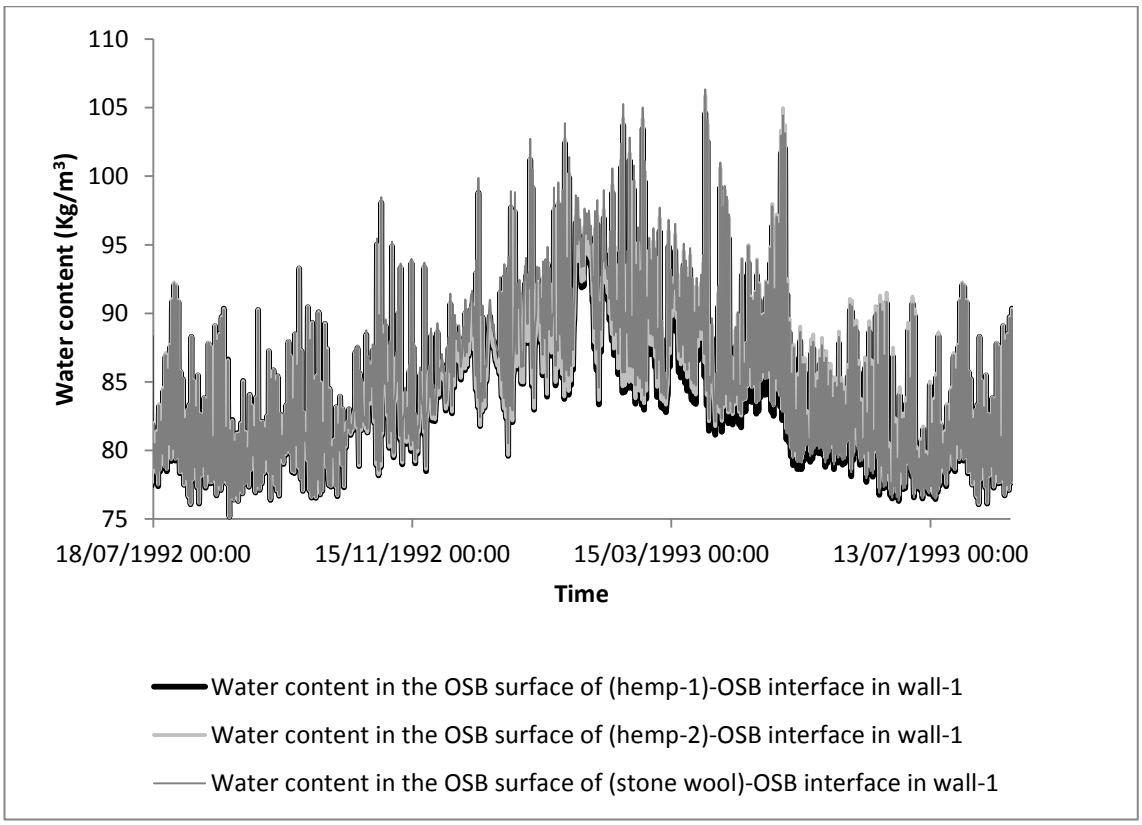


**Figure 8.54: Water content in the insulation-OSB interfaces in wall-1 in Birmingham.**

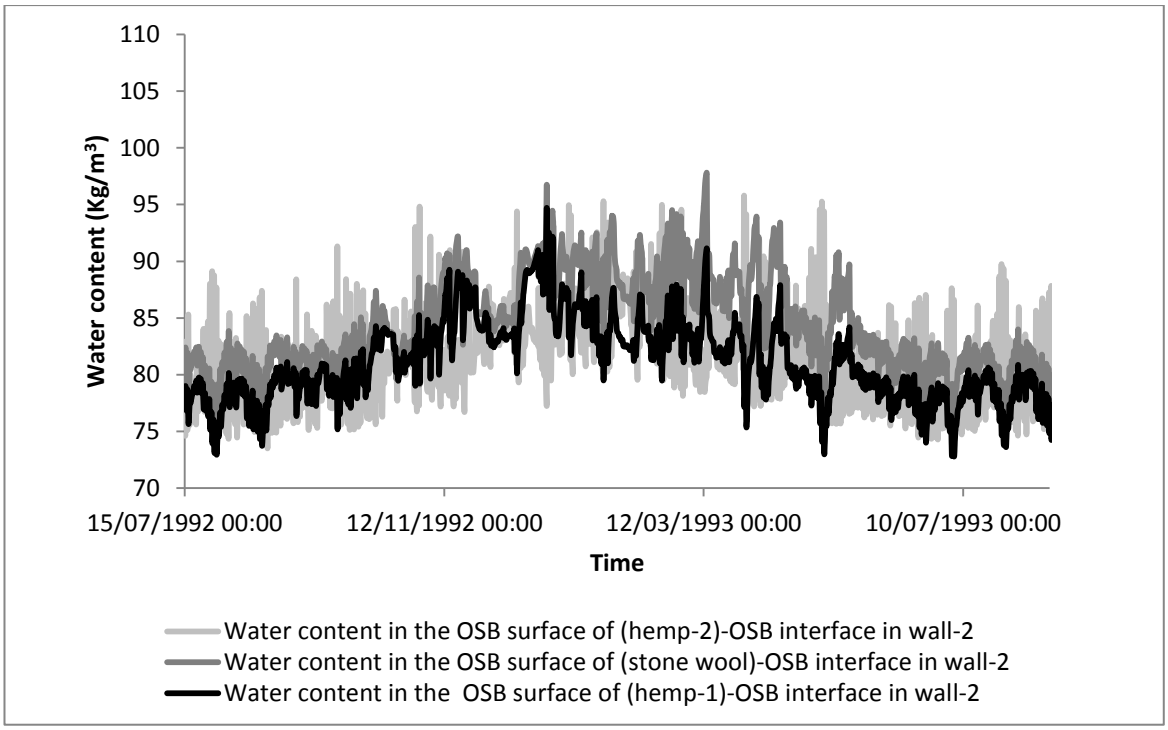


**Figure 8.55: Water content in the insulation-OSB interfaces in wall-2 in Birmingham.**

### *8.6.2.3 Mould spore germination and mould growth*

The water content in the mould spores in relation to the critical water content for mould spore germination is shown in Figures 8.56 to 8.61. The hygrothermal conditions in the insulation-OSB interfaces in relation to the Sedlbauer's isopleth are shown in the Figures 8.62 to 8.67.

***Wall-1***

Figures 8.56, 8.58 and 8.60 show that, for hemp-1, hemp-2 and stone wool insulation materials in the wall-1, the water content in the spores is higher than the critical water content for mould spore germination for 46%, 53% and 53% time of the analysed year, respectively. As for the hygrothermal conditions in wall-1, as shown in Figures 8.62, 8.64 and 8.66, there are occurrences when the hygrothermal conditions are between the LIM isopleth and the 2-day isopleths for hemp-1 and hemp-2 insulation materials and between the LIM isopleth and 1-day isopleth for stone wool insulation.

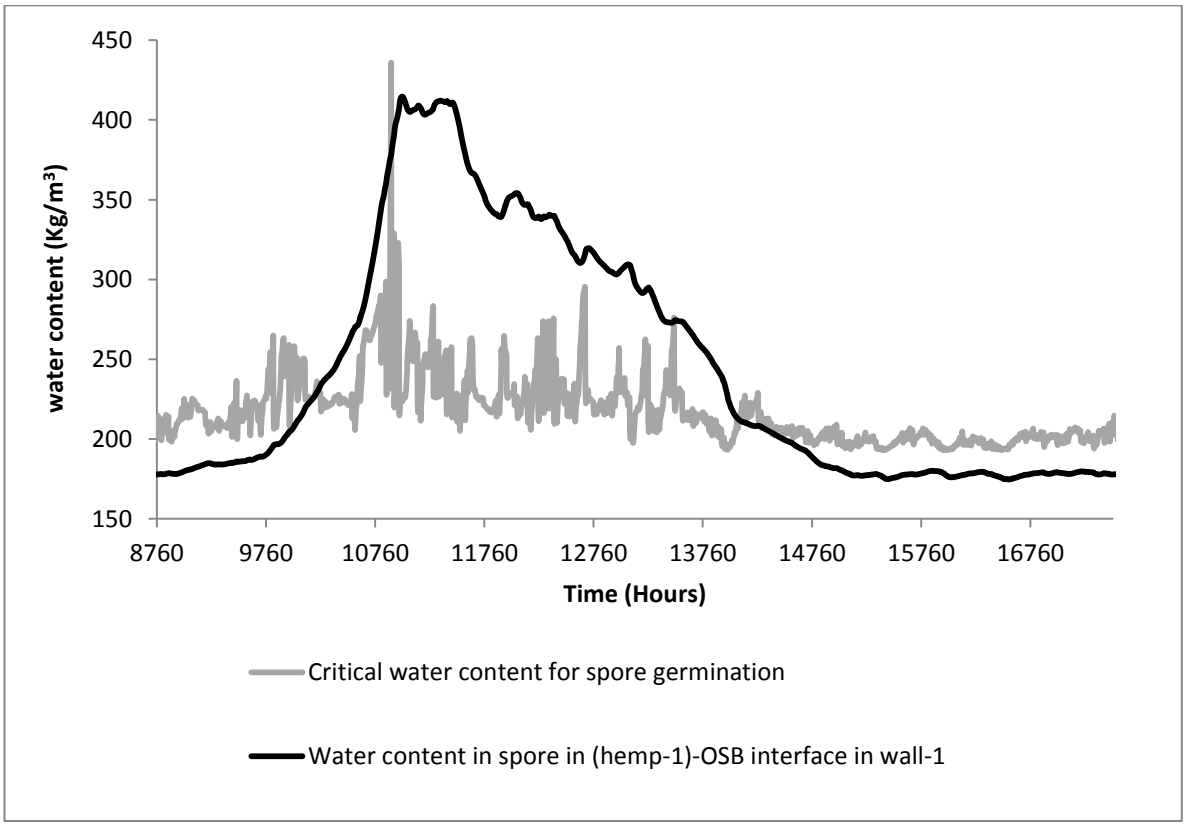


**Figure 8.56: Estimated and critical water content in the mould spore in the (hemp-1)-OSB interfaces in wall-1 in Birmingham.**

***Wall-2***

In wall-2, water content in the mould spores is always below the critical water content for all three insulation materials, as shown in Figures 8.57, 8.59 and 8.61 and the hygrothermal conditions are also always below the LIM isopleth, as shown in Figures 8.63, 8.65 and 8.67.

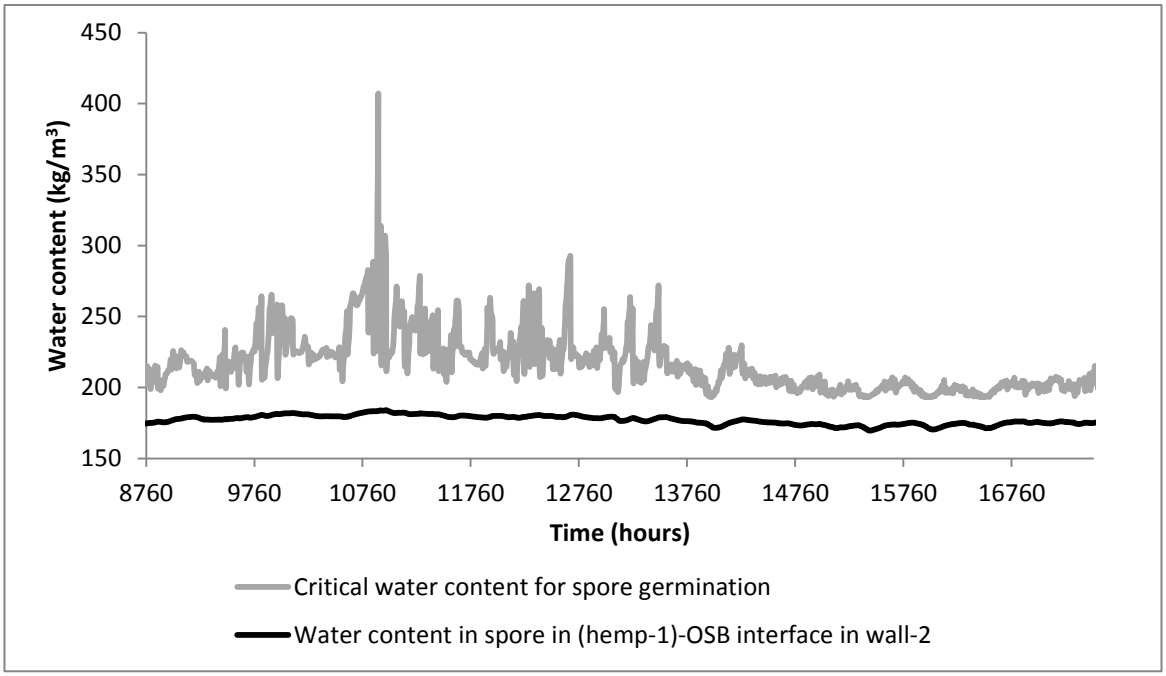


**Figure 8.57: Estimated and critical water content in the mould spore in the (hemp-1)-OSB interface in wall-2 in Birmingham.**

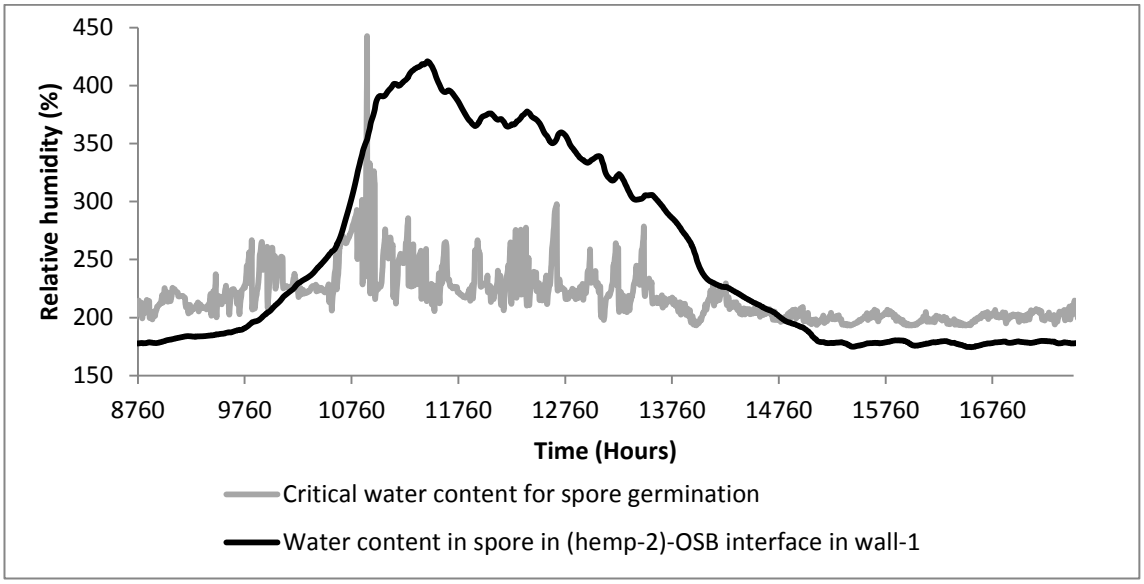


**Figure 8.58: Estimated and critical water content in the mould spore in the (hemp-2)-OSB interface in wall-1 in Birmingham.**

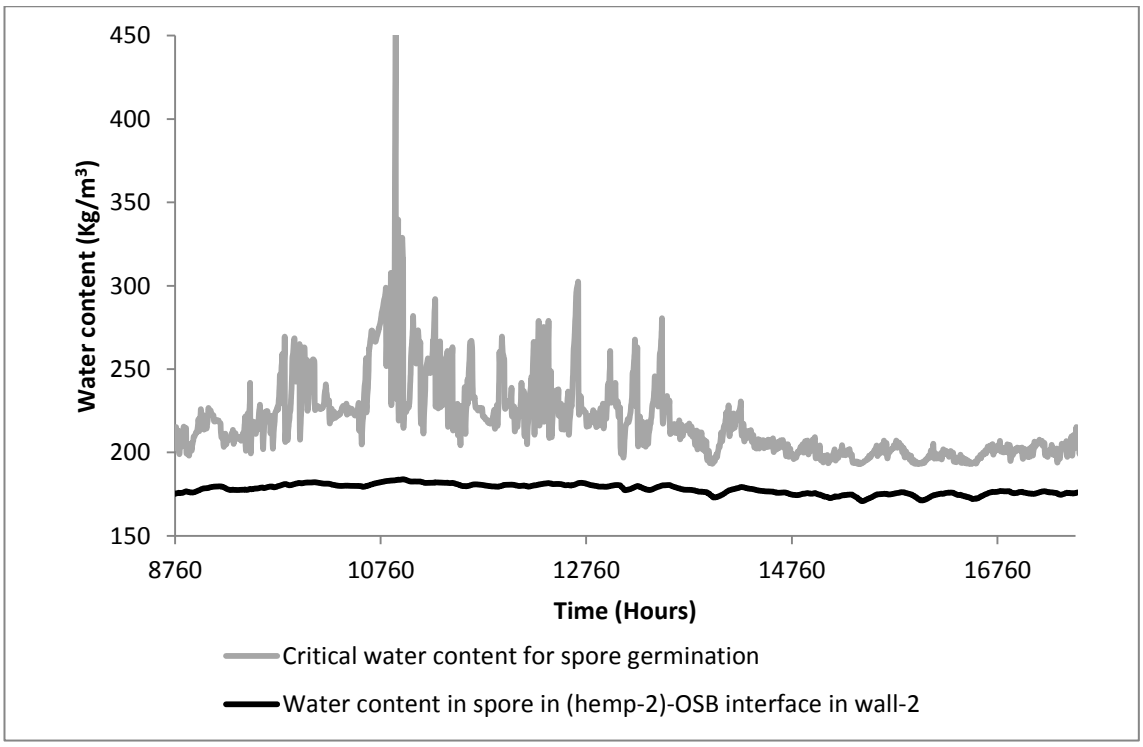


**Figure 8.59: Estimated and critical water content in the mould spore in the (hemp-2)-OSB interface in wall-2 in Birmingham.**

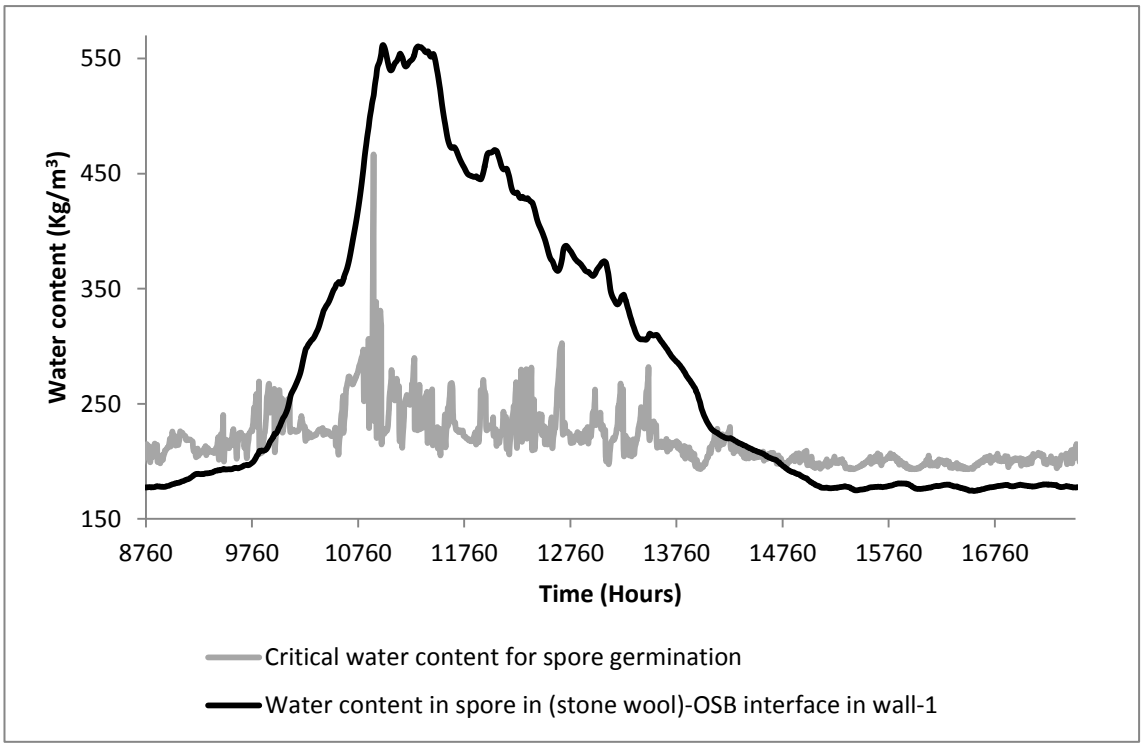


**Figure 8.60: Estimated and critical water content in the mould spore in the (stone wool)-OSB interface in wall-1 in Birmingham.**

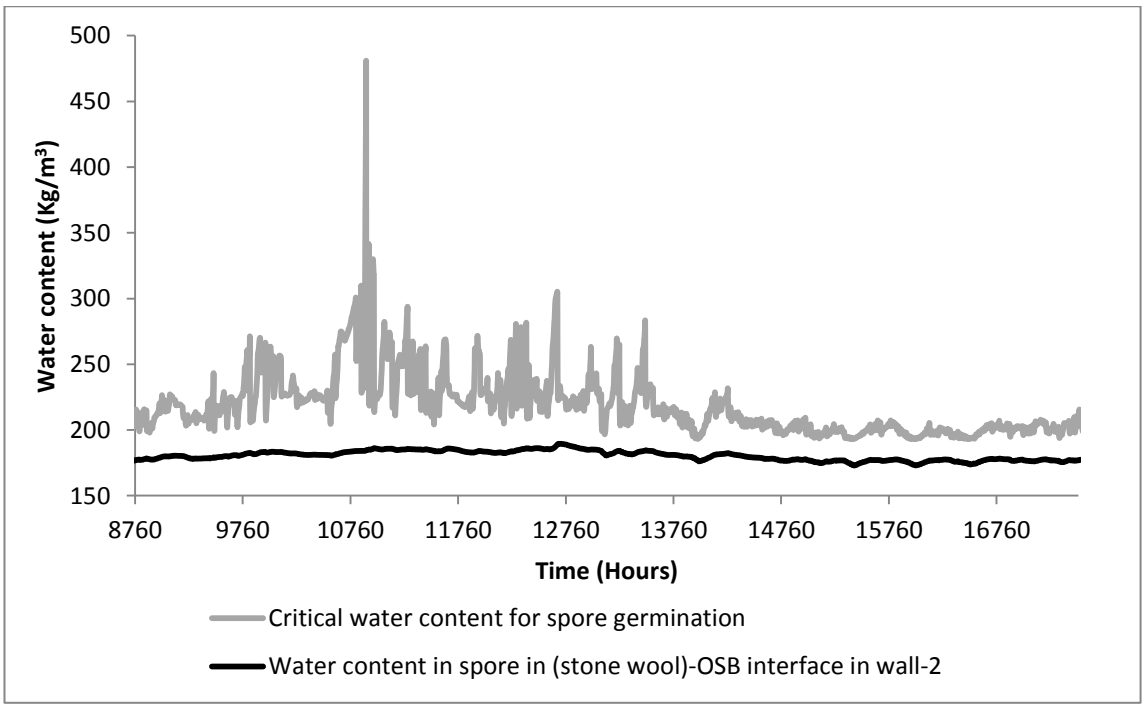


**Figure 8.61: Estimated and critical water content in the mould spore in the (stone wool)-OSB interface in wall-2 in Birmingham.**

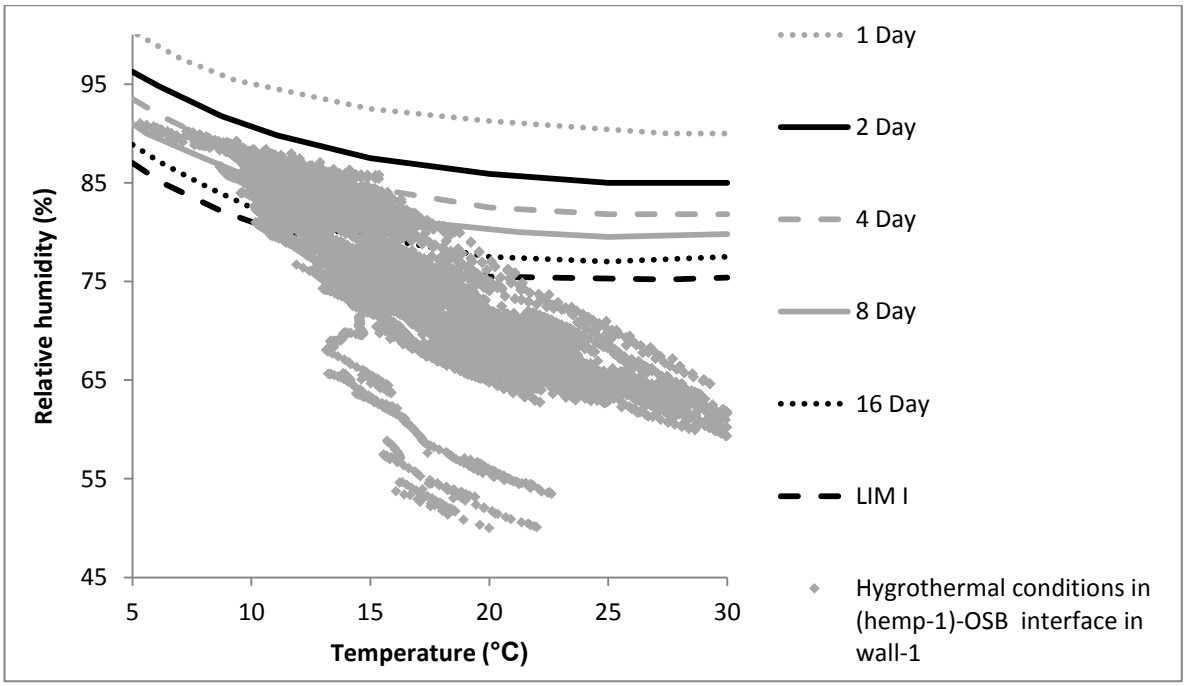


**Figure 8.62: Hygrothermal condition in the (hemp-1)-OSB interface in wall-1 in Birmingham.**

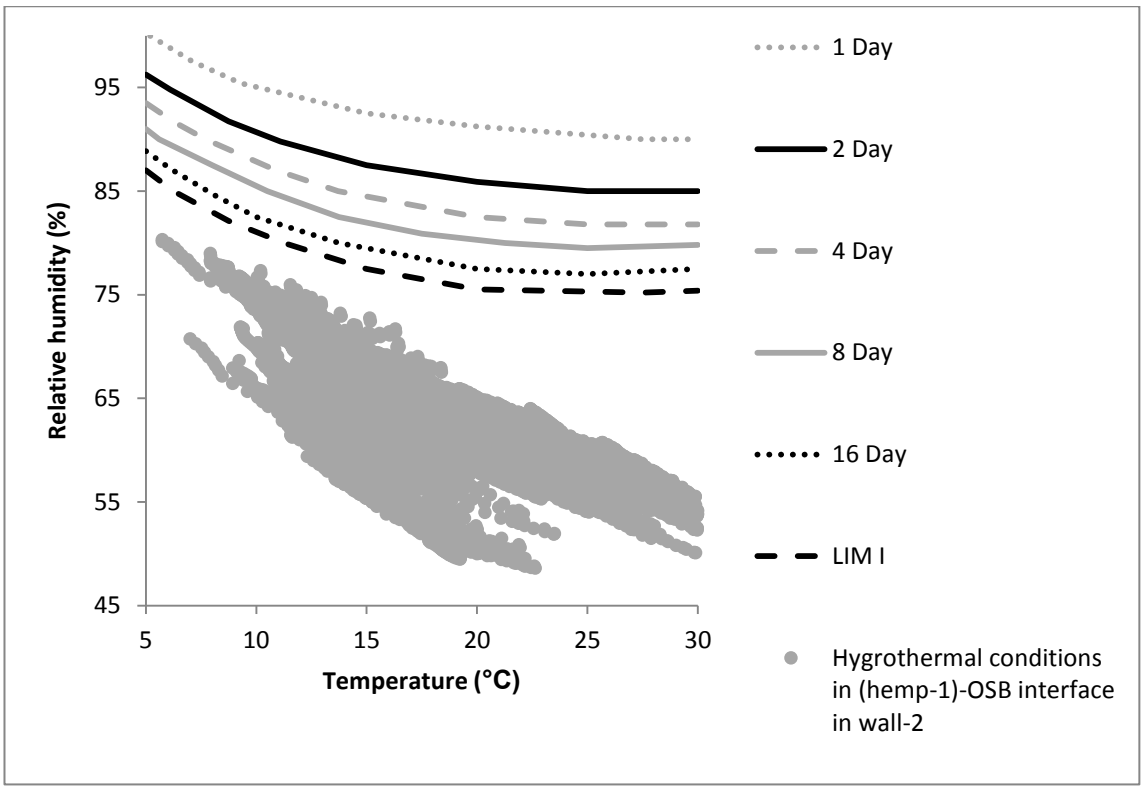


**Figure 8.63: Hygrothermal condition in the (hemp-1)-OSB interface in wall-2 in Birmingham.**

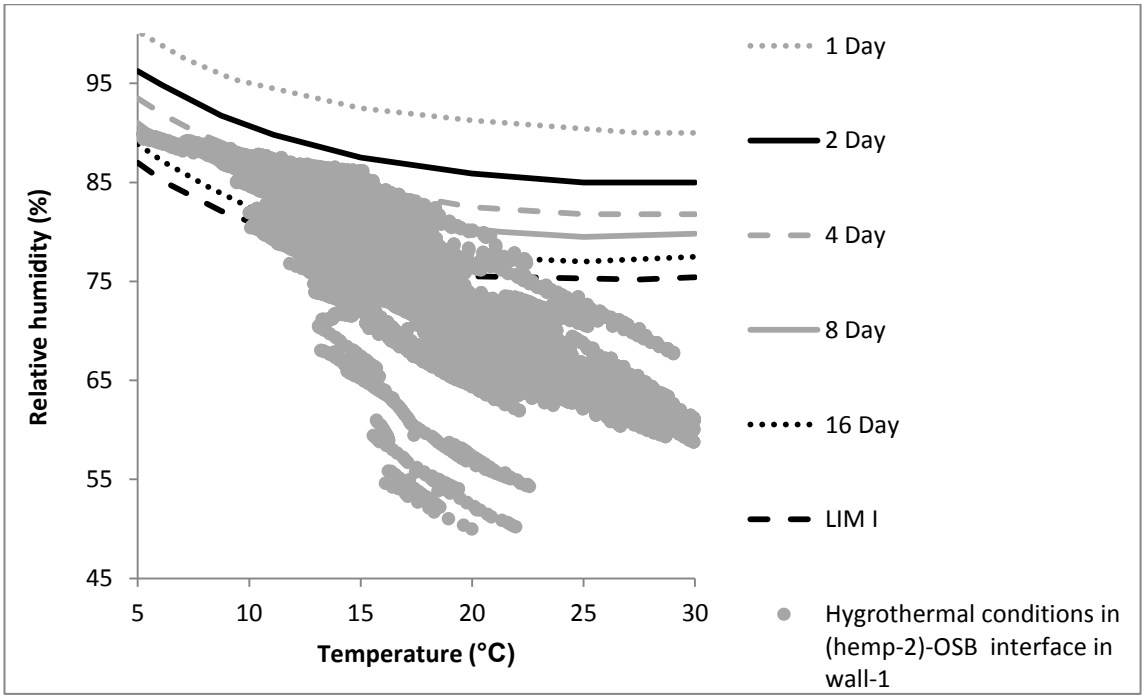


**Figure 8.64: Hygrothermal condition in the (hemp-2)-OSB interface in wall-1 in Birmingham.**

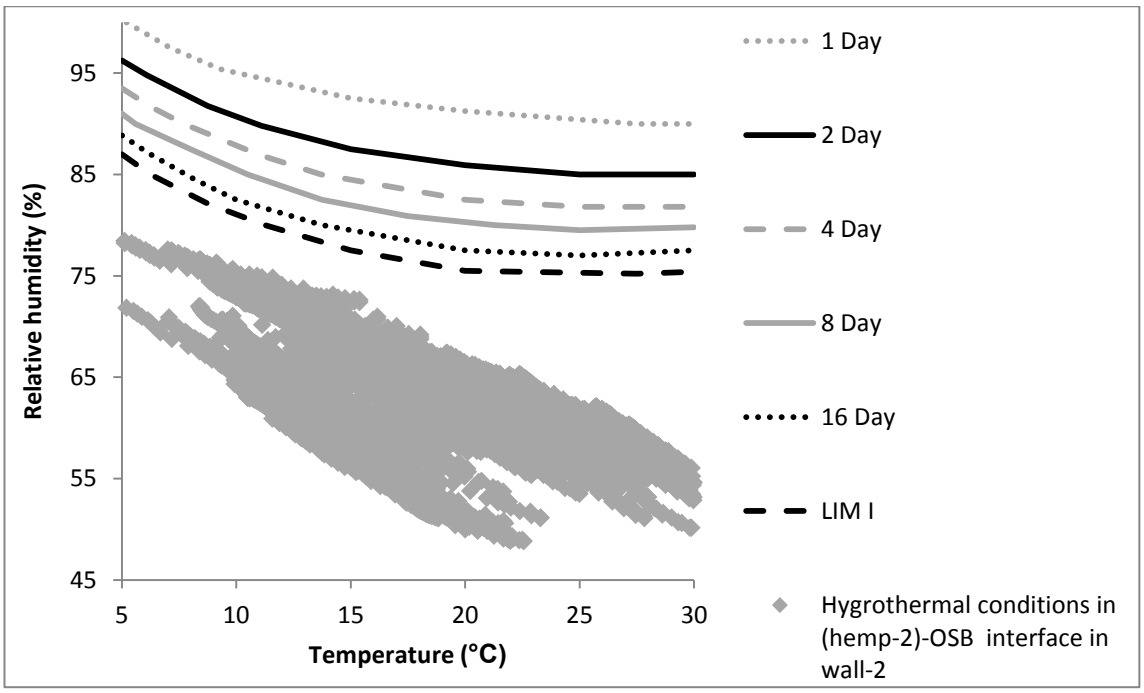


**Figure 8.65: Hygrothermal condition in the (hemp-2)-OSB interface in wall-2 in Birmingham.**

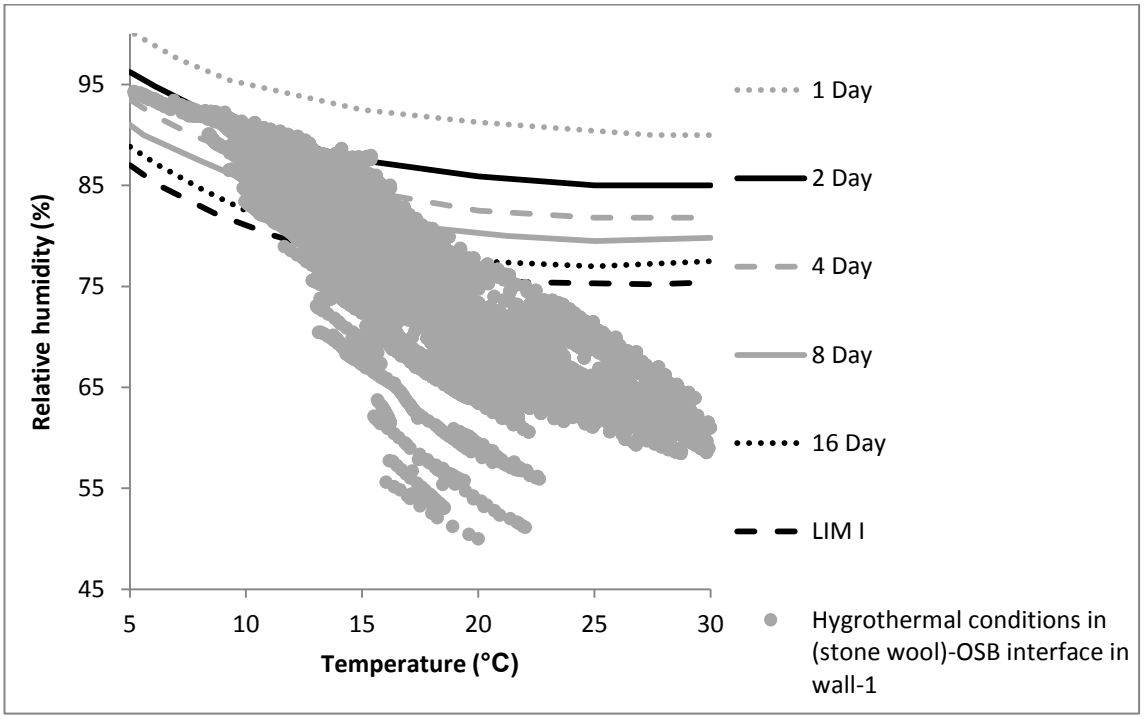


**Figure 8.66: Hygrothermal condition in the (stone wool)-OSB in wall-1 in Birmingham.**

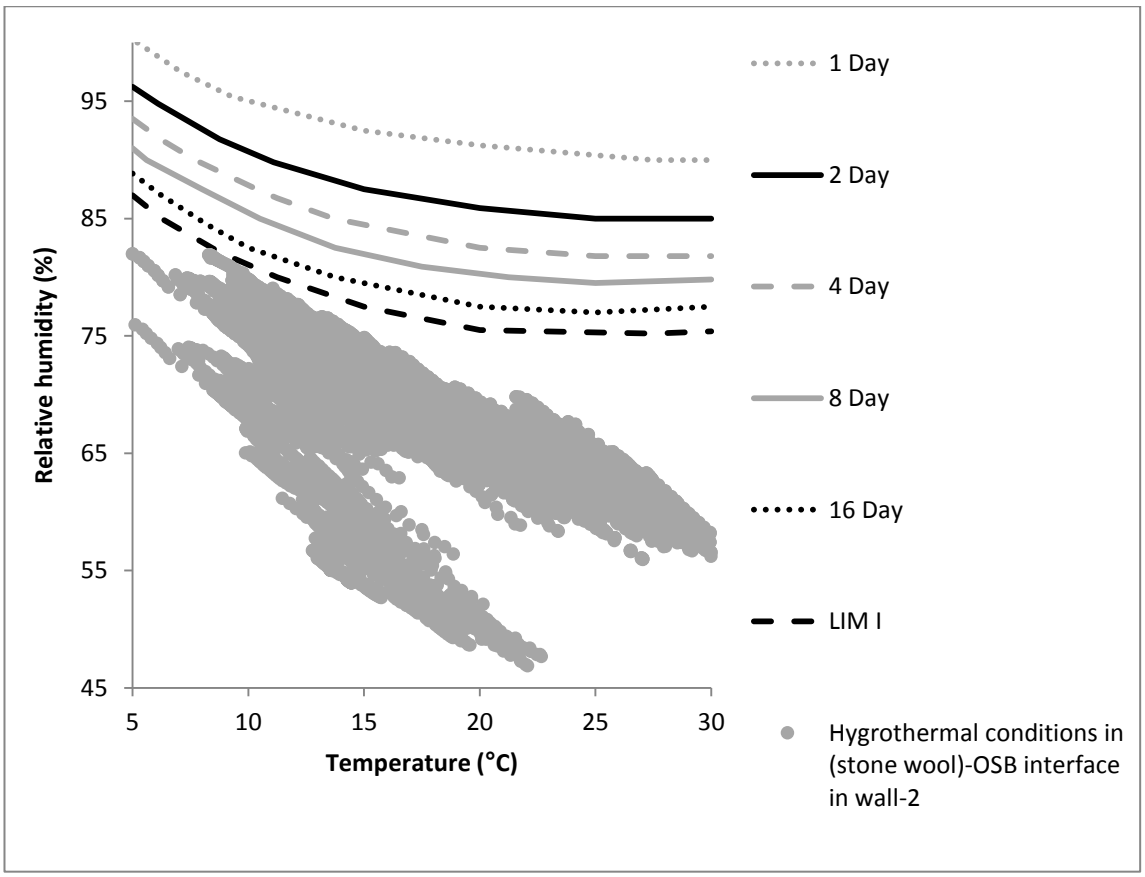


**Figure 8.67: Hygrothermal condition in the (stone wool)-OSB interface in wall-2 in Birmingham.**

### *8.6.2.4 Mould index and mould growth*

Figures 8.68 and 8.69 show the mould index and amount of mould growth, respectively. For wall-1, mould index and the amount of mould growth is the highest in stone wool and the lowest in hemp-1 insulation. It implies that hemp insulations are more effective than stone wool insulation in delaying mould growth. For wall-2, the mould index and the rate of mould growth are zero for all the insulation materials. Since wall-2 is with vapour barrier and accidental leakage is not taken into account, the WUFI-Bio software did not predict any mould growth.

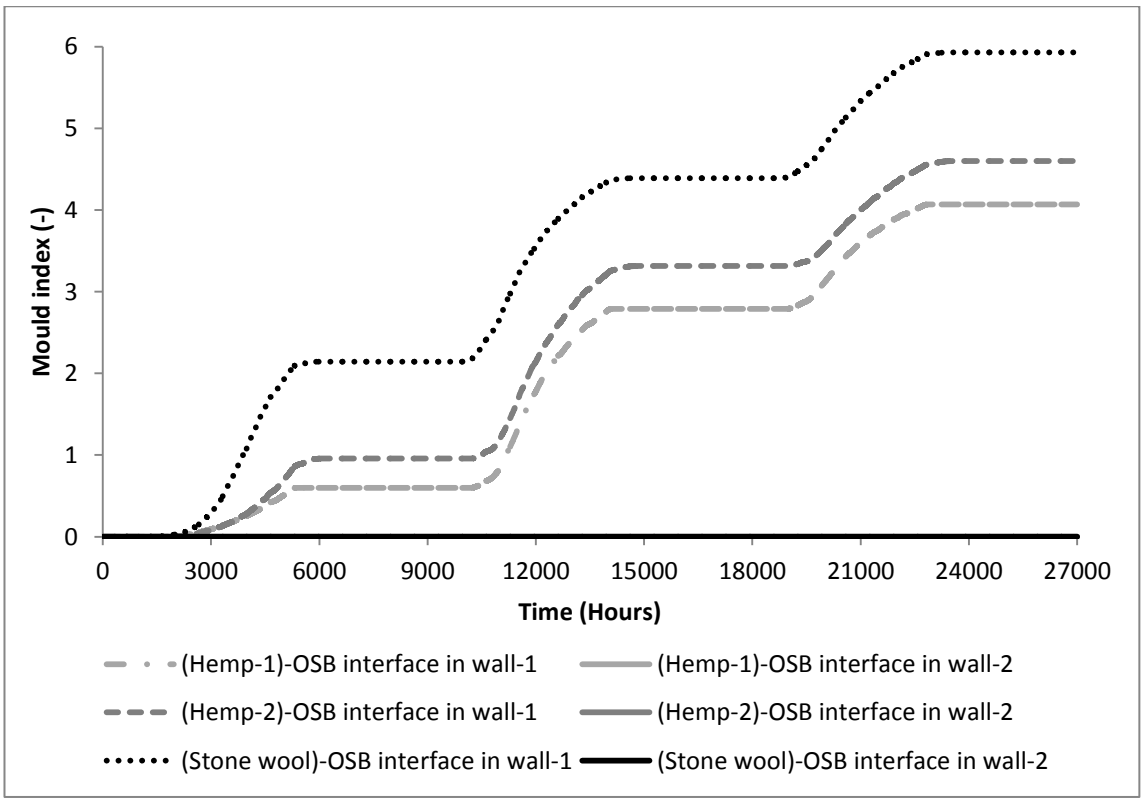


**Figure 8.68: Predicted mould index in the insulation-OSB interfaces of wall-1 and wall-2 in Birmingham.**

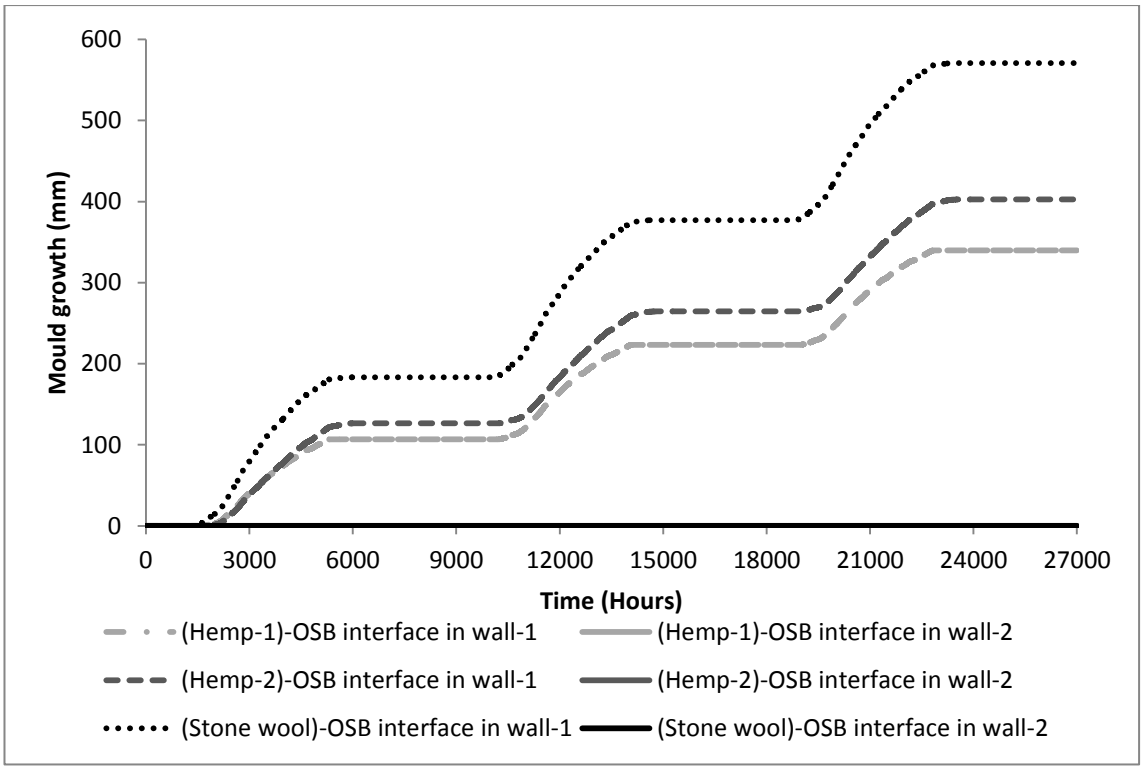


**Figure 8.69: Predicted mould growth in the insulation-OSB interfaces of wall-1 and wall-2 in Birmingham.**

### *8.6.2.5 Thermal conductivity of the insulations*

Figure 8.70 shows the equivalent thermal conductivity values of the insulation materials in wall-1 and wall-2. The lowest equivalent thermal conductivity values were observed in hemp-2 and stone wool insulation materials.

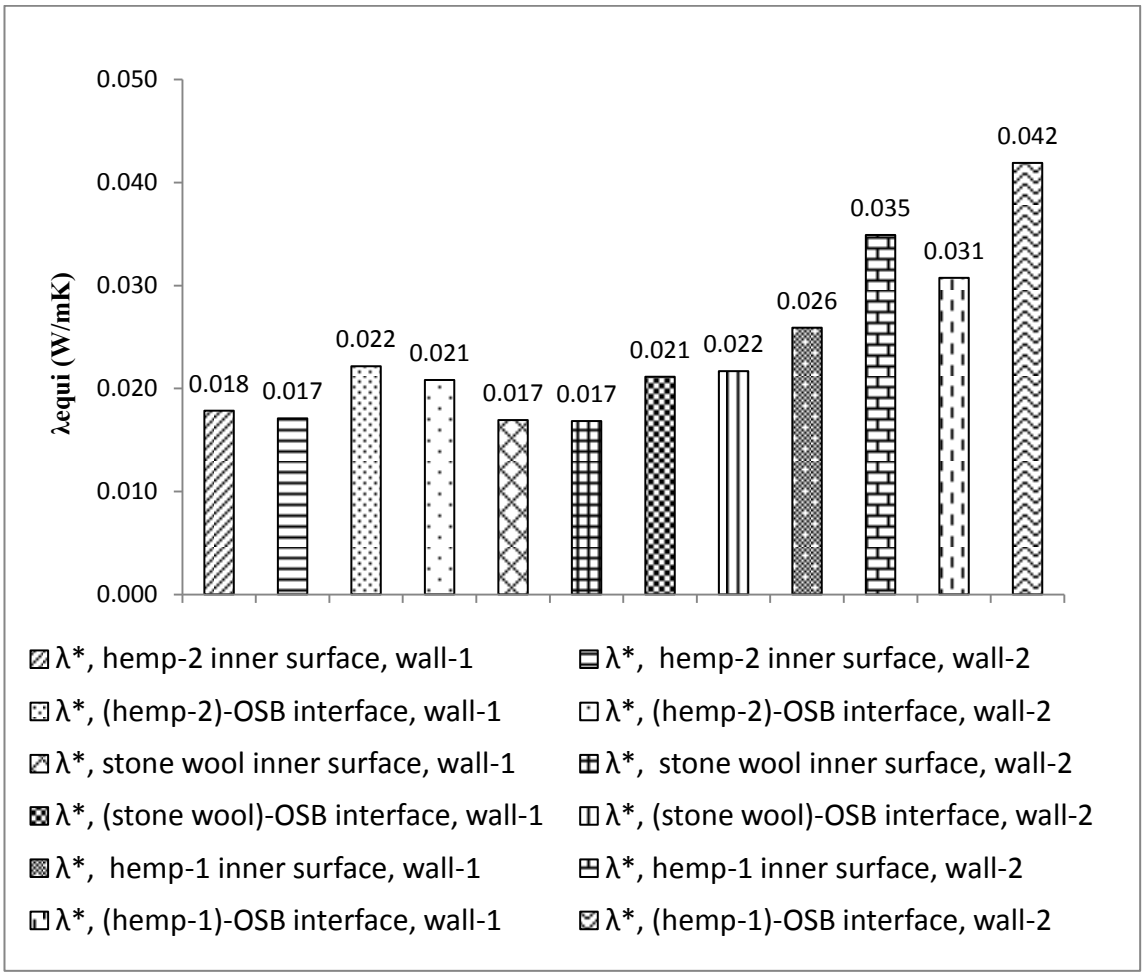


**Figure 8.70: Equivalent thermal conductivity values of the insulations in wall-1 and wall-2 in Birmingham.**

In hemp-2 insulation, the equivalent thermal conductivity values are 0.018 W/mK and 0.017 W/mK for wall-1 and wall-2, respectively. For stone wool insulation, the equivalent thermal conductivity value is 0.017 W/mK for both wall-1 and wall-2. All the equivalent thermal conductivity values mentioned above were determined from the heat flux measured on the inner surface. The highest equivalent thermal conductivity values were observed in hemp-1 insulation The values are 0.035 W/mK for wall-1 and 0.042 W/mK for wall-2 with heat flux measured in the (hemp-1)-OSB interfaces and on the inner surface respectively. It can be observed that thermal conductivity values determined from the heat flux readings in the insulation-OSB interfaces are always higher

that the thermal conductivity values determined from the heat flux reading at the inner surfaces, irrespective of the walls types. In all the cases, except for the value determined for hemp-1 insulation from the heat flux in (hemp-1)-OSB interface in wall-2, equivalent thermal conductivity values are below the manufacturers' declared thermal conductivity values.

### *8.6.3 Solid brick wall in Edinburgh*

#### *8.6.3.1 Relative humidity*

Figure 8.71 shows the relative humidity conditions in the (hemp-1)-brick, (hemp-1)-air and (hemp-1)-lime interfaces in wall-3, wall-4, wall-5, wall-7 and wall-8. It can be observed that the relative humidity conditions in the (hemp-1)-brick interface remains 99% for about 25% and 100% of the analysed period in wall-3 and wall-4, respectively. The relative humidity in the hemp-1)-lime interface is 99% for more than 25% and 80% of the analysed period in wall-7 and wall-8, respectively. However, in the (hemp-1)-air interface in wall-5, the relative humidity is about 94% for about 35% of the total period. The simulation cannot be performed for the (hemp-1)-air interface in wall-6 as the simulation software crashed repetitively and failed to perform the task. This may be due to the fact that to calculate moisture interaction of a stagnant air layer between hemp-1 insulation and the brick wall was out of the range of the WUFI software capability and this led to convergence failure.

It can be noted that, during the period of May 1994 to September 1994, the 'drying out' or decrease of relative humidity is quicker in wall-3, wall-5 and wall-7, which are walls without vapour barriers, than in the walls with vapour barrier. Similar observations can be made for hemp-2 and stone wool insulation materials, as shown in Figures 8.72 and 8.73.

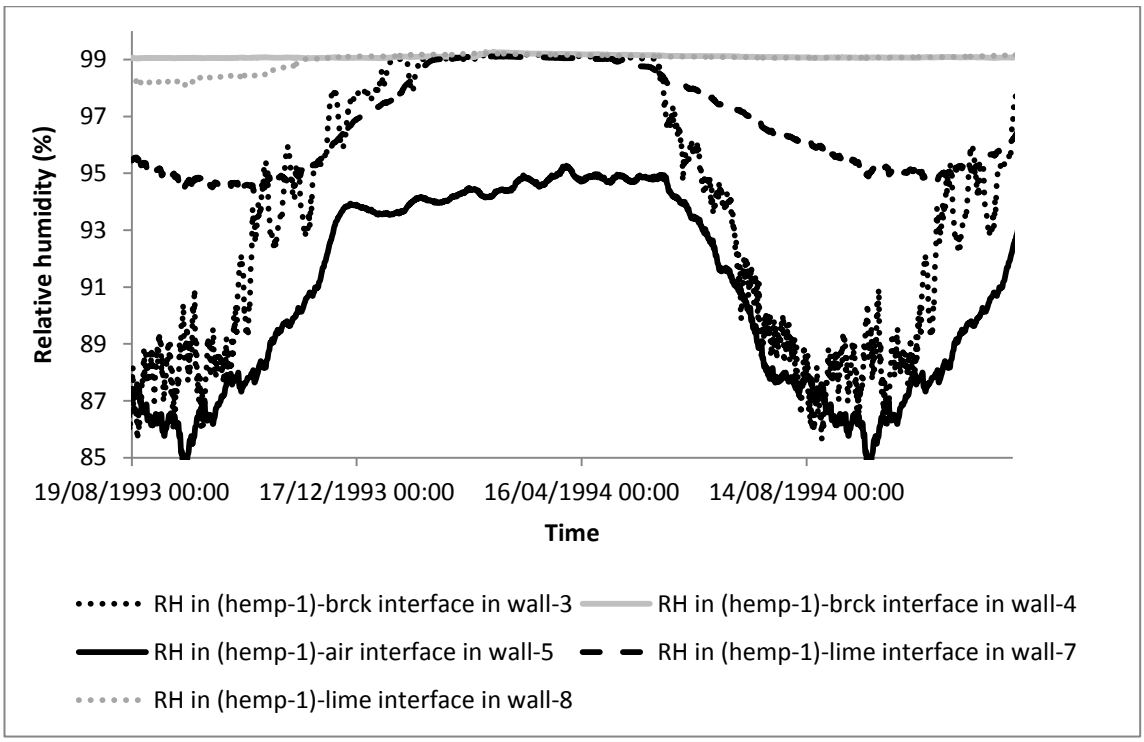


**Figure 8.71: Relative humidity in the (hemp-1)-brick, (hemp-1)-air and (hemp-1)-lime interfaces in walls with and without vapour barrier in Edinburgh.**

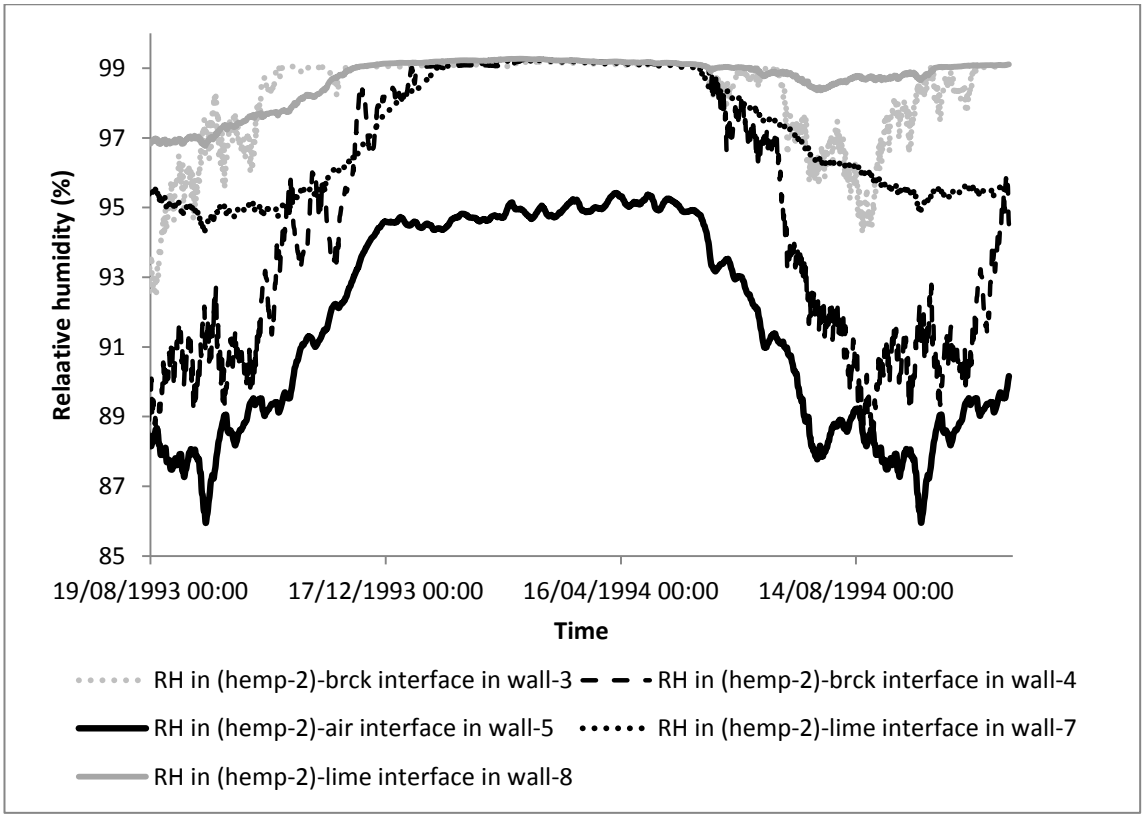


**Figure 8.72: Relative humidity in the (hemp-2)-brick, (hemp-2)-air and (hemp-2)-lime interfaces in walls with and without vapour barrier in Edinburgh.**

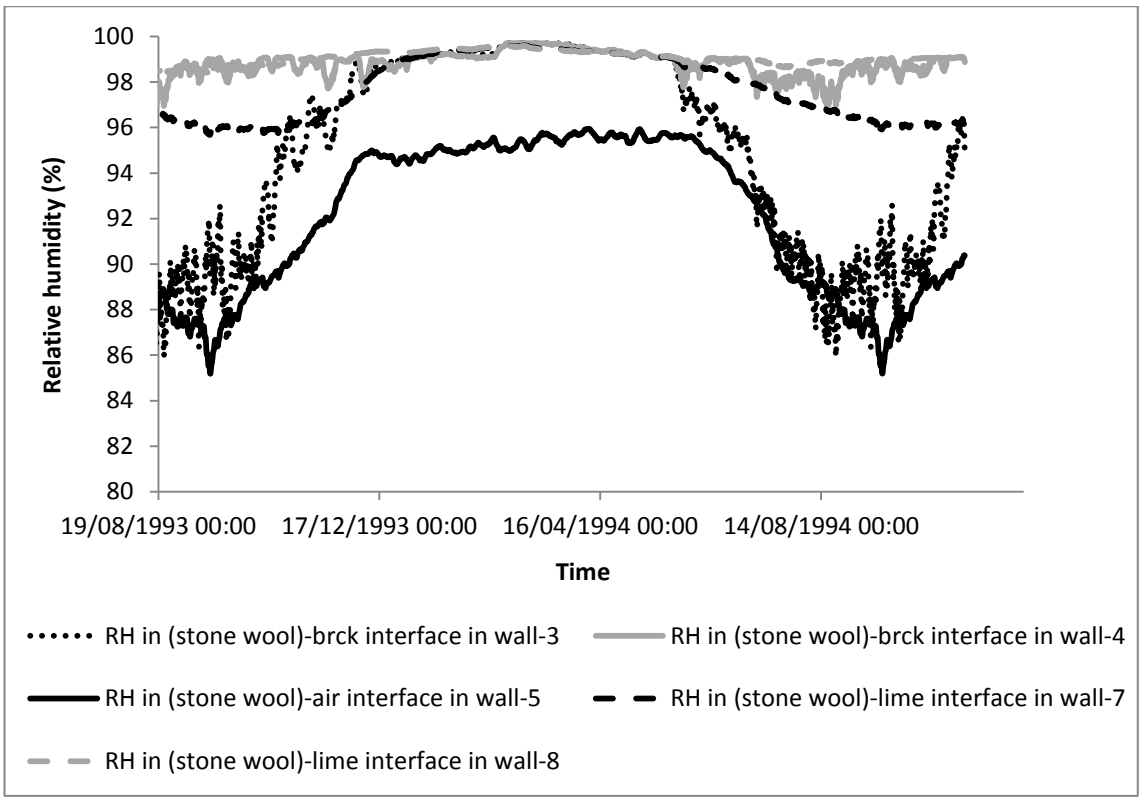


**Figure 8.73: Relative humidity in the (stone wool)-brick, (stone wool)-air and (stone wool)-lime interfaces in walls with and without vapour barrier in Edinburgh.**

Figures 8.74 and 8.75 show the relative humidity in the inner surface of the hemp-2 insulation in wall-7 and wall-8. Figure 8.74 shows the long-term trend over four years' time. It can be observed that the relative humidity in the inner surface of the insulation in wall-8 keeps increasing in the long-term while the relative humidity in the inner surface in wall-7 is always stable. Figure 8.75 shows the relative humidity conditions in the inner surface of insulation materials in wall-7 and wall-8 during 1994. It can be observed that the relative humidity in the inner surface of hemp-2 in wall-8 is about 9% higher than that in wall-7 during the month of July 1994. It can also be noticed in Figure 8.74 that, this difference in relative humidity between the inner surfaces of wall-7 and wall-8 increases gradually and there is a likelihood that sudden change in internal temperature may lead to summer condensation on the vapour barrier of wall-8. It is plausible that similar pattern will appear for other walls where insulations are installed directly on the brick.

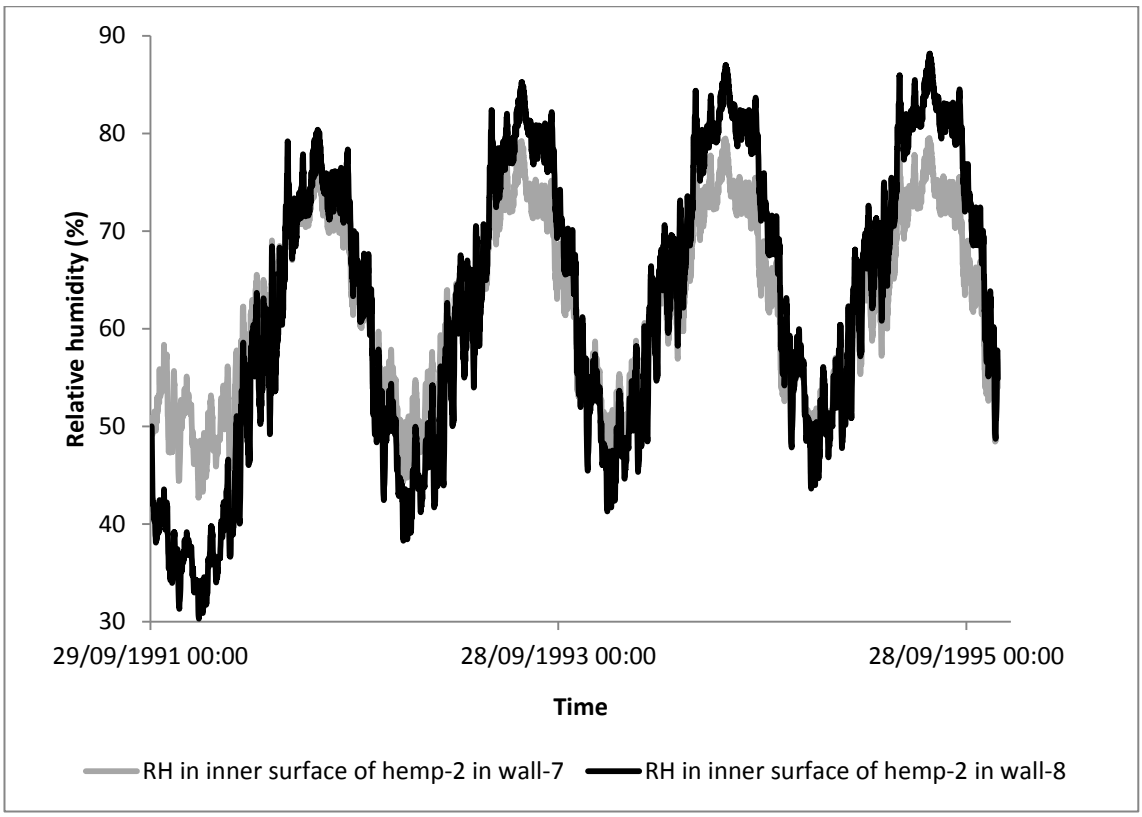


**Figure 8.74: Relative humidity in the hemp-2 inner surface of the wall-7 and wall-8 in Edinburgh during October 1991 to November 1995.**

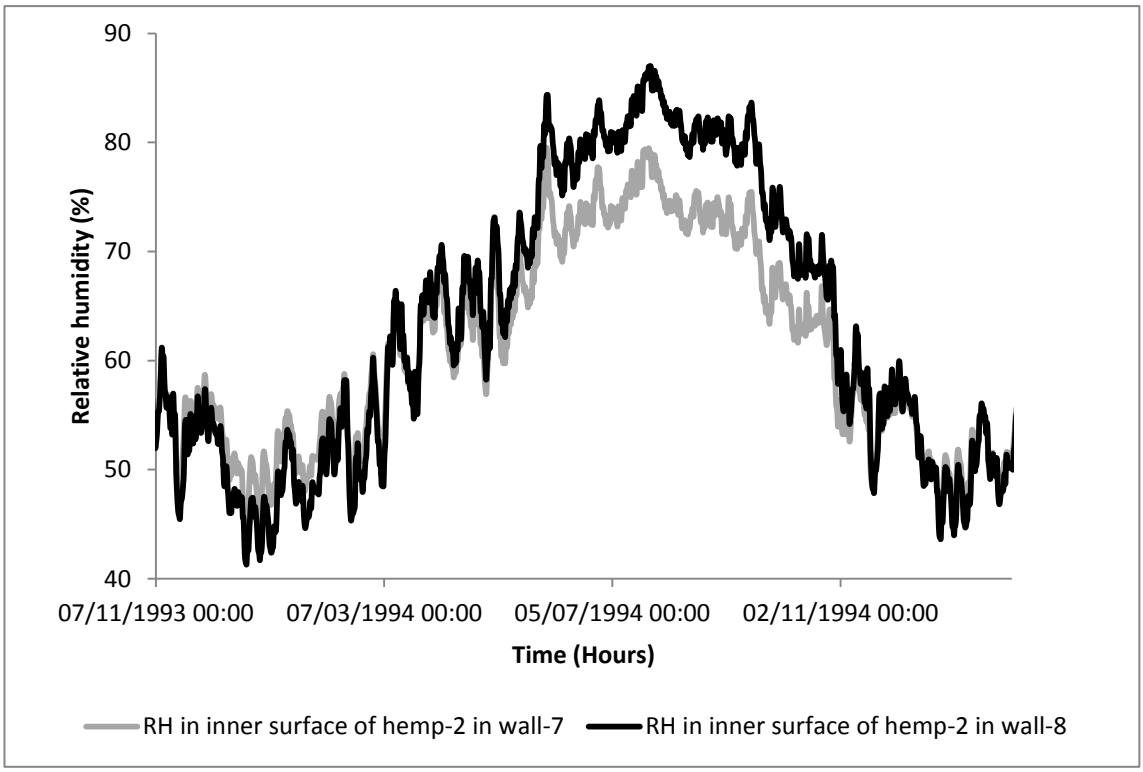


**Figure 8.75: Relative humidity in the hemp-2 inner surface of the wall-7 and wall-8 in Edinburgh during 1994.**

The comparisons of relative humidity conditions in the different walls, with and without vapour barrier, showed that, the vapour open wall with air gap between the insulation and brick performed better than the other types. Based on this observation, the most suitable wall type, the wall-5, was selected to examine the likelihood of mould spore germination and mould growth. If the most suitable wall type does not perform effectively in limiting mould growth, then there is no need to explore the other scenarios.

#### *8.6.3.2 Mould spore germination and mould growth*

Figure 8.76 shows the hygrothermal conditions in the (hemp-2)-air interface of wall-5 in terms of Sedlbauer's isopleth. Figure 8.77 shows the estimated and critical water content in the mould spore in the (hemp-2)-air interface of wall-5 in Edinburgh. It is apparent from Figures 8.76 and 8.77 that there is high likelihood of mould spore germination in the (hemp-2)-air interface. On the other hand, Figures 8.78 and 8.79 show that there is also high likelihood of mould growth in the (hemp-2)-air interface. Based on these results, it can be predicted that there will be a higher probability of mould spore germination and mould growth in the wall interfaces where the relative humidity is as high as shown in subsection 8.5.3.1.

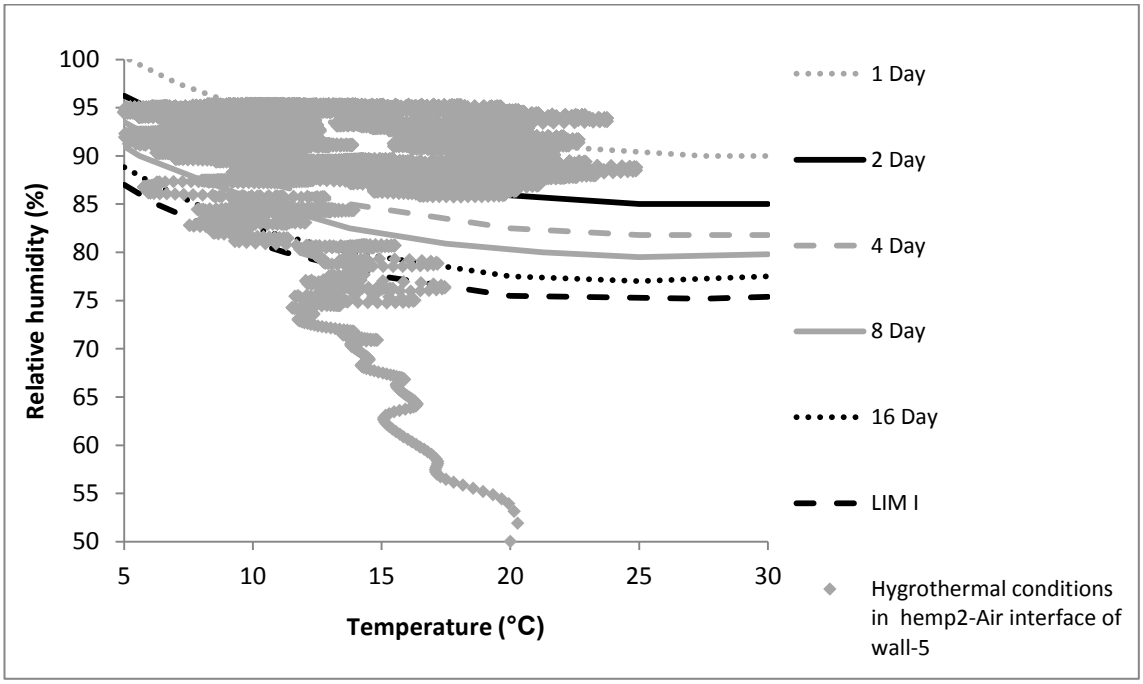


**Figure 8.76: Hygrothermal condition in the (hemp-2)-air interface of wall-5 in Edinburgh.**

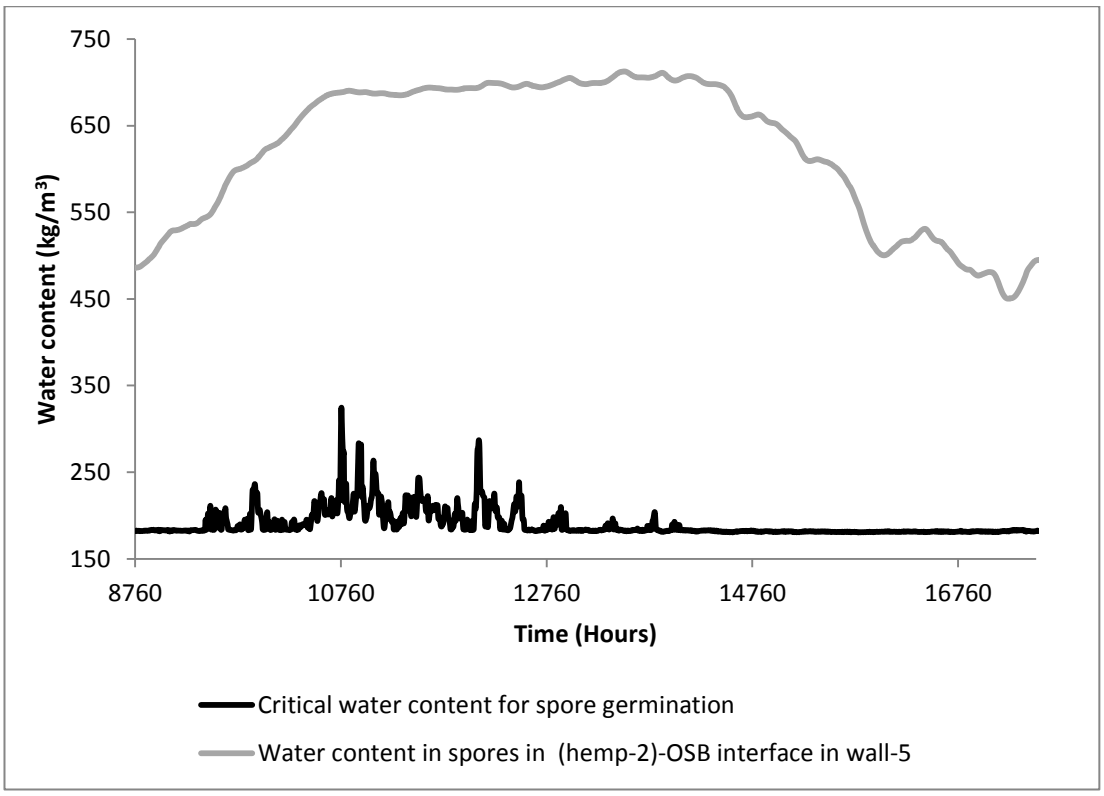


**Figure 8.77: Estimated and critical water content in the mould spore in the (hemp-2)-air interface of wall-5 in Edinburgh.**

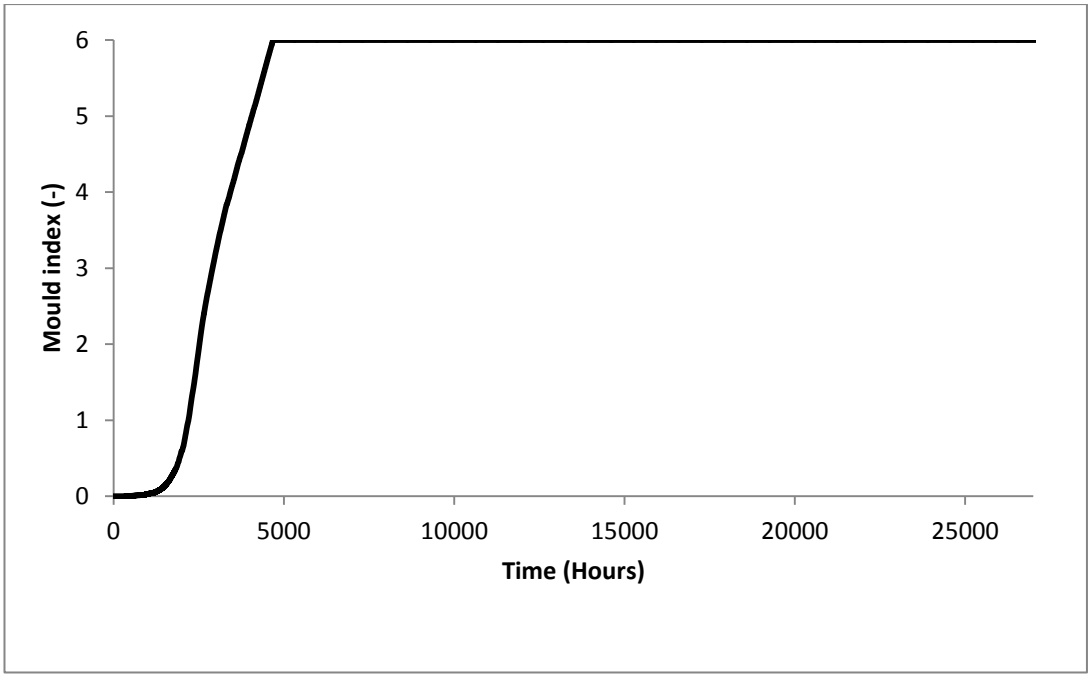


**Figure 8.78: Predicted mould index in the (hemp-2)-air interface of wall-5 in Edinburgh.**

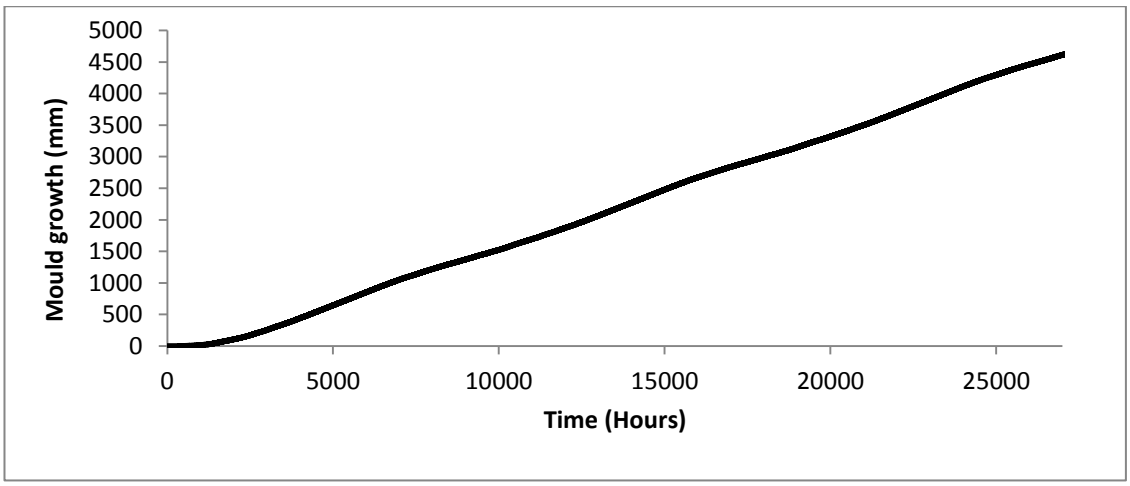


**Figure 8.79: Predicted mould growth in the (hemp-2)-air interface of wall-5 in Edinburgh.**

### *8.6.3.3 Equivalent U-value of the walls*

Figures 8.80, 8.81 and 8.82 show the equivalent U-value of the walls incorporating hemp-1, hemp-2 and stone wool insulation materials, respectively. For hemp-1 and hemp-2 insulation materials, the lowest U-values of the walls were obtained in wall-5 and wall-7. For the stone wool insulation, the lowest U-value was found in wall-5. Both wall-5 and wall-7 were without vapour barriers.

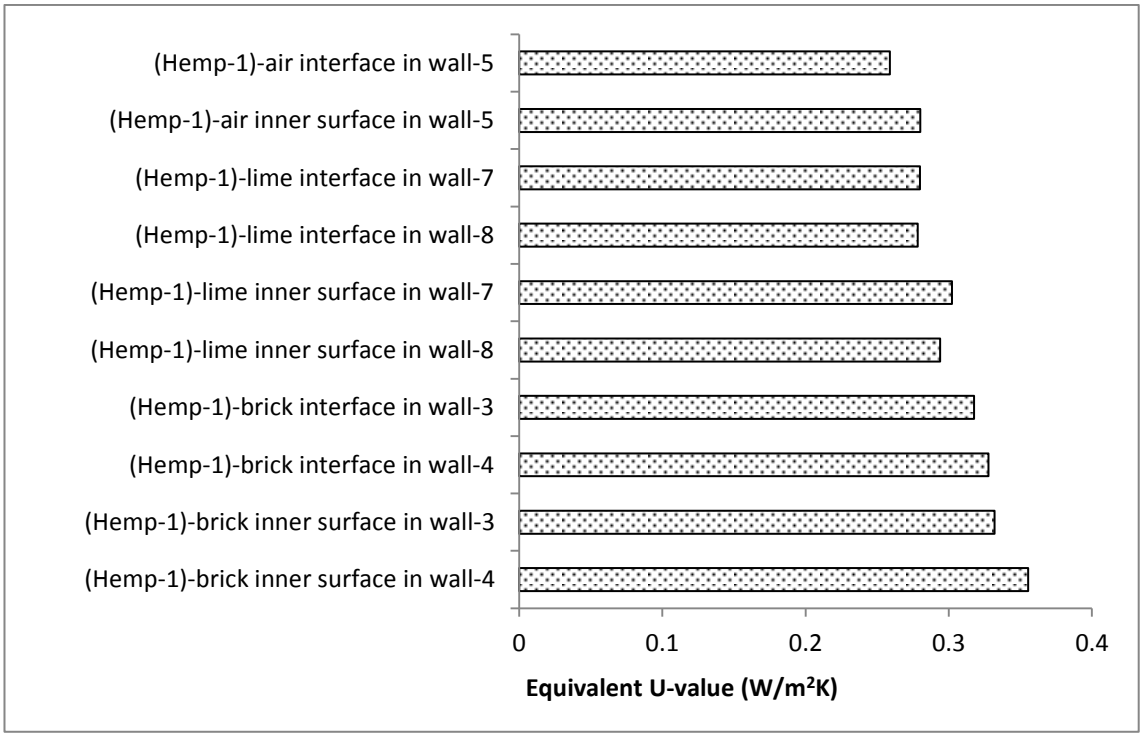


**Figure 8.80: Equivalent U-values of walls incorporating hemp-1 insulations in Edinburgh.**

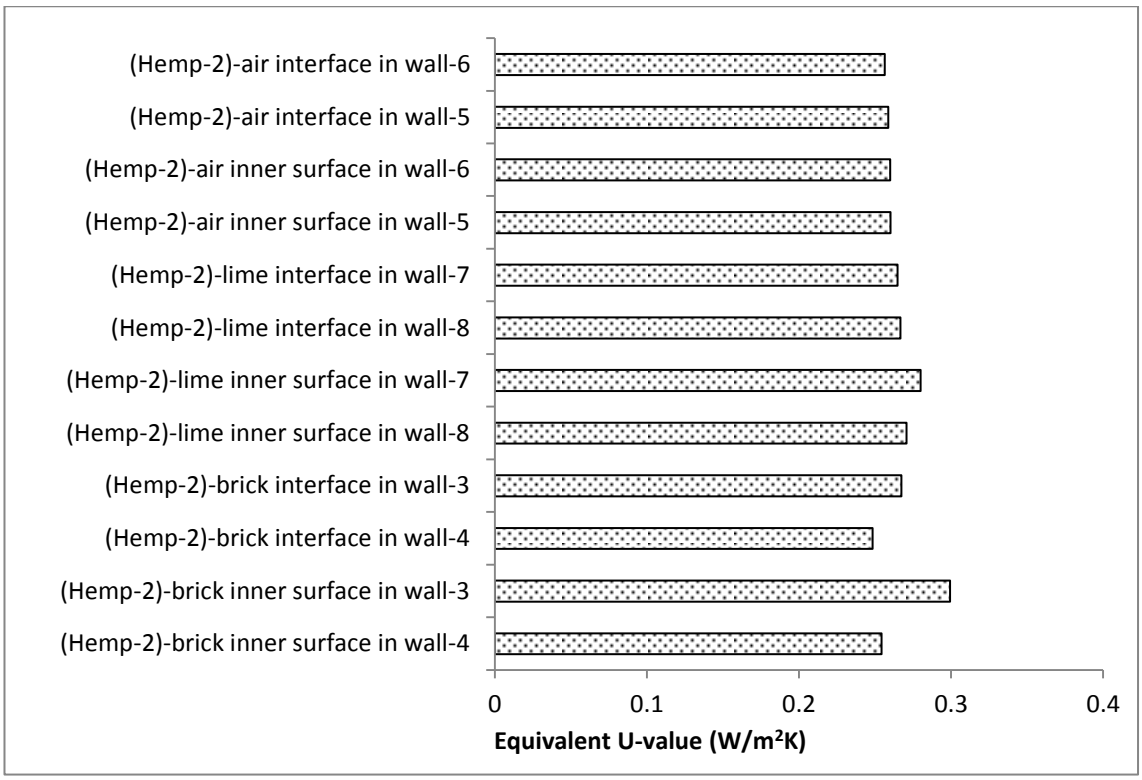


**Figure 8.81: Equivalent U-values of walls incorporating hemp-2 insulations in Edinburgh.**

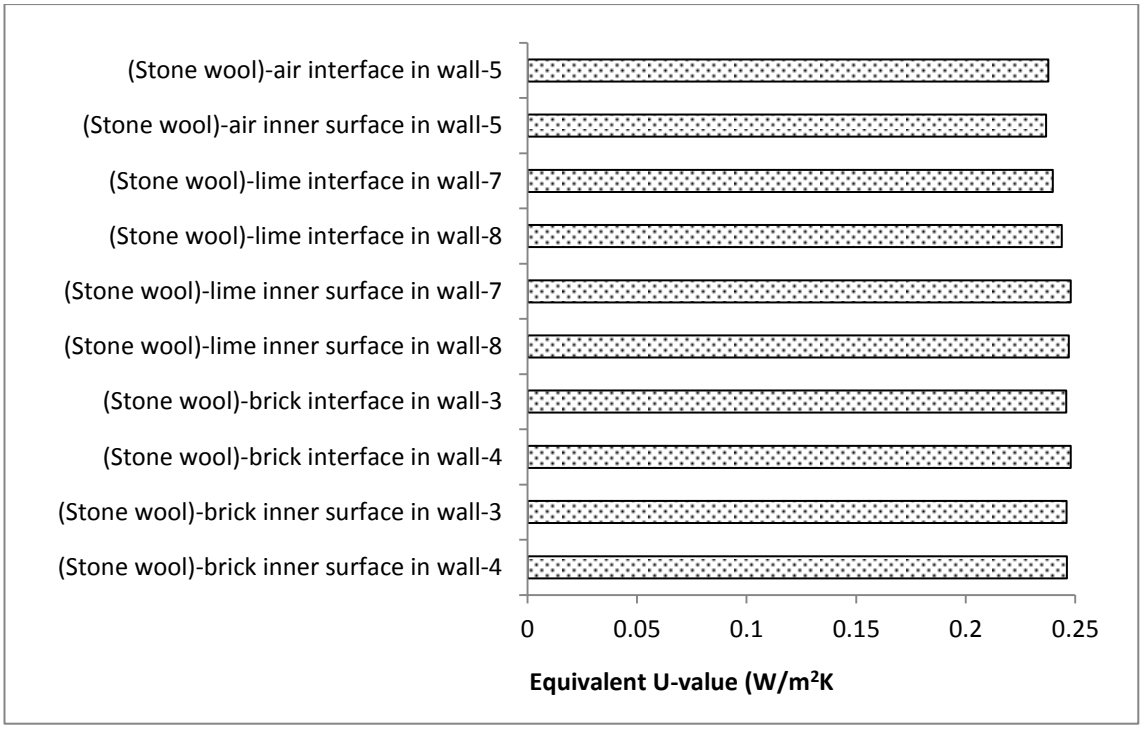


**Figure 8.82: Equivalent U-values of walls incorporating stone wool insulations in Edinburgh.**

### *8.6.4 Solid brick wall in Birmingham*

#### *8.6.4.1 Relative humidity*

Figure 8.83 shows the relative humidity conditions in the (hemp-1)-brick, (hemp-1)-air and (hemp-1)-lime interfaces in wall-3 to wall-8. It can be observed that the relative humidity conditions in the (hemp-1)-brick interface remained at 99% for about 45% and 100% of the analysed period in wall-3 and wall-4, respectively. The relative humidity in the (hemp-1)-lime interface was 99% for about 58% and 100% of the analysed period in wall-5 and wall-6. In the (hemp-1)-air interface of the wall-7, the highest relative humidity was about 94% for about 45% of the analysed period. In the (hemp-1)-air interface of wall-8, the relative humidity was between 94% and 97% during the total period of simulation. It is also observed that during the period of May 1994 to July 1994, the 'drying out' or decrease of relative humidity was quicker in walls without vapour barriers than in those with vapour barriers.

Comparable observations can be made for hemp-2 and stone wool insulation materials as shown in Figures 8.84 and 8.85.

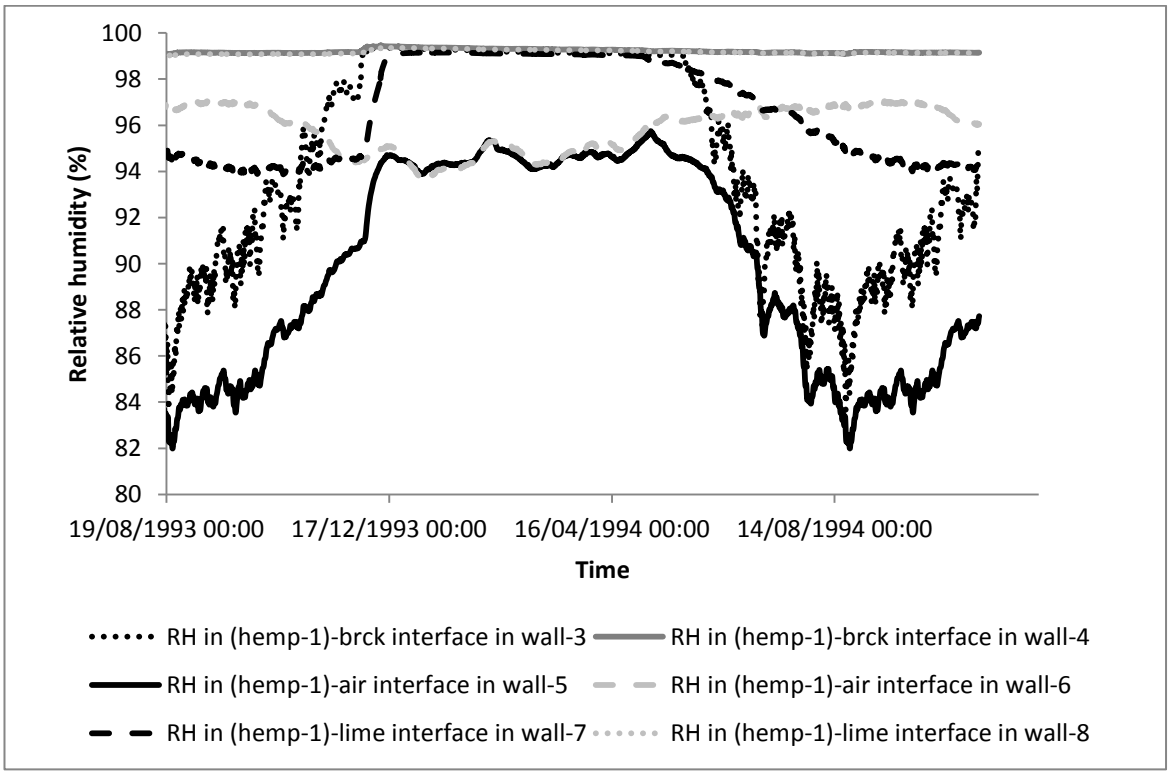


**Figure 8.83: Relative humidity in the (hemp-1)-brick, (hemp-1)-air and (hemp-1)-lime interfaces of solid brick walls in Birmingham.**

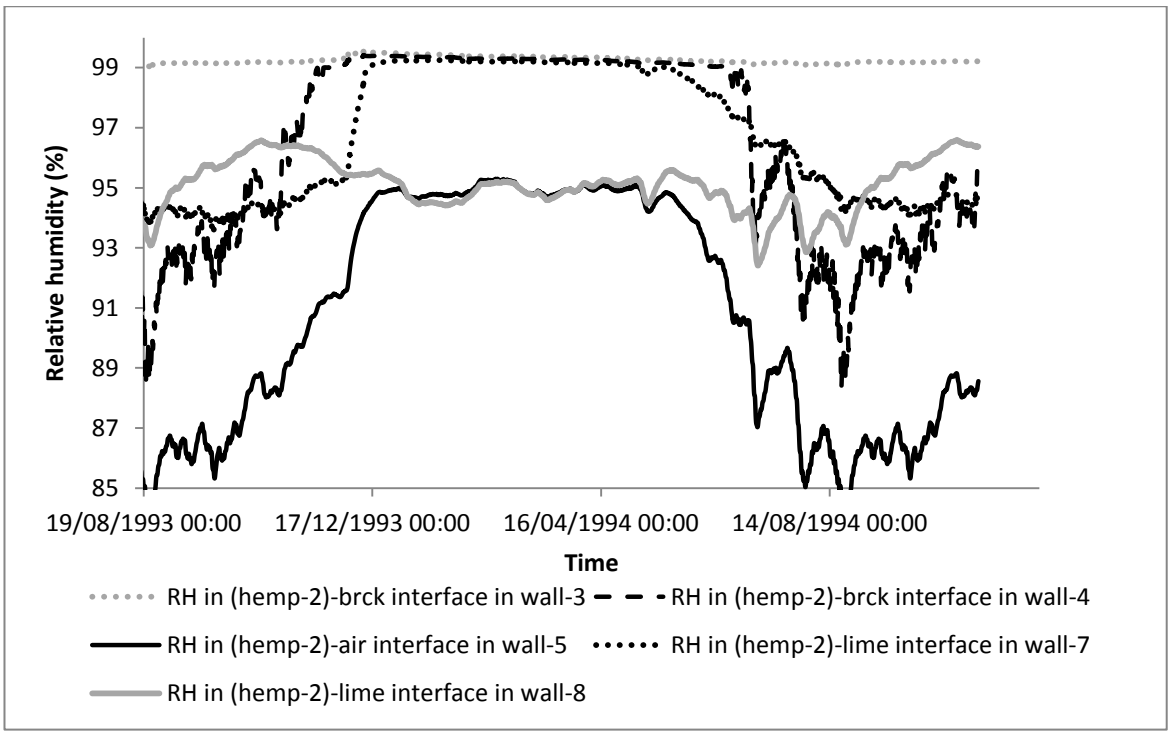


**Figure 8.84: Relative humidity in the (hemp-2)-brick, (hemp-2)-air and (hemp-2)-lime interfaces of solid brick walls in Birmingham.**

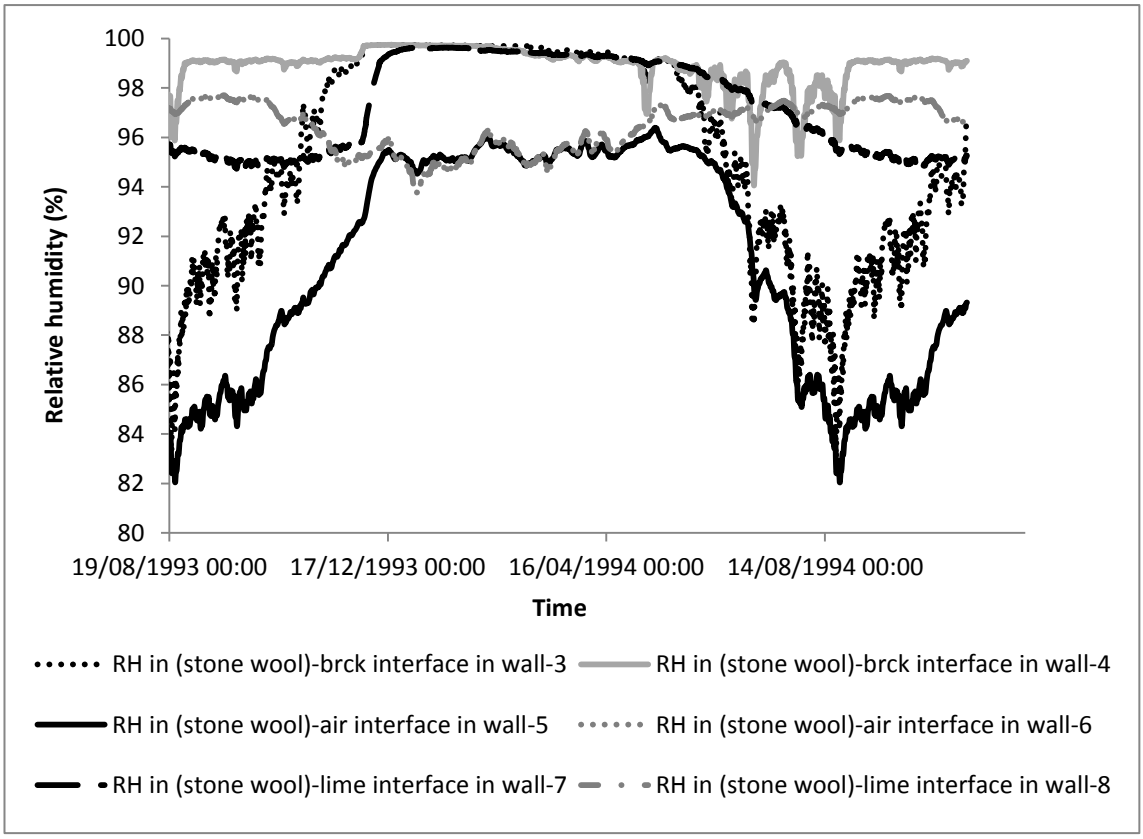


**Figure 8.85: Relative humidity in the (stone wool)-brick, (stone wool)-air and (stone wool)-lime interfaces of solid brick walls in Birmingham.**

### *8.6.4.2 Mould spore germination and mould growth*

The comparisons of relative humidity conditions in the different walls showed that the vapour open wall with air gap between the insulation and brick performed better than the other types in terms of limiting the increase of relative humidity in the interface of the insulation and the adjacent layer. For this reason, one of these better performing walls, wall-5, was chosen to assess the hygrothermal conditions in the insulation-air interface in relation to the likelihood of mould spore germination and mould growth. Figure 8.86 shows the hygrothermal conditions in the (hemp-2)-air interface of wall-5 in terms of Sedlbauer's isopleth. Figure 8.87 shows the predicted water content of the mould spore. From these two Figures, it is clear that the germination of mould spore is highly likely even in wall-5.

It is plausible that the other wall types will perform worse since the relative humidity is higher in the interfaces of the insulation materials and the adjacent layers in all the other walls.

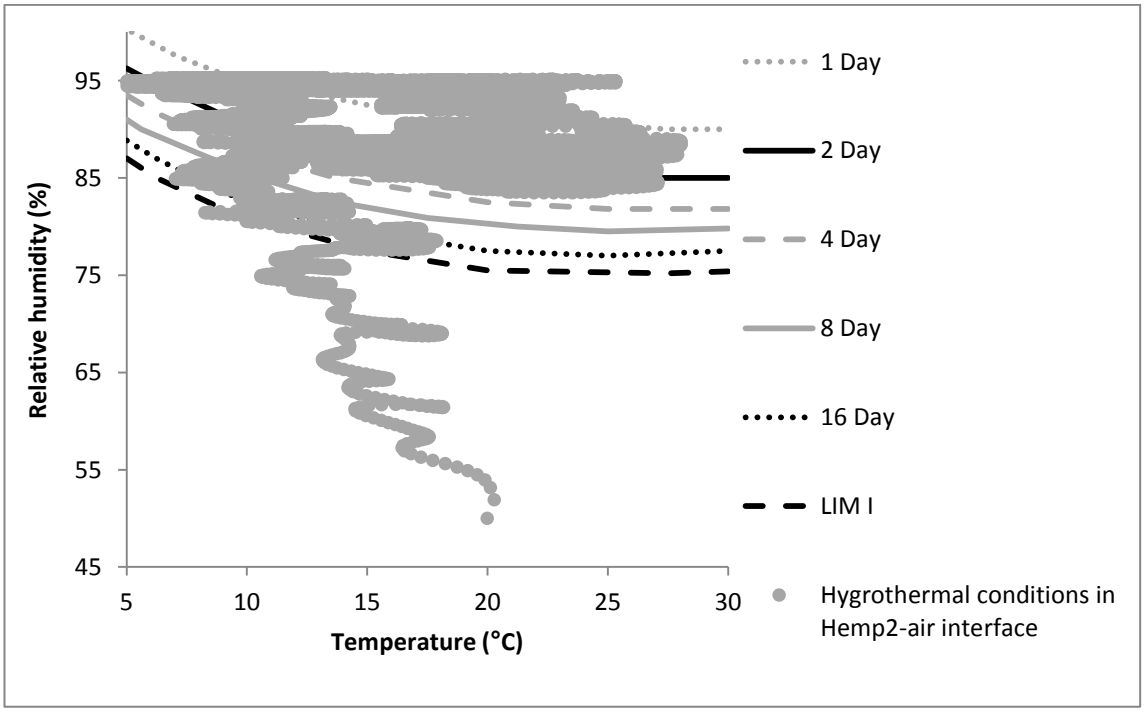


**Figure 8.86: Hygrothermal condition in the (hemp-2)-air interface of the wall-5 in Birmingham.**

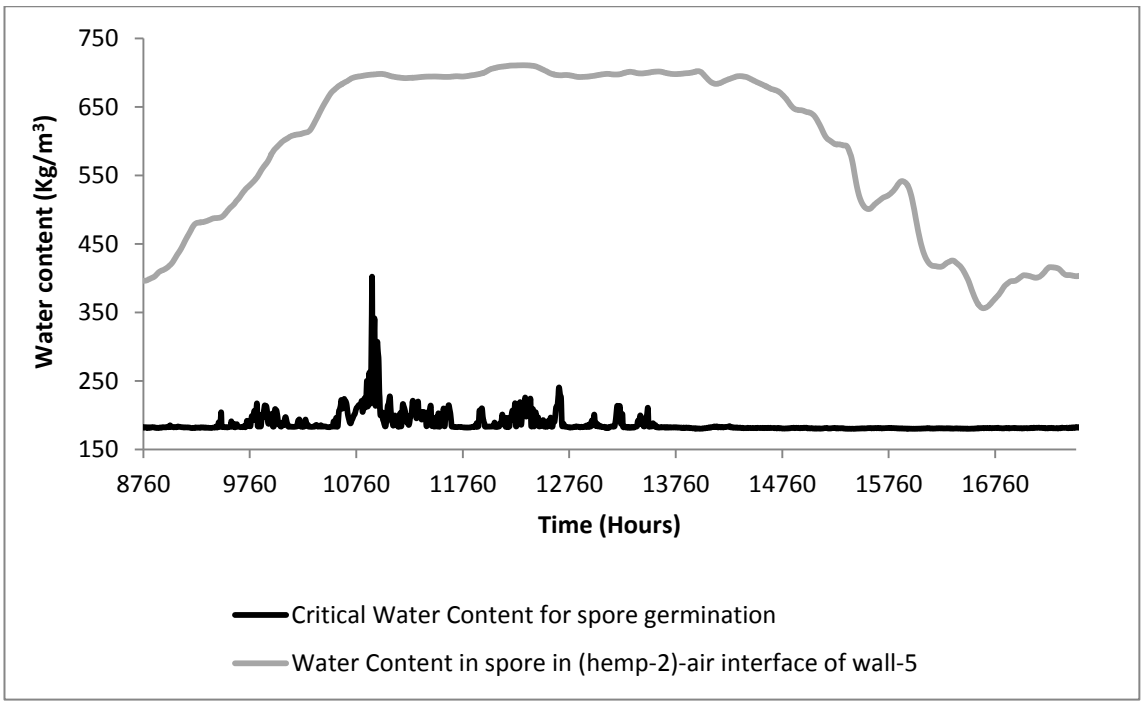


**Figure 8.87: Estimated and critical water content in the mould spore in the (hemp-2)-air interface of wall-5 in Birmingham.**

Figures 8.88 and 8.89 show the mould index and mould growth, respectively. According to these predictions, high level of mould growth can be expected after about 7 months.

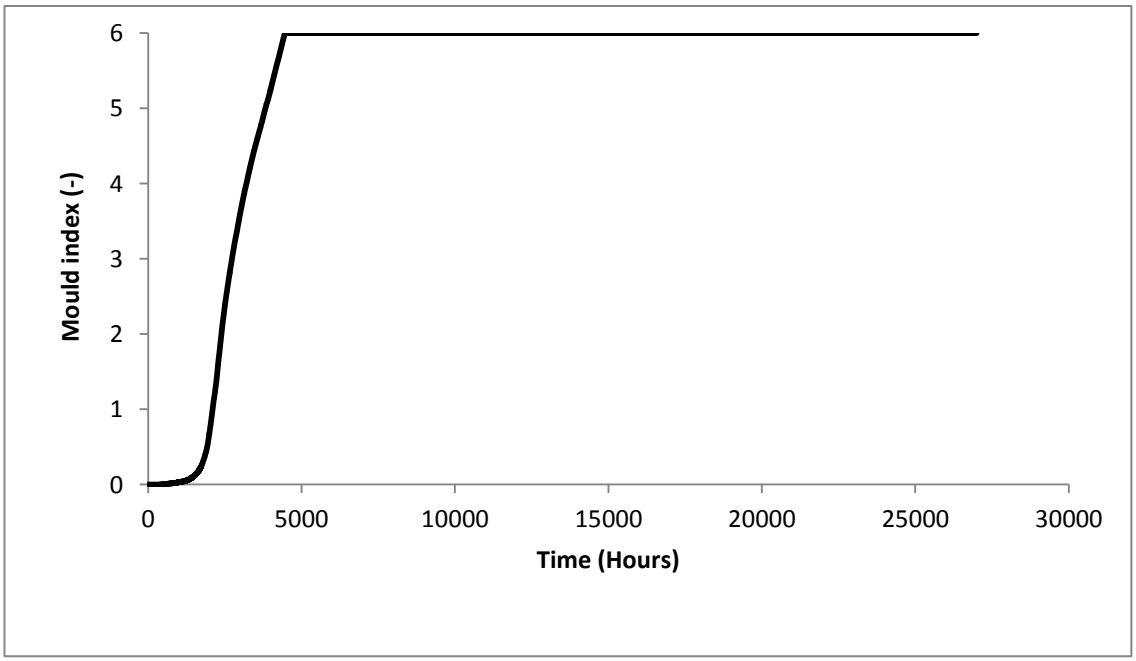


**Figure 8.88: Predicted mould index in the (hemp-2)-air interface of wall-5 in Birmingham.**

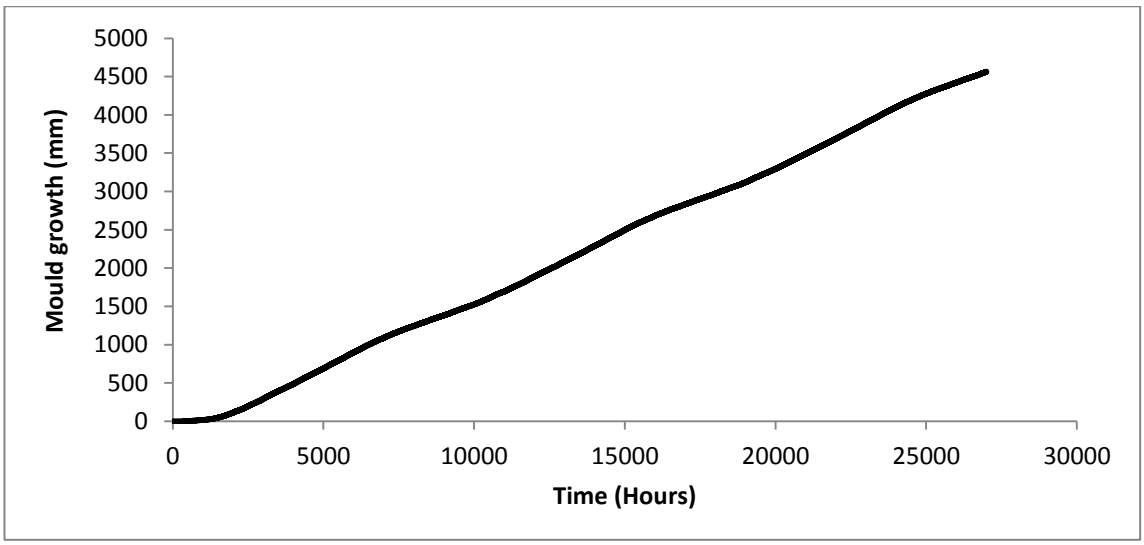


**Figure 8.89: Predicted mould growth in the (hemp-2)-air interface of wall-5 in Birmingham.**

### *8.6.4.3 Equivalent U-values of the walls*

The equivalent U-values of the walls incorporating hemp-1, hemp-2 and stone wool insulations are shown in Figures 8.90, 8.91 and 8.92, respectively. For hemp-1 insulation, the lowest equivalent U-value is observed in wall-5 and wall-7.

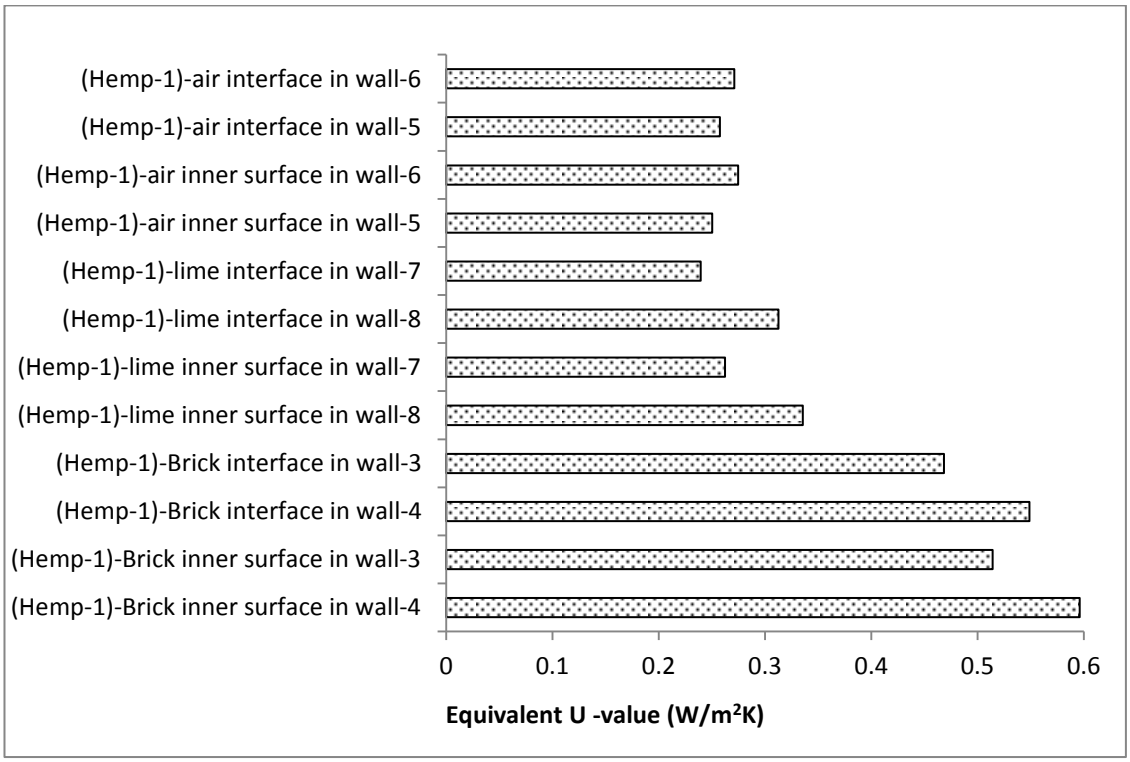


**Figure 8.90: Equivalent U-values of walls incorporating hemp-1 insulations in Birmingham.**

For hemp-2 insulation, the lowest equivalent U-value is obtained in wall-7. For stone wool insulation, the lowest equivalent U-value is also found in wall-7. All the abovementioned walls are without vapour barriers.

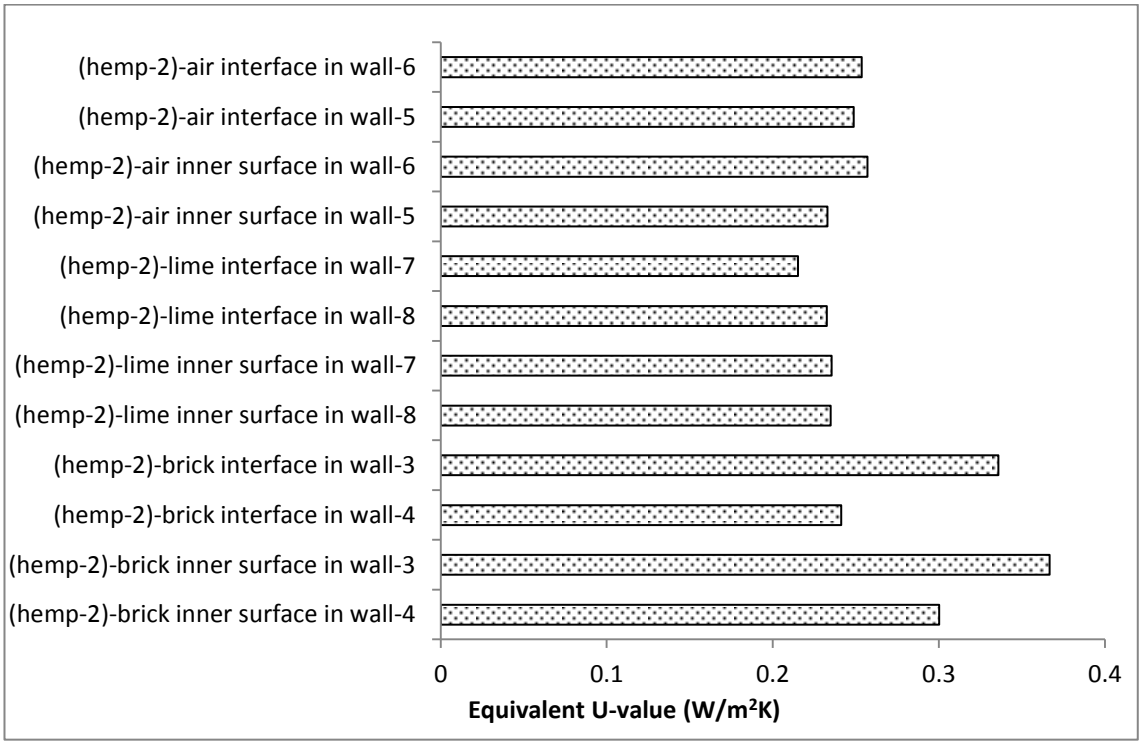


**Figure 8.91: Equivalent U-values of walls incorporating hemp-2 insulations in Birmingham.**

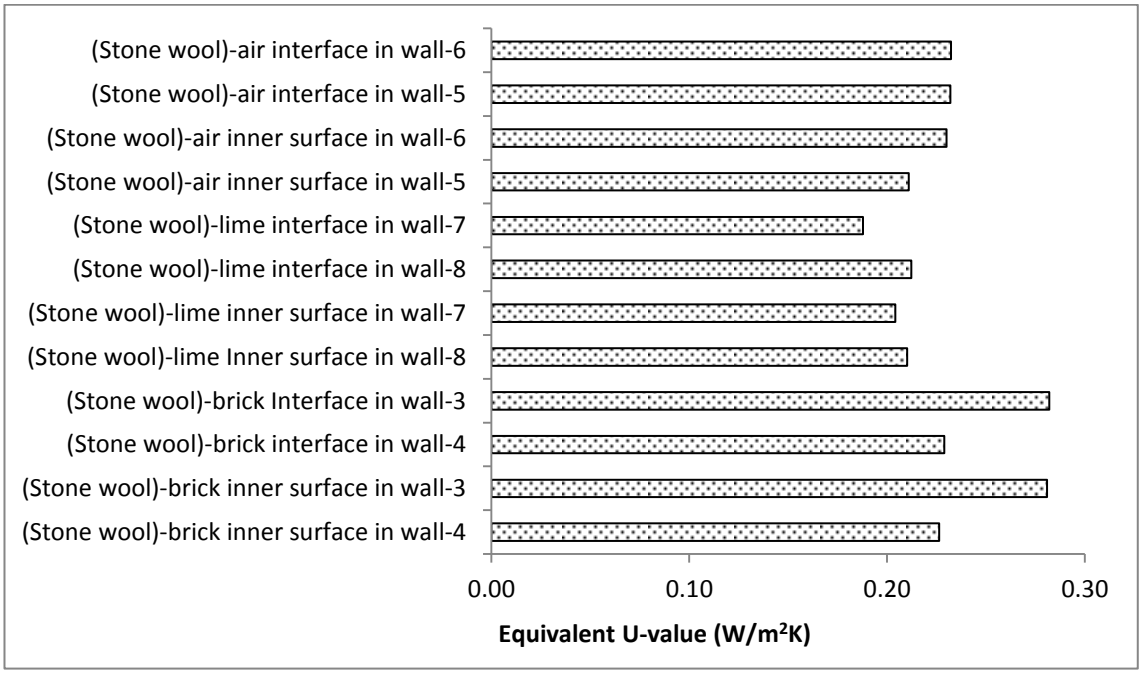


**Figure 8.92: Equivalent U-values of walls incorporating stone wool insulations in Birmingham.**

## 8.7 Chapter summary

Hygrothermal simulations were performed in the WUFI and WUFI-Bio software to determine the hygrothermal performance of hemp-1, hemp-2 and stone wool insulations incorporated in timber frame and solid brick walls of various configurations. The key indicators of the hygrothermal performance of the insulations were: likelihood of interstitial condensation and mould growth and equivalent thermal conductivity and U-value.

### *8.7.1 Condensation, mould spore germination and growth*

Numerical simulations in the WUFI software show that condensation is unlikely in the insulation-OSB interfaces of the timber frame walls, with and without vapour barriers. Mould spore germination and mould growth are likely in the walls without vapour barrier, as the high relative humidity conditions are adequate for encouraging mould spore germination. The highest amount of mould growth in the timber frame wall is predicted in wall-1, which is the wall without vapour barrier incorporating stone wool insulation. The rate of mould growth is higher in the weather condition of Edinburgh than that in Birmingham.

In the insulated brick walls with vapour barriers (wall-4, wall-6 and wall-8), condensation is most likely to occur almost over the entire year, irrespective of the type of insulation installed. However, the insulated brick wall without vapour barrier (the wall-5, with air gap between the insulation and the brick wall) is predicted to be the only wall type where condensation does not seem to be likely. However, even in this best-case scenario, the interface between the insulation and the air layer is susceptible to mould growth because of high relative humidity, with the geographical location of the wall having negligible effect, as shown in Figure 8.93.

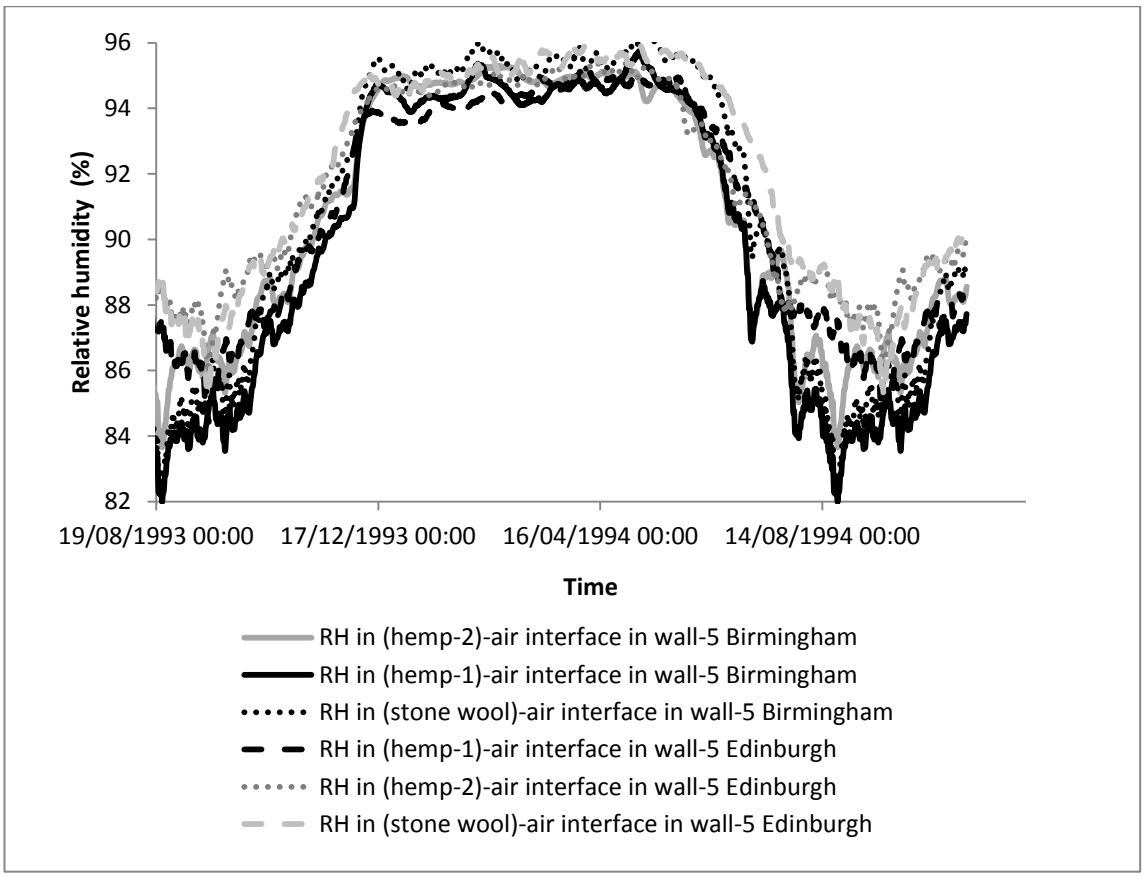


**Figure 8.93: The relative humidity the insulation-air interfaces of wall-5 in Edinburgh and Birmingham.**

### *8.7.2 Equivalent thermal conductivity and U-value*

The equivalent thermal conductivity values of the insulation materials were determined for timber frame walls (wall-1 and wall-2). Except for hemp-1 insulation in Birmingham in wall-2, where equivalent thermal conductivity value was 0.042 W/mK, equivalent thermal conductivity values never exceeded the manufacturers' declared values. Thus, based on the results of the WUFI hygrothermal simulations for wall-1 to wall-8, the thermal performance of hemp-1, hemp-2 and stone wool insulation does not decline in high relative humidity conditions except for hemp-1 insulation in wall-2 in Birmingham.

For solid brick walls, based on the dry U- values of the component materials, the U-value of wall-3 and wall-4 was 0.28 W/m$^2$K, the U-value of wall-5 and wall-6 was 0.29 W/m$^2$K and the U-value of wall-7 and wall-8 was 0.29 W/m$^2$K. In Edinburgh, the predicted U-values were lower than the dry U-values for hemp-2 and stone wool insulation materials. The only exception was wall-4 with hemp-2 insulation, which showed 3% higher equivalent U-value than the

predicted U-value. Thus, in the climatic conditions of Edinburgh, all the insulations are showing excellent thermal performance.

For hemp-1 insulation in Edinburgh, the predicted U-values of the wall-3, wall-4, wall-5, wall-6 and wall-7 exceeded the dry U-values by 18%, 27%, 9%, 13% and 3%. In Birmingham, the U-values of the wall-5 and wall-6 were always lower than the dry U-values. In wall-3 and wall-4 insulation was directly applied on the solid wall surface. Thus, in relation to thermal performance, direct interior application of insulation on solid wall will result in poor performance.

However, the WUFI software does not take into account the potential aging and slumping of the insulation materials and the subsequent change in their thermal conductivity values. The WUFI software also does not calculate the heat loss by convective air transmission through cracks and holes. Therefore, the results derived from the WUFI simulations need to be considered within the context of the limitations of this software.

# Chapter 9

# Conclusions and Recommendations

## 9.1 Overall conclusions

The UK government has committed to reduce greenhouse gas emissions by 80% compared to the 1990 baseline by the year 2050. Any deep cut in greenhouse gas emissions in the UK has to start with the building industry as it is responsible for 55% of the total $CO_2$ emission in the UK. The highest amount of energy in the building industry is used for space heating as most of the 7.7 million domestic buildings with solid brick wall and about 7.6 million of the 19 million domestic buildings with cavity walls in the UK are uninsulated. To reduce greenhouse gas emissions by 80% by the year 2050, the older buildings need to be thermally refurbished and new buildings need to be adequately insulated with such insulation products that are sustainable, renewable and low-carbon. Hemp insulation is one of the few insulation materials that come from renewable source and carry low embodied energy. However, there is a substantial void in knowledge of the thermal and hygric performance of hemp insulation that can be backed up by documented evidence. This gap in knowledge is a significant market barrier for hemp insulation products.

This thesis has contributed to filling the void in knowledge on the hygrothermal performance of hemp based thermal insulations in the context of the United Kingdom. The key objectives of this investigation was to assess the heat and moisture management capacities of hemp insulations in timber frame wall panels, solid brick walls and loft spaces and to put the findings of the assessments into the wider context of the hygrothermal performance of conventional insulations by comparing hemp insulation's hygrothermal performance with that of stone wool. The assessments were conducted using detailed laboratory-based experiments, in situ experimental monitoring and computer based numerical hygrothermal simulations. The key findings in this thesis are critically summarised below.

### *9.1.1 Hygric material properties of hemp insulations*

The hygric properties of hemp insulations that have been determined in steady state hygrothermal conditions in the laboratory are: adsorption-desorption isotherm, moisture buffering capacity, vapour diffusion resistance factor and water absorption coefficient.

In terms of the material properties, one of the key findings during the laboratory-based experiment is that the hemp insulations show 'excellent' ($MBV_{practical} \geq 2$) and 'good' ($2 > MBV_{practical} \geq 1$) moisture buffering capacity in relation to the 'Moisture Buffer Value Classes'. Moisture buffering capacity of hemp insulations can be very useful in moderating the relative humidity and thereby mitigating the risk of condensation inside walls and in the loft spaces. Moisture buffering capacity of hemp insulations can also be potentially utilised in interior spaces when the insulations are used in vapour open walls. Compared to hemp insulation, mineral insulations, such as stone wool, have a negligible buffering capacity due to their non-hygroscopic nature.

Hemp insulations can adsorb 22%-56% moisture of their dry weight at 95% relative humidity, depending on the make of the hemp insulations, while stone wool can only adsorb 1% moisture of its dry weight at 95% relative humidity. The moisture adsorption capacity combined with negligible hysteresis contributes to hemp insulation's 'good' and 'excellent' moisture buffering performance. However, in relation to moisture adsorption at high relative humidity, there are significant differences between the different makes of the hemp insulations researched in this thesis. This is due to the make of the hemp fibre insulations and the differences in the methods of hemp fibre extraction.

The vapour diffusion resistance factors of hemp insulations are largely similar to that of stone wool insulation and other fibrous insulations. However, some hemp insulations have shown high standard deviations (about 43% from the mean value) among the samples during the experimental determination of vapour diffusion resistance factor. This may be due to the non-homogenous nature of some of the hemp insulation samples. The water absorption coefficients of hemp-2, hemp-3, hemp-4 and hemp-5 insulation materials are equal to 0.03 kg/(m2√s) while the water absorption coefficient of hemp-1 is 0.04 kg/(m2√s), which is 33% higher than that of the other hemp insulations.

During the A value tests, it has been observed that long-term contact with liquid water can harden the surface of the hemp insulation and increase the density of that surface. This change in surface structure may have implication on the thermal conductivity and vapour diffusion resistance factor of hemp insulations.

### *9.1.2 Moisture management of hemp insulations*

Moisture management of hemp insulations in dynamic, quasi steady state and in situ hygrothermal conditions were studied through a wide variety of laboratory-based and in situ experiments.

An experimental dual-insulation set up and associated method of data analysis have been developed by the author during the course of the research to determine and compare the hygrothermal performances of two different insulations exposed to similar hygrothermal boundary conditions. The findings of experiments reflect the hygrothermal conditions in the insulation interfaces reasonably accurately in terms of comparing the moisture management potential of the two insulations, as verified by the results of the in situ tests. It was observed from the laboratory-based dynamic and quasi steady state hygrothermal experiments that, when exposed to high relative humidity, the likelihood and frequency of interstitial condensation was higher in the stone wool insulations than in the hemp insulations. It confirms that hemp has better moisture management capacity in dynamic hygrothermal conditions. These findings are further supported by the results of the steady state hygric tests of the moisture buffering and adsorption capacity of hemp insulations, as described in sections 4.1 and 4.2 of chapter four. During the laboratory based experiments, it was also observed that critical relative humidity conditions for mould growth remain shorter during the wetting up and longer during the drying up periods in the external surface of hemp-2 insulation than that in stone wool insulation.

A timber frame test building was built from scratch by the author to study the heat and moisture management capacity of hemp and stone wool insulations. An in situ experimental method was also developed by the author to study the hygrothermal properties of the insulation in a range of interior relative humidity conditions. In situ assessment of hygrothermal properties of hemp and stone wool in timber frame wall panels confirms the findings of the laboratory-based

experiments for the moisture management capacities of these two insulations. The likelihood of frequent condensation was observed in the external faces of the insulations in vapour open timber frame panels incorporating stone wool, while there was no likelihood of condensation in the hemp insulations.

Numerical simulations using the WUFI hygrothermal software show that condensation is unlikely in the timber frame structure. In solid brick walls, condensation is unlikely only in the walls with air gaps between the insulation and the brick wall (wall-5 and wall-6).

### *9.1.3 Mould spore germination and mould growth*

To explore the potential of mould spore germination, the hygrothermal data gathered from the in situ experiments in timber frame wall panels have been analysed in relation to Sedlbauer's isopleths. The findings of the first test show that mould spore germination is possible in the external faces of insulations in timber frame wall panels incorporating hemp insulations. Mould germination is likely in both the walls with and without vapour barriers. When hemp insulation has been compared with stone wool insulation in vapour open wall panels during one of the in situ tests, it has been found that stone wool is more susceptible to mould spore germination than hemp insulation.

Despite these predictions of mould spore germination, no visible evidence of mould growth was observed in the external faces of insulations when the insulations were dismantled. Nevertheless, further observation with a digital microscope revealed some possible traces of mould on one of the OSB panels, but the sample was not cultured for further confirmation.

Numerical simulations using the WUFI hygrothermal software and the analysis of the hygrothermal output data in WUFI-Bio software show that mould growth is likely in the timber frame wall without vapour barrier while there is no likelihood of mould growth in the wall with vapour barrier. Clearly the findings about the implausibility of mould spore germination in the wall with vapour barrier established by numerical simulations do not agree with the findings for the same type of wall panels during the in situ tests.

Hygrothermal analysis of the results obtained from the numerical simulations using the WUFI software shows that mould growth is also likely in the

insulation-brick, insulation-air and insulation-lime interfaces of all the selected solid brick wall types. Therefore, as far as the results of the WUFI software are concerned, the application of these insulations on solid brick walls does not seem feasible in relation to the hygric performance of the insulations. The finding is applicable to walls incorporating either hemp or stone wool insulation. However, the rate of mould growth is the highest in the walls insulated with stone wool. Therefore, compared to stone wool, hemp insulation is less susceptible to mould growth. Based on the hygrthermal simulations, it seems that anti-fungal treatment of the insulations should be considered to mitigate the risk of mould growth. However, the results of the hygrothermal simulations must be considered within the context of the limitations of the software.

### *9.1.4 Thermal conductivity and U-value*

Thermal conductivity values of the insulation materials were determined using steady state, dynamic, quasi steady state and in situ hygrothermal boundary conditions. It was observed that the thermal conductivity values of insulation materials at ranges of related humidity conditions could be dependent on the method used to determine the thermal conductivity values.

Thermal conductivity values were measured in steady state thermal conditions using the Fox 600 hot plate. The results have shown that the thermal conductivity of hemp-5 insulation is 0.039 W/mK at 10% relative humidity and 0.043 W/mK at 80% relative humidity, respectively. However, it is demonstrated in subsection 6.4 of chapter six that this method, when applied to measuring the thermal conductivity of moist insulation after steady state heat flux is established, causes moisture gradient along the depth of the sample and does not necessarily represent the thermal conductivity of homogenously moistened insulations.

Equivalent thermal conductivity values of both hemp and stone wool insulations were determined in vapour open condition in the laboratory applying a new experimental method using the principles of measuring average heat flux and average temperature difference. When the method was applied in dynamic hygrothermal boundary conditions (henceforth mentioned as the first test), it was found that the equivalent thermal conductivity of hemp-2 insulation varied between 0.035 W/mK and 0.046 W/mK (31% increase) for the relative humidity

ranging between 50%-80%. The equivalent thermal conductivity values of stone wool insulation varied between 0.053 W/mK and 0.068 W/mK (28% increase) for the relative humidity ranging between 50%- 80% during the first test. The average equivalent thermal conductivity of hemp-2 was 0.038 W/mK and that of the stone wool insulation was 0.054 W/mK, which were 0% and 42%, respectively, higher than the manufacturers' declared values.

The new experimental method was also applied in quasi steady state hygrothermal boundary conditions, henceforth mentioned as the second test. It was found that the thermal conductivity of hemp-2 insulation varied between 0.039 W/mK and 0.062 W/mK for the relative humidity ranges of 33%-100% (59% increase). At 80% relative humidity, the thermal conductivity of hemp insulation was 0.056 W/mK. Considering that about 9% error can occur in the thermal conductivity readings, the upper limit of the thermal conductivity of hemp insulation at 80% relative humidity during the first test in the dynamic hygrothermal boundary condition was about 0.050 W/mK. The thermal conductivity value of 0.05 W/mk was also the lower limit of the thermal conductivity of hemp-2 insulation at 80% relative humidity, determined during the second test in quasi steady state hygrothermal boundary conditions. Similarly, the upper limit of the average thermal conductivity of hemp-2 insulation during the first test was about 0.041 W/mK and the lower limit of the average thermal conductivity during the second test was about 0.043 W/mK. Hence, taking the possible errors in reading into account, the thermal conductivity values of hemp-2 insulation determined in dynamic hygrothermal conditions is potentially similar to thermal conductivity values of hemp-2 insulation determined in quasi steady state hygrothermal boundary conditions.

For stone wool insulation, it was found during the test in quasi steady state hygrothermal boundary condition that the equivalent thermal conductivity values could vary between 0.040 W/mK and 0.028 W/mK (30% decrease) for the relative humidity range of 33% to 100%. At 80% relative humidity, the equivalent thermal conductivity of stone wool insulation was determined as 0.035 W/mK. During the first test in dynamic hygrothermal boundary condition, equivalent thermal conductivity of stone wool at 80% relative humidity was 0.68 W/mK. It seems that during the second test the condensation that occurred at some locations of the stone wool exterior surface did not coincide with the

placement of the heat flux sensor. Hence, the heat flux sensor failed the register the heat flux by enthalpy flow. It may also be possible that, during the second test, when condensation occurred at the outer surface of stone wool insulation, the heat released from phase change was partially directed towards the insulation. Thus, the equivalent thermal conductivity of stone wool insulation in a vapour open setup in high relative humidity may become difficult to assess in a consistent manner. Condensation can occur very quickly on the exterior surface of stone wool and can influence the magnitude and direction of heat flux.

However, during the 'loft test' the average equivalent thermal conductivity of hemp-1 and hemp-4 insulations were determined as 0.028 W/mK and 0.034 W/mK, respectively, while the average equivalent thermal conductivity of stone wool was determined as 0.052 W/mK. These equivalent thermal conductivity values of the insulations support the results of the first test in dynamic hygrothermal boundary conditions.

During the in situ tests, it was found that in the timber frame structure, equivalent thermal conductivity of hemp-1, hemp-2 and stone wool insulations were always below or equal to the manufacturers' declared thermal conductivity values. This finding is very significant as it shows that the average thermal conductivity of the insulation materials during service conditions do not deteriorate from the manufacturers' declared values.

These aforementioned findings in relation to the equivalent thermal conductivity values of the insulation in timber frame walls were further supported by the equivalent thermal conductivity values determined using the analysed output data of the WUFI simulation software. Equivalent thermal conductivity values of the insulation materials were determined for timber frame walls (wall-1 and wall-2). Except for the hemp-1 insulation in a Birmingham climate in wall-2, where the equivalent thermal conductivity value was 0.042 W/mK, the equivalent thermal conductivity values of the insulations in all other cases never exceeded the manufacturers' declared values. It is to be noted that 0.042 W/mK is also within the error range of the manufacturer's declared value of thermal conductivity of hemp-1 insulation.

For solid brick walls, based on the dry U- values of the component materials, the following U values were obtained: the U-value of wall-3 and wall-4 was 0.28 W/m$^2$K, of wall-5 and wall-6 was 0.29 W/m$^2$K and of wall-7 and wall-8 was 0.29 W/m$^2$K. In an Edinburgh climate, the predicted U-values, based on analysis of the output data from the WUFI software, were lower than the dry U-values for hemp-2 and stone wool insulation materials, with the only exception of wall-4 with hemp-2 insulation, which showed 3% higher equivalent thermal conductivity value than the dry U-value. For hemp-1 insulation in Edinburgh, the predicted U-values of wall-3, wall-4, wall-5, wall-6 and wall-7 exceed the dry U-values by 18%, 27%, 9%, 13% and 3%, respectively. In Birmingham, the U-values of wall-5 and wall-6 were always lower than the dry U-values.

However, the WUFI software did not take into account the potential slumping and degradation of some of the insulation types and the subsequent change in thermal conductivity values. The WUFI software also did not calculate the heat loss by convective air transmission through cracks and holes. Therefore, the results derived from the WUFI simulations need to be considered within the context of the limitations of this numerical simulation software.

## 9.2 Contribution to knowledge

This thesis has made original contributions to knowledge in terms of assessing the hygrothermal performance of hemp insulations. These contributions are outlined below.

### *9.2.1 Moisture management of hemp insulation*

This thesis, for the first time to the author's knowledge, has established by laboratory-based and in situ experiments that hemp insulation reduces the frequency and magnitude of interstitial condensation in the building envelope (walls and roofs). The 'excellent' and 'good' moisture buffering capacity of hemp insulations is also established through laboratory based experiments.

### *9.2.2 Experimental setup for visual inspection of condensation*

This thesis, for the first time to the author's knowledge, has presented a dual insulation experimental set up in a dynamic hygrothermal hot box where condensation in insulations can be visually identified. This is a simplified but effective way to visually compare the hygric performances of two different

insulation materials in a way that can be readily recognised by the scientific and the non-scientific community.

### *9.2.3 Experimental determination of the equivalent thermal conductivity of hemp insulations in the laboratory*

During the course of the research, a new method of determining equivalent thermal conductivity of hemp insulations in vapour open conditions and in a range of relative humidity conditions was developed. This method portrayed the heat transfer phenomena through hemp insulation in service condition more accurately than the conventional methods. The equivalent thermal conductivity values obtained using the new method agrees with the equivalent thermal conductivity data obtained in service conditions. However, this method needs further technical refinement and benchmarking.

### *9.2.4 In situ measurement of equivalent thermal conductivity of hemp insulations*

During the course of the research, the equivalent thermal conductivity values of hemp and stone wool insulations in a timber frame test building were determined in a range of interior relative humidity conditions. Equivalent thermal conductivity values of hemp insulations were also determined for timber frame wall panels, with and without vapour barrier. It was established that the equivalent thermal conductivity of hemp insulations did not exceed the manufacturers' declared values. To the author's knowledge, no such in situ approach to determining in situ equivalent thermal conductivity value of hemp insulation in a range of relative humidity conditions was taken before.

During the in situ determination of equivalent thermal conductivity of insulation materials, it was also found that the equivalent thermal conductivity values could differ based on the placement of the heat flux meter, either on the surface of the internal plaster board or in the insulation-OSB interface (near the external surface of the insulation). The assumed reason for the variation was phase change of moisture in the insulation-OSB interface. This finding was not reported before by other researchers.

## 9.3 Industrial benefits from the research

The following industrial benefits are anticipated from the research:

- The documented evidence of heat and moisture management capacity of hemp insulations can be utilised by the insulation industry to improve the performance of bio-based fibrous insulation materials and promote them to the target market.
- The documented evidence of the moisture and heat management capacity of hemp insulations can be used by the industry for the purpose of product certification, warranty, insurance etc.
- The documented evidence of the moisture and heat management capacity of hemp insulations can be used to gain recognition for hemp insulations as sustainable and efficient insulation materials from the UK government and the relevant non-government establishments.
- Documented evidence of the moisture and heat management capacity of hemp insulations can be used by the industry to obtain funding from the government and other stakeholders to conduct further research to develop bio-based fibrous insulation prototypes.

## 9.4 Recommendations for further work

### *9.4.1 Improvement of the dual insulation set up*

An experimental method and setup have been developed to determine equivalent thermal conductivity of insulations when the insulations are directly exposed to high relative humidity and temperature gradient. The experimental method can also be used to study heat and moisture transfer in a dual insulation setup, developed by the author, where two insulation materials are exposed to identical hygrothermal boundary conditions. The experimental method and setup need further testing and further technical refinement so that thermal conductivity can also be determined without causing any condensation in the insulation-acrylic interface. One of the potential ways of doing this is to keep both sides of the insulations vapour open and to maintain similar vapour pressure on both sides of the insulations in presence of a temperature gradient.

### *9.4.2 Long-term monitoring of hygrothermal performance*

Long-term monitoring of in situ hygrothermal performance of the insulation materials will be useful to study the mould growth potential, risk of condensation

and changes in thermal conductivity values due to potential compaction, slumping and natural degradation of the insulations. Long term monitoring will be particularly helpful in relation to the insulated solid brick walls as these walls take longer period to have dynamic equilibrium with the hygrothermal boundary condition due to their high hygric and thermal mass.

### *9.4.3 Hygrothermal simulation in a heat, air and mass (HAM) transfer software*

The WUFI software does not include the air balance equation in its algorithm. Hence, any air layer is considered as stagnant in the WUFI software. However, air flow through the cracks and holes can play an important role in convective heat and moisture transfer, particularly in vapour open constructions. Numerical modelling of these situations will require the use of the HAM software particularly suited to bio-based fibrous insulation materials. No HAM software as such was commercially available during the course of this research.

**References**

ACE (2012): Dead CERT. Framing a sustainable transition to the Green Deal and the Energy Company Obligation. London: ACE.

Arundel, A. V., Sterling, E.M., Biggin, J. H., Sterling, T.D. (1986) 'Indirect health effects of relative humidity indoor environments', *Environmental Health Perspectives*, 65, pp. 351-361.

Balbuena, P. B., Gubbins, K. E.(1993) 'Theoretical Interpretation of Adsorption Behavior of Simple Fluids in Slit Pores', *Langmuir*, 9, pp.1801-1814.

Batty, W. J., O'Callaghan, P. W., Probert, S. D., Gregory S. (1981) 'Water-vapour diffusion through fibrous thermal insulants', *Applied Energy*, 8(3), pp. 193-204.

Berg, B., L. (2009) *Qualitative Research Methods for the Social Sciences*. 7th edn. Boston MA: Pearson Education Inc.

Blahovec, J. and Yanniotis, S. (2008) 'Modified Classification of Sorption Isotherms', *Journal of Food Engineering,* 9, pp. 72-77.

Boardman, B. (2007) *Home truths: A Low-carbon Strategy to Reduce UK Housing Emission by 80% by 2050*, Environmental Change Institute, University of Oxford, Oxford.

Bocsa, I. & Karus, M. (1998) *The cultivation of hemp: botany, varieties, cultivation and harvesting.* Sebastapol, Calif: Hemptech; Dartington: Green Books.

Bomberg, M. T., Trechsel, H. R. & Achenbach, P. R. (2009) General Principles for Design of Building Enclosures with Consideration of Moisture Effects. In

Trechsel, H. R. & Bomberg, M. T. (Eds.) *Moisture Control in Buildings: The Key Factor in Mold Prevention.* 2nd ed. West Conshohocken, ASTM International.

Bourie, M. (2003) *Hemp: A short History of the Most Misunderstood plant and its uses and abuses,* New York: Firefly Book.

Brown, L. R. (2011) *World on the Edge: How to Prevent Environmental and Economic Collapse.* New York: W. W. Norton.

Bryman, A. (2008) *Social Research Methods.* 3rd edn. Oxford:Oxford University Press.

BS EN 12429 (1996) *Thermal insulating products for building applications: Conditioning to moisture equilibrium under specified temperature and humidity conditions*. London: British Standards Institute.

BS EN 12086 (1997) *Thermal insulating products for building applications - Determination of water vapour transmission properties*. London: British Standards Institute.

BS EN 12429 (1998) *Thermal insulating products for building applications - Conditioning to moisture equilibrium under specified temperature and humidity conditions*. London: British Standards Institute.

BS EN ISO 12571 (2000) *Hygrothermal performance of building materials and products. Determination of hygroscopic sorption properties*. London: British Standards Institute.

BS EN ISO 15148 (2002) *Hygrothermal performance of building materials and products - Determination of water absorption coefficient by partial immersion*. London: British Standards Institute.

BS EN ISO 104566 (2007) *Building materials and products - Hygrothermal properties -Tabulated design values and procedures for determining declared and design thermal values.* London: British Standards Institute.

BS EN 15026 (2007) *Hygrothermal performance of building components and building elements. Assessment of moisture transfer by numerical simulation.* London: British Standards Institute.

BS ISO 2219 (2010) *Thermal insulation products for buildings. Factory-made products of expanded cork (ICB)- Specification*. London: British Standards Institute.

Caleb (2012) *Non-Domestic Buildings: The missed opportunity.* Available at: www.chrispearson.net/epic_downloads/non_domestic_buildings.pdf *(Accessed: 20 June 2008).*

Campbell Scientific (2012) *CR1000:Measurement and Control Datalogger.* Available at: http://www.campbellsci.co.uk/cr1000 (Accessed: 8 November 2012).

Centre for the Build Environment (2013) *The Renewable Houses.* Available at:

http://www.renewable-house.co.uk/RH/downloads/brochure.pdf (Acessed: 3 January 2013).

Cerolini, S., D'orazio, M., Di Perna, C. & Stazi, A. (2009) Moisture buffering capacity of highly absorbing materials. Energy and Buildings, 41, pp.164-168.

Ceri and Newman (2011) *Hygrothermal conditions of a residence in LLanberis.* Unpublished data.

Cohan, L. H. (1938) Sorption Hysteresis and the Vapour Pressure of Concave Surfaces. *Journal of American Chemical Society,* 60**,** pp. 433-435.

CIBSE (2012) *Weather Data Packages.* Available at: https://www.cibseknowledgeportal.co.uk/weather-data (Accessed: 2 July 2012).

Christian, J., E. (2009) Moisture Source. In Trechsel, H. R. & Bomberg, M. T. (Eds.) *Moisture Control in Buildings: The Key Factor in Mold Prevention.* 2nd ed. West Conshohocken, ASTM International.

Collet, F., Achchaq, F., Djellab, K. & Marmoret, B. H. (2011) Water Vapor Properties Of Two Hemp Wools Manufactured With Different Treatments. *Construction and Building Materials,* 25**,** 1079-1085.

Condon, J. B. (2006) Surface area and porosity determinations by physisorption: measurements and theory, Amsterdam ; Oxford: Elsevier.

DCLG (2006) *Building a greener future: towards zero carbon development: consultation.* Wetherby*:* Communities and Local Government Publications.

DECC (2012) *Revised estimates of Home Insulation Levels in Great Britain: April 2012*. London: Dept. of Energy and Climate Change.

Donohue, M. (2012) *Adsorption Isotherms with Hysteresis Loops*. Available at: http://www.nigelworks.com/mdd/PDFs/Hysteresis.pdf (Accessed: 28 June 2012).

Douglas J. Gardner,D.J.,Oporto, G. S., Ryan Mills, R. and My Ahmed Said Azizi Samir, M.A.S.A. (2008) 'Adhesion and Surface Issues in Cellulose and Nanocellulose', *Journal of Adhesion Science and Technology.* 22, pp. 545-567.

*EL-WIN-USB Windows Control Software* (2013) Avilable at: www.lascarelectronics.com/data-logger/easylogger-software.php (Accessed: 14 July 2012)

Flanagan, R. & Jewell, C. (2003) The risk of mould damage over the whole life of a Building. Reading, University of Reading.

Forest Product Laboratory (1944) *Fiber-saturation point of woo.* Available at: http://www.treesearch.fs.fed.us/pubs/32430 (Accessed: 2 October 2012).

Garcia-Jaldon, C., Dupeyre, D. And Vignon,M. R. (1998) 'Fibres from semi-retted hemp bundles by steam Explosion treatment' *Biomass and Bioenergy*, 14(3), pp. 251-260.

Gardner, D. J., Oporto, G. S., Mills, R. & Samir, M. A. S. A. (2008) Adhesion and Surface Issues in Cellulose and Nanocellulose. *Journal of Adhesion Science and Technology,* 22, pp.545-567.

Glass, J.,Dainty, A. R. J.,Gibb, A.G.F. (2008) 'New build: Materials, techniques, skills and innovation'. *Energy Policy,* 36, pp.4534-4538.

Great Britain. *Climate Change Act 2008*: *Chapter 27*. (2008) London: The Stationery Office.

Halliday, S. (2008) *Sustainable Construction,* Amsterdam ; London, Butterworth- Heineman.

Hamby, D.M. (1994) A review of techniques for parameter sensitivity analysis of environmental models. *Environmental Monitoring and Assessment*, 32, pp.135-154.

Hedlin, C., P. (1988) Heat Transfer in a Wet Porous Thermal Insulation in a Flat Roof. *Journal of Building Physics,* 11(3), pp. 165-168.

Hemp Technology (2012) *Growing Hemp.* Available at: http://www.hemptechnology.co.uk/growing.htm (Accessed: 30 November 2012).

*Hemp Technology* (2012) *What we do.* Available at: http://www.hemptechnology.co.uk/what.htm (Accessed: 30 November 2012).

Hens, H. S. L. C. (2007) *Building physics - heat, air and moisture : fundamentals and engineering methods with examples and exercises,* Berlin, Ernst & Sohn.

Heseltine, E. and Rosen, J. (Eds.) (2009) *WHO guidelines for indoor air quality: dampness and mould,* Copenhagen, WHO Regional Office for Europe.

Hill, C. A. S., Norton, A. & Newman, G. (2009) Water vapor sorption behavior of natural fibers. *Journal of Applied Polymer Science,* 112**,** pp.1524-1537.

Hoang,C. P., Kinney, K. A., Corsi, R. L., Szaniszlo, P. J. (2010) Resistance of green building materials to fungal growth, International Biodeterioration & Biodegradation, 64 , pp.104-113.

Holm, A. (2001) 'Drying of an AAC flat roof in different climates. Computational sensitivity analysis versus material property measurements', CIB World Building Congress, Wellington 2-6 April. Wellington International Council for Building.

IEA-Annex 14 (1991). Condensation and energy, Acco, Leuven: 1991.

IEA (2011) *2011: Key World Energy Statistics.* France: OREGRAPH.

IEA (2008) *World Energy Outlook 2008 Fact Sheet: Global Energy Trends: Where Are We Headed Without New Policies And What Does It Mean?.* Available at: http://www.iea.org/weo/docs/weo2008/fact_sheets_08.pdf (Accessed: 30 November 2012).

IES (2013) *Virtual Environment User Guides* [Online]. Available at: http://www.iesve.com/support/userguides (Accessed: 2 January 2013).

IGT (2010) *Low carbon construction: final report*. London: Dept. of Business, Innovation and Skills.

IPCC (2007) *Climate Change 2007: The Physical Science Basis. Contribution of Working Group I to the Fourth Assessment Report of the Intergovernmental Panel on Climate*. Cambridge: Cambridge University Press.

ISO 10051 (1996).*Thermal insulation - Moisture effects on heat transfer - Determination of thermal transmissivity of a moist material.* Geneva: International Organization for Standardization.

ISO 14040 (2006) *Environmental management -- Life cycle assessment -- Principles and framework.* Geneva: International Organization for Standardization.

ISO 8301 (1991) *Thermal insulation-Determination of steady-state thermal resistance and related properties -Heat flow meter apparatus*. Geneva: International Organization for Standardization.

ISO 9869 (1994) *Thermal insulation - Building elements - In-situ measurement of thermal resistance and thermal transmittance.* Geneva: International Organization for Standardization.

ISO 24353 (2008) *Hygrothermal performance of building materials and products - Determination of moisture adsorption/desorption properties in response to humidity variation*. Switzerland: International Organization for Standardization.

IUPAC (2012) 'Compendium of Chemical Terminology: Gold Book' [Online]. Available at: http://goldbook.iupac.org/PDF/goldbook.pdf (Accessed: 1 April 2012).

JIS A 1470-1 (2002) Test method of adsorption/desorption efficiency for building materials to regulate an indoor humidity - part 1: response method of humidity.

Karamanos, A., Hadiarakou, S. & Papadopoulos, A. M. (2008) 'The Impact of Temperature and Moisture on the Thermal Performance of Stone Wool', *Energy and Buildings,* 40**,** pp.1402-1411.

Karamanos, A., Papadopoulos, A. & Anastasellos, D. (2004) 'Heat transfer phenomena in fibrous insulating materials' [online]. Available at:

http://www.geolan.gr/sappek/docs/publications/article_6.pdf (Accessed: 1 April 2012).

Klamer, M., Morsing, E., Husemoen, T. (2004) 'Fungal growth on different insulation materials exposed to different moisture regimes' International Biodeterioration & Biodegradation ,54, pp.277-282.

Korjenic, A., Petránek, V., Zach, J. & Jitka, H., J (2011) Development and performance evaluation of natural thermal-insulation materials composed of renewable resources. *Energy and Buildings,* 43**,** pp.2518-2523.

Kostic, M. M., Pejic,B.M., B. M., Asanovica,K. A., Aleksicb,V.A., Skundrica, P.D. (2010) 'Effect of hemicelluloses and lignin on the sorption and electric properties of hemp fibers' *Industrial Crops and Products*, pp.32, 169-174.

Krus, M. & Sedlbauer. K. (2012) 'Hygrothermal Properties of Ecological Insulation Materials - A Closer Look', Fraunhofer Institute of Building Physics.

Kumaran, M. K., Mukhopadhyaya, P. & Nicole, N. (2006) Determination of Equilibrium Moisture Contents of Building Materials: Some Practical Difficulties. *Journal of ASTM International,* 3**,** pp.1-9.

Kummel, R. (2011) *The Second Law of Economics: Energy, Entropy, and the Origins of Wealth.* London: Springer.

Kunzel, H., M., Holm, A., Sedbaucer, K., Antretter, F., Ellinger, M. (2004) *Moisture buffering effects of interior linings made from wood and wood based product*, Germany: Fraunhofer Institute of Building Physics.

Kunzel, H. M. (1995) *Simultaneous heat and moisture transport in building components: one and two dimensional calculation using simple parameters*. PhD thesis. Fraunhofer Institute of Building Physics.

Kymalainen, H. R., Hautala, M., Kuisma, R. & Pasila, A. (2001) Capillarity of flax/linseed (*Linum usitatissimum* L.) and fibre hemp (*Cannabis sativa* L.) straw fractions. *Industrial Crops and Products* 14**,** pp.41-50.

Langlais, C. & Kiarsfeld, S. (1984) Heat and Mass Transfer in Fibrous Insulations. *Journal of Building Physics,* 8**,** pp.49-79.

Latif, E., Tucker, S., Newport, D., Wijeyesekera, D. C. (2010) 'Potential for Research on Hemp Insulation in the Uk construction Sector', Advances in Computing and Technology: 5th Annual Conference, London 27 January. London: UEL.

Latif, E. (2011) 'an experimental comparison between the thermal performances of hemp fibre and stone wool insulation samples in a range of hygrothermal conditions', International Conference on Built Environment in Developing Countries: 5th Annual Conference, Penang, Malaysia 6-7 December. Penang: USM.

Latif, E., Pruteanu, M. and Rhydwen, G. R., Wijeyesekera, D. C., Tucker, S., Newport, D., Ciupala, M. A. (2011) 'Thermal Conductivity Of Building Materials: An Overview of its Determination', Advances in Computing and Technology: 6th Annual Conference, London 26 January. London: UEL.

Mackenzie, F., Pout, C., Shorrock, L., Matthews, A. & Henderson, J. (2010) *Energy efficiency in new and existing buildings : comparative costs and $CO_2$ savings.* Bracknell: IHS BRE Press.

May, N., Newman, G. (2008) *Critique of the Green Guide to Specification.* Available at: http://www.goodhomes.org.uk/downloads/pages/GHA%20Critique%20of%20the%20Green%20Guide%20to%20Specification%20-%20051208.pdf (Acessed: 3 January 2013).

McMullan, R. (2007) *Environmental science in building*. 6th edn. Palgrave Macmillan: Basingstoke.

Meteonorm (2012*) Meteonorm dataset.* Available at: http://meteonorm.com/products/meteonorm-dataset/ (Accessed: 2 July 2012).

Met Office (2012) *Rank ordered statistics.* Available at: http://www.metoffice.gov.uk/climate/uk/datasets/ (Accessed: 2 July 2012).

Met Office (2013) *UK climate.* Available at: http://www.metoffice.gov.uk/climate/uk/summaries (Accessed: 4 January 2013).

Monahan, J., Powell J.C. (2011) 'An embodied carbon and energy analysis of modern methods of construction in housing: A case study using a lifecycle assessment framework'. *Energy and Buildings*, 43, pp.179-188.

Murphy, R. J. and Norton, A. (2008) *Life Cycle Assessment of Natural Fibre Insulation Materials,* London: NNFCC.

Nicolajsen, A. (2005) Thermal transmittance of a cellulose loose-fill insulation material. *Building and Environment,* 40**,** pp. 907-914.

Nilsson, D., Svennerstedt, B., Wretfors, C. (2005) 'Adsorption Equilibrium Moisture Contents of Flax Straw, Hemp Stalks and Reed Canary Grass', *Biosystems Engineering*, 91 (1), pp. 35-43.

Norton, A. J. (2008) The Life Cycle Assessment and Moisture Sorption Characteristics of Natural Fibre Thermal Insulation Materials. *School of the Environment & Natural Resources.* Bangor, Bangor University.

NTP (2010) *Draft Report on Carcinogens Substance Profile for Glass Wool Fibers (Respirable) as a Class*. Available at: http://ntp.niehs.nih.gov/NTP/roc/twelfth/2010/DrftSubProfiles/GWF20100421.pdf (Accessed: 5 December 2012)

Nyame-asiamah, F., Patel, N. (2009) 'Research methods and methodologies for studying organisational learning'. *European and mediterranean conference on information systems 2009 (emcis2009),* july 13-14 2009, crowne plaza hotel, Izmir.

Nykter, M. (2006) Microbial quality of hemp (cannabis sativa l.) and flax (linum usitatissimum l.) from plants to thermal insulation'. Helsinki, University of Helsinki.

Okubayashia,S., Griesserb, U. J., and Bechtolda, T. (2004) 'kinetic study of moisture sorption and desorption on lyocell fibers', *Carbohydrate Polymers*, 58, pp. 293-299.

Oreszczyn, T., Ridley, I., Hong, S. H., Wilkinson, P. (2006) 'Mould and winter indoor relative humidity in low income households in England'. *Indoor and Built Environment,* 15 (2), pp. 125-135.

Osborne, M. (2012) *Adsorption* Isotherms. Available at: http://www.ceet.niu.edu/cecourse/UEET%20235/isotherms (Accessed: 12 July 2012).

Padfield, T (1998) *The role of Absorbent building materials in moderating changes of relative humidity*. PhD thesis. The Technical University of Denmark, Denmark [Online]. Available at: http://www.natmus.dk/cons/tp/phd/tp_phd.pdf (Accessed: 15 September, 2009)

Padfield, T and Jensen L. (2009) 'Humidity buffering by absorbent materials' [online]. Available at: http://www.conservationphysics.org/wallbuff/buffer_performance.pdf (Accessed: 1 February 2012).

Palaniappan, M. and Gleickin, P. H. (2009) 'Peak Water', in Gleick, P. H. (ed.) *The World's Water 2008-2009: The Biennial Report on Freshwater Resources,* Washington: Island Press, pp. 1-16.

Passivhaus (2012) *The Passivhaus Standard*. Available at: http://www.passivhaus.org.uk/standard.jsp?id=122 (Accessed: 30 November 2012).

Pavlik, Z. & Cerny, R. (2009) Hygrothermal performance study of an innovative interior thermal insulation system. *Applied Thermal Engineering,* 29, pp. 1941-1946.

Rao, J., Fazio, P., Bartlett, K.,Yang, D. (2009) 'Experimental evaluation of potential trannsport of mold spores from moldy studs in full-size wall assemblies', *Building and Environment,* 44, pp. 1568-1577.

Rasmussen, T. V., Nicolajsen, A. (2005) 'Assessment of the performance of organic and mineral-based insulation products used in exterior walls and attics in dwellings' Building and Environment, 42, pp. 829-839.

Rode, C. (2005). *Moisture buffering of building materials*, BYG DTU R-126, Denmark: Technical University of Denmark.

Roels, S. & Janssen, H. (2006) A Comparison of the Nordtest and Japanese Test Methods for the Moisture Buffering Performance of Building Material. *Journal of Building Physics,* 30**,** pp. 137-161.

Roulac, J. & Hemptech (Firm) (1997) *Hemp horizons : the comeback of the world's most promising plant.* White River Junction, Vt.: Chelsea Green Pub.

Salin, A. J. (2010) Inclusion of the Sorption Hysteresis Phenomenon in Future Drying Models. Some Basic Considerations. *The Future of Quality Control for Wood & Wood Products:The Final Conference of COST Action E53.* Edinburgh.

Sandberg, P. I. (2009) Effects of Moisture on the Thermal Performance of Insulating Materials. IN TRECHSEL, H. R. & BOMBERG, M. T. (Eds.) *Moisture Control in Buildings: The Key Factor in Mold Prevention.* 2nd ed. West Conshohocken, ASTM International, pp. 28-39.

Sedlbauer, K., Krus, M. & Breuer, K. (2003) 'Mould Growth Prediction with a New Biohygrothermal Method and its Application in Practice'. *Materials Conference.* Lodz.

Smith, H. H. (2012) 'Fiber Saturation Point: A New Definition' [Online]. Available at: http://ir.library.oregonstate.edu/xmlui/bitstream/handle/1957/5433/Fiber_Saturation_ocr.pdf?sequence=1 (Accesses: 22 April, 2012).

Snoeyink , V. l., Summers , R. S. (1999) Adsorption of organic compounds, in American Water Works Association ed. Water Quality and Treatment: A Handbook of Community Water Supplies, Fifth Edition, McGraw-Hill Inc.,US; 5th edition.

Southern, J. R. (1986) Summer condensation within dry lined solid walls. *Building Service Engineering Research and Technology,* 7**,** pp. 101-106.

Spitz, C., Mora, L., Wurtz, E., Jay, A. (2012) Practical application of uncertainty analysis and sensitivity analysis on an experimental house*. Energy and Buildings*, 55, pp. 459-470.

Struik, P. C., Amaducci, S., Bullard, M. J., Stutterheim, N. C., Venturi, G. & Cromack, H. T. H. (2000) 'Agronomy of fibre hemp (Cannabis sati6a L.) in Europe', *Industrial Crops and Products,* 11**,** pp. 107-118.

Svennberg, K. (2006) *Moisture Buffering in the Indoor Environment*. PhD thesis. Lund University, Sweden.

Tian, W., (2013) A review of sensitivity analysis methods in building energy analysis. *Renewable and Sustainable Energy Reviews*, 20, pp. 411–419.

Time, B. (1998) *Hygroscopic moisture transfer in wood*. PhD thesis, Norwegian University of Science and Technology.

Timmermann , E.O. (2003) 'Multilayer sorption parameters: BET or GAB values?', *Colloids and Surfaces A: Physicochem. Eng. Aspects*, 220, pp.235-260.

Tobiasson, W. (2009) Roofs. . In Trechsel, H. R. & Bomberg, M. T. (Eds.) *Moisture Control in Buildings: The Key Factor in Mold Prevention.* 2nd ed. West Conshohocken, ASTM International.

Trechsel, H. R. & Vigener, N. W. (2009) Investigating Moisture Damage Caused by Building Envelope Problems. In Trechsel, H. R. & Bomberg, M. T. (Eds.) *Moisture Control in Buildings: The Key Factor in Mold Prevention.* 2nd ed. West Conshohocken, ASTM International

Tsongas, G. (2009) Case Studies Of Moisture Problems In Residences. In Trechsel, H. R. & Bomberg, M. T. (Eds.) *Moisture Control in Buildings: The Key Factor in Mold Prevention.* 2nd ed. West Conshohocken, ASTM International.

UNEP (2010) *The Emissions Gap Report. Are the Copenhagen Accord Pledges Sufficient to Limit Global Warming to 2° C or 1.5° C? A preliminary assessment.*

UNEP( 2012) *Global Environment Outlook 5: Environment for the Future We Want.* Malta: Progress Press Ltd.

Utley, J. & Shorrock, L. (2012) *Ninety Years of Housing 1921-2011: Trends relating to living standards, energy use and carbon emissions.* Bracknell: IHS BRE Press.

Vereecken, E. & Roels, S. (2012) Review of mould prediction models and their influence on mould risk evaluation. *Building and Environment,* 51**,** 296-310.

Viitanen, H., Vinha, J., Salminen, K., Ojanen, T., Peuhkuri, R., Paajanen, L. & Lahdesmaki, K. (2010) *Moisture and Bio-deterioration Risk of Building Materials and Structures,* 33**,** 201-224.

Woolley, T (2012) Details of wall build ups, confidential report to the TSB AA089J Energy Efficient Bio-Based Natural Fibre Insulation, Bangor University, Bangor, 7 September.

Xie, Y., Hill, C. A. S., Jalaludin, Z., Simon, S. F., Norton, A. J. & Newman, G. (2011) The dynamic water vapour sorption behaviour of natural fibres and kinetic analysis using the parallel exponential kinetics model. *Journal of Material Science,* 46**,** pp.479-489.

Ye, Z., Wells, C. M., Carrington, C. G. & Hewitt, N. J. (2006) Thermal conductivity of wool and wool–hemp insulation. *International Journal of Energy Research,* 30**,** pp.37-49.

Yoshino, H., Mitamura, T. & Hasegawa, K. (2009) Moisture buffering and effect of ventilation rate and volume rate of hygrothermal materials in a single room under steady state exterior conditions. *Building and Environment* ,44, pp.1418-1425.

# Appendix A

## Hot wire method for measuring thermal conductivity

[This description is taken from the paper published by Latif *et al.* (2011)]

The hot-wire method is used for measuring the thermal conductivity of bulk materials and materials with low thermal conductivity (Carslaw and Jaeger, 1959).

The mathematical model of hot wire method is based on the assumption that hot wire is a continuous line source and by providing constant heating power through thermal impulses it generates cylindrical coaxial isotherms in an infinite homogenous medium with initial equilibrium condition. The transient temperature can be expressed through the following equation:

$$T_{(r,t)} = [\, q/(4\pi\lambda)]*[\ln(4\alpha t/r^2) + r^2/(4\alpha t) - 1/4\{r^2/(4\alpha t)\} - \cdots - У] \qquad [A.1]$$

Where, λ is thermal conductivity (w/m-k), Q is power supply per unit length (W/m), α is thermal diffusivity of the conductive material, r is the radial position where temperature is measured, t is the time between the heat generation and measuring the temperature and У is Euler's constant (0.5772156). Assuming that the terms inside the parentheses in equation A1 is negligible at a sufficient period of time and When $(r^2/(4\alpha t) << 1$, it is possible to express equation A.1 with good approximation as:

$$T_{(r,t)} = [Q/(4\pi\lambda)]*[\ln(4\alpha t/r^2) - У] \qquad [A.2]$$

$$T_{(r,t)} = [Q/(4\pi\lambda)]*[\ln t + \ln(4\alpha/r^2) - У] \qquad [A.3]$$

Therefore temperature variation for time $t_1$ and $t_2$ can be expressed as:

$$\Delta T = [Q/(4\pi\lambda)]* [\ln(\, t_2/t_1)\,] \qquad [A.4]$$

Using this method, an experimental apparatus was developed by Franco (2007), for the measurement of thermal conductivity of insulators (figure A.1).

The line source of heat is placed on the plane surface separating two half spaces: the sample medium and the insulating medium. The temperature rise of the wire is measured as a function of time by means of two T-type thermocouples. In the comparative method the temperatures $\Delta T_A$ and $\Delta T_B$ of a hot wire on the boundary surface of a reference medium and a medium of unknown thermal conductivity $\lambda_B$ are measured at times, $t_1$ and $t_2$ respectively. If the $\lambda$ of the reference material is close to that of the materials to be tested, the value of the unknown medium can be calculated by the following equation:

$$\lambda_B - \lambda_A = KP^*(1/\Delta T_B - 1/\Delta T_A) \qquad [A.5]$$

Otherwise, if different thermal power inputs are used for the two tested materials:

$$\lambda_B - \lambda_A = K^*(P_B/\Delta T_B - P_A/\Delta T_A) \qquad [A.6]$$

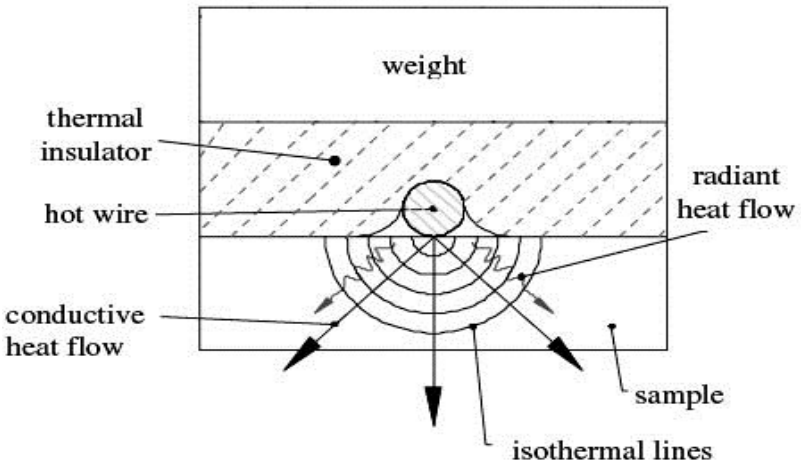


**Figure A.1: Transient hot wire apapratus**

In semi-absolute method a least-squares fit of the recorded temperature difference vs. the thermal conductivity data in accordance with Eqs. A.5 and A.6 is performed and the curve is used directly for deriving the thermal conductivity of the material.

**Heat transfer analyzer**

In thermal analyazers like Isomet 2140 (figure 7) or Quickline$^{tm}$-30, transient line source (for needle probe) or transient plain source technique (for disc shaped

surface probe) is applied based on ASTM D5334-08. Thermal conductivity is determined from power input and time dependant temperature variation. The thermal equation applied is similar to those of transient hot wire and transient plain source method.

**Figure A.2: Isomet Heat Analyzer at CAT**

**Transient Hot wire method and steady state hot wire method**

Transient hot wire method can render inaccurate result for fibrous insulation materials for two reasons: anisotropy and interlinked pore structure. For anisotropy, one-directional or radial heat transfer equation can provide incorrect result. For inter-linked pore structure (lei *et al*., 2010), convection current is likely to be created by heated air during heat flux intervention by the hot-plate or hot-wire, while the transient equations do not take into account heat transfer by convection. For most other insulations, it provides quick and reliable results with smaller samples.

Steady state hot wire method can provide inaccurate heat flow value, especially for anisotropic materials due to heat loss towards the longitudinal direction- the governing equation is developed on the basis of infinite length of heat source. However, it is a useful method for some bulk insulation materials (refractory) because of reduced measuring time and need for smaller samples.

# Appendix B

Thermal conductivity of insulation materials: Comparison of the results obtained by using an Isomet 2104 Heat Transfer Analyzer with the results obtained from Fox 600 hot plate

**Table B.1: Material properties of the insulations.**

| **Insulations** | **Size (mm)** | **Thickness (mm)** | **Density (Kg/m$^3$)** |
|---|---|---|---|
| Stone wool | 450X450 | 98 | 57.4 |
| Fibre glass | 450X450 | 100 | 15.2 |
| Celotex | 450X450 | 50.9 | 27.5 |
| EPS | 450X450 | 48.2 | 19.8 |
| Sheep wool-1 | 450X450 | 98 | 20 |
| Sheep wool-2 | 450X450 | 100 | 30.3 |
| Hemp-5.1 | 450X450 | 100 | 39.7 |
| Hemp -5.2 | 450X450 | 60 | 50.7 |
| Wood fibre-1 | 450X450 | 100 | 60.4 |
| Wood fibre- 2 | 450X450 | 80 | 140.2 |
| Wood fibre- 2 | 450X450 | 21 | 169.4 |

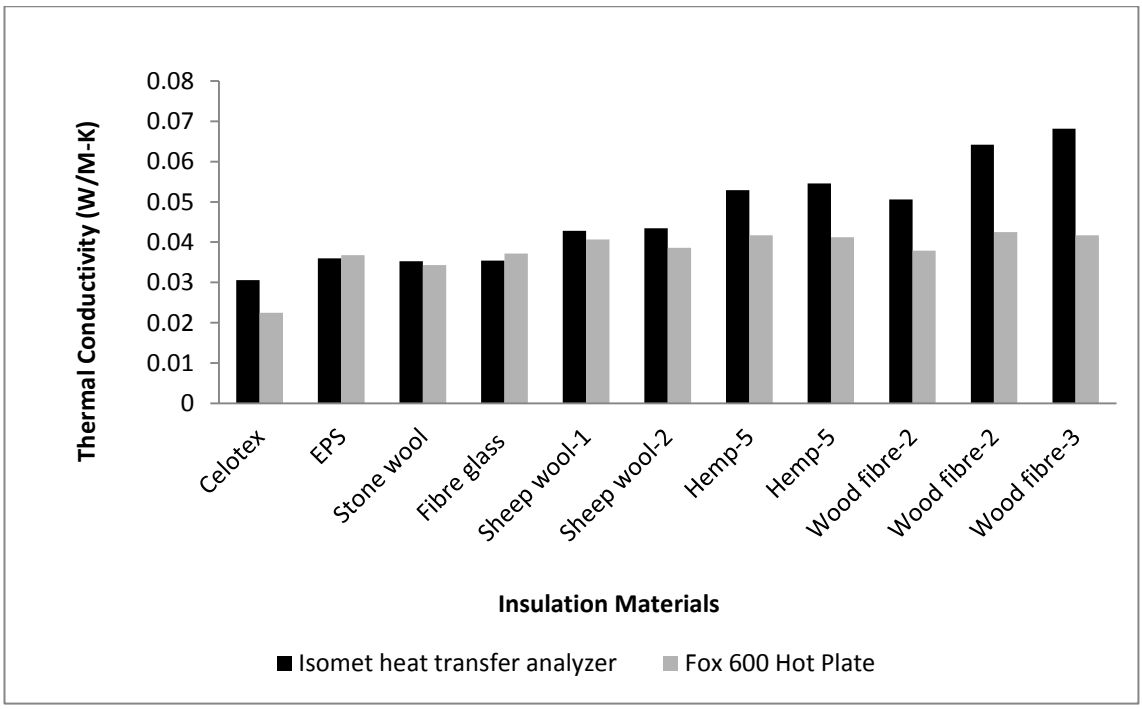


**Figure B.1: Conductivity readings at 23 °C temperature and 50% relative humidity.**

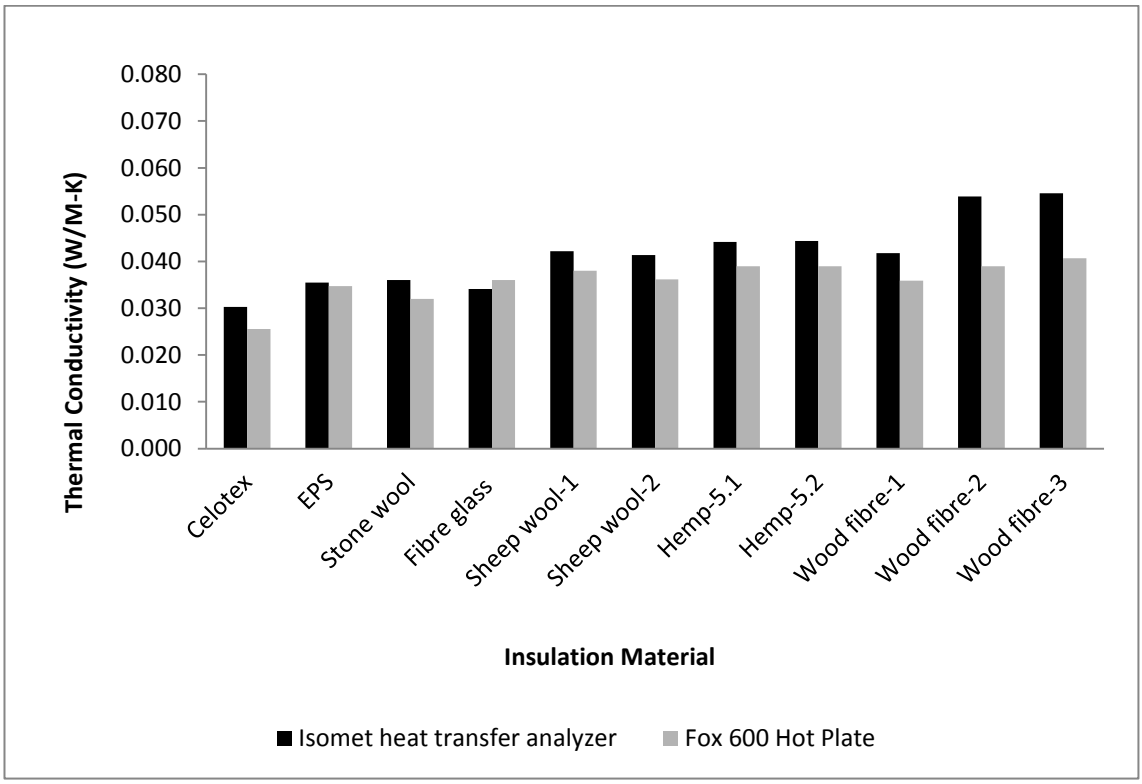


**Figure B.2: Conductivity readings at 90 °C temperature and 10% relative humidity.**

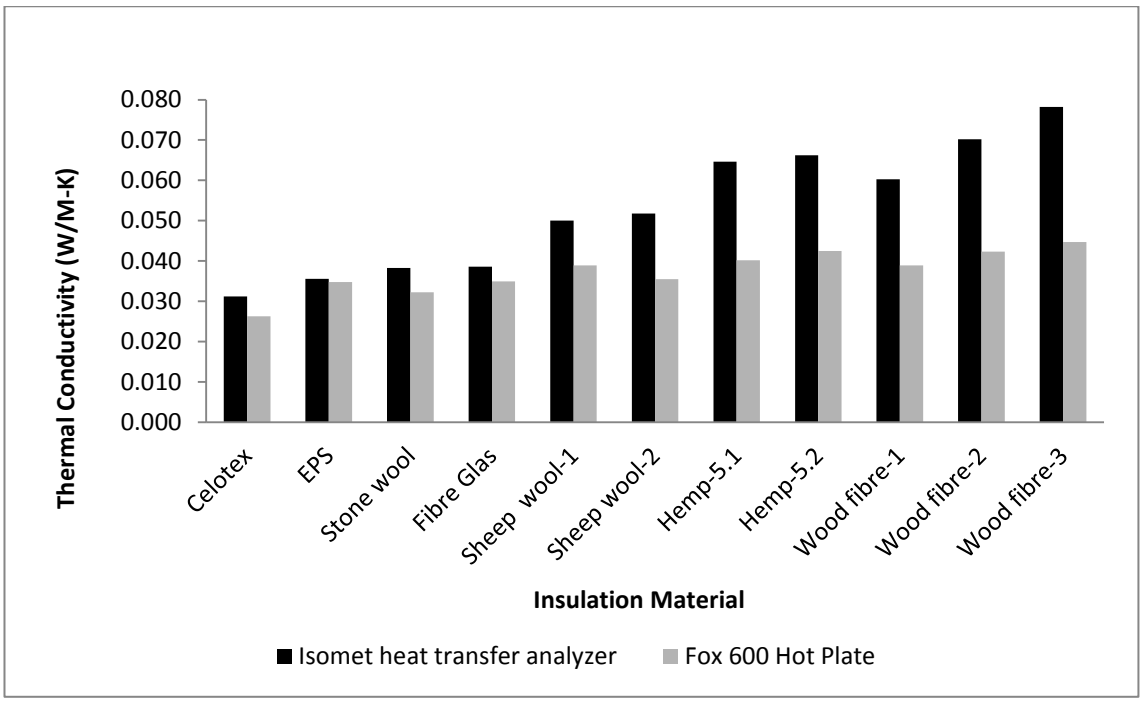


**Figure B.3: Conductivity readings at 10 °C temperature and 80% relative humidity.**

# Appendix C

## Some proposed 'rule of thumb' methods of measuring moisture dependent thermal conductivity of hemp

### C.1 Using a constant as conductivity supplement

Moisture dependent conductivity can be approximated using the following expression:

$\lambda s = \lambda + aw$

Where ,

$\lambda_s$ = Moisture dependent conductivity (W/mK)

$\lambda$ = Thermal conductivity at dry condition (W/mK)

a = Thermal conductivity supplement (-)

w = equilibrium moisture content

For hemp insulation if dry thermal conductivity is taken as 0.039, and if the thermal conductivity supplement is taken as 0.046 then the approximation of the thermal conductivity will be as shown in Table B.1.

**Table C.1: Thermal conductivity of hemp insulation determined by using thermal conductivity supplement.**

| Relative Humidity (%) | Moisture Content (Kg/kg)% | Thermal Conductivity supplement, a (-) | Dry Thermal Conductivity $\lambda$ (W/mK) | Thermal Conductivity $\lambda_s$ (W/mK) | Experimental result of Moisture Dependent Conductivity $*\lambda_{exp}$ (W/mK) |
|---|---|---|---|---|---|
| 0 | 0 | 0.046 | 0.039 | 0.039 | |
| 20 | 2.39 | 0.046 | 0.039 | 0.040 | |
| 30 | 4.89 | 0.046 | 0.039 | 0.041 | |
| 33 | 5.10 | 0.046 | 0.039 | 0.041 | 0.036 |
| 40 | 5.53 | 0.046 | 0.039 | 0.042 | |
| 50 | 7.05 | 0.046 | 0.039 | 0.042 | |
| 56 | 7.50 | 0.046 | 0.039 | 0.042 | 0.041 |
| 70 | 12.09 | 0.046 | 0.039 | 0.044 | |
| 80 | 20.76 | 0.046 | 0.039 | 0.049 | 0.050 |
| 95 | 51.88 | 0.046 | 0.039 | 0.063 | |
| 98 | 60.81 | 0.046 | 0.039 | 0.067 | 0.056 |

### C.2 Using an effective thermal conductivity value for adsorbed moisture

Moisture dependent conductivity is also approximated using the following expression:

$\lambda_e = (\lambda_1 m_1 + \lambda_2 m_2)/(m_1 + m_2)$

Where

$m_1$ = unit mass of the dry insulation (Kg)

$m_2$ = mass of moisture in insulation for unit mass of dry insulation (Kg)

$\lambda$ = thermal conductivity of dry insulation (W/mK)

$\lambda_2$ = 0.1 (W/mK), effective thermal conductivity value

The results of thermal conductivity using this equation is shown in Table B.2.

**Table C.2: Thermal conductivity of hemp insulation determined by using effective thermal conductivity value.**

| Relative Humidity (%) | Unit Weight of Dry Insulation $m_1$(kg) | Adsorbed water for unit dry mass $m_2$ (Kg) | Dry Thermal Conductivity $\lambda$ (W/mK) | Thermal Conductivity $\lambda_e$ (W/mK) | Experimental result of Moisture Dependent Conductivity $\lambda_{exp}$ (W/mK) |
|---|---|---|---|---|---|
| 0 | 0 | 0.046 | 0.039 | 0.039 | |
| 20 | 2.39 | 0.046 | 0.039 | 0.040 | |
| 30 | 4.89 | 0.046 | 0.039 | 0.042 | |
| 33 | 5.10 | | 0.039 | 0.042 | **0.036** |
| 40 | 5.53 | 0.046 | 0.039 | 0.042 | |
| 50 | 7.05 | 0.046 | 0.039 | 0.043 | |
| 56 | 7.50 | | 0.039 | 0.043 | **0.041** |
| 70 | 12.09 | 0.046 | 0.039 | 0.046 | |
| 80 | 20.76 | 0.046 | 0.039 | 0.050 | **0.050** |
| 95 | 51.88 | 0.046 | 0.039 | 0.060 | |
| 98 | 60.81 | 0.046 | 0.039 | 0.062 | **0.056** |

### C.3 Design value

Value of the building material or product in specific internal and external condition. As far as effect of moisture on conductivity is concerned, the relationship between these two values can be expressed as:

$\lambda_2 = \lambda_1 * F_m$ ,Where $F_m = e^{fu(u2-u1)}$ [C.1]

where, $\lambda_1$ is declared conductivity, $\lambda_2$ is design conductivity, $f_u$ is the moisture conversion coefficient mass by mass, $u_1$ is the moisture content mass by mass of the first set of conditions, $u_2$ is the moisture content mass by mass of the second set of conditions.

Moisture conversion coefficient (0.05) has been taken as equal to that of cellulose fibre as that was the nearest value available for organic fibres. Another moisture conversion factor of 0.85 is also used as it gives values that are more consistent with experimental and other approximated values. The results are show in Table B.3.

**Table C.3: Design values of thermal conductivity of hemp insulation.**

| Relative Humidity (%) | Experimental Conductivity $\lambda_{exp}$ (W/mK) | Design Value of Conductivity $^*\lambda_{Design}$ ( $f_u$ =0.5), (W/mK) |
|---|---|---|
| 0 | | 0.039 |
| 20 | | 0.039 |
| 30 | | 0.040 |
| 33 | **0.036** | 0.040 |
| 40 | | 0.040 |
| 50 | | 0.040 |
| 56 | **0.041** | 0.040 |
| 70 | | 0.041 |
| 80 | **0.050** | 0.043 |
| 95 | | 0.051 |
| 98 | **0.056** | 0.053 |

Figur C.1 shows that most of the apporoximations are not far from the experimental result or from each other. The differences are more pronounced at 95% and 98% relative humidity.

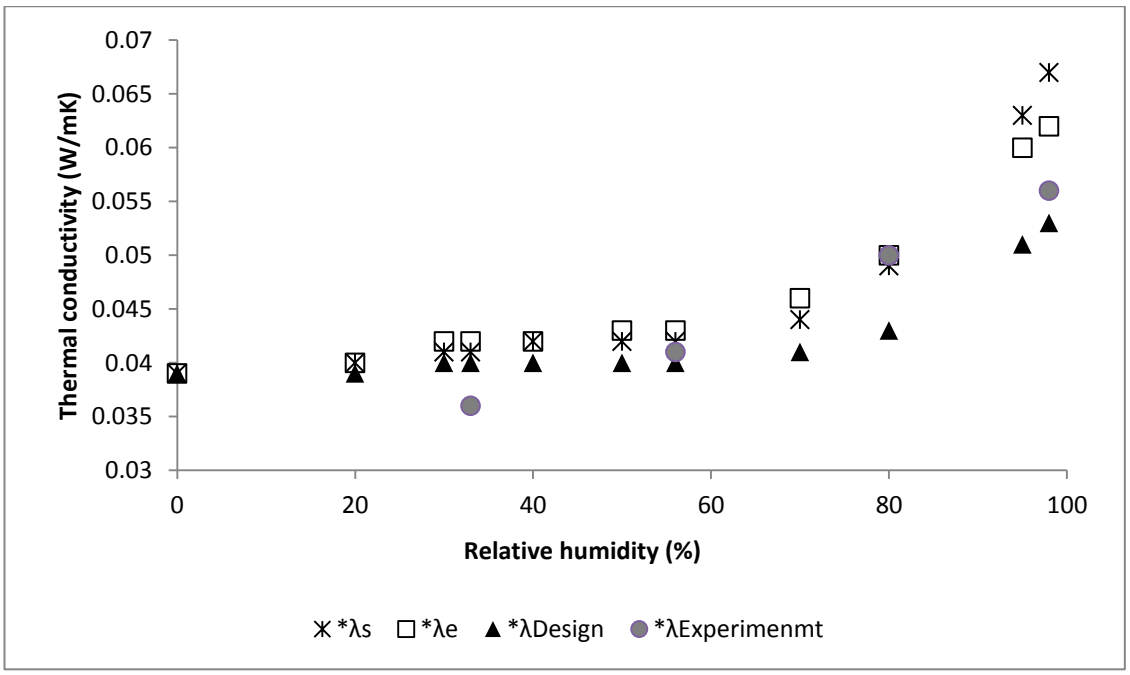


**Figure C.1: Thermal conductivity of hemp insulation determined by using thermal conductivity supplement.**

Since conductivity approximation based on moisture sorption (including the design values for conductivity) closely resembles the experimental result, it seems that in hemp insulation heat flow by mass diffusion and phase change is less dominant. However, as sorption is very high in hemp insulation, there may be some effect of sorption enthalpy which needs to be taken into account.

# Appendix D

Thermal and daylight images of the test buliding

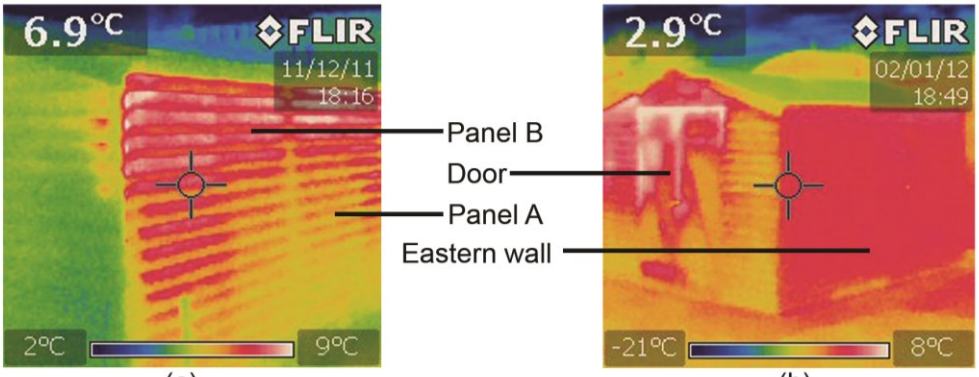


(a) (b)

D.1: Thermal images showing (a) wall panel location, (b) eastern wall, without insulations.

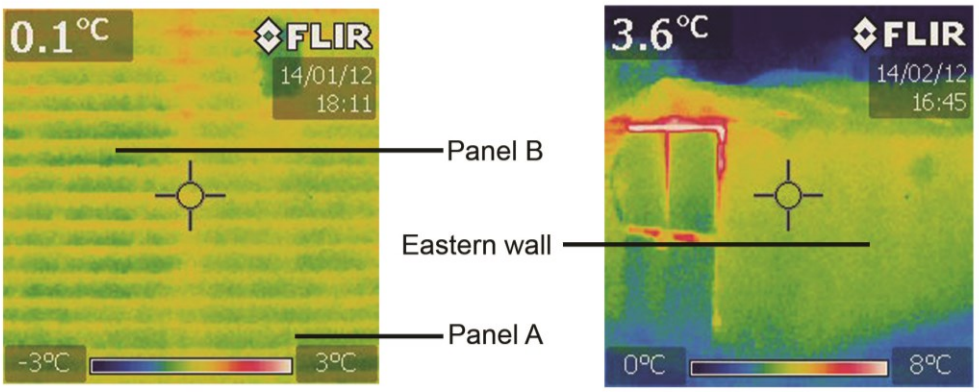


(a) (b)

D.2: Thermal images showing (a) wall panel location, (b) eastern wall, with insulations.


D.3: Illustration showing the test buiding and the the residential buidings at the east side of the test buiding.

# Appendix E

Whole building energy use

## E.1 Introduction

The Insulations used in the walls and loft of a Passivhaus are thicker than the insulation incorporated in a conventional wall to meet the fabric heat loss requirements set for the Passivhaus.

If hemp insulation is used in a in a vapour open construction with the thickness of insulation resembling a Passivhaus, it can be assumed that the thicker hemp insulation will work as a hygric and thermal mass and will influence the amount of heating and cooling load of the building. This assumption was tested for the weather conditions of Edinburgh and Birmingham.

## E.2 Material and method

Hemp-2 and stone wool insulations were selected for the study. The material properties are provided in chapter five. Two different numerical tools were used in this study. These are:

- The WUFI software
- The IES (Integrated Environmental Solution) Virtual Environment software

The WUFI software was discussed in chapter four and chapter nine. The IES virtual environment is a software package consisting of a number of energy related simulation tools to address dynamic thermal properties, air flow, lighting, lifecycle analysis, computational fluid dynamics etc. in relation to buildings. The dynamic thermal simulation was performed by the ApacheSim software tool with solar shading analysis done by the SunCast and air flow by infiltration and ventilation calculated by the Macroflow tool. The IES uses the transient heat balance equations in its algorithm. The further details of the governing equation can be found in the website of IES (2013).

To determine the effect of moisture adsorption by hemp-2 insulation on the whole house energy use in Edinburgh, the following method was used:

- Hygrothermal simulation was carried out in the WUFI software for the weather condition of Edinburgh.
- From the analysed data of water content in the hemp-2 insulation, average water content in the insulation was determined. The water content was determined as 7.6 kg/m$^3$.
- From average content of the insulation, the density and the heat capacity of the (hemp insulation and water) matrix was determined. The modifies density of the moistened insulation was determined as 57.6 kg/m$^3$ and the modified heat capacity was calculated as 1943 J/kgK based on the heat capacity of water as 4200J/kgK.
- For the purpose of simplification, similar water content data was used for Birmingham during the input of hemp-2 material data in the IES software.

The wall section and the moisture content in the insulation are shown in Figures E.1 and E.2, respectively. The buildings incorporating dry hemp-2, moistened hemp-2 and stone wool insulations are henceforth called as building-1, building-2 and building-3, respectively.

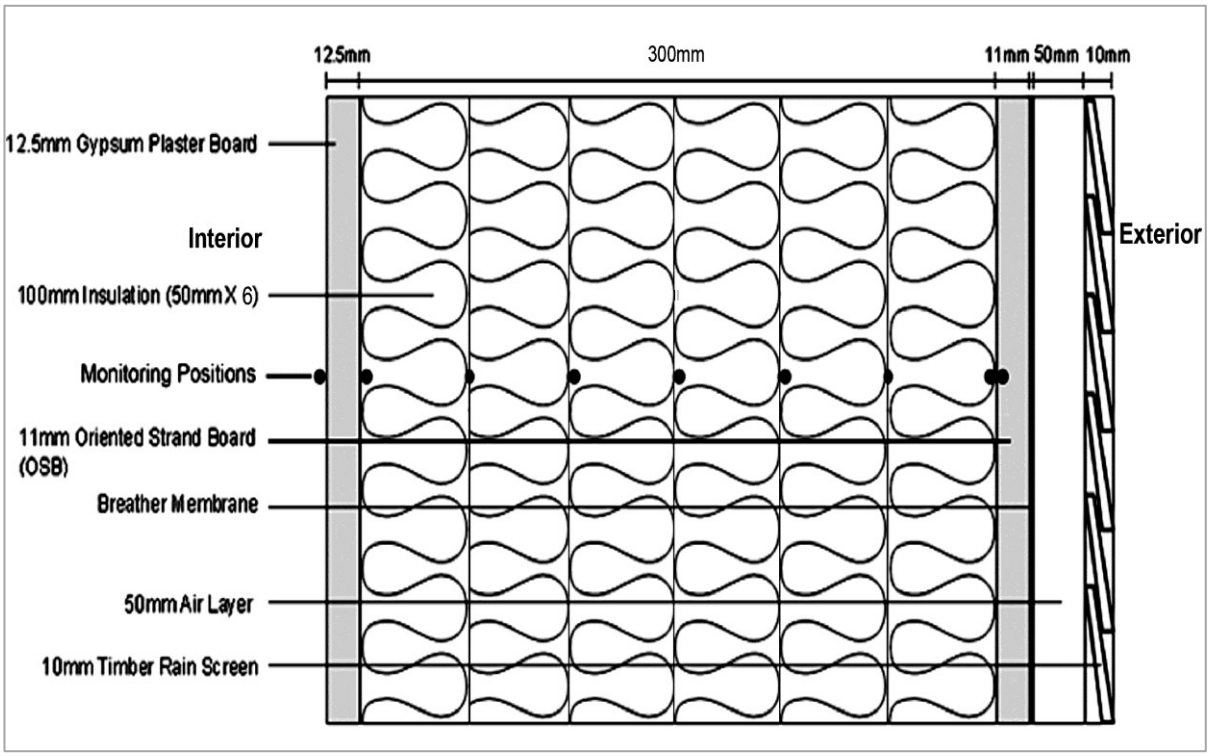


**Figure E.1: The wall section.**

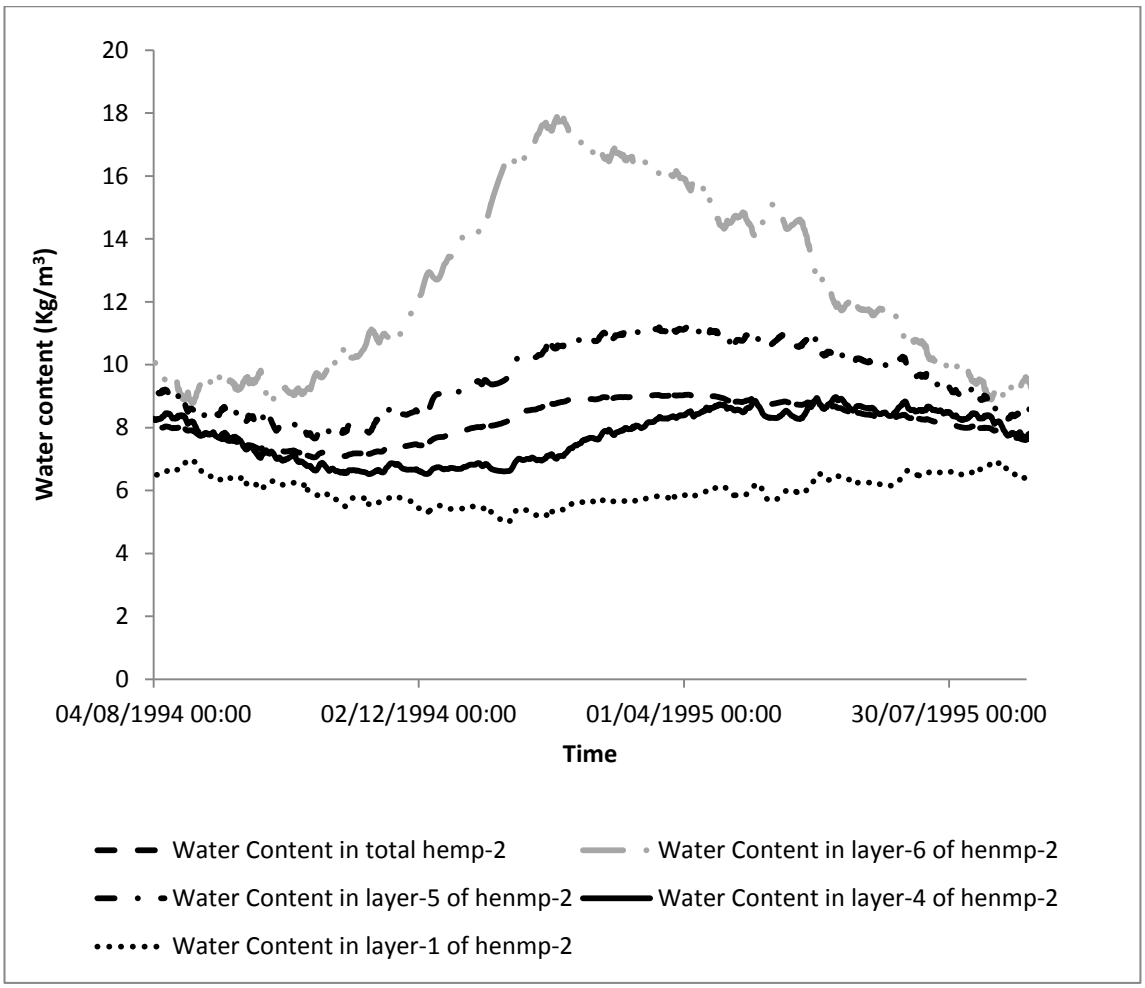


**Figure E.2: Moisture content in hemp-2 insulation.**

Dynamic thermal simulation was run in the IES Virtual Environment 2012 for three notional houses incorporating dry hemp, moistened hemp and stone wool insulation for the weather condition of Edinburgh and Birmingham. The simulation was run for one year with a preconditioning period of sixty days

The plan and the IES software image of the buildings are shown in Figure E.3 and E.4, respectively. As shown in Figure E.3, the notional building has two windows in the south wall with each window having the dimension of dimension of (2 X 2) m. There is a door in the north wall. The height of the building is 7 m, the ground floor is 4 m and the loft space is 3 m.

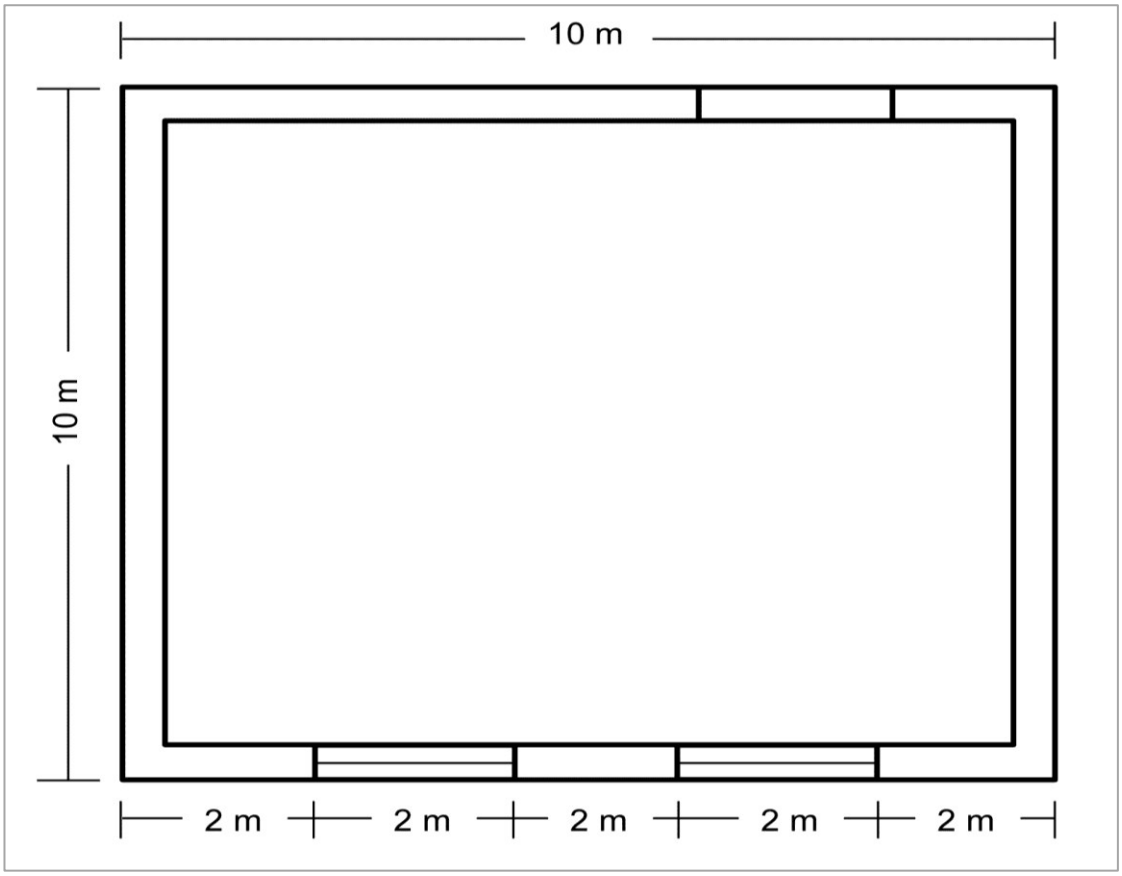


**Figure E.3: The plan of the notional building for the IES software.**

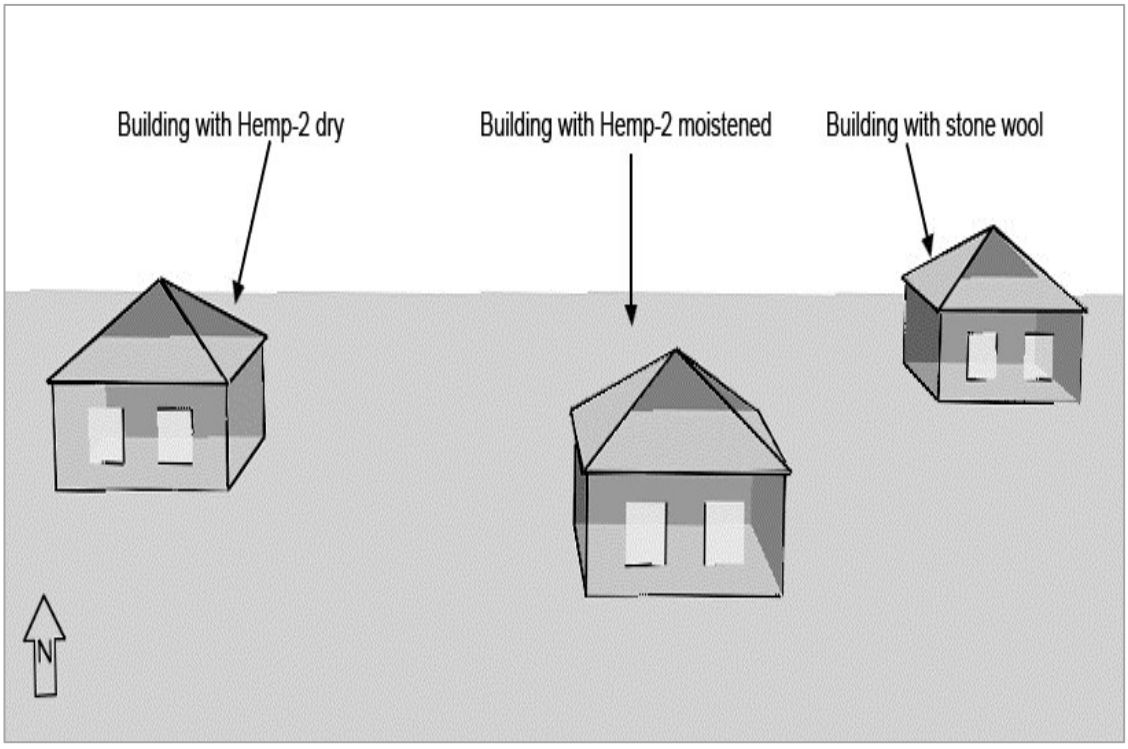


**Figure E.4: The IES software image of the simulated buildings.**

### E.3. Results and discussion

Figures E.5 to E.7 show the space conditioning sensible loads for the selected buildings for the weather conditions of Edinburgh and Birmingham. It can be observed that, in Edinburgh, the space conditioning sensible load of building-2 is 2.3% and 2.1% higher than that of building-1 and building-3, respectively. In Birmingham, the space conditioning sensible load of building-2 is 2.27% and 1.2% higher than that of building-1 and building-3, respectively. However, a closer observation of the monthly space condition loads reveal that, in Edinburgh, in summer time of June, July and August, the space conditioning sensible load of building-2 is lower than of building-3 by 4% and higher than that of building-1 by 1.97%. In Birmingham, in summer time of June, July and August, the space conditioning sensible load of building-2 is lower than that of building-3 by 7.5% and higher than that of building-1 by 1.75%. Thus, the moistened hemp-2 insulation is performing better than the stone wool insulation during the summer months. It can be assumed that, the heat capacity of the moistened hemp-2 insulation can be fully utilized when cooling degree days increase due to the global warming.

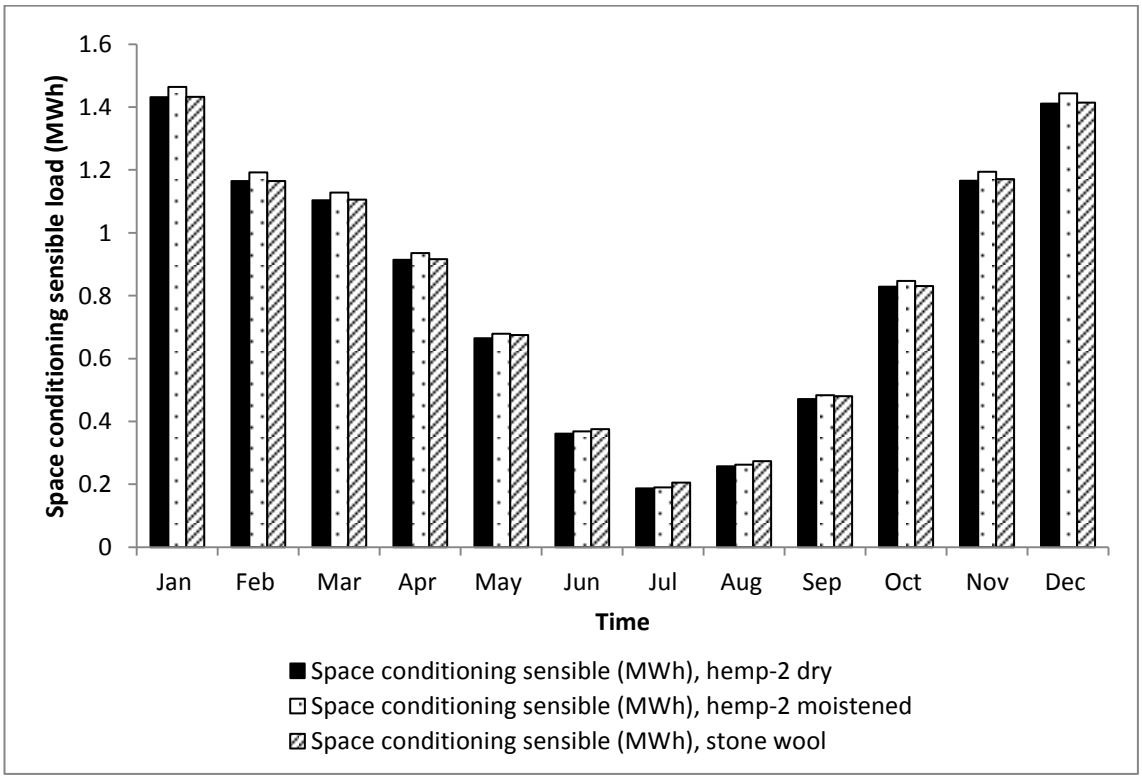


**Figure E.5: The monthly space conditioning sensible loads of the selected buildings in Edinburgh.**

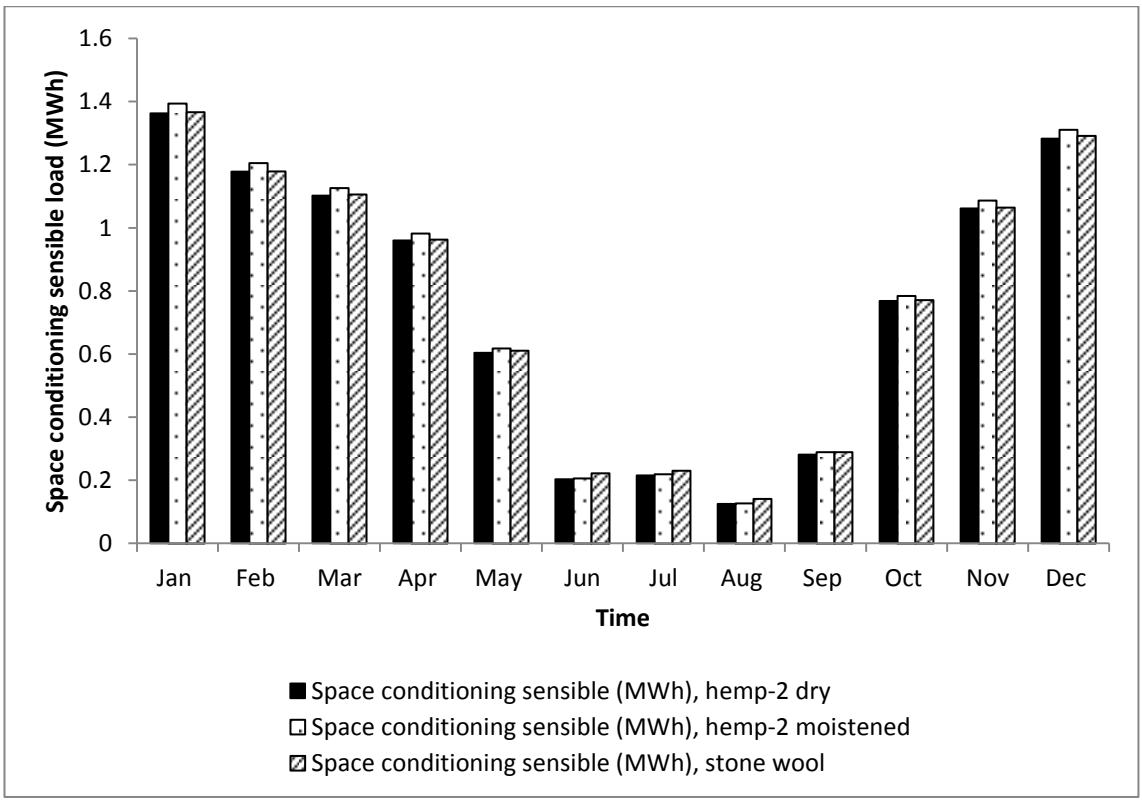


**Figure E.6: The monthly space conditioning sensible loads of the selected buildings in Birmingham.**

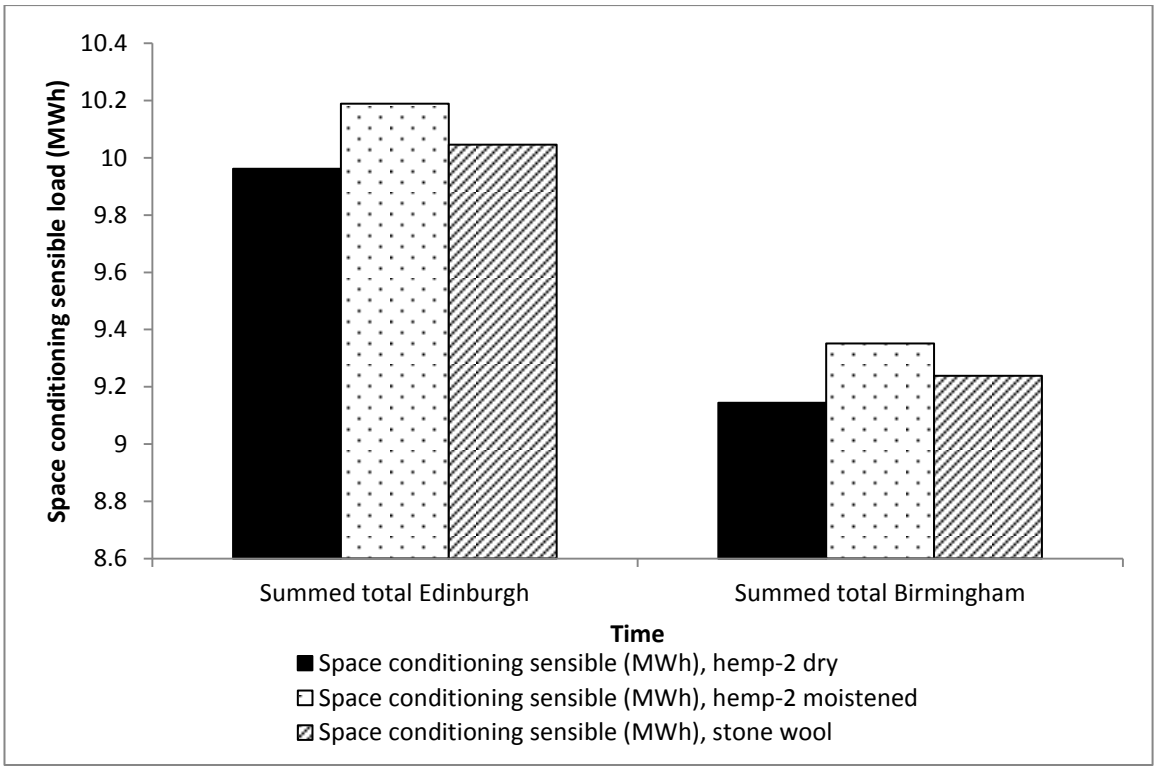


**Figure E.7: The yearly space conditioning sensible loads of the selected buildings in Edinburg and Birmingham, respectively.**

### E.4 Conclusions

The objective of the study was to examine the effect of thermal mass of moistened hemp-2 insulation on whole building energy use. It was found that, although the total space condition load of building-2 (with moistened hemp-2 insulation) was higher than that of building-1 (with dry hemp-2 insulation) and building-3 (with stone wool insulation) by 2.3% and 2.1%, respectively, in Edinburgh and 2.27% and 1.2%, respectively in Birmingham. However, it was also found that during the summer months of June, July and August the cumulative space condition load of building-2 was lower than that in building-3 by 3% and 7.5% for Edinburgh and Birmingham, respectively. Based on this result, it can be assumed that moistened hemp insulations will be more effective in saving energy when cooling degree-days increase as a result of the global warming.

# Appendix F

Data derived from the sensitivity analysis

**Table F.1: Effect of change of parameter values (%) on change of water content (%) in hemp-2 from the base case.**

| | Effect of change of water content in Hemp-2 from the base case (%) | | | | | |
|---|---|---|---|---|---|---|
| | **(-5)%** | **5%** | **(-10)%** | **10%** | **(-20)%** | **20%** |
| **Adsorption isotherm** | -4.90610 | 4.89765 | -9.88740 | 9.79508 | -19.68055 | 19.56251 |
| **μ value[1]** | 0.18678 | -0.21674 | 0.42064 | -0.40186 | 0.86782 | -0.77406 |
| **Absorption** | -0.00620 | 0.00959 | -0.01067 | 0.01573 | -0.02630 | 0.03045 |
| **MTC[2]** | 0.52428 | -0.50285 | 1.04103 | -0.96487 | 2.15995 | -2.16937 |
| **Density** | -0.01086 | 0.01373 | -0.02763 | 0.02672 | -0.06511 | 0.05704 |
| **Heat capacity** | -0.01086 | 0.01373 | -0.02763 | 0.02672 | -0.06511 | 0.05704 |
| **Porosity** | 0.00071 | -0.00022 | 0.00009 | | 0.00065 | |

**Table F.2: Effect of change of parameter values (%) on change of relative humidity (%) in (hemp-2)-OSB interface from the base case.**

| | Change of relative humidity in (Hemp-2)-OSB interface from the base case (%) | | | | | |
|---|---|---|---|---|---|---|
| | **(-5)%** | **5%** | **(-10)%** | **10%** | **(-20)%** | **20%** |
| **Adsorption isotherm** | 0.06832 | -0.04465 | 0.07818 | -0.10488 | 0.22273 | -0.24336 |
| **μ value** | 0.08171 | -0.11163 | 0.21921 | -0.21641 | 0.43989 | -0.38034 |
| **Absorption** | 0.03159 | -0.01805 | 0.05356 | -0.03277 | 0.09055 | -0.08564 |
| **MTC** | 0.23507 | -0.21826 | 0.45579 | -0.42044 | 0.97738 | -0.90919 |
| **Density** | 0.00403 | 0.02085 | 0.00208 | 0.00041 | -0.02861 | 0.03989 |
| **Heat capacity** | 0.00630 | 0.02085 | 0.00130 | 0.02185 | -0.01734 | 0.02582 |
| **Porosity** | 0.01142 | -0.00004 | -0.02810 | | -0.01238 | |

**Figure F.3: Effect of change of parameter values (%) on change of water content (%) in (hemp-2)-OSB interface from the base case.**

| | Change of water content in (Hemp-2)-OSB interface from the base case (%) | | | | | |
|---|---|---|---|---|---|---|
| | (-5)% | 5% | (-10)% | 10% | (-20)% | 10% |
| Adsorption isotherm | -4.57209 | 4.63922 | -9.42244 | 9.15017 | -18.77091 | 17.95231 |
| μ value | 0.46107 | -0.61932 | 1.21902 | -1.18505 | 2.46139 | -2.10293 |
| Absorption | 0.19215 | -0.13811 | 0.32732 | -0.24630 | 0.59361 | -0.59879 |
| MTC | 1.20000 | -1.18316 | 2.41852 | -2.28675 | 5.35186 | -4.89921 |
| Density | 0.02265 | 0.08977 | 0.02024 | -0.01112 | -0.11485 | 0.16492 |
| Heat capacity | 0.03280 | 0.08977 | 0.01677 | 0.08877 | -0.06294 | 0.09945 |
| Porosity | 0.05322 | -0.00039 | -0.13064 | | -0.05689 | |

**Table F.4: Effect of change of parameter values (%) on change of temperature (%) in hemp-2 from the base case.**

| | Change of temperature in Hemp-2 from the base case (%) | | | | | |
|---|---|---|---|---|---|---|
| | (-5)% | 5% | (-10)% | 10% | (-20)% | (20)% |
| Adsorption isotherm | 0.00730 | -0.00737 | 0.02998 | -0.01702 | 0.01913 | -0.03795 |
| μ value | 0.00825 | -0.01006 | 0.02009 | -0.01518 | 0.04698 | -0.02738 |
| Absorption | 0.00354 | -0.00466 | 0.00599 | -0.00785 | 0.01406 | -0.01604 |
| MTC | -0.10212 | 0.09818 | -0.20029 | 0.18964 | -0.38521 | 0.50799 |
| Density | 0.00278 | -0.00407 | 0.00755 | -0.00791 | 0.01704 | -0.01535 |
| Heat capacity | 0.00278 | -0.00407 | 0.00755 | -0.00791 | 0.01704 | -0.01535 |
| Porosity | -0.00013 | 0.00002 | -0.00001 | | -0.00006 | |

1. μ value: vapour diffusion resistance factor.
2. MTC: moisture dependent thermal conductivity.

# Appendix G

Conference presentations and publications

**Conference presentations**

North Wales European Research Seminar on Renewable Construction Materials: Black Mountain Insulation and Faenol Fawr Hotel Rhyl, 3-5 December, 2012 (Invited presenter).
**"Heat and Moisture Management of Hemp Insulations"**

ISDRC17: Columbia University, New York, 8-10 May, 2011
**"Fibrous Hemp Insulation: An Initial Study of its Hygric and Thermal Properties"**

ICBEDC 2010: USM, Penag, Malaysia, 1-2 December
**''An investigation into the thermal impact of adding an operable thermal insulation layer to an uninsulated metal roof in a free- running building'.**

Science Symposium 2010: CAT, Machynlleth, 9 October
"**Variable Thermal Conductivity of Fibrous Insulation Materials"**

AC & T 2010: London, 27 January
**'Potential for research on hemp insulation in the UK construction sector'**

Natural Fibre 09: London, 14-16 December
**'The potential of hemp insulation in the UK construction sector'**

## List of publications

Latif, E. (2011) 'an experimental comparison between the thermal performances of hemp fibre and stone wool insulation samples in a range of hygrothermal conditions', International Conference on Built Environment in Developing Countries: 5th Annual Conference, Penang, Malaysia 6-7December. Penang: USM.

Latif, E., Tucker, S, Wijeyesekera, D. C. (2011) Fibrous hemp insulation: An initial study of its thermal and hygric properties, International Sustainable Development Research Society (ISDRS): 17th Annual Conference, New York 08-10 May. New York: Columbia University.

Latif, E., Pruteanu, M. and Rhydwen, G. R., Wijeyesekera, D. C., Tucker, S., Newport, D., Ciupala, M. A. (2011) 'Thermal Conductivity Of Building Materials: An Overview of its Determination', Advances in Computing and Technology: 6th Annual Conference, London 26 January. London: UEL.

Latif, E., Tucker, S., Newport, D., Wijeyesekera, D. C. (2010) 'An investigation into the thermal impact of adding an operable thermal insulation layer to an uninsulated metal roof in a free- running building', International Conference on Built Environment in Developing Countries:4th Annual Conference, Penang, Malaysia 2-3 December. Penang: USM.

Latif, E., Tucker, S., Newport, D., Wijeyesekera, D. C. (2010) 'Potential for Research on Hemp Insulation in the Uk construction Sector', Advances in Computing and Technology: 5th Annual Conference, London 27 January. London: UEL.

## Contribution to research report

Tucker, S. and Latif, E. (2012) *Milestone Report: The functional performance of bio-based insulation products.* Unpublished Commercially Confidential Report, University of East London.

# Appendix H

Reference of the current research

Woolley, T. (2013) *Low Impact Building: Housing Using Renewable Materials,* Oxford: Wiley-Blackwell.

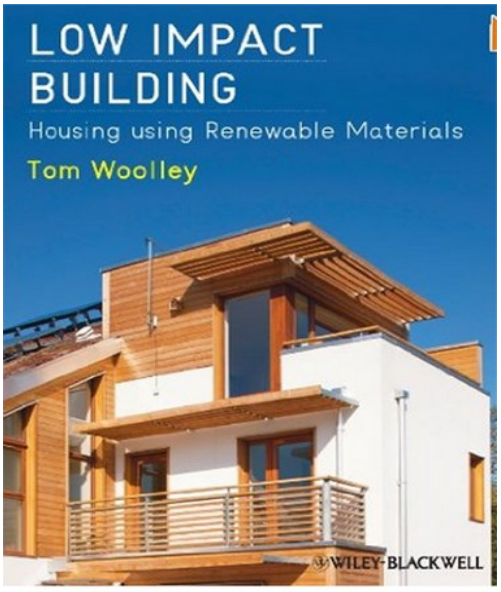


## Thermal mass and energy performance in buildings

A key factor in the ability of materials to handle moisture is their mass as well as their hygroscopic characteristics. Natural materials seem to perform better than synthetic products.

> …natural fibre insulations … will actively absorb up to 10% of their mass volume as water in changing humidities. This compares with only 1% with mineral wool insulation, and none with plastic insulations of any sort.
>
> (May undated)

Mass and moisture levels are important in understanding the thermal performance of insulation and building fabric. There is some evidence that wall and roof constructions using natural renewable materials perform better than similar constructions using synthetic materials because of their ability to deal with moisture.

Recent experiments in a climate chamber at the Centre for Alternative Technology being carried out by Tucker and Eshrar (Tucker 2012) show some very interesting results where thermal performance has been correlated with relative humidity. When natural insulation materials were compared with manmade fibres, (MMMF) in conditions of high humidity, water condensation was observed in the climate chamber with the MMMF, but hemp and sheep's wool were able to handle the extra moisture. Thermal insulation performance appears to deteriorate when MMMFs become wet, but this is not the case with some natural materials; indeed, the thermal performance may even improve slightly when additional moisture is present. This may be because water is a good medium to store heat and so the insulation materials, if they can handle moisture, can also appear to hold heat for longer.

This, like so many aspects of natural and renewable materials, is counterintuitive, because we have been taught that water is bad for building materials. Thermal conductivity is measured in hotbox tests in a

# Appendix I

# Published works

Published work I.1

---

# POTENTIAL FOR RESEARCH ON HEMP INSULATION IN THE UK CONSTRUCTION SECTOR

E Latif [*], D C Wijeyesekera [*], D Newport [*], S Tucker [**]

[*] *School of Computing, Information Technology and Engineering, University of East London*
[**] *Graduate School of Environment, Centre for Alternative Technology, Machynlleth, UK.*
*eshrar@eshrar.com, {d.c.wijeyesekera, D.J.Newport}@uel.ac.uk, simon.tucker@cat.org.uk*

**Abstract:** Hemp based thermal insulation has the potential to reduce CO2 emissions from buildings and to be 'carbon-negative' in its production and manufacture. Hemp has been in use to produce bio-based natural fibre insulation in the UK in recent years. With further development in hemp agronomy, production process and selection of raw materials in the production, hemp-based insulation materials are likely to become environmentally and functionally superior products to other insulation materials developed from petrochemical and mineral based sources. This paper looks at the research works on the present and future housing scenario in the UK, reductions in embodied energy of insulation materials, techniques for increasing thermal performance and ways in which the environmental impact can be lessened.

## 1. Introduction:

The United Kingdom, under its Climate Change Act 2008, has established the grand target of reducing greenhouse gases by ensuring that the net UK carbon account for the year 2050 will be at least 80% lower than the 1990 baseline. This new approach is important in relation to playing the UK's part in avoiding a global temperature rise of more than 2° Celsius by stabilizing atmospheric $CO_2$ concentration to 400 ppm. On September 2009, UK scientists predicted that the global average temperature could rise by 4°C as early as 2060 (British Broadcasting Corporation, 2009) which requires more robust mitigation strategies.

In the United Kingdom, the domestic sector is the second largest consumer of energy with annual consumption of 28.5% of the total energy and it represents 27% of total greenhouse gas (GHG) emissions (Boardman, 2007). The domestic sector with most of the existing buildings, according to the former Department for Business, Enterprise & Regulatory Reform (BERR), uses four times more energy than the commercial sector and seven times more than public administration (BERR, 2008). Therefore to keep up with the UK government's GHG reduction target, it is imperative that the residential sector becomes pro-active in reducing its energy consumption.

## 2. Why insulation matters:

GHG emissions from buildings can be reduced by the following methods: using materials with low embodied energy during building construction and maintenance, minimising energy consumption, using low-carbon and renewable energy in building operation, and reducing the emissions of non-$CO_2$ GHG gases.

The thermal envelope of a building determines the relationship between the exterior and interior of a building in terms of heat or mass transfer (Givoni, 1998, p.107). Therefore the use of energy depends much on the level of thermal protection of the building envelope. Thermal protection can

be increased by using insulation with better thermal performance, draught proofing and using efficient glazing.
The UK Carbon Attribution Model (Jackson et al, 2005) shows that, of the total carbon emissions of 176.4 million tonnes of carbon (MtC) in the UK, space heating represents 24 MtC and is mainly emitted directly in the home. This is the second highest emission after 'Recreation and Leisure'. This finding conforms with the study by Building Research Establishment (BRE) which highlighted that cost-effective measures could save 25% energy of which 65.4% savings could be achieved by improved insulation standards for the thermal envelope (Halliday, 2008, p.63).

## 3. British Houses and insulation: Present Context and Future Scenario:

The market for building thermal insulation in the UK can be viewed from two perspectives:

- Insulation market based on the elements of the thermal envelopes of buildings.
- Insulation market based on building types and numbers in 2050.

These two scenarios are discussed below:

### 3.1 Market based on the major thermal envelope elements of buildings:

The major elements of the thermal envelopes of buildings are walls and roofs and most of the thermal insulation market concentrates on insulating and draught-proofing these two elements. Based on a recent report (Mintel, 2007), Table 3.1 is developed to explain the trends in the insulation market for different elements of building envelopes.

Table 3.1 Market for thermal insulation based on the major elements of building thermal envelope.

| | % Market share in 2006 | Market share in 2006 by £ million |
|---|---|---|
| Cavity | 20% | 153.8 |
| Loft | 21% | 158.7 |
| Draught Proofing | 16% | 121.2 |
| Roof | 19% | 144.9 |
| Internal Wall | 6% | 46 |
| External Wall | 6% | 43.5 |
| Floor | 8% | 62 |
| Other | 4% | 31 |

### 3.2 Market based on building types and numbers in 2050:

At present there are about 25.6 million dwellings in the United Kingdom with an average floor area of 74$m^2$/dwelling. About 17 million of these houses are with cavity walls and cavity-walls are uninsulated in 8.5 million of these houses. About 5 million houses are built of solid brick walls and most of these lack wall-insulation. According to one estimate, there were 6.3 million homes in England without any or with very minimal loft insulation in 2005 (Boardman, 2007).
It has been estimated that the total numbers of British houses in 2050 will be 31.8 million (74$m^2$/dwelling) of which 20.6 million will be from the existing housing stock and about 11.2 million will be new-builds. It can be estimated that, of this existing housing stock, about 6.8 million houses will require cavity wall (or internal) insulation and 4 million houses will require solid wall insulation. In total, by 2050, 10.8 million older houses and 11.2 million new houses will require insulation in the envelope.

be increased by using insulation with better thermal performance, draught proofing and using efficient glazing.

The UK Carbon Attribution Model (Jackson et al, 2005) shows that, of the total carbon emissions of 176.4 million tonnes of carbon (MtC) in the UK, space heating represents 24 MtC and is mainly emitted directly in the home. This is the second highest emission after 'Recreation and Leisure'. This finding conforms with the study by Building Research Establishment (BRE) which highlighted that cost-effective measures could save 25% energy of which 65.4% savings could be achieved by improved insulation standards for the thermal envelope (Halliday, 2008, p.63).

## 3. British Houses and insulation: Present Context and Future Scenario:

The market for building thermal insulation in the UK can be viewed from two perspectives:

- Insulation market based on the elements of the thermal envelopes of buildings.
- Insulation market based on building types and numbers in 2050.

These two scenarios are discussed below:

### 3.1 Market based on the major thermal envelope elements of buildings:

The major elements of the thermal envelopes of buildings are walls and roofs and most of the thermal insulation market concentrates on insulating and draught-proofing these two elements. Based on a recent report (Mintel, 2007), Table 3.1 is developed to explain the trends in the insulation market for different elements of building envelopes.

Table 3.1 Market for thermal insulation based on the major elements of building thermal envelope.

| | % Market share in 2006 | Market share in 2006 by £ million |
|---|---|---|
| Cavity | 20% | 153.8 |
| Loft | 21% | 158.7 |
| Draught Proofing | 16% | 121.2 |
| Roof | 19% | 144.9 |
| Internal Wall | 6% | 46 |
| External Wall | 6% | 43.5 |
| Floor | 8% | 62 |
| Other | 4% | 31 |

### 3.2 Market based on building types and numbers in 2050:

At present there are about 25.6 million dwellings in the United Kingdom with an average floor area of 74$m^2$/dwelling. About 17 million of these houses are with cavity walls and cavity-walls are uninsulated in 8.5 million of these houses. About 5 million houses are built of solid brick walls and most of these lack wall-insulation. According to one estimate, there were 6.3 million homes in England without any or with very minimal loft insulation in 2005 (Boardman, 2007).

It has been estimated that the total numbers of British houses in 2050 will be 31.8 million (74$m^2$/dwelling) of which 20.6 million will be from the existing housing stock and about 11.2 million will be new-builds. It can be estimated that, of this existing housing stock, about 6.8 million houses will require cavity wall (or internal) insulation and 4 million houses will require solid wall insulation. In total, by 2050, 10.8 million older houses and 11.2 million new houses will require insulation in the envelope.

## 4. British insulation market and need for low-energy insulation:

By 2050, in line with the 80% GHG reduction scenario, about 22 million houses in the UK need to be insulated. This indicates a robust market for insulation materials and a potentially huge amount of material and energy flow through the supply chain. Therefore it has to be ensured that the insulation materials do not become an environmental burden per se by carrying high embodied energy, depleting non-renewable natural resources during production and creating environmental and health hazards during and after installation.
Many argue that synthetic and mineral based insulation materials are unsustainable as these products use a lot of fossil fuel and non-renewable resources during production while there is a strong commitment by the UK government to reduce energy-use (Bevan et al, 2008). One of the peak oil predictions states that conventional oil production appears to have peaked in 2005 (Hopkins, 2008) and a downward trend has begun. Therefore it can be argued that a shift from a hydrocarbon economy to a carbohydrate economy in terms of production and use of insulation is necessary.

## 5. Types and forms of Insulation materials:

Insulation materials are classified mainly on the basis of forms and in some cases on the basis of any functional attribute. Based on a previous study (Al-Homoud, 2005) (Sustainability Victoria, 2009), Table 5.1 is developed to show the major types of insulation materials and their applications.

Table 5.1 Types of Insulations based on form.

| Type | Main Products | Use |
|---|---|---|
| Rigid Boards | Polystyrene (Styrofoam, EPS, EPS-Foil), polyurethane, polyisocyanurate, Fibreglass, Phenolic Foam. | Walls, flat roofs, loft, pitched roof and perimeter insulation. |
| Batts and Blankets | Glass fibre, Mineral wool, Natural wool, Natural fibre, Polyester matt | Flat roof, pitched roof, loft, timber floor, framed wall. |
| Loose Fill to be blown-in and poured-in | Glass fibre, Mineral wool, Natural wool. (natural wool is not applicable to cavity type) | Flat roof, pitched roof, loft, framed and masonry wall |
| Reflective | Plastic film, Aluminium foil with glass fibre reinforcement, Aluminium foils on polyethylene bubbles, Multi-cell foil batts, | Flat roof, pitched roof, loft, framed wall (but not all products are suitable for all the uses). |
| Poured-in with concrete | Perlite, vermiculite | Masonry wall, loft space. |
| Foamed or sprayed in-place | Polyurethane, polyisocyanurate, Phenolic Foam. | Pitched roof, flat roof, loft space, wall and floor. |
| Blocks and Hollow forms | Aerated blocks, Hollow EPS blocks and panels filled with concrete. | Masonry wall insulation |
| Weather-proof house-wrap | Polyethylene fibres sheeting added to buildings during construction. | Flat roof, pitched roof, framed wall. |

Another useful categorisation of insulation materials is based on organic and inorganic materials as shown in Table 5.2.

Table 5.2 Types of Insulations based on organic/inorganic variations.

| Organic Insulation | Inorganic Insulations |
|---|---|
| Fibrous materials like hemp fibre, cotton, wood, cellulose, synthetic fibre etc. | Fibrous materials like glass fibre and rock wool. |
| Cellular material like polyurethane, foamed rubber etc.polystyrene, polyisocyanurate. | Cellular materials like calcium silicate, ceramic products, bonded perlite and vermiculite. |

However the classification mentioned in Tables 5.1 and 5.2 does not provide a clear perspective of environmental aspects of insulation materials. Hence, a broad-brush ecological classification of insulation materials is proposed in Table 5.3.

Table 5.3 Types of Insulations based on sourcing.

| Natural insulation | Synthetic and mineral insulation |
|---|---|
| Bio-based insulation: Plant and wood based insulations like hemp fibre insulation, cork diffutherm, etc. | Synthetic insulation: Various non-natural polymers like polyurethane polystyrene, polyisocyanurate etc. |
| Animal based insulation: wool insulation like thermafleece. | Mineral insulation: Glass fibre and rock wool insulation |

## 6. Bio insulations and hemp:

Bio-based natural insulation materials have been in use ever since the advent of man-made dwellings. Thatched roofs are considered to be the earliest kind of roofing systems (Encyclopaedia Britannica, 2009). Straw-Bale buildings were first built in the late 1800s (Woolley, 2006, p.71), (Borer and Harris, 1998, p.104). Cork barks had been used as roof covering in the 1st century AD and the Spanish people used to line the inner surfaces of stone houses with cork (Thomas, 1928, p.25). In contrast, hemp fibre insulation is a comparatively recent innovation even though hemp fibres had been processed in China since the 28th century BC and used in Europe since the 16th century for producing marine cordages, twines, textiles and papers. The importance of hemp as a fibre crop declined in the 19th century. The interest has been renewed recently in Germany, France, the Netherlands, the UK, Spain and Italy, and some other countries (Struik et al., 2000). Cautiousness is required to interpret the word 'hemp', as historically the term has been used to refer to the bast and leaf fibres of different plants including 'true' hemp (cannabis sativa), manila hemp, sisal, henequen, Indian Sunn etc (Imperial Economic Committee, 1932, p.9).

## 7. Hemp Botany, Agronomy and Hemp Fibre:

The word 'hemp' in this paper refers to 'industrial hemp' that contains a very low level of delta-9 THC (tetrahydrocannbinol) and therefore is not a psychoactive substance. Hemp is an annual crop and belongs to the Cannabinaceae family. The stalk height and thickness depend on the following factors: daily exposure to sunlight, geographical race, soil condition and available nutrients, supply of water, spacing of plants and the sex of the plant. Hemp crops require minimal biocide, suppress weeds and require limited amounts of fertiliser (Van der Werf, 1994). In the

UK, hemp is planted in late spring and sometimes reaches a height of 3 metres by August. Highest yields of 9 tonnes per hectare have been achieved in the UK. Hemp grown for fibre produces 29% fibre, 66.7% shive and 4.3% dust by mass (Murphy et al, 2008). Hemp straw can be retted in the field, or unretted straw can be processed in the factory. Hemp can be grown in a number of rotational situations. Nitrogen is a vital component of the yield. There are two possible harvest routes. These are dual hemp when both seed and straw are harvested and hemp for straw.

The stem of hemp consists of wood and bast tissue. Bast tissue forms the exterior layer of the stalk and functions as the plant's transport system. In bast tissue, groups of fibre cells are formed whose outer cell walls are strengthened with a thick layer of cellulose. The main purpose of these fibre cells is the reinforcement of the stalk by providing tensile strength and torque resistance. Fibre cells are held together in bundles by pectin. This bond is broken down during processing by biological, mechanical or chemical mechanisms. In addition to primary bast fibres, hemp forms secondary fibre bundle systems to provide elasticity and stability. The secondary fibre bundles are shorter in length and diameter and less valuable than the Primary fibres. Bast fibres are used as raw materials of thermal insulations.

## 8. Performance requirements for crop based construction materials:

Some critical performance requirements to determine the best application for crop-based construction materials (Van Wyk, 2007), are:

- **Economic performance**: Low embodied energy in manufacture and in use, low water use in manufacture, low wastage in manufacture and in assembly, and recycling potential.
- **Social performance**: Overcoming consumer resistance, health and safety during manufacture and assembly, facilitating the participation of small, medium and micro enterprises, rural workers and women in the supply chain and life-cycle.
- **Environmental performance:** Bio-degradability of the material at the end of its life-cycle, using materials with low toxicity levels and low emission.

The strength of the above analysis lies in the identification of social performance. Any discussion of economic potential of hemp insulation will be inadequate if social performance is not considered.

## 9. Life Cycle Assessment (LCA) of the insulation materials:

LCA is the compilation and evaluation of the inputs, outputs and potential environmental impacts throughout a product's life cycle, from raw material acquisition through production, use, end-of-life treatment, recycling and final disposal (ISO, 2006). The four phases of a LCA study are: Goal and Scope Definition, Life Cycle Inventory Analysis (LCI), Life Cycle Impact Assessment (LCIA), and Interpretation.

### 9.1 The LCA of hemp insulation:

A cradle to grave assessment of Natural Fibre Insulation (NFI) materials based on ISO 14040 standards for LCA has been carried out recently (Murphy et al, 2008). A comparison has been made between the following insulation materials: RockWool (Mineral Wool), Thermafleece (Sheep

influences energy use and thermal comfort in the building. The second is the longevity of the envelope in terms of its ability to cope with moisture. Some current researchers (Pavlík, Z.and C˘erny, R., 2009) are looking at these performances in terms of their contribution to air quality, tempering of internal air humidity and avoidance of mold growth, as well as the thermal performance.

- **Application:** It is important to recognise the different needs of new-build and refurbishment markets. For example, the thermal refurbishment of an old building requires thin insulation and a dry method of installation. Therefore research, in this case, needs to be directed towards developing rigid insulation boards.
- **Hybrid hemp insulation:** Novel insulation material like PCM (Phase Change Materials, for better thermal storage capacity), aerogel (for better λ value) or aeroclay (98% air and 2% clay) can be incorporated into the fibre matrix of hemp. However, in all cases the following issues need to be considered:
  - The hygrothermal performance of the hybrid material, with respect to moisture transfer and condensation.
  - The potential risk of producing a 'monstrous hybrid' (Mcdonough et al, 2009) mixture of materials, both technical and biological.
  - The viability of producing hybrid insulation while there is market presence of aerogel and PCM insulation as plaster board and other forms.
  - Health issues with regards to using nano particles.

## 11. Conclusion:

In the UK about 11 million older houses need to be insulated which can be the potential refurbishment market for hemp insulation. In addition about another 11 million new houses will be built by 2050 requiring a huge amount of insulation. With the increasing awareness of low-energy and environmentally benign goods, eco-efficient bio-based natural fibre insulation materials hold the prospect of being successful mainstream products. However, to enter into the mainstream market, the products have to be economically competitive, thermally efficient and contextually relevant. Some research potential that can determine the future of hemp insulation is therefore explored.

## References


Al-Homoud M. S., "Performance characteristics and practical applications of common building thermal insulation materials", *Building and Environment,* 40, 2005, pp. 353-366.

Bevan, R. & Woolley, T., *Hemp lime construction: a guide to building with hemp lime composites,* Bracknell, IHS BRE Press 2008.

Boardman, B., *Home truths: A Low-carbon Strategy to Reduce UK Housing Emission by 80% by 2050*, Environmental Change Institute, University of Oxford, Oxford 2007.

Borer, P., Harris, C., Preston, G. & Foo, B., *The whole house book: ecological building design and materials,* Machynlleth, Centre for Alternative Technology, 1998.

Encyclopaedia Britannica, "roof" [Online]. Available at: http://www.britannica.com /EBchecked/topic/509178/ roof (Accessed: 10 October 2009), 2009.

BERR *Digest of United Kingdom Energy Statistics 2008,* London: The Stationery Office, 2008.

Givoni, B., Climate *considerations in building and urban design,* New York, London, Van Nostrand Reinhold, 1998.

Halliday, S., Sustainable *Construction,* Amsterdam; London, Butterworth-Heineman, 2008.

Hendrickson, C. T., Lave, L. B. & Matthews, H. S., Environmental *life cycle assessment of goods and services : an input-output approach,* Washington, D.C., Resources for the Future , Chichester : John Wiley [distributor], 2006.

Hopkins, R., The *transition handbook: from oil dependency to local resilience,* Totnes, Green, 2008.

ISO, *ISO 14040: Environmental management-life cycle assessment -principles and framework.* Geneva, International Organisation for Standardization, 2006.

Imperial Economic Committee, *Hemp Fibre,* London, His Majesty's Stationery Office, 1932.

Jackson, T., Papathanasopoulou, E., Bradley, P. and Druckman, A., Attributing *UK carbon emissions to functional Consumer needs: methodology and pilot Results.* [Online]. Available at: http://www.surrey.ac.uk/resolve/Docs/WorkingPapers/RESOLVE_WP_01-07.pdf (Accessed: 10 August 2009), 2005

Mcdonough, W. & Braungart, M., *Cradle to Cradle: remaking the way we make things,* New York, North Point Press, 2002.

Mintel, Performance characteristics and practical applications of common building thermal insulation materials, Thermal *Insulation (Industrial Report) - UK*, UK, MBD Ltd., 2007.

Murphy, R. J. and Norton, A., *Life Cycle Assessment of Natural Fibre Insulation Materials,* London, NNFCC, 2008.

Pavlík, Z., C˘erny, R.," Performance characteristics and practical applications of common building thermal insulation materials Hygrothermal performance study of an innovative interior thermal insulation system", *Applied Thermal Engineering*, 29, 2009, pp. 1941-1946.

Struik, P.C., Amaducci, S., Bullard, M..J., Stutterheim, N.C., Venturi, G., Cromack, H.T.H., "Agronomy of fibre hemp (Cannabis sati6a L.) in Europe", *Industrial Crops and Products,*11, 2000, p.107-118.

Sustainability Victoria, *Insulation Types*, Available at: http://www.sustainability.vic.gov.au/ resources/ documents/insulation_types.pdf (Accessed: 25 October, 2009), 2009.

Thomas, P. E., Cork *Insulation*, Chicago, Nickerson & Collins Co., 1928

Van der Werf, H., "Crop Physiology of Fibre Hemp (*Cannabis sativa* L)", PhD thesis, Wageningen University, 1994.

Van Wyk, L., "The Application of Natural Fibre Composites in Construction: A Research Case Study", *Sixth International Conference on Composite Science and Technology,* Durban, South Africa, 22-24 January 2007, ICCST, 2007.

Woolley, T., Natural *building: a guide to materials and techniques,* Ramsbury, Crowood, 2006.

# Appendix I

Published work I.2

---

# THERMAL CONDUCTIVITY OF BUILDING MATERIALS: AN OVERVIEW OF ITS DETERMINATION

E Latif [*], M Pruteanu [***] and G R Rhydwen [*],
D C Wijeyesekera [*], S Tucker [**], M A Ciupala [*], D Newport [*]

[*] *School of Computing, Information Technology and Engineering, University of East London,*
[**] *Graduate School of Environment, Centre for Alternative Technology, Machynlleth, UK*
[***] *Technical University of Iaşi, Romania*

*ranyl@hotmail.co.uk, eshrarlatif@hotmail.com, pruteanu_marian@yahoo.com*
*{d.c.wijeyesekera ,m.a.ciupala, d.j.newport}@uel.ac.uk, simon.tucker@cat.org.uk*

**Abstract: A** range of instruments are available to measure thermal conductivity of building materials. Some of these tools are heat-flow meter, hot plate, hot box and heat transfer analyzer. Thermal conductivity data derived by using different instruments can be different from each other. Implication of these variations in thermal conductivity is significant in terms of commercial profile of the insulations and also in terms of calculating energy saving in large scale use of that specific insulation. Thus it is important to know which of the measuring instrument for thermal conductivity can produce relatively accurate and representative result. This paper firstly looks at the methods and instrument for measuring thermal conductivity of building materials and secondly compares and analyses the results of testing thermal conductivity of fibrous insulations using a heat analyzer and a hot plate.

## 1. Introduction:

Thermal conductivity is defined as the rate of heat transfer through the unit thickness of a material per unit area per unit temperature difference. The unit of thermal conductivity is w/m-K. Thermal conductivity is lowest in gas phase of a material and highest in solid phase. Heat conduction in a solid phase occurs through the energy transport by flow of electrons and through molecular vibration. In steady state condition, thermal conductivity is a good indicator of the heat conduction through a material, but in transient condition, diffusivity ($\alpha$ in $m^2/s$) of a material gives a better indication of how quickly heat propagates through a material. In transient condition, thermal conductivity data of a material is still needed since diffusivity is a function of conductivity and volume heat capacity. Thermal conductivity is usually measured in a steady state condition, however the process is time consuming and complex, especially in case

of materials with higher heat capacity. A quicker method requires the measurement of heat transfer in transient condition since steady state cannot be reached in a short period of time. This paper compares steady state and transient methods of measuring thermal conductivity.

## 2. Governing thermal Equations:

The primary equation of thermal conductivity at macroscopic level based on Fourier's law is:

$$Q_x = -K_x A \partial T/\partial x \qquad [w] \qquad (1)$$
$$q_x = -k_X \partial T/\partial x \qquad [w/m^2] \qquad (2)$$

Where $Q_x$ is heat transfer and $q_x$ is heat transfer rate ($W/m^2$) in x direction per unit area (normal to the direction of heat flow); $k_X$ is thermal conductivity (W/m.K) towards the x direction and $\partial T/\partial x$ is the temperature gradient in the same direction.
The internal thermal conductivity derived from the equation (1) or (2) is for steady state heat flow and temperature variation. Based on the Fouriers' law and the first law of thermodynamics, the following partial differential heat equation is developed for one dimensional transient heat flow where heat capacity of the conductive material is taken into account:

$$\partial^2 T/\partial x^2 + g/k = (1/\alpha) * (\partial T/\partial t) \qquad (3)$$

where α is the diffusivity of the conductive material, $\partial T$ is differential temperature, K is conductivity and g is internal heat generation.
For three dimensional Cartesian co-ordinate system, the heat balance equation is as follows:

$$\partial^2 T/\partial x^2 + \partial^2 T/\partial y^2 + \partial^2 T/\partial z^2 + g/K = (1/\alpha)(\partial T/\partial t) \qquad (4)$$

In steady state condition temperature difference is not changing in time ($\partial T/\partial t$), and if there is no internal heat generation, equation (3) and (4) can be written respectively as :

$$\partial^2 T/\partial x^2 = 0 \qquad (5)$$
$$\partial^2 T/\partial x^2 + \partial^2 T/\partial y^2 + \partial^2 T/\partial z^2 = 0 \qquad (6)$$

The transient heat flow equations are used in dynamic thermal simulation software while the conventional measuring instruments for thermal conductivity are based on equation (1). Next section describes the conditions in measuring thermal conductivity based on time and determination of heat input.

## 3. Variations of Conditions in Measuring Thermal conductivity:

### 3.1 Measurement of Heat Flow and Conductivity:

- Absolute Method: In determining thermal conductivity, when heat flux is measured directly from power input.
- Comparative Method: When heat flux measurement is done indirectly during determining thermal conductivity.

### 3.2 Temperature Difference and Conductivity:

- Steady state: When temperature gradient does not change in time.
- Transient: When temperature gradient changes in time, it is called a transient method.

Next two sections look at instruments and methods in measuring conductivity.

## 4. Steady state methods for measuring thermal conductivity:

### 4.1 Hot Box :

Calibrated and Guarded hot box methods are used according to BS EN ISO 8990:1996 (1998). Thermal conductance and resistance

are calculated on the basis of the power input in the metering box and the resultant difference of environmental temperature between hot and cold side boxes. However, thermal conductivity only for flat, opaque and homogeneous materials can be derived from thermal resistance data using the following equation:

$$\lambda = d/R_s. \quad (7)$$

Air temperatures can be used instead of environmental temperature when there is no significant different between air temperature and radiant temperature

**4.1.1 Calibrated HotBox***:* In calibrated hot box (Figure 1, left) the envelope of the hot box is comprised of materials of high thermal resistance so that there is minimal heat loss ($\Phi_3$) through the metering wall. If the flanking loss is $\Phi_4$, and the total power input is $\Phi_p$ , then the equation for total heat flow rate $\Phi_1$ through specimen will be,

$$\Phi_1 = \Phi_p - \Phi_3 - \Phi_4 \quad (8)$$
where $\Phi_3 \leq (10\% \text{ of } \Phi_p)$

The metering box walls are thermally insulated, air and vapour-tight. Thermopiles are used to determine heat loss through metering walls, thermocouples are used to measure specimen surface temperature. Electric resistance heaters are recommended for heat supply. Temperature of the cold side chamber is controlled by refrigeration unit.

**4.1.2 Guarded Hot Box**: In a guarded hot box (Figure 1, right), the metering chamber is surrounded by a guard box. The environment of guard box is controlled to minimize heat flow through the metering box wall and lateral heat flow in the specimen. If the lateral loss is $\Phi_2$, and the total power input is $\Phi_p$ , then the equation for total heat flow rate $\Phi_1$ through specimen will be,

$$\Phi_1 = \Phi_p - \Phi_3 - \Phi_2 \quad (9)$$
where $\Phi_3 \leq (10\% \text{ of } \Phi_p)$

**4.1.3 Calculation for Calibrarted and Guarded Hot Box :** The basic equation for U (thermal transmittance, w/m$^2$-K) value are:

$$\Phi = U * A * dT, \quad (10)$$
$$U = \Phi / A (T_2 - T_1) \quad (11)$$
$$R = [(T_1 - T_2)/ \Phi] * A \quad (12)$$

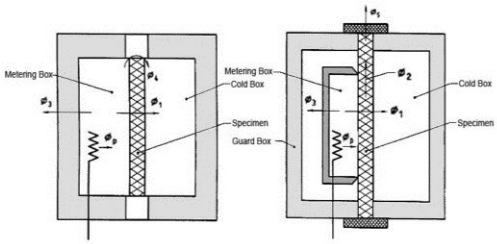


Figure 1. Calibrated and Guarded Hot Box (BS EN ISO 8990:1996, 1998)

In the above equations, A= surface area (m$^2$) of insulation, R= thermal resistance (m$^2$-K/w). Determining the temperature difference can be complicated. If the thermal resistance of the specimen is much higher than its surface thermal resistance or if forced convection is used in such a way that $h_c$ is greater than $Eh_r$ then the difference of air temperatures in hot and cold side box contribute to negligible errors in measurements. In all other cases difference of environmental temperature has to be taken into account. The equation for environmental temperature $T_n$ is:

$$T_n = (Eh_r * T'_r) /( Eh_r + h_c) + (hc * T_a)/ ( Eh_r + h_c) \quad (13)$$

Where, $h_c$ = 3.0 w/m$^2$k (heat transfer coefficient for convection), $h_r = 4\sigma T^3_m$ (heat transfer coefficient for radiation), $\sigma$ = 5.97 * $10^{-8}$ w/m$^2$k$^4$ (Stephan Boltzmann constant), $T_m = ( T'_r + T_s)/2$, and $1/E = 1/\varepsilon_1 + 1/\varepsilon_2 - 1$, $\varepsilon$ and $\varepsilon_2$ are the emissivities of the

baffle and specimen respectively. In absence of data for $h_c$, the following equation is used to determine $T_n$:

$$T_n = [(T_a * \Phi/A) + Eh_r (T_a - T'_r) T_s] / [(\Phi/A) + Eh_r (T_a - T'_r)] \quad (14)$$

$$U = \Phi/A(T_{n1} - T_{n2}) \quad (15)$$

### 4.2. Guarded Hot Plate and Heat Flow Meter:

The hot and cold surfaces of hot plate and heat flow meter are directly in touch with the insulation surfaces which eliminate the need for measuring radiant heat. The U value is determined from Equation (10), (11) and (12). The critical issue is how the heat flow rates and temperature differences are accurately measured. Hot plate and heat flow meter uses different method for measuring heat flow rates according to BS EN 12667: 2001(2002). A brief description of both the equipments is provided below:

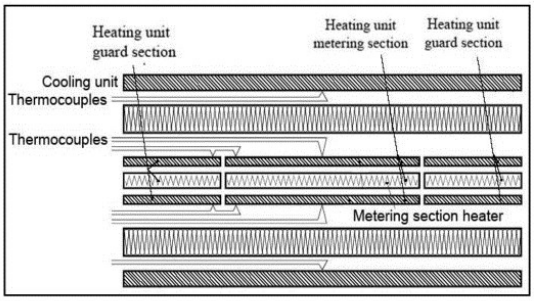


Figure 2. Guarded Hot Plate (BS EN 12667:20012002)

**4.2.1. Guarded hot plate apparatus:** Here heat flow rate is determined from the power input to the heating unit. In a **t**wo-specimen guarded hot plate (see figure 2) two specimens are sandwiched between a central flat plate heating unit and two peripheral flat plate cooling unit (see figure 2a). Heating unit has a metering unit at the centre and two guard units on both sides. The cooling unit is similar to the size of the heating unit. Heat flow rate is determined by measuring the average electric power supplied to the metering area. Temperature difference can be measured from the surface thermocouples of the heating and cooling units. Thermal resistance is calculated from the equation (12). Thermal conductivity can be measured from the following equation:

$$\lambda_t, \lambda^* \text{ or } \lambda = U * d \quad (16)$$

where, $\lambda_t$ = Thermal transmissivity, $\lambda^*$ = hygrothermal transmissivity and $\lambda$ = thermal conductivity. Equation (16) is valid for follwing criteria:

- The material is homogeneous,
- For homogeneous anisotropic material, the ratio of conductivity measured in a direction parallel to the surface and normal to the surface is not more than two (in any order), and
- At any one mean temperature thermal resistance is independent of the temperature difference across the specimen

**4.2.2 Heat flow meter apparatus:** Here density of heat flow rate is calculated by measuring heat flow through the insulation materials using heat flow meters. The measured heat flow is then multiplied by a calibration factor to get the density of heat flow rate. Thermal resistance is determined from the following equation:

$$R = (T_1 - T_2) / (f * e_h) \quad (17)$$

where: $f$ is the calibration factor of the heat flow meter; $e_h$ is the heat flow meter output; $T_1$ and $T_2$ are the temperatures at hot and cold sides. Thermal conductivity can be measured from the equation (16) .

### 4.3. Pope, Zawilski and Tritt's method:

Pope, Zawilski and Tritt (2002) developed a

device that uses steady-state absolute thermal conductivity measurements in lessened time. Thermal conductivity measurements are made using electronics and data acquisition software that allows stabilization of temperature. Once temperature is stable, a small power of current is independently put into each strain gauge until the heat flow is uniform and stable. The power and ΔT are recorded. Then current through the heater is slightly increased, the temperature difference allowed to equilibrate, and then the power and ΔT are again recorded. This sequence is repeated several times, resulting in a power verses ΔT sweep at a given temperature. This power sweep is then fit to a straight line, the slope being proportional to the thermal conductivity. Measuring period is 24–48 hours.

### 4.4. Steady state hot-wire method (radial flow method):

In radial heat flow method heat is generated along the axis of a cylinder, when steady-state condition is reached, radial temperature isotherm is measured at two different radii. If there is no longitudinal heat loss, thermal conductivity λ is:

$$\lambda = [Q/(2\pi l \Delta T)]\ln(r_2/r_1) \qquad (18)$$

In practical applications, central heat source is of finite length, therefore end guard is used and correction is applied. This method is also applied as comparative method by having concentric cylinders of known and unknown conductivity with a central heat source. Slack and Glassbrenner (Tritt and Weston, 2005, p.194) used this method to measure thermal conductivity of germanium (figure 3) taking heat flow reading from power input (absolute method) and temperature readings at the centre and the periphery. One of the present authors also

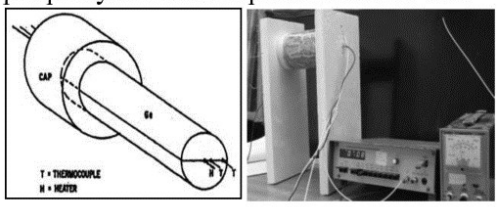


Figure 3. Slack and Glassbrenner's device (Tritt and Weston, 2005, p.194) and Radial flow device (Pruteanu,2010, p.11).

(Pruteanu, 2010) used the method (absolute) to measure thermal conductivity of straw using two concentric tubes (Figure 5). A hot wire method is especially useful in high temperature where longitudinal methods can fail due to radiative heat losses from the heater and the sample surfaces.

## 5. Transient Methods:

### 5.1 Hot wire method for measuring thermal conductivity:

The transient hot-wire method is used for measuring the thermal conductivity of liquids and low thermal conductivity materials (Carslaw and Jaeger, 1959). Here conductivity can be obtained as a function of temperature, time and heat flow without knowing the diffusivity and the distance. The mathematical model of hot wire method is based on the assumption that hot wire is a continuous line source and by providing constant heating power through thermal impulses it generates cylindrical coaxial isotherms in an infinite homogenous medium with initial equilibrium condition. The transient temperature can be expressed through the following equation:

$$T_{(r,t)} = [\, q/(4\pi\lambda)]*[\ln(4\alpha t/r^2) + r^2/(4\alpha t) - 1/4\{r^2/(4\alpha t)\} - \cdots - y] \qquad (19)$$

Where, λ is thermal conductivity (w/m-k), Q is power supply per unit length (W/m), α is thermal diffusivity of the conductive material, r is the radial position where tempera ture is measured, t is the time between the heat generation and measuring the temperature and У is Euler's constant Assuming that the terms inside the parentheses in equation (10) is negligible at a sufficient period of time and When equation (10) with good approximation as: $(r^2/(4\alpha t) << 1$, it is possible to express

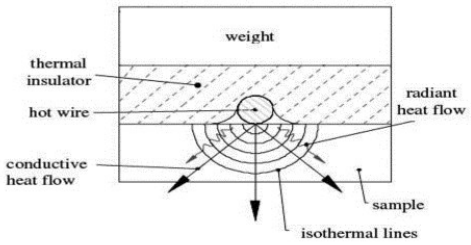


Figure 4. Transient hot wire apparatus (Franco, 2007, p.2499).

$$T_{(r,t)} = [Q/(4\pi\lambda)]*[\ln(4\alpha t/r^2) - У] \quad (20)$$
$$T_{(r,t)} = [Q/(4\pi\lambda)]*[\ln t + \ln(4\alpha/r^2) - У] \quad (21)$$

Therefore temperature variation for time $t_1$ and $t_2$ can be expressed as:

$$\Delta T = [Q/(4\pi\lambda)]* [\ln( t_2/t_1) ] \quad (22)$$

### 5.2 Thermal Analyzer:

In thermal analyazers like Isomet 2140 or Quickline$^{tm}$-30 transient line source (for needle probe) or transient plain source technique (for disc shaped surface probe) is applied based on ASTM D5334 - 08. Conductivity is determined from power input and time dependant temperature variation. The thermal equation applied is similar to those of transient hot wire and transient plain source method.

## 6 Advantages and Disadvantages of the methods:

### 6.1 Hot Box, hot plate and heat flow meter:

It is difficult to measure thermal conductivity of insulations in moist condition accurately in these equipments because of the moisture gradient created by the induced temperature difference (Clarke and Yaneske, 2009). These methods are also time-consuming. For dry insulations, hot box can provide reliable results although readings can be distorted due to radiation heat loss in very high temperature measurements. Hot plate and heat flow meter is not recommended for non-homogenous materials. Heat flow meter uses heat flux meters which are comparative instruments that calculate heat flux from temperature- there can be errors in heat flux reading in addition to any error induced by a hot plate method.

### 6.2 Transient Hot wire method:

Transient hot wire method can render inaccurate result for some insulation materials for two reasons: anisotropy and interlinked pore structure. For anisotropy, one-directional or radial heat transfer equation can provide incorrect result. For inter-linked pore structure (Lei et al, 2010), convection current is likely to be created by heated air during heat flux intervention by the hot-plate or hot-wire, while the transient equations do not take into account heat transfer by convection. For most other insulations, it provides quick and reliable results with smaller samples.

### 6.3 Steady state hot wire method:

Steady state hot wire method can provide inaccurate heat flow value for anisotropic materials due to heat loss towards the longitudinal direction since the governing equation is developed on the basis of infinite length of heat source. However, it is a useful method for some bulk insulation materials (refractory) because of reduced measuring time and need for smaller samples.

## 7. An experimental study of thermal conductivity:

Two of the present authors (Tucker S and Latif E) have carried out a comparison study of measured conductivity of various fibrous insulation materials in three hygrothermal regimes. For the purpose of this paper, comparison data at 23°C temperature and 50% relative humidity is presented in figure. The experiment was carried out with two devices: Isomet Heat Analyzer (transient method) and Fox 600 Hot Plate (steady state method). Conductivity measurements in steady state method were carried out by Gary Newman and Dick Salisbury of Plant Fibre Technology Ltd.

Measurements were taken by both equipments when the insulation materials had reached Equilibrium Moisture Content (EMC) with 23°C temperature and 50% relative humidity. EMCs for insulation materials were attained by exposing the material to the selected hygrothermal regime in climate chambers and by following the process prescribed in BS EN 12429 (1996).

It can be observed from Figure 5 that there are considerable agreements between the thermal conductivity data for glass wool, stone wool and lamb wool insulation measured by the two equipments. However, thermal conductivity data of hemp fibre and wood fibre insulation measured in Isomet Heat Analyzer is significantly higher than that in Fox 600 Hot Plate. It seems to be a significant finding that the two equipments do not agree in readings only for cellulose based fibrous insulations. It is not possible without further research to ascertain the reason behind this discrpency. However, two assumptions can be made. It can be assumed that the hydrofillic nature of the cellulose insulation materials as opposed to the hydrophobic nature of the mineral and synthetic fibre insulation may contribute to this behaviour. It can also be assumed that, since steady state measurents require a temperature gradient of 20°C between the

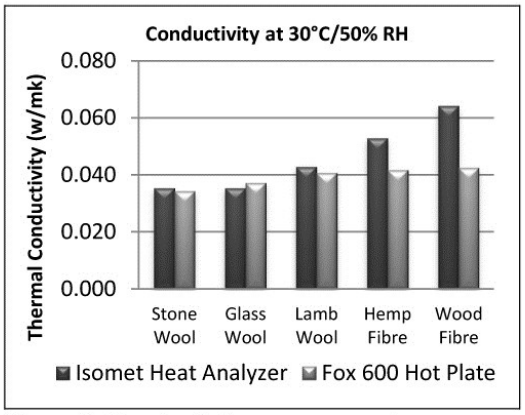

Figure 5. Conductivity measurements.

two sides of the sample insulation and since it takes at least about 72 hrs to reach steady state condition -moisture can be removed or migrated in the mean time resulting in measuring in a condition similar to dry state. In any case, steady state and transient methods provide different values for similar cellulose-based fibrous insulation materials in the stated thermal regime.

## 8. Conclusions:

Thermal conductivity of insulations can be determined by steady state and transient methods. Hot box, hot plate and heat flow meter devices are time consuming; require bigger samples and are not very accurate in

measuring moisture dependent conductivity. However these methods are reliable in measuring dry thermal conductivity. There is not much data available on reliability of steady state methods which are relatively speedier. Transient methods are convenient for regular measurement of conductivity; moisture dependent conductivity might be measured without seriously affecting moisture gradient, however this method is not suitable for non homogenous materials. The authors' experiment shows that significant variations exist between certain transient method and steady state method in terms of the data obtained for thermal conductivity of cellulose-based fibrous insulation materials.

## 9. References:


BS EN 12429, "Thermal insulating products for building applications: Conditioning to moisture equilibrium under specified temperature and humidity conditions", British Standard Institute, 1996.

BS EN 12667:2001, "Thermal performance of building materials and products- Determination of thermal resistance by means of guarded hot plate and heat flow meter methods- Dry and moist products of high and medium thermal resistance", British Standards Institute, 2002.

BS EN ISO 8990:1996, "Thermal insulations- Determination of steady-state thermal transmission properties –Calibrated and Guarded hot box", British Standards Institute, 1998.

Carslaw, H.S., Jaeger, J.C., Conduction *of Heat in Solids*, second ed., Clarendon Press, 1959.

Clarke, J. A., Yaneske, P. P. "A rational approach to the harmonisation of the thermal properties of building materials", *Building and Environment,* 44, 2009, pp. 2046-2055.

Franco, A., "An apparatus for the routine measurement of thermal conductivity of materials for building application based on a transient hot-wire method", *Applied Thermal Engineering,* 27, 2007, pp. 2495-2504.

Lei, Z., Zhu, S., Pan, N., "Transient methods of thermal properties measurement on fibrous materials", *Journal of Heat Transfer,* 132, 2010, pp. 1-7.

Pope, A.L., Zawilski, B., Tritt, T.M., Description of removable sample mount apparatus for rapid thermal conductivity measurements, Cryogenics 41 (2001), 725-731, Elsevier Ltd., 2002.

Pruteanu, M., "Investigations regarding the thermal conductivity of straw", *Bulletin of the Polytechnic Institute of Jassy*, Construction. Architecture Section, Tome LVI(LX), Fasc. 3, 2010, pp. 9-16.

Tritt, T. M., Weston, D., "Measurement techniques and considerations for determining thermal conductivity of bulk materials", in Tritt, T. M. (ed.) *Thermal Conductivity: Theory, Properties and Applications*, New York, Spinger, 2005.

Xamán, J., Lira, L., Arce, J., "Analysis of the temperature distribution in a guarded hot plate apparatus for measuring thermal conductivity", A*pplied Thermal Engineering,* 29, 2009, pp. 617-623.

# Appendix I

## Published work I.3

---

### AN EXPERIMENTAL COMPARISON BETWEEN THE THERMAL AND HYGRIC PERFORMANCES OF HEMP FIBRE AND STONE WOOL INSULATION SAMPLES IN A RANGE OF HYGROTHERMAL CONDITIONS

**Eshrar Latif**[1]
[1,] CITE, University of East London, UK
eshrarlatif@hotmail.com

**ABSTRACT:** Thermal Insulations are the most cost effective means of controlling heat transfer through the building envelopes and thereby of saving heating or cooling energy both in developed and developing countries. The synthetic and mineral insulation materials are produced from non-renewable sources and their embodied energy is high due to the production process. Bio-based insulations like fibrous hemp, on the other hand, are produced from renewable materials and their embodied energy is comparatively low. However there are commercial claims that mineral insulations do not change their conductivity significantly in different hygrothermal conditions whereas the bio-insulations do meaning that bio-based insulations are poor thermal performer at dynamic environmental conditions. The present experiment compares the moisture dependent conductivity of and heat flux through a sample of stone wool and a sample of fibrous hemp insulation simultaneously by exposing both the insulations to similar boundary conditions in a hygrothermal hot box at one side and in cooler air at the other side. The external surfaces of the insulations have been covered with 3mm clear acrylic sheet to replicate a cooler surface and to monitor if interstitial condensation occurs. Heat flux sensors, relative humidity and temperature probes are used to monitor the surface and internal condition in the insulations. Both the samples are of about similar thickness and of similar dry thermal conductivity according to the manufacturers claim. The test has been run for about three weeks' time. It has been found that interstitial condensation occurs in the rock wool insulation very quickly and total heat loss through the rock wool insulation is also comparatively higher for a range of hygrothermal boundary conditions. Thermal conductivity is also higher in the rock wool insulation than in the hemp fibre insulation in most of the times. Condensation can lead to mould growth and rotting of vulnerable elements of envelope assembly and higher conductivity can lead to higher energy use. These findings are contrary to the industry claims that bio-based insulations perform poorly in higher humidity.

**Keywords:** Insulation, Condensation, Conductivity, Heat Flux.

### 1. INTRODUCTION

Two widely discussed topic of a building envelop system is its thermal conductivity and the risk of interstitial condensation. Thermal conductivity and diffusivity can contribute to the amount of energy needed for space heating and cooling, on the other hand condensation can lead to structural damage and mold growth within the building envelope. Another important issue is sustainability and energy use of building materials. It has been found that energy use in building can be significantly lessened by using thermal insulations in building envelopes.

However, a sustainable thermal insulation has to be produced from a renewable source, has to be bio-degradable, should carry low embodied energy and should not perform worse than the conventional insulation materials. Hemp fibre insulation ticks most of the boxes to be claimed as a sustainable insulation, however there is doubt about its thermal and hygric performance as it is a comparatively new insulation material. Bio-based fibrous material are still being improved and developed on the basis of its performance evaluation. The aim of the present study is to contribute to the knowledge of the hygrotheral performance of a sample of commercially available hemp insulation and compare its performance with a commercially available sample of stone wool insulation with reference to interstitial condensation and thermal conductivity. This will also contribute to making informed decisions during specifying and buying insulations in an industry where vagueness, claims and counter claims about the hygrothermal performance of insulations and even about what constitutes sustainability make it necessary to establish some robust knowledge about the materials.

## 2. THE SAMPLE INSULATION MATERIALS

A sample of stone wool and a sample of fibrous hemp insulation are used in the experiment. The properties of the materials are given in the table 1 below:

*Table 1. Material Properties*

| | Measured Dimension (mm X mm) | Measured Thickness (mm) | Declared Conductivity (W/M-K) | Measured Density at 50% RH ($Kg/m^3$) | Measured Density at 10% RH ($Kg/m^3$) |
|---|---|---|---|---|---|
| Hemp | 650X320 | 120 | 0.044 | 49 | 46 |
| Stone Wool | 660X320 | 110 | 0.044 | 23 | 23 |

## 3. DESCRIPTION OF THE EXPERIMENTAL SETUP

The experimental setup consists of the following equipment and sensors:

### 3.1 Climate Chamber

The climate chamber is manufactured by Temperature Applied Sciences Ltd . Temperature range is -65°C to 150°C and the humidity range is 10% to 98%. There is a port hole on the left wall of the climate to connect it to any external facility.

### 3.2 Insulated Cell or the Hygrothermal Hot Box

The total dimension of the cell with the insulation is 1460 mm X 1460mm X1460 mm. The internal dimension of the cell is 860mm X 860mm X 860mm and the cell is covered by 300mm thick EPS insulation. There is an opening at the front with the dimension of 860mm X 860mm. Insulation can be placed on this opening or insulation can be placed on a separate insulated framework which is 350mm in thickness with 860mmX860mm opening and with an external dimension of 1460mm X 1460mm. The Insulated cell is equipped with a resistive micro heater that can create a temperature of up to 40°C. For this experiment, the cell is linked to the climate chamber with an insulated PVC pipe of 65mm diameter. The insulated cell is called the hygrothermal hotbox as temperature and moisture can be reasonably controlled inside it by controlling the temperature and humidity of the climate chamber and by controlling the internal heater of the hygrothermal hot box.

### 3.3 Air Conditioner

A 2.5KW portable air conditioner has been used to lower the external temperature. The temperature control range is 15°C to 25°C.

### 3.4 Temperature and Humidity Sensors

CS215 Temperature & Relative Humidity Probe from Campbell Scientific is used to measure temperature and humidity together. The accuracy of humidity measurement is (at 25°C) ±2% over 10-90% RH, ±4% over 0–100% RH, the accuracy of temperature measurement is ±0.9°C over -40° to +70°C. For temperature measurements only some PT100 probes (platinum resistance thermometer) from Campbell Scientific have also been used to measure temperature. The measurement range is - 200°C to 650°C and accuracy is ±0.1°C at 0°C and ± 0.19°C at 100°C. In addition to these sensors some temperature and humidity data loggers (EL-USB-2) by Lascar Electronics have been used. The temperature measurement range is -35°C to 80°C and accuracy is ± 0.5°C. The humidity measurement range is 0% to 100% and accuracy is ±3%.

### 3.5 Heat Flux Sensors

The Heat flux sensor HFP01(using thermopile to measure voltage in response to heat flux) developed by Hukseflux has been used to measure heat flux through the insulation. The measurement range is between -2000 w/$m^2$ to +2000 w/$m^2$ and the accuracy is ±5%.

### 3.6 CR1000 Data Logger

CR1000 data logger has been used for gathering data from the CS215 probes , PT100/3 probes and Hukseflux heat flux sensors. The data can be viewed by the PC400 software. CR 1000 logger and the PC400 software (developed by Campbell Scientific) are also used to control the temperature, amplitude and temperature hysteresis of the internal heater of the hygrothermal hotbox. The CR1000 data logger has an MTBF (mean time between failures) of 975 years.

## 4. MATERIAL PREPARATION AND INSTRUMENTATION

Each of the insulation samples have been fitted with one heat flux sensor, four temperature and humidity sensors, two temperature sensors and one Isomet needle probe. All the sensors are threaded to the external surfaces and three internal layers of the insulations so that there is no displacement of the sensors during the experiment. The insulations are partially sliced and opened up along its depth (along the section) to accommodate the sensors. Once the sensors are properly placed the partially opened layers are joined together with cotton threads. The figure one below shows the schematic of the arrangement.

## 5. CALIBRATION OF SENSORS AND PROBES:

The temperature and moisture sensors are checked for calibration and it has been find that the results are within the range of error. For heat flux sensors it has been found that there is variation between the readings of the two heat flux sensors, the readings of the one sensor is adjusted numerically so that the error in minimized. The details are not provided of the calibration process due to the shortage of space.

## 6. EXPERIMENTAL SETUP

The two insulation samples are places side by side in a 30mm EPS frame and the samples are separated by a 30mm layer of EPS insulation. The wires from all the sensors run through a channel at the upper part of the frame and the wires are linked to the CR1000 data logger. Some of the temperature and Humidity Loggers (EL-USB-2) are independent and data from those loggers are extracted once the experiment is done. The outer surface of the dual insulations is covered with a 3mm clear acrylic- the intention is to make the condensation visible and the evidence can be visually recorded if it occurs at the interface of the acrylic and any of the insulations. The duel-insulations with the frame is placed in front of a hot-box (which we are calling a hygrothermal hot-box). The hot-box is connected to a climate chamber where temperature and humidity can

be programmed or be manually controlled. There is a temperature and relative humidity sensor

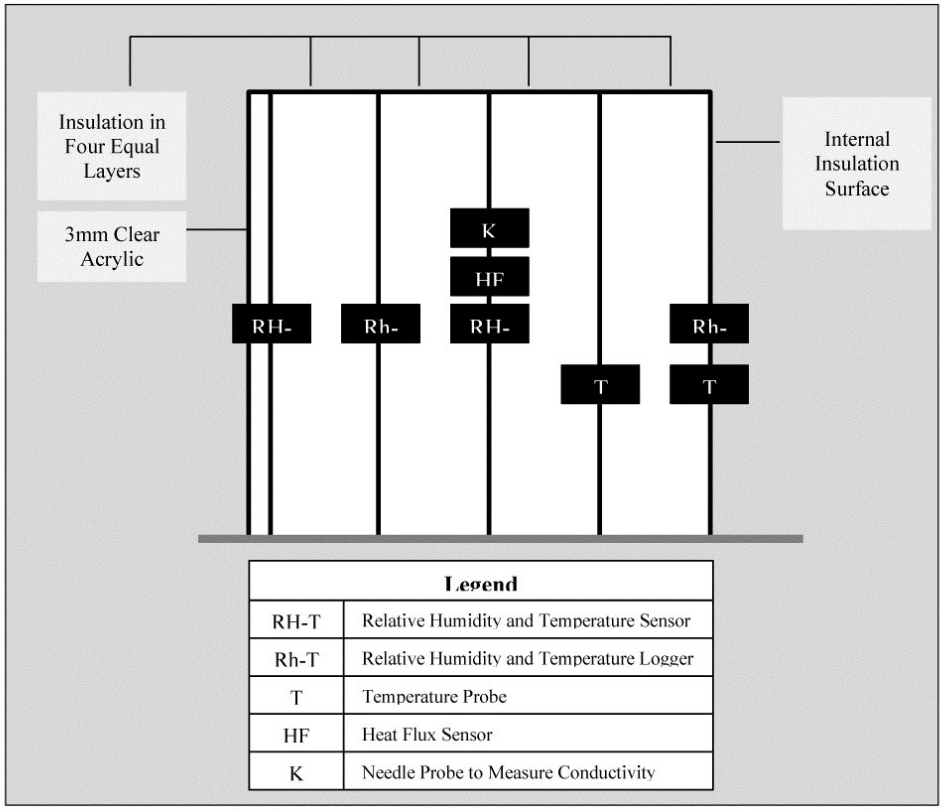


*Figure 1. Sensors across the Insulation Section*

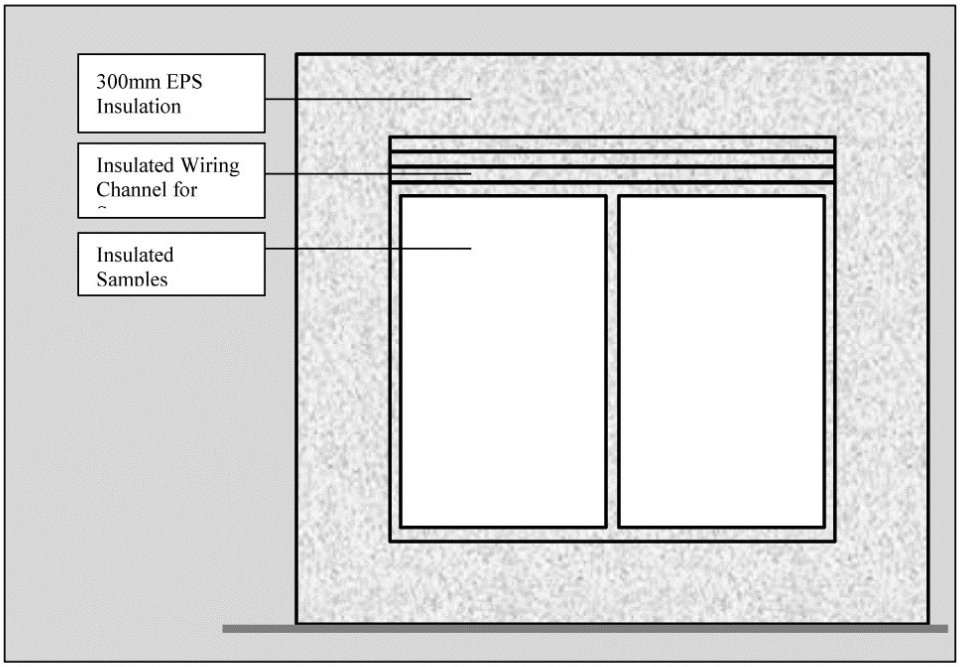


*Figure 2. Front View of the Duel-Insulation Setup*

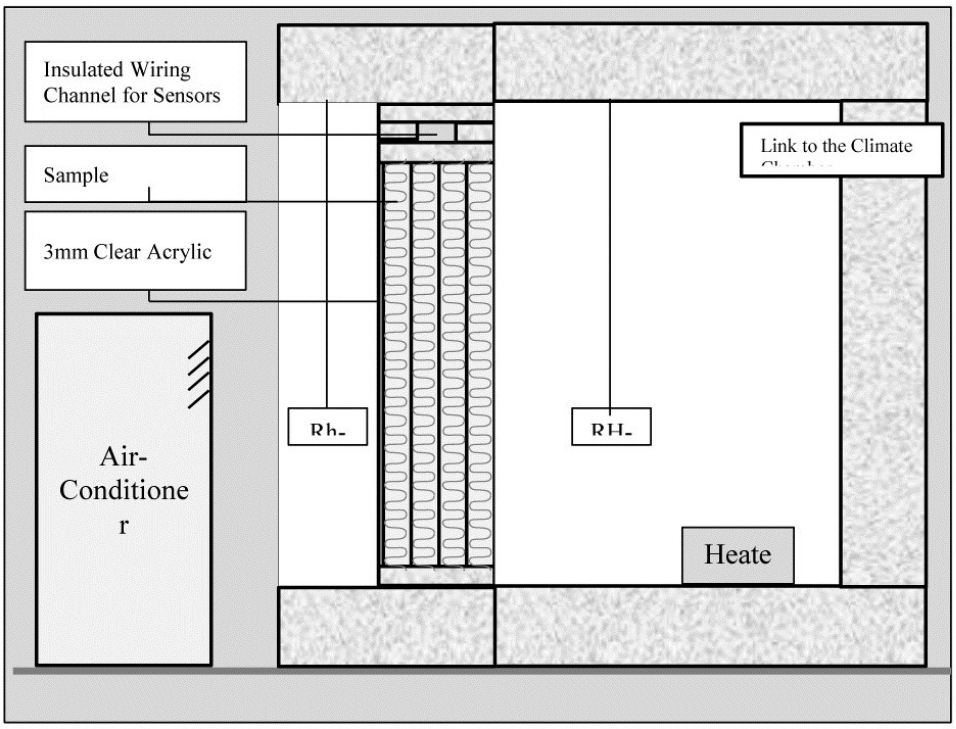


*Figure 1. Sectional drawing of the setup with the sample insulations*

inside the hygrothermal hot box and another temperature and humidity logger outside the hot-box. The acrylic sheet is glued to the duel insulation frame with silicon sealant to make sure that there is no moisture release to the outside and that there is no moisture interaction between the insulations.

## 7. EXPERIMENTAL METHOD:

The insulations are exposed to dynamic Relative Humidity (RH) varying from 35% RH to 80% RH. Internal temperature at the dynamic hot box is kept at around 35°C and the external temperature is kept between 15° to 22°C. Temperature difference between the interior and exterior of the insulation is attempted to be maintained between 10°C to 20°C so that uni-directional heat flux can be achieved. Effective thermal conductivity is measured from heat flux and surface temperature differences following Fourier's law of conductivity. Interstitial condensation can be easily viewed once it has occurred in the internal surfaces of the acrylic sheet. Occurrence of interstitial condensation is also checked numerically by calculating the due point temperature at the interface and comparing them with the actual temperature of the surfaces.

## 8. RESULT AND DUSCUSSION:

### 8.1 Interstitial Condensation:

During the total period of 22 days of experimental run, interstitial condensation was visually observed behind the clear acrylic of rock stone insulation twice. When the condensation was first noticed (assuming that the condensation might have happened earlier) the relative humidity probe registered Around 86% relative humidity and when the condensation was noticed for the second time the relative humidity probe registered about 93% relative humidity, this clearly shows the limitation of the probes to sense actual interstitial condensation on the adjacent surfaces. However why and when condensation has occurred can be explained by determining the vapour pressure gradient along the insulation layers and comparing the mathematically determined due point temperature with the surface temperature. It can be easily seen that in the acrylic surface cover of hemp insulation temperature is always higher than the dew-point temperature and in the acrylic surface cover of the stone wool insulation the surface temperature is lower than the dew point temperature during the times when condensation was observed. No condensation was observed in the inner surface of the acrylic behind the hemp insulation (see figure 4) during these periods which can also be explained by dew-point analysis as explained earlier. When the condensation was noticed the climate chambers were switched off so that relative humidity inside the hygrothermal climate chamber could go down which eventually could induce the relative humidity inside the insulations to go down along the vapour pressure gradient. Figure 5 shows the relative humidity on the external surfaces of stone wool and of hemp insulations before, during and after the second occurrence of condensation. From figure 5 and figure 6 it can also be observed that peak humidity near the outer surface of stone wool is about 10% higher than the peak humidity near the outer surface of hemp insulation for about 60 hours. However although both of the insulations are exposed to the similar external and internal temperature and humidity boundary condition, when the climate chamber was switched of the drop of humidity in the external surface of stone wool insulation was very steep at the beginning while the drop in humidity in the outer surface of hemp insulation is very steady. Although there is a clear correlation visible between the fluctuation of external temperature and the fluctuation of humidity in the outer surface of rock wool, still the sudden drop of relative humidity in stone wool external surface can better be explained by the vapour diffusion resistance factor and sorption isotherm of the materials. Vapour diffusion resistance factor of the

stone wool and the hemp fibre insulation have been measured by the author following BS EN 1208:1997 (British Standards Institute, 1997). The relevant findings are presented in the table 2. From present authors tests for the specific insulation samples the vapour diffusion resistance factor of hemp is measured as 1.29 and of stone wool is measured as 1.36 in wet cup test. However, BS EN ISO 1046:2007 (British Standards Institute, 2007) provides tabulated design values of a number of building materials and according to that the vapour diffusion resistance factor of mineral wool (for density range of 10-200 Kg/$m^3$) in wet cup test is 1, no data is provided for hemp insulation. However vapour permeability can vary in thermal insulation if bulk density changes (Betty et al, 1981). Hence from the present author's test it can be assumed that the vapour diffusion resistance factors of both the materials are about similar. Another important humidity and moisture related property of the material is moisture holding capacity (which can be determined from sorption-desorption nisotherm) which can vary among insulation materials. Moisture holding capacity of insulation materials are measured by exposing the materials to a range of humidity

*Figure 4. Condensation is Clearly Visible on Stone Wool Surface on the Left.*

conditions until equilibrium moisture content is reached in accordance with table C.2 of BS EN 12429:1998 (British Standards Institute, 1998) for the determination of equilibrium moisture content and BS EN ISO12571:2000

(British Standards Institute, 2000) for the climatic chamber method for determining sorption properties. The findings are shown in figure 8. It is very clear that while stone wool does not adsorb moisture at all, hemp fibre has a very high moisture adsorption capacity. Both the insulations have similar diffusion resistance factor but hemp has higher moisture holding capacity, therefore when the Acrylic is used as a vapour barrier and higher vapour pressure is created in the hotbox, in stone wool vapour goes straightaway to the acrylic layer and since the stone wool does not absorb or adsorb moisture, vapour pressure becomes higher near the acrylic and also in the air gaps of the mineral fibres. On the other hand, in hemp insulation vapour propagation becomes a factor of vapour permeability and moisture adsorption capability resulting in lesser vapour near the acrylic barrier and in the air voids between the fibres. Therefore while condensation occurred at the outer surface of stone wool, at the same time internal humidity and vapour pressure shows a damping effect inside the hemp insulation because of its vapour resistance and moisture holding capacity. From figure 6 it can be observed that the humidity gradient in stone wool instantaneously followed the internal humidity gradient except at the external layer where condensation occurred (see figure 7). On the other hand humidity gradient inside the hemp insulation was steadier during the whole time and is less affected by the humidity gradient inside the hotbox.

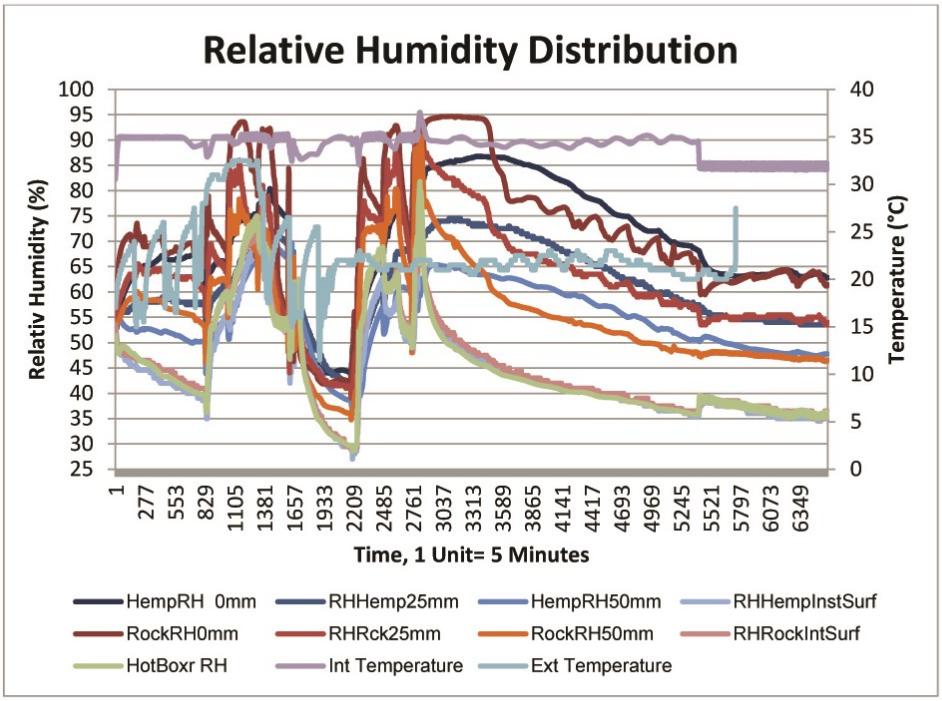

*Figure 5. Relative Humidity Distribution Across the Insulation During the Experiment.*

*Table 2. Vapour Transmission Properties*

| Material | W, Water Vapour Permeance ($mg/m^2h.Pa$) | Z, Water Vapour Resistance (1/W) | δ, Water Vapour Permeability | μ, Water Vapour Diffusion Resistance Factor | $S_d$, Water Vapour Equivalent Air Layer Thickness (m) |
|---|---|---|---|---|---|
| Hemp | 9.93 | 0.102 | 0.558 | 1.29 | 0.072 |
| Stone wool | 6.51 | 0.154 | 0.455 | 1.36 | 0.108 |

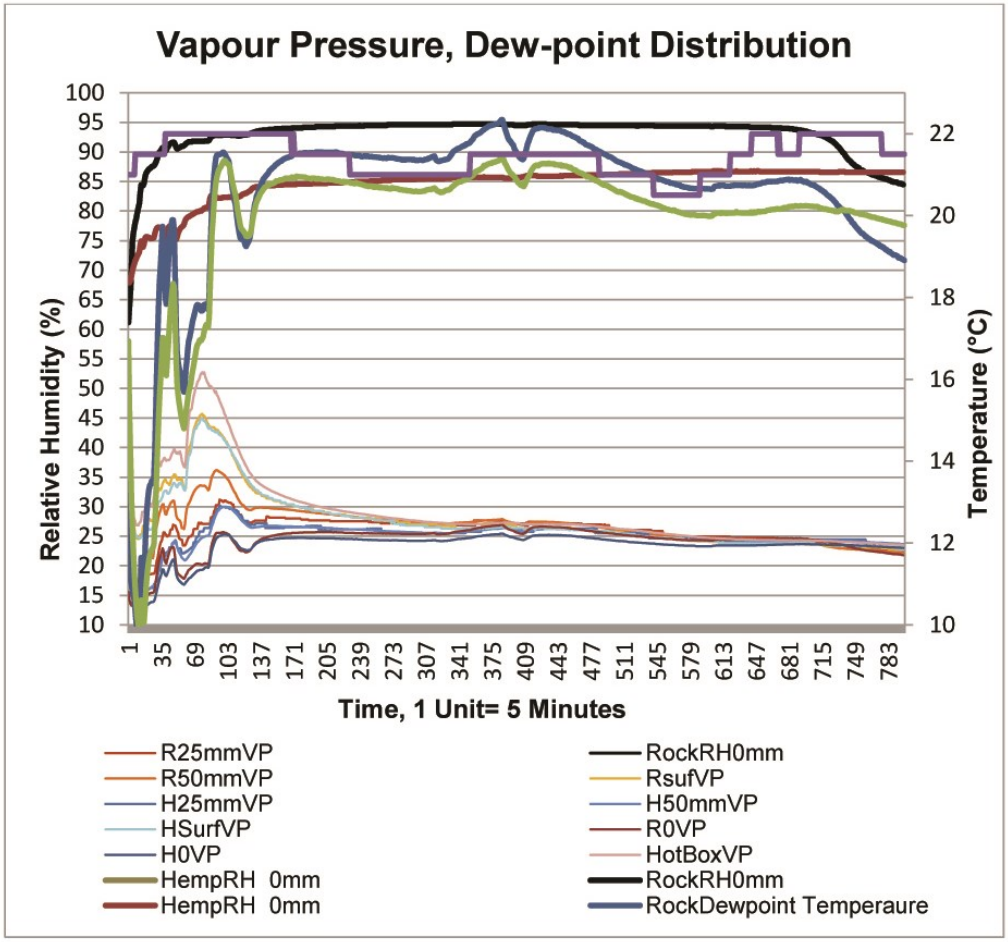


*Figure 6. Vapour Pressure, Dew-point Temperatures and Acrylic Surface Temperature*

*Table 3. Conductivity of Hemp and Stone Wool*

| Average Relative Humidity(%) | Average Conductivity of Hemp | No of Data | Standard Deviation | Average Conductivity of Stone Wool | No of Data | Standard Deviation |
|---|---|---|---|---|---|---|
| 35-45 | 0.052 | 422 | 0.002 | 0.055 | 475 | 0.001 |
| 40-50 | 0.050 | 602 | 0.002 | 0.053 | 270 | 0.002 |
| 45-55 | 0.050 | 2465 | 0.002 | 0.052 | 1975 | 0.002 |
| 50-60 | 0.050 | 3165 | 0.002 | 0.053 | 3339 | 0.002 |
| 55-65 | 0.049 | 1026 | 0.002 | 0.054 | 2401 | 0.002 |
| 60-70 | 0.048 | 2416 | 0.003 | 0.054 | 1029 | 0.002 |
| 65-75 | 0.048 | 1555 | 0.004 | 0.054 | 943 | 0.002 |
| 70-80 | 0.047 | 130 | 0.006 | 0.054 | 1301 | 0.002 |

## 9. CONCLUSIONS

One sample of a commercially hemp insulation and one sample of a commercially available stone wool insulation is hygrothermally tested in a duel-insulation setup. It has been observed that for the specific insulation samples, and for the places the setup and assembly is applicable, condensation can occur much earlier in the moisture barrier interface of stone wool insulation than in hemp insulation. It has also been observed that moisture dependent conductivity of hemp insulation is comparatively lower than the moisture dependent conductivity of stone wool insulation in moist of the humidity ranges.

## 10. REFERENCES


Batty, W. J., O'Callaghan, P. W., Probert S. D., and Gregory S. (1981) 'Water-vapour diffusion through fibrous thermal insulants', *Applied Energy*, 8(3), pp. 193-204.

British Standards Institute (1997) BS EN 12086: *Thermal insulating products for building applications - Determination of water vapour transmission properties. Bsol.bsigroup.com* [Online]. Available at: https://bsol.bsigroup.com/ (Accessed: 25July 2011).

British Standards Institute (1998) BS EN 12429: *Thermal insulating products for building applications -Conditioning to moisture equilibrium under specified temperature and humidity conditions. Bsol.bsigroup.com* [Online]. Available at: https://bsol.bsigroup.com/ (Accessed: 07January 2011).

British Standards Institute (2000) BS EN ISO12571: *Hygrothermal performance of building materials and products -Determination of hygroscopic sorption properties. Bsol.bsigroup.com* [Online]. Available at: https://bsol.bsigroup.com/ (Accessed: 10June 2010).

British Standards Institute (2007) BS EN ISO 10456: *Building materials and products-Hygrothermal properties- Tabulated design values and procedures for determining declared and design thermal values. Bsol.bsigroup.com* [Online]. Available at: https://bsol.bsigroup.com/ (Accessed: 27July 2011).